MYCORRHIZOSPHERE COMMUNICATION: MYCORRHIZAL FUNGI AND ENDOPHYTIC FUNGUS-PLANT INTERACTIONS

EDITED BY: Erika Kothe and Katarzyna Turnau
PUBLISHED IN: Frontiers in Microbiology

frontiers Research Topics

ISSN 1664-8714
ISBN 978-2-88945-739-7
DOI 10.3389/978-2-88945-739-7

About Frontiers

Frontiers is more than just an open-access publisher of scholarly articles: it is a pioneering approach to the world of academia, radically improving the way scholarly research is managed. The grand vision of Frontiers is a world where all people have an equal opportunity to seek, share and generate knowledge. Frontiers provides immediate and permanent online open access to all its publications, but this alone is not enough to realize our grand goals.

Frontiers Journal Series

The Frontiers Journal Series is a multi-tier and interdisciplinary set of open-access, online journals, promising a paradigm shift from the current review, selection and dissemination processes in academic publishing. All Frontiers journals are driven by researchers for researchers; therefore, they constitute a service to the scholarly community. At the same time, the Frontiers Journal Series operates on a revolutionary invention, the tiered publishing system, initially addressing specific communities of scholars, and gradually climbing up to broader public understanding, thus serving the interests of the lay society, too.

Dedication to Quality

Each Frontiers article is a landmark of the highest quality, thanks to genuinely collaborative interactions between authors and review editors, who include some of the world's best academicians. Research must be certified by peers before entering a stream of knowledge that may eventually reach the public - and shape society; therefore, Frontiers only applies the most rigorous and unbiased reviews.
Frontiers revolutionizes research publishing by freely delivering the most outstanding research, evaluated with no bias from both the academic and social point of view. By applying the most advanced information technologies, Frontiers is catapulting scholarly publishing into a new generation.

What are Frontiers Research Topics?

Frontiers Research Topics are very popular trademarks of the Frontiers Journals Series: they are collections of at least ten articles, all centered on a particular subject. With their unique mix of varied contributions from Original Research to Review Articles, Frontiers Research Topics unify the most influential researchers, the latest key findings and historical advances in a hot research area! Find out more on how to host your own Frontiers Research Topic or contribute to one as an author by contacting the Frontiers Editorial Office: researchtopics@frontiersin.org

MYCORRHIZOSPHERE COMMUNICATION: MYCORRHIZAL FUNGI AND ENDOPHYTIC FUNGUS-PLANT INTERACTIONS

Topic Editors:
Erika Kothe, Friedrich Schiller University Jena, Germany
Katarzyna Turnau, Jagiellonian University in Krakow, Poland

Ectomycorrhizal root exemplifying the intimate association between plant and fungus in a mutually beneficial symbiosis. Image: Piotr Mleczko.

Cover image: Main background: Leszek Glasner/Shutterstock.com. Bottom right image: Piotr Mleczko.

The specific interactions of fungi with plants include the mutually beneficial mycorrhizal symbioses and an increasing number of case studies, where endophytic fungi communicate with their host plant to allow for beneficial interactions. The omics methods development has allowed for a substantial increase in knowledge that emphasized in many cases the intricate interplay between the symbiotic partners. In addition to the direct interactions, the mycorrhizosphere comes into view, as

the fungal soil mycelium is interacting with the community outside the host plant, transferring signals also to the host. This Research Topic encompasses research on both major types of mycorrhizal interactions, endo- and ectomycorrhiza, and includes communication with the environment in which both partners interact with soil microbes. The mycorrhizosphere is in the center of molecular biology and modern ecological research, greatly fostered by the possibilities of genetic manipulation.

Citation: Kothe, E., Turnau, K., eds. (2019). Mycorrhizosphere Communication: Mycorrhizal Fungi and Endophytic Fungus-Plant Interactions. Lausanne: Frontiers Media. doi: 10.3389/978-2-88945-739-7

Table of Contents

SECTION III

PHYTOPATHOGENIC INTERACTIONS

SECTION IV

ENVIRONMENTAL INTERACTIONS

frontiers in Microbiology

EDITORIAL
published: 05 December 2018
doi: 10.3389/fmicb.2018.03015

Editorial: Mycorrhizosphere Communication: Mycorrhizal Fungi and Endophytic Fungus-Plant Interactions

Erika Kothe[1]* *and Katarzyna Turnau*[2]

[1] Institute of Microbiology, Friedrich Schiller University, Jena, Germany, [2] Institute of Environmental Sciences, Jagiellonian University in Krakow, Kraków, Poland

Keywords: mycorrhiza, endophyte, fungus-plant interactions, mycorrhizophere, communication

Editorial on the Research Topic

Mycorrhizosphere Communication: Mycorrhizal Fungi and Endophytic Fungus-Plant Interactions

PLANT MYCOBIOMES

Plants do not exist as single entities but should rather be considered to form a complex community with microbes and other organisms where plant tissues form diverse niches for microbes. One major relationship concerns plant-fungal interactions that range from pathogenicity to mutually beneficial symbioses. A balanced state (homeostasis) of these interactions is essential for maintaining the plant as well as an overall healthy state of the environment. Mycorrhizal associations are well-studied examples of root-fungal mutually beneficial symbiosis (Ferlian et al., 2018; Gehring and Johnson, 2018). The reasons for establishing a mutual symbiosis are only just beginning to be understood at the molecular level (Mello and Balestrini). Communication between endo- and ecto-mycorrhiza and their respective host plants (Raudaskoski and Kothe, 2015; Luginbuehl and Oldroyd, 2017; Garcia et al., 2018, and citations therein) and the effects on phytohormone levels and localized delivery (see Boivin et al., 2016; MacLean et al., 2017) have been the focus of several recent reports. But even so, a full understanding of these relationships will only be gained by investigating the effects of different strains of the same fungal species (Sharma et al.).

For roots, as well as above-ground plant tissues, endophytic fungi can be considered as examples of specific co-evolution, provided the term "endophytic" is used in its *sensu strictu* (for a detailed comment, see Kothe and Dudeja, 2011). To prove endophytic behavior, Koch's postulates need to be observed, and tissue specificity for re-infection may be used as a method to discriminate real endophytes from mere co-occurrence (Wężowicz et al., 2017; Domka et al., 2018; Ważny et al., 2018). The traits of endophytes that do not lead to symptoms in a healthy plant clearly delineate them from phytopathogenic fungi, however, caution is necessary because their effect on the symbiosis can vary with the species/variety of the partner and environmental conditions. For endophytic fungi, knowledge is much more limited as compared to mycorrhiza, although a role for strigolactone signaling is presented by Rozpądek et al.

Temporal shifts in plant-associated fungal populations are known to occur. An example from mycorrhizal symbiosis is for young trees with endomycorrhizal symbionts that are later replaced by specific ectomycorrhizal associations (Knoblochová et al., 2017; Bachelot et al., 2018). Within 4 weeks, vesicles and hyphae are visible in the roots of *Picea abies* and *Pinus sylvestis* leading to increased main-root development and up to a 300% increase in secondary roots.

OPEN ACCESS

Edited by:
Anna Maria Pirttilä,
University of Oulu, Finland

Reviewed by:
Tamás Papp,
University of Szeged, Hungary

***Correspondence:**
Erika Kothe
erika.kothe@uni-jena.de

Specialty section:
This article was submitted to Fungi and Their Interactions, a section of the journal Frontiers in Microbiology

Received: *12 September 2018*
Accepted: *22 November 2018*
Published: *05 December 2018*

Citation:
Kothe E and Turnau K (2018) Editorial: Mycorrhizosphere Communication: Mycorrhizal Fungi and Endophytic Fungus-Plant Interactions. Front. Microbiol. 9:3015. doi: 10.3389/fmicb.2018.03015

These effects alone will increase the potential at a later stage for formation of ectomycorrhiza, which is the only form of mycorrhiza seen in mature pine and spruce. After the ectomycorrhiza is established, a succession of fungal partners appears. First, fast-growing, broad host-range, reproduction-strategy fungi are attracted; later, slower growing, but more specific, ectomycorrhizal fungi, acting by capacity strategy, are recruited. For spruce, that would lead to replacement of, e.g., *Cenococcum geophilum* (see de Freitas Periera et al.) or *Pisolithus tinctorius* by host-specific fungi like *T. vaccinum*.

MULTI-OMICS IN FUNGAL-PLANT MOLECULAR COMMUNICATION

The mycobionts and their hosts will constantly communicate to establish and maintain the symbiosis. Signals are perceived and result in changes in gene expression. With excreted proteins or metabolites, the partner is stimulated. A multi-level interaction thus will be visible with changed transcriptome, proteome, and metabolome patterns. These can be visualized with techniques such as transcriptomics (Fiorilli et al., 2016; Nagabhyru et al., 2018), proteomics (Sebastiana et al., 2017; Shrivastava et al., 2018), metabolomics (Hill et al., 2018; Maciá-Vicente et al., 2018), or combinations thereof (e.g., Larsen et al., 2016). Since secreted proteins may be important for the signal exchange, secretomics can be expected to identify effector proteins exchanged between symbiont and host (Doré et al., 2015; Wagner et al., 2015). Volatiles exchanged address a subgroup of metabolites for signal exchange (Ditengou et al., 2015; Pistelli et al., 2017). And a combination of translatome and proteome data (Sharma et al.), as well as multi-omics have proven to substantially improve the quality of prediction for the symbiotic molecular network (Vijayakumar et al., 2016).

Interactions between symbiotic fungus and plant in production of secondary metabolites (Ludwig-Müller, 2015; González-Menéndez et al., 2016) shows the intricate relationship between the symbiotic partners. In addition to the dual interaction, the communication is expanded with additional fungi or bacteria which co-occur in the environment.

MULTI-PARTNER INTERACTIONS

Usually, plant and fungus are not alone in the partnership, but additional interactions with bacteria or other fungi will influence the outcome of these associations in nature. This complex relationship is reflected in the concept of the mycorrhizosphere, where plant roots and hyphae of the mycorrhizal partner encounter other soil microorganisms. These additional interactions in the vicinity of the root need to be considered in studies of cross-talk (Vannini et al., 2016; Wagner et al., 2016).

Phytohormones produced in the mycorrhizosphere may alter the physiology of the symbiotic partners and aid formation of new mycorrhiza (Wagner et al., 2015). For example, the ectomycorrhizal *Tricholoma vaccinum* produces the auxin indole-3-acetic acid (IAA), which stimulates mycorrhization (Krause et al., 2015). In addition, the exogenous presence of the phytohormone promotes branching, which leads to an increased Hartig-net formation during symbiosis (Krause et al., 2015). Moreover, ectomycorrhization can be reversed by associated fungi that produce IAA-inhibiting compounds (Hause and Saarschmidt, 2009). With soil zygomycetes, a tripartite interaction occurs in which the zygomycete-derived metabolite, D-orenone, induces a transporter that allows for increased excretion of IAA by the mycorrhizal fungus, *T. vaccinum* (Wagner et al., 2016). Soil bacteria are also capable of auxin biosynthesis, mostly upon tryptophan induction *via* root exudates. Since IAA increases branching of ectomycorrhizal fungi, some have been termed mycorrhiza-helper bacteria (Frey-Klett et al., 2016). It is now clear that multi-partner communication systems have evolved and are present in any habitat.

Like symbionts, phytopathogens also act *via* phytohormes, e.g., by inducing systemic-acquired resistance in host plants (Scholz et al.). Similar mechanisms of cross-talk can be inferred from comparison of pathosystems to endophytic or mycorrhizal symbiosis.

MOLECULAR RESPONSES TO ENVIRONMENTAL STRESSES

In addition to biotic interactions shaping the plant mycobiome, abiotic factors certainly influence the mutual, commensal or pathogenic interaction. Environmental conditions may influence plant mycobiomes, and these effects are more likely observed under detrimental conditions, such as nutrient limitation, drought, salinity, or other stresses, for example metal toxicity (Kumar and Verma, 2018; Shi et al., 2018). The molecular background of stress recognition and signal transduction within endomycorrhiza is reported by Sun et al. and an example of endophytes altering phosphate mobility in the mycorrhizosphere is given by Baum et al. The molecular background of stress recognition and signal transduction with an endomycorrhizal association is reported by Sun et al. as is an example of endophytes changing phosphate mobilities in the mycorrhizosphere (Baum et al.).

Environmental stresses, like metal contamination in the ground, to name just one example, can be buffered by mycorrhizal and endophytic associations. A molecular role has been shown for hydrophobins, small amphipatic proteins that decorate the cell wall of air-exposed mycelium. A study by Sammer et al. on the up-regulation of different hydrophobins during the life cycle of the mycorrhizal fungus exposed to metal contamination illustrates their protective effect. In that study, the biotic interaction is also characterized by volatiles and exudates from the host tree inducing mycorrhiza-associated hydrophobin genes (Sammer et al., 2016).

Transporter production, as well as intracellular storage of metals, illustrate specific adaptive responses in fungi. Many fungi are able to carry increased metal loads if grown on metal-contaminated substrate. A prominent example is the mushrooms

that showed high cesium content when collected from the fall-out areas after the Chernobyl accident. A molecular explanation is now available for this observation (see Benes et al.). For metals that are not only toxic, but essential for growth at lower concentrations, e.g., zinc, require the presence of a specific uptake and storage system. Indeed, for zinc, such a system has been described with the ectomycorrhizal fungus *Suillus luteus* (Coninx et al.). As an additional twist, there are fungi that influence mutual symbioses of bacteria with plants. An example of this is shown by Thiem et al. where the influence of microbiome, including the mycobiome, on the actinorrhizal interaction between *Frankia* and alder (*Alnus glutinosa*) under salinity is demonstrated.

APPLICATIONS FOR GROWING DEMANDS ON SUSTAINABLE AGRICULTURE AND FORESTRY

Anthropogenic impact, including industrial pollution and both conventional and organic agriculture, has already affected the soil microbiome, leading to decreases in soil quality and the nutritional value of crops. In doing so, it has created the necessity to use a range of chemicals, such as fertilizers and pesticides, to avoid the spread of unwanted pathogenic microbes. These substances not only affect plant-microbial foes but also the friendly microbes that help the plant to establish homeostasis and attain the nutritional quality of products that support the health of the consumers. The twenty first century brings us possibilities to develop new and innovative methods to rebuild soil tilth and to renovate the plant microbiota (see, e.g., Verzeaux et al., 2017; Campos et al., 2018). However, to be successful, we need an increased understanding by both food and wood producers on the molecular communication between fungi and the host plant, resulting in competitive advantages specifically under abiotic stress. The results may provide solutions for the problems aggravating sustainable agriculture and forestry, especially under the ever-changing environmental conditions (Shinde et al., 2018).

The re-introduction of protective microbes can be achieved through bioaugmentation strategies, which allow them to create optimal conditions for crop growth under harsh conditions (see Treu and Falandysz, 2017) and a reduction in the use of water, fertilizers, and pesticides. The most common plant inhabitants are endophytes that, when properly selected, can be a potent tool against pathogens and abiotic factors (see French, 2017). They also support mycorrhizae, which in turn contribute to plant growth and induce tolerance to salinity, pollution, drought, extreme temperatures, elevated CO_2, etc. (see, e.g., Dhawi et al., 2017). The provision of well-selected microbes and the application of appropriate agricultural/forestry practices, both of which are feasible now, can decrease the current intensive use of fertilizers while maintaining an environment that is conducive to human health. Although nowadays the interaction of fungi and bacteria with plants is better understood, there is still a need for greater insight into the interplay between bacteria and fungi, fungi with other fungi, and their interactions with plants. Furthermore, building stronger bridges between bacteriologists and mycologists will help to benefit from their complementary skills, as exemplified by the work on the roles of strigolactones (see, De Cuyper and Goormachtig, 2017).

AUTHOR CONTRIBUTIONS

All authors listed have made a substantial, direct and intellectual contribution to the work, and approved it for publication.

REFERENCES

Bachelot, B., Uriarte, M., Muscarella, R., Forero-Montaña, J., Thompson, J., McGuire, K., et al. (2018). Associations among arbuscular mycorrhizal fungi and seedlings are predicted to change with tree successional status. *Ecology* 99, 607–620. doi: 10.1002/ecy.2122

Boivin, S., Fonouni-Farde, C., and Frugier, F. (2016). How auxin and cytokinin phytohormones modulate root microbe interactions. *Front. Plant Sci.* 7:1240. doi: 10.3389/fpls.2016.01240

Campos, P., Borie, F., Cornejo, P., López-Ráez, J. A., López-García, Á., and Seguel, A. (2018). Phosphorus acquisition efficiency related to root traits: is mycorrhizal symbiosis a key factor to wheat and barley cropping? *Front. Plant Sci.* 9:752. doi: 10.3389/fpls.2018.00752

De Cuyper, C., and Goormachtig, S. (2017). Strigolactones in the Rhizosphere: friend or foe? *Mol. Plant Microbe Interact.* 30, 683–690. doi: 10.1094/MPMI-02-17-0051-CR

Dhawi, F., Datta, R., and Ramakrishna, W. (2017). Proteomics provides insights into biological pathways altered by plant growth promoting bacteria and arbuscular mycorrhiza in sorghum grown in marginal soil. *Biochim. Biophys. Acta Proteins Proteom.* 1865, 243–251. doi: 10.1016/j.bbapap.2016.11.015

Ditengou, F. A., Müller, A., Rosenkranz, M., Felten, J., Lasok, H., van Doorn, M. M., et al. (2015). Volatile signalling by sesquiterpenes from ectomycorrhizal fungi reprogrammes root architecture. *Nat. Commun.* 6:6279. doi: 10.1038/ncomms7279

Domka, A., Rozpądek, P., Ważny, R., and Turnau, K. (2018). *Mucor* sp. - an endophyte of Brassicaceae capable of surviving in toxic metal-rich sites. *J. Basic Microbiol.* doi: 10.1002/jobm.201800406. [Epub ahead of print].

Doré, J., Perraud, M., Dieryckx, C., Kohler, A., Morin, E., Henrissat, B., et al. (2015). Comparative genomics, proteomics and transcriptomics give new insight into the exoproteome of the basidiomycete *Hebeloma cylindrosporum* and its involvement in ectomycorrhizal symbiosis. *New Phytol.* 208, 1169–1187. doi: 10.1111/nph.13546

Ferlian, O., Biere, A., Bonfante, P., Buscot, F., Eisenhauer, N., Fernandez, I., et al. (2018). Growing research networks on mycorrhizae for mutual benefits. *Trends Plant Sci.* 23, 975–984. doi: 10.1016/j.tplants.2018.08.008

Fiorilli, V., Belmondo, S., Khouja, H. R., Abbà, S., Faccio, A., Daghino, S., et al. (2016). RiPEIP1, a gene from the arbuscular mycorrhizal fungus *Rhizophagus irregularis*, is preferentially expressed *in planta* and may be involved in root colonization. *Mycorrhiza* 26, 609–621. doi: 10.1007/s00572-016-0697-0

French, K. E. (2017). Engineering mycorrhizal symbioses to alter plant metabolism and improve crop health. *Front. Microbiol.* 8:1403. doi: 10.3389/fmicb.2017.01403

Frey-Klett, P., Garbaye, J., and Tarkka, M. (2016). The mycorrhiza helper bacteria revisited. *New Phytol.* 176, 22–36. doi: 10.1111/j.1469-8137.2007.02191.x

Garcia, K., Delaux, P. M., Cope, K. R., and Ané J. M. (2018). Molecular signals required for the establishment and maintenance of ectomycorrhizal symbioses. *New Phytol.* 208, 79–87. doi: 10.1111/nph.13423

Gehring, C. A., and Johnson, N. C. (2018). Beyond ICOM8: perspectives on advances in mycorrhizal research from 2015 to 2017. *Mycorrhiza* 28, 197–201. doi: 10.1007/s00572-017-0818-4

González-Menéndez, V., Pérez-Bonilla, M., Pérez-Victoria, I., Martín, J., Muñoz, F., Reyes, F., et al. (2016). Multicomponent analysis of the differential induction of secondary metabolite profiles in fungal endophytes. *Molecules* 21:234. doi: 10.3390/molecules21020234

Hause, B., and Saarschmidt, S. (2009). The role of jasmonates in mutualistic symbioses between plants and soil-borne microorganisms. *Phytochemistry* 70, 1589–1599. doi: 10.1016/j.phytochem.2009.07.003

Hill, E. M., Robinson, L. A., Abdul-Sada, A., Vanbergen, A. J., Hodge, A., and Hartley, S. E. (2018). Arbuscular mycorrhizal fungi and plant chemical defence: effects of colonisation on aboveground and belowground metabolomes. *J. Chem. Ecol.* 44, 198–208. doi: 10.1007/s10886-017-0921-1

Knoblochová, T., Kohout, P., Püschel, D., Doubková, P., Frouz, J., Cajthaml, T., et al. (2017). Asymmetric response of root-associated fungal communities of an arbuscular mycorrhizal grass and an ectomycorrhizal tree to their coexistence in primary succession. *Mycorrhiza* 27, 775–789. doi: 10.1007/s00572-017-0792-x

Kothe, E., and Dudeja, S. S. (2011). Editorial: plant-microbe interactions. *J. Basic Microbiol.* 51:4. doi: 10.1002/jobm.201190002

Krause, K., Henke, C., Asiimwe, T., Ulbricht, A., Klemmer, S., Schachtschabel, D., et al. (2015). Biosynthesis and secretion of indole-3-acetic acid and its morphological effects on *Tricholoma vaccinum*-spruce ectomycorrhiza. *Appl. Environ. Microbiol* 81, 7003–7011. doi: 10.1128/AEM.01991-15

Kumar, A., and Verma, J. P. (2018). Does plant-microbe interaction confer stress tolerance in plants: a review? *Microbiol. Res.* 207, 41–52. doi: 10.1016/j.micres.2017.11.004

Larsen, P. E., Sreedasyam, A., Trivedi, G., Desai, S., Dai, Y., Cseke, L. J., et al. (2016). Multi-omics approach identifies molecular mechanisms of plant-fungus mycorrhizal interaction. *Front. Plant Sci.* 6:1061. doi: 10.3389/fpls.2015.01061

Ludwig-Müller, J. (2015). Plants and endophytes: equal partners in secondary metabolite production? *Biotechnol. Lett.* 37, 1325–1334. doi: 10.1007/s10529-015-1814-4

Luginbuehl, L. H., and Oldroyd, G. E. D. (2017). Understanding the arbuscule at the heart of endomycorrhizal symbioses in plants. *Curr. Biol.* 27, R952–R963. doi: 10.1016/j.cub.2017.06.042

Maciá-Vicente, J. G., Shi, Y. N., Cheikh-Ali, Z., Grün, P., Glynou, K., Kia, S. H., et al. (2018). Metabolomics-based chemotaxonomy of root endophytic fungi for natural products discovery. *Environ. Microbiol.* 20, 1253–1270. doi: 10.1111/1462-2920.14072

MacLean, A. M., Bravo, A., and Harrison, M. J. (2017). Plant signaling and metabolic pathways enabling arbuscular mycorrhizal symbiosis. *Plant Cell* 29, 2319–2335. doi: 10.1105/tpc.17.00555

Nagabhyru, P., Dinkins, R. D., and Schardl, C. (2018). Transcriptomics of *Epichloë*-grass symbioses in host vegetative and reproductive stages. *Mol. Plant Microbe Interact*. doi: 10.1094/MPMI-10-17-0251-R. [Epub ahead of print].

Pistelli, L., Ulivieri, V., Giovanelli, S., Avio, L., Giovannetti, M., and Pistelli, L. (2017). Arbuscular mycorrhizal fungi alter the content and composition of secondary metabolites in *Bituminaria bituminosa* L. *Plant Biol.* 19, 926–933. doi: 10.1111/plb.12608

Raudaskoski, M., and Kothe, E. (2015). Novel findings on the role of signal exchange in arbuscular and ectomycorrhizal symbioses. *Mycorrhiza* 25, 243–252 doi: 10.1007/s00572-014-0607-2

Sammer, D., Krause, K., Gube, M., Wagner, K., and Kothe, E. (2016). Hydrophobins in the life cycle of the ectomycorrhizal basidiomycete *Tricholoma vaccinum*. *PLoS ONE* 11:e0167773. doi: 10.1371/journal.pone.0167773

Sebastiana, M., Martins, J., Figueiredo, A., Monteiro, F., Sardans, J., Peñuelas, J., et al. (2017). Oak protein profile alterations upon root colonization by an ectomycorrhizal fungus. *Mycorrhiza* 27, 109–128. doi: 10.1007/s00572-016-0734-z

Shi, W., Zhang, Y., Chen, S., Polle, A., Rennenberg, H., and Luo, Z. B. (2018). Physiological and molecular mechanisms of heavy metal accumulation in nonmycorrhizal versus mycorrhizal plants. *Plant Cell Environ.* doi: 10.1111/pce.13471. [Epub ahead of print].

Shinde, S., Naik, D., and Cumming, J. R. (2018). Carbon allocation and partitioning in *Populus tremuloides* are modulated by ectomycorrhizal fungi under phosphorus limitation. *Tree Physiol.* 38, 52–65. doi: 10.1093/treephys/tpx117

Shrivastava, N., Jiang, L., Li, P., Sharma, A. K., Luo, X., Wu, S., et al. (2018). Proteomic approach to understand the molecular physiology of symbiotic interaction between *Piriformospora indica* and *Brassica napus*. *Sci. Rep.* 8:5773. doi: 10.1038/s41598-018-23994-z

Treu, R., and Falandysz, J. (2017). Mycoremediation of hydrocarbons with basidiomycetes-a review. *J. Environ. Sci. Health B* 52, 148–155. doi: 10.1080/03601234.2017.1261536

Vannini, C., Carpentieri, A., Salvioli, A., Novero, M., Marsoni, M., Testa, L., et al. (2016). An interdomain network: the endobacterium of a mycorrhizal fungus promotes antioxidative responses in both fungal and plant hosts. *New Phytol.* 211, 265–275. doi: 10.1111/nph.13895

Verzeaux, J., Hirel, B., Dubois, F., Lea, P. J., and Tétu, T. (2017). Agricultural practices to improve nitrogen use efficiency through the use of arbuscular mycorrhizae: basic and agronomic aspects. *Plant Sci.* 264, 48–56. doi: 10.1016/j.plantsci.2017.08.004

Vijayakumar, V., Liebisch, G., Buer, B., Xue, L., Gerlach, N., Blau, S., et al. (2016). Integrated multi-omics analysis supports role of lysophosphatidylcholine and related glycerophospholipids in the *Lotus japonicus-Glomus intraradices* mycorrhizal symbiosis. *Plant Cell Environ.* 39, 393–415. doi: 10.1111/pce.12624

Wagner, K., Krause, K., David, A., Kai, M., Jung, E. M., Sammer, D., et al. (2016). Influence of zygomycete-derived D'orenone on IAA signalling in *Tricholoma*-spruce ectomycorrhiza. *Environ. Microbiol.* 18, 2470–2480. doi: 10.1111/1462-2920.13160

Wagner, K., Linde, J., Krause, K., Gube, M., Köstler, T., Sammer, D., et al. (2015). *Tricholoma vaccinum* host communication during ectomycorrhiza formation. *FEMS Microbiol. Ecol.* 91:fiv120. doi: 10.1093/femsec/fiv120

Ważny, R., Rozpądek, P., Jędrzejczyk, R. J., Śliwa, M., Stojakowska, A., Anielska, T., et al. (2018). Does co-inoculation of *Lactuca serriola* with endophytic and arbuscular mycorrhizal fungi improve plant growth in a polluted environment? *Mycorrhiza* 28, 235–246. doi: 10.1007/s00572-018-0819-y

Wężowicz, K., Rozpądek, P., and Turnau, K. (2017). Interactions of arbuscular mycorrhizal and endophytic fungi improve seedling survival and growth in post-mining waste. *Mycorrhiza* 27, 499–511. doi: 10.1007/s00572-017-0768-x

Conflict of Interest Statement: The authors declare that the research was conducted in the absence of any commercial or financial relationships that could be construed as a potential conflict of interest.

frontiers in Microbiology

REVIEW
published: 15 February 2018
doi: 10.3389/fmicb.2018.00216

Recent Insights on Biological and Ecological Aspects of Ectomycorrhizal Fungi and Their Interactions

Antonietta Mello and Raffaella Balestrini*

Institute for Sustainable Plant Protection (IPSP), Torino Unit, National Research Council, Turin, Italy

The roots of most terrestrial plants are colonized by mycorrhizal fungi. They play a key role in terrestrial environments influencing soil structure and ecosystem functionality. Around them a peculiar region, the mycorrhizosphere, develops. This is a very dynamic environment where plants, soil and microorganisms interact. Interest in this fascinating environment has increased over the years. For a long period the knowledge of the microbial populations in the rhizosphere has been limited, because they have always been studied by traditional culture-based techniques. These methods, which only allow the study of cultured microorganisms, do not allow the characterization of most organisms existing in nature. The introduction in the last few years of methodologies that are independent of culture techniques has bypassed this limitation. This together with the development of high-throughput molecular tools has given new insights into the biology, evolution, and biodiversity of mycorrhizal associations, as well as, the molecular dialog between plants and fungi. The genomes of many mycorrhizal fungal species have been sequenced so far allowing to better understanding the lifestyle of these fungi, their sexual reproduction modalities and metabolic functions. The possibility to detect the mycelium and the mycorrhizae of heterothallic fungi has also allowed to follow the spatial and temporal distributional patterns of strains of different mating types. On the other hand, the availability of the genome sequencing from several mycorrhizal fungi with a different lifestyle, or belonging to different groups, allowed to verify the common feature of the mycorrhizal symbiosis as well as the differences on how different mycorrhizal species interact and dialog with the plant. Here, we will consider the aspects described before, mainly focusing on ectomycorrhizal fungi and their interactions with plants and other soil microorganisms.

Keywords: ectomycorrhizae, plant–microbe interactions, symbiosis, cell wall, mycorrhizal fungi

OPEN ACCESS

Edited by:
Erika Kothe,
Friedrich Schiller University Jena, Germany

Reviewed by:
Mika Tapio Tarkka,
Helmholtz-Zentrum für Umweltforschung (UFZ), Germany
Gwen-Aelle Grelet,
Landcare Research, New Zealand

****Correspondence:***
Antonietta Mello
antonietta.mello@ipsp.cnr.it

Specialty section:
This article was submitted to Fungi and Their Interactions, a section of the journal Frontiers in Microbiology

Received: *17 October 2017*
Accepted: *30 January 2018*
Published: *15 February 2018*

Citation:
Mello A and Balestrini R (2018) Recent Insights on Biological and Ecological Aspects of Ectomycorrhizal Fungi and Their Interactions. Front. Microbiol. 9:216. doi: 10.3389/fmicb.2018.00216

INTRODUCTION

The roots of most terrestrial plants are colonized by mycorrhizal fungi. They play a key role in terrestrial environments providing to plants an improvement in mineral nutrient uptake and earning in return carbon compounds (Brundrett, 2009). Mycorrhizal interactions are usually classified on the basis of the features of the symbiotic interfaces and of the taxonomic identity of the plant and fungal symbionts (Smith and Read, 2008). Among mycorrhizal symbioses

(see van der Heijden et al., 2015 for a review), ectomycorrhizae are established by the mycelia of fungi almost exclusively belonging to the so called "higher fungi," i.e., Basidiomycetes and Ascomycetes, whose ecological strategies have been revisited by Tedersoo and Smith (2013). Ectomycorrhizal (ECM) fungi are present all over the world, and their host plants include most angiosperm and gymnosperm trees, as well as shrubs (Bonfante, 2010). Some ECM plants are economically important timber-producing tree species, while some ECM fungi are represented by the economically important truffles and porcini (Mello et al., 2015a). Between plant and soil there is a very specific environment, the ectomycorrhizosphere, in which diverse communities of microorganisms – fungi and bacteria – interact. It is known that ECM fungi have a key role in nitrogen cycling, particularly in boreal and temperate forests, and that they can help their host plants to tolerate abiotic stresses. ECM assemblages provide benefits for inorganic nitrogen uptake under environmental constraints, through stress activation of distinct ECM fungal taxa. This suggests that these taxa are functionally diverse and opens new opportunities to characterize the ECM fungal identities (Pena and Polle, 2014). Furthermore, Gehring et al. (2017) demonstrated that tree genetics determines fungal partner communities that confer drought tolerance, highlighting the interlinked importance of the genetics of a tree and its microbiome.

The development of an ECM symbiosis requires morphological changes in the two partners, to allow the formation of the symbiotic structures, through the regulation of several genes (Martin et al., 2007; Kohler et al., 2015). From the first work in which cDNA arrays were used to study gene expression in the ECM symbiosis between *Eucalyptus globulus* and *Pisolithus tinctorius* (Voiblet et al., 2001), important progress has been done in the comprehension of the mechanisms involved in the ectomycorrhiza development. Information on the functional diversity of the ECM interactions has been highlighted, leading to the discovery of many genes coding for plant/fungus symbiosis-regulated proteins. Among them, several mycorrhiza-induced small-secreted proteins (MiSSPs) that may act as effectors and are required for symbiosis establishment have been identified (Plett et al., 2011, 2014a; Kohler et al., 2015; Martin et al., 2016 for a review). Additionally, Pellegrin et al. (2015) showed, through a bioinformatics pipeline, that the secretome of ECM fungi is enriched in SSPs in comparison to other species with a different life style. Shared- and lifestyle-specific SSPs have been identified in saprotrophic and ECM fungi, and the ECM-specific SSPs could be a signature of the ECM symbiosis lifestyle. This would suggest they have a role in a molecular dialog with host plants, leading to the formation of a functional ectomycorrhiza (Pellegrin et al., 2015; Garcia and Ané, 2016 for a commentary).

Despite similar anatomical patterns, the sequenced ECM genomes showed that differences are present in symbiosis regulated genes, revealing a diversity in the manner by which symbiotic fungi interact with their partners and suggesting the use of different molecular toolboxes to dialog with the host plant (Martin et al., 2008, 2010; Kohler et al., 2015; Peter et al., 2016). Remarkably, the role of MiSSPs (such as MiSSP7) to control host plant defense reactions has been elegantly demonstrated in *Laccaria bicolor* and *Populus trichocarpa* interaction (Plett et al., 2011, 2014b), while such fungal effectors have not been found among the upregulated transcripts in *Tuber melanosporum* ECMs (Martin et al., 2010), suggesting that different mechanisms may be involved in the development and maintaining of the ECM symbiosis. Transcript profiling of ECM roots from different plant/fungus interactions suggests that similar functional gene categories appear to be up-regulated, although these genes are not the same in the several ECM fungal species (Kohler et al., 2015). The availability of more genome sequences from ECM fungi also confirms that they have a reduced set of genes encoding plant cell wall degrading enzymes (PCWDEs) (Kohler et al., 2015), as already suggested from the genome sequence of the first two sequenced mycorrhizal fungi, i.e., *L. bicolor* and the black truffle *T. melanosporum*, respectively (Martin et al., 2008, 2010). In addition to genomic features and transcriptomic profiles, epigenetic variation is considered an important player in the evolution of biological diversity, and epigenetic regulatory systems have an important role in the response to environmental stimuli and stress factors (Zhong, 2016). The availability of the genome sequences from several fungal species will allow the understanding on how DNA methylation regulatory components are evolved in ECM fungi, and the role of the epigenetic mechanisms to cope with different environmental conditions through modifications of gene expression mediated by DNA methylation and transposon activity profiles. Considering that DNA methylation in fungi lead to transposable elements (TEs) silencing, comparative methylome and transcriptome analyses have been performed in a TE-rich organism such as the ECM fungus *T. melanosporum* (Chen et al., 2014), suggesting that a reversible methylation mechanism functions in truffles to cope with the multitude of TEs present in its genome. Information derived from these analyses, whether extended to individuals from different geographical areas, may also provide a new tool to explain intraspecific variability and adaptation to different environments and, in the case of truffles, commercially organoleptic properties (i.e., aroma).

An ECM root is a complex organ, formed not only by two individuals, plant and fungus, but also by two fungal pseudotissues: the mantle (i.e., the sheat), which develops outside the root, and the Hartig net, which colonizes the apoplastic space between root cells (Balestrini et al., 2012; Balestrini and Kottke, 2016). The two ECM compartments are thought to be functionally different. This has been first demonstrated by a study on *Amanita muscaria* ectomycorrhizae, where the mantle was manually dissected from the ectomycorrhizal root, revealing a differential expression for two fungal genes coding for a phenylalanine ammonium lyase (*AmPAL*) and a hexose transporter (*AmMst1*) (Nehls et al., 2001). While the first (*AmPAL*) was mainly expressed in the mantle, the expression of *AmMst1* increased in the Hartig net. More recently, the combination of a laser microdissection (LMD) approach, which allows the collection of the two ECM fungal compartments, with microarray gene expression analysis, revealed a specificity in the transcript profiles, reflecting a functional specificity for these two ECM compartments, e.g., that the mantle is the

responsible for the mineral elements (i.e., nitrogen) and water uptake from soil, while the expression of several transporters is enhanced in the Hartig net (Hacquard et al., 2013). In the last years, different reviews have been focused on the molecular signals (mechanisms) underlying the ECM development and functioning (Garcia et al., 2015; Martin et al., 2016). A role of flavonoids and hormones in the signaling pathway during the early stages of the ECM establishment has been proposed since several years (Garcia et al., 2015 and references therein). More recently, two plant flavonoids have been suggested to trigger the expression of a fungal effector (MiSSP7, see below) in *L. bicolor* (Plett et al., 2014a). It has been also reported that accumulation at the root apex and redistribution of auxin, which is a hormone produced by both the symbiotic partners, may play a role to stimulate lateral short root development required for the ECM formation (Felten et al., 2009). Martin et al. (2016) have recently speculated that secreted fungal MiSSPs may interact with auxin, gibberellin, and salicylate receptors to alter root development. Moreover, increased concentrations of ethylene and jasmonic acid repressed fungal colonization, with an impact on the development of the ECM roots (Plett et al., 2014b). However, the effective involvement of plant hormones in ECM establishment and maintenance has to be still fully elucidated (Garcia et al., 2015).

Here, some specific aspects related to the biology and ecology of the ECM fungi will be considered, starting with their *in situ* dynamics to the symbiotic interface creation, before and after their genome sequencing and the advent of the environmental genomics.

Given that truffles are of high economic interest, crossing several research fields ranging from taxonomy to truffle cultivation, and are the first edible ECM fungi whose genome has been sequenced, extensive research has been focused on them in order to understand their life cycle and thus to increase their production. For this reason, particular attention will be given to some insights highlighted by the sequencing of the black truffle *T. melanosporum* genome.

IDENTIFICATION OF ECTOMYCORRHIZAL FUNGI: FROM THE PAST TO THE PRESENT

The identification of ECM fungi has generally been focused on the macro- and microscopic examination of fruiting bodies and only since the early 1990s these fungi have also been characterized by DNA-based methods. At the beginning, most of the identification of fruiting bodies has involved restriction analyses of the internal transcribed spacer (ITS) region producing ITS-RFLP database from sporocarp samples (Horton and Bruns, 2001). The next step has been the direct sequence analysis of the ITS region and its deposit in GenBank or EMBL. Specific primers have been then developed for the identification of many fungal species upon increase of sequences number (Gardes et al., 1991). Amicucci et al. (1998) designed ITS primers for the identification of five species of white truffles, *T. magnatum* Pico, *T. borchii* Vittad., *T. maculatum* Vittad., *T. dryophilum* Berk. & Br. and *T. puberulum* Berk. & Br. that have similar morphological characteristics, but different organoleptic qualities and economic value. At this regard, Mello et al. (2006) designed ITS primers for the identification of the marketable boletes *Boletus edulis* Bull.: Fr. *sensu stricto*, *B. aereus* Bull.: Fr, *B. pinophilus* Pila ìt et Dermek and *B. aestivalis* Fr. (all classified as *B. edulis* s.l.), which are hardly distinguishable on the basis of their morphology and considered as the most frequently eaten fungi among those harvested in natural conditions in Europe. Once the molecular tools as sequencing and specific primers have been available, they have allowed typing the ECM tips, usually after sorting these in morphotypes. This method has, thereafter, been used in many studies on EM community structure and spatial distribution since the pioneering work of Gardes et al. (1991). According to Kaldorf et al. (2004), roughly 90% of all ectomycorrhizas of aspen clones in experimental fields was represented by *Cenococcum geophilum*, *Laccaria* sp., *Phialocephala fortinii*, two different Thelephoraceae, and one member of the Pezizales. Murat et al. (2005) sorted 335 mycorrhizal root tips collected in a truffle-ground into 39 morphotypes, on the basis of color, mantle shape and surface texture, presence of cystidia, and EM branching pattern, providing novel information on the ectomycorrhizal and endophytic species living in a *T. magnatum* truffle-ground. Above all, the finding of the few *T. magnatum* mycorrhizae in a non-productive period for this fungus, and in a non-productive area, suggested that there is not a direct linkage between mycorrhizae and fruiting bodies. Since mycorrhizal networks permit interactions among trees, their architecture has been investigated by multi-locus microsatellite DNA, leading to the identification of the trees and fungal genets connected in a multi-aged old-growth forest (Beiler et al., 2010). In order to study functional diversity among ECM fungi *in situ*, the activities of enzymes involved in the degradation and nutrient release from soil organic matter have been used (Courty et al., 2010; Pritsch and Garbaye, 2011). Combining enzymatic activities and stable isotope assays of root tips Tedersoo et al. (2012) have tried to assess the functional aspects of tropical ECM fungi. This study demonstrates that the ECM fungus may affect both potential enzymatic activities and $\delta^{15}N$ patterns of ECM tips in relation to phylogeny and exploration type (i.e., contact, short distance, medium-distance fringe and long-distance types; cf. Agerer, 2001).

As each ECM species is specialized in exploiting specific resources of the soil ecosystem, investigations have been thereafter focused on the spatial distribution of the extraradical mycelium. It interconnects plant rootlets in the forest ecosystems, forming the 'wood wide web' (Martin et al., 2016). Tracking the distribution of a given ECM fungus is considered difficult, since fruiting bodies do not reflect the distribution of ground networks (Dahlberg, 2001). The detection of the mycelium in soil has been possible thanks to the advent of new methods that have led to the direct extraction and amplification of DNA from this environment. *Hebeloma cylindrosporum* was the first ECM fungus to be detected in soil, within 50 cm from the fruiting bodies (Guidot et al., 2002). Using the β-tubulin gene as a marker, Zampieri et al. (2010) could show that the mycelium of *T. magnatum* is more widespread than was inferred

from the distribution of its fruiting bodies and ectomycorrhizae. Thanks to the progress of real-time PCR techniques, that has been optimized to quantify ECM mycelium of several ECM fungi (Iotti et al., 2014), De la Varga et al. (2012) quantified *B. edulis* extraradical mycelium in a Scots pine forest and found positive correlation between the concentration of mycelia and the presence of mycorrhizae of *B. edulis*, but not with the productivity of fruiting bodies, in the investigated samples. Given that knowledge of the annual dynamics of the mycelium of ectomycorrhizal fungi in forests soils is important in the carbon cycle, the mobilization of soil nutrients, and in the interactions of different components (plants, fungi, microfauna, and microorganisms) of the ecosystem, De la Varga et al. (2013) investigated with the same approach, the seasonal dynamics of *B. edulis* and *Lactarius deliciosus* extraradical mycelium in pine forests of central Spain. Soil mycelial dynamics of both species resulted to be strongly dependent on the weather, with an increase of biomass during the coldest months of the year.

Once it has been possible detecting mycelium of a given species and tracing its distribution, research has moved toward genet localization not only of sporocarps but also of the subterranean parts, i.e., the ectomycorrhizae and the extraradical mycelia. Studies based on the analysis of the genet structure of sporocarps, have proved that early stage fungi such as *Hebeloma* and *Laccaria* formed many small genets, and late stage fungi such as *Cortinarius* formed a few large genets (Hirose et al., 2004). Using a polymorphic microsatellite marker specific for *Suillus grevillei*, Zhou et al. (2001) demonstrated that the development of *S. grevillei* sporocarps is correlated with that of extra-radical mycelia and ectomycorrhizae of the same genet, which are distributed in a narrow area, however, no *S. grevillei* mycelia and mycorrhizae were detected close to the area where *S. grevillei* sporocarps emerged in the previous year, thus suggesting that subterranean genets change location year after year. Also Guidot et al. (2001) found a spatial congruence of above- and below-ground distribution for *H. cylindrosporum*, and the tendency of the same genets to be dominant above and below ground. Interestingly, it has been possible proving the interconnection between a single genet and different plants. At this regard, Lian et al. (2006) showed that each genet detected in the mycelial mats of *Tricholoma matsutake* colonized from three to seven trees in a natural *Pinus densiflora* forest.

All these studies have been focused on the individual recognition of ectomycorrhizal fungi clarifying many aspects of their population biology (for a review see Dowhan et al., 2011). The introduction of high-throughput sequencing techniques and the suitability of studying (micro)organisms directly *in situ* (metagenomics or environmental genomics) has provided new information on ECM fungal communities by 'barcodes' of ITS regions in several biomes/ecosystems, e.g., tropical African forests (Tedersoo et al., 2010); Swedish spruce plantations (Wallander et al., 2010); truffle grounds (Mello et al., 2011); transgenic poplar plantations (Danielsen et al., 2012); ECM roots in the Svalbard (Blaalid et al., 2012, 2014); an urban landscape (Lothamer et al., 2014); boreal and tropical forests (Clemmensen et al., 2013; McGuire et al., 2013a); a forest dominated by oaks in Japan (Toju et al., 2013); *Pinus sylvestris*-dominated plots across three study areas in Estonia (Hiiesalu et al., 2017).

In parallel with the development of the next-generation sequencing systems such as 454 Genome sequencer (introduced in 2005, it uses real-time sequencing-by-synthesis pyrosequencing technology), the Illumina platform (utilizes a sequencing-by-synthesis approach coupled with bridge amplification on the surface of a flow cell) and Ion Torrent PGM (relies on the real-time detection of hydrogen ion concentration, released as a by-product when a nucleotide is incorporated into a strand of DNA by the polymerase action), new tools such as FUNGuild, have been developed to taxonomically parse fungal OTUs by ecological guild independent of sequencing platform or analysis pipeline. Using a database and an accompanying bioinformatics script, Nguyen et al. (2015) demonstrated the application of FUNGuild to three high-throughput sequencing datasets from different habitats: forest soils, grassland soils, and decomposing wood. Several pipelines provided as web services have been produced for processing fungal ITS metabarcoding using 454-sequenced amplicons, such as CLOTU (Kumar et al., 2011), SCATA[1], PLUTOF (Abarenkov et al., 2010). Once the Illumina MiSeq platform for fungal metabarcoding has become very popular (starting with research by Bokulich et al., 2013; McGuire et al., 2013b; Schmidt et al., 2013), Bálint et al. (2014) developed a pipeline for cleaning up fungal ITS metabarcoding data generated on this platform.

An investigation of community–environment relationships in truffle grounds of the ECM fungus *T. melanosporum*, sampled in two areas, one devoid of vegetation (known as brulé in French and where fruitingbodies of this fungus are usually collected), and outside the brulé, has shown that Ascomycota were the dominant phylum in the brulé, and that their number decreased moving from inside the brulé to outside, while the number of Basidiomycota increased (Mello et al., 2011). Furthermore, this work provides comparison of the two ITS regions, ITS1 and ITS2, for fungal communities assessment. Changes in ECM fungal communities have been registered in many investigations (Mello et al., 2015b). Hui et al. (2011) have observed, in a Finnish forest, that a long-term exposition to Pb contamination can result in a shift in the composition of the ECM community associated with *P. sylvestris* L., as well as an increase in the abundance of the OTUs corresponding to the *Thelephora* genus and a decrease in the frequency of OTUs assigned to *Pseudotomentella*, *Suillus*, and *Tylospora*. In the Siberian tundra Gittel et al. (2013) have verified a decrease in ECM fungi abundance and an increase of bacteria in buried soils because of the low temperature and anoxia of these sites. ECM fungal communities of a temperate oak forest soil resulted to be affected by seasonality and soil depth (Voříšková et al., 2014). Rincón et al. (2015) revealed a highly compartmentalized and contrasted response of fungal communities of *Pinus sylvestris* in France and Spain with different response of fungal sub-assemblages in soil vs. roots and lifestyle. High-throughput sequencing analysis of fungal communities in temperate beech forests in Germany showed that distance decays of soil-inhabiting and root-associated fungal assemblages differ,

[1]http://scata.mykopat.slu.se/

and identified explanatory environmental variables (Goldmann et al., 2016).

Although many sophisticated bioinformatics tools are available, high-throughput assessment of species richness and evenness in a fungal community (including ectomycorrhizal fungi) remains still a technical challenge, because of the methodological biases and the limitations of markers. According to Lindahl et al. (2013) the major benefit of high-throughput methods relies in their capacity to unearth the main fungal colonizers in large numbers of samples, since not always singletons represent authentic rare taxa. A global soil sampling in 365 sites across the world, followed by DNA metabarcoding, revealed representatives of all major phyla and classes of fungi in all ecosystems but with relative proportions variable several fold across biomes, in addition to several deeply divergent class-level fungal lineages that had not yet been described or previously sequenced (Tedersoo et al., 2014). The overall richness of soil fungi increased toward the equator, however, functional differences were observed between fungal communities in forested and tree-less ecosystems. In fact, richness of ECM fungi head a peak at mid latitudes, especially in temperate forests and Mediterranean biomes of the Northern Hemisphere, in accordance with the dominance at mid latitudes of Pinaceae, which is the oldest family of ECM plants (**Figure 1**). Data from this paper clearly determine climatic factors as the main drivers of fungal diversity and community composition, and greatly advance our understanding of global fungal diversity patterns. Beside this, they alert us on the impact of climate change on the consequences of altered soil microorganism communities and highlight the lack of data from understudied tropical and subtropical ecosystems (Tedersoo et al., 2014). Moving from a global scale analysis to the tripartite associations between roots, fungi and bacteria, that are known to influence plant health and growth (Bonfante and Anca, 2009), Marupakula et al. (2017) identify the different bacterial communities associated with different types of ECM associations, providing clue for more detailed functional studies of specific combinations of ECM fungi and bacteria. Furthermore the study shows as N additions impact fungal–bacterial interactions at the ectomycorrhizal root tip level in different soil horizons, likely influencing patterns of carbon allocation to roots. The study of microbe–microbe interactions is recently also taking advantage of a combination of -omics with direct process measurements (e.g., stable isotope probing 'SIP') to map functions and relationships in complex communities. Musat et al. (2016) review how is might be possible now to track microbial interactions with NanoSIMS (Nano secondary ion mass spectrometry), that has the potential to provide quantitative measures of organic matter-mineral-microbial interactions and biogeochemical processing at the macro- and microaggregate or single-cell scale. Regarding this approach, Worrich et al. (2017) demonstrate that mycelium-forming fungi and oomycetes provide nitrogen, carbon and water to bacteria in dry and oligotrophic environments, thus helping them and contributing to ecosystem functioning in stressed conditions.

Anyway, the parallel increase of data output from high-throughput sequencing and of databases of entire genomes will move the research toward direct analysis of meta-genomes and meta-transcriptomes of complex fungal communities (Kuske and Lindahl, 2013). However, Marmeisse et al. (2013) pointed out that ribosomal genes, whose copy number is potentially variable, do not reflect the real pool of organisms in a community and auspicate more rigorous methodologies to assess the ecological questions related to fungal communities. Another limit of DNA metabarcoding is that the number of sequenced species is still a limitation to the precise taxonomic identification of soil fungal sequences.

So far, the meta-genomes studied, included the soil meta-genome, have isolated only bacterial and archaeal genes but not eukaryotic ones (Marmeisse et al., 2017). These authors clearly explain in their review that the reason of this lack is due to the dilution of eukaryotic genes of interest in the total metagenome, the large size of eukaryotic genomes and the strategy of cloning and expressing environmental DNA in bacteria. Besides listing the reasons to care about eukaryotic environmental nucleic acids (most of commercial enzymes and metabolites come from eukaryotes; eukaryotes are highly diverse at both local and global scales and have diverse gene repertoires), Marmeisse et al. (2017) review how metatranscriptomics is an alternative approach to access to environmental eukaryotes, starting with the isolation of their mRNAs that are distinguishable from those of bacteria having the poly-(A) tails lacking in bacteria messages. The systematic sequencing of eukaryotic metatranscriptomes from forest soil has been first applied by Damon et al. (2012), so resulting to be still in its infancy. Although most sequences coming from this approach cannot be affiliated to any taxon, it provides functional data despite of the barcoding of soil communities, in addition to unique products of biotechnological interest. A novel fungal family of oligopeptide transporters has been identified by functional metatranscriptomics of soil eukaryotes by Damon et al. (2011). Within the framework of the DOE Joint Genome Institute Community Sequencing Program, a challenging large-scale metatranscriptomics project - 'Metatranscriptomics of Forest Soil Ecosystems'[2] – to explore the interaction of forest trees with communities of soil fungi, including ectomycorrhizal symbionts, has started. This project aims to sequence the metatranscriptome of soil fungi of ecosystems from the boreal, temperate and mediterranean forests. But fungal ecology is also taking benefits from environmental proteomics (Bastida et al., 2009; Schneider et al., 2012; Zampieri et al., 2016). This approach provides insights into the metabolically active species and the composition and functionality of microbial communities. Keiblinger et al. (2016) eloquently review the opportunities and limits of this approach and discuss how linking phylogenetics and functionality can help learn more on microbial ecology and on potential soil metabolic pathways. Within the –omics, also metabolomics has been applied to soil. Jones et al. (2014) obtained the metabolic profiles of communities living in soils from a range of former mine sites in the United Kingdom to assess the effects of pollution. Although each –omics approach provides valuable information separately, only network-based approaches and combination of data can

[2]http://mycor.nancy.inra.fr/blogGenomes/?page_id=3262

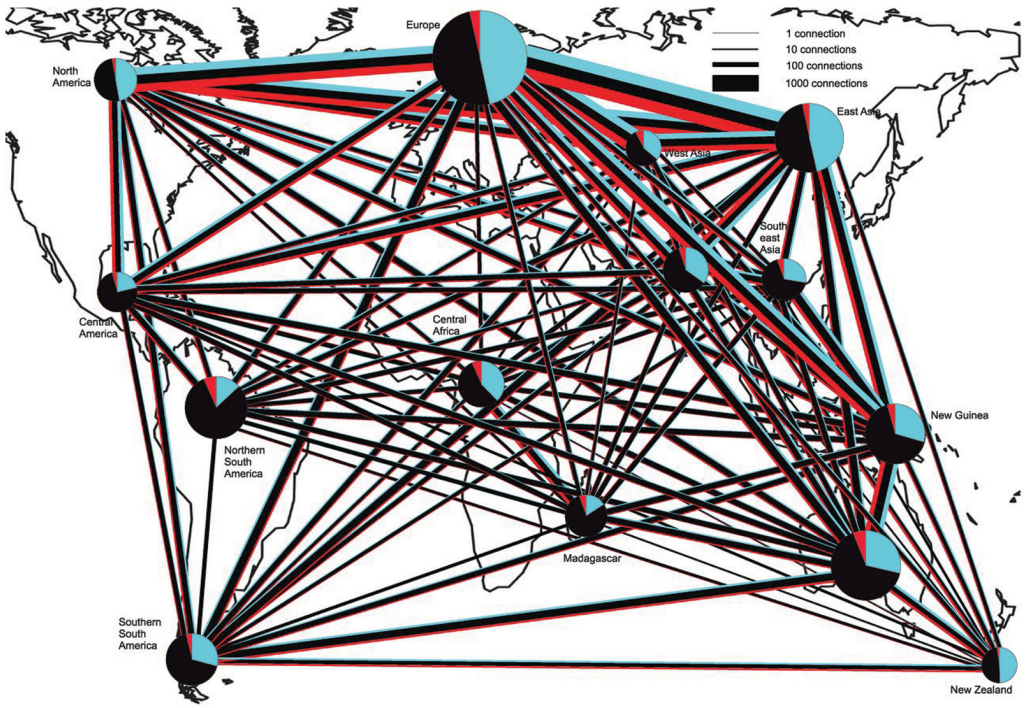

FIGURE 1 | Connectedness of biogeographic regions by shared OTUs of EcM fungi, saprotrophs, and plant pathogens. Blue, EcM fungi; Black, saprotrophs; and red, plant pathogens. The width of lines and diameter of pie charts are proportional to the square root of the number of connections and sample size (number of sites), respectively. Pie charts indicate the number of OTUs found in each region. OTUs with a single sequence per site and OTUs belonging to Hypocreales and Trichocomaceae (in which the ITS region is too conservative for species-level discrimination) were excluded. Figure modified from Tedersoo et al. (2014).

lead to the understanding of microbiomes. Below an example of a combination of data from genomics, metagenomics and metaproteomics.

TOOLS FROM *T. melanosporum* GENOME SEQUENCE FOR DECIPHERING ITS *IN SITU* DYNAMICS

In the last years, the biology and the ecology of truffles have greatly increased, thanks to many new scientific insights and technologies as the sequencing of *T. melanosporum* genome.

Regarding the life cycle, truffles have been considered for long-time self-fertile (Bertault et al., 1998). This opinion could not be tested in absence of an experimental system, based on spore germination, and therefore of the classical breeding of the resulting mycelia (Mello et al., 2005). Only thanks to the *T. melanosporum* genome sequencing, it has been possible to discover that *T. melanosporum* has a heterothallic organization (Martin et al., 2010; Rubini et al., 2011a). Heterothallic organization with a MAT locus structured in two idiomorphs harbored by different strains was also found in other truffles: *T. borchii* and *T. indicum* (Belfiori et al., 2013, 2016). That means that for truffle reproduction it is necessary that strains of opposite mating type meet. Since these discoveries, the spatio-temporal distribution of these strains in soil and in mycorrhizae has been investigated by numerous authors. The distribution of mating type genes of *T. melanosporum* has been first investigated in *T. melanosporum* natural plantation by Rubini et al. (2011b) who reported that, contrary to what is expected, strains with opposite mating types were never present on the same root apparatus, while both mating types were detected in the soil of the plantation. The same authors showed in experiments of inoculation of host plants in controlled conditions that the coexistence of both types on the roots of the same host plant can happen, but lasts until their competition excludes one of the two mating types. According to Iotti et al. (2012) the competition between strains of different mating types seems related to a self-/non-self-recognition system acting before hyphal contact rather than to the presence of a heterokaryon incompatibility (HI) system which leads to the death of the heterokaryotic cells in incompatible reactions. In support of this fact, Rubini et al. (2014) reports that orthologs of the genes controlling HI in other filamentous ascomycetes are present also in the *T. melanosporum* genome, but they lack the key functional domains involved in the HI process. Zampieri et al. (2012) could detect mating type genes for *T. melanosporum* under productive and formally productive trees but, generally, not under unproductive trees, so suggesting that the presence of the two mating types in soil can be a promising predictor of the fertility of truffle orchards and, hopefully of the *T. melanosporum* production when other abiotic and biotic factors are favorable. Mating type distribution of *T. melanosporum* has also been investigated in artificially planted truffiéres in Australia to increase ascoma

production (Linde and Selmes, 2012). Since the discovery of the *T. melanosporum* heterothallism, inoculation techniques for production of seedlings with mycelia of opposite mating type are envisaged to improve truffle productivity (Rubini et al., 2014). This modern approach has been recently applied by Iotti et al. (2016) who produced *T. borchii* fruiting bodies starting from the mycorrhization of plants with mycelial pure culture.

The spatial genetic structure of *T. melanosporum* populations at a small scale has been investigated in two productive *T. melanosporum* orchards, one located in the northern France and the other in central Italy thanks to polymorphic SSR markers searched in the *T. melanosporum* genome and mating type genes (Murat et al., 2013). The analysis of the genetic profiles of ectomycorrhizae using both SSR and mating type markers, and the monitoring of the distribution of *T. melanosporum* mycelia of the two mating types in the soil allowed the authors to demonstrate a pronounced spatial genetic structure of *T. melanosporum*, characterized by non-random distribution of small genets. Several small *T. melanosporum* genets that shared the same mating types could be found on the same host plant, suggesting that the genet distributional pattern is related to the allelic configuration of the MAT locus. However, the factors involved in truffle sexual reproduction are difficult to search due to the impossibility of manipulating truffle *in vitro* (Le Tacon et al., 2015). In *T. melanosporum*, the female gametes are ascogonia (MAT1-1 or MAT1-2) produced by a haploid mycelium forming the ectomycorrhizal root tips from which the peridium and the sterile tissue of the gleba constituting the truffle develop. After the fertilization from germinating ascospores acting as male genotypes, a diploid transitory phase occurs (that cannot be detected in mature ascocarps), followed by a meiosis phase that ends in the formation of a mature truffle (De la Varga et al., 2017). **Figure 2** shows a laser microdissection (LMD) experiment coupled with RT-PCR analysis using mating-type genes on different cell-type populations collected from a *T. melanosporum* fruiting body, i.e., vegetative hyphae and reproductive structures (asci containing the ascospores). As confirmation of the heterotallism in *T. melanosporum* (Rubini et al., 2011a), transcripts corresponding to the first mating type gene (MAT1-1-1) can be observed in both LMD samples, while those corresponding to the second mating type gene (MAT 1-2-1) can only be detected in the reproductive compartment.

From the ecological point of view, the development of the ECM symbiosis and of the fruiting bodies of *T. melanosporum* is associated to the formation of a burnt area (known by the French word brulé), characterized by little vegetation around their host plants because of the phytotoxic effects generated by the truffle metabolites and volatile organic compounds (Splivallo et al., 2011). Metagenomics data applied to French truffle-grounds have showed a reduced fungal biodiversity, a dominance of *T. melanosporum* and a reduced presence both of the ECM Basidiomycota and of bacteria belonging to *Pseudomonas* and Flavobacteriaceae inside the brulé, together with a reduction of richness of arbuscular mycorrhizal fungi (Napoli et al., 2010; Mello et al., 2011, 2013, 2015b; Mello and Zampieri, 2017). In order to relate microbial community composition to ecological processes happening in the brulé, Zampieri et al. (2016) applied a metaproteomics analysis to the brulé previously characterized by metagenomics, and cross-referenced the resulting proteins with a database they constructed, incorporating the metagenomics data for the organisms previously identified in this soil, including the black truffle *T. melanosporum*. The resulting proteins were categorized and assigned to the organisms living in the brulé, leading to discover that the soil inside the brulé contained a larger number of proteins compared with the soil outside the brulé, of which more proteins from herbaceous plants (despite the scarce vegetation typical of such a niche), and more biological processed, mostly of them related to responses to multiple types of stress from most of the brulé components. Thus, although the brulé has a reduced diversity of plant and microbial species, it seems to be a very active environment, characterized by broad stress responses and in particular by herbaceous plants. From these results Zampieri et al. (2016) hypothesize that volatile organic compounds, may elicit stress and defense responses in fungi, bacteria, and above all in the herbaceous plants inside the

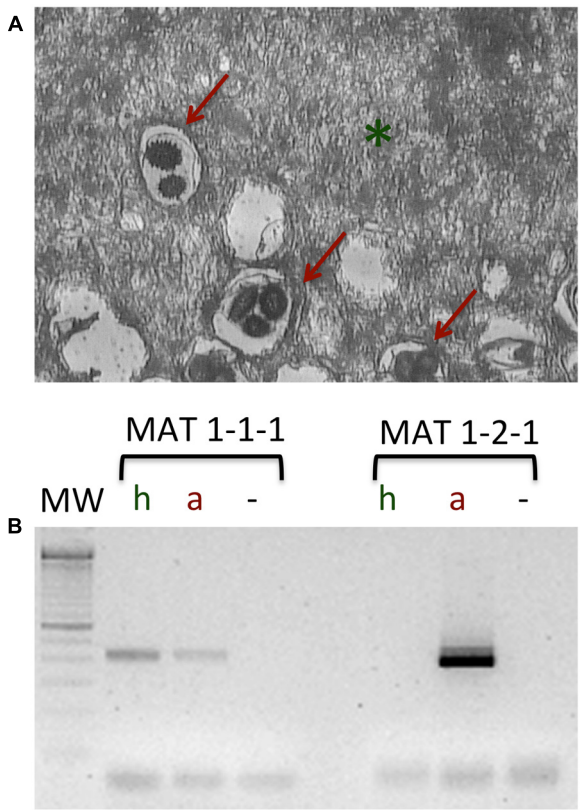

FIGURE 2 | Laser microdissection on the *T. melanosporum* fruiting body as described in Sillo et al. (2013). **(A)** Section of the inner part (gleba) of a *T. melanosporum* fruiting body. The vegetative hyphae (green asterisk) and reproductive structure, i.e., the asci (red arrows) can be distinguished. **(B)** RT-PCR analysis of the microdissected samples (hyphae, h; asci containing the ascospores, a; –, negative control). Using specific primers for MAT1-1-1 and MAT1-2-1, a fragment of the expected size can be observed in both LMD samples (h and a) for the first mating type gene (MAT1-1-1), while the transcripts corresponding to the second mating type gene (MAT 1-2-1) can only be detected in the reproductive compartment (a).

brulé. At this regard, already Splivallo et al. (2007) had showed that *Arabidopsis*, exposed to volatile organic compounds under laboratory conditions, produced an oxidative burst.

Taking in the all, the combination of metagenomics and metaproteomics has provided a powerful tool to reveal functioning of a complex phenomenon associated to an ECM fungus, as the brulé. Since metaproteomics is the study of all the proteins expressed by the organisms within an ecosystem at a specific time will surely help, together with different -OMIC approaches, to understand the ecological regulation of environmental processes.

FROM THE MORPHOLOGICAL OBSERVATIONS TO THE IDENTIFICATION OF GENES POTENTIALLY INVOLVED IN THE SYMBIOTIC INTERFACE CREATION

For many years, the interest of researchers has been dedicated to reveal, through morphological observations, the changes in hyphal growth and remodeling of the root and hyphal cell walls during ECM development (Balestrini and Kottke, 2016). At morphological level, the symbiotic interface in an ectomycorrhiza is formed by the plant and fungal cell walls in direct contact, because the ECM fungus remains apoplastic (Peterson and Massicotte, 2004; Balestrini and Bonfante, 2014; Balestrini and Kottke, 2016; **Figure 3**). The use of *in situ* affinity techniques that utilize specific probes for fungal and plant cell wall components has allowed information to be obtained on the cell wall composition at the plant/fungus interface (Balestrini et al., 1996; Peterson and Massicotte, 2004; Balestrini and Bonfante, 2014; Balestrini and Kottke, 2016). Several fungal proteins localized on the fungal cell wall in the ectomycorrhizal basidiomycete *P. tinctorius* have been observed to be highly increased during eucalypt root colonization, such as symbiosis-regulated acidic polypeptides (SRAPs) and hydrophobins (Laurent et al., 1999; Martin et al., 1999; Tagu et al., 2001). In the ectomycorrhizal ascomycete *T. borchii*, a secreted phospholipase A2 (TbSP1) has been also localized on the fungal cell wall and a role during ECM development has been proposed (Soragni et al., 2001; Miozzi et al., 2005). A homolog gene (*TmelPLA2*) has been also identified in *T. melanosporum* genome and this gene was one of the most upregulated transcripts during the colonization of *Corylus avellana* roots (Balestrini et al., 2012), in agreement with the previous data. More recently, the information derived from the several mycorrhizal genomes sequencing and the transcriptomics data on different ECM symbioses allowed the identification of novel fungal cell wall components with a putative role in the interaction with the host plant. A genome-wide inventory of hydrophobins, i.e., fungal small secreted proteins associated with the outer surface of the cell wall and able to mediate the interaction between the fungus and the environment (Whiteford and Spanu, 2002), have been obtained from *L. bicolor* where it has been demonstrated that the expression of these genes changed depending on the life-cycle stage and on the host root environment (Plett et al., 2012). A weak up-regulation of one of the four putative hydrophobin genes identified in *T. melanosporum* genome, has been also reported in its ECMs (Balestrini et al., 2012). A role for these proteins in the formation of the symbiotic interface and/or in the hyphal aggregation required for the formation of the symbiotic structures has been hypothesized (Balestrini and Bonfante, 2014). Interestingly, genes coding for putative chitin deacetylases (CDAs), which are enzymes belonging to the carbohydrate esterase 4 (CE4) family[3] that are involved in the chitin conversion to chitosan, have been also reported as upregulated in *T. melanosporum* (Balestrini et al., 2012) and *L. bicolor* (Veneault-Fourrey et al., 2014) ectomycorrhizae, suggesting a role in the symbiosis establishment. The role(s) of CE4 enzymes in ectomycorrhizae is still unknown, but on the basis of their expression profiles, it has been suggested that some of them are involved in cell wall synthesis, whereas others are perhaps involved in fungal colonization to avoid plant defense responses (Veneault-Fourrey et al., 2014). CE4 can be in fact involved in cell wall formation, but a role in the reduction of chitin oligomers elicitor activity through their de-acetylation has been also proposed during plant–pathogen interactions. Additionally, chitin de-acetylation to chitosan in pathogen fungal structures could also have a function to protect fungal cell wall plant from chitinases (Tsigos et al., 2000). The presence of a chitin-binding domain in *TmelPDA3,* one of the *T. melanosporum* upregulated genes, should also be highlighted, considering that a role for chitin-binding proteins has been also proposed in pathogenic fungi to protect the fungal cell wall from chitinases produced by host plants. This has been reported for the biotrophic fungal pathogen *Cladosporium fulvum* that secrets the apoplastic effector Avr4, which is a chitin-binding lectin that functions to protect the integrity of the fungal cell wall against chitinases (van den Burg et al., 2006; Malinovsky et al., 2014). Genome-wide transcriptome profiling allowed to demonstrate that several genes related to cell wall modification, significantly regulated during ectomycorrhiza formation, are involved in fungal cell wall processing, suggesting an extensive remodeling when the fungus is in contact with the host plant cells in agreement with the view of fungal cell wall as a highly dynamic structure (Veneault-Fourrey et al., 2014). Additionally, several expansin-like genes have been identified in the *L. bicolor* genome and several of them were found to be regulated during ECM development, suggesting a role as complement of the enzyme set involved in fungal and/or plant cell wall modification. One expansin-gene (*LbEXP1*) was first showed as the most highly induced CAZyme in ECM tissues (Martin et al., 2008) and then localized on the fungal cell wall, both in the Hartig net and mantle hyphae, suggesting a role in the fungal cell wall remodeling during symbiosis structures development (Veneault-Fourrey et al., 2014).

A subtle remodeling of the root cell wall in response to the contact with the ECM fungus has been reported years ago (Balestrini et al., 1996; Balestrini and Bonfante, 2014 for a review). A localized degradation of pectin has been suggested

[3]http://www.cazy.org/CE4.html

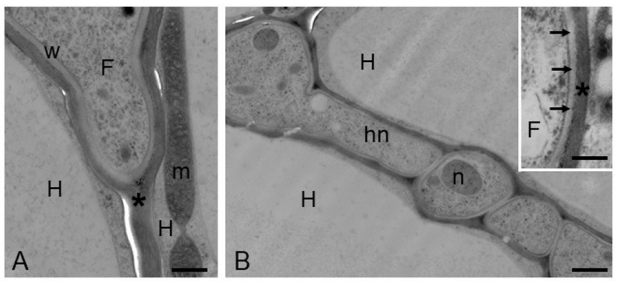

FIGURE 3 | Hazelnut-*T. melanosporum* ectomycorrhizal root. Ectomycorrhizal roots have been prepared for the transmission electron microscopy using the high-pressure freezing and freeze substitution. **(A)** A fungal hypha (F) penetrates between two host cells (H). The asterisk marks the plant cell wall. m, mitochondria; w, fungal cell wall. Bar, 0.60 μm. **(B)** Hartig net (Hn) in a fully developed mycorrhiza. Hyphae develop among plant cells (H), and their cell walls are in direct contact with the plant cell walls, showing a simple interface. Bar, 1.2 μm. (Inset) Magnification of the contact zone between plant (asterisk) and fungal cell wall (arrows). F, fungus. Bar, 0.50 μm.

during fungal colonization, according with the growth of the ECM fungus through the middle lamella and with the expression of fungal genes acting on these plant cell-wall components (Balestrini and Kottke, 2016; Sillo et al., 2016). In addition to a remodeling of the middle lamella, a soft remodeling of the plant cell wall through the loosening of cellulose has been also suggested during *L. bicolor* ECM development. Considering ectomycorrhizae at different stages of the interactions it was possible to verify that *L. bicolor* CAZymes acting on several plant cell wall components are expressed at a different developmental stage (Veneault-Fourrey et al., 2014). Recently, Doré et al. (2017), working on different developmental stages of the ECM interaction between *H. cylindrosporum* and *Pinus pinaster*, showed that genes coding for extracellular proteins, such as MiSSPs and CAZymes, were over-represented among the genes up-regulated upon pre-infectious interaction, suggesting that these specific proteins are host-induced and might play essential function(s) in the early fungal response to host root. Remarkably, the expression of some of these genes has been reported in the Hartig net compartment in *T. melanosporum* and *C. avellana* ECMs (Hacquard et al., 2013). Looking at the plant genes, Sebastiana et al. (2014) also reported that several genes coding enzymes involved in cell wall biosynthesis and modification were found to be differentially expressed in ectomycorrhizal cork oak roots with respect to non-colonized roots. In detail, cell wall-related glycosylhydrolases (GH), which are required for the modification of cell wall polysaccharides and are involved in wall loosening and elongation, were mostly up-regulated in oak ECM roots. By contrast, cell wall-related glycosyltransferases (GT), involved in the synthesis of non-cellulosic polysaccharides as part of the biosynthetic machinery to synthesize the complex plant cell-wall polysaccharides, resulted to be mostly down-regulated. Overall, these plant regulated genes might be involved in the remodeling of the plant cell wall required to facilitate hyphae penetration between cells and fungal accommodation (Sillo et al., 2016), but they might be also involved in maintaining the cell wall thickness during the changes in the architecture of host colonized cells, i.e., radial elongation (Sebastiana et al., 2014), requiring the addition of newly synthesized polysaccharides. Interestingly, an activation of cellulose synthesis in oak colonized roots has been also suggested, and transcripts corresponding to plant expansins, which are known to be involved in cell wall loosening and cell enlargement, were found to be up-regulated in ECM roots (Sebastiana et al., 2014).

However, although many studies suggest a role for the proteins regulated in symbiosis, functional analyses with the aim to highlight the function of these proteins are still lacking, as well as the nature of the cell wall remodeling during the ectomycorrhiza establishment and development.

CONCLUSION AND PERSPECTIVES

In conclusion, genomic and transcriptomic sequencing projects starting with the first mycorrhizal genome sequencing (i.e., that of *L. bicolor*) have allowed the identification of the common core of ECM symbiosis-related genes, as determinants of the symbiotic lifestyle, as well as the identification of species-specific traits. However, genome sequencing is only the first step to obtain information on how an organism interacts with the environment and with other organisms. The combination of functional, structural, cellular, and bioinformatics approaches is providing knowledge on the function of genes/proteins and permits to reconstruct the pathways of an organism in specific growth conditions, and in its natural environment. In fact, metagenomics, metatranscriptomics and metaproteomics studies are currently and fast providing a powerful mean for the analysis of environmental microorganisms without the need of culturing them. At the question: "can -omics provide insight into microbial ecology that cannot be achieved using traditional methods?", Jansson and Prosser (2013) and Prosser (2015) reply that although -omics generate a large amount of 'big data' experiments that test hypotheses on microbe-environment associations may allow more direct identification and analysis of the ecological processes. The large volume of sequence data involved in the ECM symbiosis, provide a reference database for an estimation of the ECM fungal taxa number and their ecology.

The next crucial research will be linking molecular and metabolic data to key processes such as the exchange of nutrients, the plant protection against stresses and diseases and the genes responsible of the symbiosis.

AUTHOR CONTRIBUTIONS

RB has contributed on the molecular and cellular interactions in the ectomycorrhizal symbiosis, with particular attention on the cell walls of the two symbionts. AM has contributed on the biodiversity of ectomycorrhizal fungi, their population dynamics and their interactions with other soil microorganisms.

ACKNOWLEDGMENTS

The authors thank Fabiano Sillo for providing the results illustrated in the **Figure 2** and Antonella Faccio for the preparation of the ectomycorrhizal roots with high-pressure freezing and freeze substitution in the laboratory of Robert Roberson (Arizona State University) during a Short Term Mobility program funded by the CNR. They are grateful to Marco Chiapello for modifications of original Figure 1 from Tedersoo et al. (2014).

REFERENCES

Abarenkov, K., Tedersoo, L., Nilsson, R. H., Vellak, K., Saar, I., Veldre, V., et al. (2010). PlutoF — a web based workbench for ecological and taxonomic research, with an online implementation for fungal ITS sequences. *Evol. Bioinform.* 6, 189–196. doi: 10.4137/EBO.S6271

Agerer, R. (2001). Exploration types of ectomycorrhizae. *Mycorrhiza* 11, 107–114. doi: 10.1007/s005720100108

Amicucci, A., Zambonelli, A., Giomaro, G., Potenza, L., and Stocchi, V. (1998). Identification of ectomycorrhizal fungi of the genus *Tuber* by species-specific ITS primers. *Mol. Ecol.* 7, 273–277. doi: 10.1046/j.1365-294X.1998.00357.x

Balestrini, R., and Bonfante, P. (2014). Cell wall remodelling in mycorrhizal symbiosis: a way towards biotrophism. *Front. Plant Sci.* 5:237. doi: 10.3389/fpls.2014.00237

Balestrini, R., Hahn, M. G., and Bonfante, P. (1996). Location of cell-wall components in ectomycorrhizae of *Corylus avellana* and *Tuber magnatum*. *Protoplasma* 191, 55–69. doi: 10.1007/BF01280825

Balestrini, R., and Kottke, I. (2016). "Structure and development of ectomycorrhizal roots," in *Molecular Mycorrhizal Symbiosis*, ed. F. Martin (Oxford: Wiley-Blackwell), 47–61. doi: 10.1002/9781118951446.ch4

Balestrini, R., Sillo, F., Kohler, A., Schneider, G., Faccio, A., Tisserant, E., et al. (2012). Genome-wide analysis of cell wall-related genes in *Tuber melanosporum*. *Curr. Genet.* 58, 165–177. doi: 10.1007/s00294-012-0374-6

Bálint, M., Schmidt, P. A., Sharma, R., Thines, M., and Scmitt, I. (2014). An Illumina metabarcoding pipeline for fungi. *Ecol. Evol.* 4, 2642–2653. doi: 10.1002/ece3.1107

Bastida, F., Moreno, J. L., Nicolas, C., Hernandez, T., and Garcıa, C. (2009). Soil metaproteomics: a review of an emerging environmental science. Significance, methodology and perspectives. *J. Soil Sci.* 60, 845–859. doi: 10.1111/j.1365-2389.2009.01184.x

Beiler, K. J., Durall, D. M., Simard, S. W., Maxwell, S. A., and Kretzer, A. M. (2010). Architecture of the wood-wide web: *Rhizopogon* spp. Genets link multiple Douglas-fir cohorts. *New Phytol.* 185, 543–553. doi: 10.1111/j.1469-8137.2009.03069.x

Belfiori, B., Riccioni, C., Paolocci, F., and Rubini, A. (2013). Mating type locus of Chinese black truffles reveals heterothallism and the presence of cryptic species within the Tuber indicum species complex. *PLOS ONE* 8:e82353. doi: 10.1371/journal.pone.0082353

Belfiori, B., Riccioni, C., Paolocci, F., and Rubini, A. (2016). Characterization of the reproductive mode and life cycle of the whitish truffle *T. borchii*. *Mycorrhiza* 26, 515–527. doi: 10.1007/s00572-016-0689-0

Bertault, G., Raymond, M., Berthomieu, A., Callot, G., and Fernandez, D. (1998). Trifling variation in truffles. *Nature* 394, 734–734. doi: 10.1038/29428

Blaalid, R., Carlsen, T., Kumar, S., Halvorsen, R., Ugland, K. I., Fontana, G., et al. (2012). Changes in the root-associated fungal communities along a primary succession gradient analysed by 454 pyrosequencing. *Mol. Ecol.* 21, 1897–1908. doi: 10.1111/j.1365-294X.2011.05214.x

Blaalid, R., Davey, M. L., Kauserud, H., Carlsen, T., Halvorsen, R., Høiland, K., et al. (2014). Arctic root- associated fungal community composition reflects environmental filtering. *Mol. Ecol.* 23, 649–659. doi: 10.1111/mec.12622

Bokulich, N. A., Thorngate, J. H., Richardson, P. M., and Mills, D. A. (2013). Microbial biogeography of wine grapes is conditioned by cultivar, vintage, and climate. *Proc. Natl. Acad. Sci. U.S.A.* 25, E139–E148. doi: 10.1073/pnas.1317377110

Bonfante, P. (2010). "Plant-fungal interactions in mycorrhizas," in *Encyclopedia of Life Sciences (ELS)* (Chichester: John Wiley & Sons Ltd.).

Bonfante, P., and Anca, J. A. (2009). Plants, mycorrhizal fungi and bacteria: a network of interactions. *Annu. Rev. Microbiol.* 63, 363–383. doi: 10.1146/annurev.micro.091208.073504

Brundrett, M. C. (2009). Mycorrhizal associations and other means of nutrition of vascular plants: understanding the global diversity of host plants by resolving conflicting information and developing reliable means of diagnosis. *Plant Soil* 320, 37–77. doi: 10.1007/s11104-008-9877-9

Chen, P.-Y., Montanini, B., Liao, W.-W., Morselli, M., Jaroszewicz, A., Lopez, D., et al. (2014). A comprehensive resource of genomic, epigenomic and transcriptome sequencing data for the black truffle *Tuber melanosporum*. *Gigascience* 3:25. doi: 10.1186/2047-217X-3-25

Clemmensen, K. E., Bahr, A., Ovaskainen, O., Dahlberg, A., Ekblad, A., Wallander, H., et al. (2013). Roots and associated fungi drive long-term carbon sequestration in boreal forest. *Science* 339, 1615–1618. doi: 10.1126/science.1231923

Courty, P. E., Buée, M., Diedhiou, A. G., Frey-Klett, P., Le Tacon, F., Rineau, F., et al. (2010). The role of ectomycorrhizal communities in forest ecosystem processes: new perspectives and emerging concepts. *Soil Biol. Biochem.* 42, 679–698. doi: 10.1016/j.soilbio.2009.12.006

Dahlberg, A. (2001). Community ecology of ectomycorrhizal fungi: an advancing interdisciplinary field. *New Phytol.* 150, 555–562. doi: 10.1046/j.1469-8137.2001.00142.x

Damon, C., Lehembre, F., Oger-Desfeux, C., Luis, P., Ranger, J., and Fraissinet-Tachet, L. (2012). Metatranscriptomics Reveals the diversity of genes expressed by eukaryotes in forest soils. *PLOS ONE* 7:e28967. doi: 10.1371/journal.pone.0028967

Damon, C., Vallon, L., Zimmermann, S., Haider, M. Z., Galeote, V., Dequin, S., et al. (2011). A novel fungal family of oligopeptide transporters identified by functional metatranscriptomics of soil eukaryotes. *ISME J.* 5, 1871–1880. doi: 10.1038/ismej.2011.67

Danielsen, L., Thürmer, A., Meinicke, P., Buée, M., Morin, E., Martin, F., et al. (2012). Fungal soil communities in a young transgenic poplar plantation form a rich reservoir for fungal root com- munities. *Ecol. Evol.* 2, 1935–1948. doi: 10.1002/ece3.305

De la Varga, H., Águeda, B., Ágreda, T., Martínez-Peña, F., Parladé, J., and Pera, J. (2013). Seasonal dynamics of *Boletus edulis* and *Lactarius deliciosus* extraradical mycelium in pine forests of central Spain. *Mycorrhiza* 23, 391–402. doi: 10.1007/s00572-013-0481-3

De la Varga, H., Águeda, B., Martínez-Peña, F., Parladé, J., and Pera, J. (2012). Quantification of extraradical soil mycelium and ectomycorrhizas of *Boletus edulis* in a Scots pine forest with variable sporocarp productivity. *Mycorrhiza* 22, 59–68. doi: 10.1007/s00572-011-0382-2

De la Varga, H., Le Tacon, F., Lagoguet, M., Todesco, F., Varga, T., Miquel, I., et al. (2017). Five years investigation of female and male genotypes in perigord black truffle (*Tuber melanosporum* Vittad.) revealed contrasted reproduction strategies. *Environ. Microbiol.* 19, 2604–2615. doi: 10.1111/1462-2920.13735

Doré, J., Kohler, A., Dubost, A., Hundley, H., Singan, V., and Peng, Y. (2017). The ectomycorrhizal basidiomycete *Hebeloma cylindrosporum* undergoes early waves of transcriptional reprogramming prior to symbiotic structures differentiation. *Environ. Microbiol.* 19, 1338–1354. doi: 10.1111/1462-2920.13670

Dowhan, G. W., Vincenot, L., Gryta, H., and Selosse, M. A. (2011). Population genetics of ectomycorrhizal fungi: from current knowledge to emerging directions. *Fungal Biol.* 115, 569–597. doi: 10.1016/j.funbio.2011.03.005

Felten, J., Kohler, A., Morin, E., Bhalerao, R. P., Palme, K., Martin, F., et al. (2009). The ectomycorrhizal fungus *Laccaria bicolor* stimulates lateral root formation in poplar and Arabidopsis through auxin transport and signaling. *Plant Physiol.* 151, 1991–2005. doi: 10.1104/pp.109.147231

Garcia, K., and Ané, J. M. (2016). Commentary on "Comparative analysis of secretomes from ectomycorrhizal fungi with an emphasis on small-secreted proteins". *Front. Plant Sci.* 7:1734. doi: 10.3389/fmicb.2016.01734

Garcia, K., Delaux, P. M., Cope, K., and Ané, J. M. (2015). Molecular signals required for the establishment and maintenance of ectomycorrhizal symbioses. *New Phytol.* 208, 79–87. doi: 10.1111/nph.13423

Gardes, M., White, T. J., Fortin, J. A., Bruns, T. D., and Taylor, J. W. (1991). Identification of indigenous and introduced symbiotic fungi in ectomycorrhizae by amplification of nuclear and mitochondrial ribosomal DNA. *Can. J. Bot.* 69, 180–190. doi: 10.1139/b91-026

Gehring, C. A., Sthultz, C. M., Flores-Rentería, L., Whipple, A. V., and Whitham, T. G. (2017). Tree genetics defines fungal partner communities that may confer drought tolerance. *Proc. Natl. Acad. Sci. U.S.A.* 114, 11169–11174. doi: 10.1073/pnas.1704022114

Gittel, A., Bárta, J., Kohoutová, I., Mikutta, R., Owens, S., Gilbert, J., et al. (2013). Distinct microbial communities associated with buried soils in the Siberian tundra. *ISME J.* 8, 841–853. doi: 10.1038/ismej.2013.219

Goldmann, K., Schröter, K., Pena, R., Schöning, I., Schrump, M., Buscot, F., et al. (2016). Divergent habitat filtering of root and soil fungal communities in temperate beech forests. *Sci. Rep.* 6:31439. doi: 10.1038/srep31439

Guidot, A., Debaud, J. C., and Marmeisse, R. (2001). Correspondence between genet diversity and spatial distribution of above- and below-ground populations of the ectomycorrhizal fungus *Hebeloma cylindrosporum*. *Mol. Ecol.* 10, 1121–1131. doi: 10.1046/j.1365-294X.2001.01265.x

Guidot, A., Debaud, J. C., and Marmeisse, R. (2002). Spatial distribution of the below-ground mycelia of an ectomycorrhizal fungus inferred from specific quantification of its DNA in soil samples. *FEMS Microbiol. Ecol.* 42, 477–486. doi: 10.1111/j.1574-6941.2002.tb01036.x

Hacquard, S., Tisserant, E., Brun, A., Legué, V., Martin, F., and Kohler, A. (2013). Laser microdissection and microarray analysis of *Tuber melanosporum* ectomycorrhizas reveal functional heterogeneity between mantle and Hartig net compartments. *Environ. Microbiol.* 15, 1853–1869. doi: 10.1111/1462-2920.12080

Hiiesalu, H., Bahram, M., and Tedersoo, L. (2017). Plant species richness and productivity determine the diversity of soil fungal guilds in temperate coniferous forest and bog habitats. *Mol. Ecol.* 26, 4846–4858. doi: 10.1111/mec.14246

Hirose, D., Kikuchi, J., Kanzaki, N., and Futai, K. (2004). Genet distribution of sporocarps and ectomycorrhizas of *Suillus pictus* in a Japanese white pine plantation. *New Phytol.* 164, 527–541. doi: 10.1111/j.1469-8137.2004.01188.x

Horton, T. R., and Bruns, T. D. (2001). The molecular revolution in ectomycorrhizal ecology: peeking into the black-box. *Mol. Ecol.* 10, 1855–1871. doi: 10.1046/j.0962-1083.2001.01333.x

Hui, N., Jumpponen, A., Niskanen, T., Liimatainen, K., Jones, K. L., Koivula, T., et al. (2011). EcM fungal community structure, but not diversity, altered in a Pb-contaminated shooting range in a boreal coniferous forest site in Southern Finland. *FEMS Microbiol. Ecol.* 76, 121–132. doi: 10.1111/j.1574-6941.2010.01038.x

Iotti, M., Leonardi, M., Lancellotti, E., Salerni, E., Oddis, M., Leonardi, P., et al. (2014). Spatio-temporal dynamic of *Tuber magnatum* mycelium in natural trufflegrounds. *PLOS ONE* 9:e115921. doi: 10.1371/journal.pone.0115921

Iotti, M., Piattoni, F., Leonardi, P., and Hall, J. R. (2016). First evidence for truffle production from plants inoculated with mycelial pure cultures. *Mycorrhiza* 26, 793–798. doi: 10.1007/s00572-016-0703-6

Iotti, M., Rubini, A., Tisserant, E., Kholer, A., Paolocci, F., and Zambonelli, A. (2012). Self/nonself recognition in *Tuber melanosporum* is not mediated by a heterokaryon incompatibility system. *Fungal Biol.* 116, 261–275. doi: 10.1016/j.funbio.2011.11.009

Jansson, J., and Prosser, J. I. (2013). Microbiology: the life beneath our feet. *Nature* 494, 40–41. doi: 10.1038/494040a

Jones, O. A., Sdepanian, S., Lofts, S., Svendsen, C., Spurgeon, D. J., Maguire, M. L., et al. (2014). Metabolomic analysis of soil communities can be used for pollution assessment. *Environ. Toxicol. Chem.* 33, 61–64. doi: 10.1002/etc.2418

Kaldorf, M., Renker, C., Fladung, M., and Buscot, F. (2004). Characterization and spatial distribution of ectomycorrhizas colonizing aspen clones released in an experimental field. *Mycorrhiza* 14, 295–306. doi: 10.1007/s00572-003-0266-1

Keiblinger, K. M., Fuchs, S., Zechmeister-Boltenstern, S., and Riedel, K. (2016). Soil and leaf litter metaproteomics-a brief guideline from sampling to understanding. *FEMS Microbiol. Ecol.* 92, 1–18. doi: 10.1093/femsec/fiw180

Kohler, A., Kuo, A., Nagy, L. G., Morin, E., Barry, K. W., Buscot, F., et al. (2015). Convergent losses of decay mechanisms and rapid turnover of symbiosis genes in mycorrhizal mutualists. *Nat. Genet.* 47, 410–415. doi: 10.1038/ng.3223

Kumar, S., Carlsen, T., Mevik, B. H., Enger, P., Blaalid, R., Shalchian-Tabrizi, K., et al. (2011). CLOTU: an online pipeline for processing and clustering of 454 amplicon reads into OTUs followed by taxonomic annotation. *BMC Bioinformatics* 12:182. doi: 10.1186/1471-2105-12-182

Kuske, C. R., and Lindahl, B. D. (2013). "Metagenomics for study of fungal ecology," in *Ecological Genomics of the Fungi*, ed. F. Martin (Hoboken, NJ: Wiley- Blackwell). doi: 10.1186/1471-2105-12-182

Laurent, P., Voiblet, C., Tagu, D., De Carvalho, D., Nehls, U., and De Bellis, R. (1999). Cell wall acidic polypeptides in *Pisolithus tinctorius* are up-regulated during the development of *Eucalyptus globulus* ectomycorrhizal. *Mol. Plant Microbe Interact.* 12, 862–871. doi: 10.1094/MPMI.1999.12.10.862

Le Tacon, F., Zeller, B., Plain, C., Hossann, C., Bréchet, C., Martin, F., et al. (2015). Study of nitrogen and carbon transfer from soil organic matter to *Tuber melanosporum* mycorrhizas and ascocarps using 15N and 13C soil labelling and whole-genome oligoarrays. *Plant Soil* 395, 351–373. doi: 10.1007/s11104-015-2557-7

Lian, C., Narimatsu, M., Nara, K., and Hogetsu, T. (2006). *Tricholoma matsutake* in a natural *Pinus densiflora* forest: correspondence between above- and below-ground genets, association with multiple host trees and alteration of existing ectomycorrhizal communities. *New Phytol.* 171, 825–836. doi: 10.1111/j.1469-8137.2006.01801.x

Lindahl, B. D., Nilsson, R. H., Tedersoo, L., Abarenkov, K., Carlsen, T., Kjøller, R., et al. (2013). Fungal community analysis by high-throughput sequencing of amplified markers – a user's guide. *New Phytol.* 199, 288–299. doi: 10.1111/nph.12243

Linde, C. C., and Selmes, H. (2012). Genetic diversity and mating type distribution of *Tuber melanosporum* and their significance to truffle cultivation in artificially planted truffieìres in Australia. *Appl. Environ. Microbiol.* 78, 6534–6539. doi: 10.1128/AEM.01558-12

Lothamer, K., Brown, S. P., Mattox, J. D., and Jumpponen, A. (2014). Comparison of root-associated communities of native and non-native ectomycorrhizal hosts in an urban landscape. *Mycorrhiza* 24, 267–280. doi: 10.1007/s00572-013-0539-2

Malinovsky, F. G., Fangel, J. U., and Willats, G. T. (2014). The role of the cell wall in plant immunity. *Front. Plant Sci.* 5:178. doi: 10.3389/fpls.2014.00178

Marmeisse, R., Kellner, H., Fraissinet-Tachet, L., and Luis, P. (2017). Discovering protein-coding genes from the environment: time for the eukaryotes? *Trends Biotechnol.* 35, 824–835. doi: 10.1016/j.tibtech.2017.02.003

Marmeisse, R., Nehls, U., Opik, M., Selosse, M. A., and Pringle, A. (2013). Bridging mycorrhizal genomics, metagenomics and forest ecology. *New Phytol.* 198, 343–346. doi: 10.1111/nph.12205

Martin, F., Aerts, A., Ahrén, D., Brun, A., Danchin, E. G., Duchaussoy, F., et al. (2008). The genome of *Laccaria bicolor* provides insights into mycorrhizal symbiosis. *Nature* 452, 88–92. doi: 10.1038/nature06556

Martin, F., Kohler, A., and Duplessis, S. (2007). Living in harmony in the wood underground: ectomycorrhizal genomics. *Curr. Opin. Plant Biol.* 10, 204–210. doi: 10.1016/j.pbi.2007.01.006

Martin, F., Kohler, A., Murat, C., Balestrini, R., Coutinho, P. M., Jaillon, O., et al. (2010). Périgord black truffle genome uncovers evolutionary origins and mechanisms of symbiosis. *Nature* 464, 1033–1038. doi: 10.1038/nature08867

Martin, F., Kohler, A., Murat, C., Veneault-Fourrey, C., and Hibbett, D. S. (2016). Unearthing the roots of ectomycorrhizal symbioses. *Nat. Rev. Microbiol.* 14, 760–773. doi: 10.1038/nrmicro.2016.149

Martin, F., Laurent, P., De Carvalho, D., Voiblet, C., Balestrini, R., Bonfante, P., et al. (1999). Cell wall proteins of the ectomycorrhizal basidiomycete *Pisolithus tinctorius*: identification, function and expression in symbiosis. *Rev. Fungal Genet. Biol.* 27, 161–174. doi: 10.1006/fgbi.1999.1138

Marupakula, S., Mahmood, S., Jernberg, J., Nallanchakravarthula, S., Fahad, Z. A., and Finlay, R. D. (2017). Bacterial microbiomes of individual ectomycorrhizal *Pinus sylvestris* roots are shaped by soil horizon and differentially sensitive to

nitrogen addition. *Environ. Microbiol.* 19, 4736–4753. doi: 10.1111/1462-2920.13939

McGuire, K. L., Allison, S. D., Fierer, N., and Treseder, K. K. (2013a). Ectomycorrhizal-dominated boreal and tropical forests have distinct fungal communities, but analogous spatial patterns across soil horizons. *PLOS ONE* 8:e68278. doi: 10.1371/journal.pone.0068278

McGuire, K. L., Payne, S. G., Palmer, M. I., Gillikin, C. M., Keefe, D., and Kim, S. J. (2013b). Digging the New York City skyline: soil fungal communities in green roofs and city parks. *PLOS ONE* 8:e58020. doi: 10.1371/journal.pone.0058020

Mello, A., Ding, G. C., Piceno, Y. M., Napoli, C., Tom, L. M., DeSantis, T. Z., et al. (2013). Truffle brûlés have an impact on the diversity of soil bacterial communities. *PLOS ONE* 8:e61945. doi: 10.1371/journal.pone.0061945

Mello, A., Ghignone, S., Vizzini, A., Sechi, C., Ruiu, P., and Bonfante, P. (2006). ITS primers for the Identification of marketable boletes. *J. Biotechnol.* 121, 318–329. doi: 10.1016/j.jbiotec.2005.08.022

Mello, A., Lumini, E., Napoli, C., Bianciotto, V., and Bonfante, P. (2015a). Arbuscular mycorrhizal fungal diversity in the *Tuber melanosporum* brûlé. *Fung Biol.* 19, 518–527. doi: 10.1016/j.funbio.2015.02.003

Mello, A., Murat, C., Vizzini, A., Gavazza, V., and Bonfante, P. (2005). *Tuber magnatum* Pico, a species of limited geographical distribution: its genetic diversity inside and outside a truffle ground. *Environ. Microbiol.* 7, 55–65. doi: 10.1111/j.1462-2920.2004.00678.x

Mello, A., Napoli, C., Murat, C., Morin, E., Marceddu, G., and Bonfante, P. (2011). ITS-1 *versus* ITS-2 pyrosequencing: a comparison of fungal populations in truffle grounds. *Mycologia* 103, 1184–1193. doi: 10.3852/11-027

Mello, A., and Zampieri, E. (2017). Who is out there? What are they doing? Application of metagenomics and metaproteomics to reveal soil functioning. *Ital. J. Mycol.* 46, 1–7.

Mello, A., Zampieri, E., and Balestrini, R. (2015b). "Ectomycorrhizal fungi and their applications," in *Plant Microbes Symbiosis: Applied Facets*, ed. N. K. Arora (New Delhi: Springer).

Miozzi, L., Balestrini, R., Bolchi, A., Novero, M., Ottonello, S., and Bonfante, P. (2005). Phospholipase A2 up- regulation during mycorrhiza formation in *Tuber borchii*. *New Phytol.* 167, 229–238. doi: 10.1111/j.1469-8137.2005.01400.x

Murat, C., Rubini, A., Riccioni, C., De la Varga, H., Akroume, E., Belfiore, B., et al. (2013). Fine-scale spatial genetic structure of the black truffle (*Tuber melanosporum*) investigated with neutral microsatellites and functional mating type genes. *New Phytol.* 199, 176–187. doi: 10.1111/nph.12264

Murat, C., Vizzini, A., Bonfante, P., and Mello, A. (2005). Morphological and molecular typing of the belowground fungal community in a natural *Tuber magnatum* truffle–ground. *FEMS Microbiol. Lett.* 245, 307–313. doi: 10.1016/j.femsle.2005.03.019

Musat, N., Musat, F., Weber, P. K., and Pett-Ridge, J. (2016). Tracking microbial interactions with NanoSIMS. *Curr. Opin. Biotechnol.* 41, 114–121. doi: 10.1016/j.copbio.2016.06.007

Napoli, C., Mello, A., Borra, A., Vizzini, A., Sourzat, P., and Bonfante, P. (2010). *Tuber melanosporum*, when dominant, affects fungal dynamics in truffle grounds. *New Phytol.* 185, 237–247. doi: 10.1111/j.1469-8137.2009.03053.x

Nehls, U., Mikolajewski, S., Magel, E., and Hampp, R. (2001). Carbohydrate metabolism in ectomycorrhizas: gene expression, monosaccharide transport and metabolic control. *New Phytol.* 150, 533–541. doi: 10.1046/j.1469-8137.2001.00141.x

Nguyen, N. H., Song, Z., Bates, S. T., Branco, S., Tedersoo, L., and Menke, J. (2015). FUNGuild: an open annotation tool for parsing fungal community datasets by ecological guild. *Fungal Ecol.* 20, 241–248. doi: 10.1016/j.funeco.2015.06.006

Pellegrin, C., Morin, E., Martin, F. M., and Veneault-Fourrey, C. (2015). Comparative analysis of secretomes from ectomycorrhizal fungi with an emphasis on small-secreted proteins. *Front. Microbiol.* 6:1278. doi: 10.3389/fmicb.2015.01278

Pena, R., and Polle, A. (2014). Attributing functions to ectomycorrhizal fungal identities in assemblages for nitrogen acquisition under stress. *ISME J.* 8, 321–330. doi: 10.1038/ismej.2013.158

Peter, M., Kohler, A., Ohm, R. A., Kuo, A., Krützmann, J., Morin, E., et al. (2016). Ectomycorrhizal ecology is imprinted in the genome of the dominant symbiotic fungus *Cenococcum geophilum*. *Nat. Commun.* 7:12662. doi: 10.1038/ncomms12662

Peterson, R. L., and Massicotte, H. B. (2004). Exploring structural definitions of mycorrhizas, with emphasis on nutrient-exchange interfaces. *Can. J. Bot.* 82, 1074–1088. doi: 10.1139/b04-071

Plett, J. M., Daguerre, Y., Wittulsky, S., Vayssières, A., Deveau, A., Melton, S. J., et al. (2014a). The effector MiSSP7 of the mutualistic fungus *Laccaria bicolor* stabilizes the *Populus* JAZ6 protein and represses JA-responsive genes. *Proc. Natl. Acad. Sci. U.S.A.* 111, 8299. doi: 10.1073/pnas.1322671111

Plett, J. M., Khachane, A., Ouassou, M., Sundberg, B., Kohler, A., and Martin, F. (2014b). Ethylene and jasmonic acid act as negative modulators during mutualistic symbiosis between *Laccaria bicolor* and Populus roots. *New Phytol.* 202, 270–286. doi: 10.1111/nph.12655

Plett, J. M., Gibon, J., Kohler, A., Duffy, K., Hoegger, P. J., Velagapudi, R., et al. (2012). Phylogenetic, genomic organization and expression analysis of hydrophobin genes in the ectomycorrhizal basidiomycete *Laccaria bicolor*. *Fungal Genet. Biol.* 49, 199–209. doi: 10.1016/j.fgb.2012.01.002

Plett, J. M., Kemppainen, M., Kale, S. D., Kohler, A., Legue, V., Brun, A., et al. (2011). A secreted effector protein of *Laccaria bicolor* is required for symbiosis development. *Curr. Biol.* 21, 1197–1203. doi: 10.1016/j.cub.2011.05.033

Pritsch, K., and Garbaye, J. (2011). Enzyme secretion by ECM fungi and exploitation of mineral nutrients from soil organic matter. *Ann. For. Sci.* 68, 25–32. doi: 10.1007/s13595-010-0004-8

Prosser, J. (2015). Dispersing misconceptions and identifying opportunities for the use of 'omics' in soil microbial ecology. *Nat. Rev. Microbiol.* 13, 439–446. doi: 10.1038/nrmicro3468

Rincón, A., Santamaría-Pérez, B., Rabasa, S. G., Coince, A., Marçais, B., and Buée, M. (2015). Compartmentalized and contrasted response of ectomycorrhizal and soil fungal communities of Scots pine forests along elevation gradients in France and Spain. *Environ. Microbiol.* 17, 3009–3024. doi: 10.1111/1462-2920.12894

Rubini, A., Belfiori, B., Riccioni, C., Arcioni, S., Martin, F., and Paolocci, F. (2011a). Isolation and characterization of MAT genes in the symbiotic ascomycete *Tuber melanosporum*. *New Phytol.* 189, 710–722. doi: 10.1111/j.1469-8137.2010.03492.x

Rubini, A., Belfiori, B., Riccioni, C., Arcioni, S., Martin, F., and Paolocci, F. (2011b). *Tuber melanosporum*: mating type distribution in a natural plantation and dynamics of strains of different mating types on the roots of nursery-inoculated host plants. *New Phytol.* 183, 723–735. doi: 10.1111/j.1469-8137.2010.03493.x

Rubini, A., Riccioni, C., Belfiori, B., and Paolocci, F. (2014). Impact of the competition between mating types on the cultivation of *Tuber melanosporum*: romeo and Juliet and the matter of space and time. *Mycorrhiza* 24, 19–27. doi: 10.1007/s00572-013-0551-6

Schmidt, P. A., Bálint, M., Greshake, B., Bandow, C., Römbke, J., and Schmitt, I. (2013). Illumina metabarcoding of a soil fungal community. *Soil Biol. Biochem.* 65, 128–132. doi: 10.1016/j.soilbio.2013.05.014

Schneider, T., Keiblinger, K. M., Schmid, E., Sterflinger-Gleixner, K., and Ellersdorfer, G. (2012). Who is who in litter decomposition? Metaproteomics reveals major microbial players and their biogeochemical functions. *ISME J.* 6, 1749–1762. doi: 10.1038/ismej.2012.11

Sebastiana, M., Vieira, B., Lino-Neto, T., Monteiro, F., Figueiredo, A., Sousa, L., et al. (2014). Oak root response to ectomycorrhizal symbiosis establishment: RNA-Seq derived transcript identification and expression profiling. *PLOS ONE* 9:e98376. doi: 10.1371/journal.pone.0098376

Sillo, F., Fangel, J. U., Henrissat, B., Faccio, A., Bonfante, P., Martin, F., et al. (2016). Understanding plant cell-wall remodelling during the symbiotic interaction between *Tuber melanosporum* and *Corylus avellana* using a carbohydrate microarray. *Planta* 244, 347–359. doi: 10.1007/s00425-016-2507-5

Sillo, F., Gissi, C., Chignoli, D., Ragni, E., Popolo, L., and Balestrini, R. (2013). Expression and phylogenetic analyses of the Gel/Gas proteins of *Tuber melanosporum* provide insights into the function and evolution of glucan remodeling enzymes in fungi. *Fungal Genet. Biol.* 53, 10–21. doi: 10.1016/j.fgb.2013.01.010

Smith, S. E., and Read, D. J. (2008). *Mycorrhizal Symbiosis*, 3rd Edn. London: Academic.

Soragni, E., Bolchi, A., Balestrini, R., Gambaretto, C., Bonfante, P., and Ottonello, S. (2001). Nutrient regulated expression of a secretable surface protein gene in the ectomycorrhizal fungus *Tuber borchii*. *EMBO J.* 20, 5079–5090. doi: 10.1093/emboj/20.18.5079

Splivallo, R., Novero, M., Bertea, C. M., Bossi, S., and Bonfante, P. (2007). Truffle volatiles inhibit growth and induce an oxidative burst in *Arabidopsis thaliana*. *New Phytol.* 175, 417–424. doi: 10.1111/j.1469-8137.2007.02141.x

Splivallo, R., Ottonello, S., Mello, A., and Karlovsky, P. (2011). Truffle volatiles: from chemical ecology to aroma biosynthesis. *New Phytol.* 189, 688–699. doi: 10.1111/j.1469-8137.2010.03523.x

Tagu, D., De Bellis, R., Balestrini, R., De Vries, O. M. H., Piccoli, G., Stocchi, V., et al. (2001). Immuno-localization of hydrophobin HYDPt-1 from the ectomycorrhizal basidiomycete *Pisolithus tinctorius* during colonization of *Eucalyptus globulus* roots. *New Phytol.* 149, 127–135. doi: 10.1046/j.1469-8137.2001.00009.x

Tedersoo, L., Bahram, M., Põlme, S., Kõljalg, U., Yorou, N. S., and Wijesundera, R. (2014). Global diversity and geography of soil fungi. *Science* 346:1256688. doi: 10.1126/science.1256688

Tedersoo, L., Naadel, T., Bahram, M., Pritsch, K., Buegger, F., Leal, M., et al. (2012). Enzymatic activities and stable isotope patterns of ectomycorrhizal fungi in relation to phylogeny and exploration types in an afrotropical rain forest. *New Phytol.* 195, 832–843. doi: 10.1111/j.1469-8137.2012.04217.x

Tedersoo, L., Nilsson, R. H., Abarenkov, K., Jairus, T., Sadam, A., Saar, I., et al. (2010). 454 Pyrosequencing and Sanger sequencing of tropical mycorrhizal fungi provide similar results but reveal substantial methodological biases. *New Phytol.* 188, 291–301. doi: 10.1111/j.1469-8137.2010.03373.x

Tedersoo, L., and Smith, M. E. (2013). Lineages of ectomycorrhizal fungi revisited: foraging strategies and novel lineages revealed by sequences from belowground. *Fungal Biol. Rev.* 27, 83–99. doi: 10.1016/j.fbr.2013.09.001

Toju, H., Yamamoto, S., Sato, H., Tanabe, A. S., Gilbert, G. S., and Kadowaki, K. (2013). Community composition of root- associated fungi in a *Quercus*-dominated temperate forest: "codominance" of mycorrhizal and root-endophytic fungi. *Ecol. Evol.* 3, 1281–1293. doi: 10.1002/ece3.546

Tsigos, I., Martinou, A., Kafetzopoulos, D., and Bouriotis, V. (2000). Chitin deacetylases: new, versatile tools in biotechnology. *Trends Biotechnol.* 18, 305–312. doi: 10.1016/S0167-7799(00)01462-1

van den Burg, H. A., Harrison, S. J., Joosten, M. H., Vervoort, J., and de Wit, P. J. (2006). *Cladosporium fulvum* Avr4 protects fungal cell walls against hydrolysis by plant chitinases accumulating during infection. *Mol. Plant Microbe Interact.* 19, 1420–1430. doi: 10.1094/MPMI-19-1420

van der Heijden, M. G. A., Martin, F. M., and Selosse, M. A. (2015). Mycorrhizal ecology and evolution: the past, the present, and the future. *New Phytol.* 205, 1406–1423. doi: 10.1111/nph.13288

Veneault-Fourrey, C., Communa, C., Kohler, A., Morin, E., Balestrini, R., Plett, J., et al. (2014). Genomic and transcriptomic analysis of *Laccaria bicolor* CAZome reveals insights into polysaccharides remodelling during symbiosis establishment. *Fungal Genet. Biol.* 72, 168–181. doi: 10.1016/j.fgb.2014.08.007

Voiblet, C., Duplessis, S., Encelot, N., and Martin, F. (2001). Identification of symbiosis-regulated genes in *Eucalyptus globulus–Pisolithus tinctorius* ectomycorrhiza by differential hybridization of arrayed cDNAs. *Plant J.* 25, 181–191. doi: 10.1046/j.1365-313x.2001.00953.x

Vořišková, J., Brabcová, V., Cajthaml, T., and Baldrian, P. (2014). Seasonal dynamics of fungal communities in a temperate oak forest soil. *New Phytol.* 201, 269–278. doi: 10.1111/nph.12481

Wallander, H., Johansson, U., Sterkenburg, E., Brandstr€om-Durling, M., and Lindahl, B. D. (2010). Production of ectomycorrhizal mycelium peaks during canopyclosure in Norway spruce forests. *New Phytol.* 187, 1124–1134. doi: 10.1111/j.1469-8137.2010.03324.x

Whiteford, J. R., and Spanu, P. D. (2002). Hydrophobins and the interactions between fungi and plants. *Mol. Plant Pathol.* 3, 391–400. doi: 10.1046/j.1364-3703.2002.00129.x

Worrich, A., Stryhanyuk, H., Musat, N., König, S., Banitz, T., Centler, F., et al. (2017). Mycelium-mediated transfer of water and nutrients stimulates bacterial activity in dry and oligotrophic environments. *Nat. Commun.* 8:15472. doi: 10.1038/ncomms15472

Zampieri, E., Chiapello, M., Daghino, S., Bonfante, P., and Mello, A. (2016). Soil metaproteomics reveals an inter-kingdom stress response to the presence of black truffles. *Sci. Rep.* 6:25773. doi: 10.1038/srep25773

Zampieri, E., Murat, C., Cagnasso, M., Bonfante, P., and Mello, A. (2010). Soil analysis reveals the presence of an extended mycelial network in a *Tuber magnatum* truffle–ground. *FEMS Microbiol. Ecol.* 71, 43–49. doi: 10.1111/j.1574-6941.2009.00783.x

Zampieri, E., Rizzello, R., Bonfante, P., and Mello, A. (2012). The detection of mating type genes of *Tuber melanosporum* in productive and non productive soils. *Appl. Soil Ecol.* 57, 9–15. doi: 10.1016/j.apsoil.2012.02.013

Zhong, X. (2016). Comparative epigenomics: a powerful tool to understand the evolution of DNA methylation. *New Phytol.* 210, 76–80. doi: 10.1111/nph.13540

Zhou, Z., Miwa, M., Matsuda, Y., and Hogetsu, T. (2001). Spatial distribution of the subterranean mycelia and ectomycorrhizae of *Suillus grevillei* Genets. *J. Plant Res.* 114, 179–185. doi: 10.1007/PL00013981

Conflict of Interest Statement: The authors declare that the research was conducted in the absence of any commercial or financial relationships that could be construed as a potential conflict of interest.

frontiers in Microbiology

ORIGINAL RESEARCH
published: 13 February 2018
doi: 10.3389/fmicb.2018.00141

Secretome Analysis from the Ectomycorrhizal Ascomycete *Cenococcum geophilum*

Maíra de Freitas Pereira[1,2†], Claire Veneault-Fourrey[1,3†], Patrice Vion[1], Fréderic Guinet[1,3], Emmanuelle Morin[1], Kerrie W. Barry[4], Anna Lipzen[4], Vasanth Singan[4], Stephanie Pfister[2], Hyunsoo Na[4], Megan Kennedy[4], Simon Egli[2], Igor Grigoriev[4], Francis Martin[1], Annegret Kohler[1] and Martina Peter[2*]*

[1] Institut National de la Recherche Agronomique, Unité Mixte de Recherche 1136 Interactions Arbres, Microorganismes, Laboratoire D'excellence Recherches Avancés sur la Biologie de l'Arbre et les Ecosystémes Forestiers, Centre Institut National de la Recherche Agronomique-Lorraine, Champenoux, France, [2] Swiss Federal Research Institute WSL, Forest Dynamics, Birmensdorf, Switzerland, [3] Université de Lorraine, Unité Mixte de Recherche 1136 Interactions Arbres-Microorganismes, Vandoeuvre les Nancy, France, [4] United States Department of Energy Joint Genome Institute, Walnut Creek, CA, United States

OPEN ACCESS

Edited by:
Erika Kothe,
Friedrich Schiller Universität Jena, Germany

Reviewed by:
Stefano Ghignone,
Istituto per la Protezione Sostenibile delle Piante (CNR), Italy
Nuria Ferrol,
Consejo Superior de Investigaciones Científicas (CSIC), Spain

***Correspondence:**
Annegret Kohler
annegret.kohler@inra.fr
Martina Peter
martina.peter@wsl.ch

† These authors have contributed equally to this work.

Specialty section:
This article was submitted to Fungi and Their Interactions, a section of the journal Frontiers in Microbiology

Received: *22 November 2017*
Accepted: *22 January 2018*
Published: *13 February 2018*

Citation:
de Freitas Pereira M, Veneault-Fourrey C, Vion P, Guinet F, Morin E, Barry KW, Lipzen A, Singan V, Pfister S, Na H, Kennedy M, Egli S, Grigoriev I, Martin F, Kohler A and Peter M (2018) Secretome Analysis from the Ectomycorrhizal Ascomycete Cenococcum geophilum. Front. Microbiol. 9:141. doi: 10.3389/fmicb.2018.00141

Cenococcum geophilum is an ectomycorrhizal fungus with global distribution in numerous habitats and associates with a large range of host species including gymnosperm and angiosperm trees. Moreover, *C. geophilum* is the unique ectomycorrhizal species within the clade Dothideomycetes, the largest class of Ascomycetes containing predominantly saprotrophic and many devastating phytopathogenic fungi. Recent studies highlight that mycorrhizal fungi, as pathogenic ones, use effectors in form of Small Secreted Proteins (SSPs) as molecular keys to promote symbiosis. In order to better understand the biotic interaction of *C. geophilum* with its host plants, the goal of this work was to characterize mycorrhiza-induced small-secreted proteins (MiSSPs) that potentially play a role in the ectomycorrhiza formation and functioning of this ecologically very important species. We combined different approaches such as gene expression profiling, genome localization and conservation of MiSSP genes in different *C. geophilum* strains and closely related species as well as protein subcellular localization studies of potential targets of MiSSPs in interacting plants using in tobacco leaf cells. Gene expression analyses of *C. geophilum* interacting with *Pinus sylvestris* (pine) and *Populus tremula* × *Populus alba* (poplar) showed that similar sets of genes coding for secreted proteins were up-regulated and only few were specific to each host. Whereas pine induced more carbohydrate active enzymes (CAZymes), the interaction with poplar induced the expression of specific SSPs. We identified a set of 22 MiSSPs, which are located in both, gene-rich, repeat-poor or gene-sparse, repeat-rich regions of the *C. geophilum* genome, a genome showing a bipartite architecture as seen for some pathogens but not yet for an ectomycorrhizal fungus. Genome re-sequencing data of 15 *C. geophilum* strains and two close relatives *Glonium stellatum* and *Lepidopterella palustris* were used to study sequence conservation of MiSSP-encoding genes. The 22 MiSSPs showed a high presence-absence polymorphism among the studied *C. geophilum* strains suggesting an evolution through gene gain/gene loss.

Finally, we showed that six CgMiSSPs target four distinct sub-cellular compartments such as endoplasmic reticulum, plasma membrane, cytosol and tonoplast. Overall, this work presents a comprehensive analysis of secreted proteins and MiSSPs in different genetic level of *C. geophilum* opening a valuable resource to future functional analysis.

Keywords: *Cenococcum geophilum*, small secreted proteins, ectomycorrhiza, symbiosis, interaction

INTRODUCTION

Symbiotic plant–fungal interactions are predominant in worldwide soils and have important roles in the global colonization by land plants. In forest soils, the ectomycorrhizal (ECM) symbiosis is the dominant form of a mutualistic interaction between the fine roots of trees and fungal hyphae. This interaction allows the exchange of nutrients and water between partners and increases the disease resistance of host plants (Smith and Read, 2010). Approximately 20,000 ECM fungi from diverse fungal clades and about 6,000 tree species worldwide are able to form this association (van der Heijden et al., 2015; Martin et al., 2016). Although the ECM lifestyle evolved independently several times from ancestral saprotrophs (Hibbett et al., 2000; Kohler et al., 2015) the arisen symbiotic organ and mutualistic interaction is surprisingly similar each time. Recent genomic and transcriptomic studies indicate the convergent evolution of a symbiosis toolkit with two major features of the ECM lifestyle: a reduced number of plant cell wall degrading enzymes as compared to saprotrophic ancestors in the genome and in the transcriptome the accumulation of lineage-specific transcripts possibly involved in the biotic interaction (Kohler et al., 2015; Martin et al., 2016).

Ectomycorrhiza formation is a process controlled by different genetic and environment factors (Tagu et al., 2002; Smith and Read, 2010; Kohler et al., 2015; Martin et al., 2016). A molecular communication between fungi and plant is a prerequisite for establishment of a symbiotic interaction (Plett and Martin, 2011; Martin et al., 2016). In order to manipulate host defenses and enable colonization, the secretion of small proteins is a known mechanism of pathogenic fungal–host interactions. It has been observed in mycorrhizal interactions as well but their role is still poorly understood (Martin et al., 2008, 2016; Garcia et al., 2015; Plett and Martin, 2015). Fungal genome availability allowed comparative analyses across different lifestyles including saprotrophic, mycorrhizal, pathogenic and endophytic ones revealing that all fungal genomes encode for small-secreted proteins (SSPs), which are defined as proteins of <300 amino-acids containing a signal-peptide (Martin et al., 2008, 2010, 2016; Kohler et al., 2015; Pellegrin et al., 2015; Kamel et al., 2017). Despite some overlap among shared SSPs in ECM fungi and saprotrophic fungi based on sequence similarities, many genes encoding SSPs are orphan genes and are unique to each ECM species (Kohler et al., 2015; Pellegrin et al., 2015). To understand the role of SSPs in the mycorrhiza development, both gene expression studies as well as functional analyses are necessary. So far, only two SSPs, a Mycorrhizae induced Small Secreted Protein of 7Kda (MiSSP7) in *Laccaria bicolor*, an ECM fungus and the secreted protein 7 (SP7) in *Rhizophagus irregularis* (previously known as *Glomus intraradices*), an arbuscular mycorrhizal fungus have been functionally characterized, and in both cases, the secreted effector targeted to the host plants nucleus and reshuffled plant defense pathways (Kloppholz et al., 2011; Plett et al., 2011, 2014).

One of the most abundant ECM fungi is the ascomycete *Cenococcum geophilum* Fr. showing a worldwide distribution through numerous habitats, environments and geographic regions and associating with a large variety of host species including gymnosperms and angiosperms (Trappe, 1962; LoBuglio, 1999; Obase et al., 2017). *C. geophilum* forms characteristic black monopodial or dichotomous ectomycorrhizas with darkly pigmented, emanating hyphae, as well as resistance propagules known as sclerotia, but sexual structures have never been found (Trappe, 1962; LoBuglio, 1999; Obase et al., 2017). Although being a broadly distributed fungus, the biology of *C. geophilum* is poorly understood. Studies on the fine-scale diversity of *C. geophilum* populations revealed a high level of genetic polymorphism and this can help to explain the large amount of physiological and phenotypic differences reported among *C. geophilum* isolates from similar as well as diverse geographic regions (LoBuglio, 1999; Douhan et al., 2007; Obase et al., 2017). Likewise, the variability in genome size, ploidy level and gene polymorphism among *C. geophilum* isolates support the evidence of possible cryptic sexual recombination and speciation (Spatafora et al., 2012; Bourne et al., 2014). *C. geophilum* is the only ECM fungus belonging to the clade of Dothideomycetes, the largest class of Ascomycota with a high level of ecological diversity, including many devastating plant pathogens and saprotrophs (LoBuglio, 1999; Ohm et al., 2010).

The recent genome sequencing of a *C. geophilum* strain revealed a large size of 178 Mbp and is predicted to encode for 14,748 gene models (Peter et al., 2016). Transcript profiling of *C. geophilum* genes expressed in pine ectomycorrhizal root tips revealed the upregulation of genes encoding membrane transporters, including aquaporin water channels and sugar transporters in symbiosis. Also, MiSSPs were highly induced or even specifically expressed in symbiotic tissues as seen for

Abbreviations: CAZymes, Carbohydrate-Active Enzymes; CBM, Carbohydrate binding modules; CDS, Coding DNA sequence; CEG, Core eukaryotic genes; ECM, Ectomycorrhiza; ER-Endoplasmic reticulum; FDR, False discovery rate; FIR, Intergenic flanking region; FPKM, Fragment Per Kilobase of exon model per Million mapped reads; GAPDH, Glyceraldehyde-3-phosphate dehydrogenase; GEO, Gene Expression Omnibus; GFP, Green fluorescent protein; GH, Glycoside hydrolase; GDR, gene-dense repeat-poor region; GSR, gene-sparse repeat-rich region; GT, glycosyl transferase; ITS, Internal transcribed spacer; MiSSP, Mycorrhizae induced Small Secreted Protein; SP, Secreted Protein; SiP-Signal Peptide; SSP, Small Secreted Proteins; TE, Transposable Elements; TPM, Transcripts per million.

other ECM fungi (Kohler et al., 2015; Peter et al., 2016). Furthermore, comparative genome analysis of *C. geophilum* with sequenced Dothideomycetes and a set of other fungi revealed that eight of the symbiosis-induced (>5 fold) SSPs are unique to *Cenococcum* and might play an important role in the fungal-plant interaction as seen for effector genes (Peter et al., 2016). One of the most striking features of the *C. geophilum* genome is its massively increased size compared to other sequenced Dothideomycetes (Peter et al., 2016). The 3–4 times larger genome of this ECM species is explained by the proliferation of transposable elements (TE), which make up 75% of the genome (Peter et al., 2016). Increased genome sizes due to TE bursts have been observed for other mycorrhizal fungi such as *Tuber melanosporum* and *Rhizophagus irregularis* (Kohler and Martin, 2016), but also for many biotrophic plant pathogens (Raffaele and Kamoun, 2012; Stukenbrock and Croll, 2014). In plant pathogens, these TEs are often not randomly spread over the genome but cluster in repeat-rich chromosomal segments that evolve at accelerated rates than the rest of the genome due to diverse mechanisms such as TE-activity and TE silencing machineries (Raffaele and Kamoun, 2012). Also, genes implicated in virulence and host adaptation such as effector genes tend to localize in repeat-rich, faster evolving regions (Raffaele and Kamoun, 2012). Even within species, substantial presence/absence polymorphisms have been observed for such genes in proximity of TEs for a plant pathogen, being a source of variation and driving local adaptation (Hartmann and Croll, 2017). Such a two-speed genome has convergently evolved in plant pathogenic fungi in independent lineages such as the oomycetes and the Dothideomycetes (Dong et al., 2015) but has not been observed for mycorrhizal fungi so far.

In order to better understand the biotic interaction of *C. geophilum* with its host plants, the goal of this work was to analyze whether *C. geophilum* is secreting MiSSPs as mean of communication with its host plants and narrow down the repertoire of candidate effectors for further demonstration. The specific objectives were (i) to assess the regulation of the *C. geophilum* secretome in ectomycorrhizal root tips formed with two different host plants, the gymnosperm *Pinus sylvestris* (pine) and the angiosperm *Populus tremula* × *Populus alba*-INRA clone 717-1-B4 (poplar) through transcriptomic analyses (ii) to identify candidate symbiosis effector genes and study their genomic localization, (iii) to study presence-absence polymorphism in candidate effectors by analyzing 15 re-sequenced *C. geophilum* strains and two closely related Dothideomycetes genomes to elucidate their evolution and conservation and (iv) to obtain a first glimpse of the possible role as effectors for a selection of MiSSPs by studying their potential target within the host plant cell through sub-cellular localization experiments in *Nicotiana benthamiana* leaf cells.

MATERIALS AND METHODS

Microorganisms Growth Condition

Cenococcum geophilum isolates originating from different sites (**Supplementary Table S1**) were kept in Petri dishes (100 × 20 mm) containing *Cenococcum* medium, a modified MMN medium containing casein (Trappe, 1962), at 25°C and transferred to new culture medium every 20 days. *Escherichia coli* (subcloning efficiency DH5a competent cells; Invitrogen, Carlsbad, CA, U.S.A.) and *Agrobacterium tumefaciens* (electrocompetent strain GV3101) were conserved at −80°C and they were grown in LB and YEPD medium at 37 and 28°C, respectively.

Plant Growth Condition and Ectomycorrhiza Formation

In vitro interaction systems were established between *C. geophilum* isolate 1.058, of which the genome is available (http://genome.jgi.doe.gov/Cenge3/Cenge3.info.html) and Scots pine (*Pinus sylvestris*) or hybrid poplar (*Populus tremula* × *Populus alba*; INRA clone 717-1-B4) respectively. Pine seeds [*P. sylvestris* provenance VS/Leuk (31/10) WSL] were superficially disinfected in a laminar flux hood by immersion in H_2O_2 for 30 min, followed by three rinses with sterile distilled water. The seeds were germinated in modified MMN medium described by Brun et al. (1995), with low nitrogen and phosphorus during seven days for observation of contamination. After seed germination, the plants were transferred to Petri dishes containing modified MMN and covered with a cellophane membrane (135 mm). Approximately ten agar disks containing fungal mycelium of *C. geophilum* 1.58 were placed in the vicinity of the roots. The dishes were incubated in a growth chamber at 25°C with 16 h light/day for 90 days (**Supplementary Figures S1A,B,E**).

The hybrid poplar (*Populus tremula* × *Populus alba*; INRA clone 717-1-B4) was micropropagated *in vitro* in Murashige and Skoog (MS) medium (Murashige and Skoog, 1962), with hormone supplements to synchronize rhizogenesis as described by Felten et al. (2009). In parallel, the MNM medium with low phosphorus and nitrogen (Brun et al., 1995) was covered with cellophane membranes and inoculated with 10–12 agar disks containing fungal mycelium at 25°C for 20 days. Following this, two hybrid poplar plants per dish were transferred onto the fungal mycelium. The Petri dishes were incubated in a growth chamber at 25°C with 16 h light/day for 60 days (**Supplementary Figures S1C–E**).

For both experiments, pure cultures of *C. geophilum*, pine and hybrid poplar grown in identical conditions were used as experimental controls, and the assays were conducted in minimum of three replicates. After the indicated period of time, Petri dishes were opened and the different tissues were collected for RNA analyses as follows: Single mycorrhizal root tips were collected in a 1.5 ml tube and immediately frozen in liquid nitrogen. Extramatrical mycelium surrounding roots and emanating from pine ECMs was scratched from the cellophane using a scalpel and if present, sclerotia formed in these dishes were separately collected and also immediately frozen in liquid nitrogen. For pure culture controls, free-living mycelium or fine root tips, respectively, were collected at the same time and manner as indicated for synthesis Petri dishes.

RNA Extraction and Illumina Sequencing and Data Analysis

Total RNA from mycorrhizal roots, sclerotia, extramatrical mycelium, fungal, and plant controls were extracted with the RNeasy Plant Mini kit (Qiagen, Courtaboeuf, France), including a DNase I (Qiagen) treatment, according to the manufacturer's instructions to eliminate traces of genomic DNA. Assays for the quantification and integrity check were conducted using an Experion Automated Electrophoresis Station (Bio-Rad, Hercules, CA, USA) or Agilent 2100 Bioanalyzer system (Agilent, Santa Clara, CA, USA).

Preparation of libraries and 2 × 150 bp Illumina HiSeq2000/2500 mRNA sequencing (RNA-Seq) was performed by the Joint Genome Institute (JGI) facilities. Raw reads were filtered and trimmed using the JGI QC pipeline (see **Supplementary Table S2**). Using BBDuk, raw reads were evaluated for artifact sequence by kmer matching (kmer = 25), allowing 1 mismatch and detected artifact was trimmed from the 3′ end of the reads. RNA spike-in reads, PhiX reads and reads containing any Ns were removed. Quality trimming was performed using the phred trimming method set at Q6. Finally, following trimming, reads under the length threshold were removed (minimum length 25 bases or 1/3 of the original read length—whichever is longer). Filtered reads from each library were aligned to *C. geophilum* v 2.0 reference transcripts available at the JGI database (http://genome.jgi.doe.gov/Cenge3/Cenge3.info.html). FeatureCounts was used to generate the raw gene counts and only primary hits assigned to the reverse strand were included in the raw gene counts (Liao et al., 2014). Raw gene counts were used to evaluate the level of correlation between biological replicates using Pearson's correlation and determine which replicates would be used in the DGE analysis. FPKM (Fragment Per Kilobase of exon model per Million mapped reads) and TPM (transcripts per million) normalized gene counts were also provided. DESeq2 (version 1.10.0), including an independent filtering procedure by default, was used to determine which genes were differentially expressed between pairs of conditions (Love et al., 2014). The parameters used to call a gene differentially expressed between conditions were fold change > log1 and FDR $p < 0.05$. A gene with a FPKM > 1 was considered as expressed. The complete RNA-Seq data was submitted to GEO (GSE108831 and GSE108866). For selecting MiSSPs as well as for comparisons among different synthesis systems, we added RNA-Seq data of a semi-sterile greenhouse trial growing *P. sylvestris* with *C. geophilum* 1.58 in pots (Peter et al., 2016; GEO Accession GSE83909). Here, pine trees were pre-grown for 2 months in pots containing a 1:2 double-autoclaved mixture of quartz sand and sieved forest topsoil before being inoculated by *C. geophilum* 1.58 mycelia and grown for another 3 months before harvesting ECMs. As pure culture fungal control, 2-months-old mycelium grown as indicated above on agar Petri dishes was used (Peter et al., 2016).

Genome Architecture and Gene Density Analysis

Genomic distances between two genes and genome architecture heatmaps were generated according to Saunders et al. (2014). These results were binned according to log (length) and plotted as a 2-dimensional heatmap using Excel. Plotting the abundance of genes according to their 5′ and 3′ flanking intergenic lengths indicate local gene density (**Figure 3**). In *C. geophilum* genome, we defined two contrasting regions: one gene-dense repeat-poor (GDR) containing a high number of genes (gene-dense) combined with short 3′ and 5′ flanking regions indicating a low level of repeats (repeat-poor), whereas the gene-sparse repeat-rich (GSR) region is characterized by a low number of genes displaying long 5′ and/or 3′ flanking regions. We also represent, according to local gene density, the distribution of gene expression induction in ECM root tips compared to free-living mycelium (log2 fold change) or their level of expression (fpkm values).

DNA Extraction, Genome Re-sequencing of *Cenococcum geophilum* Isolates and Presence–Absence Analyses of Selected SSPs

To study the presence/absence polymorphism of selected SSPs, data of 15 recently re-sequenced strains of *C. geophilum* was used. The 15 strains originated from diverse locations in Switzerland, France, Poland and Finland (**Supplementary Table S1**). For genomic DNA sequencing, mycelia were grown in liquid culture containing *Cenococcum* medium for 3–4 weeks after which they were harvested, pulverized in liquid nitrogen and stored at −80°C until processing. DNA was extracted using the PowerMax Soil DNA isolation kit (MOBIO/QIAGEN CA, USA) according to the manufacturer's instructions and using around 2 g of mycelia. Library construction and sequencing was performed at the Joint Genome Institute (JGI) using Illumina HiSeq 2500 and 2 × 100 bp read length sequencing in two different lanes. Between 26 and 48 million raw reads were generated corresponding to a 15–27x coverage. CLC genomic workbench 10 was used to de novo assembly the 15 genomes with the following parameters: Mapping mode: map reads to contigs; minimum contig lenght: 500; Mismatch cost = 2; Insertion cost = 3; Deletion cost = 2; length fraction = 1.0; Similarity fraction = 0.9. A summary is given in **Supplementary Table S3** and sequence contigs for the different strains and for all MiSSPs studied are compiled in **Supplementary File 1** (http://mycor.nancy.inra.fr/IMGC/CenococcumGenome/download/Supplementary_data_1.fa.gz).

Screening for presence–absence polymorphism of the 22 selected *C. geophilum* MiSSPs and 22 Core eukaryotic genes–CEG (**Supplementary Table S4**) in the 15 re-sequenced strains was done by conducting a BLASTN search against the *de novo* assemblies and the reference genome 1.58 (https://genome.jgi.doe.gov/Cenge3/Cenge3.home.html). Further, the genome data of the closest related species, *Glonium stellatum* (https://genome.jgi.doe.gov/Glost2/Glost2.info.html) and *Lepidopterella palustris* (https://genome.jgi.doe.gov/Leppa1/Leppa1.home.html) was used to compare *C. geophilum* SSP sequences for polymorphism (Peter et al., 2016). A gene was considered as affected if the deletion event was overlapping >90% of the gene. To check presence–absence polymorphism in gene duplications, manual alignments was done using the INRA Multalin interface (Corpet, 1988). The presence of a *C. geophilum* MiSSP in the respective *de*

novo assembly contigs was defined as the lowest e-value accession (E-value) combined with the greatest HSP length (number of nucleotides in the reference genome–Cg1.58).

The variability in presence–absence patterns of the 22 selected MiSSP genes among *C. geophilum* isolates was examined with principal coordinate analyses (PCO) using the Jaccard similarity index. Variation explained in these patterns by phylogenetic clade (3 levels), country (4 levels) and forest type (4 levels) of isolate origin were assessed using the PERMANOVA routine (Anderson, 2001) implemented in the software Primer7 using 9,999 unrestricted permutations of raw data as well as by Monte Carlo tests (Clarke and Gorley, 2015). Phylogenetic analysis was performed using the online software phylogeny.fr from concatenated sequences of *C. geophilum* GAPDH and ITS using default parameters (Dereeper et al., 2008). In short, MUSCLE was used to align sequences and Gblocks for curation. Phylogeny was performed using a maximum likelihood algorithm using PhyML and branch confidence indices were calculated based on an approximate likelihood ratio test. ITS and GAPDH sequences are given in **Supplementary Table S5**.

Validation of SSP Gene Presence–Absence in Different *Cenococcum Geophilum* Isolates by PCR

We validated gene presence–absence polymorphism for some selected *C. geophilum* MiSSPs using direct amplification of target genes including upstream and downstream regions. The primers were designed using Primer 3.0 (Untergasser et al., 2012) from a conserved flanking sequences of each gene (**Supplementary Table S6**). PCR reactions were performed with OneTaq® DNA Polymerases according to the manufacturer's instructions (New England Biolabs, Mass, USA) and amplicons run on 1% agarose gels. Each PCR reaction was purified with QIAquick PCR Purification Kit (Qiagen, Courtaboeuf, France) and the PCR product verified by sequencing (Eurofins, Ebersberg, Germany).

Cloning Procedures and Plasmids Used for Localization Experiments

The open reading frame (ORF) coding the mature form (i.e., without the signal peptide) of 22 *C. geophilum* selected MiSSPs were synthetized by GeneCust Europe (Ellange, Luxembourg). The vectors were designed with *att* sites accomplish to gene sequence to be compatible with PCR Cloning System with Gateway® Technology. The entry clone (*C. geophilum* MiSSP vectors) was utilize in LR recombination reaction with pB7WGF2 (C-terminal fusion with GFP) destination vector to create an expression clone (Karimi et al., 2002). The vectors were amplified in *E. coli* (DH5a competent cells; Invitrogen, Carlsbad, CA, USA). Sequences of DNA fragments inserted in vectors obtained by PCR were verified by sequencing (Eurofins genomics, Ebersberg, Germany) before to clone in *A. tumefaciens* (electrocompetent strain GV3101). For colocalization studies, we used a set of markers fused to mCherry protein developed by Nelson et al. (2007).

Transient Protein Expression in *Nicotiana benthamiana* Leaf Cells

N. benthamiana plants were grown in phytotron at 22°C under 16-h day and 8-h night conditions. *A. tumefaciens* GV3101 was used to deliver T-DNA constructs into leaf cells of 4–6 weeks-old *N. benthamiana* plants, following the agroinfiltration method previously described (Win et al., 2011). Overnight-grown bacterial cultures were resuspend into 10 ml of infiltration buffer (10 mM MgCl2, 10 mM MES, pH 5.6, 200 µM acetosyringone), optical density at 600 nm (OD600) adjusted at 0.1. Bacteria were incubated at 28°C during 2 h under 50 rpm. For all co-transformations, *A. tumefaciens* strains were mixed in a 1:1 ratio in infiltration buffer to a final OD 600 of 0.2. The leaves were collected 2 days after infiltration for further protein isolation or microscopy analysis.

Live-Cell Imaging by Laser-Scanning Confocal Microscopy

Small pieces of leaves were mounted in Perfluorodecalin 95% (Sigma-Aldrich, Saint Louis, MO, USA) and water between a slide and a coverslip and were immediately observed. Live-cell imaging was performed with a Zeiss LSM780, confocal microscope system, using 10× (air) and 40× (water immersion) objectives. The GFP was excited at 488 nm, whereas the mCherry was excited at 561 nm. Specific emission signals corresponding to the GFP and the mCherry were collected between 505–525 and 580–620 nm, respectively. Each construct gave a similar localization pattern across at least three independent observations. After observation, leaves were frozen in liquid nitrogen and were conserved at −80° C for further use.

Total Protein Isolation and Immunoblotting

N. benthamiana leaves were harvested 2 days after infiltration, were frozen in liquid nitrogen, and were ground into powder with mortar and pestle. Total protein extraction was performed by reducing and denaturing proteins from the leaf powder 10 min at 95°C in Laemmli buffer (0.5 M Tris-HCl, pH 6.8, 10 mM dithiothreitol [DTT], 2% SDS, 20% glycerol) in order to avoid *in vitro* nonspecific degradation of the fusion proteins. Proteins were separated by 15–20% SDS-PAGE (Mini-PROTEAN® TGX™ Gels) and transferred onto a nitrocellulose membrane using Trans-Blot Turbo Transfer System (Bio-Rad, CA, USA). Transfert efficiency was assessed by Red Ponceau staining. GFP detection was performed in a single step using a GFP (B2): sc-9996 horseradish peroxidase (HRP)-conjugated antibody (Santa Cruz Biotechnology, Santa Cruz, CA, USA). Protein bands on immunoblots were detected using Clarity ECL Western Blot Substrate (Bio-Rad, CA, USA) using the manufacturer's protocol.

RESULTS

Host-Dependent Gene Expression Changes of *Cenococcum geophilum* Secreted Protein-Encoding Genes

The *C. geophilum* genome contains a total of 595 predicted secreted proteins (SP) including 227 Small Secreted Proteins

(SSPs, <300 aa), 120 Carbohydrate-Active Enzymes (CAZymes), 13 lipases, 27 proteases, and 208 other SPs (Peter et al., 2016).

To study host dependent changes in the gene expression of secreted proteins we performed RNA-Seq analyses on *C. geophilum* ECM roots from *P. sylvestris* and *P. tremula x alba* and *C. geophilum* free living mycelium grown in *in vitro* systems. We complemented the analysis with samples from extramatrical mycelium of pine ECM and sclerotia.

The majority of SPs were expressed in all tissues (88–93%). For 30 (5%) of them, no transcripts were detected in any of the conditions studied. The expression of 221 transcripts was significantly regulated in ECM root tips as compared to free-living mycelium in the *in vitro* systems (FC > log1, FDR $p < 0.05$; **Figure 1**; **Supplementary Table S7**). In interaction with pine roots, 114 SSPs were up- and 70 down-regulated, while in contact with poplar roots 107 SSPs were up- and only 20 down-regulated compared to control free-living mycelium (**Figure 1B**). The majority of genes were similarly regulated in the interaction with both host trees (**Figure 1A**). Among the most highly up-regulated transcripts in both interactions were SSPs (e.g., Cenge3:660401, Cenge3:693798, Cenge3:698167), but also secreted CAZymes (GH131, CBM1-GH45, CBM18-CE4-CBM18) (**Supplementary Table S7**). Interestingly, the up-regulated transcripts of pine ECM were significantly enriched in CAZymes, whereas for poplar ECM, they were enriched in SSPs (**Figure 1B**). We further analyzed the host-dependent expression levels of these 221 SPs in ECM of the different hosts. If the expression values varied less then five times between the two hosts, we considered a transcript as used in both interactions; with a more then five-fold difference, the transcript was considered as more important for either of the two host interactions (**Supplementary Table S8**). The majority

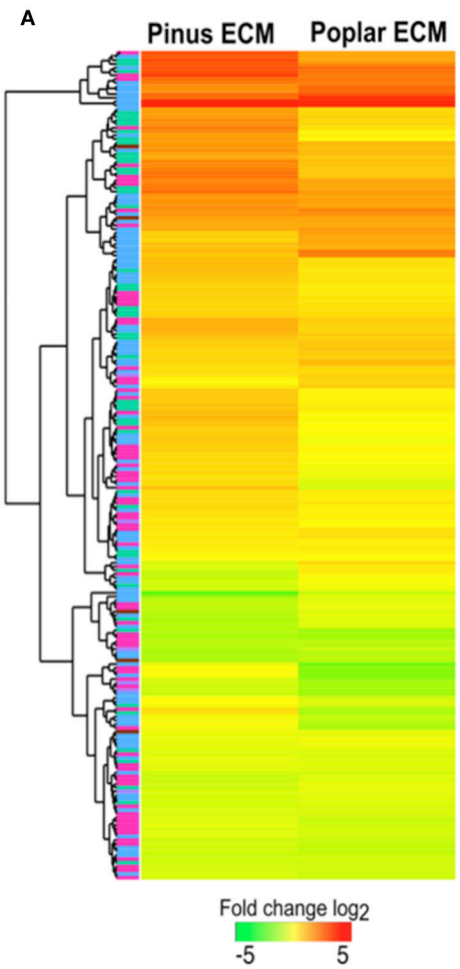

B

	Pinus ECM[Ŧ]	Poplar ECM[Ŧ]
UP		
Total	114	107
SSP	46	53*
Cazymes	33*	28
Proteases	2	1
Lipases	2	2
Others	31	23
DOWN		
Total	70	20
SSP	27	6
Cazymes	7	4
Proteases	4	1
Lipases	3	1
Others	29	8

[Ŧ]compared to the respective free-living mycelium

*enriched compared to genome (Fisher-Test $p<0.05$)

FIGURE 1 | Changes in *C. geophilum* gene expression in pine and poplar ECM compared to free-living mycelium. Secretome transcripts significantly regulated (log2 fold > 1; FDR $p < 0.05$) in minimum one of the mycorrhizal systems to free-living mycelium were included in the analysis. **(A)** Fold change of gene expression was calculated for pine and poplar ECMs compared to the mean free-living mycelium expression value. Log2 transformed data were subjected to R Package Heatmap2 for clustering. Regulation levels range from pale to saturated colors (red for induction; green for repression). A column on the left side indicates by color the class of the secreted protein predicted for each gene. **(B)** Number of transcripts regulated in pine and poplar ECMs by secreted protein class. *SP class enriched compared to the number present in the genome (Fisher-test for enrichment $p < 0.05$). Data are provided in **Supplementary Table S7**.

of the genes (134/147 up-regulated, 76/83 down-regulated) were similarly expressed in ECM root tips of both host plants (**Figure 2**). None of the SPs was specific for one interaction; that is, showing no expression (value 0) when interacting with the other host tree. However, significantly higher expression was observed for two SSPs in interaction with poplar (Cenge3:573854; Cenge3:294776) and for one SSP and several CAZymes in interaction with pine roots (Cenge3:28058; CBM1-GH45, GH12, CBM1-GH5-4, GH28, GT90) (**Supplementary Table S7**). Interestingly, when comparing the different synthesis systems used, i.e., *in vitro* agar Petri dishes for pine and poplar and a semi-sterile pot system for pine (Peter et al., 2016), it seems that the system had a more pronounced impact on gene expression changes in interactions than had the host identity. Clearly more

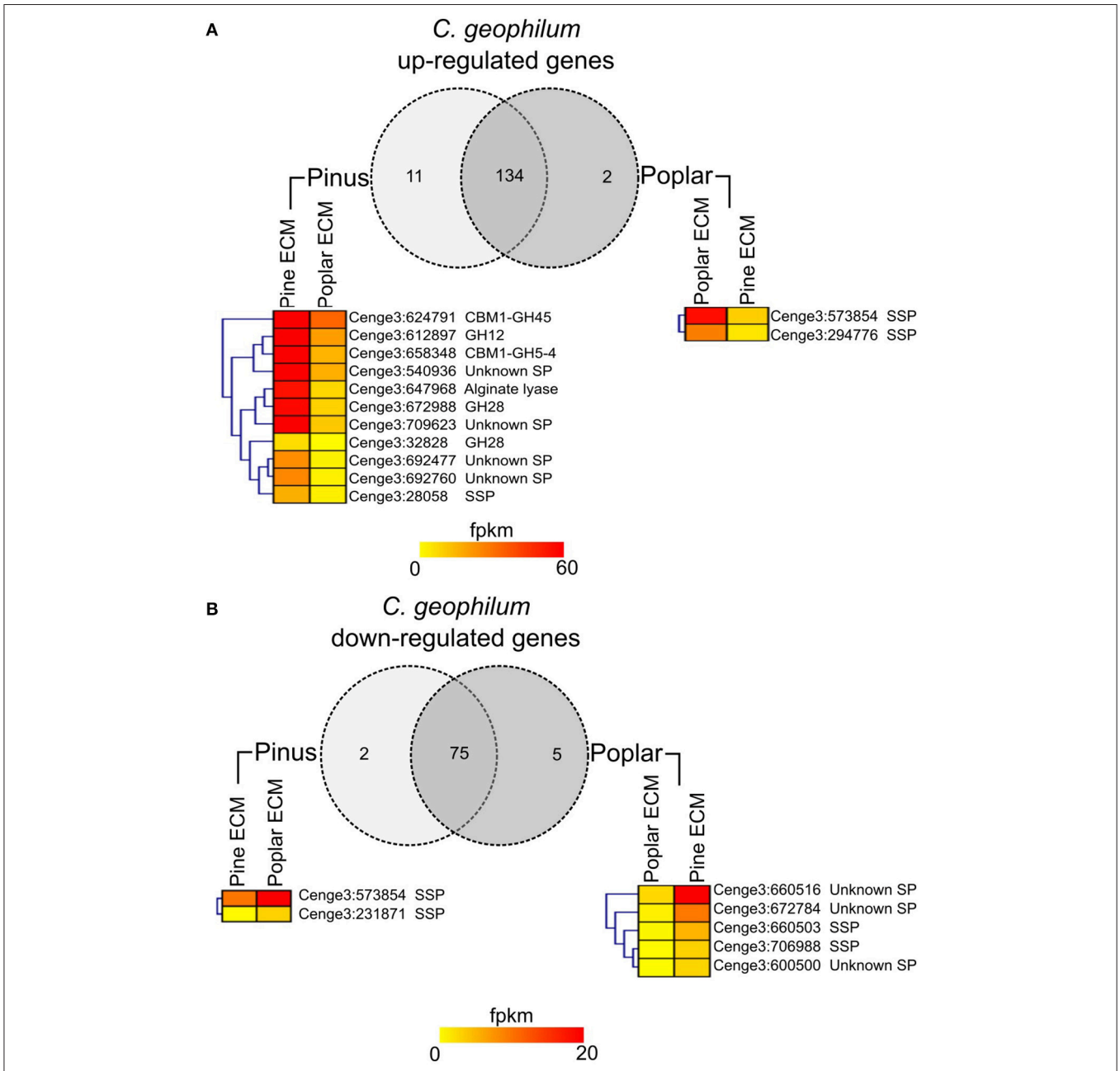

FIGURE 2 | Host specific secretome of *C. geophilum*. Transcripts up-regulated **(A)** or down-regulated **(B)** in pine and/or poplar ECMs compared to free-living mycelium and their expression values (fpkm) in mycorrhizal tissue. Genes coding for secreted proteins were considered as used in both interactions if the expression difference was <5-fold. The expression was considered as more specific for one host tree if the expression differences was >5-fold. The expression of genes showing a more then 5-fold difference is shown in heatmaps for pine and poplar ECM. Note that the expression in some cases is <1 fpkm but never zero. Note that eight transcripts that were up-regulated in one and down-regulated in the other ECM were counted two times.

C. geophilum genes were commonly up-regulated in ECM of pine and poplar from the *in vitro* system (41 genes) as compared to commonly up-regulated genes in pine ECM using the different systems (6 genes; **Supplementary Figure S2**).

Selecting Mycorrhiza Induced Small Secreted Proteins (MiSSPs) for Further Characterization

We further focused on *C. geophilum* MiSSPs in order to identify candidate effector proteins for the interaction between *C. geophilum* and its host trees. A set of 22 MiSSPs, induced (>2.5 fold) in the interaction between *C. geophilum* and *P. sylvestris* under semi-sterile greenhouse conditions was selected from Peter et al. (2016) (**Table 1**). The predicted protein size of these MiSSPs ranged from 58 to 275 aa, containing no (e.g., Cenge3:664950 and Cenge3:679266) to 10.61% of cysteine residues (Cenge3:666290). Only six MiSSP sequences contain known domains or sequence homology to known proteins such as the SnoaL domain (PF12680, PF13577; Cenge3: 677330), the cupin domain (PF00190, PF07883; Cenge3:552209), the Ubiquitin 3 binding protein But2 C-terminal domain (PF09792; Cenge3:677232 and Cenge3:658610) or the "secreted in xylem 1" (Six1) protein of *Fusarium oxysporum* (Cenge3:698167; Rep et al., 2004). Eight MiSSPs were specific to *C. geophilum* while the others share sequence similarity with genes from other Dothideomycetes fungi (**Table 1**). Three pair of duplications were present within the selected MiSSPs showing sequence similarities from 77–95 to 72–93% for nucleotide and protein sequences, respectively (**Supplementary Figure S3**). Expression studies showed that some of these MiSSPs were also up-regulated in sclerotia formed in *in vitro* synthesis dishes and in extramatrical mycelium emanating from the ECM root tips (**Table 1**).

Genome of *Cenococcum geophilum* Displays a Bipartite Architecture with MiSSPs Present in Both Regions

Due to richness in transposable elements found in the *C. geophilum* genome, we measured for each gene the distance to the neighboring genes at both 5′ and 3′ end. This method is used as a proxy to detect repeat-rich regions, assuming that the larger the intergenic region is the more repetitive sequences are present (Raffaele et al., 2010b). *C. geophilum* genome displayed two types of regions: repeat-rich, gene-sparse regions (GSR) and repeat-poor, gene-dense (GDR) regions, with a cut-off for 5′ and/or 3′ intergenic region length at >6,495 bp (**Figure 3**). This indicates a "two-speed" genome for *C. geophilum* as seen for some pathogenic fungi. In order to test whether gene position and environment could impact the *in planta* gene regulation, we measured the distribution of all *C. geophilum* genes for their expression induction and repression in ectomycorrhizal root tips compared to free-living mycelium according to local gene density. We observed that *in planta* regulated (either induced or repressed) genes are scattered all over the genome independently of the type of region. Neither did the host (pine vs poplar) nor the environmental condition (greenhouse vs. *in vitro*) influence this observation (**Supplementary Figures S4A–C**). Furthermore, gene location had an impact on the median level of gene expression (rpkm). Genes located in GSR (repeat-rich) tended to be expressed at a lower level than genes located in GDR (repeat-sparse) (**Supplementary Figure S4D**). This suggests an impact of repeats on the gene expression level.

One third (34%) of the genes encoding for the predicted *C. geophilum* secretome were located in GSR, which parallels the proportion found for the full-predicted proteome (33%; **Supplementary Figure S5**). Within the secretome, the categories "SSPs" and "other SPs" tended to show more members in GSR (37%) compared to the secreted CAZymes, lipases or proteases (28, 23, and 33%, respectively; **Supplementary Figure S5**) but no significant enrichment was observed. Again, we did not notice a difference in *in planta* gene regulation whether secretome-encoding genes were located in GDR or GSR (data not shown).

The 22 *C. geophilum* MiSSPs were present in both types of regions (**Figure 3**). Interestingly, when MiSSPs are duplicated, one copy is located in the GDR and one in GSR. Two duplications likely occurred at the same event since the genes were neighbors in both compartments but with invaded repeats in the repeat-rich region (**Supplementary Figure S6**).

MiSSP Encoding Genes Show Presence–Absence Polymorphism across *Cenococcum geophilum* Isolates

Re-sequencing data from *C. geophilum* isolates originating from different European countries (Switzerland, France, Poland and Finland) and genome data of closely related species, *Glonium stellatum* and *Lepidopterella palustris* allowed to compare SSP sequences for polymorphism (presence–absence) among fungal strains. For seven MiSSPs, PCR amplifications were performed to verify the presence or absence and PCR products were sequenced. Six *C. geophilum* MiSSPs (Cenge3:666290, Cenge3:723230, Cenge3:664950, Cenge3:28058, Cenge3:661585 and Cenge3:667330) were present in all *C. geophilum* isolates but were missing in either *G. stellatum* or *L. palustris* or in both (**Figure 4**, **Supplementary Table S9**). Two MiSSPs (Cenge3:668273 and Cenge3:552209) and all analyzed CEGs were present in all *C. geophilum* isolates as well as in *G. stellatum* and *L. palustris*. All other MiSSPs were dispersed among *C. geophilum* isolates. Most conserved MiSSPs (6 of 8; 75%), i.e., those that are present in all *C. geophilum* strains, localized in GDR, whereas only 36% (5 of 14) of the non-conserved MiSSPs did (**Figure 4C**). The entire set of 22 MiSSPs were present in only three of the four isolates originating from the same site as the sequenced strain. Based on phylogeny analysis using the internal transcribed spacer (ITS) and the glyceraldehyde-3-phosphate dehydrogenase (GAPDH) as marker genes (Obase et al., 2016), these three strains were closely related to the sequenced one and clustered within the clade 5 according to the nomenclature of Obase et al. (2016) (**Figure 4A**; **Supplementary Figure S7**). The clades 5 and 6 likely correspond to cryptic species and within clade 5, even more subdivisions are indicated based on species delimitation analyses (Obase et al., 2016; here divided in clade 5a and 5b). When looking at similarities in presence–absence of the 22 MiSSPs

TABLE 1 | List of 22 MiSSPs candidates selected of *Cenococcum geophilum* and *Pinus sylvestris* ectomycorrhiza.

						Transcript evidence (FC log2)				
Protein ID	**INTERPRO/putative function-best hit**	**Size (aa)**	**SP length**	**Cystein %**	**Presence in others Dothideomycetes fungi†**	**Semi-steril synthesis**	***In vitro* synthesis**			
						***P. sylvestris* ECM**	***P. sylvestris* ECM**	***P. tremula* x *P. alba* ECM**	**Extramatricial mycelium**	**Sclerotia**
28058	–	209	20	8.17	Yes	2.49	−0.92	2.5		
331593	_	81	21	6.25	No	1.42	−0.02	−0.7		
552209	Cupin domain, manganese ion binding/spherulin-like	275	20	1.46	Yes	4.41	2.1	0.87		
634429	Protein of unknown function DUF4237	224	18	1.79	Yes	2.43	3.6	3.6	x	x
636312	Duplication of Cenge3:660403	249	19	3.23	Yes	1.93	0.46	0.74		
658610	Ubiquitin 3 binding protein But2, C-terminal	186	19	1.08	Yes	3.55	−0.25	−0.82		x
659287	–	136	20	7.41	Yes	3.66	1.2	0.6		
659858	Duplication of Cenge3:660401	58	19	3.51	No	4.3	0.95	1.2		
660401	Duplication of Cenge3:659858	58	19	3.51	No	8.08	9.4	5.9		
660403	Duplication of Cenge3:636312	249	19	3.23	Yes	6.53	0.68	−0.074		
661585	_	194	22	4.66	Yes	5.4	3.5	2.3		x
664950	_	72	19	0	No	1.21	0.21	−0.39		
666290	–	180	22	10.61	Yes	2.95	2	3		x
667330	NTF2-like domain, Polyketide cyclase SnoaL-like domain	172	19	0.58	Yes	3.75	3.8	2.9		x
668273	–	204	19	0.99	Yes	3.53	2.7	3.4		x
670497	_	199	17	5.05	Yes	2.89	−0.041	0.15		
677232	Ubiquitin 3 binding protein But2, C-terminal	204	18	1.48	Yes	7.53	−6.2	−1.6		
679266	Duplication of Cenge3:693798	131	20	0	No	5.94	2.5	4.9		x
680403	_	135	20	1.49	No	7.88	1.5	5.4		x
693798	Duplication of Cenge3:679266	239	21	0.84	No	7.18	8.4	6.5		x
698167	*Fusarium* secreted in xylem protein 1	259	23	3.88	No	8.21	8.1	6.9		x
723230	–	96	23	2.11	Yes	2.52	0.3	0.26		

† *Presence in other Dothideomycetes of which genome sequences are available (https://genome.jgi.doe.gov/dothideomycetes/dothideomycetes.info.html) determinated by Blastp analysis.*
FC, Fold change; SiP, Signal Peptide; ECM, ectomycorrhizal roots. GDR, Gene dense region; GSR, Gene sparse region.

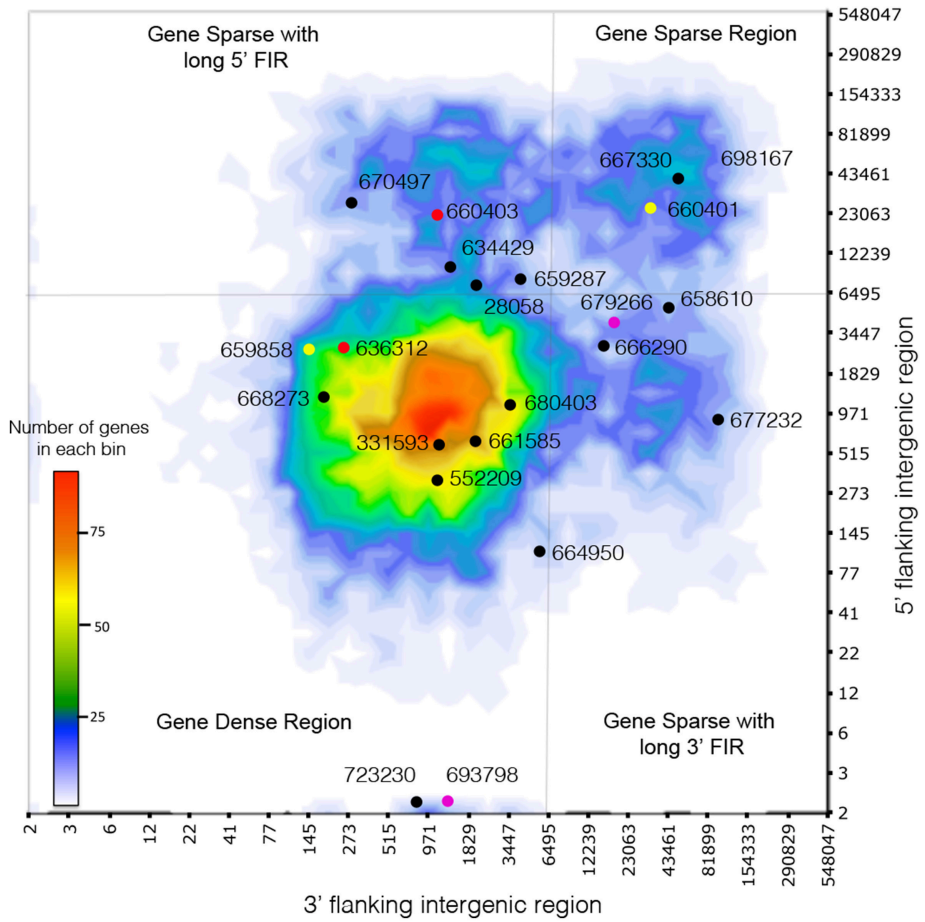

FIGURE 3 | *Cenococcum geophilum* genome architecture. Distribution of distances of the closest repetitive genomic element on 5′ and 3′ sides for all genes (heatmap) and the genes encoding the 22 *C. geophilum* MiSSPs. Genes represented with the same color correspond to gene duplications. Gray lines delineate 5′ and 3′ intergenic flanking region (FIR) at 6495 bp to highlight long 5′ and 3′ intergenic flanking region and the gene-sparse repeat-rich regions (GSR) vs. the gene-dense repeat-poor region (GDR).

among the 16 *C. geophilum* isolates, clade affiliation explained best the polymorphism, whereas country origin marginally and the forest type (and therefore potential plant host) did not significantly explain these patterns (**Supplementary Figure S8**).

C. geophilum MiSSPs Accumulate in Distinct Plant Subcellular Compartments

To determine possible *in planta* subcellular location of the 22 *C. geophilum* MiSSP, we cloned their coding DNA sequence (CDS) without the signal peptide (mature form of protein) in an expression vector to obtain MiSSPs fused to a green fluorescent protein (GFP) and expressed them into tobacco leaf cells. 21 *C. geophilum* MiSSP::GFP fusions emitted a detectable fluorescent signal using confocal microscope (**Figure 5**). The fluorescent signals of Cenge3:552209-GFP, Cenge3:667330-GFP, and Cenge3:659858-GFP accumulated in the plasma membrane, endoplasmic reticulum, and tonoplast, respectively. The signals of Cenge3:679266-GFP and Cenge3:634429-GFP accumulated in small cytosolic bodies (**Figure 5**). The displayed fluorescent signal in specific subcellular compartments was markedly different from GFP controls and the localization was confirmed by co-expression of specific organelle plant markers (Nelson et al., 2007; **Figure 5**). All other *C. geophilum* SSP-GFP showed an uninformative subcellular distribution in the nucleus and cytosol as did the GFP control (**Supplementary Figure S9**). It is important to consider that these localizations were obtained using a 35S promoter and GFP (a protein with triple size of our protein of interest) as a tag. Both actions could result to different localization from those observed when MiSSPs are delivered by the symbiont. Immunoblotting experiments demonstrated both protein production and the integrity for 20 fusion proteins displayed a band at the expected protein size, confirming their integrity. In contrast, one fusion protein (Cenge3:698167) showed no detectable fluorescent signal and no bands on the immunoblots and another (Cenge3:679266) was localized at cytosolic bodies but the integrity could not be confirmed (**Supplementary Figure S10**). In conclusion, we showed that four distinct subcellular compartments are targeted

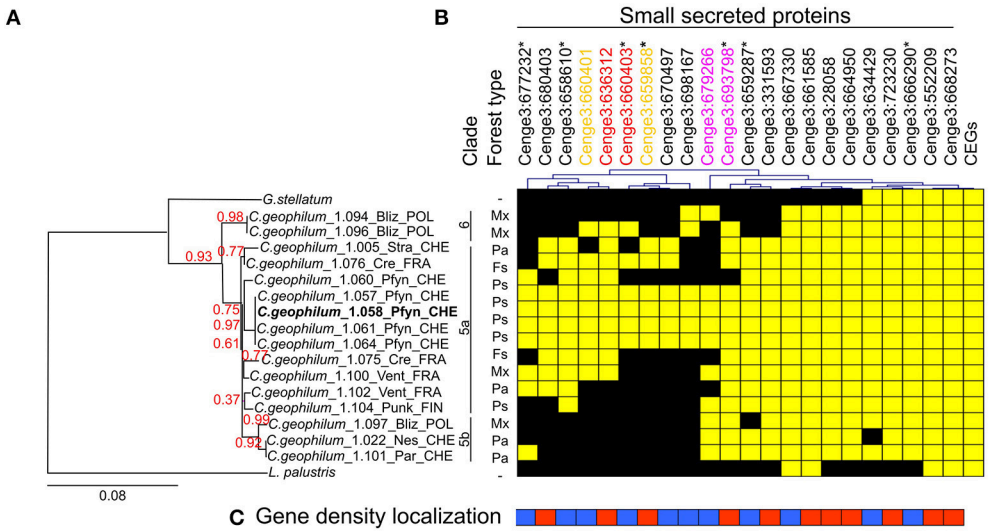

FIGURE 4 | Distribution of genes encoding SSPs among *Cenococcum geophilum* isolates and two closely related species, *Glonium stellatum* and *Lepidopterella palustris*. **(A)** Phylogenetic tree reconstructed based on concatenated nucleotide sequence of the internal transcribed sequence (ITS) and glyceraldehyde-3-phosphate dehydrogenase (GAPDH) gene using PhyML-maximum likelihood. The tree was rooted by *L. palustris* and branch confidence indices were calculated by an approximate likelihood ratio test. The scale bar indicates the number of nucleotide substitutions per site. Three distinct clades are indicated and numbered according to Obase et al. (2016) including a possible subdivision of clade 5 (left). The forest type in which the strains were isolated is indicated as *Picea abies* (Pa), *Pinus sylvestris* (Ps), *Fagus sylvatica* (Fs) and Mixed Forest (Mx). **(B)** Presence (yellow) or absence (black) of genes are indicated for 22 MiSSPs and 22 core eukaryotic genes (CEGs) across the *C. geophilum* strains and the two closely related species. **(C)** Gene density localization is indicated for 22 MiSSPs present in gene sparse (blue) or gene dense region (red). Asterisks next to the Protein IDs indicate that the presence–absence was confirmed by PCR. Presence–absence patterns are hierarchically clustered (top). Color code for gene duplication was indicated (top).

by the selected *C. geophilum* MiSSPs, including the plasma membrane, tonoplast, cytosol and endoplasmic reticulum.

DISCUSSION

Cenococcum geophilum is a cosmopolitan ECM fungus well known for its extremely wide range of host plants and habitats (LoBuglio, 1999). Although some intraspecific variation in host specificity may exist among different isolates of *C. geophilum* as indicated by a re-synthesis experiment of this species (Antibus et al., 1981) and as known for other generalist ECM species (Le Quéré et al., 2004), the studied *C. geophilum* 1.58 isolate forms ECMs with diverse hosts both gymnosperms (*Pinus sylvestris, Picea abies*) and angiosperms (*Populus* spp., *Quercus* spp.; M. Peter unpublished). To understand its communication strategy with different symbiotic partners, we compared the gene regulation of secreted proteins and found that the same gene sets were used and similarly expressed in ECMs of *C. geophilum* formed with either host. Only very few genes were differentially expressed, which is astonishing for so different trees as are the gymnosperm pine and the angiosperm poplar. Only few studies about host specific interactions are available from ECM systems. The generalist *Laccaria bicolor* also expressed a core gene regulon when interacting with the two different hosts *Pseudotsuga menziesii* and *Populus trichocarpa* but almost 80% of the about 4,000 up-regulated genes were specific to one of the host trees, among which many secreted proteins (Plett et al., 2015). On the contrary, a very similar set of genes was expressed in compatible interactions between species of the *Suillus* genus, considered as specialists on *Pinaceae*, interacting with different *Pinus* species and significant differences were mainly observed in incompatible interactions (Liao et al., 2016). Generalists such as the root endophyte *Pirifomospora indica* (Lahrmann et al., 2013) and the plant pathogen *Sclerotinia sclerotiorum* (Guyon et al., 2014) clearly induced host-specific gene sets whereas the specialist barley powdery mildew pathogen *Blumeria graminis* f. sp. *hordei* expressed very similar gene sets when interacting with divergent hosts such as monocots and dicots (Hacquard et al., 2013). Being a very broad generalist, we therefore expected *C. geophilum* to rather show a host-specific regulon, which was not the case with only 8% of all up-regulated genes being host-specific. More work is needed to see whether such a uniform response of *C. geophilum* holds true for other host trees and in more natural systems such as in greenhouse trials. The small set of differentially regulated genes likely corresponds to the fine-tuning necessary for the interaction with each host tree. A more than five-fold higher difference in transcript abundance was detected mainly for CAZymes during the interaction between *C. geophilum* and pine and for MiSSPs in *C. geophilum* poplar ECM. Since pine and poplar roots have different cell wall compositions (Sarkar et al., 2009), a different set of cell-wall loosening enzymes could be necessary for the penetration of hyphae and development of the Hartig net. For instance, the two GH28 acting on pectins, a GH5-4 acting on hemi-/cellulose and a GH45 a cellulase with similarity to plant expansins that have an important role in plant cell wall loosening (Cosgrove, 2000)

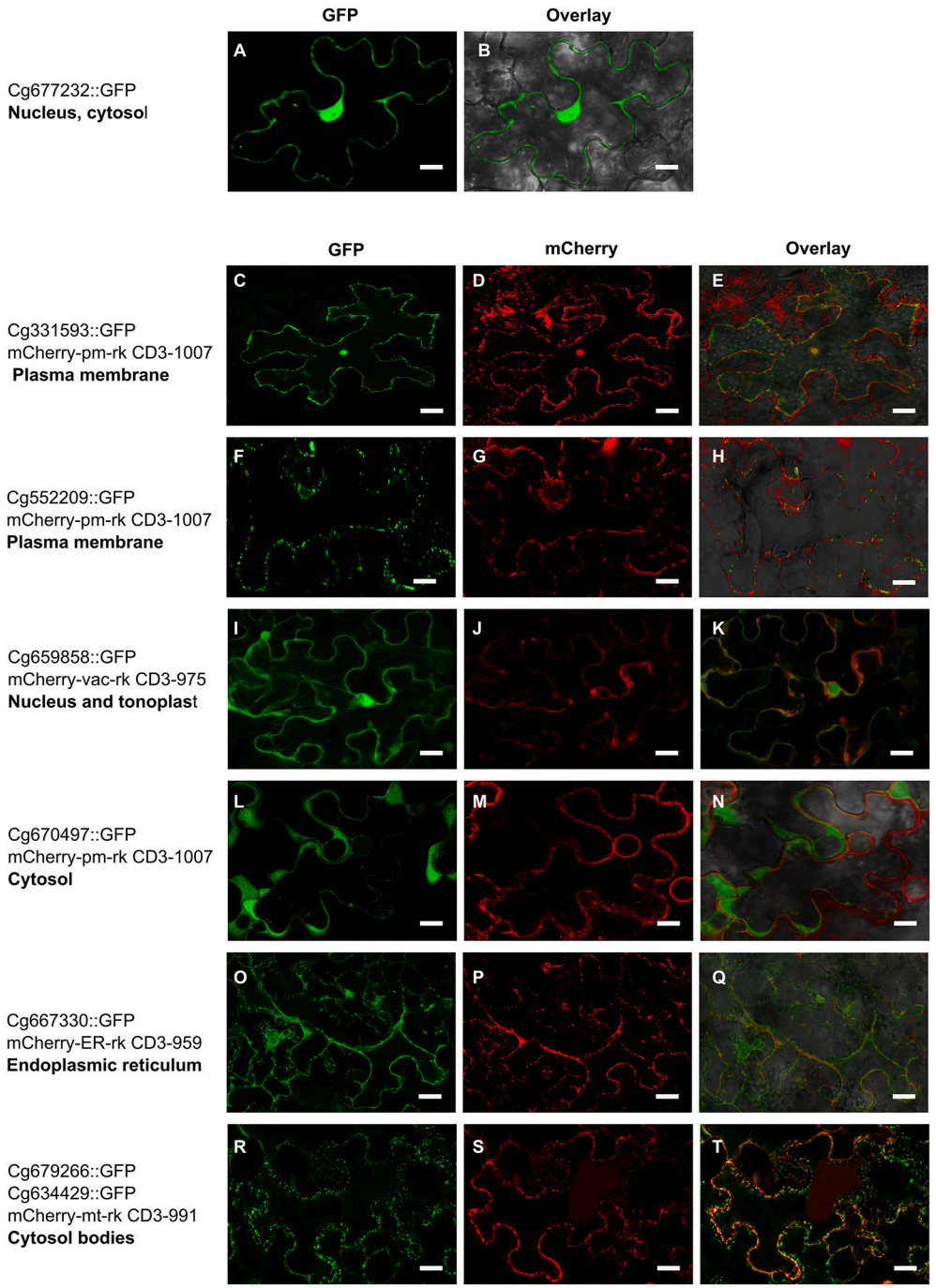

FIGURE 5 | *Cenococcum geophilum* MiSSP candidates accumulate in different subcellular compartments Live cell imaging of six MiSSP:GFP fusion proteins accumulating in specific organelle localization. For each MiSSP:GFP fusion proteins tGFP, mCherry and the overlay are shown. **(A–B)** A representative image for fusion proteins accumulating in the nucleoplasm and cytosol is shown. **(C–H)** Plasma membrane, **(I–K)** tonoplast, **(L–M)** cytosol, **(O–Q)** endoplasmic reticulum and **(R–T)** cytosolic bodies in *Nicotiana benthamiana* leaf cells.

are among the more highly expressed genes in pine ECM. The colonization of the gymnosperm *P. menziesii* by *L. bicolor* was also accompanied by a high number of differentially expressed CAZymes with increased abundances; among these were GH5 and GH28. On the opposite, *L. bicolor* interacting with poplar roots under semi-sterile greenhouse conditions expressed a dozen of SSPs specifically in interaction with poplar (Plett et al., 2015), which fits well with our observations.

Expression profiling data from *in vitro* ECM produced in this work revealed that several MiSSPs up-regulated in greenhouse (Peter et al., 2016) were not regulated in the *in vitro* syntheses even when interacting with the same host tree. This suggests that environmental factors are equally important for the regulation of MiSSPs. Proteomic analysis of the secretome of *Hebeloma cylindrosporum* free-living mycelium revealed that 17% of the secreted proteins were SSPs (Doré et al., 2015). These SSP-encoding genes were differentially regulated in ECM root tips and depending on the environmental conditions. Likewise, gene profiling of extramatrical mycelium and sclerotia of *C. geophilum* performed in the present study showed that some MiSSPs were not only up-regulated in the ECM root tip itself, but also in other fungal tissues in the presence of a host plant, which indicates that they are induced by the host plant but play a role in biological processes not directly linked to the fungal-plant communication at the symbiotic interface. All these data strengthen the concept that fungal SSPs not only play an important role as candidate effector genes in fungal-plant interactions, but also in the adaptation to their environment and saprotrophic growth (Doré et al., 2015).

C. geophilum is the first ectomycorrhizal fungus showing a bipartite genome architecture with repeat-rich, gene-poor regions and vice versa. This genome compartmentalization refers to regions with uneven mutation rates, GC-content and gene density with the gene-sparse, repeat-rich compartments evolving at higher rates (Raffaele and Kamoun, 2012; Plissonneau et al., 2017). This phenomenon has first been described for the oomycete *Phytophtora infestans* genome (Haas et al., 2009) and recently, a convergence toward similar genome architecture has been demonstrated in phylogenetically unrelated fungal plant pathogens such as *Leptosphaeria maculans* (Rouxel et al., 2011; Grandaubert et al., 2014) and *Zymoseptoria triticii* (Stukenbrock et al., 2010). In all these plant-pathogens, the two-speed-genome explained genomic plasticity in order to increase and adapt the repertoire of effector/avirulence genes (Möller and Stukenbrock, 2017). The rapidly evolving compartment in pathogen genomes is largely controlled by transposable elements (Plissonneau et al., 2017) being hot spots for duplication, deletion, and recombination as well as local mutagenesis through TE-silencing mechanisms such as repeat induced point mutation (RIP; Dong et al., 2015). The high content of transposable elements in *C. geophilum* (75% of genome; Peter et al., 2016) might therefore also play an important role in genome adaptation and since TEs are arranged in different compartments, these might also evolve at different rates. Moreover, in plant pathogens, genes implicated in virulence and host adaptation such as effector genes tend to localize in repeat-rich, faster evolving regions (Raffaele and Kamoun, 2012). The genes coding for the selected 22 MiSSPs of *C. geophilum* are localized not only in repeat rich but also in gene dense regions. This is true also for other *in planta*-induced genes and differs from what has been found for the pathogenic oomycete *P. infestans* (Raffaele et al., 2010a). We noticed that conserved MiSSPs are rather located in gene-dense regions, whereas those that are dispersed among *C. geophilum* isolates are more often found close to repeats. This indicates that these MiSSPs might evolve at different rates. Likewise, duplicated MiSSPs that each have a member in both regions show different presence–absence patterns among *C. geophilum* isolates, and are therefore evolving differentially. Subcellular localization analyses for one of the three duplications indicate that the duplicated genes might have different functions since one member targeted the tonoplast within the plant cell (Cenge3:659858) whereas the other showed no specific localization (Cenge3:660401). Interestingly, gene expression and regulation for duplicated genes located in either repeat-rich regions or gene-dense regions were different, indicating that TEs might affect promotor regions and thereby gene regulation and/or that duplicated genes play different roles in the fungal-host interaction. Clearly more population genomic and functional studies are needed to elucidate the evolutionary rate of change of these duplications and its functional significance for adaptation.

Intra- and interspecies comparisons of MiSSP presence revealed that some MiSSPs are conserved not only in *C. geophilum* isolates but also in saprotrophic relatives. Distinct factors can contribute to secretome variation and evolution such as host specificity, phylogenetic history and lifestyle (Kohler et al., 2015; Pellegrin et al., 2015; Liao et al., 2016; Kamel et al., 2017). The genomes of ECM fungi analyzed so far, share a large set of SSPs with brown and white rot fungi and litter decayers (Kohler et al., 2015; Pellegrin et al., 2015; Martin et al., 2016) and these are likely involved in conserved processes such as developmental changes (e.g., hyphal aggregation in mycelia and fruiting body formation), saprotrophic growth or soil environmental interactions, as indicated by the present and other gene expression studies (Doré et al., 2015). Further, intraspecific analyses show that several species-specific MiSSPs found in the reference genome 1.58 are absent in other *C. geophilum* strains. This dispersion of MiSSPs within *C. geophilum* isolates, which to some extend reflect phylogenetic sub-clades, suggests that gene gain and loss may be an important driver of evolution as shown for pathogenic fungi (Syme et al., 2013; van Dam et al., 2016; Hartmann and Croll, 2017). Whether sub-clades identified with commonly used phylogenetic marker genes do reflect cryptic species, needs to be evaluated using genome-wide polymorphism analyses of additional isolates of *C. geophilum* populations. Likewise, the role mating, but also TE activity, which has been suggested as possible driver of cryptic speciation in plant systems (Bonchev and Parisod, 2013), play in microevolutionary processes within this taxon remains to be determined.

Over the past 5 years, information about secretome repertoires with a particular emphasis on SSPs became available for fungi with different ways of life (Guyon et al., 2014; Lo Presti et al., 2015; Pellegrin et al., 2015; Kamel et al., 2017). However, only a few studies provide data regarding the role of these fungal SSPs in mutualistic plant-microbe interactions. One limitation is that the majority of SSPs are orphan genes that have no domains of known function. Tools to assess their functional role are scarce for species that cannot be transformed and easily handled in the laboratory, as are mycorrhizal fungi. One available approach to elucidate their role is to first identify their subcellular localization in an heterologous system and then try to identify their potential targets (Alfano, 2009). Confocal microscopy assays revealed that

five *C. geophilum* MiSSPs over the 22 tested target distinct sub-cellular compartments, such as plasma membrane, cytosol, endoplasmic reticulum and tonoplast.

Only six MiSSPs showed known domains or homology to other proteins. For example, the cupin domain containing MiSSP, which was conserved in all fungal strains studied here, localized to the plasma membrane and was only induced in ECM of pine. This domain is found in a wide variety of functionally diverse proteins in eukaryotes and prokaryotes (Dunwell et al., 2000) which does not allow speculating about possible functions of this MiSSP. A second MiSSP contains a NTF2 super family domain, probably similar to the one in SnoaL polyketide cyclase. These domains are found in several organisms, including filamentous fungal phytopathogens and present different functions within the proteins, including both enzymatic and non-enzymatic versions (Eberhardt et al., 2013; Deng et al., 2017). This MiSSP was conserved among *C. geophilum* isolates and *L. palustris* and localized in plant endoplasmic reticulum. The third MiSSP was the most highly expressed and up-regulated (Cenge3:698167) in ECM roots and to a lower degree in root-associated sclerotia in all ECM experiments. Unfortunately, sub-cellular localization experiments were unsuccessful for this particular MiSSP. It shows similarity (66%) to the "secreted in xylem 1" (Six1) effector of the asexual, soil inhabiting ascomycete *Fusarium oxysporum* that can switch from a saprotrophic to a pathogenic lifestyle infecting plant roots (Rep et al., 2004). Although several studies have been performed on this protein, the exact function of it is still unclear. This protein (and homologs of it) has been shown to be secreted in root xylem vessels, the gene expression being induced in early root infection only by living cells and that it plays a role in virulence (Rep et al., 2004; Van Der Does et al., 2008; Li et al., 2016). Only strains of the polyphyletic formae speciales lycopersici causing tomato wilt have the genomic region containing Six1 (Van Der Does et al., 2008). In *C. geophilum*, this MiSSP was only present in a few strains and it remains to be determined, whether it is highly expressed in ECM roots of all these strains and what role it could play in the symbiotic fungal-plant interaction.

None of the MiSSPs analyzed in this work were predicted to localize in the nucleus. We expected such a localization as the two symbiotic effectors characterized in mycorrhizal fungi so far, MiSSP7 and SP7, and many effectors from pathogens target the nucleus (Kloppholz et al., 2011; Plett et al., 2011; Petre et al., 2015). Two MiSSPs (Cenge3:679266 and Cenge3:634429) formed cytosolic bodies and the irregularity of the bodies suggesting that they might be artefactual aggregates, as proposed for localization of rust effectors (Petre et al., 2015; Qi et al., 2018). It is important to consider that these localizations were obtained using GFP as a tag, which can interfere with MiSSPs localization as it is a large fluorescent tag of ∼27 kDa (Varden et al., 2017). However, the proportion of informative localizations as well as identified compartments are consistent with similar studies on SSPs of filamentous plant-pathogenic fungi (Caillaud et al., 2012; Chaudhari et al., 2014; Petre et al., 2015, 2016; Germain et al., 2017; Varden et al., 2017; Qi et al., 2018). Next steps now are to localize the MiSSPs in root cells of host plants and to search for direct plant targets using co-immunoprecipitation/mass spectrometry. The confirmation that a MiSSP is an authentic symbiotic effector requires the demonstration that it is essential for symbiosis development and that it has the ability to interfere with a host component to conclusively support symbiosis. A promising approach in this respect is to use double stranded interfering (dsi) RNA to knock down transcription of MiSSPs, a method successfully applied in fungal-plant systems for which efficient transformation protocols are lacking (Wang et al., 2016).

AUTHOR CONTRIBUTIONS

Conceived and designed the experiments: MP, AK, CV-F, FM, MdFP, and KB; Performed the experiments: MdFP, PV, FG, SP, HN, and MK; Analyzed sequence data: MdFP, EM, AK, CV-F, VS, AL, and MP; Drafted the manuscript: MdFP, AK, CV-F, and MP; Revised the manuscript: MdFP, MP; AK, CV-F, SE, IG, and FM. All authors read and approved the final manuscript.

ACKNOWLEDGMENTS

We would like to thank Barbara Meier and Ursula Oggenfuss for the great help in the set-up of the mycorrhization systems at WSL. This project was supported by grants from the French National Agency of Research (ANR) as part of the "Investissement d'Avenir program (ANR-11_LABX-0002-01) of Labex ARBRE (CFP15) and the WSL within the frame of the ARBRE/WSL project 'Blacksecret' as well as by the Region Lorraine Research Council who provided a 6-month researcher grant to MFP and the EC-supported Network of Excellence Evoltree (GOCE-016322 to MP).

SUPPLEMENTARY MATERIAL

The Supplementary Material for this article can be found online at: https://www.frontiersin.org/articles/10.3389/fmicb.2018.00141/full#supplementary-material

Supplementary Figure S1 | Ectomycorrhiza formed by *Cenococcum geophilum* and their host plants. Morphological characteristics of typical ectomycorrhiza formed by *C. geop*hilum in interaction with *Pinus sylvestris* **(A)** and *Populus tremula L.* × *Populus alba* L.-INRA 717) **(C)**. Cross-sections of ectomycorrhiza roots of both system shows a presence of the Hartig net between epidermal and cortex cells in both interactions **(B,D)**. Percentage of ectomycorrhiza formation between *C. geophilum* and *P. sylvestris* and *C. geophilum* and *P. tremula* × *P. alba* **(E)**.

Supplementary Figure S2 | Comparison of *C. geophilum* gene expression changes in greenhouse pine ECM, *in vitro* pine ECM and *in vitro* poplar ECM. Venn diagram based on the comparison of secreted proteins regulated in at least one experiment: ECM formed by *C. geophilum* with *Pinus sylvestris* [*in vitro* synthesis or greenhouse (Peter et al., 2016)] and *C. geophilum* with *Populus tremula* × *Populus alba* L.-INRA 717 (*in vitro* synthesis). Note that the age of control mycelium was different: *C. geophilum* with *P. sylvestris* [*in vitro* synthesis = 90 days, *C. geophilum* with *P. sylvestris* greenhouse = 15 days; *C. geophilum* with *Populus tremula* × *P. alba in vitro* synthesis = 60 days. Data are provided in **Supplementary Table S6**.

Supplementary Figure S3 | Nucleotide **(A–C)** and protein **(D–F)** alignments of duplications of candidate MiSSPs in the *C. geophilum* genome. **(A,D)** Cenge3:636312 and Cenge3:660403, **(B,E)** Cenge3:679266 and Cenge3:693798, **(C,F)** Cenge3:660401 and Cenge3:659858. Protein ID from Joint Genome Institute (JGI).

Supplementary Figure S4 | Distribution of gene expression induction in ectomycorrhizal root tips compared to free-living mycelium according to local gene density for all genes. The median **(A)**, minimum **(B)** or maximum **(C)** induction (log_2 ratio ECM vs. FLM) values associated to genes in each bin are shown as a color-coded heat map. **(D)** Distribution of the average gene expression level in ectomycorrhizal root tips according to local gene density. The median values for gene expression in each bin are shown as a color-coded heat map. Data are presented for ECM root tips of *C. geophilum* and *P. sylvestris*-semi-sterile under greenhouse conditions (left column) or *in vitro* system (middle column) and for *C. geophilum- Populus tremula x alba in vitro* (right column).

Supplementary Figure S5 | Percentage and number of genes found in gene-dense repeat sparse or gene sparse repeat rich regions for the proteome and the secretome of *C. geophilum*. The secretome was categorized into functional categories (proteases, lipases, CAZymes, SSPs and other secreted proteins). Enrichment tests were not significant.

Supplementary Figure S6 | Genomic landscape of compartments on scaffold 21 and 23 of *Cenococcum geophilum* harboring duplications of MiSSPs in gene-dense and gene-poor, repeat-rich regions. Displays are extracted from the genome viewer of the Joint Genome Institute (JGI) website (https://genome.jgi.doe.gov/Cenge3/Cenge3.home.html) showing tracks of base position, GC content, predicted genes (GeneCatalog; dark blue), and predicted repetitive regions (black, 3 tracks) discovered by RepeatScout and masked by RepeatMasker.

Supplementary Figure S7 | Phylogenetic tree of *C. geophilum* strains and the closest relative *Glonium stellatum* reconstructed based on concatenated nucleotide sequences of the internal transcribed spacer (ITS) and the glyceraldehyde-3-phosphate dehydrogenase (GAPDH) using PhyML-maximum likelihood. In addition to the 15 *C. geophilum* strains from the present study, six representative strains of the six clades from the study of Obase et al. (2016) were included in the analysis. Branch confidence indices were calculated using an approximate likelihood ratio test. The scale bar indicates the number of nucleotide substitutions per site. Three distinct clades are indicated and numbered according to Obase et al. (2016) including a possible subdivision of clade 5 (left). *Glonium stellatum* was designated as the outgroup.

Supplementary Figure S8 | Variability in presence/absence of 22 MiSSP genes among 16 *C. geophilum* isolates. The first two axes of a principal coordinate analysis based on the Jaccard similarity index are provided. Each symbol represents an isolate originating from the given country with isolates closer to each other showing more similar presence/absence patterns. In **(A)**, different symbols indicate the phylogenetic clade the isolate are grouped into based on a concatenated dataset of the ITS and GADPH regions (Obase et al., 2016). In **(B)**, different symbols indicate the forest type with the dominating tree species: Mx, mixed forest; Pa, *Picea abies*; Fs, *Fagus sylvatica;* Ps, *Pinus sylvestris*. **(C)** PERMANOVA table showing the effects of phylogenetic clade, country of origin and forest type of isolation on the MiSSP presence/absence patterns in the 16 *C. geophilum* isolates. Analyses were performed with the Primer-E software (Clarke and Gorley, 2015).

Supplementary Figure S9 | Candidate effectors with no informative localization *in planta*. Representative images corresponding to the 13 fusion proteins accumulating in the nucleoplasm and the cytosol. The fusion proteins were transiently expressed in *Nicotiana benthamiana* leaf cells by agroinfiltration. Live-cell imaging was performed with a laser-scanning confocal microscope 2 days after infiltration. The green fluorescent protein (GFP) was excited at 488 nm. GFP (green) fluorescence was collected at 505–525 nm.

Supplementary Figure S10 | Immunoblots of CgMiSSPs:GFP fusion proteins in *N. benthamiana* leaves. GFP detection was performed in a single step by a GFP-HRP conjugated antibody. The theoretical size of each fusion protein (SSP+GFP) is indicated between parentheses in kiloDalton (kDa). Page rulers and corresponding sizes in kiloDalton (kDa) are indicated on the blots. White asterisks indicate specific protein bands.

Supplementary Table S1 | *Cenococcum geophilum* and other fungal strains used in this work.

Supplementary Table S2 | Main features of *C. geophilum* RNAseq data.

Supplementary Table S3 | Main features of *C. geophilum* re-sequencing data.

Supplementary Table S4 | Core eukaryotic genes selected for presence/absence polymorphism analysis.

Supplementary Table S5 | Concatenated and separated sequences of *C. geophilum* glyceraldehyde 3-phosphate dehydrogenase (GAPDH) and internal transcribed spacer (ITS).

Supplementary Table S6 | List of primers used to amplify seven MiSSPs in *C. geophilum* mycelium.

Supplementary Table S7 | Genes encoding small secreted proteins regulated in the interaction between *Cenococcoccum geophilum* and *Pinus sylvestris* or *Populus tremula* × *alba* as compared to free-living mycelium (FLM).

Supplementary Table S8 | Expression comparison of genes encoding secreted proteins significantly regulated in the interaction between *Cenococcum geophilum* and *Pinus sylvestris* or *Populus tremula* × *alba*. A fold change between Pine and Poplar ECM was calculated and a cut-off 5 fold was established to show specificity expression in each tissue.

Supplementary Table S9 | Blast results of *C. geophilum* 1.58 MiSSP candidates against de novo assemblies of *C. geophilum* strains. The genes that are absent in respective strains based on e-value and HSP length are marked in red. A fasta file with respective contigs is available (**Supplementary File 1**).

Supplementary File 1 | *C. geophilum* nucleotide sequences contig containing MiSSPs of respective *C. geophilum* strains.

REFERENCES

Alfano, J. R. (2009). Roadmap for future research on plant pathogen effectors. *Trends Microbiol.* 10, 805–813. doi: 10.1111/j.1364-3703.2009.00588.x

Anderson, M. J. (2001). A new method for non-parametric multivariate analysis of variance. *Austral Ecol.* 26, 32–46. doi: 10.1111/j.1442-9993.2001.01070.pp.x

Antibus, R. K., Croxdale, J. G., Miller, O. K., and Linkins, E. (1981). Ectomycorrhizal fungi of *Salix rotundifolia*. III. Resynthesized mycorrhizal complexes and their surface phosphatase activities. *Canad. J. Bot.* 59, 2458–2465. doi: 10.1139/b81-297

Bonchev, G., and Parisod, C. (2013). Transposable elements and microevolutionary changes in natural populations. *Mol. Ecol. Resour.* 13, 765–775. doi: 10.1111/1755-0998.12133

Bourne, E. C., Mina, D., Gonçalves, S. C., Loureiro, J., Freitas, H., and Muller, L. A. H. (2014). Large and variable genome size unrelated to serpentine adaptation but supportive of cryptic sexuality in *Cenococcum geophilum*. *Mycorrhiza* 24, 13–20. doi: 10.1007/s00572-013-0501-3

Brun, A., Chalot, M., Finlay, R. D., and Soderstrom, B. (1995). Structure and function of the ectomycorrhizal association between *Paxillus involutus* (Batsch) Fr. and *Betula pendula* Roth. I. dynamics of mycorrhiza formation. *New Phytol.* 129, 487–493. doi: 10.1111/j.1469-8137.1995.tb04319.x

Caillaud, M.-C., Piquerez, S. J. M., Fabro, G., Steinbrenner, J., Ishaque, N., Beynon, J., et al. (2012). Subcellular localization of the Hpa RxLR effector repertoire identifies a tonoplast-associated protein HaRxL17 that confers enhanced plant susceptibility. *Plant J.* 69, 252–265. doi: 10.1111/j.1365-313X.2011.04787.x

Chaudhari, P., Ahmed, B., Joly, D. L., and Germain, H. (2014). Effector biology during biotrophic invasion of plant cells. *Virulence* 5, 703–709. doi: 10.4161/viru.29652

Clarke, K., and Gorley, R. (2015). *PRIMER v7, User Manual/Tutorial*.

Corpet, F. (1988). Multiple sequence alignment with hierarchical clustering. *Nucleic Acids Res.* 16, 10881–10890. doi: 10.1093/nar/16.22.10881

Cosgrove, D. J. (2000). Loosening of plant cell walls by expansins. *Nature* 407, 321–326. doi: 10.1038/35030000

Deng, C. H., Plummer, K. M., Jones, D. A. B., Mesarich, C. H., Shiller, J., Taranto, A. P., et al. (2017). Comparative analysis of the predicted secretomes of *Rosaceae scab* pathogens *Venturia inaequalis* and *V. pirina* reveals expanded effector families and putative determinants of host range. *BMC Genomics* 18:339. doi: 10.1186/s12864-017-3699-1

Dereeper, A., Guignon, V., Blanc, G., Audic, S., Buffet, S., Chevenet, F., et al. (2008). Phylogeny. fr, robust phylogenetic analysis for the non-specialist. *Nucleic Acids Res.* 36(Suppl. 2), W465–W469. doi: 10.1093/nar/gkn180

Dong, S., Raffaele, S., and Kamoun, S. (2015). The two-speed genomes of filamentous pathogens, Waltz with plants. *Curr. Opin. Genet. Devel.* 35, 57–65. doi: 10.1016/j.gde.2015.09.001

Doré, J., Perraud, M., Dieryckx, C., Kohler, A., Morin, E., Henrissat, B., et al. (2015). Comparative genomics, proteomics and transcriptomics give new insight into the exoproteome of the basidiomycete *Hebeloma cylindrosporum* and its involvement in ectomycorrhizal symbiosis. *New Phytol.* 208, 1169–1187. doi: 10.1111/nph.13546

Douhan, G. W., Huryn, K. L., and Douhan, L. I. (2007). Significant diversity and potential problems associated with inferring population structure within the *Cenococcum geophilum* species complex. *Mycologia* 99, 812–819. doi: 10.1080/15572536.2007.11832513

Dunwell, J. M., Khuri, S., and Gane, P. J. (2000). Microbial relatives of the seed storage proteins of higher plants, conservation of structure and diversification of function during evolution of the cupin superfamily. *Microbiol. Mol. Biol. Rev.* 64, 153–179. doi: 10.1128/MMBR.64.1.153-179.2000

Eberhardt, R. Y., Chang, Y., Bateman, A., Murzin, A. G., Axelrod, H. L., Hwang, W. C., et al. (2013). Filling out the structural map of the NTF2-like superfamily. *BMC Bioinformatics* 14:327. doi: 10.1186/1471-2105-14-327

Felten, J., Kohler, A., Morin, E., Bhalerao, R. P., Palme, K., Martin, F., et al. (2009). The ectomycorrhizal fungus Laccaria bicolor stimulates lateral root formation in poplar and Arabidopsis through auxin transport and signaling. *Plant Physiol.* 151, 1991–2005. doi: 10.1104/pp.109.147231

Garcia, K., Delaux, P.-M., Cope, K. R., and Ané, J.-M. (2015). Molecular signals required for the establishment and maintenance of ectomycorrhizal symbioses. *New Phytol.* 208, 79–87. doi: 10.1111/nph.13423

Germain, H., Joly, D. L., Mireault, C., Plourde, M. B., Letanneur, C., Stewart, D., et al. (2017). Infection assays in Arabidopsis reveal candidate effectors from the poplar rust fungus that promote susceptibility to bacteria and oomycete pathogens. *Mol. Plant Pathol.* 19, 191–200. doi: 10.1111/mpp.12514.

Grandaubert, J., Lowe, R. G. T., Soyer, J. L., Schoch, C. L., Van de Wouw, A. P., Fudal, I., et al. (2014). Transposable element-assisted evolution and adaptation to host plant within the *Leptosphaeria maculans-Leptosphaeria biglobosa* species complex of fungal pathogens. *BMC Genomics* 15, 1–27. doi: 10.1186/1471-2164-15-891

Guyon, K., Balagué, C., Roby, D., and Raffaele, S. (2014). Secretome analysis reveals effector candidates associated with broad host range necrotrophy in the fungal plant pathogen *Sclerotinia sclerotiorum*. *BMC Genomics* 15:336. doi: 10.1186/1471-2164-15-336

Haas, B. J., Kamoun, S., Zody, M. C., Jiang, R. H. Y., Handsaker, R. E., Cano, L. M., et al. (2009). Genome sequence and analysis of the Irish potato famine pathogen *Phytophthora infestans*. *Nature* 461, 393–398. doi: 10.1038/nature08358

Hacquard, S., Kracher, B., Maekawa, T., Vernaldi, S., Schulze-Lefert, P., and Ver Loren van Themaat, E. (2013). Mosaic genome structure of the barley powdery mildew pathogen and conservation of transcriptional programs in divergent hosts. *Proc. Natl. Acad. Sci. U.S.A.* 110, E2219–E2228. doi: 10.1073/pnas.1306807110

Hartmann, F. E., and Croll, D. (2017). Distinct trajectories of massive recent gene gains and losses in populations of a microbial eukaryotic pathogen. *Mol. Biol. Evol.* 34, 2808–2822. doi: 10.1093/molbev/msx208

Hibbett, D., Gilbert, L.-B., and Donoghue, M. J. (2000). Evolutionary instability of ectomycorrhizal symbioses in basidiomycetes. *Nature* 407, 506–508. doi: 10.1038/35035065

Kamel, L., Tang, N., Malbreil, M., San Clemente, H., Le Marquer, M., Roux, C., et al. (2017). The comparison of expressed candidate secreted proteins from two arbuscular mycorrhizal fungi unravels common and specific molecular tools to invade different host plants. *Front. Plant Sci.* 8, 1–18. doi: 10.3389/fpls.2017.00124

Karimi, M., Inzé, D., and Depicker, A. (2002). GATEWAY vectors for Agrobacterium-mediated plant transformation. *Trends Plant Sci.* 7, 193–195. doi: 10.1016/S1360-1385(02)02251-3

Kloppholz, S., Kuhn, H., and Requena, N. (2011). A secreted fungal effector of glomus intraradices promotes symbiotic biotrophy. *Current Biol.* 21, 1204–1209. doi: 10.1016/j.cub.2011.06.044

Kohler, A., Kuo, A., Nagy, L. G., Morin, E., Barry, K. W., Buscot, F., et al. (2015). Convergent losses of decay mechanisms and rapid turnover of symbiosis genes in mycorrhizal mutualists. *Nat. Genet.* 47, 410–415. doi: 10.1038/ng.3223

Kohler, A. and Martin, F. (2016). "The evolution of the mycorrhizal lifestyles–a genomic perspective," in *Molecular Mycorrhizal Symbiosis*, ed F. Martin (Hoboken, NJ: John Wiley & Sons, Inc.), 87–106. doi: 10.1002/9781118951446.ch6

Lahrmann, U., Ding, Y., Banhara, A., Rath, M., Hajirezaei, M. R., Döhlemann, S., et al. (2013). Host-related metabolic cues affect colonization strategies of a root endophyte. *Proc. Natl. Acad. Sci. U.S.A.* 110, 13965–13970. doi: 10.1073/pnas.1301653110

Le Quéré, A., Schutzendubel, A., Rajashekar, B., Canback, B., Hedh, J., Erland, S., et al. (2004). Divergence in gene expression related to variation in host specificity of an ectomycorrhizal fungus. *Mol. Ecol.* 13, 3809–3819. doi: 10.1111/j.1365-294X.2004.02369.x

Li, E., Wang, G., Xiao, J., Ling, J., Yang, Y., and Xie, B. (2016). A SIX1 homolog in *Fusarium oxysporum* f. sp. conglutinans is required for full virulence on cabbage. *PLoS ONE* 11:e0152273. doi: 10.1371/journal.pone.0152273

Liao, H. L., Chen, Y., and Vilgalys, R. (2016). Metatranscriptomic study of common and host-specific patterns of gene expression between pines and their symbiotic ectomycorrhizal fungi in the genus Suillus. *PLoS Genet.* 12:e1006348. doi: 10.1371/journal.pgen.1006348

Liao, Y., Smyth, G. K., and Shi, W. (2014). featureCounts, an efficient general purpose program for assigning sequence reads to genomic features. *Bioinformatics* 30, 923–930. doi: 10.1093/bioinformatics/btt656

LoBuglio, K. F. (1999). *Cenococcum. Ectomycorrhizal Fungi Key Genera in Profile.* Berlin; Heidelberg: Springer, 287–309.

Lo Presti, L., Lanver, D., Schweizer, G., Tanaka, S., Liang, L., Tollot, M., et al. (2015). Fungal effectors and plant susceptibility. *Annu. Rev. Plant Biol.* 66, 513–545. doi: 10.1146/annurev-arplant-043014-114623

Love, M. I., Huber, W., and Anders, S. (2014). Moderated estimation of fold change and dispersion for RNA-seq data with DESeq2. *Genome Biol.* 15:550. doi: 10.1186/s13059-014-0550-8

Martin, F., Aerts, A., Ahrén, D., Brun, A., Danchin, E. G. J., Duchaussoy, F., et al. (2008). The genome of Laccaria bicolor provides insights into mycorrhizal symbiosis. *Nature* 452, 88–92. doi: 10.1038/nature06556

Martin, F., Kohler, A., Murat, C., Balestrini, R., Coutinho, P. M., Jaillon, O., et al. (2010). Périgord black truffle genome uncovers evolutionary origins and mechanisms of symbiosis. *Nature* 464, 1033–1038. doi: 10.1038/nature08867

Martin, F., Kohler, A., Murat, C., Veneault-Fourrey, C., and Hibbett, D. S. (2016). Unearthing the roots of ectomycorrhizal symbioses. *Nature Rev. Microbiol.* 14, 760–773. doi: 10.1038/nrmicro.2016.149

Möller, M., and Stukenbrock, E. H. (2017). Evolution and genome architecture in fungal plant pathogens. *Nat. Rev. Microbiol.* 15, 756–771. doi: 10.1038/nrmicro.2017.76

Murashige, T., and Skoog, F. (1962). A revised medium for rapid growth and bio assays with tobacco tissue cultures. *Physiol. Plant.* 15, 473–497. doi: 10.1111/j.1399-3054.1962.tb08052.x

Nelson, B. K., Cai, X., and Nebenführ, A. (2007). A multicolored set of *in vivo* organelle markers for co-localization studies in Arabidopsis and other plants. *Plant J.* 51, 1126–1136. doi: 10.1111/j.1365-313X.2007.03212.x

Obase, K., Douhan, G. W., Matsuda, Y., and Smith, M. E. (2017). *Progress and Challenges in Understanding The Biology, Diversity, and Biogeography of Cenococcum geophilum*. Cham: Springer.

Obase, K., Douhan, G. W., Matsuda, Y., and Smith, M. E. (2016). Revisiting phylogenetic diversity and cryptic species of *Cenococcum geophilum* sensu lato. *Mycorrhiza* 26, 529–540. doi: 10.1007/s00572-016-0690-7

Ohm, R. A., de Jong, J. F., Lugones, L. G., Aerts, A., Kothe, E., Stajich, J. E., et al. (2010). Genome sequence of the model mushroom Schizophyllum commune. *Nat. Biotechnol.* 28, 957–963. doi: 10.1038/nbt.1643

Pellegrin, C., Morin, E., Martin, F. M., and Veneault-Fourrey, C. (2015). Comparative analysis of secretomes from ectomycorrhizal fungi with

an emphasis on small-secreted proteins. *Front. Microbiol.* 6:1278. doi: 10.3389/fmicb.2015.01278

Peter, M., Kohler, A., Ohm, R. A., Kuo, A., Krützmann, J., Morin, E., et al. (2016). Ectomycorrhizal ecology is imprinted in the genome of the dominant symbiotic fungus *Cenococcum geophilum*. *Nat. Commun.* 7:12662. doi: 10.1038/ncomms12662

Petre, B., Saunders, D. G. O., Sklenar, J., Lorrain, C., Krasileva, K. V., Win, J., et al. (2016). Heterologous expression screens in *Nicotiana benthamiana* identify a candidate effector of the wheat yellow rust pathogen that associates with processing bodies. *PLoS ONE* 11:e0149035. doi: 10.1371/journal.pone.0149035

Petre, B., Saunders, D. G. O., Sklenar, J., Lorrain, C., Win, J., Duplessis, S., et al. (2015). Candidate effector proteins of the rust pathogen melampsora *Larici-Populina* target diverse plant cell compartments. *Mol. Plant-Microbe Interact.* 28, 689–700. doi: 10.1094/MPMI-01-15-0003-R

Plett, J. M., Daguerre, Y., Wittulsky, S., Vayssières, A., Deveau, A., Melton, S. J., et al. (2014). Effector MiSSP7 of the mutualistic fungus Laccaria bicolor stabilizes the populus JAZ6 protein and represses jasmonic acid (JA) responsive genes. *Proc. Natl. Acad. Sci. U.S.A.* 111, 8299–8304. doi: 10.1073/pnas.1322671111

Plett, J. M., Kemppainen, M., Kale, S. D., Kohler, A., Legué, V., Brun, A., et al. (2011). A secreted effector protein of laccaria bicolor is required for symbiosis development. *Curr. Biol.* 21, 1197–1203. doi: 10.1016/j.cub.2011.05.033

Plett, J. M., and Martin, F. (2011). Blurred boundaries, lifestyle lessons from ectomycorrhizal fungal genomes. *Trends Genet.*27, 14–22. doi: 10.1016/j.tig.2010.10.005

Plett, J. M., and Martin, F. (2015). Reconsidering mutualistic plant-fungal interactions through the lens of effector biology. *Curr. Opin. Plant Biol.* 26, 45–50. doi: 10.1016/j.pbi.2015.06.001

Plett, J. M., Tisserant, E., Brun, A., Morin, E., Grigoriev, I. V., Kuo, A., et al. (2015). The mutualist Laccaria bicolor expresses a core gene regulon during the colonization of diverse host plants and a variable regulon to counteract host-specific defenses. *Mol. Plant Microbe Interact.* 28, 261–273. doi: 10.1094/MPMI-05-14-0129-FI

Plissonneau, C., Benevenuto, J., Mohd-Assaad, N., Fouché, S., Hartmann, F. E., and Croll, D. (2017). Using population and comparative genomics to understand the genetic basis of effector-driven fungal pathogen evolution. *Front. Plant Sci.* 8, 1–15. doi: 10.3389/fpls.2017.00119

Qi, M., Grayczyk, J. P., Seitz, J. M., Lee, Y., Link, T. I., Choi, D., et al. (2018). Suppression or activation of immune responses by predicted secreted proteins of the soybean rust pathogen Phakopsora pachyrhizi. *Mol. Plant Microbe. Interact.* 31, 163–174. doi: 10.1094/MPMI-07-17-0173-FI

Raffaele, S., Farrer, R. A., Cano, L. M., Studholme, D. J., MacLean, D., Thines, M., et al. (2010a). Genome evolution following host jumps in the irish potato famine pathogen lineage. *Science* 330, 1540–1543. doi: 10.1126/science.1193070

Raffaele, S., and Kamoun, S. (2012). Genome evolution in filamentous plant pathogens, why bigger can be better. *Nat. Rev. Microbiol.* 10, 417–430. doi: 10.1038/nrmicro2790

Raffaele, S., Win, J., Cano, L. M., and Kamoun, S. (2010b). Analyses of genome architecture and gene expression reveal novel candidate virulence factors in the secretome of *Phytophthora infestans*. *BMC Genomics* 11:637. doi: 10.1186/1471-2164-11-637

Rep, M., Van Der Does, H. C., Meijer, M., Van Wijk, R., Houterman, P. M., Dekker, H. L., et al. (2004). A small, cysteine-rich protein secreted by *Fusarium oxysporum* during colonization of xylem vessels is required for I-3-mediated resistance in tomato. *Mol. Microbiol.* 53, 1373–1383. doi: 10.1111/j.1365-2958.2004.04177.x

Rouxel, T., Grandaubert, J., Hane, J. K., Hoede, C., van de Wouw, A. P., Couloux, A., et al. (2011). Effector diversification within compartments of the *Leptosphaeria maculans* genome affected by repeat-induced point mutations. *Nat. Commun.* 2:202. doi: 10.1038/ncomms1189

Sarkar, P., Bosneaga, E., and Auer, M. (2009). Plant cell walls throughout evolution, towards a molecular understanding of their design principles. *J. Exp. Bot.* 60, 3615–3635. doi: 10.1093/jxb/erp245

Saunders, D. G. O., Win, J., Kamoun, S., and Raffaele, S. (2014). "Two-dimensional data binning for the analysis of genome architecture in filamentous plant pathogens and other eukaryote," in *Methods in Molecular Biology, Vol. 1127, 2nd Edn.,* eds P. R. J. Birch, J. T. Jones, and J. I. B. Bos (New York, NY: Springer Science), 29–51.

Smith, S. E., and Read, D. J. (2010). *Mycorrhizal Symbiosis*. Cambridge, MA: Academic Press.

Spatafora, J. W., Owensby, C. A., Douhan, G. W., Boehm, E. W., and Schoch, C. L. (2012). Phylogenetic placement of the ectomycorrhizal genus Cenococcum in Gloniaceae (Dothideomycetes). *Mycologia* 104, 758–765. doi: 10.3852/11-233

Stukenbrock, E. H., and Croll, D. (2014). The evolving fungal genome. *Fungal Biol. Rev.* 28, 1–12. doi: 10.1016/j.fbr.2014.02.001

Stukenbrock, E. H., Jørgensen, F. G., Zala, M., Hansen, T. T., McDonald, B. A., and Schierup, M. H. (2010). Whole-genome and chromosome evolution associated with host adaptation and speciation of the wheat pathogen *Mycosphaerella graminicola*. *PLoS Genet.* 6:e1001189. doi: 10.1371/journal.pgen.1001189

Syme, R. A., Hane, J. K., Friesen, T. L., and Oliver, R. P. (2013). Resequencing and comparative genomics of *Stagonospora nodorum*, sectional gene absence and effector discovery. *G3* 3, 959–969. doi: 10.1534/g3.112.004994

Tagu, D., Lapeyrie, F., and Martin, F. (2002). The ectomycorrhizal symbiosis, genetics and development. *Plant Soil* 244, 97–105. doi: 10.1023/A:1020235916345

Trappe, J. M. (1962). *Cenococcum Graniforme-Its Distribution, Ecology, Mycorrhiza Formation, and Inherent Variation.* Ph. D thesis, University of Washington, 148.

Untergasser, A., Cutcutache, I., Koressaar, T., Ye, J., Faircloth, B. C., Remm, M., et al. (2012). Primer3—new capabilities and interfaces. *Nucleic Acids Res.* 40:e115. doi: 10.1093/nar/gks596

van Dam, P., Fokkens, L., Schmidt, S. M., Linmans, J. H. J., Kistler, H. C., Ma, L. J., et al. (2016). Effector profiles distinguish formae speciales of *Fusarium oxysporum*. *Environ. Microbiol.* 18, 4087–4102. doi: 10.1111/1462-2920.13445

Van Der Does, H. C., Lievens, B., Claes, L., Houterman, P. M., Cornelissen, B. J. C., and Rep, M. (2008). The presence of a virulence locus discriminates *Fusarium oxysporum* isolates causing tomato wilt from other isolates. *Environ. Microbiol.* 10, 1475–1485. doi: 10.1111/j.1462-2920.2007.01561.x

van der Heijden, M. G. A., Martin, F. M., Selosse, M.-A., and Sanders, I. R. (2015). Mycorrhizal ecology and evolution, the past, the present, and the future. *New Phytol.* 205, 1406–1423. doi: 10.1111/nph.13288

Varden, F. A., De la Concepcion, J. C., Maidment, J. H., and Banfield, M. J. (2017). Taking the stage, effectors in the spotlight. *Curr. Opin. Plant Biol.* 38, 25–33. doi: 10.1016/j.pbi.2017.04.013

Wang, M., Weiberg, A., Lin, F.-M., Thomma, B. P. H. J., Huang, H.-D., and Jin, H. (2016). Bidirectional cross-kingdom RNAi and fungal uptake of external RNAs confer plant protection. *Nat. Plants* 2:16151. doi: 10.1038/nplants.2016.151

Win, J., Kamoun, S., and Jones, A. M. E. (2011). Purification of effector–target protein complexes via transient expression in *Nicotiana benthamiana*. *Plant Immunity Methods Protocols* 712, 181–194. doi: 10.1007/978-1-61737-998-7_15

Conflict of Interest Statement: The authors declare that the research was conducted in the absence of any commercial or financial relationships that could be construed as a potential conflict of interest.

frontiers in Microbiology

ORIGINAL RESEARCH
published: 28 November 2017
doi: 10.3389/fmicb.2017.02320

The *SlZRT1* Gene Encodes a Plasma Membrane-Located ZIP (Zrt-, Irt-Like Protein) Transporter in the Ectomycorrhizal Fungus *Suillus luteus*

Laura Coninx[1], Anneleen Thoonen[1], Eli Slenders[2], Emmanuelle Morin[3], Natascha Arnauts[1], Michiel Op De Beeck[1†], Annegret Kohler[3], Joske Ruytinx[1] and Jan V. Colpaert[1]*

[1] Environmental Biology, Centre for Environmental Sciences, Hasselt University, Hasselt, Belgium, [2] Biomedical Research Institute, Hasselt University, Hasselt, Belgium, [3] Institut National de la Recherche Agronomique, Laboratoire d'Excellence ARBRE, UMR 1136, Université de Lorraine Interactions Arbres/Microorganismes, Champenoux, France

OPEN ACCESS

Edited by:
Erika Kothe, Universität Jena, Germany

Reviewed by:
Marcela Claudia Pagano, Universidade Federal de Minas Gerais, Brazil
Oswaldo Valdes-Lopez, Universidad Nacional Autónoma de México, Mexico

***Correspondence:**
Joske Ruytinx
joske.ruytinx@uhasselt.be

†Present address:
Michiel Op De Beeck, Microbial Ecology, Department of Biology, Lund University, Lund, Sweden

Specialty section:
This article was submitted to Fungi and Their Interactions, a section of the journal Frontiers in Microbiology

Received: *24 August 2017*
Accepted: *10 November 2017*
Published: *28 November 2017*

Citation:
Coninx L, Thoonen A, Slenders E, Morin E, Arnauts N, Op De Beeck M, Kohler A, Ruytinx J and Colpaert JV (2017) The SlZRT1 Gene Encodes a Plasma Membrane-Located ZIP (Zrt-, Irt-Like Protein) Transporter in the Ectomycorrhizal Fungus Suillus luteus. Front. Microbiol. 8:2320. doi: 10.3389/fmicb.2017.02320

Zinc (Zn) is an essential micronutrient but may become toxic when present in excess. In Zn-contaminated environments, trees can be protected from Zn toxicity by their root-associated micro-organisms, in particular ectomycorrhizal fungi. The mechanisms of cellular Zn homeostasis in ectomycorrhizal fungi and their contribution to the host tree's Zn status are however not yet fully understood. The aim of this study was to identify and characterize transporters involved in Zn uptake in the ectomycorrhizal fungus *Suillus luteus,* a cosmopolitan pine mycobiont. Zn uptake in fungi is known to be predominantly governed by members of the ZIP (Zrt/IrtT-like protein) family of Zn transporters. Four ZIP transporter encoding genes were identified in the *S. luteus* genome. By in silico and phylogenetic analysis, one of these proteins, SlZRT1, was predicted to be a plasma membrane located Zn importer. Heterologous expression in yeast confirmed the predicted function and localization of the protein. A gene expression analysis via RT-qPCR was performed in *S. luteus* to establish whether *SlZRT1* expression is affected by external Zn concentrations. *SlZRT1* transcripts accumulated almost immediately, though transiently upon growth in the absence of Zn. Exposure to elevated concentrations of Zn resulted in a significant reduction of *SlZRT1* transcripts within the first hour after initiation of the exposure. Altogether, the data support a role as cellular Zn importer for SlZRT1 and indicate a key role in cellular Zn uptake of *S. luteus*. Further research is needed to understand the eventual contribution of SlZRT1 to the Zn status of the host plant.

Keywords: *Suillus luteus*, mycorrhiza, zinc transporter, zinc homeostasis, zinc deficiency, metal uptake

INTRODUCTION

Zinc (Zn) is an essential micronutrient required by all living organisms (Eide, 2006). Due to its unique set of chemical properties, Zn plays both a functional and a structural role in many proteins. The metal is characterized by a small radius and has thus a highly concentrated charge (Clemens, 2006a). Furthermore, Zn is a Lewis acid with a high affinity for ligands with sulfur- (S),

nitrogen- (N), and oxygen- (O) containing functional groups (Clemens, 2006a). Due to its full d-subshell, Zn is also able to interact with these ligands more flexibly than other transition metals (Berg and Shi, 1996). By supporting a tetrahedral coordination geometry, Zn allows proteins to quickly shift conformations in biological reactions. These properties combined with its lack of redox activity, explain why Zn is a valuable structural element (e.g., Zn finger proteins) and a catalyst for many enzymes (e.g., hydrolytic enzymes) (Frausto da Silva and Williams, 2001). However, the same properties that make Zn an indispensable nutrient can also induce toxicity (Clemens, 2006b). When present in excess, Zn can cause protein damage and inactivation by uncontrolled high-affinity binding to functional groups within proteins (Clemens, 2006b). For this reason, it is necessary for living cells to tightly regulate Zn concentrations in the cytoplasm. The physiological concentration range of Zn between deficiency and toxicity is extremely narrow and organisms are consequently equipped with a number of homeostatic mechanisms to tightly regulate cytoplasmic Zn concentrations (Eide, 2006). Especially transporter proteins play a crucial role in maintaining Zn homeostasis (Eide, 2006).

In eukaryotes most of the Zn transport is achieved by two protein families: the ZIP (Zrt/Irt-like protein) and CDF (Cation Diffusion Facilitator) transporter families (Gaither and Eide, 2001). Proteins belonging to the ZIP transporter family increase cytoplasmic Zn levels by transporting Zn across the plasma membrane or by mobilizing stored Zn from intracellular compartments. Whereas members of the CDF family transport Zn in the direction opposite to that of the ZIP proteins. Efflux or compartmentalization of Zn is promoted by transporting Zn from the cytoplasm into the lumen of an organelle or out of the cell (Gaither and Eide, 2001).

Transporters belonging to the ZIP family typically possess 5 to 8 transmembrane domains (TMDs). The protein sequence is most conserved in TMD IV and the region adjacent to TMD IV (Eng et al., 1998). The ZIP family can be divided into four subfamilies based on a higher degree of sequence similarity: the ZIP I, ZIP II, GufA and LIV-I subfamily (Guerinot, 2000; Gaither and Eide, 2001). Members of the ZIP family are well-studied in *Saccharomyces cerevisiae*, which is an excellent fungal model system to investigate Zn uptake and efflux (Zhao and Eide, 1996). Currently, four ZIP Zn transporter genes have been identified in baker's yeast: *ZRT1, ZRT2, ZRT3,* and *YKE4*. The yeast *ZRT1* gene was the first influx Zn transporter gene from any organism to be characterized at the molecular level (Zhao and Eide, 1996). The *ZRT1* gene encodes a high-affinity Zn uptake system induced by Zn limitation, whereas the ZRT2 transporter corresponds to a low-affinity uptake system that is active in Zn repleted cells (Eide, 1996; Zhao and Eide, 1996). Zn uptake in yeast is predominantly governed by these two plasma membrane-located transporters (Eide, 1996; Zhao and Eide, 1996). Both transporters are included in the ZIP I subfamily (Gaither and Eide, 2001). The third characterized yeast ZIP protein, ZRT3, belongs to the GufA ZIP subfamily (Gaither and Eide, 2001). This transporter localizes to the vacuolar membrane and mobilizes Zn under Zn deficiency (MacDiarmid et al., 2000). Lastly, Kumánovics et al. (2006) characterized YKE4, a bidirectional Zn transporter in the endoplasmic reticulum (ER) of *S. cerevisiae*, which regulates Zn concentrations in the ER and cytoplasm. YKE4 is a LIV-I subfamily transporter (Gaither and Eide, 2001).

Additional to the research in yeast, other ZIP transporters and mechanisms of Zn homeostasis in fungi are primarily characterized and studied in human fungal pathogens. Membrane Zn importers of the ZIP I subfamily have been shown to be crucial for the acquisition of Zn and the virulence of several human pathogenic fungi (Crawford and Wilson, 2015). This was observed in *Candida albicans* for the Zn transporter CaZRT1 (Citiulo et al., 2012), in *Cryptococcus neoformans* for CnZIP1 (Do et al., 2016) and in *Aspergillus fumigatus* for AfZrfC (Amich et al., 2014). These transporters enable pathogenic fungi to overcome Zn deficiency within the Zn-limited host environment (Jung, 2015). Zn and fungal ZIP transporters are therefore considered to be key players in this kind of pathogenic host-microbe interactions.

In the current study we aim to identify plasma membrane localized Zn importers and their role in cellular Zn homeostasis in the ectomycorrhizal fungus *Suillus luteus*. Ectomycorrhizae are mutualistic host-microbe interactions between tree roots and ectomycorrhizal fungi. The mycobiont offers the tree a balanced nutrient supply in exchange for photosynthetic sugar (Martin et al., 2016). Although Zn is not expected to be a key regulator of ectomycorrhizal development nor to be extremely scarce at the symbiotic interface, availability of this element may have an impact on the fitness of both individual symbiotic partners and the mutualism in particular environments. Micronutrient deficiencies are rarely observed in natural forests but severe Zn deficiency in tree plantations has been reported previously (Thorn and Robertson, 1987; Boardman and McGuire, 1990). Moreover, trees are sensitive to high soil Zn concentrations. We previously demonstrated that well-adapted ectomycorrhizal fungi can protect host trees from Zn toxicity when Zn is present in excess (Adriaensen et al., 2004, 2006). An improved knowledge on the mechanisms of cellular Zn homeostasis in ectomycorrhizal fungi, going beyond the general focus on detoxification by vacuolar sequestration and including Zn uptake and deficiency, will be the first step toward a better understanding of the contribution of ectomycorrhizal fungi to host tree Zn homeostasis.

MATERIALS AND METHODS

Fungal Strains and Culture Conditions

The monokaryotic *S. luteus* isolate UH-Slu-Lm8-n1 (Kohler et al., 2015) and the dikaryotic isolate UH-Slu-P4 (Colpaert et al., 2004) were used in this study. Cultures were maintained on solid Fries medium according to Colpaert et al. (2004). Preceding Zn exposure assays, 1-week-old exponentially growing mycelia were harvested and liquid cultures were initiated and maintained according to Nguyen et al. (2017). Three gram of spherical mycelia grown for 1 week in liquid culture were transferred to petri dishes containing 25 ml modified liquid Fries medium supplemented with 0, 20, 500, or 1000 μM $ZnSO_4 \cdot 7H_2O$. These Zn concentrations were chosen to induce Zn deficiency, Zn

sufficiency and mild Zn toxicity (Ruytinx et al., 2017). The petri dishes were incubated on a shaking incubator at 23°C. Metal exposure was performed in triplicate. Mycelia (400 mg) were sampled at 0, 1, 2, 4, 8, and 24 h after initiation of exposure, flash frozen in liquid nitrogen and stored at −70°C.

ZIP Identification and Phylogenetic Tree Construction

The *S. luteus* reference genome was searched for ZIP transporter encoding genes. A BLASTp search using characterized fungal ZIP transporters (Supplementary Table 1) and a Pfam domain search were performed at the *S. luteus* genome portal at MycoCosm of the Joint Genome Institute (JGI)[1] (Grigoriev et al., 2012; Kohler et al., 2015). Full-length amino acid sequences of previously characterized ZIP transporters were obtained from the transporter classification database[2], the Swissprot database[3] and the National Center for Biotechnology Information (NCBI) server[4]. All sequences, including the newly identified *S. luteus* ZIP sequences, were aligned with the Multiple Alignment using Fast Fourier Transform (MAFFT) alignment logarithm version 7 (Katoh and Standley, 2013) and imported into the Molecular Evolutionary Genetics Analysis (MEGA) package version 6.06 (Tamura et al., 2013). A phylogenetic tree was constructed using the neighbor-joining (NJ) method (Poisson correction model for distance computation) to infer evolution of the identified *S. luteus* ZIP transporters and to predict their function more precisely.

Cloning of *SlZRT1*

Total RNA was extracted from *S. luteus* mycelium ground in liquid nitrogen using the RNeasy Plant Mini kit (Qiagen, Germany) and a cDNA library was constructed using the SMARTer cDNA synthesis kit (Clontech, United States) according to the manufacturer's instructions. Specific primers were designed for amplification of the full-length coding sequence of *SlZRT1* (left: 5′ CCT CAAACTATGTCAGATTTAAATT 3′; right: 5′ TGCCCA ACGCCCCAGGAGC 3′). The PCR reaction contained: 10x High Fidelity PCR buffer, 0.2 mM dNTP-mixture, 2 mM $MgSO_4$, 0.2 μM *SlZRT1* forward and reverse primer, 5 ng cDNA and 0.5 U Platinum Taq High Fidelity DNA polymerase (Invitrogen, United States). RNase-free water was added to obtain a final reaction volume of 30 μl. The following PCR cycling conditions were used: 2 min at 95°C; 35 cycles of 30 s at 95°C + 30 s at 56°C + 1 min at 68°C, and 1 cycle of 3 min at 68°C. 5 μl of the PCR product was visualized on an agarose gel to verify the reaction specificity and the length of the amplicon. The remaining 25 μl PCR product was purified using the GeneJET PCR Purification Kit (ThermoScientific, United States). The purified PCR-product was cloned into the gateway entry vector pCR8/GW/TOPO (Invitrogen) and subsequently transferred by the Gateway LR-clonase II Enzyme Mix (Invitrogen) to destination vectors pYES-DEST52 (Invitrogen, United States) and pAG426GAL-ccdB-EGFP (Alberti et al., 2007) for functional analysis in yeast. The insert was sequenced in both directions to verify correct orientation and fusion.

Yeast Mutant Complementation and Subcellular Localization

SlZRT1 was heterologous expressed in *S. cerevisiae*. Yeast strains used are CM30 (MATα, ade6, can1-100, his3-11, 15 leu2-3, trp1-1, ura3-52) and CM34 or Δzrt1Δzrt2 (CM30, zrt1::LEU2, zrt2::HIS3) (MacDiarmid et al., 2000). Yeast cells were transformed according to the LiAc/PEG method as described by Gietz and Woods (2002). Transformed yeast cells were selected on synthetic defined medium without uracil [SD-URA; 0.7% w/v yeast nitrogen base (Difco), 2% w/v D-glucose, and 0.2% w/v Yeast Synthetic Drop-out Mix without uracil (Sigma)]. Plates were incubated at 30°C.

For metal tolerance assays, transformed yeasts were grown to mid log phase (OD_{600} ± 1.5) in liquid SD-URA medium with 2% w/v D-galactose instead of D-glucose (induction medium). Yeast cells were pelleted, washed with sterile distilled water, and adjusted to $OD_{600} = 1$. A 1/10 dilution series was prepared (10^0, 10^{-1}, 10^{-2}, and 10^{-3}). Drop assays were performed for three independent yeast clones on SD-URA control induction medium (1 mM Zn) and induction medium supplemented with 50, 100, or 200 μM ethylenediaminetetraacetic acid (EDTA) (MacDiarmid et al., 2000). For subcellular localization of SlZRT1::EGFP fusion proteins, yeast transformants were grown to mid-log phase $OD_{600} = 1$ on induction medium. Plasma membrane of the cells was stained at 0°C by FM4-64 (Molecular Probes, Invitrogen) according to Vida and Emr (1995). Afterward, a 3 μl droplet of yeast cells was analyzed at 0°C with a Zeiss LSM 510 META laser scanning confocal microscope (Carl Zeiss, Jena, Germany), using a Zeiss 40x NA1.1 water immersion objective (C-Apochromat 40x/1.1 W Corr., Carl Zeiss). Enhanced green fluorescent protein (EGFP) fluorescence analysis was performed with the 488 nm excitation line of an argon-ion laser and a band-pass 500–550 nm emission filter. FM4-64 (ThermoFisher) fluorescence analyses were performed with a 543 nm HeNe laser and a long-pass 560 nm emission filter. Image processing was carried out with ImageJ (NIH, Bethesda, MD, United States) software.

Zn Content Analysis of Transformed Yeast

Transformed yeast cells were cultured at 30°C in liquid induction medium without Zn until culture saturation. Three rounds of Zn deprivation were completed by re-inoculating 0.5 ml of saturated yeast suspension to new Zn-less induction medium. Zn-starved cells were grown to mid log phase (OD_{600} ± 1.5) and diluted to $OD_{600} = 1$. One ml of yeast suspension was added to Erlenmeyer flasks containing 20 ml liquid induction medium without Zn and medium supplemented with 500 μM Zn (repletion). Zn treatments were performed for five independent yeast clones. Cultures were allowed to grow for 24 h at 30°C. Yeast cells were collected by centrifugation, washed three times with 20 mM $PbNO_3$ and milli-Q water. Afterward cells were resuspended

[1] http://genome.jgi.doe.gov/Suilu2/Suilu2.home.html

[2] http://www.tcdb.org/

[3] http://www.uniprot.org/

[4] http://www.ncbi.nlm.nih.gov/

in 0.5 ml of milli-Q water, frozen (−20°C) and lyophilized. Lyophilized cells were acid digested (HNO_3/HCl) and Zn content was determined by inductively coupled plasma optical emission spectrometry (ICP-OES).

RNA Extraction, cDNA Synthesis, and qPCR

Total RNA was extracted from mycelium pulverized in liquid nitrogen using the RNeasy Plant Mini Kit (Qiagen). The TURBO DNA-free kit [Invirtogen (Life Technologies), United States] was used to perform a desoxyribonuclease (DNase) treatment to remove residual genomic DNA. RNA integrity and absence of DNA contamination was verified via agarose gel analysis. RNA concentration and purity were evaluated on a NanoDrop ND-1000 Spectrophotometer (Isogen Life Science, the Netherlands). One μg of each RNA sample was converted to cDNA with the Primescript RT Reagent Kit (Perfect Real Time) (TaKaRa Clontech, United States). A 10-fold dilution of the cDNA was prepared in 1/10 diluted Tris-EDTA (TE) buffer and stored at −20°C.

Real-time reverse transcription polymerase chain reaction (qRT-PCR) was performed in a 96-well optical plate with an ABI PRISM 7500 Fast Real-Time PCR System (Life Technologies) according to Ruytinx et al. (2016). A *SlZRT1* specific primer pair was designed using Primer3 (Rozen and Skaletsky, 2000) (5′ GCCAAACGGACAAACTGG 3′; 5′ GACAGGCACGGAGATGAAAG 3′; efficiency = 92.1%). Data were expressed relative to the sample with the highest expression level via the formula $2^{-(Ct-Ctmin)}$ and normalized using five reference genes (*TUB1, ACT1, GR975621, AM085296,* and *AM085296*). Reference genes were selected previously by Ruytinx et al. (2016) and their stability was confirmed within the current experimental conditions using GeNorm (Vandesompele et al., 2002). A normalization factor was calculated as the geometric mean of the relative expression levels of the reference genes. Mean values of four biological replicates were calculated, rescaled to the control condition (20 μM Zn) within each time point and log2 transformed. A two-way analysis of variance (ANOVA) followed by a Tukey's HSD test was run in "R" version 3.2.2 (R Core Team, 2015) to assess differences in *SlZRT1* expression level.

RESULTS

Identification of a ZIP Transporter in *S. luteus*

The BLASTp search of the *S. luteus* genome (UH-Slu-Lm8-n1 v2.0) with characterized fungal ZIP transporters identified four *S. luteus* genes (protein IDs 720881, 22926, 229544, and 811220) predicted to encode ZIP proteins. A NJ phylogenetic tree including previously characterized ZIP transporters was constructed to predict the function of the newly identified *S. luteus* genes. The different ZIP subfamilies are well-supported in the tree as indicated by high bootstrap values (>90; **Figure 1**). Three of the identified *S. luteus* proteins (IDs 720881, 22926, and 229544) cluster within the ZIP I subfamily. Within this subfamily, proteins with ID 720881 and 22926 cluster together with the *S. cerevisiae* Zn importers ScZRT1 and ScZRT2; the protein with ID 229544 clusters with *S. cerevisiae* ATX2, a Golgi transporter involved in manganese (Mn) homeostasis. The fourth identified *S. luteus* gene encodes a protein (ID 811220) clustering close to the *S. cerevisiae* YKE4 (ER localized Zn transporter) within the LIV-1 subfamily of ZIP transporters. We were not able to detect a member of the Guf A and ZIP II subfamily of ZIP transporters within the *S. luteus* reference genome.

One identified *S. luteus* gene, encoding the protein with ID 22926 was selected for further analysis because of its high sequence similarity with the yeast Zn importers ScZRT1 and SpZRT1. Reciprocal BLASTp suggest the *S. luteus* protein to be orthologous to the high-affinity Zn importers ScZRT1 and SpZRT1 and was therefore named SlZRT1. *SlZRT1* is predicted to have a 1398 bp open reading frame with eight exons encoding a 338 amino acid polypeptide. The encoded peptide shows several characteristics that are typical for proteins belonging to the ZIP family (**Figure 2**). Eight TMDs were predicted by the topology program TMHMM and a long variable cytoplasmic loop is present between TMD3 and TMD4. A histidine rich motif $HXX(HX)_3$, suggested to function as Zn binding site, is present in the variable cytoplasmic loop of SlZRT1 and two other histidines that are typically conserved in ZIP transporters were identified (**Figure 2**). One of these conserved histidines is located in the conserved TMD4, which contains the ZIP signature sequence described by Eng et al. (1998). SlZRT1 matches 13 of the 15 amino acids of this ZIP signature sequence.

Functional Analysis of *SlZRT1* in Yeast

SlZRT1 was heterologous expressed in yeast to confirm that it encodes a plasma membrane-located ZIP Zn importer, which was predicted by the phylogenetic analysis. **Figure 3** and **Supplementary Figure 1** illustrate that transformation with *SlZRT1* partly restored the growth of the zinc-uptake-deficient yeast strain Δzrt1Δzrt2 on medium supplemented with different concentrations of EDTA. Transformation with the empty vector did not result in complementation of the Zn deficient phenotype (**Figure 3** and **Supplementary Figure 1**). Expression of the SlZRT1::EGFP fusion protein indicates a localization of SlZRT1 on the plasma membrane. Yeast cells transformed with SlZRT1::EGFP showed a bright green fluorescent ring surrounding the cells, which co-localized with FM4-64 plasma membrane staining (**Figure 4**).

Zn and Fe Content Analysis of Transformed Yeast

Zn and Fe content were measured in Zn starved (**Figure 5A**) and Zn replete (**Figure 5B**) yeast cells in order to obtain more insight into the function of SlZRT1. **Figure 5A** illustrates that Δzrt1Δzrt2 yeast mutants transformed with *SlZRT1* contained the same amount of Zn as the wild type (WT) yeast after starvation (0 μM Zn) while Δzrt1Δzrt2 mutants transformed with the empty vector had a significantly lower

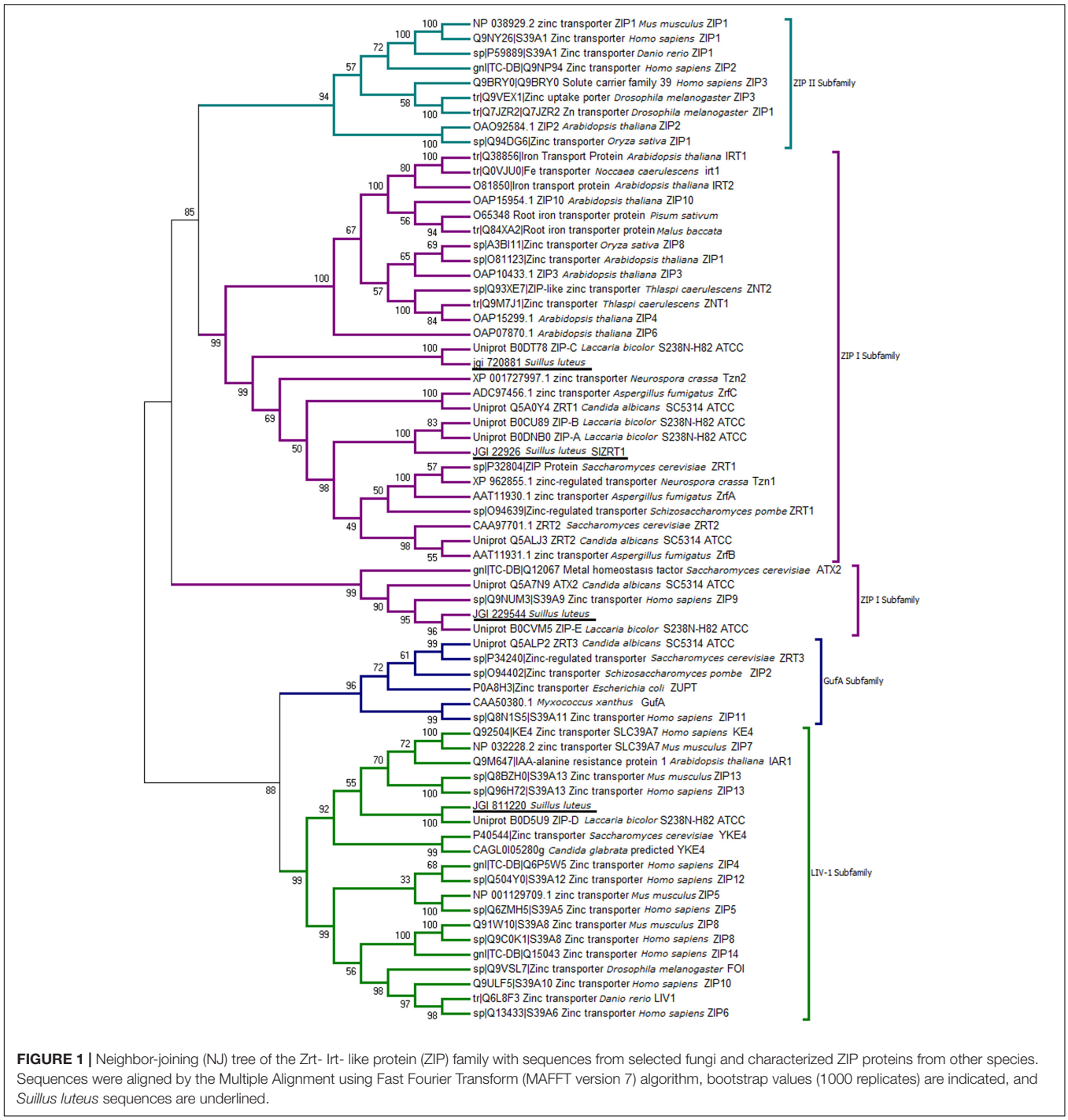

FIGURE 1 | Neighbor-joining (NJ) tree of the Zrt- Irt- like protein (ZIP) family with sequences from selected fungi and characterized ZIP proteins from other species. Sequences were aligned by the Multiple Alignment using Fast Fourier Transform (MAFFT version 7) algorithm, bootstrap values (1000 replicates) are indicated, and *Suillus luteus* sequences are underlined.

Zn content. Similarly, 24 h after Zn repletion (500 μM Zn) *SlZRT1* transformed yeast mutants and WT yeast accumulated significantly more Zn than empty vector transformed yeast mutants (**Figure 5B**). A small difference in Zn accumulation was observed between WT yeast cells and *SlZRT1* transformed Δzrt1Δzrt2 yeast cells. Additionally the Fe content in the yeast transformants was analyzed, since some ZIP transporters can also use Fe as a substrate. Yet, no significant differences in Fe content were observed among the yeast transformants exposed to 0 or 500 μM Zn (**Supplementary Figures S2A,B**).

SlZRT1 Gene Expression Analysis in *S. luteus*

In *S. luteus*, *SlZRT1* gene expression was determined at early time points (0, 1, 2, 4, 8, and 24 h) after exposure to different concentrations of Zn [0, 20 (control), 500, and 1000 μM]

FIGURE 2 | Alignment of SlZRT1 and ScZRT1 protein sequences. The eight transmembrane domains (TMDs) predicted by topology prediction program TMHMM2.0 are indicated in green, the putative metal binding domains in blue, the ZIP signature sequence as described by Eng et al. (1998) in red, and two conserved histidines with an asterisk (located in TMD4 and TMD5).

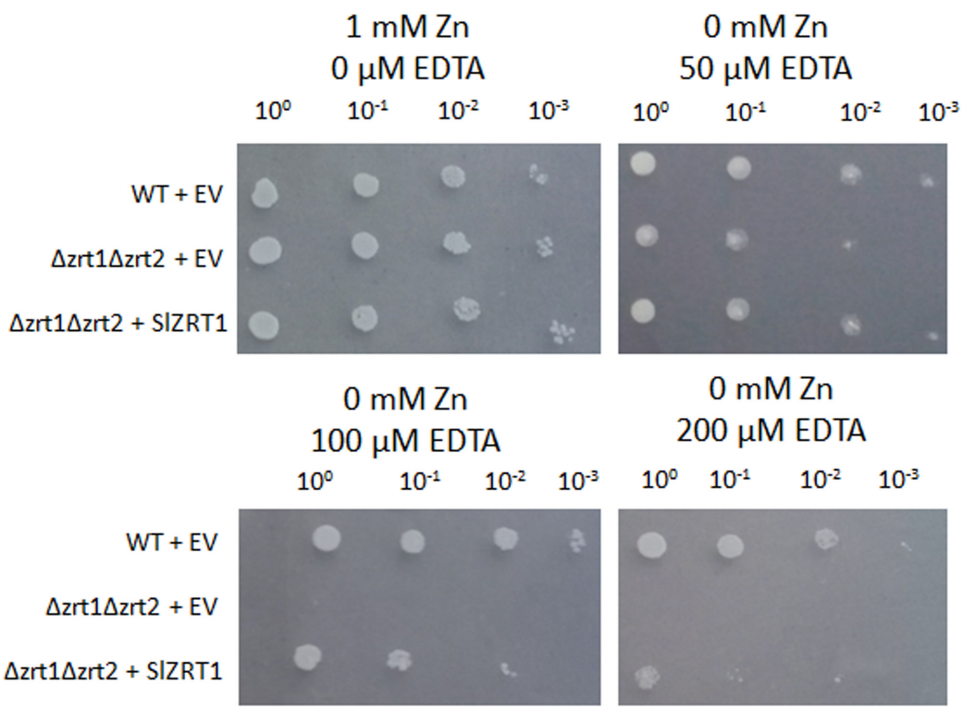

FIGURE 3 | Functional complementation of the zinc-uptake-deficient yeast strain Δzrt1 Δzrt2 by SlZRT1. Wild type (WT) and mutant yeast cultures with an OD_{600} = 1 were 10-fold serial diluted (10^0, 10^{-1}, 10^{-2}, and 10^{-3}) and spotted on control (1 mM Zn) or ethylenediaminetetraacetic acid (EDTA) supplemented synthetic drop-out (SD) medium. The WT strain was transformed with the empty vector (EV, pYES-DEST52; Invitrogen), the mutant strain Δzrt1 Δzrt2 with either the EV or the vector containing *SlZRT1*. The experiment was carried out for three independent clones and pictures were taken after 4 days of growth.

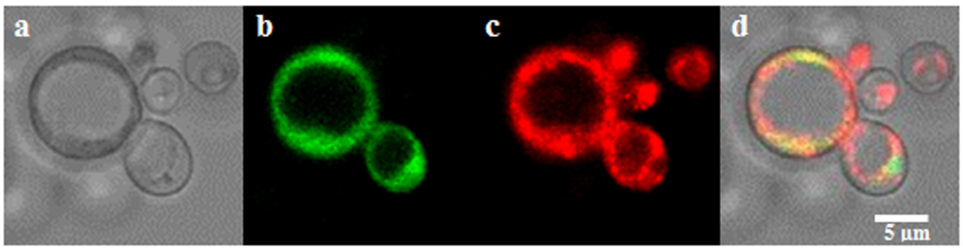

FIGURE 4 | Localization of the SlZRT1:EGFP fusion protein to the plasma membrane in yeast **(a–d)**. **(a)** Bright field image, **(b)** EGFP fusion protein, **(c)** FM4-64 plasma membrane staining, and **(d)** merged images. SlZRT1:EGFP and FM4-64 plasma membrane staining co-localize.

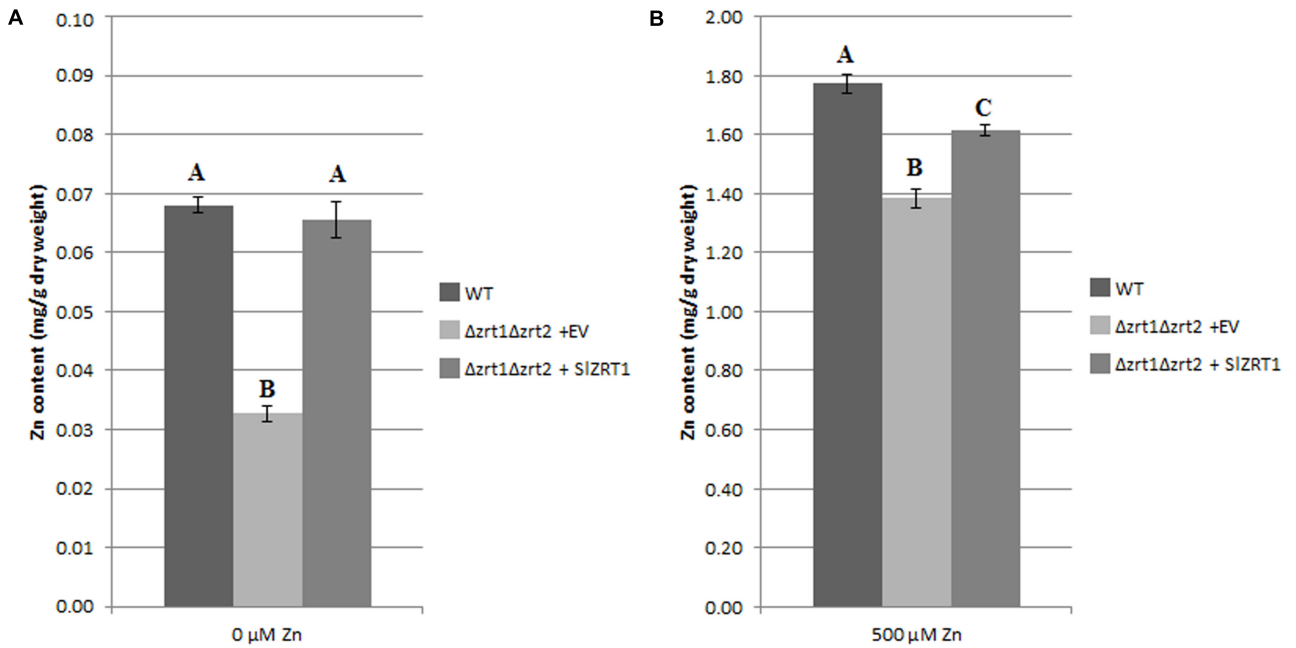

FIGURE 5 | Intracellular Zn concentrations in transformed yeast cells **(A,B)**. The WT strain was transformed with the EV (pYES-DEST52, Invitrogen), the mutant strain with either the EV or the vector containing *SlZRT1*. Data are the average ± SE of five biological replicates, significant differences ($p < 0.05$) are indicated by different letters. **(A)** In control conditions (0 µm Zn), **(B)** after exposure to Zn (500 µM).

to assess the role of the *SlZRT1* in Zn homeostasis. Results clearly illustrate that mRNA levels of *SlZRT1* are dependent of external Zn concentration (**Figure 6**). Exposure to mildly toxic Zn concentrations (500 and 1000 µM) results in an almost immediate significant downregulation of *SlZRT1* gene expression. The expression patterns upon exposure to 500 and 1000 µM Zn are similar regardless differences in external Zn concentrations. In contrast, in the absence of external Zn, *SlZRT1* expression is quickly induced to reach a maximum level after 2 h, declines to control levels after 4 h and tends to be higher again in the long term (24 h).

DISCUSSION

Transition metals, such as Zn, Fe, Mg, are essential to all living organisms. However, when present in excess these metals may become toxic. To overcome metal toxicity, it is crucial for cells to tightly control cytoplasmic metal concentrations (Eide et al., 2005). Metal transporter proteins play a crucial role in the regulation of cytoplasmic metal concentrations and cellular metal homeostasis (Migeon et al., 2010). Among fungi, mechanisms involved in Zn homeostasis are mostly studied in *S. cerevisiae*. Transporters of the ZIP family were shown to be vital to prevent Zn deficiency in this species (Eide, 2006) and several other fungi (Kiranmayi et al., 2009; Jung, 2015). *S. cerevisiae* possess two plasma membrane localized Zn importers of the ZIP family (ScZRT1 and ScZRT2) and one tonoplast localized ZIP transporter (ScZRT3) for re-mobilization of vacuolar stored Zn. In the current study, we identified four ZIP transporter encoding genes in the genome of the ectomycorrhizal fungus *S. luteus*. Three of the newly identified proteins are members of the ZIP I subfamily of ZIP transporters, one belongs to the LIV-1 subfamily (**Figure 1**). With the exception of ScZRT3, a tonoplast transporter

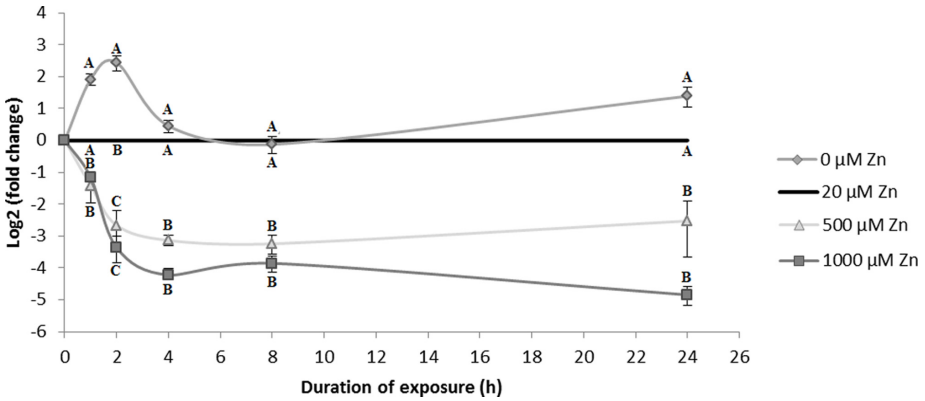

FIGURE 6 | *SlZRT1* gene expression in *S. luteus* mycelium after 0, 1, 2, 4, 8, and 24 h exposure to different concentrations of Zn. Data are the average ± SE of three biological replicates and expressed as fold change to the control condition (20 µM Zn) within each time point. Mean values were log2 transformed. Significant differences ($p < 0.05$) within each time point are indicated by different letters.

involved in Zn mobilization from the vacuole, homologs for all characterized *S. cerevisiae* ZIP transporters were identified within the *S. luteus* genome. So far, no homologs for the ScZRT3 protein have been identified in members of the Basidiomycota. Nevertheless, several basidiomycetes including *S. luteus* store excess Zn into their vacuoles (Sacky et al., 2016; Ruytinx et al., 2017). Transporters belonging to other protein families likely evolved in these species to re-mobilize stored Zn in absence of external environmental Zn. In accordance with what has been found in other fungi, there was no member of the ZIP II subfamily of ZIP transporters detected in *S. luteus*. This subfamily consists mainly of metazoan representatives (Guerinot, 2000).

Reciprocal BLASTp suggested the *S. luteus* protein with ID 22926, named SlZRT1 to be orthologous to the *S. cerevisiae* ScZRT1 transceptor. ScZRT1 functions as a high-affinity Zn uptake transporter and receptor (Schothorst et al., 2017). Together with its homolog, the plasma membrane transporter ScZRT2, ScZRT1 is responsible for Zn uptake in Zn deficient yeast cells (Gaither and Eide, 2001). SlZRT1 and ScZRT1 show 39% sequence identity. An important difference in the sequence of SlZRT1 and ScZRT1 is found within the putative Zn binding domain (histidine rich domain, HRD) localized within the cytoplasmic loop between TMD3 and TMD4 (**Figure 2**). SlZRT1's binding domain (HDVHGHGHG) shows a HXX additional to the classical $(HX)_3$ domain of ScZRT1 (HDHTHD). This difference might correspond to an altered affinity toward Zn and/or a modified function of the protein. Mutation of the histidines in the HRD of ScZRT1 results in a 70% reduction in the maximum uptake rate of ScZRT1 (V_{max}), whereas the substrate concentration at which the reaction rate is half of V_{max} (K_m) remains unaffected (Gitan et al., 2003). Also for other ZIP1 subfamily transporters a reduction in Zn uptake due to mutation of histidines in the HRD was observed (Mao et al., 2007) and some of these histidines are even necessary for the protein to be functional, i.e., able to transport Zn across the plasma membrane (Milon et al., 2006).

Heterologous expression and subcellular localization in yeast are common experimental procedures to study eukaryotic gene function and protein localization (Zhao and Eide, 1996; Mokdad-Gargouri et al., 2012). Heterologous expression of *SlZRT1* in the Δzrt1Δzrt2 yeast double mutant, which is defective in Zn uptake, resulted in an almost complete restoration of the phenotype (**Figure 3**) and SlZRT1::EGFP fusion proteins localize at the plasma membrane of yeast cells (**Figure 4**). These results support a role as plasma membrane localized Zn transporter for the SlZRT1 protein. However, kinetics of the transporter might be different from the ScZRT1 protein. SlZRT1 did not fully complement ScZRT1 as observed in the drop assays (**Figure 3**) and Zn starved *SlZRT1* transformed Δzrt1Δzrt2 yeast cells accumulate less Zn within 24 h after Zn replenishment than WT yeast cells do (**Figure 5**). No significant differences in Fe content were observed (**Supplementary Figure 2**), indicating a high Zn specificity of the transporter.

In yeast, *ScZRT1* expression is regulated both at the transcriptional and the post-transcriptional level by Zn (Gitan and Eide, 2000). Post-translationally, Zn induces the removal of ScZRT1 from the plasma membrane via ubiquitination (Gitan et al., 2003). After endocytosis the protein is degraded in the vacuole. This regulatory system ensures a rapid shutdown of Zn uptake in yeast cells exposed to high concentrations of Zn (Gitan and Eide, 2000). In *S. luteus SlZRT1* expression is regulated by excess Zn. *SlZRT1* expression level is significantly lower after exposure to potentially toxic concentrations of Zn (500 and 1000 µM) as compared to the control (20 µM) and this already 1 h after initiation of the exposure (**Figure 6**). In contrast, absence of external Zn results in a rapid accumulation of *SlZRT1* mRNA. Two hours after initiation of Zn starvation in *S. luteus* mycelium, *SlZRT1* gene expression peaks and declines again to reach control levels after 4 h of growth in absence of Zn. After 24 h of growth in the absence of Zn, the *SlZRT1* expression level in *S. luteus* mycelium is slightly higher again compared to the level in mycelium grown in control conditions. These fluctuations in expression level could possibly reflect the cell's Zn status. A similar expression pattern, though delayed in time was detected by Schothorst et al. (2017) in *S. cerevisiae* for *ScZRT1*

in conditions of Zn deprivation. *ScZRT1* transcripts peak at 2 days under Zn deprivation and decline again afterward. A fast transcriptional response on limited environmental Zn concentrations is common for plasma membrane localized Zn transporters of the ZIP I subfamily. Induction of transcription in the absence of external Zn was reported previously for fungal ZIP I subfamily Zn importers which were identified in Ascomycota (ScZRT1 of *Schizosaccharomyces pombe,* ZrfA, ZrfB and ZrfC *of Aspergillus fumigatus,* Tzn1 and Tzn2 of *Neurospora crassa,* CaZRT1 and CaZRT2 of *Candida albicans*) and in Basidiomycota (CgZIP1 and GgZIP2 of *Cryptococcus gattii*) (Dainty et al., 2008; Kiranmayi et al., 2009; Jung, 2015).

Altogether, our data support a function as plasma membrane localized Zn importer with an important role in Zn homeostasis of *S. luteus* for SlZRT1. Likely, SlZRT1 is responsible for an adequate supply of Zn to the cell when environmental Zn is limited. With our current data, we cannot conclude on a role for SlZRT1 as Zn receptor for signaling in order to adjust primary metabolism to external Zn availability. Such a role was reported recently for ScZRT1 (Schothorst et al., 2017) and is certainly worth investigation in *S. luteus* and mycorrhizal fungi in general. Ectomycorrhizal fungi are well-known to offer their host plant a balanced nutrient supply by efficiently collecting limited nutrients and reducing the transfer of excess, potentially toxic elements. In relation to Zn, ectomycorrhizal fungi in general, and *S. luteus* in particular, are reported to protect their host plant from Zn toxicity (Colpaert et al., 2011). As trees in general do not tolerate high Zn soil concentrations, this protective feature of *S. luteus* is interesting for phytoremediation purposes. Further research is needed to better understand the regulation and function of *SlZRT1* within the *S. luteus* – host ectomycorrhizal association and to assess the contribution of SlZRT1 to the Zn status of the host plant.

AUTHOR CONTRIBUTIONS

LC, JR, and JC designed the study. LC, AT, ES, and NA performed the experiments. LC, EM, AK, and JR analyzed the data. LC and JR wrote the manuscript. LC, ES, NA, MODB, JR, and JC contributed in manuscript editing. All authors read and approved the final version of the manuscript.

FUNDING

This work was financially supported by the Research Foundation Flanders (FWO Project G079213N). LC holds a Flanders Innovation & Entrepreneurships Ph.D. fellowship (IWT Project 141461) and her research visit at INRA Grand Est Nancy was funded by the Laboratory of Excellence Advanced Research on the Biology of Tree and Forest Ecosystems (ARBRE; grant No. ANR-11-LABX-0002-01). Part of the computations were performed at the INRA Grand Est-Nancy Ecogenomics facilities. The Mycorrhizal Genomics Initiative is supported by the French National Institute for Agricultural Research (INRA), the US Department of Energy (DOE) Joint Genome Institute (JGI; Office of Science of the US Department of Energy), the Region Lorraine Research Council and the European Commission [European Regional Development Fund (ERDF)].

ACKNOWLEDGMENTS

We thank Carine Put, Ann Wijgaerts, and Brigitte Vanacken for their technical assistance. Stefan Gobert for his assistance with the confocal microscopy. We are also grateful to Prof. Dr. David Eide for kindly providing the yeast mutant.

SUPPLEMENTARY MATERIAL

The Supplementary Material for this article can be found online at: https://www.frontiersin.org/articles/10.3389/fmicb.2017.02320/full#supplementary-material

FIGURE S1 | Functional complementation of the zinc-uptake-deficient yeast strain Δzrt1Δzrt2 by SlZRT1::EGFP. Wild type (WT) and mutant yeast cultures with an $OD_{600} = 1$ were 10-fold serial diluted (10^0, 10^{-1}, 10^{-2}, and 10^{-3}) and spotted on control (1 mM Zn) or ethylenediaminetetraacetic acid (EDTA) supplemented synthetic drop-out (SD) medium. The WT strain was transformed with the empty vector (EV, pAG306GAL-ccdB-EGFP; Alberti et al., 2007), the mutant strain Δzrt1Δzrt2 with either the EV or the vector containing *SlZRT1:GFP*. The experiment was carried out for three independent clones and pictures were taken after 4 days of growth.

FIGURE S2 | Fe concentration in transformed yeast cells **(A,B)**. The WT strain was transformed with the EV (pYES-DEST52, Invitrogen), the mutant strain with either the EV or the vector containing *SlZRT1*. Data are the average ± SE of five biological replicates, significant differences ($p < 0.05$) are indicated by different letters. **(A)** In control conditions (0 μm Zn), **(B)** after exposure to Zn (500 μM).

REFERENCES

Adriaensen, K., van der Lelie, D., Van Laere, A., Vangronsveld, J., and Colpaert, J. V. (2004). A zinc-adapted fungus protects pines from zinc stress. *New Phytol.* 161, 549–555. doi: 10.1046/j.1469-8137.2003.00941.x

Adriaensen, K., Vangronsveld, J., and Colpaert, J. V. (2006). Zinc-tolerant *Suillus bovinus* improves growth of Zn-exposed *Pinus sylvestris* seedlings. *Mycorrhiza* 16, 553–5 58. doi: 10.1007/s00572-006-0072-7

Alberti, S., Gitler, A. D., and Lindquist, S. (2007). A suite of gateway cloning vectors for highthroughput genetic analysis in *Saccharomyces cerevisiae*. *Yeast* 24, 913–919. doi: 10.1002/yea.1502

Amich, J., Vicentefranqueira, R., Mellado, E., Ruiz-Carmuega, A., Leal, F., and Calera, J. A. (2014). The ZrfC alkaline zinc transporter is required for *Aspergillus fumigatus* virulence and its growth in the presence of the Zn/Mn-chelating protein calprotectin. *Cell. Microbiol.* 16, 548–564. doi: 10.1111/cmi.12238

Berg, J., and Shi, Y. (1996). The galvanization of biology: a growing appreciation for the roles of zinc. *Science* 271, 1081–1085. doi: 10.1126/science.271.5252.1081

Boardman, R., and McGuire, D. O. (1990). The role of zinc in forestry. II. Zinc deficiency and forest management: effect on yield and silviculture of plantations in South Australia. *For. Ecol. Manage.* 37, 207–218. doi: 10.1016/0378-1127(90)90055-G

Citiulo, F., Jacobsen, I. D., Miramon, P., Schild, L., Brunke, S., Zipfel, P., et al. (2012). *Candida albicans* scavenges host zinc via pra1 during endothelial invasion. *PLOS Pathog.* 8:e1002777. doi: 10.1371/journal.ppat.1002777

Clemens, S. (2006a). Evolution and function of phytochelatin synthases. *J. Plant Physiol.* 163, 319–332. doi: 10.1016/j.jplph.2005.11.010

Clemens, S. (2006b). Toxic metal accumulation, responses to exposure and mechanisms of tolerance in plants. *Biochimie* 88, 1707–1719. doi: 10.1016/j.biochi.2006.07.003

Colpaert, J. V., Muller, L. A. H., Lambaerts, M., Adriaensen, K., and Vangronsveld, J. (2004). Evolutionary adaptation to Zn toxicity in populations of suilloid fungi. *New Phytol.* 162, 549–559. doi: 10.1111/j.1469-8137.2004.01037.x

Colpaert, J. V., Wevers, J. H. L., and Adriaensen, K. (2011). How metal-tolerant ecotypes of ectomycorrhizal fungi protect plants from heavy metal pollution. *Ann. For. Sci.* 68, 17–24. doi: 10.1007/s13595-010-0003-9

Crawford, A., and Wilson, D. (2015). Essential metals at the host-pathogen interface: nutritional immunity and micronutrient assimilation by human fungal pathogens. *FEMS Yeast Res.* 15:fov071. doi: 10.1093/femsyr/fov071

Dainty, S. J., Kennedy, C., Watt, S., Bähler, J., and Whitehall, S. K. (2008). Response of *Schizosaccharomyces pombe* to zinc deficiency. *Eukaryot. Cell.* 7, 454–464. doi: 10.1128/EC.00408-07

Do, E., Hu, G., Caza, M., Kronstad, J., and Jung, W. (2016). The ZIP family zinc transporters support the virulence of *Cryptococcus neoformans*. *Med. Mycol.* 54, 605–615. doi: 10.1093/mmy/myw013

Eide, D. (1996). The ZRT2 gene encodes the low affinity Zinc transporter in *Saccharomyces cerevisiae*. *J. Biol. Chem.* 271, 23203–23210. doi: 10.1074/jbc.271.38.23203

Eide, D. (2006). Zinc transporters and the cellular trafficking of zinc. *Biochim. Biophys. Acta* 1763, 711–722. doi: 10.1016/j.bbamcr.2006.03.005

Eide, D., Clark, S., Nair, M. T., Gehl, M., Gribskov, M., Guerinot M., et al. (2005). Characterization of the yeast ionome: a genome-wide analysis of nutrient mineral and trace element homeostasis in *Saccharomyces cerevisiae*. *Genome Biol.* 6:R77 doi: 10.1186/gb-2005-6-9-r77

Eng, B. H., Guerinot, M. L., Eide, D., and Saier, M. H. (1998). Sequence analyses and phylogenetic characterization of the ZIP family of metal ion transport proteins. *J. Membr. Biol.* 166, 1–7. doi: 10.1007/s002329900442

Frausto da Silva, J. J. R., and Williams, R. J. P. (2001). *The Biological Chemistry of the Elements*, 2nd Edn. Oxford: Clarendon Press, 800.

Gaither, L. A., and Eide, D. J. (2001). Eukaryotic zinc transporters and their regulation. *Biometals* 14, 251–270. doi: 10.1023/A:1012988914300

Gietz, D. R., and Woods, R. A. (2002). Transformation of yeast by lithium acetate/single-stranded carrier DNA/polyethylene glycol method. *Methods Enzymol.* 350, 87–96. doi: 10.1016/S0076-6879(02)50957-5

Gitan, R. S., and Eide, D. J. (2000). Zinc-regulated ubiquitin conjugation signals endocytosis of the yeast ZRT1 zinc transporter. *Biochem. J.* 346, 329–336. doi: 10.1042/bj3460329

Gitan, R. S., Shababi, M., Kramer, M., and Eide, D. J. (2003). A cytosolic domain of the yeast zrt1 zinc transporter is required for its post-translational inactivation in response to Zinc and Cadmium. *J. Biol. Chem.* 278, 39558–39564. doi: 10.1074/jbc.M302760200

Grigoriev, I. V., Nordberg, H., Shabalov, I., Aerts, A., Cantor, M., Goodstein, D., et al. (2012). The genome portal of the department of energy joint genome institute. *Nucleic Acids Res.* 42, D26–D31. doi: 10.1093/nar/gkr947

Guerinot, M. L. (2000). The ZIP family of metal transporters. *Biochim. Biophys. Acta* 1465, 190–198. doi: 10.1016/S0005-2736(00)00138-3

Jung, W. H. (2015). The Zinc transport systems and their regulation in pathogenic fungi. *Mycobiology* 43, 179–183. doi: 10.5941/MYCO.2015.43.3.179

Katoh, K., and Standley, D. M. (2013). MAFFT multiple sequence alignment software version 7: improvements in performance and usability. *Mol. Biol. Evol.* 30, 772–780. doi: 10.1093/molbev/mst010

Kiranmayi, P., Tiwari, A., Sagar, K. P., Haritha, A., and Mohan, P. M. (2009). Functional characterization of tzn1 and tzn2-zinc transporter genes in *Neurospora crassa*. *Biometals* 22, 441–420. doi:10.1007/s10534-008-9177-0

Kohler, A., Kuo, A., Nagy, L. G., Morin, E., Barry, K. W., Buscot, F., et al. (2015). Convergent losses of decay mechanisms and rapid turnover of symbiosis genes in mycorrhizal mutualists. *Nat. Genet.* 47, 410–415. doi: 10.1038/ng.3223

Kumánovics, A., Poruk, K. E., Osborn, K. A., Ward, D. M., and Kaplan, J. (2006). YKE4 (YIL023C) encodes a bidirectional zinc transporter in the endoplasmic reticulum of *Saccharomyces cerevisiae*. *J. Biol. Chem.* 281, 22566–22574. doi: 10.1074/jbc.M604730200

MacDiarmid, C. W., Gaither, L. A., and Eide, D. (2000). Zinc transporters that regulate vacuolar zinc storage in *Saccharomyces cerevisiae*. *EMBO J.* 19, 2845–2855. doi: 10.1093/emboj/19.12.2845

Mao, X., Kim, B., Wang, F., Eide, D. J., and Petris, M. J. (2007). A histidine-rich cluster mediates the ubiquitination and degradation of the human zinc transporter, hZIP4, and protects against zinc cytotoxicity. *J. Biol. Chem.* 282, 6992–7000. doi: 10.1074/jbc.M610552200

Martin, F., Kohler, A., Murat, C., Veneault-Fourrey, C., and Hibbett, D. S. (2016). Unearthing the roots of ectomycorrhizal symbioses. *Nat. Rev. Microbiol.* 14, 760–773. doi: 10.1038/nrmicro.2016.149

Migeon, A., Blaudez, D., Wilkins, O., Montanini, B., Campbell, M., Richaud, P., et al. (2010). Genome-wide analysis of plant metal transporters, with an emphasis on poplar. *Cell. Mol. Life Sci.* 67, 3763–3784. doi: 10.1007/s00018-010-0445-0

Milon, B., Wu, Q., Zou, J., Costello, L. C., and Franklin, R. B. (2006). Histidine residues in the region between transmembrane domains III and IV of hZip1 are required for zinc transport across the plasma membrane in PC-3 cells. *Biochim. Biophys. Acta* 1758, 1696–1701. doi: 10.1016/j.bbamem.2006.06.005

Mokdad-Gargouri, R., Abdelmoula-Soussi, S., Hadiji-Abbès, N., Amor, I. Y., Borchani-Chabchoub, I., and Gargouri, A. (2012). Yeasts as a tool for heterologous gene expression. *Methods Mol. Biol.* 824, 359–370. doi: 10.1007/978-1-61779-433-9_18

Nguyen, H., Rineau, F., Vangronsveld, J., Cuypers, A., Colpaert, J. V., and Ruytinx, J. (2017). A novel, highly conserved metallothionein family in basidiomycete fungi and characterization of two representative SlMTa and SlMTb genes in the ectomycorrhizal fungus *Suillus luteus*. *Environ. Microbiol.* 19, 2577–2587. doi: 10.1111/1462-2920.13729

R Core Team (2015) *R: A Language and Environment for Statistical Computing*. Vienna: R Foundation for Statistical Computing.

Rozen, S., and Skaletsky, H. (2000). Primer3 on the WWW for general users and for biologist programmers. *Methods Mol. Biol.* 132, 365–386.

Ruytinx, J., Coninx, L., Nguyen, H., Smisdom, N., Morin, E., Kohler, A., et al. (2017). Identification, evolution and functional characterization of two Zn CDF-family transporters of the ectomycorrhizal fungus *Suillus luteus*. *Environ. Microbiol. Rep.* 9, 419–427. doi: 10.1111/1758-2229.12551

Ruytinx, J., Remans, T., and Colpaert, J. V. (2016). Gene expression studies in different genotypes of an ectomycorrhizal fungus require a high number of reliable reference genes. *PeerJ Prep.* 4:e2125v1.

Sacky, J., Leonhardt, T., and Kotrba, P. (2016). Functional analysis of two genes coding for distinct cation diffusion facilitators of the ectomycorrhizal Zn-accumulating fungus *Russula atropurpurea*. *Biometals* 29, 349–363. doi: 10.1007/s10534-016-9920-x

Schothorst, J., Zeebroeck, G. V., and Thevelein, J. M. (2017). Identification of Ftr1 and Zrt1 as iron and zinc micronutrient transceptors for activation of the PKA pathway in *Saccharomyces cerevisiae*. *Microb. Cell* 4, 74–89. doi: 10.15698/mic2017.03.561

Tamura, K., Stecher, G., Peterson, D., Filipski, A., and Kumar, S. (2013). MEGA6: molecular evolutionary genetics analysis version 6.0. *Mol. Biol. Evol.* 30, 2725–2729. doi: 10.1093/molbev/mst197

Thorn, A. J., and Robertson, E. D. (1987). Zinc deficiency in *Pinus radiata* at cape Karikari, New Zealand. *N. Z. J. For. Sci.* 17, 129–132.

Vandesompele, J., De Preter, K., Pattyn, F., Poppe, B., Van Roy, N., De Paepe, A., et al. (2002). Accurate normalization of real-time quantitative RT-PCR data by geometric averaging of multiple internal control genes. *Genome Biol.* 3, research0034.1–research0034.11. doi: 10.1186/gb-2002-3-7-research0034

Vida, T. A., and Emr, S. D. (1995). A new vital stain for visualizing vacuolar membrane dynamics and endocytosis in yeast. *J. Cell Biol.* 128, 779–792. doi: 10.1083/jcb.128.5.779

Zhao, H., and Eide, D. (1996). The yeast ZRT1 gene encodes the zinc transporter protein of a high-affinity uptake system induced by zinc limitation. *Proc. Natl. Acad. Sci. U.S.A.* 93, 2454–2458. doi: 10.1073/pnas.93.6.2454

Conflict of Interest Statement: The authors declare that the research was conducted in the absence of any commercial or financial relationships that could be construed as a potential conflict of interest.

frontiers in Microbiology

ORIGINAL RESEARCH
published: 05 March 2018
doi: 10.3389/fmicb.2018.00091

Arbuscular Mycorrhizal Fungal 14-3-3 Proteins Are Involved in Arbuscule Formation and Responses to Abiotic Stresses During AM Symbiosis

Zhongfeng Sun[1], Jiabin Song[1], Xi'an Xin[1], Xianan Xie[2] and Bin Zhao[1]**

[1] State Key Laboratory of Agricultural Microbiology, College of Life Science and Technology, Huazhong Agricultural University, Wuhan, China, [2] State Key Laboratory for Conservation and Utilization of Subtropical Agro-Bioresources, College of Forestry and Landscape Architecture, South China Agricultural University, Guangzhou, China

OPEN ACCESS

Edited by:
Erika Kothe,
Friedrich-Schiller-Universität Jena, Germany

Reviewed by:
Raffaella Balestrini,
Consiglio Nazionale delle Ricerche (CNR), Italy
Maria Rapala-Kozik,
Jagiellonian University, Poland

***Correspondence:**
Bin Zhao
binzhao@mail.hzau.edu.cn
Xianan Xie
30004537@scau.edu.cn

Specialty section:
This article was submitted to Fungi and Their Interactions, a section of the journal Frontiers in Microbiology

Received: 18 September 2017
Accepted: 16 January 2018
Published: 05 March 2018

Citation:
Sun Z, Song J, Xin X, Xie X and Zhao B (2018) Arbuscular Mycorrhizal Fungal 14-3-3 Proteins Are Involved in Arbuscule Formation and Responses to Abiotic Stresses During AM Symbiosis. Front. Microbiol. 9:91. doi: 10.3389/fmicb.2018.00091

Arbuscular mycorrhizal (AM) fungi are soil-borne fungi belonging to the ancient phylum Glomeromycota and are important symbionts of the arbuscular mycorrhiza, enhancing plant nutrient acquisition and resistance to various abiotic stresses. In contrast to their significant physiological implications, the molecular basis involved is poorly understood, largely due to their obligate biotrophism and complicated genetics. Here, we identify and characterize three genes termed *Fm201*, *Ri14-3-3* and *RiBMH2* that encode 14-3-3-like proteins in the AM fungi *Funneliformis mosseae* and *Rhizophagus irregularis*, respectively. The transcriptional levels of *Fm201*, *Ri14-3-3* and *RiBMH2* are strongly induced in the pre-symbiotic and symbiotic phases, including germinating spores, intraradical hyphae- and arbuscules-enriched roots. To functionally characterize the *Fm201*, *Ri14-3-3* and *RiBMH2* genes, we took advantage of a yeast heterologous system owing to the lack of AM fungal transformation systems. Our data suggest that all three genes can restore the lethal *Saccharomyces cerevisiae bmh1 bmh2* double mutant on galactose-containing media. Importantly, yeast one-hybrid analysis suggests that the transcription factor RiMsn2 is able to recognize the STRE (CCCCT/AGGGG) element present in the promoter region of *Fm201* gene. More importantly, Host-Induced Gene Silencing of both *Ri14-3-3* and *RiBMH2* in *Rhizophagus irregularis* impairs the arbuscule formation in AM symbiosis and inhibits the expression of symbiotic *PT4* and *MST2* genes from plant and fungal partners, respectively. We further subjected the AM fungus-*Medicago truncatula* association system to drought or salinity stress. Accordingly, the expression profiles in both mycorrhizal roots and extraradical hyphae reveal that these three 14-3-3-like genes are involved in response to drought or salinity stress. Collectively, our results provide new insights into molecular functions of the AM fungal 14-3-3 proteins in abiotic stress responses and arbuscule formation during AM symbiosis.

Keywords: arbuscular mycorrhiza, abiotic stresses, *Funneliformis mosseae*, *Rhizophagus irregularis*, *Fm201*, host-induced gene silencing, 14-3-3 proteins

INTRODUCTION

Arbuscular mycorrhizal (AM) fungi, belonging to the ancient phylum Glomeromycota, are soil-borne microbes and capable of establishing the most widespread mutualistic association, namely AM symbiosis, with more than 80% terrestrial flowering plant species (Simon et al., 1993; Remy et al., 1994). Due to the obligate biotrophic nature, AM fungi need to consume plant photosynthates (Bago et al., 2000) and lipids to complete their life cycle (Bravo et al., 2017; Jiang et al., 2017), and reciprocally AM fungi significantly contribute to plant growth not only by enhancing mineral nutrient uptake and water acquisition from surrounding soil, but also protecting plants against fungal pathogens (Smith and Read, 2008; Jung et al., 2012; Chitarra et al., 2016) and a variety of abiotic stresses (Augé, 2001; Schützendübel and Polle, 2002; Lenoir et al., 2016). Therefore, AM fungi are key endosymbionts of the plant symbiosis and have significant impacts on plant productivity and ecosystem function (Van der Heijden et al., 1998), and are of great interest for the sustainable agricultural development (Gianinazzi et al., 2010).

The formation of a functional AM symbiosis requires successive stages between AM fungal and host symbionts at both physiological and molecular levels (Genre et al., 2005; Bonfante and Genre, 2010). Specifically, the development of arbuscular mycorrhiza consists of three major distinct stages through the progression of AM fungal hyphae during root colonization (Genre et al., 2005; Harrison, 2012; Gutjahr and Parniske, 2013). Arbuscules are generally thought to be the primary sites for nutrients exchange between the two symbionts (Parniske, 2008; Bonfante and Genre, 2010). In this symbiotic interface, the host membrane surrounding an arbuscule, known as the periarbuscular membrane (PAM), harbors AM-specific Pi transporters that acquire Pi released from the arbuscule (Harrison et al., 2002; Javot et al., 2007a). Outside the roots, the extraradical mycelia of AM fungi can extend the soil substratum beyond the depletion zone of the rhizosphere to uptake nutrients (particularly Pi and N) and water from the surrounding soils (Govindarajulu et al., 2005; Javot et al., 2007b; Li et al., 2013).

Despite their great importance, the underlying signaling events during initiation and formation of AM symbiosis are not well understood (Paszkowski, 2006; Bonfante and Requena, 2011; Gutjahr and Parniske, 2013; Oldroyd, 2013; Schmitz and Harrison, 2014; Bonfante and Genre, 2015). In contrast to a plethora of discoveries on morphological and chemical features in AM fungi, the molecular basis involved is still largely unknown, partially due to the limited available genomic resources. Many genome-wide gene expression analysis have been employed recently in order to understand the underlying molecular mechanisms of the AM formation. These studies mainly focused on the host plants (recently reviewed in Salvioli and Bonfante, 2013), whereas only a few investigations addressed the fungi partners (Requena et al., 2002; Breuninger and Requena, 2004; Cappellazzo et al., 2007; Kikuchi et al., 2014). Major progress has been recently achieved using transcriptomics and genomics data of *Rhizophagus irregularis* (Tisserant et al., 2012; Tisserant et al., 2013; Lin et al., 2014) and *Gigaspora* genus (Salvioli et al., 2016; Tang et al., 2016).

Using the suppression subtractive hybridization library (SSH) strategy, Breuninger and Requena (2004) firstly found some ESTs of fungal genes which were induced in the appressorium stage may display potential roles in this stage of *Funneliformis mosseae*. In this case, an EST tag termed 201, which encodes a 14-3-3 like protein in fungi, shows a significant up-regulation in the appressorium stage of AM symbiosis (Breuninger and Requena, 2004). Recently, Tisserant et al. (2012) released the first genome-wide overview of the transcriptional profiles of the various fungal tissues of *R. irregularis*. Particularly, a large number of fungal non-redundantly expressed transcripts was investigated in spores, intraradical mycelia (IRM), extraradical mycelia (ERM), and arbuscules. Interestingly, the transcripts encoding *R. irregularis* 14-3-3 proteins were inducible in both IRM and ERM.

14-3-3 proteins are highly conserved and dimeric proteins with a subunit mass of approximate 30 KDa (van Heusden and Steensma, 2006). These proteins are named based on the fraction number after EDTA-cellulose chromatography and the position after subsequent starch gel-electrophoresis (Moore, 1967). The first description of the function of 14-3-3 protein is substantially comparable to the 'activator' protein, that is important in the regulation of serotonin and noradrenaline biosynthesis in the brain (Ichimura et al., 1987). Moreover, 14-3-3 proteins form homo- or hetero-dimers by two subunits harboring the independent ligand-binding channels. Until now, it is extensively studied that these proteins generally serve as adapters, chaperones, activators, or repressors in the regulation of signal transduction pathways by reorganization of specific phosphoserine/phosphothreonine-inclusive binding motifs phosphorylated by protein kinase A (Smith et al., 1998; van Heusden, 2009; Smith et al., 2011; Parua and Young, 2014). Additionally, 14-3-3 proteins also play important roles in the pseudohyphal growth of *Saccharomyces cerevisiae* and the pathogenic fungal infection, such as *Ustilago maydis* (Gancedo, 2001; Rispail et al., 2009; Ballou et al., 2013; Liu et al., 2015). These known 14-3-3 proteins have also been implicated in several signaling cascades responding to biotic and abiotic stresses in plants (Roberts et al., 2002; Lozano-Duran and Robatzek, 2015; Li et al., 2016), suggesting that these proteins may display distinct roles during eukaryotes life cycle (Liu et al., 2015). So far, at least two distinct 14-3-3 subunits have been characterized in fungi (Darling et al., 2005; Hermeking and Benzinger, 2006). Porcel et al. (2006) identified a gene *Gi14-3-3* (currently *Ri14-3-3*) from the AM fungus *R. irregularis*, encoding a 14-3-3 protein subunit that is enhanced under drought stress during AM symbiosis, being the first 14-3-3 protein from AM fungus reported so far. Additionally, recent work has provided new evidence for the potential involvement of *Ri14-3-3* gene in the interaction between maize and *R. irregularis* under drought stress (Li et al., 2016). However, the molecular mechanisms of *Ri14-3-3* gene in enhancing plant resistance to drought stress are still unclear.

To further advance our understanding of the roles of 14-3-3 proteins in fungal symbionts during AM symbiosis, we here report three novel fungal genes, so called *Fm201*, *Ri14-3-3* and *RiBMH2*, which encode 14-3-3-like proteins from *F. mosseae* (BEG12) and *R. irregularis* (DAOM197198), respectively. *14-3-3*

genes are strongly induced in the early stage of AM symbiosis. Moreover, the expression of *14-3-3* genes are regulated in response to drought and osmotic stresses. To further characterize these AM fungal *14-3-3* genes, we validated the capability of these genes to complement the metabolic deficient Δ*bmhs* mutant (*bmh1* and *bmh2* double mutant) in a yeast heterologous expression system. We also provided insights into the regulatory mechanism between 14-3-3 protein and Msn2 transcription factor from AM fungi and further proved the existence of two distinct 14-3-3 subunits in AM fungi. More importantly, in the absence of stable transformation protocols for AM fungi (Helber and Requena, 2008; Helber et al., 2011), host-induced gene silencing (HIGS) of the two *14-3-3* genes in *R. irregularis*, whereby these genes are silenced in the AM fungal symbiont by expressing an RNA interference construct in the host, provides a potential tool to address the function of 14-3-3 proteins in obligate biotrophic AM fungi. Collectively, our results provide new insights into molecular functions of the AM fungal 14-3-3 proteins in stress responses and arbuscule formation during AM symbiosis.

RESULTS

Identification of *Fm201* Gene From *Funneliformis mosseae*

In the previous study, transcript abundance of 201-tag was significantly enhanced at the early appressorium stage of AM symbiosis (Breuninger and Requena, 2004). The amino acid sequence of 201-tag exhibits a high similarity (∼97%) with the Ri14-3-3 protein from *R. irregularis* (Breuninger and Requena, 2004; Tisserant et al., 2012). With the aim to confirm if this fungal 14-3-3 protein is involved in AM symbiosis, a DNA clone of 1.5 kb in length was obtained by inverse PCR from the cloning procedures on *F. mosseae* genomic DNA based on the 201-tag. The isolated fragment with 5′ end and upstream region was highly similar to the sequence of *Ri14-3-3* gene from *R. irregularis* (Porcel et al., 2006). Since the 5′ and 3′ end sequences of this gene are not available, 5′ and 3′ RACE experiments on RNA pools of *F. mosseae* germinating spores were subsequently performed to obtain the full-length CDS sequence. A 1,401 bp full-length cDNA sequence of *Fm201*, covering the 5′UTR (188 bp) and 3′UTR (411 bp), was thus identified (Accession number: KM258580). The corresponding genomic sequence of *Fm201* gene is 1,685 bp in length, containing seven exons and seven introns (Supplementary Figure S1). Interestingly, *Fm201* gene contains a 100 nt intron in the 5′ UTR and two transcriptional variants of 3′UTRs (61 and 411 nt in length, respectively). These unusual features of AM fungal 14-3-3 gene firstly reported in the present study may suggest important roles in the regulation of *Fm201* expression during AM symbiosis.

Fm201 Protein Is Conserved Among Eukaryotes

To further investigate the phylogenetic and structural features of the Fm201 protein from AM fungi, we exploited the phylogenetic placement and 3D structure of Fm201 protein using bioinformatics strategy. The *in silico* analysis revealed that the open reading frame (ORF) of *Fm201* gene consists of 804 bp corresponding to 267 amino acids with a predicted molecular weight of approximate 30 kDa. A phylogeny of basal fungi and 14-3-3 proteins from *Homo sapiens* clearly supports Fm201 as a sister clade to Ri14-3-3 (**Figure 1A**), indicative of the conserved evolutionary origin of the *14-3-3* genes in AM fungi, whereas the RiBMH2 protein from *R. irregularis* belongs to the closer relative of the yeast BMH2 (**Figure 1A**). Compared to the 14-3-3 proteins from *H. sapiens*, Fm201 protein still shares a very high homology. This also demonstrates that 14-3-3 proteins are highly conserved in eukaryotes. As a conserved protein, Fm201 protein shares 97% similarities with Ri14-3-3 protein from AM fungi. The amino acid sequence of Fm201 was compared with BMHs from *S. cerevisiae*, 14-3-3s from *R. irregularis* and *H. sapiens* 14-3-3 epsilon and a high homology with over 72% identity at the amino acid level was observed (Supplementary Figure S2).

We further carried out the Homology modeling using *Homo sapiens* 14-3-3 epsilon (80.52% identity in amino acid sequences) as a model. The predicted three-dimensional conformation of Fm201 indicates that Fm201 is a typical 14-3-3 protein with 9 alpha helices and 8 loops, with the highly homologous α3, α5, α7, and α9 putatively forming its amphipathic ligand-binding grooves (**Figure 1C**). Fm201 homologous dimers could form a typical C-shape cup, which provides a basic structure of 14-3-3 dimers for implementing its function (**Figure 1D**).

14-3-3 Proteins Restore Metabolic Activity of *S. cerevisiae* Δ*bmhs* Mutant

To gain further insights into the function of 14-3-3, a *S. cerevisiae* heterologous expression system was exploited. Since Fm201 shares 82.3% identity at the amino acid sequence with both BMH1 and BMH2 in *S. cerevisiae* (see Supplementary Figure S2), the ORF of *Fm201* was cloned into pMR-12 under the control of the *Gal7* promoter and replaced *S. cerevisiae BMH1*. To test if Fm201 can restore the metabolic activity of *S. cerevisiae* Δ*bmhs* mutant, as referred in Materials and Methods (also see Supplementary Table S1). *S. cerevisiae* Δ*bmhs* mutant with pMR-12-*Fm201* cannot grow on YPD with 2% glucose as the sole carbon source. However, cell growth was recovered when using 2% galactose as the sole carbon source (**Figure 2**). Similar results were observed when replacing *Fm201* with *Ri14-3-3* or *RiBMH2* (**Figure 2**). These data confirmed that Fm201 has similar function as BMH1 in *S. cerevisiae*.

Functional Dissection of CREs on Promoter of *Fm201* (pFm201) in *S. cerevisiae*

14-3-3 proteins have been reported to participate in pseudohyphal growth and resistance in yeast (Roberts et al., 1997; Hurtado and Rachubinski, 2002). However, the roles of these 14-3-3 proteins in mycorrhizal fungi are largely unknown. It has been observed that expression specificity of plant 14-3-3 genes in response to various stresses is largely promoter

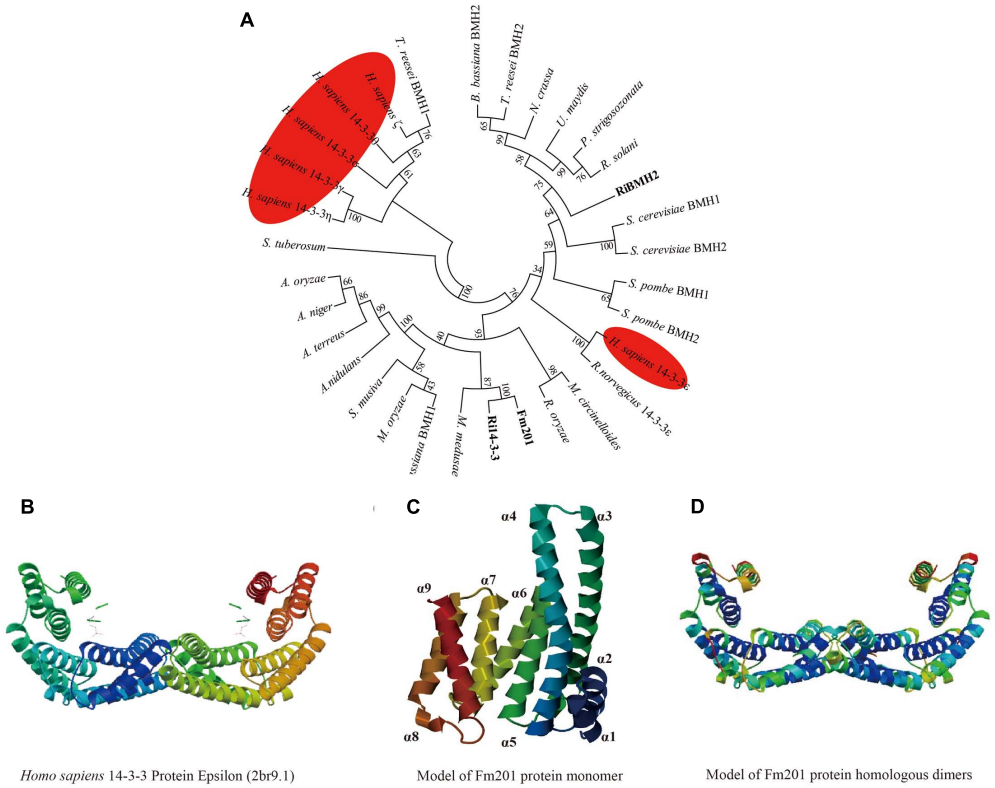

FIGURE 1 | *In silico* analysis of Fm201 protein and its homologs from AM fungi. **(A)** The unrooted phylogenetic tree was constructed based on multiple sequence alignment of 14-3-3 proteins in fungal species and *Homo sapiens*. The phylogenetic relationships were analyzed by Neighbor-joining method with MEGA v6.0 software. Bootstrap values were calculated using 1,000 replicates. 14-3-3 proteins from mycorrhizal fungi are highlighted in bold and their homologs from *H. sapiens* are colored red. **(B)** Predicted structure of *Homo sapiens* 14-3-3 epsilon (2br9A) dimers. **(C,D)** Homology modeling of Fm201 monomer and homodimer using *Homo sapiens* 14-3-3 epsilon (2br9A) as reference.

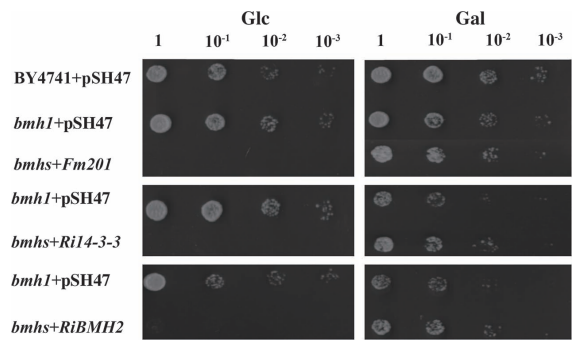

FIGURE 2 | 14-3-3 proteins from mycorrhizal fungi restore the growth of *S. cerevisiae* Δ*bmhs* mutant on galactose-contained media. Ten-fold serial dilutions of yeast cells (the wild-type BY4741, Δ*bmh1* mutant or Δ*bmhs* mutant) carrying different constructs (the empty vector pSH47, the full-length cDNA of *Fm201, Ri14-3-3, or RiBMH2*) were grown on SD/-Ura plates with 2% glucose or galactose as carbon source. Expression of *Fm201*, *Ri14-3-3*, or *RiBMH2* gene is controlled by galactose-inducible Gal7 promoter.

dependent (Aksamit et al., 2005). To analyze the putative CREs (Cis-Regulatory Elements) located in the promoter region of *Fm201*, a 1.5 kb length promoter sequence upstream of *Fm201* coding region (pFm201) was analyzed via Yeastract database[1]. The CREs present in pFm201 were compared with pBMH1, pBMH2 from *S. cerevisiae* and pRiBMH2 in *R. irregularis* (van Heusden, 2009) (**Table 1**). Many common CREs in corresponding sites shared by pFm201 and pBMHs have been shown to be recognized by many transcriptional factors (Bruckmann et al., 2004; van Heusden, 2009). In the present study, two CREs possiblely recognized by Msn2 and STE12 were chosen for further investigations. Msn2 is an STRE element (AGGGG/CCCCT) binding transcription factor, which is supposed to be related to fungal infection and resistance to abiotic stress in other filamentous fungi (Schmitt and Mcentee, 1996; Seidl et al., 2004; Elfving et al., 2014; Zhang et al., 2014). STE12, so-called GintSTE, is the transcriptional factor that has been reported in mycorrhizal fungi and is believed to be an indispensable component in the early process of mycorrhizal fungi infection (Tollot et al., 2009; Tang et al., 2016). The common and shared CREs present upstream of *Fm201*, *RiBMH2* and *S. cerevisiae BMHs* imply that 14-3-3 proteins in AM fungi may be involved in the regulation of resistance to abiotic stress and hyphal growth in AM fungi as BMHs in *S. cerevisiae*.

[1]http://www.yeastract.com/

TABLE 1 | Predicted motifs on the *Fm201* gene promoter compared with that of *RiBMH2*, *ScBMH1* and *ScBMH2**

Transcription factors	Motif	*ScBMH1*	*ScBMH2*	*Fm201*	*RiBMH2*
Ash1p	YTGAT	-510F	-955F, -881R, -1173R, -1252R	-951F, -1164F, -522R, -664R, -748R, -794R, -1098R, -1164R, -1200R,-1216R, -1238R	-1094F, -1071F, -1034F, -977F, -616F, -436F, -165F, -131F, -157R, -354R, -491R, -789R, -932R, -1178R
Bas1p, Gcn4p	TGACTC	-324R			-403F, -800R
Cbf1p	RTCACRTG	-388R		-1285F	
Fkh1p, Fkh2p	RYMAAYA	-300F, -512R, -520R	-981F, -955R, -965R, -997R	-22F, -277F, -717F, -721F, -1387F, -1499F, -774R, -1552 R	-1491F, -1453F, -1118F, -945F, -599F, -514F, -505F, -496F, -492F, -425F, -369F, -344R, -523R, -1132R,
Gcn4p	TTGCGCAA	-506FR			-355FR
Gcn4p	CACGTG	-389FR		-937FR	
Gcr1p	CWTCC	-292F, -314R, -348R, -378F	-1074F, -924F	-384F,-279R,-1284R, -1482R	-313R
Mot3p	TMGGAA	-67R	-1361F, -1283R		-1320F, -1312F,
Mot3p	AAGAGG	-290R, -316F, -376R	-1024R		
Mot3p	AAGGWT		-1300R	-221F,-856F,-1020F, -1129R	-1326F, -378F
Nrg1p	CCCTC		-921F	-1037R	
Msn2p**	**CCCCT**	**-212R, -420R, -429R**		**-490F**	**-985F, -1173R**
Pho4p	CACGTK	-389FR			
Rgt1p	CGGANNA	-335R	-1360F, -1073R	-1070F, -786R	-1127F
Rpn4p	GGTGGCAAA	-304F			
Rtg1p, Rtg3p	GTCAC	-388R	-1069R	-1270F,-1285F	-147F, -249R, -185R
Stb5p	CGGNS	-270F, -277F, -282R, -305F, -330F, -382F, -539F	-1078F, -1055F, -1127R	-121F, -345F, -1070F,-87R,-1435R,-1535R	-1189F, -308F, -301F, -289F, -262F
Ste12p**	**TGAAACA**		**-1222R**	**-1322R,**	**-1159R**
Tec1p	CATTCT		-873F, -1381F	-969F, -329R, -963R	-1080R
Yap1p	TKACAAA	-187f	-715F	-861R	-521R

*1.5 kb length promoter sequences of RiBMH2 and Fm201 were chosen to analysis the predicted motifs. The promoter sequence of Ri14-3-3 has not yet been released.
** Words in bold are transcription factor verified in the report.

Due to the lack of stable genetic transformation approaches in the AM fungi, it is technically challenging to knockout *Fm201* gene to confirm the biological function in the early stages during symbiosis (Sanders, 1999; Maldonado-Mendoza et al., 2001). To probe the possible function of Fm201 protein, we employed the site-specific mutagenesis and yeast one-hybrid system to initially explore the essential region of *Fm201* promoter. Compared to the site-specific mutagenesis of STRE (CCCCT/AGGGG) located in pFm201(pFm201-ΔSTRE), pFm201 is more sensitive to abiotic stresses, osmotic pressure and drought stress (**Figure 3A**). This result indicates that the STRE element of pFm201 could be recognized by Msn2 in *S. cerevisiae*. Although there is no any report, to our knowledge, about the functional properties of RiMsn2 factor mentioned as RiMsn4 in *R. irregularis*, it may play a major role in eukaryotic abiotic stress response and hyphae differentiation (Tisserant et al., 2013; Zhang et al., 2014).

A yeast one-hybrid system was also performed to confirm the interaction between GintSTE and RiMsn2 with CREs on pFm201 (**Figure 3B**). As shown in **Figure 3B**, yeast cells harboring pFm201 with STRE element and RiMsn2 or GintSTE protein grew well, whereas growth of the cells carrying RiMsn2 or GintSTE and *Fm201* promoter without STRE element as negative controls were severly inhibited under the same conditions. These data suggest that GintSTE and RiMsn2 proteins interact with the STRE element of *Fm201* gene, the similar results were also acquired from the promoter of *RiBMH2* (data not shown). It is therefore reasonable to speculate that GintSTE and RiMsn2 proteins positively regulate the expression of *14-3-3* genes in presymbiotic stage through the binding between GintSTE/RiMsn2 and pFm201.

14-3-3 Genes Are Highly Induced in Germinating Spores and Early Stages of Symbiosis

Due to the obligate biotrophic and asexual multinucleate nature of the AM fungi (Sanders, 1999; Maldonado-Mendoza et al., 2001), it is difficult to generate mutants and overexpression

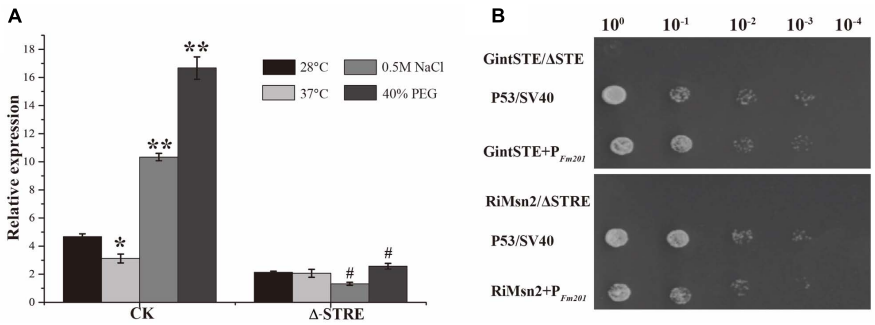

FIGURE 3 | Promoter activity analysis of *Fm201* gene in Yeast. **(A)** Real-time RT-PCR quantification of *Fm201* gene expression in yeast under different abiotic stress treatments. CK indicates the full-length promoter sequence of Fm201 gene. Lines with a significant ratio to the express rate of each group in 28°C. Error bars indicate the means of three biological replicates with SD values. Data shown are averages ± SD; $n = 3$. (#, $*p < 0.05$, $**p < 0.01$). **(B)** Yeast one-hybrid analysis of the interaction between GintSTE or RiMsn2 with *Fm201* promoter (pFm201). Yeast carrying both pGBKT7-P53 and pGADT7-SV40 was used as the positive control. pHis2- ΔSTRE with pGADT7-Rec2-RiMsn2 and pHis2- ΔSTE with pGADT7-Rec2-GintSTE were used as negative controls. Δ-STRE indicates the deletion of STRE elements located in pFm201 promoter, Δ-STE indicates the deletion of GintSTE binding sites located in pFm201 promoter. 10-fold serial dilutions of yeast cells were spotted on plates containing 2% Glc as carbon source.

strains to analyze the biological functions of Fm201 protein during AM fungal infection. To obtain further insights into the expression profile of *Fm201* gene during the colonization process, we performed a time-course analysis of *Medicago truncatula* roots inoculated with *F. mosseae* in the pot system, then sampled at 12, 18, 25, and 50 days post-inoculation (dpi) and also collected the quiescent spores and germinated spores. Morphological analyses of mycorrhizal roots showed almost majority of the appressoria and intraradical hyphae at 12–18 dpi. More arbuscules were obviously detected starting from 25 dpi, while the abundance of arbuscules decreased at 50 dpi (**Figure 4A**), the mycorrhizal colonization of the root samples was also calculated as described by Trouvelot et al. (2015) (data not shown). The transcript abundance of *Fm201* gene in *F. mosseae* at different stages were also analyzed by qRT-PCR. As shown in **Figure 4B**, the transcript abundance of *Fm201* was obviously higher in germinating spores than in quiescent spores, the transcript abundance of *Fm201* is ∼40% lower in 50 dpi than in 25 dpi when arbuscules decreased. This expression pattern was similar with fungal colonization in early stages of symbiosis, especially during the hyphopodium formation and root penetration (see **Figures 4A,D**). The similar results of *RiBMH2* and *Ri14-3-3* were also obtained from quiescent spores, germinated spores and sampled at 8, 12, 18, 40 days post-inoculation (dpi) by *R. irregularis* (**Figure 4C**). The expression levels of both *RiBMH2* and *Ri14-3-3* obviously increased accompanying the infection process and arbuscules initiation, as demonstrated by the parallel increased transcriptional levels of *MtStbM1* (**Figure 4E**), the host plant subtilase-encoding gene which is considered as a molecular marker of arbuscular mycorrhiza development (Wegel et al., 2007; Takeda et al., 2009).

Knock-Down of *14-3-3* Impairs the Arbuscule Formation in AM Symbiosis

Because of the obligate property of mycorrhizal fungi, the effect of Δ*Fm201* mutant on the establishment and maintenance of mycorrhizal symbiosis cannot be confirmed *in vivo*. RNAi technique has been successfully utilized to inhibit *Ri14-3-3* encoding a homologous protein of *Fm201* as described above in *R. irregularis* induced by hairy root lines of *M. truncatula* during symbiosis (Nowara et al., 2010; Helber et al., 2011). A 262 bp cDNA sequence from *R. irregularis Ri14-3-3* gene was cloned into pK7GWIWG2 (II) RR according to the approach mentioned in Materials and Methods. The Host-Induced Gene Silencing (HIGS) results of *Ri14-3-3* showed no significant influence on the intraradical structures of *R. irregularis* within the roots, when compared with the control roots (**Figure 5A**).

Since the draft of *R. irregularis* genome was recently released (Tisserant et al., 2013; Lin et al., 2014), we cloned and identified the coding sequence of another 14-3-3 protein subunit termed *RiBMH2* (EXX69786.1). The existence of this novel 14-3-3 protein subunit may explain the nice arbuscule observed in HIGS of *Ri14-3-3*. Thus, the HIGS experiment targeting both *Ri14-3-3* and *RiBMH2* was designed to address this issue. Mycorrhizal phenotype analysis uncovered that the arbuscules are defective. The almost collapsed arbuscules were present in the hairy root of *Ri14-3-3/RiBMH2* RNAi plants, when these two genes were both strongly repressed. Furthermore, the mycorrhizal colonization of each group was also calculated. The data suggests that the abundance of arbuscules in RNAi roots was also significantly lower than that in the control roots (**Figures 5A–C**). Moreover, the expression levels of symbiotic *MtPT4* and *RiMST2*, which are considered as molecular markers of the functioning of arbuscules (Harrison et al., 2002; Helber et al., 2011), are significantly reduced in the *Ri14-3-3/RiBMH2* RNAi roots relative to the control roots (**Figures 5D,E**), indicating that knock-down of both *Ri14-3-3* and *RiBMH2* has a significant effect on the symbiotic phenotype of AM symbiosis. These results also suggest that RiBMH2 may be required for arbuscule formation in AM symbiosis. It also provides a direct evidence that AM fungal 14-3-3 proteins play important roles during AM symbiosis.

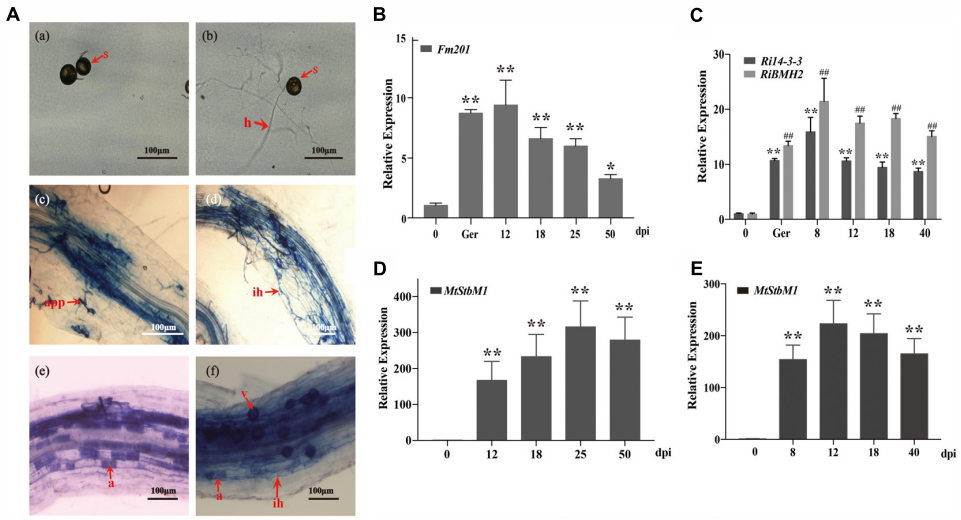

FIGURE 4 | Transcript profiles of 14-3-3 genes in quiescent spores, germinating spores and during different symbiotic stages. **(A)** Optical micrographs of the morphological structures of *F. mosseae* BEG12 during different stages of mycorrhizal symbiosis. Spore (s), hyphae (h), appressorium (app), arbuscule (a), and Vesicle (v) are shown. Scale bars represent 100 μm. **(B)** Expression fold change of *Fm201* from the AM fungus *F. mosseae*. Transcript abundance of *Fm201* was evaluated by real time RT-PCR in different fungal tissues: quiescent spores (0), germinating spores (ger), uninfected *M. truncatula* roots (Uninfected) and mycorrhizal roots (12–50 dpi). *Fm201* gene is expressed as a ratio relative to *FmActin* gene from *F. mosseae.* Lines with a significant ratio to the express rate of *Fm201* in quiescent spores. **(C)** Expression fold change of *Ri14-3-3* and *RiBMH2* from *R. irregularis*. Transcript abundance of *Ri14-3-3* and *RiBMH2* was evaluated by qRT-PCR in different fungal tissues: quiescent spores (0), germinating spores (ger), uninfected *M. truncatula* roots (Uninfected) and mycorrhizal roots (8–40 dpi). *Ri14-3-3* and *RiBMH2* gene is expressed as a ratio relative to *RiActin* gene from *R. irregularis.* Lines with a significant ratio to the express rate of *Ri14-3-3* or *RiBMH2* in quiescent spores. **(D)** The transcript abundance of *MtSbtM1* in *M. truncatula* relative to *MtTEF* in mycorrhizal roots infected by *F. mosseae* (12–50 dpi). **(E)** The transcript abundance of *MtSbtM1* in *M. truncatula* relative to *MtTEF* in mycorrhizal roots infected by *R. irregularis* (8–40 dpi). Error bars indicate the means of three biological replicates with SD values. Data shown are averages ± SD; $n = 3$. (#, $^{*}p < 0.05$, ##, $^{**}p < 0.01$).

14-3-3 Genes Are Up-Regulated in Response to Salinity and Drought Stresses During AM Symbiosis

To further investigate the potential roles of 14-3-3 proteins in response to salinity and drought stresses, the transcript profiles of *14-3-3s* in mycorrhizal roots and external hyphae were analyzed by qRT-PCR after 150 mM NaCl treatment for various time (**Figures 6A,C**). The transcript abundance of *14-3-3* shows slight but significant increase after 1.5 h and relatively stable within 24 h in mycorrhizal roots. In addition, the transcription profile of *Fm201* in extraradical hyphae treated with NaCl shows more rapid induction than in intraradical mycelia. To determine whether *14-3-3* genes are responsive to drought stress, the transcript abundance of *14-3-3* genes under 1/2 water holding capacity of drought treatment was also compared (**Figures 6B,D**). Unlike salinity stress treatment, the transcript abundance of *14-3-3* genes show a ∼4 fold and ∼7 fold up regulation in mycorrhizal roots and extraradical hyphae, respectively. These findings suggest that *Fm201* may be responsible for the crosstalk between plant and *R. intraradices* under salinity and/or drought stresses.

DISCUSSION

In terrestrial ecosystems, AM symbiosis is considered to be the most widespread ecologically and agriculturally mutualistic beneficial association among plant symbioses. Despite their great importance in both ecology and agriculture, advance in understanding the molecular basis of AM symbiosis from the fungal aspect is slow until the release of the transcriptomic data of several AM fungal species (Tisserant et al., 2012; Salvioli et al., 2016; Tang et al., 2016) and genomic data of *R. irregularis* (Tisserant et al., 2013; Lin et al., 2014), biological functions of only a few genes have been characterized during interaction with plants. In such a context, we focus on the characterization of the *14-3-3* genes from AM fungi based on its higher expression during the colonization process.

AM Fungal 14-3-3 Proteins Are a Conserved Feature of Glomeromycota

According to bioinformatics analyses, 14-3-3s from AM fungi are typical 14-3-3 proteins with higher similarity to the known 14-3-3 sequences of yeast and human. Additionally, Fm201 protein is conserved across eukaryotes based on the phylogenetic relationships among AM fungi and other basal eukaryotic species as well as the conserved 3D homology structures between *F. mosseae* and human (Yang et al., 2006). Therefore, it is of interest to find that two similar sequences were found in the recently released genome and transcriptome of another AM fungus, *R. irregularis* (Tisserant et al., 2012, 2013). Since the sequences of the two additional genes, the so called *Ri14-3-3* and *RiBMH2*, are complete with the full-length of CDSs, and the percentage of identity is relatively high (∼97%), the three AM

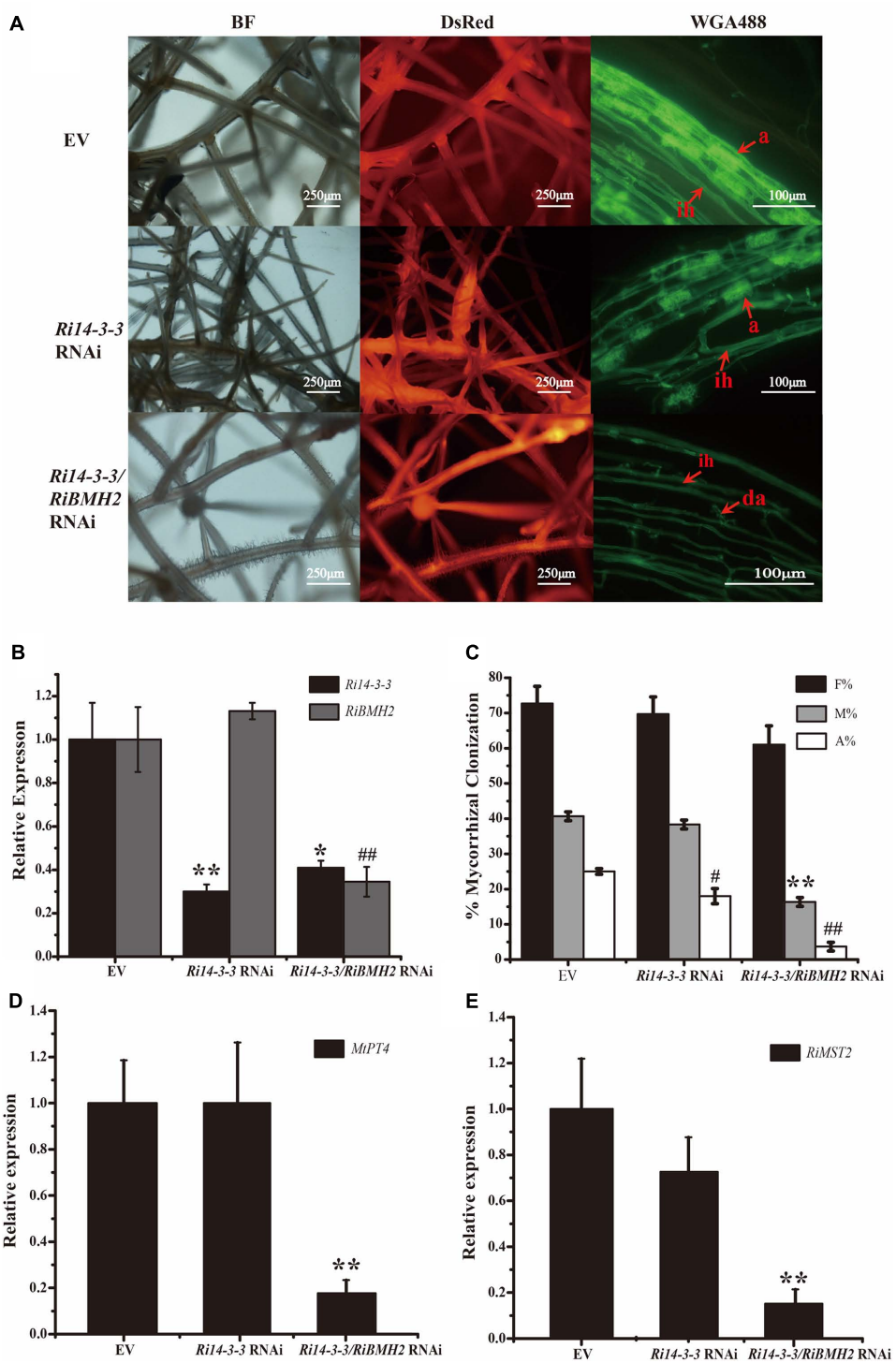

FIGURE 5 | Mycorrhizal symbiotic phenotypes of Host-Induced Gene Silencing of *Ri14-3-3* and *RiBMH2*. **(A)** Hairy root transformation of *M. truncatula* with empty vector (EV), *Ri14-3-3* RNAi vector, or *Ri14-3-3/BMH2* RNAi vector. Transgenic hairy roots were infected by AM fungi and the mycorrhizal phenotypes were observed with fluorescence microscope. a, mature arbuscules; ad, arbuscule degradation; ih, internal hyphae. **(B)** Transcript abundance change of *Ri14-3-3* and *RiBMH2* in transgenic hairy roots as measured by qRT-PCR using *RiActin* gene as the reference gene. **(C)** Mycorrhization level was analyzed by WGA 488 staining of hairy roots at 30 dpi with *R. irregularis*. F%, frequency of colonization; M%, intensity of mycorrhiza; A%, arbuscule abundance. **(D)** Expression levels of *MtPT4* in control (EV) and RNAi lines were determined by real-time RT-PCR. The *M. truncatula MtTEF* gene was used as the reference gene. **(E)** Transcript accumulation of *RiMST2* in control (EV) and RNAi mycorrhizal roots measured by real-time RT-PCR. The *R. irregularis RiActin* gene was used as endogenous control. Three technical replicates were analyzed. Asterisks indicate statistically significant differences from respective control lines. Error bars indicate the means of three biological replicates with SD values. Data shown are averages ± SD; $n = 3$. (#, *$p < 0.05$, ##, **$p < 0.01$).

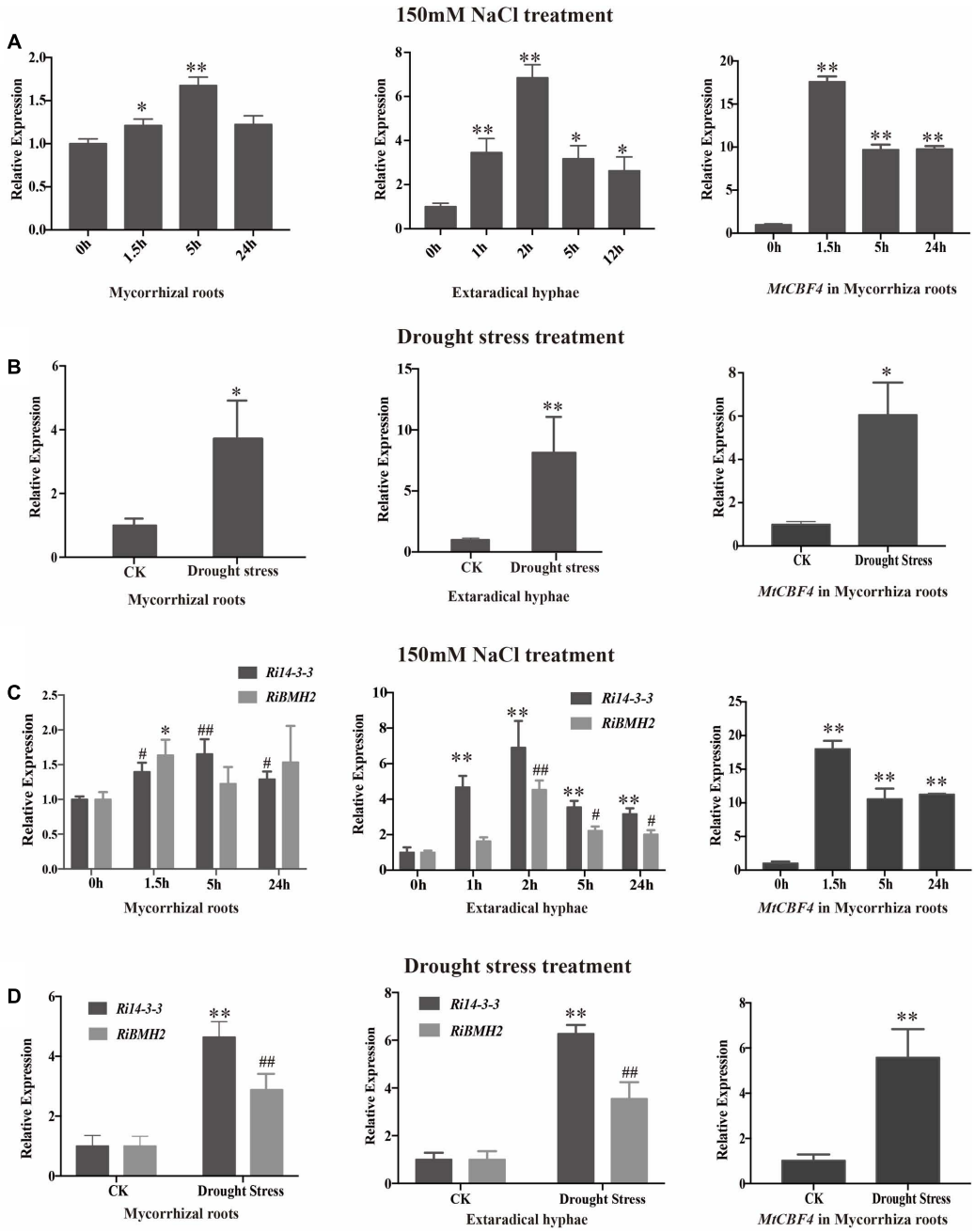

FIGURE 6 | The transcript profile of *14-3-3* in AM symbiosis under drought and osmotic stresses. **(A)** Expression fold change of *Fm201* and *MtCBF4* in mycorrhizal roots, external hyphae or after exposure to osmotic stress treated by 150 mM NaCl for different hours. **(B)** Expression fold change of *Fm201* and *MtCBF4* in mycorrhizal roots, external hyphae under drought stress. **(C)** Expression fold change of *Ri14-3-3, RiBMH2* and *MtCBF4* in mycorrhizal roots, external hyphae after exposure to osmotic stress treated by 150 mM NaCl for different hours. Lines with a significant ratio to the express rate of *Ri14-3-3, RiBMH2 or MtCBF4* in 0 h. **(D)** Expression fold change of *Ri14-3-3, RiBMH2, MtCBF4* in mycorrhizal roots, external hyphae. The *FmActin*, *RiActin* or *MtTEF* was used as the reference gene. Three biological replicates were analyzed. Asterisks indicate statistically significant differences from respective control lines. Lines with a significant ratio to the express rate of *Ri14-3-3, RiBMH2 or MtCBF4* in CK. Error bars indicate the means of three biological replicates with SD values. Data shown are averages ± SD; $n = 3$. (#, $^{*}p < 0.05$, ##, $^{**}p < 0.01$).

fungal proteins share the same nine α-helix domain topologies. Among them, *Ri14-3-3* gene from *R. irregularis* has been firstly reported by Porcel et al. (2006). Moreover, RNA-seq data presented a significant induction *in planta* phase compared to spores (Tisserant et al., 2012). Only the investigation within genomic and transcriptomic data in AM fungi will clarify whether *Fm201*-related sequences are a general feature among fungi. Consistent with the previous *in silico* analyses, these three Fm201,

Ri14-3-3 and RiBMH2 are able to complement the yeast *BMH1* and *BMH2* double mutants. This finding is in agreement with those data reported in the earlier studies (van Heusden et al., 1995, 1996), indicating that these genes identified above encode the functional 14-3-3-like proteins in AM fungi. Further studies need to be carried out to confirm whether these 14-3-3-like proteins identified are a conserved feature of Glomeromycota and whether they may have an essential role in the intraradical phase during interaction with the host plants.

The transcription of *14-3-3* genes show a clear increase in the germinating spores as well as the intraradical phase in both *R. irregularis* and *F. mosseae*. The data stemming from the time-course experiment presented that the relatively higher transcription levels were achieved in the phases of root penetration and arbuscules formation, while the expression levels of *Fm201* and *Ri14-3-3* are obviously reduced compared with *RiBMH2* in the degenerating mycorrhizal roots. In addition, we also correlated the *Fm201* mRNA abundance with the morphological structures of *F. mosseae* inside the roots (at 12–50 dpi). The results of *Fm201* transcription patterns also suggest that it may play an important role in the germination and hyphopodium formation of *F. mosseae*, which was also proposed by Breuninger and Requena (2004) through SSH of AM symbiosis at the early stage. In addition, transcript levels of *Fm201* remain higher during the symbiotic stage (see **Figure 4B**), suggesting that this 14-3-3 protein may also play important roles during AM symbiosis, especially the formation of arbuscule besides the root penetration stage. It is thus speculated that the expression of *14-3-3s* are, to some extent, related to root penetration and arbuscules formation. This hypothesis is supported by the evidence that *14-3-3* transcripts were present in both the laser micro-dissected arbuscule-containing cells and the IRM including intercellular hyphae (Tisserant et al., 2012). Overall these data implicate a relationship between AM fungal 14-3-3 related genes and intraradical hyphal growth and arbuscule differentiation.

Two AM Fungal 14-3-3 Protein Subunits Have the Impacts on the Success of Arbuscular Mycorrhizal Colonization and Arbuscule Formation

The potential involvement of AM fungal 14-3-3 genes *Ri14-3-3* and *RiBMH2* in the *in planta* phase of the colonization process was also supported by the HIGS of *Ri14-3-3* and/or *RiBMH2* during the *M. truncatula–R. irregularis* mycorrhizal symbiosis. Lacking the stable genetic transformation protocols for AM fungi, HIGS was confined to AM fungi (Helber et al., 2011; Xie et al., 2016).

The data of the knock-down of both *Ri14-3-3* and *RiBMH2* genes by HIGS resulting in the impaired arbuscule formation of *R. irregularis* suggest the significance of these AM fungal 14-3-3 proteins for AM symbiosis. Connecting with the transcripts of *RiBMH2* during *M. truncatula–R. irregularis* mycorrhizal symbiosis, *RiBMH2* may be required for the development of AM symbioses and the arbuscule differentiation within roots. However, the *Ri14-3-3* RNAi roots colonized by *R. irregularis* exhibited a considerable arbuscule abundance as compared with control mycorrhizal roots. These findings suggest that the AM functionality or arbuscule formation is redundantly regulated by the two 14-3-3-like genes in *R. irregularis*. Nevertheless, we here propose that *RiBMH2* is essential for arbuscule formation, whereas *Ri14-3-3* could be involved in the colonization process but not AM functionality. This hypothesis is supported by the evidence that the transcripts of *MtPT4* and *RiMST2*, two symbiotic genes responsible for arbuscule functionality, were strongly reduced in *Ri14-3-3*/*RiBMH2* RNAi roots, while they were not repressed in *Ri14-3-3* RNAi roots. Although *Ri14-3-3* homologous gene *RiBMH2* is identified in the *R. irregularis* draft genome (Tisserant et al., 2013; Lin et al., 2014) and *RiBMH2* was not down-regulated in *Ri14-3-3* RNAi roots (see **Figure 5B**), the normal AM fungal structures observed in this HIGS system indicate a novel but unknown role for *Ri14-3-3* in the establishment of AM symbiosis. Based on the above findings and the previous study (Liu et al., 2015), we hypothesize that RiBMH2-mediated signal could be an important signal in the control of arbuscules formation and *R. irregularis* hyphal growth within roots. This unknown signal relayed by RiBMH2 serves as the essential signal to ensure the metabolic activity of *R. irregularis* in the hyphal growth and/or arbuscule differentiation during symbiosis. In the absence of this RiBMH2-mediated signal, the arbuscules are impaired, and growth of the fungus is prevented. The *R. irregularis* itself needs to activate 14-3-3 protein RiBMH2 in response to the environmental clues to meet demands during fungal growth and division. In addition, our functional analysis in yeast cells suggested that *Ri14-3-3* and *RiBMH2* encode functional signal proteins involved in growth induction (see **Figures 2B,C**), indicating that these two proteins may play potential roles in signal transduction during the colonization process and arbuscule formation, respectively. Thus, we can speculate the involvement of Ri14-3-3 in fine-tuning fungal growth in the intraradical phase responding to the external stimuli, moreover, RiBMH2 may be indispensable for arbuscules differentiation. This complex mechanism by which arbuscular mycorrhizas are formed in roots requires the elaborate control of the two AM fungal 14-3-3 proteins in the intraradical phase during cross-talk with host plant.

Remarkably, these results from the HIGS experiments revealed that one 14-3-3 protein subunit can adjust its own expression quantity to offset the adverse influence caused by the lack of another 14-3-3 protein subunit. This conclusion is consistent with the previous results derived from yeast system (van Heusden et al., 1995). Based on this point, it is reasonable to hypothesize that the AM fungal 14-3-3 proteins are indispensable for the symbiosis functioning.

Involvement of AM Fungal 14-3-3 Proteins in Msn2/STRE Element-Mediated Signaling Pathway

The knockdown of both *Ri14-3-3* and *RiBMH2* by HIGS exhibits somewhat distinct phenotypes, i.e., fewer arbuscule abundance and impaired arbuscules (see **Figures 5A,C**), repression of the

endosymbiosis functioning with regard to transcription of the symbiotic *MtPT4* and *MST2* genes (see **Figures 5D,E**). We hypothesize that there exists a positive feedback mechanism in the potential signaling pathway in *R. irregularis*. It is also proposed that the CREs upstream of a gene always show close relationship with its function, especially for the regulatory proteins (Carey et al., 2012; Petrov et al., 2012), although most CREs are composed of short sequences which may be very abundant in eukaryotic genomes (van Heusden, 2009). As expected, we observed some conserved motifs including STRE elements in the promoters of two AM fungal 14-3-3 genes *Fm201* and *RiBMH2* (see **Table 1**), as predicted by YEASTRACT database, in comparison with the promoters of yeast *BMH1* and *BMH2*. Interestingly, the deletion of STRE (CCCCT/AGGGG) element in the promoter of Fm201 showed significantly reduced levels of the reporter gene mRNAs when expressed in yeast cells (see **Figure 3A**). These hypotheses mentioned above are also supported by the fact that the orthologous *Fm201* gene promoter with STRE element (pFm201) directly interacts with transcription factor Msn2 in yeast cells (see **Figure 3B**). Furthermore, this recognition between RiMsn2 and pFm201 may contribute to the induction of *Fm201* in extraradical hyphae in response to the salinity (150 mM NaCl treatment) stress (see **Figure 6A**). Therefore, based on the site-specific mutagenesis and the yeast one-hybrid analyses, the transcription of AM fungal 14-3-3-like genes during AM symbiosis is Msn2/STRE-element dependent. The zinc finger DNA-binding proteins Msn2 and Msn4 serve as the key factors that controlling fungal growth and stress responses in different fungal species (Martinez-Pastor et al., 1996; Schmitt and Mcentee, 1996; Liu et al., 2013; Zhang et al., 2014). In addition, the Msn2-controlled and STRE-driven gene *Fm201* and *RiBMH2* from *F. mosseae* and *R. irregularis*, respectively, are positively regulated in response to drought stress during AM symbiosis (see **Figures 6B,D**), reinforcing that AM fungal 14-3-3 genes participate in the Msn2/STRE element-mediated signaling pathway in AM fungal symbiont during AM symbiosis.

Overall these data presented in this study provided new insights into the signaling function of the 14-3-3 proteins in AM fungal cells during crosstalk with host plants. Based on the aforementioned data, we also propose the hypothesis that abiotic stresses such as salinity and drought affect a Msn2/STRE-mediated signaling pathway governing the expression of AM fungal 14-3-3 proteins that promoted fungal colonization and arbuscule formation within roots (see **Figure 7**). In the first version of the scheme for abiotic stresses induced signaling, it has been proposed that 14-3-3 proteins preferentially expressed in the intraradical phase are involved in AM fungal colonization process and arbuscule functionality by the regulation of Msn2/STRE-mediated signaling pathway that may control the fungal growth and arbuscule lifespan during AM symbiosis.

Further studies, such as characterizing the precise roles of the novel *RiMsn2* gene identified in this work, validating the protein-protein interactions in the Msn2-mediated signaling pathway and the biochemical functions of core components of this pathway, and determining the direct evidence of Msn2-dependent mechanisms in *R. irregularis*, are needed to define the underlying stress response mechanisms in AM symbionts. Furthermore, the RNA-seq data and gene expression analyses show that both *R. irregularis* and *Gigaspora margarita* contain multiple distinct MAPK (Mitogen-activated protein kinase)-related proteins (Tisserant et al., 2012; Salvioli et al., 2016; Xie et al., 2016), indicative of the presence of MAPK signaling cascade in AM fungi to respond to external stresses stimuli and adapt to environmental fluctuation. Thus, a major goal in this field will be to uncover a master MAPK protein regulating the AM fungal growth and differentiation during symbiosis under various abiotic stresses.

In summary, we showed that *Fm201*, *Ri14-3-3* and *RiBMH2*, three genes from two different AM fungi, are preferentially expressed in the intraradical phase and may have impacts on the success of AM colonization and arbuscule formation. Our data also presented that Msn2 protein governs the *Fm201*

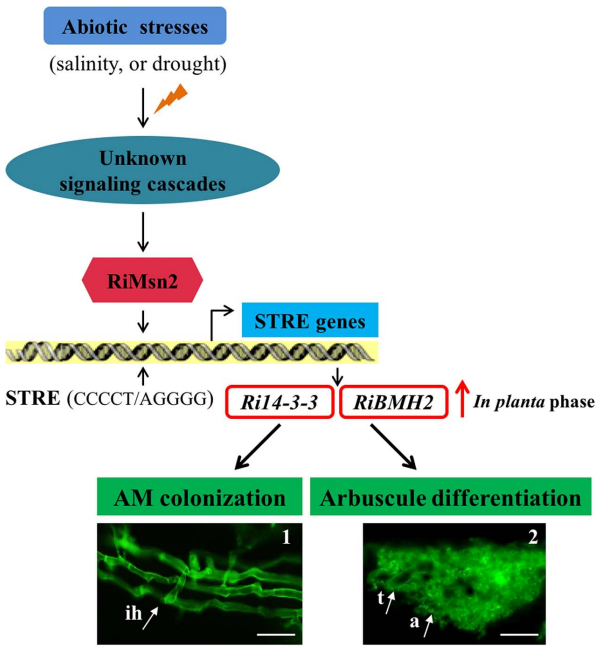

FIGURE 7 | Proposed Working Model of two 14-3-3 proteins in *R. irregularis*. Schematic representation of the abiotic stresses-induced signaling cascades in AM fungi and the involvement of *Ri14-3-3* and *RiBMH2* genes in the RiMsn2/STRE-mediated signaling pathway during AM symbiosis. In AM fungi, the unknown signaling cascades are triggered by the external stress stimuli such as salinity or drought; then the core component RiMsn2 factor is activated by the upstream of potential cascades. The functional RiMsn2 is translocated to the nuclear to recognize the STRE (Stress response element) (CCCCT/AGGGG) on the AM fungal genome. Meanwhile, in the *in planta* phase, transcription of the STRE genes, including Ri14-3-3 and RiBMH2, are clearly induced after this interaction between RiMsn2 and STRE. Thus, the expression of Ri14-3-3 and RiBMH2 proteins are involved in or essential for AM colonization and arbuscule differentiation within roots. The black arrows indicate the positive interactions, while the red arrow suggests the induction of *Ri14-3-3* and *RiBMH2* genes in the *in planta* phase. The images 1 and 2 represent the intraradical hyphae and arbuscule from WGA488 staining. ih, intraradical hyphae; t, trunk; a, arbuscule. Scale bars represent 25 μm.

gene transcription, indicating that AM fungal 14-3-3 gene identified is involved in Msn2 factor/STRE element-mediated signaling pathway. Importantly, host-induced gene silencing of both *Ri14-3-3* and *RiBMH2* impairs the arbuscule differentiation within roots, indicating that the two AM fungal 14-3-3 protein subunits are required for arbuscule formation. Additionally, these AM fungal 14-3-3 genes are up-regulated in response to salinity and drought stresses during AM symbiosis. Based on these new findings, we propose that the AM fungal *14-3-3* genes are essential for the interaction between AM fungi and host plants, and are potentially involved in enhancing plant salinity and drought tolerance by Msn2/STRE element-controlled signaling.

MATERIALS AND METHODS

Biological Materials and Growth Conditions

A-grade spores of *R. irregularis* DAOM197198 were purchased from Agronutrition (Carbonne, France). Spores of *F. mosseae* BEG12 were kindly provided by the International Bank of Glomeromycota (IBG, Dijon, France) and collected from *Medicago truncatula* pot cultures by wet sieving to isolate genomic DNA and total RNA. Spores surface sterilized by 2% chloramine T, and then immersed in a solution containing 0.02% streptomycin and 0.02% gentamycin for 10 min (Besserer et al., 2008). Germinated spores of *F. mosseae* were selected from acetone solution containing 10^{-8}mol/L GR24 (10^{-9}mol/L GR24 for *R. irregularis* in two days) in 25°C dark incubator. Quiescent spores, germination spores and mycorrhizal roots (at 10, 18 25, 50 dpi for *F. mosseae*; 8, 12, 18, 40 dpi for *R. irregularis*) were harvested. After washing in sterile water, all materials described above were immediately frozen in liquid nitrogen and stored at −80°C before nucleic acid extraction.

The water-holding capacity of the soil was computated before planting. The soil was weighed before plant, watered uniformly until flowed from the bottom. Keep the pot suspended in midair for 1 day before weighing. The increase weight of soil after waterd is water-holding capacity. *M. truncatula* mycorrhizal roots inoculated with AM fungi were treated with NaCl (0.5 M) to 150 mM in final concentration (Calculate according to 70% of water holding capacity in soil) (Giovannetti et al., 2001; Li et al., 2011). Drought treatment was measured by 1/2 water-holding capacity treatment which was proved drought stress treatment to *M. truncatula* in previous experiments. Mycorrhizal roots and extraradical hyphae from sandwich system were harvested at 1.5, 5, 24 h after treatments (Abdel Latef and Chaoxing, 2011; Estrada et al., 2012) to monitor the transcript profiles of *14-3-3* genes under different abiotic stresses by qRT-PCR analysis.

Fm201 promoter-YGFP chimeric gene in *S. cerevisiae* BY4741 was treated with NaCl (500 mM), $CuSO_4$ (50 mM), $CdCl_2$ (0.2 mM), PEG4000 (25%), and 37°C abiotic stresses in YPD medium and then harvested after 1h treatments (Vido et al., 2001).

DNA and RNA Extraction, RT-PCR and Real Time RT-PCR

The total DNA was isolated from AM fungal sporescarps as described by Zézé et al. (1994). Total RNA of different AM fungal tissues was extracted with TRIzol reagent (Invitrogen) according to the protocol. Surface-sterilized spores were placed into 1.5 ml RNase free microtube and then frozen in liquid nitrogen, 0.3ml TRIzol solution was immediately added to the microtube. Electric mill (TIANGEN OSE-Y20, Beijing, China) and Phase Lock Gel (TIANGEN, Beijing, China) were used to make sure the quality of RNA. Total RNA yields and concentrations were measured by the Thermo NanoDrop 2000 spectrophotometer (Thermo). To remove residual genomic DNA, each total RNA sample was treated with RNase-free DNaseI (Thermo) according to the manufacturer's instructions. The first cDNA strand was synthesized as described in RevertAid First Strand cDNA Synthesis Kit (Thermo).

Transcript profiles of AM fungal genes *Fm201*, *Ri14-3-3*, and *RiBMH2* as well as host plant genes *MtSbtM1* and *MtCBF4* in different symbiotic stages and under abiotic stresses were studied by qRT-PCR using ViiA 7 system (Life Technologies, United States), three biological replications were performed. The expression levels were normalized to transcripts of the β-*actin* gene of *F. mosseae* or *R. irregularis* and to transcripts of the *MtTEF* gene of *M. truncatula* (Hohnjec et al., 2005). Before real time RT-PCR, gene-specific primers for all target genes were validated on genomic DNA and cDNA. Total RNA was isolated from AM roots comprised plant and fungal materials. The specificity of the primer pairs were also confirmed via PCR method on *M. truncatula* total DNA. No amplification signals were present on plant DNA. The primers sequences for all genes studied in this work are provided in Supplementary Table S2. qRT-PCR was performed using SYBR Green Real-time PCR Master Mix (TOYOBO, Japan) according to the manufacturer's instructions. Each 10 μl reaction contained 1 μl of the synthesized cDNA (cDNA pool was diluted to 200 μl), 5 μl SYBR Green Real-time PCR Master Mix, 0.5 μl each primer(10 μM), 3 μl ddH_2O. PCR program consisted of a 30 s incubation at 95°C to active the hot-start recombinant Taq DNA polymerase, followed by 40 cycles of 10 s at 95°C, 15 s at 57°C, and 20 s at 72°C. The relative levels of transcripts were calculated by using the $2^{-\Delta\Delta ct}$ method (Livak and Schmittgen, 2001).

Cloning of *Fm201* Gene From *F. mosseae*

The *Fm201* EST sequence was obtained from NCBI (Accession number: CF803281), (Breuninger and Requena, 2004). Reverse PCR was utilized to get the 5′ flanking sequence of *Fm201* gene. The gene-specific primers 201F and 201R were designed to amplify the partial DNA fragment of *Fm201* according to the available sequence of *Fm201* EST. Genomic DNA of *F. mosseae* was digested by FastDigest restriction enzyme *Xho*I (Thermo). DNA fragments were self-ligated by T_4 DNA ligase, and the reaction was carried out in a final volume of 20 μl containing 0.5 μl digested DNA fragments, 2 μl 10× buffer, 0.5 μl T_4 DNA ligase (Thermo), 17 μl ddH_2O, incubated for 12 h at 10°C. Nest-PCR was performed in this experiment, 0.5 μl ligated

production was used as PCR template, the specific primers used in the first PCR reaction were 201RF1 and 201RR1, products from first PCR reaction were diluted to 1/1000 as the template for the second PCR reaction, and specific primer 201RF2 and 201RR2 were used.

RACE as a classic method to rapidly obtain the 5′ and 3′ ends of the *Fm201* gene (Scotto-Lavino et al., 2006a,b). 3′RACE was carried out on the total RNA from *F. mosseae* sporecarps by using primer Q_T. Two pairs of primers RACE201F/Q_O and RACE201F2/Q_I were used for the subsequent nest PCR reactions, respectively. Due to the high A/T containing feature of AM fungi genomic DNA, the dGTP and Q_C replaced the dATP and Q_T used in classic 5′RACE, responsively. The first cDNA strand was obtained from *F. mosseae* sporocarps by using specific primer RACE201R1. Primers Q_C, Q_o and RACE201R2 were used as the first PCR cycle primers, while primers Q_I and RACE201R3 were used as the second PCR cycle. Transfast *pfu* DNA polymerase (Transgen, Beijing, China) was used in the PCR reactions mentioned above, PCR products were cloned into pEASY-Blunt vector (Transgen, Beijing, China) and sequenced.

Plasmids Construction

Plasmid pMR12 was generated from pMRI-11(Xie et al., 2014), the promoter of Gal7 was amplified from the genome DNA of *S. cerevisiae* BY4741 by PCR using the specific primers P_{Gal7}F/P_{Gal7}R. P_{Gal7} and pMR-11 were digested with both *Sac*I and *Spe*I, respectively, then the digests were cloned into target vector pMR-11. To address the regulation of CREs located in the promoter of *Fm201*, the expression profiles of YGFP reporter were conducted in *S. cerevisiae* BY4741. Monoclonal vector pUG35 carrying a YGFP reporter is used in yeast heterologous systems (Cormack et al., 1997). Two restriction sites were *Sac*I and *Xba*I, which were added to the start codon upstream sequence of *Fm201* (pFm201) by using primers 201PFn (n = 1,2,3,4) and 201PR1, then cloned into pUG35 to replace P_{MET-25} to produce a series of 5′ truncated promoters-reporter vectors. pFm201 targeted deletion of *cis*-element was conducted by using SOE-PCR method (Ho et al., 1989). The specific primers used are provided in Supplementary Table S2). The site-directed mutation promoter sequences were also cloned into pUG35 as the promoter truncated verification vectors. qRT-PCR was used for monitoring transcriptional efficiency of *Fm201*, the *Ura* gene of pUG35 was chosen as the internal standard, primers UraF, UraR, YGFPF, YGFPR were used in this experiment (Peter et al., 2006).

Yeast One-Hybrid Screening

Yeast one hybrid experiment was carried out using the Matchmaker One-hybrid System (Clontech), the ORF of *GintSTE* was cloned from cDNA of *Rhizophagus irregularis* by using primers RiSTE12F and RiSTE12R, and cloned into pGADT7-rec2. Two same 272 bp length promoter fragments contained STE12 targeted *cis*-element STRE were cloned into pHIS2 in tandem, the same fragment only lacking the *cis*-element STRE was also inserted into the pHIS2 as a negative control. Yeast one-hybrid experiment of Msn2 was carried out in the same way and the primers RiMsn2F and RiMsn2R were used as mentioned in Supplementary Table S2.

Plasmids for yeast one-hybrid were co-transformed into yeast Y187 strain. Y187 cells carrying the target plasmids were cultivated in SD medium lacking leucine and tryptophan, and were also gradiently inoculated at 1.0 OD_{600} on SD medium lacking leucine, histidine and tryptophan and supplemented with 30 mM 3-AT, which is a competitive inhibitor of the His3 protein.

HIGS of *R. irregularis* 14-3-3 Genes in Hairy Root Lines of *M. truncatula*

The RNAi-target sequences of *Ri14-3-3* and *RiBMH2* were amplified by the specific primers Ri14-3-3F/Ri14-3-3R and RiBMH2ATG/RiBMH2F. The PCR products were cloned to the linearized pDONR221 used CloneExpressII (Vazyme, Nanjing, China), then the LR reaction was done to recombine the target sequences into the pK7GWIWG2(II)RR according to the instructions in Gateway protocol.

Agrobacterium rhizogenes Msu440-mediated root transformation was performed following the method as described in *Medicago Truncatula* Handbook (International Committee, 2006). *In vitro* hairy roots were cultured on EM plates containing Benzyl penicillin (200 mg/L) for three times. The root tip (2∼3 cm in length) was used for each subculture. The root was re-cultured in the M medium without antibiotics for half a month. The hairy root lines without bacteria were re-cultured in new M medium for mycorrhization. Mycorrhizal hairy root of *P. crispum* without DsRed tag was cut into small pieces (∼3 mm) and placed around the hairy root of *M. truncatula* harboring DsRed marker as described in Supplementary Figure S3. The mycorrhizal roots with red fluorescence were harvested in one month until the external hyphae of *R. irregularis* beyond the hairy root surface of *M. truncatula*.

Quantification of Arbuscular Mycorrhizal Colonization

Mycorrhizal roots collected from pot cultures were stained with 0.1% Typan blue, while the mycorrhizal hairy roots expressing red fluorescence grown on plates were stained with WGA488, and the estimation of AM colonization was performed as described by Trouvelot et al. (2015) using MYCOCALC program[2].

In Silico Analysis of Fm201 Protein

The deduced amino acid sequence of Fm201 was analyzed with the computer program DNAstar. Multiple sequence alignments were performed by DNAMAN8. The unrooted phylogenetic tree constructed by neighbor-joining algorithm was carried out using MEGA6. The computation of physical and chemical parameters was conducted by using ProtParam tool[3]. Homology modeling of the three-dimensional structure of Fm201 protein was done with the program Swiss Model[4] using *Homo sapiens* 14-3-3ε protein (2br9A) as the template (**Figure 1B**; Yang et al., 2006). The *cis*-elements of the promoters *Fm201* and *RiBMH2* were analyzed on YEASTRACT[5] using *S. cerevisiae* S288c as the reference.

[2]http://www2.dijon.inra.fr/mychintec/Mycocalc-prg/download.html

[3]http://www.expasy.ch/tools/protparam.html

[4]http://swissmodel.expasy.org/

[5]http://www.yeastract.com/

Yeast mutant strains used in this article are constructed with the methods mentioned by van Heusden (van Heusden et al., 1995, 1996). The detail information for each strain is available at Supplementary Table S1. In the construction of *bhms-Fm201*(MATa; his3Δ1; leu2Δ0; met15Δ0; ura3Δ0; BMH1::KanMX (Gal7[*Fm201*]); BMH2::ura3), fragments of pMRI-12 which contain a KanMX and a Gal7 promoter and pSH47 which contain a Ura3 marker were used to replace BY4741, BMH1 and BMH2, respectively, by primers PMRI-12F1, PMRI-12R1 and PSH47F, PSH47R. The *bmhs*-Ri14-3-3 and *bmhs*-RiBMH2 were also built in the same way.

Statistical Analyses

Statistical analyses were performed through one-way ANOVA. Following ANOVA, Tukey's test was performed to make comparisons between treatments, using a probability level of $p < 0.05$(*, #), $0.05 \leq p < 0.01$ (**, ##). All statistical analyses were performed using SPSS statistical package (version 23.0, SPSS Inc., United States).

ACCESSION NUMBERS

The sequence data can be found in the GenBank data libraries under accession numbers. Nucleic acid sequence: *MtCBF4* (HQ110079.1), *MtStbM1* (XM_003611148.1), *MtPT4 (*AY116211.1), *Fmactin* (KM360085.1), *Fm201* (KM258580.1), *Riactin* (EXX64987.1), *RiBMH2* (*JEMT01016782.1*), *Ri14-3-3* (AM049264.1), *RiMST2* (HM143864.1), Ri14-3-3 (CAJ16742.1). Amino acid sequence: Fm201(KM258580), RiBMH2 (EXX69786.1), *R. oryzae* 14-3-3 (EIE87660.1), *M. medusa* 14-3-3 (ABS86241.1), *M. circinelloides* 14-3-3 (EPB82885.1), *A. oryzae* 14-3-3 (XP_001819291.2), *A. niger* 14-3-3 (XP_001399080.1), *S. borealis* 14-3-3 (ESZ95350.1), *M. oryzae* 14-3-3 (XP_003710925.1), *A. nidulans* (CBF81292.1), *A. terreus* 14-3-3 (XP_001212078.1), *P. strigosozonata* 14-3-3 (XP_007382290.1), *S. musiva* 14-3-3 (EMF09853.1), *B. bassiana* 14-3-3 (XP_008601347.1), *R. solani* 14-3-3 (CCO32840.1), *S. cerevisiae* BMH1 (CAA46959.1), *S. tuberosum* 14-3-3 (XP_004250139.1), *O. sativa* 14-3-3 (NP_001047234.1), *S. cerevisiae* BMH2 (CAA59275.1), *R. norvegicus* 14-3-3ε (NP_113791.1), *H. sapiens* 14-3-3ε (NP_006752.1).

AUTHOR CONTRIBUTIONS

BZ and XXie conceived this research. ZS and JS prepared the biological material for gene expression analysis. ZS and XXin performed the data analysis. ZS and XXie wrote the manuscript. BZ and XXie revised the manuscript.

FUNDING

This study was financially supported by grant from the Natural Science Foundation of China (Grant No. 31270159).

ACKNOWLEDGMENTS

We are grateful to Professor Ton Bisseling, Ph.D. U. Gueldener and Ph.D. Wenping Xie for kindly providing the pK7GWIWG2 (II) RR, pUG35 and pMR-11 plasmids, respectively. We also thank Professor Deqiang Duanmu for the constructive discussions and language corrections during the manuscript preparation.

SUPPLEMENTARY MATERIAL

The Supplementary Material for this article can be found online at: https://www.frontiersin.org/articles/10.3389/fmicb.2018.00091/full#supplementary-material

REFERENCES

Abdel Latef, A. A. H., and Chaoxing, H. (2011). Effect of arbuscular mycorrhizal fungi on growth, mineral nutrition, antioxidant enzymes activity and fruit yield of tomato grown under salinity stress. *Sci. Hortic.* 127, 228–233. doi: 10.1016/j.scienta.2010.09.020

Aksamit, A., Korobczak, A., Skala, J., Lukaszewicz, M., and Szopa, J. (2005). The 14-3-3 gene expression specificity in response to stress is promoter-dependent. *Plant Cell Physiol.* 46, 1635–1645. doi: 10.1093/pcp/pci179

Augé, R. M. (2001). Water relations, drought and vesicular-arbuscular mycorrhizal symbiosis. *Mycorrhiza* 11, 3–42. doi: 10.1007/s005720100097

Bago, B., Pfeffer, P. E., and Shachar-Hill, Y. (2000). Carbon metabolism and transport in arbuscular mycorrhizas. *Plant Physiol.* 124, 949–958. doi: 10.1104/pp.124.3.949

Ballou, E. R., Kozubowski, L., Nichols, C. B., and Alspaugh, J. A. (2013). Ras1 acts through duplicated Cdc42 and Rac proteins to regulate morphogenesis and pathogenesis in the human fungal pathogen Cryptococcus neoformans. *PLoS Genet.* 9:e1003687. doi: 10.1371/journal.pgen.1003687

Besserer, A., Bécard, G., Jauneau, A., Roux, C., and Séjalon-Delmas, N. (2008). GR24, a synthetic analog of strigolactones, stimulates the mitosis and growth of the arbuscular mycorrhizal fungus *Gigaspora rosea* by boosting its energy metabolism. *Plant Physiol.* 148, 402–413. doi: 10.1104/pp.108.121400

Bonfante, P., and Genre, A. (2010). Mechanisms underlying beneficial plant–fungus interactions in mycorrhizal symbiosis. *Nat. Commun.* 1:48. doi: 10.1038/ncomms1046

Bonfante, P., and Genre, A. (2015). Arbuscular mycorrhizal dialogues: do you speak 'plantish'or 'fungish'? *Trends Plant Sci.* 20, 150–154. doi: 10.1016/j.tplants.2014.12.002

Bonfante, P., and Requena, N. (2011). Dating in the dark: how roots respond to fungal signals to establish arbuscular mycorrhizal symbiosis. *Curr. Opin. Plant Biol.* 14, 451–457. doi: 10.1016/j.pbi.2011.03.014

Bravo, A., Brands, M., Wewer, V., Dörmann, P., and Harrison, M. J. (2017). Arbuscular mycorrhiza-specific enzymes fatm and ram2 fine-tune lipid biosynthesis to promote development of arbuscular mycorrhiza. *New Phytol.* 214, 1631–1645. doi: 10.1111/nph.14533

Breuninger, M., and Requena, N. (2004). Recognition events in AM symbiosis: analysis of fungal gene expression at the early appressorium stage. *Fungal Genet. Biol.* 41, 794–804. doi: 10.1016/j.fgb.2004.04.002

Bruckmann, A., Steensma, H. Y., Mj, T. D. M., and Van Heusden, G. P. (2004). Regulation of transcription by *Saccharomyces cerevisiae* 14-3-3 proteins. *Biochem. J.* 382, 867–875. doi: 10.1042/BJ20031885

Cappellazzo, G., Lanfranco, L., and Bonfante, P. (2007). A limiting source of organic nitrogen induces specific transcriptional responses in the extraradical

structures of the endomycorrhizal fungus *Glomus intraradices*. *Curr. Genet.* 51:59. doi: 10.1007/s00294-006-0101-2

Carey, M. F., Peterson, C. L., and Smale, S. T. (2012). Identifying cis-acting DNA elements within a control region. *Cold Spring Harb. Protoc.* 2012, 279–296. doi: 10.1101/pdb.top068171

Chitarra, W., Pagliarani, C., Maserti, B., Lumini, E., Siciliano, I., Cascone, P., et al. (2016). Insights on the impact of arbuscular mycorrhizal symbiosis on tomato tolerance to water stress. *Plant Physiol.* 171, 00307.2016. doi: 10.1104/pp.16.00307

Cormack, B. P., Bertram, G., Egerton, M., Gow, N. A., Falkow, S., and Brown, A. J. (1997). Yeast-enhanced green fluorescent protein (yEGFP): a reporter of gene expression in *Candida albicans*. *Microbiology* 143, 303–311.

Darling, D. L., Yingling, J., and Wynshaw-Boris, A. (2005). Role of 1433 proteins in eukaryotic signaling and development. *Curr. Top. Dev. Biol.* 68, 281–315. doi: 10.1016/S0070-2153(05)68010-68016

Elfving, N., Chereji, R. V., Bharatula, V., Bjorklund, S., Morozov, A. V., and Broach, J. R. (2014). A dynamic interplay of nucleosome and Msn2 binding regulates kinetics of gene activation and repression following stress. *Nucleic Acids Res.* 42, 5468–5482. doi: 10.1093/nar/gku176

Estrada, B., Barea, J. M., Aroca, R., and Ruiz-Lozano, J. M. (2012). A native Glomus intraradices strain from a Mediterranean saline area exhibits salt tolerance and enhanced symbiotic efficiency with maize plants under salt stress conditions. *Plant Soil* 366, 333–349. doi: 10.1007/s11104-012-1409-y

Gancedo, J. M. (2001). Control of pseudohyphae formation in *Saccharomyces cerevisiae*. *FEMS Microbiol. Rev.* 25, 107–123.

Genre, A., Chabaud, M., Timmers, T., Bonfante, P., and Barker, D. G. (2005). Arbuscular mycorrhizal fungi elicit a novel intracellular apparatus in *Medicago truncatula* root epidermal cells before infection. *Plant Cell* 17, 3489–3499. doi: 10.1105/tpc.105.035410

Gianinazzi, S., Gollotte, A., Binet, M. N., van Tuinen, D., Redecker, D., and Wipf, D. (2010). Agroecology: the key role of arbuscular mycorrhizas in ecosystem services. *Mycorrhiza* 20, 519–530. doi: 10.1007/s00572-010-0333-3

Giovannetti, M., Fortuna, P., Citernesi, A. S., Morini, S., and Nuti, M. P. (2001). The occurrence of anastomosis formation and nuclear exchange in intact arbuscular mycorrhizal networks. *New Phytol.* 151, 717–724. doi: 10.1046/j.0028-646x.2001.00216.x

Govindarajulu, M., Pfeffer, P. E., Jin, H., Abubaker, J., Douds, D. D., Bücking, H., et al. (2005). Nitrogen transfer in the arbuscular mycorrhizal symbiosis. *Nature* 435, 819–823. doi: 10.1038/nature03610

Gutjahr, C., and Parniske, M. (2013). Cell and developmental biology of arbuscular mycorrhiza symbiosis. *Annu. Rev. Cell Dev. Biol.* 29, 593–617. doi: 10.1146/annurev-cellbio-101512-122413

Harrison, M. J. (2012). Cellular programs for arbuscular mycorrhizal symbiosis. *Curr. Opin. Plant Biol.* 15, 691–698. doi: 10.1016/j.pbi.2012.08.010

Harrison, M. J., Dewbre, G. R., and Liu, J. (2002). A phosphate transporter from *Medicago truncatula* involved in the acquisition of phosphate released by arbuscular mycorrhizal fungi. *Plant Cell* 14, 2413–2429. doi: 10.1105/tpc.004861

Helber, N., and Requena, N. (2008). Expression of the fluorescence markers dsred and gfp fused to a nuclear localization signal in the arbuscular mycorrhizal fungus glomus intraradices. *New Phytol.* 177, 537–548. doi: 10.1111/j.1469-8137.2007.02257.x

Helber, N., Wippel, K., Sauer, N., Schaarschmidt, S., Hause, B., and Requena, N. (2011). A versatile monosaccharide transporter that operates in the arbuscular mycorrhizal fungus glomus sp is crucial for the symbiotic relationship with plants. *Plant Cell* 23, 3812–3823. doi: 10.1105/tpc.111.089813

Hermeking, H., and Benzinger, A. (2006). 14-3-3 proteins in cell cycle regulation. *Semin. Cancer Biol.* 16, 183–192. doi: 10.1016/j.semcancer.2006.03.002

Ho, S. N., Hunt, H. D., Horton, R. M., Pullen, J. K., and Pease, L. R. (1989). Site-directed mutagenesis by overlap extension using the polymerase chain reaction. *Gene* 77, 51–59. doi: 10.1007/978-1-4939-6472-7_27

Hohnjec, N., Vieweg, M. F., Pühler, A., Becker, A., and Küster, H. (2005). Overlaps in the transcriptional profiles of *Medicago truncatula* roots inoculated with two different glomus fungi provide insights into the genetic program activated during arbuscular mycorrhiza. *Plant Physiol.* 137, 1283–1301. doi: 10.1104/pp.104.056572

Hurtado, C. A., and Rachubinski, R. A. (2002). YlBMH1 encodes a 14-3-3 protein that promotes filamentous growth in the dimorphic yeast *Yarrowia lipolytica*. *Microbiology* 148, 3725–3735.

Ichimura, T., Isobe, T., Okuyama, T., Yamauchi, T., and Fujisawa, H. (1987). Brain 14-3-3 protein is an activator protein that activates tryptophan 5-monooxygenase and tyrosine 3-monooxygenase in the presence of Ca^{2+},calmodulin-dependent protein kinase II. *FEBS Lett.* 219, 79–82. doi: 10.1155/2017/3682752

International Committee (2006). *Medicago truncatula Handbook*. Ardmore, OK: Samuel Roberts Noble Foundation.

Javot, H., Penmetsa, R. V., Terzaghi, N., Cook, D. R., and Harrison, M. J. (2007a). A *Medicago truncatula* phosphate transporter indispensable for the arbuscular mycorrhizal symbiosis. *Proc. Natl. Acad. Sci. U.S.A.* 104, 1720–1725. doi: 10.1073/pnas.0608136104

Javot, H., Pumplin, N., and Harrison, M. J. (2007b). Phosphate in the arbuscular mycorrhizal symbiosis: transport properties and regulatory roles. *Plant Cell Environ.* 30, 310–322. doi: 10.1111/j.1365-3040.2006.01617.x

Jiang, Y., Wang, W., Xie, Q., Liu, N., Liu, L., Wang, D., et al. (2017). Plants transfer lipids to sustain colonization by mutualistic mycorrhizal and parasitic fungi. *Science* 356, 1172–1175. doi: 10.1126/science.aam9970

Jung, S. C., Martinez-Medina, A., Lopez-Raez, J. A., and Pozo, M. J. (2012). Mycorrhiza-induced resistance and priming of plant defenses. *J. Chem. Ecol.* 38, 651–664. doi: 10.1007/s10886-012-0134-6

Kikuchi, Y., Hijikata, N., Yokoyama, K., Ohtomo, R., Handa, Y., Kawaguchi, M., et al. (2014). Polyphosphate accumulation is driven by transcriptome alterations that lead to near-synchronous and near-equivalent uptake of inorganic cations in an arbuscular mycorrhizal fungus. *New Phytol.* 204, 638–649. doi: 10.1111/nph.12937

Lenoir, I., Fontaine, J., and Lounèshadj, S. A. (2016). Arbuscular mycorrhizal fungal responses to abiotic stresses: a review. *Phytochemistry* 123, 4–15. doi: 10.1016/j.phytochem.2016.01.002

Li, D., Zhang, Y., Hu, X., Shen, X., Ma, L., Su, Z., et al. (2011). Transcriptional profiling of *Medicago truncatula* under salt stress identified a novel cbf transcription factor mtcbf4 that plays an important role in abiotic stress responses. *BMC Plant Biol.* 11:109. doi: 10.1186/1471-2229-11-109

Li, T., Hu, Y. J., Hao, Z. P., Li, H., Wang, Y. S., and Chen, B. D. (2013). First cloning and characterization of two functional aquaporin genes from an arbuscular mycorrhizal fungus glomus intraradices. *New Phytol.* 197, 617–630. doi: 10.1111/nph.12011

Li, T., Sun, Y., Ruan, Y., Xu, L., Hu, Y., Hao, Z., et al. (2016). Potential role of d-myo-inositol-3-phosphate synthase and 14-3-3 genes in the crosstalk between zea mays and rhizophagus intraradices under drought stress. *Mycorrhiza* 26, 1–15. doi: 10.1007/s00572-016-0723-2

Lin, K., Limpens, E., Zhang, Z., Ivanov, S., Saunders, D. G., Mu, D., et al. (2014). Single nucleus genome sequencing reveals high similarity among nuclei of an endomycorrhizal fungus. *PLoS Genet.* 10:e1004078. doi: 10.1371/journal.pgen.1004078

Liu, Q., Li, J. G., Ying, S. H., Wang, J. J., Sun, W. L., Tian, C. G., et al. (2015). Unveiling equal importance of two 14-3-3 proteins for morphogenesis, conidiation, stress tolerance and virulence of an insect pathogen. *Environ. Microbiol.* 17, 1444–1462. doi: 10.1111/1462-2920.12634

Liu, Q., Ying, S. H., Li, J. G., Tian, C. G., and Feng, M. G. (2013). Insight into the transcriptional regulation of msn2 required for conidiation, multi-stress responses and virulence of two entomopathogenic fungi. *Fungal Genet. Biol.* 54, 42–51. doi: 10.1016/j.fgb.2013.02.008

Livak, K. J., and Schmittgen, T. D. (2001). Analysis of relative gene expression data using real-time quantitative PCR and the $2^{\Delta\Delta C_T}$ Method. *Methods* 25, 402–408. doi: 10.1006/meth.2001.1262

Lozano-Duran, R., and Robatzek, S. (2015). 14-3-3 proteins in plant-pathogen interactions. *Mol. Plant Microbe Interact.* 28, 511–518. doi: 10.1094/MPMI-10-14-0322-CR

Maldonado-Mendoza, I. E., Dewbre, G. R., and Harrison, M. J. (2001). A phosphate transporter gene from the extra-radical mycelium of an arbuscular mycorrhizal fungus Glomus intraradices is regulated in response to phosphate in the environment. *Mol. Plant Microbe Interact.* 14, 1140–1148. doi: 10.1094/MPMI.2001.14.10.1140

Martinez-Pastor, M. T., Marchler, G., Schuller, C., Marchler-Bauer, A., Ruis, H., and Estruch, F. (1996). The *Saccharomyces cerevisiae* zinc finger proteins Msn2p and Msn4p are required for transcriptional induction through the stress response element (STRE). *EMBO J.* 15, 2227–2235.

Moore, B. W. (1967). "Specific proteins of the nervous system," in *Physiological and Biochemical Aspects of Nervous Integration*, ed. F. D. Carlson (Englewood Cliffs, NJ: Prentice-Hall), 343–359.

Nowara, D., Gay, A., Lacomme, C., Shaw, J., Ridout, C., Douchkov, D., et al. (2010). HIGS: host-induced gene silencing in the obligate biotrophic fungal pathogen *Blumeria graminis*. *Plant Cell* 22, 3130–3141. doi: 10.1105/tpc.110.077040

Oldroyd, G. E. (2013). Speak, friend, and enter: signalling systems that promote beneficial symbiotic associations in plants. *Nat. Rev. Microbiol.* 11, 252–263. doi: 10.1038/nrmicro2990

Parniske, M. (2008). Arbuscular mycorrhiza: the mother of plant root endosymbioses. *Nat. Rev. Microbiol.* 6, 763–775. doi: 10.1038/nrmicro1987

Parua, P. K., and Young, E. T. (2014). Binding and transcriptional regulation by 14-3-3 (Bmh) proteins requires residues outside of the canonical motif. *Eukaryot. Cell* 13, 21–30. doi: 10.1128/EC.00240-13

Paszkowski, U. (2006). A journey through signaling in arbuscular mycorrhizal symbiosis 2006. *New Phytol.* 172, 35–46. doi: 10.1111/j.1469-8137.2006.01840.x

Peter, G. J., Düring, L., and Ahmed, A. (2006). Carbon catabolite repression regulates amino acid permeases in *Saccharomyces cerevisiae* via the TOR signaling pathway. *J. Biol. Chem.* 281, 5546–5552. doi: 10.1074/jbc.M513842200

Petrov, V., Vermeirssen, V., De Clercq, I., Van Breusegem, F., Minkov, I., Vandepoele, K., et al. (2012). Identification of cis-regulatory elements specific for different types of reactive oxygen species in *Arabidopsis thaliana*. *Gene* 499, 52–60. doi: 10.1016/j.gene.2012.02.035

Porcel, R., Aroca, R., Cano, C., Bago, A., and Ruiz-Lozano, J. M. (2006). Identification of a gene from the arbuscular mycorrhizal fungus glomus intraradices encoding for a 14-3-3 protein that is up-regulated by drought stress during the AM symbiosis. *Microb. Ecol.* 52, 575–582. doi: 10.1007/s00248-006-9015-2

Remy, W., Taylor, T. N., Hass, H., and Kerp, H. (1994). Four hundred-million-year-old vesicular arbuscular mycorrhizae. *Proc. Natl. Acad. Sci. U.S.A.* 91, 11841–11843. doi: 10.1073/pnas.91.25.11841

Requena, N., Mann, P., Hampp, R., and Franken, P. (2002). Early developmentally regulated genes in the arbuscular mycorrhizal fungus glomus mosseae : identification of gmgin1, a novel gene with homology to the c-terminus of metazoan hedgehog proteins. *Plant Soil* 244, 129–139. doi: 10.1023/A:1020249932310

Rispail, N., Soanes, D. M., Ant, C., Czajkowski, R., Grunler, A., Huguet, R., et al. (2009). Comparative genomics of MAP kinase and calcium-calcineurin signalling components in plant and human pathogenic fungi. *Fungal Genet. Biol.* 46, 287–298. doi: 10.1016/j.fgb.2009.01.002

Roberts, M. R., Salinas, J., and Collinge, D. B. (2002). 14-3-3 proteins and the response to abiotic and biotic stress. *Plant Mol. Biol.* 50, 1031–1039. doi: 10.1023/A:1021261614491

Roberts, R. L., Mösch, H.-U., and Fink, G. R. (1997). 14-3-3 proteins are essential for Ras/MAPK cascade signaling during pseudohyphal development in *S. cerevisiae*. *Cell* 89, 1055–1065. doi: 10.1016/S0092-8674(00)80293-7

Salvioli, A., and Bonfante, P. (2013). Systems biology and "omics" tools: a cooperation for next-generation mycorrhizal studies. *Plant Sci.* 203–204, 107–114. doi: 10.1016/j.plantsci.2013.01.001

Salvioli, A., Ghignone, S., Novero, M., Navazio, L., Bagnaresi, P., and Bonfante, P. (2016). Symbiosis with an endobacterium increases the fitness of a mycorrhizal fungus, raising its bioenergetic potential. *ISME J.* 10, 130–144. doi: 10.1038/ismej.2015.91

Sanders, I. R. (1999). Evolutionary genetics: no sex please, we're fungi. *Nature* 399, 737–739. doi: 10.1038/21544

Schmitt, A. P., and Mcentee, K. (1996). Msn2p, a zinc finger dna-binding protein, is the transcriptional activator of the multistress response in *Saccharomyces cerevisiae*. *Proc. Natl. Acad. Sci. U.S.A.* 93, 5777–5782. doi: 10.1073/pnas.93.12.5777

Schmitz, A. M., and Harrison, M. J. (2014). Signaling events during initiation of arbuscular mycorrhizal symbiosis. *J. Integr. Plant Biol.* 56, 250–261. doi: 10.1111/jipb.12155

Schützendübel, A., and Polle, A. (2002). Plant responses to abiotic stresses: heavy metal-induced oxidative stress and protection by mycorrhization. *J. Exp. Bot.* 53, 1351–1365. doi: 10.1093/jxb/53.372.1351

Scotto-Lavino, E., Du, G., and Frohman, M. A. (2006a). 3′ end cdna amplification using classic RACE. *Nat. Protoc.* 1, 2742–2745. doi: 10.1101/pdb.prot4130

Scotto-Lavino, E., Du, G., and Frohman, M. A. (2006b). 5′ end cDNA amplification using classic RACE. *Nat. Protoc.* 1, 2555–2562. doi: 10.1101/pdb.prot4131

Seidl, V., Seiboth, B., Karaffa, L., and Kubicek, C. (2004). The fungal STRE-element-binding protein Seb1 is involved but not essential for glycerol dehydrogenase (gld1) gene expression and glycerol accumulation in *Trichoderma atroviride* during osmotic stress. *Fungal Genet. Biol.* 41, 1132–1140. doi: 10.1016/j.fgb.2004.09.002

Simon, L., Bousquet, J., Levesque, R. C., and Lalonde, M. (1993). Origin and diversification of endomycorrhizal fungi and coincidence with vascular land plants. *Nature* 363, 67–69. doi: 10.1038/363067a0

Smith, A., Ward, M. P., and Garrett, S. (1998). Yeast PKA represses Msn2p/Msn4p-dependent gene expression to regulate growth, stress response and glycogen accumulation. *EMBO J.* 17, 3556–3564. doi: 10.1093/emboj/17.13.3556

Smith, A. J., Daut, J., and Schwappach, B. (2011). Membrane proteins as 14-3-3 clients in functional regulation and intracellular transport. *Physiology* 26, 181–191. doi: 10.1152/physiol.00042.2010

Smith, S., and Read, D. (2008). *Mycorrhiza Symbiosis*, 3rd Edn. San Diego, CA: Academic Press.

Takeda, N., Sato, S., Asamizu, E., Tabata, S., and Parniske, M. (2009). Apoplastic plant subtilases support arbuscular mycorrhiza development in *Lotus japonicus*. *Plant J.* 58, 766–777. doi: 10.1111/j.1365-313X.2009.03824.x

Tang, N., San Clemente, H., Roy, S., Becard, G., Zhao, B., and Roux, C. (2016). A survey of the gene repertoire of *Gigaspora rosea* unravels conserved features among glomeromycota for obligate biotrophy. *Front. Microbiol.* 7:233. doi: 10.3389/fmicb.2016.00233

Tisserant, E., Kohler, A., Dozolme-Seddas, P., Balestrini, R., Benabdellah, K., Colard, A., et al. (2012). The transcriptome of the arbuscular mycorrhizal fungus Glomus intraradices (DAOM 197198) reveals functional tradeoffs in an obligate symbiont. *New Phytol.* 193, 755–769. doi: 10.1111/j.1469-8137.2011.03948.x

Tisserant, E., Malbreil, M., Kuo, A., Kohler, A., Symeonidi, A., Balestrini, R., et al. (2013). Genome of an arbuscular mycorrhizal fungus provides insight into the oldest plant symbiosis. *Proc. Natl. Acad. Sci. U.S.A.* 110, 20117–20122. doi: 10.1073/pnas.1313452110

Tollot, M., Wong Sak Hoi, J., Van Tuinen, D., Arnould, C., Chatagnier, O., Dumas, B., et al. (2009). An STE12 gene identified in the mycorrhizal fungus Glomus intraradices restores infectivity of a hemibiotrophic plant pathogen. *New Phytol.* 181, 693–707. doi: 10.1111/j.1469-8137.2008.02696.x

Trouvelot, S., Bonneau, L., Redecker, D., van Tuinen, D., Adrian, M., and Wipf, D. (2015). Arbuscular mycorrhiza symbiosis in viticulture: a review. *Agron. Sustain. Dev.* 35, 1449–1467. doi: 10.1007/s13593-015-0329-7

Van der Heijden, M. G., Klironomos, J. N., Ursic, M., Moutoglis, P., Streitwolf-Engel, R., Boller, T., et al. (1998). Mycorrhizal fungal diversity determines plant biodiversity, ecosystem variability and productivity. *Nature* 396, 69–72. doi: 10.1038/23932

van Heusden, G. P. (2009). 14-3-3 Proteins: insights from genome-wide studies in yeast. *Genomics* 94, 287–293. doi: 10.1016/j.ygeno.2009.07.004

van Heusden, G. P., Griffiths, D. J., Ford, J. C., Chin, A. W. T. F., Schrader, P. A., Carr, A. M., et al. (1995). The 14-3-3 proteins encoded by the BMH1 and BMH2 genes are essential in the yeast *Saccharomyces cerevisiae* and can be replaced by a plant homologue. *Eur. J. Biochem.* 229, 45–53.

van Heusden, G. P., and Steensma, H. Y. (2006). Yeast 14-3-3 proteins. *Yeast* 23, 159–171. doi: 10.1002/yea.1338

van Heusden, G. P. H., van der Zanden, A. L., Ferl, R. J., and Steensma, H. Y. (1996). Four Arabidopsis thaliana 14-3-3 protein isoforms can complement the lethal yeast bmh1 bmh2 double disruption. *FEBS Lett.* 391, 252–256. doi: 10.1016/0014-5793(96)00746-6

Vido, K., Spector, D., Lagniel, G., Lopez, S., Toledano, M. B., and Labarre, J. (2001). A proteome analysis of the cadmium response in *Saccharomyces cerevisiae*. *J. Biol. Chem.* 276, 8469–8474. doi: 10.1074/jbc.M008708200

Wegel, E., Schauser, L., Sandal, N., Stougaard, J., and Parniske, M. (2007). Mycorrhiza mutants of *Lotus japonicus* define genetically independent steps during symbiotic infection. *Mol. Plant Microbe Interact.* 11, 933–936. doi: 10.1094/MPMI.1998.11.9.933

Xie, W., Liu, M., Lv, X., Lu, W., Gu, J., and Yu, H. (2014). Construction of a controllable β-carotene biosynthetic pathway by decentralized assembly strategy in *Saccharomyces cerevisiae*. *Biotechnol. Bioeng.* 111, 125–133. doi: 10.1002/bit.25002

Xie, X., Lin, H., Peng, X., Xu, C., Sun, Z., Jiang, K., et al. (2016). Arbuscular mycorrhizal symbiosis requires a phosphate transceptor in the *Gigaspora margarita* fungal symbiont. *Mol. Plant* 9, 1583–1608. doi: 10.1016/j.molp.2016.08.011

Yang, X., Wen, H. L., Sobott, F., Papagrigoriou, E., Robinson, C. V., et al. (2006). Structural basis for protein–protein interactions in the 14-3-3 protein family. *Proc. Natl. Acad. Sci. U.S.A.* 103, 17237–17242.

Zézé, A., Dulieu, H., and Gianinazzi-Pearson, V. (1994). DNA cloning and screening of a partial genomic library from an arbuscular mycorrhizal fungus *Scutellospora castanea*. *Mycorrhiza* 4, 251–254. doi: 10.1007/BF00206773

Zhang, H., Zhao, Q., Guo, X., Guo, M., Qi, Z., Tang, W., et al. (2014). Pleiotropic function of the putative zinc-finger protein MoMsn2 in *Magnaporthe oryzae*. *Mol. Plant Microbe Interact.* 27, 446–460. doi: 10.1094/MPMI-09-13-0271-R

Conflict of Interest Statement: The authors declare that the research was conducted in the absence of any commercial or financial relationships that could be construed as a potential conflict of interest.

frontiers in Microbiology

ORIGINAL RESEARCH
published: 19 March 2018
doi: 10.3389/fmicb.2018.00441

The Role of Strigolactone in the Cross-Talk Between *Arabidopsis thaliana* and the Endophytic Fungus *Mucor* sp.

Piotr Rozpądek[1], Agnieszka M. Domka[2], Michał Nosek[3], Rafał Ważny[1], Roman J. Jędrzejczyk[1], Monika Wiciarz[4] and Katarzyna Turnau[2]*

[1] Małopolska Centre of Biotechnology, Jagiellonian University, Kraków, Poland, [2] Institute of Environmental Sciences, Jagiellonian University, Kraków, Poland, [3] Institute of Biology, Pedagogical University of Kraków, Kraków, Poland, [4] Faculty of Biochemistry, Biophysics and Biotechnology, Jagiellonian University, Kraków, Poland

OPEN ACCESS

Edited by:
Mohamed Hijri, Université de Montréal, Canada

Reviewed by:
George Newcombe, University of Idaho, United States
Mika Tapio Tarkka, Helmholtz-Zentrum für Umweltforschung (UFZ), Germany

***Correspondence:**
Piotr Rozpądek
piotr.rozpadek@uj.edu.pl

Specialty section:
This article was submitted to Fungi and Their Interactions, a section of the journal Frontiers in Microbiology

Received: *31 August 2017*
Accepted: *26 February 2018*
Published: *19 March 2018*

Citation:
Rozpądek P, Domka AM, Nosek M, Ważny R, Jędrzejczyk RJ, Wiciarz M and Turnau K (2018) The Role of Strigolactone in the Cross-Talk Between Arabidopsis thaliana and the Endophytic Fungus Mucor sp. Front. Microbiol. 9:441. doi: 10.3389/fmicb.2018.00441

Over the last years the role of fungal endophytes in plant biology has been extensively studied. A number of species were shown to positively affect plant growth and fitness, thus attempts have been made to utilize these microorganisms in agriculture and phytoremediation. Plant-fungi symbiosis requires multiple metabolic adjustments of both of the interacting organisms. The mechanisms of these adaptations are mostly unknown, however, plant hormones seem to play a central role in this process. The plant hormone strigolactone (SL) was previously shown to activate hyphae branching of mycorrhizal fungi and to negatively affect pathogenic fungi growth. Its role in the plant–endophytic fungi interaction is unknown. The effect of the synthetic SL analog GR24 on the endophytic fungi *Mucor* sp. growth, respiration, H_2O_2 production and the activity of antioxidant enzymes was evaluated. We found fungi colony growth rate was decreased in a GR24 concentration dependent manner. Additionally, the fungi accumulated more H_2O_2 what was accompanied by an altered activity of antioxidant enzymes. Symbiosis with *Mucor* sp. positively affected *Arabidopsis thaliana* growth, but SL was necessary for the establishment of the beneficial interaction. *A. thaliana* biosynthesis mutants *max1* and *max4*, but not the SL signaling mutant *max2* did not develop the beneficial phenotype. The negative growth response was correlated with alterations in SA homeostasis and a significant upregulation of genes encoding selected plant defensins. The fungi were also shown to be able to decompose SL *in planta* and to downregulate the expression of SL biosynthesis genes. Additionally, we have shown that GR24 treatment with a dose of 1 μM activates the production of SA in *A. thaliana*. The results presented here provide evidence for a role of SL in the plant–endophyte cross-talk during the mutualistic interaction between *Arabidopsis thaliana* and *Mucor* sp.

Keywords: strigolactone, fungal endophytes, *Arabidopsis thaliana*, salicylic acid, symbiosis, jasmonic acid

INTRODUCTION

A growing number of evidence indicates that endophytic fungi play a significant role in plant biology (Schulz, 2006; Yuan et al., 2009; Johnson et al., 2013). Endophytic fungi facilitate water and nutrient acquisition, resistance to abiotic stress such as drought, salinity and metal stress and provide protection against pathogenic microorganisms and herbivores. Their popularity is growing, for their potential in agriculture and bioremediation (Oelmüller et al., 2009; Li et al., 2012; Johnson et al., 2013). The potential for application of beneficial fungi seems very optimistic, however, understanding the mechanisms of the interactions between plants and endophytic fungi requires extensive research.

Plant adaptation to biotic and abiotic constraints requires several adjustments in plant metabolism, morphology, life cycle *etc*. These adaptations are often mediated by phytohormones. Recently, the plant hormone strigolactone (SL) has been recognized due to its role in root and shoot architecture determination and plant interactions in the rhizosphere (Rochange, 2010; Foo and Reid, 2013; Koltai and Kapulnik, 2013; Pandya-Kumar et al., 2014; Chen et al., 2015; van Zeijl et al., 2015). SLs are carotenoid derivates synthesized from β-carotene by consecutive action of a β-carotene isomerase, two carotenoid cleavage dioxygenases: CCD7 and CCD8 (MORE AXILARY GROWTH-MAX3 and 4) respectively and an enzyme from the P450 cytochrome family: MAX1 (MORE AXILARY GROWTH1). Downstream, a LATERAL BRANCHING OXYREDUCTASE (LBO) was recently shown to convert a carlactone intermediate in the process of SL biosynthesis (Brewer et al., 2016).

Strigolactones are important in plant responses to nutrient and water deficiency (López-Ráez et al., 2008; Yoneyama et al., 2012; Foo et al., 2013; López-Ráez, 2016; Visentin et al., 2016). SL biosynthesis mutants *max3* and *max4* and the SL signaling mutant *max2* are more sensitive to drought, due to a relationship between SL and ABA (Bu et al., 2014; Ha et al., 2014). Similarly, osmotic stress had a more severe effect on the *Lotus japonicus* SL biosynthesis mutant: *Ljccd7* (Liu et al., 2015). Nitrogen and phosphorus starvation activated SL biosynthesis and exudation and available reports indicate that SL plays a role in plant adaptation to P deficiency (Umehara et al., 2008; Kohlen et al., 2011; Ruyter-Spira et al., 2011; Andreo-Jimenez et al., 2015). Symbiotic microorganisms including endophytic fungi facilitate adaptation to environmental challenges including nutrient deficiencies and drought (reviewed in Bacon and White, 2016).

Strigolactones are signaling molecules involved in plant-soil microorganism interactions (reviewed in López-Ráez, 2016; Waters et al., 2017). The best described is its action in the plant–AMF interaction. In this mutual relationship the fungus provides the plant with necessary nutrients in exchange for reduced carbon. The AMF symbiosis is widespread throughout the plant kingdom; according to available reports, the roots of over 80% of terrestrial plants are colonized by AMF (Smith and Read, 2008; Brundrett, 2009). Only a few plant families, including the Brassicaceae have lost the ability to engage in mutual symbiosis with AMF (reviewed in Venkateshwaran et al., 2013). Nevertheless, recent reports indicate that numerous members of this family harbor a wide variety of fungal symbionts, including beneficial endophytic fungi that may play a similar role in plant physiology as AMF (Barzanti et al., 2007; García et al., 2013; Card et al., 2015; Hong et al., 2015). This also allows to study the mechanisms of symbiosis with well-established plant models such as *Arabidopsis thaliana*, *Thlaspi caerulescens* etc.

Strigolactones are secreted from plant roots into the rhizosphere and act as a signal for directional growth of the hyphae, thus SL seems to facilitate the plant-AMF interaction in the pre-symbiotic stage of symbiosis (Akiyama et al., 2005; Besserer et al., 2006; Kretzschmar et al., 2012; Mori et al., 2016). Fungal mycelium treated with synthetic SL analogs exhibits a number of changes such as: hyphal branching and growth, increased respiratory activity and ATP and NADPH production, mitosis, expression of effector genes and spore germination. Additionally, SL treatment activates synthesis and release of short chain chitin oligomers which can activate the symbiotic (SYM) signaling pathway, which in turn trigger symbiotic responses in the plant (Lopez-Raez et al., 2017). According to studies with SL-biosynthesis and SL-exudation mutants of pea, petunia, rice and tomato, SL was not necessary for the establishment of the plant-AMF symbiosis, however, the colonization rate of these mutants was much lower compared to wild type plants (Gomez-Roldan et al., 2008; López-Ráez et al., 2008; Vogel et al., 2009; Koltai et al., 2010; Gutjahr et al., 2012; Kretzschmar et al., 2012). The response of different AMF species differs in respect to various SL molecules, however, doses as low as 10 nM of GR24 were shown to affect the growth pattern of the fungi (Besserer et al., 2008). Even though significant progress has been made in elucidating SL signaling and perception in *A. thaliana* and rice, the mechanism of SL perception nor signaling are not known in fungi. In *A. thaliana* the α/β hydrolase D14 was recognized as a SL receptor. SL signaling is mediated by the MAX2 (MORE AXILARY GROWTH2)/SMAXL (SUPRESOR OF MAX2 6, 7, and 8 in particular) signal transduction pathway, but no clear MAX2 or D14 homologs were found in sequenced fungal genomes including *Rhizophagus irregularis* (Waters et al., 2017).

Strigolactones are also involved in other interactions in the rhizosphere: act as a signal for rhizobacteria, as stimulants of parasitic plant seed (*Striga* sp. and *Orobanche* sp.) and pathogenic fungi (Rochange, 2010; Foo and Reid, 2013; Koltai and Kapulnik, 2013). The role of SL in plant–pathogenic fungi interactions is not clear. There are several, contradictory reports. A range of responses to the synthetic SL analog-GR24 on pathogenic fungi growth and branching were reported for the same species (Dor et al., 2011; Torres-Vera et al., 2014; Foo et al., 2016). Recently, Belmondo et al. (2017) has shown that a thioredoxin reductase is necessary for limiting *Botrytis cinerea* growth by GR24, indicating a relationship between SL and ROS (reactive oxygen species) metabolism.

The role of SL in biotic stress responses may be associated with its interaction with other phytohormones or hormone dependent signaling. In the SL deficient tomato, slccd8, reduced concentration of ABA, SA and JA were shown (Torres-Vera et al., 2014). In response to the parasitic plant *Phelipanche*

ramosa, the expression of SL biosynthetic D27 and CCD8 and SA, JA and ABA marker genes was upregulated (Torres-Vera et al., 2016). The SL signaling mutant *max2* was more susceptible to *Pectobacterium carotovorum* and *Pseudomonas syringe*, probably due to alterations in ABA metabolism (Piisilä et al., 2015). However, studies performed on SL biosynthesis and signaling garden pea mutants contradict these reports, showing no increased sensitivity to infection by the necrotrophic soilborne oomycete *Pythium irregulare* (Foo et al., 2016).

Previously, the endophytic fungus *Mucor* sp. was found to accelerate *Arabidopsis arenosa* and *A. thaliana* growth (Rozpądek et al., 2017). The fungus was also shown to improve *A. arenosa* toxic metal tolerance (Rozpądek et al., 2017). Other members of this genus improved oilseed rape growth in heavily polluted environments (Zhu et al., 2015; Zahoor et al., 2017) As recently suggested by Martin and Plett (2015), the closely related with AMF Mucoromycetes associated with extant, basal land plants, such as liverworts, hornworts and lycopods, in a symbiosis whose mutualistic nature is suspected, making this group of fungi a good model for studying the mechanisms of symbiosis.

In this study, we evaluated the role of SL in the interaction between *A. thaliana* and its fungal symbiont *Mucor* sp. It was hypothesized that SL is necessary in the development of mutualism between the two interacting organisms both as a secretory signal adjusting the *Mucor* sp. metabolism, to the mutualistic mode and a plant, intrinsic regulatory molecule. Its role was assumed to be associated with its connection to SA synthesis or signaling. Additionally, the possibility that the fungi may have an effect on SL metabolism after colonization was tested.

MATERIALS AND METHODS

Plant Cultivation

Arabidopsis thaliana WT (N6000), *max1* (N9564), *max4-1* (N9568) and *max2-2* (N9566) (more axillary branches 1, 4 and 2) mutants (all in Col-0 background) were obtained from NASC (The Nottingham Arabidopsis Stock Centre, United Kingdom). Seeds were surface sterilized with 8% NaOCl, 96% and 75% EtOH and sown to sterile 1/4 MS medium in a petri dish and placed in darkness (4°C). After 48 h seeds were transferred to a growth chamber (Panasonic MLR-352H-PE, JP) with a 16 h photoperiod, 21/17°C day/night temperature and 50% humidity. After 10 days seedlings were moved to MSR medium with no sugar (10 plants per petri dish) and inoculated with the fungus. To evaluate the effect of SL on plant biomass yield, MSR was supplemented with 1 μM of the synthetic SL analog: GR24 (StrigoLab, I) in acetone. Inoculation of *in vitro* cultures was performed by placing 2.1×10^6 *Mucor* sp. spores 5 mm from the tip of the main root. After 10–12 days of growth plants were harvested, frozen in liquid nitrogen and stored at −80°C. For biomass yield evaluation 3 separate experiments with 25–30 plants were performed. Due to differences in plant growth in between experiments, fresh weight of treated plants (E+, GR24 and E+GR24) was presented in relation to appropriate control. In all GR24 feeding experiments acetone mock control was performed.

Strigolactone Feeding Experiments, Fungi Growth, Respiration

Mucor sp. (KU234656, strain UNIJAG.PL.E50) spores (2.1×10^6) were placed in PDA (potato dextrose agar) medium supplemented with GR24. For colony growth evaluation spores were inoculated onto PDA containing 1, 10, 50, 100, 500, and 1000 nM of GR24 in 9 cm petri dishes. Colony surface area was measured after 48 h of growth in 24°C in darkness. Fungi respiration was measured with a 30 channel Micro-oxymax respirometer (Columbus Instruments, United States) between the 24 and 48 h of growth. A single O_2 measurement was performed every 2 h. Spores were placed in PDA supplemented with 50, 500, and 1000 nM of GR24 in 250 ml Duran bottles in the darkness at 24°C (growth chamber of Memmert, IPP400, United States). Fungi respiration was measured as O_2 consumption per 2 h for 24 h. The respiration rate was presented in relation to colony diameter. The experiment was run in 5 replicates. For all experiments mock (acetone) treated control was performed.

Enzyme Activity Assays

Protein Extraction and Quantification

Mucor sp. colonies grown in PDA supplemented with 1, 10, 50, 100, and 1000 nM of GR24 were harvested from media after 48 h of growth and grounded with a mortar and pestle in liquid nitrogen. For crude protein extraction, powdered mycelia were homogenized with molybdenum beads in a TissueLyzer LT (Qiagen, DE) in ice cold 100 mM HEPES-NaOH buffer (pH 7.5, 4 mM DTT, 1 mM EDTA) at 35 Hz for 15 min. The homogenizer adapter was precooled in liquid nitrogen to keep samples frozen. After extraction, samples were centrifuged for 10 min at 10,000 *g* at 4°C. Protein content was quantified according to Bradford (1976) using BSA as a standard. A separate set of fungi mycelium was prepared for each enzyme activity assay. The experiment was run in 5 replicates. For all experiments mock (acetone) treated control was performed.

Catalase Activity

The spectrophotometric measurement was performed according to the modified method described by Aebi (1984). Crude tissue extracts (10 μl) were added to 990 μl of phosphate buffer pH 7.0 containing 3 mM H_2O_2. CAT activity was determined from the decrease in absorbance at 240 nm due to CAT dependent reduction of H_2O_2. Enzyme activity was defined as 1 μmol of H_2O_2 decomposed by 1 mg of total soluble proteins per minute.

Glutathione Reductase Activity

The supernatants were analyzed for GR activity according to the modified method described by Foyer et al. (1995). Enzyme activity was determined from the decrease in absorbance at 340 nm in the reaction mixture containing TRIS-HCl (50 mM, pH 7.5) buffer, EDTA (1 mM) and GSSG (0.5 mM) in a total volume of 1 ml. Reaction was initiated with the addition of 0.15 mM NADPH.

Superoxide Dismutase Activity

Separations of soluble protein fractions were performed using native non-continuous PAGE in the buffer system described by Laemmli (1970) at 4°C and 180 V. SOD bands on 12% polyacrylamide gels were visualized according to the staining procedure described by Beauchamp and Fridovich (1971). The gels were incubated in the staining buffer for 30 min, in darkness, at room temperature and subsequently exposed to white light until SOD activity bands became visible. The gels were scanned using the office scanner Epson V700 Photo, and densitometric analysis was performed with ImageJ (NIH, United States).

Determination of H_2O_2 Concentration

For H_2O_2 assay powdered mycelia were homogenized with molybdenum beads in a TissueLyzer LT (Qiagen, DE) in ice cold 50 mM phosphate buffer pH 7.0 and at 40 Hz for 15 min. The homogenizer's adapter was precooled in liquid nitrogen to keep frozen. After extraction, samples were centrifuged for 15 min at 13,000 *g* at 4°C. H_2O_2 was assayed with Amplex® Red Hydrogen Peroxide Kit (Invitrogen) according to the manufacturer's instructions. The experiment was run in 5 replicates.

Fungi Staining, Confocal Microscopy and Plant Colonization Assessment

Plant colonization by the fungus was assessed according to Domka et al. (under review), by comparing the expression of the fungal *TEF1*α (Translation elongation factor 1-alpha) with plant *ACT7* (Actin-7) with *q*PCR. To visualize mycelium *in planta* GFP-expressing strain of *Mucor* sp. (KU234656, strain UNIJAG.PL.E50) was generated (Domka et al., under review). Visualization was performed with a confocal microscopy (Nikon Eclipse, JP) equipped with GFP filter blocks.

SL Decomposition Assay

The ability of the fungi to decompose SL *in planta* was verified by transferring 10 day old seedlings from ¼ MS medium to MSR supplemented with 1 μM GR24 fluorescent analog: GR24-BODIPY (StrigoLab, I) for 24 h to allow the plant to uptake it. Subsequently, seedlings were transferred to fresh MSR and inoculated with *Mucor* sp. Plants were harvested after 48 h of growth. Visualization of the fluorescence signal was performed with confocal microscopy (Nikon Eclipse, JP). Fluorescence was excited by 490 nm The fluorescence signal intensity was measured with ImageJ (NIH, United States). Five petri dishes with 10 seedlings for treated and not treated plants were prepared.

Salicylic Acid and Jasmonic Acid Biosynthesis Induction

To test the relationship between SL and SA and JA production, *A. thaliana* 10 day old seedlings grown in MS medium were transferred to MSR supplemented with 0, 1, 10, 50, 100, 500, 1000 nM of GR24 and harvested after 10 days of vegetation. To evaluate the impact of the fungi on SA production in SL treated plants, *A. thaliana* seedlings were transferred from MS to MSR supplemented with 1 μM GR24 and simultaneously inoculated with *Mucor* sp. (as described in "Plant cultivation"). The temporal pattern of SA production dynamics was evaluated with E+ seedlings grown in medium supplemented with GR24 for 1, 2, 5, and 10 days.

Salicylic Acid and Jasmonic Acid Concentration Measurement

Salicylic acid concentration was measured 1, 2, 5, and 10 days after transferring seedlings to MSR supplemented with 1 μM GR24. Inoculation was performed simultaneously with transfer. Unlabeled SA was purchased from Sigma-Aldrich (D). Sample preparation and HPLC analysis were carried out according to Müller et al. (2011) with modifications. Frozen plant roots (about 200 mg Fw – 30 plants per sample) was powdered in liquid nitrogen with a metal pestle in polypropylene tubes and then extracted with methanol:isopropanol:glacial acetic acid (20:79:1; v/v/v) in a 10:1 v/w ratio for 20 min in 4°C. During extraction sonification was applied. Subsequently, samples were centrifuged for 20 min in 15000 *g*. This procedure was performed 5 times to assure maximum, close to 100% extraction (from the second extraction 1 ml of extraction solution was used).

The HPLC analysis was performed using Shimadzu LCMS-2020 (JP) system equipped with an autosampler. Separation of plant extracts was performed with a Kinetex 2.6u C18 100x2.1 mm column. The total eluent flow was 0.400 ml min^{-1}. Gradient profile described in Müller et al. (2011). The MS analysis was performed using quadrupole mass spectrometer (Shimadzu) negative mode. The following MS parameters were used for analysis: DL temp. 250°C, HB temp. 200°C, detector voltage 0.95 kV, oven temp. 35°C, nebulizing gas flow 15 l min^{-1}. The external standard calibration curve method was used for determination of hormone concentration in plant tissues. Five standard solutions were prepared ranging from 0.05 to 10 ng μl^{-1}. All samples were run in 3 replicates.

Gene Expression Analysis

RNA Preparation

Total RNA was extracted from frozen in liquid nitrogen, ground leaves (from 5 plants per sample) with the Total RNA Mini Kit (Bio-Rad, United States). RNA purity and quantity was determined by Biospec-Nano (SHIMADZU, JP) The integrity of RNA was assessed with the Agilent 2100 Bioanalyzer (United States) and RNA 6000 Nano Kit (Agilent, DE).

*q*PCR

Reverse transcription was carried out on 1000 ng of total RNA, after digestion with DNase (DNA free kit, Ambion Bioscience, United States), with iScript cDNA synthesis kit (Bio-Rad, United States). For *q*PCR, probes were labeled with the EvaGreen (SsoFast EvaGreen Supermix, Bio-Rad, United States) fluorescent dye. For a single reaction 10 ng of cDNA and 150 nM of gene specific primers were used. To test amplification specificity a dissociation curve was acquired by heating samples from 60°C to 95°C. As house-keeping reference α-tubulin 5 (At5g19780) and ubiquitin 10 (At4g05320) was used. Reaction efficiency was tested by serial dilutions of cDNAs with gene specific primers (Supplementary Table 1). All samples were run in triplicates.

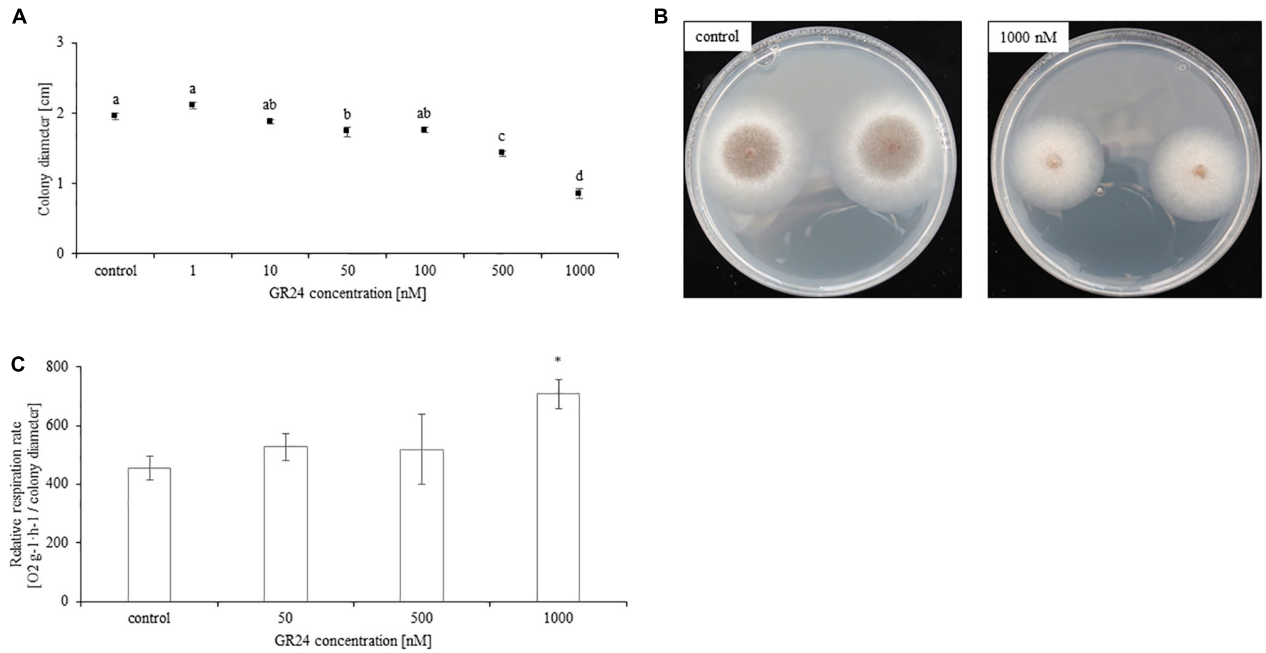

FIGURE 1 | *Mucor* sp. colony diameter measured 48 h after PDA inoculation with 2.1 × 10^6 fungi spores. The medium was supplemented with 0, 1, 10, 50, 100, 500, and 1000 nM of GR24 **(A)**. Letters above bars indicate statistically significant differences according to one-way ANOVA and Tuckey *post hoc* test (N = 10, $P \leq 0.05$). Respiration rate of Mucor sp. grown in PDA supplemented with 50, 500, and 1000 nM of GR24 and not treated control. Fungi respiration was measured as O_2 consumption per 2 h for 24 h. The respiration rate was presented in relation to colony diameter. Stars above bars represent statistically significant differences according to the student's t-test (N = 5, $P \leq 0.05$, mean value ± SE) **(B)**. Photographs illustrating *Mucor* sp. colony diameter grown for 48 h in PDA supplemented with 1000 nM GR24 **(C)**.

Expression was calculated according to Pfaffl (2001) with WT plants serving as calibrator. For gene expression analysis plants were harvested 10–12 days after inoculation. The experiment was repeated twice. In each experiment 3 samples (10 plants per sample) per variant were collected. Analysis were performed in triplicates.

Statistical Analysis

Data normality and variance homogeneity were evaluated by the Shapiro–Wilk and Levene's tests, respectively. If necessary, data were normalized with log or Box-Cox transformation. Statistical significance was determined by analysis of variance (ANOVA), followed by Tuckey or Fischer *post hoc* test ($p \leq 0.05$) as indicated in figure captions. Differences between two groups were tested by t-test. Statistical analyses were conducted using Statistica ver. 12.5 (Statsoft).

RESULTS

GR24 Inhibits Mycelium Growth and Increases the Respiration Rate

Supplementation of growth medium with GR24 significantly inhibited the growth of *Mucor* sp. Colony diameter decreased with growing concentrations of GR24. The lowest concentration which had an inhibitory effect was 50 nM. Treatment with 100 nM inhibited mycelium growth in a similar fashion, whereas treatment with concentrations of 500 and 1000 nM resulted in a gradual decline in colony diameter (**Figures 1A,B**). Additionally, as shown in **Figure 1B** treatment with 1000 nM delayed spore formation by the fungi. The respiration rate was significantly decreased only in result of treatment with 1000 nM of GR24. Lower concentrations did not significantly affect it (**Figure 1C**). Mock treatments did not differ from control.

GR24 Activates H_2O_2 Production and Alters the Activity of Antioxidant Enzymes

GR24 treatment with doses higher than 50 nM induced H_2O_2 production in the fungi mycelium. There were no difference in H_2O_2 concentration in mycelium treated with 50, 100, and 1000 nM (**Figure 2A**) The activity of GR was significantly decreased in all treatments (**Figure 2B**). The response of CAT and Cu/ZnSOD was dose dependent. Doses of 1 and 10 nM decreased enzyme activity (**Figures 2C,D**) whereas 10–1000 nM significantly increased Cu/ZnSOD, but not CAT activity (**Figures 2C,D**). Mock treatments did not differ from control.

Fungi Colonization of SL Biosynthesis Mutants

One day after inoculation fungal hyphae was detected on the surface of the root (**Figures 3A,B**). Later, the mycelium was present inside root hairs (**Figure 3C**) and inside other root

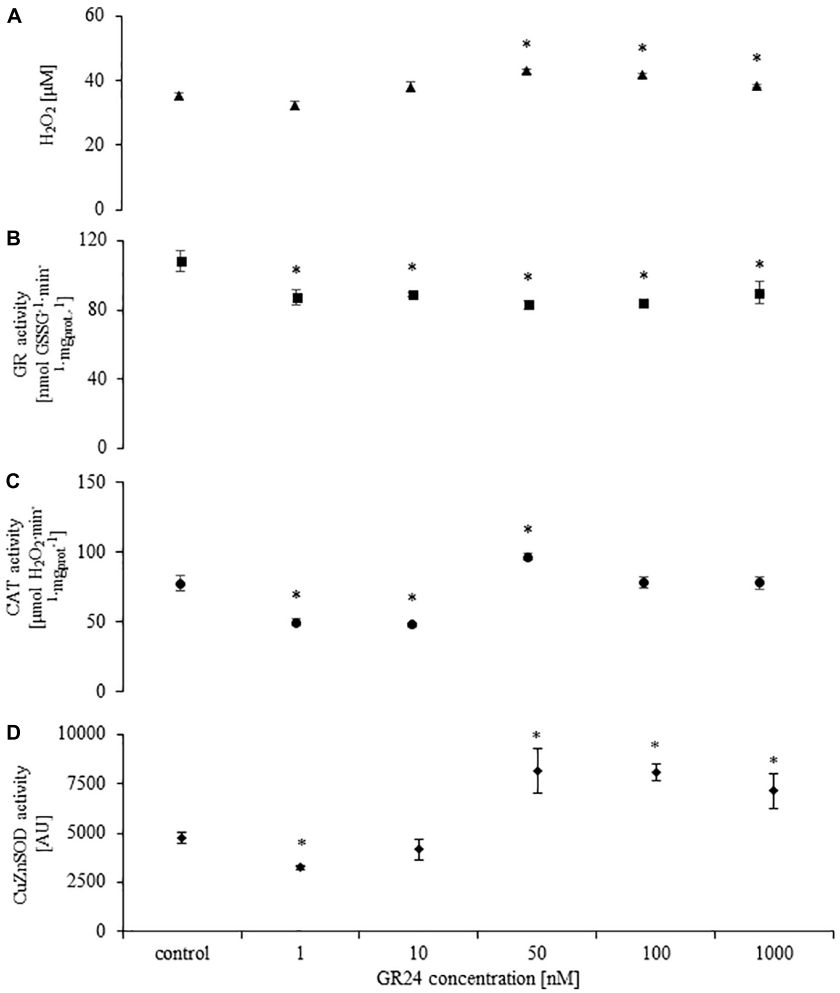

FIGURE 2 | H_2O_2 concentration **(A)**, glutathione reductase (GR; **B**), catalase (CAT; **C**), superoxide dismutase (Cu/ZnSOD; **D**) activities in *Mucor* sp. treated with 0, 1, 10, 50, 100, and 1000 nM of GR24. Stars above bars represent statistically significant differences according to the student's *t*-test $N = 5$, $P \leq 0.05$, mean value ± SE.

cells (**Figure 3D**). Colonization of *A. thaliana* tissues by *Mucor* sp. was described in detail by Domka et al. (2017, submitted). No significant changes in colonization rate were observed (**Figure 3E**).

SL Biosynthesis Mutants Do Not Develop the Beneficial Growth Phenotype Upon Inoculation

Due to differences in growth tempo between experiments, bars in **Figure 4** represent fresh weight treated plants relative to appropriate control: WT, *max1*, *max4* and *max2*. Inoculation with *Mucor* sp. improved biomass yield of WT and *max2 A. thaliana*, whereas SL biosynthesis mutants produced significantly less biomass (**Figure 4**).

Mucor sp. Decomposes GR24 *in Planta*

The fluorescence signal from GR24-BODIPY was significantly lower in E+ plants 48 h after inoculation (**Figures 5A,B**).

High Doses of GR24 Induce SA Synthesis in *A. thaliana*, But Has No Effect on JA Production

To test the relationship between SL and SA and JA production, *A. thaliana* 10 day old seedlings grown in medium MS medium were transferred to MSR supplemented with 0, 1, 10, 50, 100, 500, 1000 nM of GR24. Synthetic SL treatment had no effect on JA accumulation in plants (data not shown). SA concentration was significantly increased (close to 30-fold) in plants treated with the highest dose of GR24 (**Figure 6A**). Lower concentrations did not affect SA synthesis in *A. thaliana*. No differences in SA concentration were shown 24 hpi (hours past inoculation) (**Figure 6B**). 48 hpi GR24 treated seedlings accumulated significantly more SA. Twelve days after inoculation GR24 treated plants accumulated 25-fold more SA compared to control. Inoculation with the fungi prevented SA production by the plant (**Figure 6B**). 48 hpi SA accumulation was slightly lower than in untreated (GR24+) plants, but not significantly

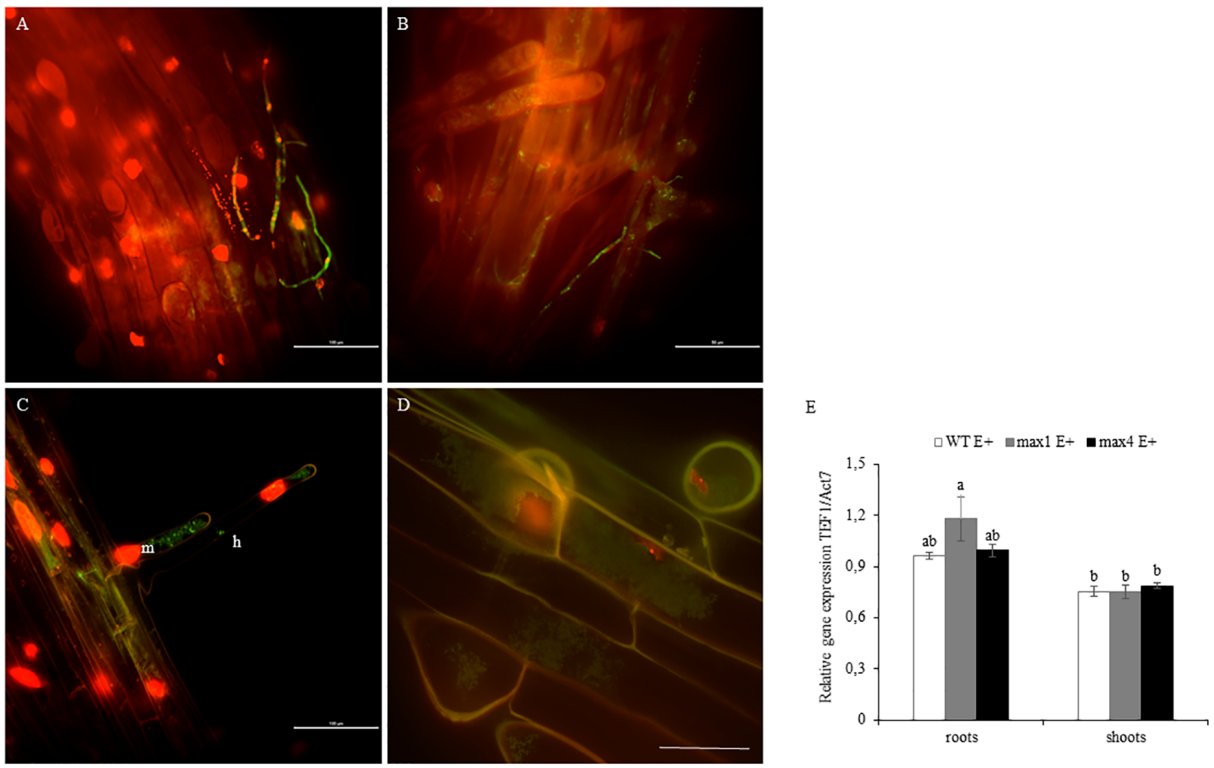

FIGURE 3 | Roots of *A. thaliana* colonized by *Mucor* sp. tagged with GFP. Fungal hyphae on the root surface, bars 100 and 50 μm respectively **(A,B)**. Mycelium (m) inside root hair (h), bar 100 μm **(C)**. Fungal mycelium (m) inside root cells, bar 50 μm **(D)**. Root colonization rate by mycelium shown as fungal TEF1α gene expression in relation to plant ACT7 gene expression. Letters above bars indicate statistically significant differences according to one-way ANOVA and Tuckey *post hoc* test ($N = 3$, $P \leq 0.05$, mean value ± SE) **(E)**.

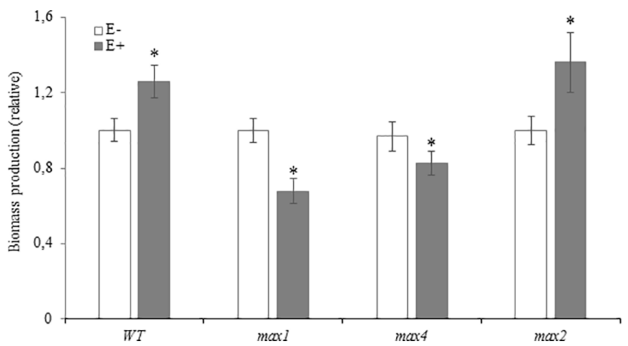

FIGURE 4 | Fresh weight of *Arabidopsis thaliana* WT and max1, max4 and max2 mutants 10 days after inoculation with *Mucor* sp., GR24 treated and inoculated with *Mucor* sp. and treated with GR24 **(A)**. Three separate experiments with 25–30 plants per genotype were performed. Due to differences in plant growth in between experiments, fresh weight of treated plants (E+, GR24 and E+GR24) was presented in relation to appropriate control (WT, max1, max4, max2). Stars above bars represent statistically significant differences according to the student's *t*-test $N = 5$, $P \leq 0.05$, mean value ± SE.

higher than in control and E+ seedlings. No differences in SA concentration were shown 12 dpi between control and E+ seedlings. Mock treatments did not differ from control.

Salicylic Acid and Jasmonic Acid Accumulation in E+ WT and *max1* and *2* Mutants

SA accumulation in *max1* mutants was significantly higher, whereas *max2* accumulated significantly less SA than in WT plants. Upon inoculation SA concentration increased in WT and *max2*. *max1* mutants responded to inoculation with decreased SA accumulation, which was significantly lower than in WT and *max2* (**Figure 6C**). No differences in JA accumulation were shown between WT, *max1* and *max2* mutants, nor did inoculation affect it (**Figure 6D**).

The Expression SL Biosynthesis Was Downregulated in E+ *Arabidopsis thaliana*

The expression of genes encoding proteins involved in SL biosynthesis: *CYP711A* (cytochrome P450, family 711, subfamily A), *D27* (beta-carotene isomerase D27-like protein) and *CCD8* (carotenoid cleavage dioxygenase 8) were significantly downregulated in inoculated WT plants, whereas genes encoding proteins involved in SL signaling were either unaffected by inoculation: *D14* (strigolactone esterase D14), *BRC1* (branched 1) (**Figure 7C**).

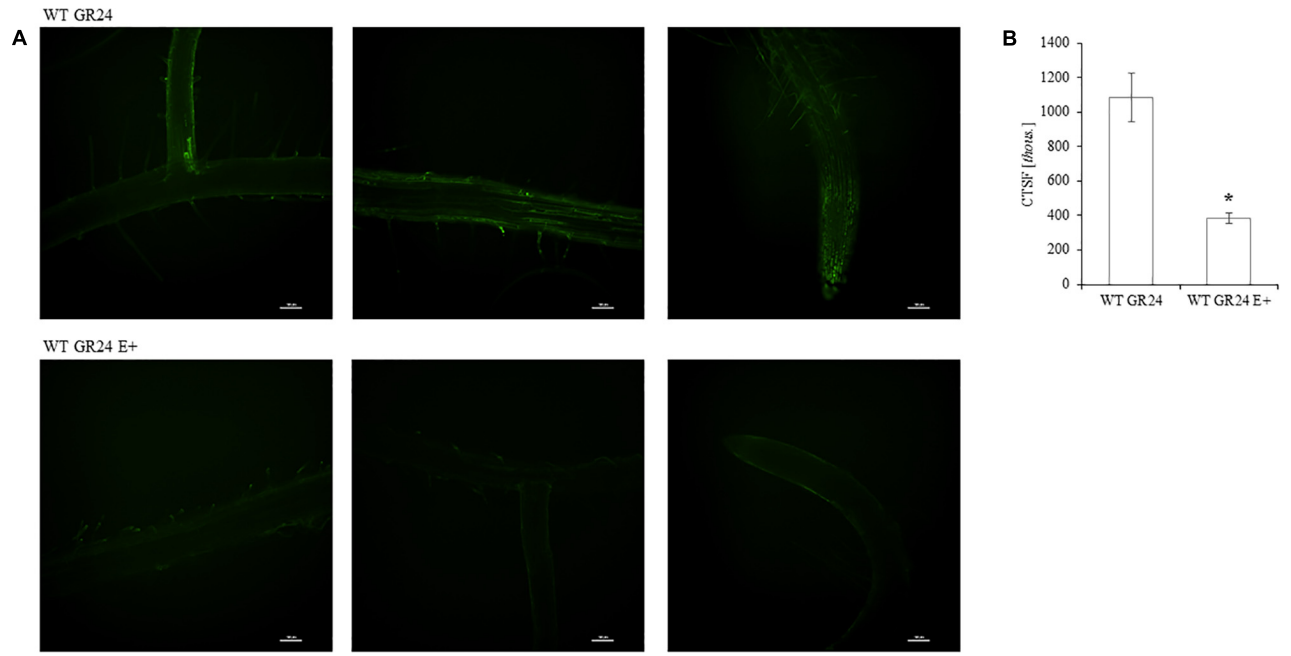

FIGURE 5 | Photographs illustrating the decomposition of the fluorescent analog GR24-BODIPY (StrigoLab, I) by *Mucor* mycelium inside roots of *A. thaliana*. Plants were fed with 1 μM GR24-BODIPY in MSR for 24 h transferred to GR24 free medium and inoculated with *Mucor* sp. **(A)**. Visualization was performed with confocal microscope and quantification of the fluorescence signal was performed 48 hpi with ImageJ-NIH. Stars above bars represent statistically significant differences according to the student's *t*-test $N = 3$, $P \leq 0.05$, mean value ± SE **(B)**.

The Expression Profiles of Plant Defense Related Genes Were Altered in *max1* and *max2* Mutants During the Interaction With *Mucor* sp.

In order to evaluate the role of SL in adjusting *A. thaliana's* defense to inoculation with *Mucor* sp. the expression of selected plant defensins was quantified (**Figure 7A**). Upon inoculation, the abundance of *PR2* mRNA was not changed in WT and *max2*. *max1* exhibited a significant upregulation of the expression of this gene. The expression of PR3 was upregulated in E+WT and E+*max1* (in *max1* more significantly then in WT), whereas in *max2* no differences in PR3 expression after inoculation were shown. No differences in the expression of PR5 between E+ and appropriate controls were shown, however, in the SL biosynthesis mutant PR5 transcript abundance was significantly higher compared to WT and *max2* (in both control and E+). Interestingly, PR5 expression in E+*max4* was significantly higher (Supplementary Figure 1).

Inoculation with *Mucor* sp. resulted in a significant upregulation in the expression of PDF1.2 in relation to relevant controls in all plants examined. Expression levels in WT and *max2* were similar, whereas PDF1.2 transcript abundance in *max1* was significantly higher (in both control and E+ plants). The expression of two defense related transcription factors WRKY25 and WRKY33 was upregulated in *max1* compared to WT plants. After inoculation their abundance rose in WT, whereas in *max1* and *max2* no differences were found. The response of SA biosynthesis genes was also altered in SL biosynthesis mutants. Genes encoding ICS1 and PAL1 were downregulated upon inoculation in *max1* E+ in relation to respective control, whereas no differences in their expression were found in WT (**Figure 7B**). The expression of the examined genes in *max4* closely resembled that in *max1* (Supplementary Figure 1).

DISSCUSION

GR24 strongly inhibited the growth of a number of phytopathogenic fungi, suggesting a role in plant defense (Dor et al., 2011). Additionally, hyphal branching was shown to be activated upon treatment with the SL analog. In this study GR24 treatment had a similar effect on the endophytes growth, but it did not affect branching (data not shown). GR24 doses used in this study were, however significantly lower compared to the concentrations used by other authors. Previously, micromolar concentrations of GR24 were shown to limit growth of mycelium (Dor et al., 2011; Belmondo et al., 2017), whereas here, 50 nM of GR24 was sufficient enough to limit colony expansion. This suggests that SL in the mutualistic interaction, imposes its effects in concentrations relatively lower compared to plant-pathogen interactions. Higher pathogen resistance to SL may have evolved due to selective pressure of this group of fungi. This, however, requires more detailed research.

Mycelium growth inhibition was accompanied by increased production/accumulation of H_2O_2 and inhibited the activity of GR which plays an important role in H_2O_2 scavenging.

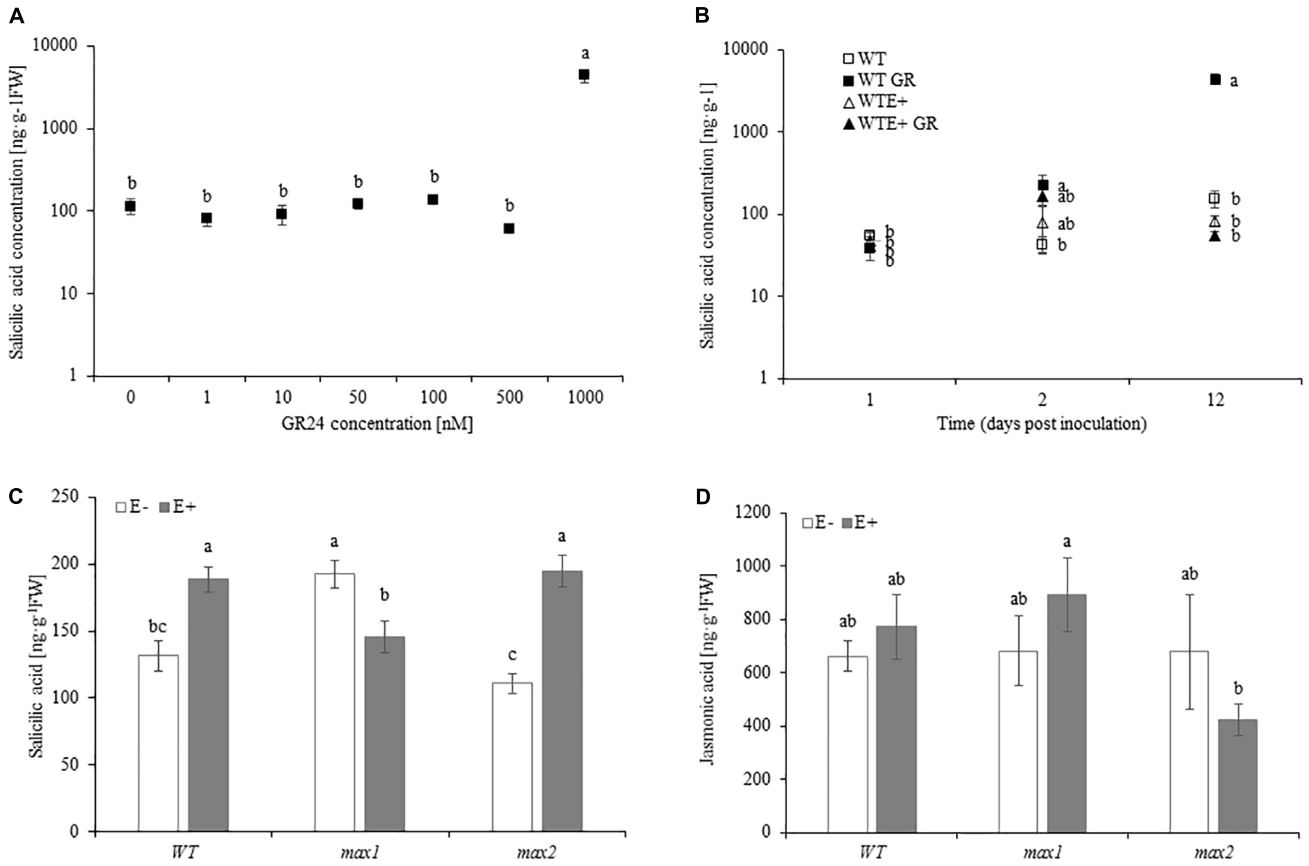

FIGURE 6 | SA accumulation in *Arabidopsis thaliana* WT grown in medium supplemented with 0–1000 nM of GR24 for 10 days **(A)**. SA accumulation in *Arabidopsis thaliana* WT grown in medium supplemented with 1000 nM of GR24 for 24 h, 48 h and 12 days **(B)**. SA **(C)** and JA **(D)** concentration in *A. thaliana* seedlings inoculated with *Mucor* sp. 10 days after inoculation. Letters above bars indicate statistically significant differences according to one-way ANOVA and Fischer *post hoc* test ($N = 3$, $P \leq 0.05$, mean value ± SE).

Lower concentrations of GR24, below 50 nM, reduced the activity of antioxidant enzymes examined, indicating that SL activates ROS production in the mycelium either directly by inducing an oxidative burst or indirectly, by reducing the activity of ROS scavenging enzymes. ROS were suggested to be necessary in limiting *B. cinerea* radial growth by GR24 (Belmondo et al., 2017). Previously, Tanaka et al. (2006) showed that by knocking out the *NOXA* gene encoding the plasmalemma bound, $O_2^{\bullet-}$ generating NADPH oxidase, the perennial ryegrass endophyte *Epichloë festucae* spreads throughout the plant causing disease symptoms. This indicated that by inducing ROS production the host plant may control its symbiotic partner. GR24 concentrations of 50 nM and above induced the production of H_2O_2 in *Mucor* sp. and activated the H_2O_2 producing/$O_2^{\bullet-}$ scavenging Cu/Zn SOD, suggesting that SL plays a role in activating ROS production during plant–fungi symbiosis.

Strigolactone are perceived by D14, a non-canonical α/β hydrolase receptor. Upon binding D14 was proposed to hydrolyse SL (Koltai and Kapulnik, 2013). The mechanism of SL perception by fungi is unknown, however, SL decomposition is not a unique plant feature. Recently it was shown that soil borne fungi from the *Trichoderma* and *Fusarium* genus were able to degrade 4 different natural and synthetic SLs including GR24. This ability is considered to be used in prevention of parasitic plant seed germination, but the biological relevance of this phenomenon is not known (Boari et al., 2016). In this study, we showed that *Mucor* sp. can also decompose GR24, both *ex planta* and more importantly *in planta*, thus it cannot be excluded that the fungi can modulate SL metabolism during the colonization process. Additionally, the results presented here show that upon inoculation, the expression of SL biosynthesis genes was downregulated in *A. thaliana*. This provides further evidence for the modulatory role of the endophytic *Mucor* sp. on SL metabolism during symbiosis establishment.

To evaluate the relevance of SL in the interaction between *A. thaliana* and *Mucor* sp. SL mutants were inoculated with the fungi. Biosynthesis mutants *max1* and *max4* responded negatively, in terms of growth to inoculation. The phenotype of *max2* (which synthesizes, but does not respond to SL) after inoculation with *Mucor* sp. resembled WT, suggesting that SL may had induced changes in *Mucor* sp. metabolism by switching it from "beneficial to parasitic mode" and MAX2 dependent

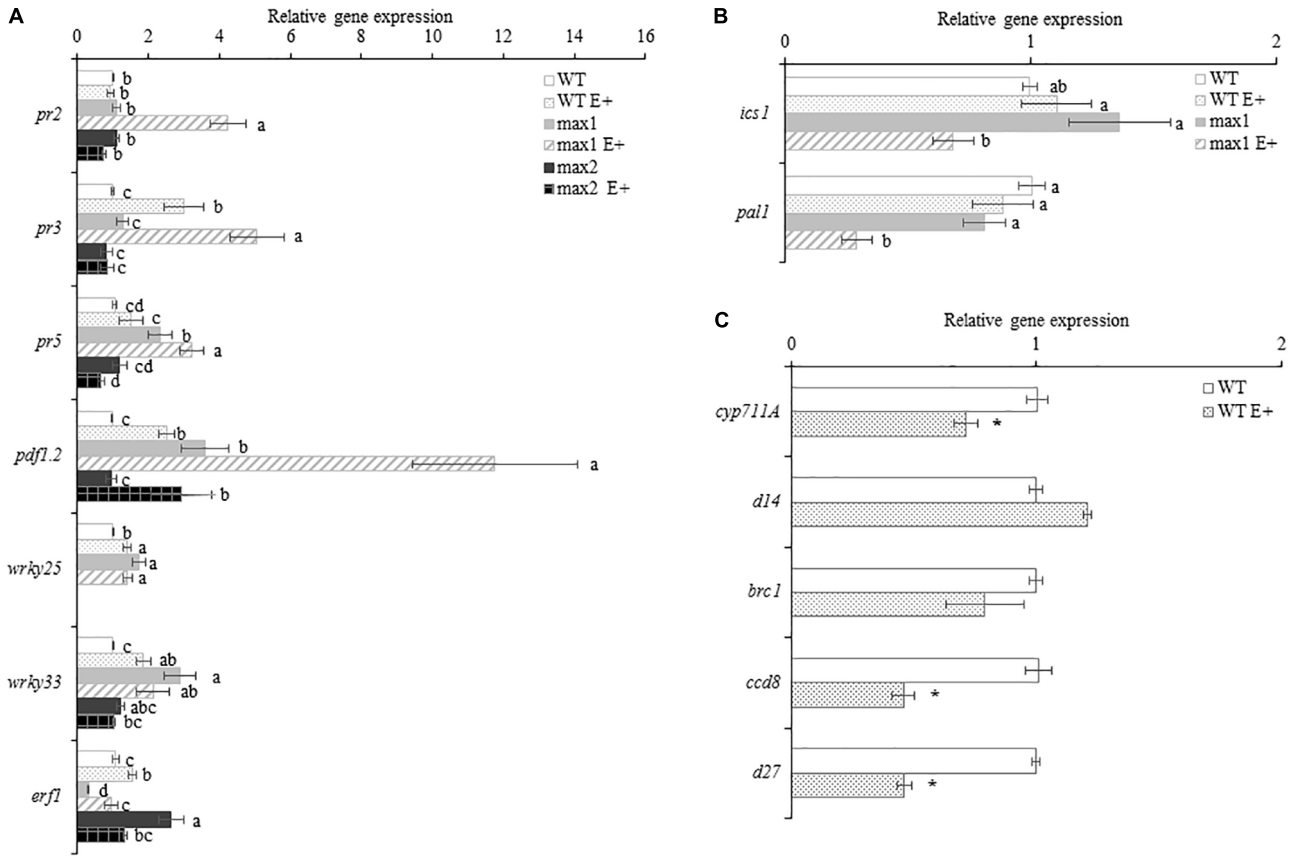

FIGURE 7 | The expression of *A. thaliana* WT, *max1* and *max2* inoculated with *Mucor sp.* (E+) defense related genes **(A)**, salicylic acid biosynthesis genes **(B)** and strigolactone biosynthesis and signaling genes **(C)** Letters above bars indicate statistically significant differences according to one-way ANOVA and Fischer *post hoc* test ($N = 6$, $P \leq 0.05$, mean value ± SE).

signaling was not necessary for the development of the beneficial phenotype. What's interesting is that the colonization rate of *max1* and *4* mutants did not differ from WT, indicating that in the absence of SL the plants did not lose ability to control colonization.

Plants control mycelium spread inside their tissues by activating a specific immune response. Selected defense mechanisms controlled by plant hormones JA, SA and ET are upregulated and others are downregulated (Jacobs et al., 2011; Lahrmann et al., 2015). A relationship between SL and these phytohormones has also been suggested (Marzec, 2016). According to the only report connecting SL to plant defense (Torres-Vera et al., 2014), SL deficiency alters defense related hormone profiles: the *Slccd8* tomato RNAi line accumulated less JA and SA. According to results presented here JA accumulation was not affected by neither SL deficiency, lack of MAX2 dependent SL signaling nor inoculation. To verify weather SL acts in controlling plant defense (possibly in the suppression of plant defense) we quantified the accumulation of SA in WT and *max* mutants inoculated with the fungus. The results indicate that, SL may act in suppressing SA production: *A. thaliana max1* and *max4* (see Supplement) accumulated significantly more SA than WT plants. At the same time, SA concentration in WT E+ and *max2* E+ increased what was coincident with deactivation of SL biosynthesis genes, suggesting that there may be a relationship between these two processes. SA biosynthesis gene expression was not changed in WT plants what indicates that other routes of SA accumulation regulation (SA catabolism for instance) had to control this process (Lahrmann et al., 2015). Exogenously applied synthetic SL activated SA synthesis in *A. thaliana* but only in concentrations of 1 μM, lower concentrations did not affect SA production in seedlings. This undermines the hypothesis of the downregulating role of SL in SA production. The physiological relevance of SL activated SA production is controversial. There are no reports indicating that plants can be exposed to such high concentrations in nature, nM and pM concentrations are usually found *in planta* (Seto et al., 2014), but 1 μM of GR24 is preferentially used in most studies using this SL analog (Marquez-Garcia et al., 2014; Passaia et al., 2014; Ito et al., 2015). In literature, there is only one report indicating that micromolar doses of GR24 can be toxic to the plant (Ito et al., 2015). No reports consider the fact that *A. thaliana* seedlings treated with GR24 can be exposed to stress (SA biosynthesis is stress responsive), nor consider the fact of SA synthesis activation upon GR24 treatment. Nevertheless, the results of SA accumulation seem

to confirm that SL serves in inhibition of SA accumulation. SA accumulated in *max1* mutants, co-cultivation of *A. thaliana* with *Mucor* sp. resulted in downregulation of SL biosynthesis genes and an increase in accumulation of SA (probably *via* a *max2* independent pathway). Additionally, we have shown that the fungus has the ability to degrade SL *in planta* what can be another routes of regulating SL content by the fungus. Several reports indicate that mycorrhizal plants prevent further root colonization by AMF possibly by altering SL production (reviewed in Steinkellner et al., 2007). The results presented here provide indirect evidence confirming that, indeed the endophytic fungus *Mucor sp.* possesses the ability to modulate SL metabolism/abundance *in planta*. Verifying the ecological significance of this phenomenon requires, however, further research. The relationship and the role of SL and SA in the establishment of the plant–fungi symbiosis is much more complicated than the picture presented above, the accumulation of SA in *max1* E+ and *max4* E+ mutants, as well as SA biosynthesis gene downregulation in E+ mutants indicates that other factors are involved in establishing the post infection equilibrium between SA and SL in plant–endophytic fungi interactions.

To further explore the relationship between SL and plant defense during the interaction between *A. thaliana* and *Mucor* sp. the expression of selected defense related genes in *A. thaliana* SL was measured. The expression of plant defensins is SA and JA inducible (Thomma et al., 1998, 1999). The expression of the tested defensins (PR2, PR3, PR5, PDF1.2) was significantly upregulated in inoculated plants under SL deficiency. Additionally, *PDF1.2* and *PR5* expression was significantly higher in the absence of the fungal stimulus providing further evidence for a link between SL and plant defense. The expression of the two defense related TFs examined also differed in WT and *max1*. WRKY25 and WRKY33 transcript abundance was higher in *max1* and did not respond to inoculation, whereas WT exhibited an activation of their expression. Surprisingly, the response of the SL signaling mutant *max2* differed from both WT and *max1*. Constitutive expression of the genes tested resembled WT, but, barely any of the genes responded to the fungi. Out of the tested genes only *PDF1.2* exhibited a response similar to that found in WT. Nevertheless, inhibition of *max2* dependent SL signaling resulted in almost complete non-responsiveness of the tested genes. The *max2* mutant produces SL and developed the beneficial phenotype upon inoculation, what indicates that SL serves both as a signal influencing the fungi and a signaling molecule controlling plant defense in response to the endophyte. It seems as though, SL MAX2 dependent signaling and activation of defense that takes place in the WT is not a necessary condition in the development of a mutual symbiosis between *A. thaliana* and *Mucor* sp. However, defense related gene expression in *max1* and *max4* mutants indicates that SL plays a role in suppressing the expression of the tested genes. The MAX2 dependent SL signaling pathway is intact in these mutants, suggesting that other factors compensate for SL under SL deficiency. Additionally, MAX2 signaling is not a unique feature of SL signal transduction. Another group of plant signaling molecules: karrikins, derived from cellulose combustion and involved in fire follower plant seed germination (among other functions) utilize MAX2 dependent signaling (Waters et al., 2014). MAX2 also targets several other proteins including the brassinosteroid target protein BRI1-EMS SUPPRESSOR1 (BES1) and the proteins from the DELLA family of GRAS transcriptional regulators involved in gibberellin signaling (Wang et al., 2013). Thus, caution needs to be taken when interpreting the response of the MAX2 mutant.

During the *A. thaliana–Mucor* sp. interaction an accumulation of defense compounds took place in WT (*PDF1.2* and *PR3*), but in significantly less quantities when compared to *max1* and *max4*. Previously, Jacobs et al. (2011) have shown that some basal defense is necessary for the establishment of the beneficial interaction between an endophytic fungus and its host plant. The results presented here seem to confirm this statement, however, there are variations in the response of *A. thaliana* to *Mucor* sp. and other fungi species in terms of activation specific defense related genes.

Upregulated defense mechanisms may not necessarily indicate a direct link between SL and defense. We can also imagine that since SL affects the fungi limiting its growth, it can also affect some unknown recognition patterns rendering the fungi recognizable as an endophyte and the upregulation of plant defense results from not recognizing the fungi as potentially beneficial. Additionally, the negative growth response of SL biosynthesis mutants suggests that in the absence of SL, a shift in resource allocation from growth to defense necessary to restrain fungi spread may take place. This, however, requires further investigations.

CONCLUSION

Recently, intense efforts are made to define the elements that allow plants to distinguish between potential symbionts and pathogens and to elucidate the plant-fungi cross-talk. Studying signals exchanged in the rhizosphere by plants and fungi is thus significantly important (Bonfante and Genre, 2010; Antolín-Llovera et al., 2014; Hayashi and Parniske, 2014). The role of SL in this process has been proposed previously. The data presented in this study indicates that SL plays a dual role in the interaction between plants and endophytic fungal symbionts. The synthetic SL analog GR24 was shown to affect the metabolism of *Mucor* sp. by limiting its growth and inducing ROS production. On the other hand, the fungus was shown to be able to decompose SL *in planta* and reduce SL biosynthesis gene expression. At the same time SL deficient *A. thaliana* mutants, but not the *max2* signaling mutant were not able to benefit from its fungal symbiont. The expression of a number of defense related genes was upregulated in SL deficient plants, suggesting a role of SL in regulating the plants immune response. However, it seems that the postulated link between SL and JA, SA is not as unequivocal as previously thought. Nevertheless, we present several lines of evidence of a direct and/or indirect relation of SL and plant defense.

Additionally, we have shown that high doses of GR24 activate SA production in *A. thaliana* and that by inoculating the plant with *Mucor* sp. we were able to prevent SA accumulation most probably by limiting root exposition to GR24 (the fungi decomposed GR24). This model represents a good illustration of the role that fungi play in natural environments. SL decomposition and possible downregulation of SL biosynthesis in the host plant limits SL availability in the soil, what in turn may have a limiting effect on parasitic plant seed germination.

AUTHOR CONTRIBUTIONS

PR designed the study, participated in experiments, analyzed the data and prepared the text of the manuscript. AD performed the *q*PCR, microscopic analyses. RW performed the *q*PCR and statistical analysis of data. RJ performed the HPLC determination of hormones. MN performed enzyme activity assays. KT was involved in designing the study and interpretation of the results. All authors were involved in the manuscript preparation and approved the manuscript prior to the submission.

FUNDING

This work was supported by NSC, Maestro Project, DEC – 2011/02/A/NZ9/00137, COST action FA1206, and Jagiellonian University funds (DS 758).

ACKNOWLEDGMENTS

The authors would like to acknowledge Teresa Anielska, Martyna Janicka, Weronika Janas (Institute of Environmental Sciences, Jagiellonian University, Kraków, Poland) and Agnieszka Bednarska (Institute of Nature Conservation, Polish Academy of Sciences, Kraków, Poland) for technical support.

SUPPLEMENTARY MATERIAL

The Supplementary Material for this article can be found online at: https://www.frontiersin.org/articles/10.3389/fmicb.2018.00441/full#supplementary-material

REFERENCES

Aebi, H. (1984). Catalase in vitro. *Methods Enzymol.* 105, 121–126. doi: 10.1016/S0076-6879(84)05016-3

Akiyama, K., Matsuzaki, K., and Hayashi, H. (2005). Plant sesquiterpenes induce hyphal branching in arbuscular mycorrhizal fungi. *Nature* 435, 824–827. doi: 10.1038/nature03608

Andreo-Jimenez, B., Ruyter-Spira, C., Bouwmeester, H. J., and Lopez-Raez, J. A. (2015). Ecological relevance of strigolactones in nutrient uptake and other abiotic stresses, and in plant-microbe interactions below-ground. *Plant Soil* 394, 1–19. doi: 10.1007/s11104-015-2544-z

Antolín-Llovera, M., Ried, M. K., and Parniske, M. (2014). Cleavage of the symbiosis receptor-like kinase ectodomain promotes complex formation with nod factor receptor 5. *Curr. Biol.* 24, 422–427. doi: 10.1016/j.cub.2013.12.053

Bacon, C. W., and White, J. F. (2016). Functions, mechanisms and regulation of endophytic and epiphytic microbial communities of plants. *Symbiosis* 68, 87–98. doi: 10.1007/s13199-015-0350-2

Barzanti, R., Ozino, F., Bazzicalupo, M., Gabbrielli, R., Galardi, F., Gonnelli, C., et al. (2007). Isolation and characterization of endophytic bacteria from the nickel hyperaccumulator plant *Alyssum bertolonii*. *Microb. Ecol.* 53, 306–316. doi: 10.1007/s00248-006-9164-3

Beauchamp, C., and Fridovich, I. (1971). Superoxide dismutase: improved assays and an assay applicable to acrylamide gels. *Anal. Biochem.* 44, 276–287. doi: 10.1016/0003-2697(71)90370-8

Belmondo, S., Marschall, R., Tudzynski, P., López Ráez, J. A., Artuso, E., Prandi, C., et al. (2017). Identification of genes involved in fungal responses to strigolactones using mutants from fungal pathogens. *Curr. Genet.* 63, 201–213. doi: 10.1007/s00294-016-0626-y

Besserer, A., Becard, G., Jauneau, A., Roux, C., and Sejalon-Delmas, N. (2008). GR24, a synthetic analog of strigolactones, stimulates the mitosis and growth of the Arbuscular Mycorrhizal Fungus *Gigaspora rosea* by boosting its energy metabolism. *Plant Physiol.* 148, 402–413. doi: 10.1104/pp.108.121400

Besserer, A., Puech-Pagès, V., Kiefer, P., Gomez-Roldan, V., Jauneau, A., Roy, S., et al. (2006). Strigolactones stimulate arbuscular mycorrhizal fungi by activating mitochondria. *PLoS Biol.* 4:e226. doi: 10.1371/journal.pbio.0040226

Boari, A., Ciasca, B., Pineda-Martos, R., Lattanzio, V. M. T., Yoneyama, K., and Vurro, M. (2016). Parasitic weed management by using strigolactone-degrading fungi. *Pest Manag. Sci.* 72, 2043–2047. doi: 10.1002/ps.4226

Bonfante, P., and Genre, A. (2010). Mechanisms underlying beneficial plant–fungus interactions in mycorrhizal symbiosis. *Nat. Commun.* 1, 1–11. doi: 10.1038/ncomms1046

Bradford, M. M. (1976). A rapid and sensitive method for the quantitation of microgram quantities of protein utilizing the principle of protein-dye binding. *Anal. Biochem.* 72, 248–254. doi: 10.1101/pdb.prodprot15

Brewer, P. B., Yoneyama, K., Filardo, F., Meyers, E., Scaffidi, A., Frickey, T., et al. (2016). LATERAL BRANCHING OXIDOREDUCTASE acts in the final stages of strigolactone biosynthesis in *Arabidopsis*. *Proc. Natl. Acad. Sci. U.S.A.* 113, 6301–6306. doi: 10.1073/pnas.1601729113

Brundrett, M. C. (2009). Mycorrhizal associations and other means of nutrition of vascular plants: understanding the global diversity of host plants by resolving conflicting information and developing reliable means of diagnosis. *Plant Soil* 320, 37–77. doi: 10.1007/s11104-008-9877-9

Bu, Q., Lv, T., Shen, H., Luong, P., Wang, J., Wang, Z., et al. (2014). Regulation of drought tolerance by the F-Box protein MAX2 in *Arabidopsis*. *Plant Physiol.* 164, 424–439. doi: 10.1104/pp.113.226837

Card, S. D., Hume, D. E., Roodi, D., McGill, C. R., Millner, J. P., and Johnson, R. D. (2015). Beneficial endophytic microorganisms of *Brassica* - A review. *Biol. Control* 90, 102–112. doi: 10.1016/j.biocontrol.2015.06.001

Chen, Z., Gao, X., Zhang, J., Bonfante, P., Genre, A., Al-Babili, S., et al. (2015). Strigolactones affect lateral root formation and root-hair elongation in *Arabidopsis*. *Planta* 6, 209–216. doi: 10.1007/s00425-010-1310-y

Dor, E., Joel, D. M., Kapulnik, Y., Koltai, H., and Hershenhorn, J. (2011). The synthetic strigolactone GR24 influences the growth pattern of phytopathogenic fungi. *Planta* 234, 419–427. doi: 10.1007/s00425-011-1452-6

Foo, E., Blake, S. N., Fisher, B. J., Smith, J. A., and Reid, J. B. (2016). The role of strigolactones during plant interactions with the pathogenic fungus *Fusarium oxysporum*. *Planta* 243, 1387–1396. doi: 10.1007/s00425-015-2449-3

Foo, E., and Reid, J. B. (2013). Strigolactones: new physiological roles for an ancient signal. *J. Plant Growth Regul.* 32, 429–442. doi: 10.1007/s00344-012-9304-6

Foo, E., Yoneyama, K., Hugill, C. J., Quittenden, L. J., and Reid, J. B. (2013). Strigolactones and the regulation of pea symbioses in response to nitrate and phosphate deficiency. *Mol. Plant* 6, 76–87. doi: 10.1093/mp/sss115

Foyer, C. H., Souriau, N., Perret, S., Lelandais, M., Kunert, K. J., Pruvost, C., et al. (1995). Overexpression of glutathione reductase but not glutathione synthetase leads to increases in antioxidant capacity and resistance to photoinhibition in poplar trees. *Plant Physiol.* 109, 1047–1057. doi: 10.1104/pp.109.3.1047

García, E., Alonso, Á., Platas, G., and Sacristán, S. (2013). The endophytic mycobiota of *Arabidopsis thaliana*. *Fungal Divers.* 60, 71–89. doi: 10.1007/s13225-012-0219-0

Gomez-Roldan, V., Fermas, S., Brewer, P. B., Puech-Pagès, V., Dun, E. A., Pillot, J.-P., et al. (2008). Strigolactone inhibition of shoot branching. *Nature* 455, 189–194. doi: 10.1038/nature07271

Gutjahr, C., Radovanovic, D., Geoffroy, J., Zhang, Q., Siegler, H., Chiapello, M., et al. (2012). The half-size ABC transporters STR1 and STR2 are indispensable for mycorrhizal arbuscule formation in rice. *Plant J.* 69, 906–920. doi: 10.1111/j.1365-313X.2011.04842.x

Ha, C. V., Leyva-Gonzalez, M. A., Osakabe, Y., Tran, U. T., Nishiyama, R., Watanabe, Y., et al. (2014). Positive regulatory role of strigolactone in plant responses to drought and salt stress. *Proc. Natl. Acad. Sci. U.S.A.* 111, 851–856. doi: 10.1073/pnas.1322135111

Hayashi, M., and Parniske, M. (2014). Symbiosis and pathogenesis: what determines the difference? *Curr. Opin. Plant Biol.* 20, v–vi. doi: 10.1016/j.pbi.2014.07.008

Hong, C. E., Jo, S. H., Moon, J. Y., Lee, J. S., Kwon, S. Y., and Park, J. M. (2015). Isolation of novel leaf-inhabiting endophytic bacteria in *Arabidopsis thaliana* and their antagonistic effects on phytophathogens. *Plant Biotechnol. Rep.* 9, 451–458. doi: 10.1007/s11816-015-0372-5

Ito, S., Nozoye, T., Sasaki, E., Imai, M., Shiwa, Y., Shibata-Hatta, M., et al. (2015). Strigolactone regulates anthocyanin accumulation, acid phosphatases production and plant growth under low phosphate condition in *Arabidopsis*. *PLoS One* 10:e0119724. doi: 10.1371/journal.pone.0119724

Jacobs, S., Zechmann, B., Molitor, A., Trujillo, M., Petutschnig, E., Lipka, V., et al. (2011). Broad-spectrum suppression of innate immunity is required for colonization of *Arabidopsis* roots by the fungus *Piriformospora indica*. *Plant Physiol.* 156, 726–740. doi: 10.1104/pp.111.176446

Johnson, L. J., De Bonth, A. C. M., Briggs, L. R., Caradus, J. R., Finch, S. C., Fleetwood, D. J., et al. (2013). The exploitation of epichloae endophytes for agricultural benefit. *Fungal Divers.* 60, 171–188. doi: 10.1007/s13225-013-0239-4

Kohlen, W., Charnikhova, T., Liu, Q., Bours, R., Domagalska, M. A., Beguerie, S., et al. (2011). Strigolactones are transported through the xylem and play a key role in shoot architectural response to phosphate deficiency in nonarbuscular mycorrhizal host Arabidopsis. *Plant Physiol.* 155, 974–987. doi: 10.1104/pp.110.164640

Koltai, H., and Kapulnik, Y. (2013). Unveiling signaling events in root responses to strigolactone. *Mol. Plant* 6, 589–591. doi: 10.1093/mp/sst057

Koltai, H., LekKala, S. P., Bhattacharya, C., Mayzlish-Gati, E., Resnick, N., Wininger, S., et al. (2010). A tomato strigolactone-impaired mutant displays aberrant shoot morphology and plant interactions. *J. Exp. Bot.* 61, 1739–1749. doi: 10.1093/jxb/erq041

Kretzschmar, T., Kohlen, W., Sasse, J., Borghi, L., Schlegel, M., Bachelier, J. B., et al. (2012). A petunia ABC protein controls strigolactone-dependent symbiotic signalling and branching. *Nature* 483, 341–344. doi: 10.1038/nature10873

Laemmli, U. K. (1970). Cleavage of structural proteins during the assembly of the head of bacteriophage T4. *Nature* 227, 680–685. doi: 10.1038/227680a0

Lahrmann, U., Strehmel, N., Langen, G., Frerigmann, H., Leson, L., Ding, Y., et al. (2015). Mutualistic root endophytism is not associated with the reduction of saprotrophic traits and requires a noncompromised plant innate immunity. *New Phytol.* 207, 841–857. doi: 10.1111/nph.13411

Li, H. Y., Wei, D. Q., Shen, M., and Zhou, Z. P. (2012). Endophytes and their role in phytoremediation. *Fungal Divers.* 54, 11–18. doi: 10.1007/s13225-012-0165-x

Liu, J., He, H., Vitali, M., Visentin, I., Charnikhova, T., Haider, I., et al. (2015). Osmotic stress represses strigolactone biosynthesis in Lotus japonicus roots: exploring the interaction between strigolactones and ABA under abiotic stress. *Planta* 241, 1435–1451. doi: 10.1007/s00425-015-2266-8

López-Ráez, J. A. (2016). How drought and salinity affect arbuscular mycorrhizal symbiosis and strigolactone biosynthesis? *Planta* 243, 1375–1385. doi: 10.1007/s00425-015-2435-9

López-Ráez, J. A., Charnikhova, T., Gómez-Roldán, V., Matusova, R., Kohlen, W., De Vos, R., et al. (2008). Tomato strigolactones are derived from carotenoids and their biosynthesis is promoted by phosphate starvation. *New Phytol.* 178, 863–874. doi: 10.1111/j.1469-8137.2008.02406.x

Lopez-Raez, J. A., Shirasu, K., and Foo, E. (2017). Strigolactones in plant interactions with beneficial and detrimental organisms: the Yin and Yang. *Trends Plant Sci.* 22, 527–537. doi: 10.1016/j.tplants.2017.03.011

Marquez-Garcia, B., Njo, M., Beeckman, T., Goormachtig, S., and Foyer, C. H. (2014). A new role for glutathione in the regulation of root architecture linked to strigolactones. *Plant Cell Environ.* 37, 488–498. doi: 10.1111/pce.12172

Martin, F., and Plett, J. M. (2015). Reconsidering mutualistic plant–fungal interactions through the lens of effector biology. *Curr. Opin. Plant Biol.* 26, 45–50. doi: 10.1016/j.pbi.2015.06.001

Marzec, M. (2016). Strigolactones as part of the plant defence system. *Trends Plant Sci.* 21, 900–903. doi: 10.1016/j.tplants.2016.08.010

Mori, N., Nishiuma, K., Sugiyama, T., Hayashi, H., and Akiyama, K. (2016). Carlactone-type strigolactones and their synthetic analogues as inducers of hyphal branching in arbuscular mycorrhizal fungi. *Phytochemistry* 130, 90–98. doi: 10.1016/j.phytochem.2016.05.012

Müller, M., Munné-Bosch, S., Pan, X., Welti, R., Wang, X., Dun, E., et al. (2011). Rapid and sensitive hormonal profiling of complex plant samples by liquid chromatography coupled to electrospray ionization tandem mass spectrometry. *Plant Methods* 7:37. doi: 10.1186/1746-4811-7-37

Oelmüller, R., Sherameti, I., Tripathi, S., and Varma, A. (2009). *Piriformospora indica*, a cultivable root endophyte with multiple biotechnological applications. *Symbiosis* 49, 1–17. doi: 10.1007/s13199-009-0009-y

Pandya-Kumar, N., Shema, R., Kumar, M., Mayzlish-Gati, E., Levy, D., Zemach, H., et al. (2014). Strigolactone analog GR24 triggers changes in PIN2 polarity, vesicle trafficking and actin filament architecture. *New Phytol.* 202, 1184–1196. doi: 10.1111/nph.12744

Passaia, G., Queval, G., Bai, J., Margis-Pinheiro, M., and Foyer, C. H. (2014). The effects of redox controls mediated by glutathione peroxidases on root architecture in *Arabidopsis*. *J. Exp. Bot.* 65, 1403–1413. doi: 10.1093/jxb/ert486

Pfaffl, M. (2001). A new mathematical model for relative quantification in real-time RT–PCR. *Nucleic Acids Res.* 29, 2003–2009. doi: 10.1093/nar/29.9.e45

Piisilä, M., Keceli, M. A., Brader, G., Jakobson, L., Jõesaar, I., Sipari, N., et al. (2015). The F-box protein MAX2 contributes to resistance to bacterial phytopathogens in *Arabidopsis thaliana*. *BMC Plant Biol.* 15:53. doi: 10.1186/s12870-015-0434-4

Rochange, S. (2010). "Strigolactones and their role in arbuscular mycorrhizal symbiosis," in *Arbuscular Mycorrhizas: Physiology and Function*, ed. Y. Kapulnik (Dordrecht: Springer), 73–90.

Rozpądek, P., Domka, A., Ważny, R., Nosek, M., Jędrzejczyk, R., Tokarz, K., et al. (2017). How does the endophytic fungus Mucor sp. improve Arabidopsis arenosa vegetation in the degraded environment of a mine dump? *Environ. Exp. Bot.* 147, 31–42. doi: 10.1016/j.envexpbot.2017.11.009

Ruyter-Spira, C., Kohlen, W., Charnikhova, T., van Zeijl, A., van Bezouwen, L., de Ruijter, N., et al. (2011). Physiological effects of the synthetic strigolactone analog GR24 on root system architecture in *Arabidopsis*: another belowground role for strigolactones? *Plant Physiol.* 155, 721–734. doi: 10.1104/pp.110.166645

Schulz, B. (2006). "Mutualistic interactions with fungal root endophytes," in *Microbial Root Endophytes*, eds B. Schulz, C. Boyale, and T. Sieber (Berlin: Springer), 261–279. doi: 10.1007/3-540-33526-9_15

Seto, Y., Sado, A., Asami, K., Hanada, A., Umehara, M., Akiyama, K., et al. (2014). Carlactone is an endogenous biosynthetic precursor for strigolactones. *Proc. Natl. Acad. Sci. U.S.A.* 111, 1640–1645. doi: 10.1073/pnas.1314805111

Smith, S., and Read, D. (2008). *Mycorrhizal Symbiosis*, 3rd Edn. Cambridge: Academic Press.

Steinkellner, S., Lendzemo, V., Langer, I., Schweiger, P., Khaosaad, T., Toussaint, J. P., et al. (2007). Flavonoids and strigolactones in root exudates as signals in symbiotic and pathogenic plant-fungus interactions. *Molecules* 12, 1290–1306. doi: 10.3390/12071290

Tanaka, A., Christensen, M. J., Takemoto, D., Park, P., and Scott, B. (2006). Reactive oxygen species play a role in regulating a fungus-perennial ryegrass mutualistic interaction. *Plant Cell* 18, 1052–1066. doi: 10.1105/tpc.105.039263

Thomma, B. P., Eggermont, K., Tierens, K. F., and Broekaert, W. F. (1999). Requirement of functional ethylene-insensitive 2 gene for efficient resistance of *Arabidopsis* to infection by *Botrytis cinerea*. *Plant Physiol.* 121, 1093–1102. doi: 10.1104/pp.121.4.1093

Thomma, B. P. H. J., Eggermont, K., Penninckx, I. A. M. A., Mauch-Mani, B., Vogelsang, R., Cammue, B. P. A., et al. (1998). Separate jasmonate-dependent and salicylate-dependent defense-response pathways in *Arabidopsis* are essential for resistance to distinct microbial pathogens. *Proc. Natl. Acad. Sci. U.S.A.* 95, 15107–15111. doi: 10.1073/pnas.95.25.15107

Torres-Vera, R., García, J. M., Pozo, M. J., and Juan, A. L. (2016). Physiological and molecular plant pathology expression of molecular markers associated

to defense signaling pathways and strigolactone biosynthesis during the early interaction tomato- *Phelipanche ramosa*. *Physiol. Mol. Plant Pathol.* 94, 100–107. doi: 10.1016/j.pmpp.2016.05.007

Torres-Vera, R., García, J. M., Pozo, M. J., and López-Ráez, J. A. (2014). Do strigolactones contribute to plant defence? *Mol. Plant Pathol.* 15, 211–216. doi: 10.1111/mpp.12074

Umehara, M., Hanada, A., Yoshida, S., Akiyama, K., Arite, T., Takeda-Kamiya, N., et al. (2008). Inhibition of shoot branching by new terpenoid plant hormones. *Nature* 455, 195–200. doi: 10.1038/nature07272

van Zeijl, A., Liu, W., Xiao, T. T., Kohlen, W., Yang, W., Bisseling, T., et al. (2015). The strigolactone biosynthesis gene DWARF27 is co-opted in rhizobium symbiosis. *BMC Plant Biol.* 15:260. doi: 10.1186/s12870-015-0651-x

Venkateshwaran, M., Volkening, J. D., Sussman, M. R., and Ané, J. M. (2013). Symbiosis and the social network of higher plants. *Curr. Opin. Plant Biol.* 16, 118–127. doi: 10.1016/j.pbi.2012.11.007

Visentin, I., Vitali, M., Ferrero, M., Zhang, Y., Ruyter-Spira, C., Novák, O., et al. (2016). Low levels of strigolactones in roots as a component of the systemic signal of drought stress in tomato. *New Phytol.* 212, 954–963. doi: 10.1111/nph.14190

Vogel, J. T., Walter, M. H., Giavalisco, P., Lytovchenko, A., Kohlen, W., Charnikhova, T., et al. (2009). SlCCD7 controls strigolactone biosynthesis, shoot branching and mycorrhiza-induced apocarotenoid formation in tomato. *Plant J.* 61, 300–311. doi: 10.1111/j.1365-313X.2009.04056.x

Wang, Y., Sun, S., Zhu, W., Jia, K., Yang, H., and Wang, X. (2013). Strigolactone/MAX2-induced degradation of brassinosteroid transcriptional effector BES1 regulates shoot branching. *Dev. Cell* 27, 681–688. doi: 10.1016/j.devcel.2013.11.010

Waters, M. T., Gutjahr, C., Bennett, T., and Nelson, D. C. (2017). Strigolactone signaling and evolution. *Annu. Rev. Plant Biol.* 68, 291–322. doi: 10.1146/annurev-arplant-042916-040925

Waters, M. T., Scaffidi, A., Sun, Y. K., Flematti, G. R., and Smith, S. M. (2014). The karrikin response system of *Arabidopsis*. *Plant J.* 79, 623–631. doi: 10.1111/tpj.12430

Yoneyama, K., Xie, X., Kim, H., Kisugi, T., Nomura, T., Sekimoto, H., et al. (2012). How do nitrogen and phosphorus deficiencies affect strigolactone production and exudation? *Planta* 235, 1197–1207. doi: 10.1007/s00425-011-1568-8

Yuan, Z., Zhang, C., and Lin, F. (2009). Role of diverse non-systemic fungal endophytes in plant performance and response to stress: progress and approaches. *J. Plant Growth Regul.* 29, 116–126. doi: 10.1007/s00344-009-9112-9

Zahoor, M., Irshad, M., Rahman, H., Qasim, M., Afridi, S. G., Qadir, M., et al. (2017). Alleviation of heavy metal toxicity and phytostimulation of *Brassica campestris* L. by endophytic Mucor sp. MHR-7. *Ecotoxicol. Environ. Saf.* 142, 139–149. doi: 10.1016/j.ecoenv.2017.04.005

Zhu, S., Tang, J., Zeng, X., Wei, B., Yang, S., and Huang, B. (2015). Isolation of *Mucor circinelloides* Z4 and *Mucor racemosus* Z8 from heavy metal-contaminated soil and their potential in promoting phytoextraction with Guizhou oilseed rap. *J. Cent. South Univ.* 22, 88–94. doi: 10.1007/s11771-015-2498-6

Conflict of Interest Statement: The authors declare that the research was conducted in the absence of any commercial or financial relationships that could be construed as a potential conflict of interest.

frontiers in Microbiology

ORIGINAL RESEARCH
published: 18 May 2018
doi: 10.3389/fmicb.2018.01012

Mixture of *Salix* Genotypes Promotes Root Colonization With Dark Septate Endophytes and Changes P Cycling in the Mycorrhizosphere

Christel Baum[1], Katarzyna Hrynkiewicz[2], Sonia Szymańska[2], Nora Vitow[1], Stefanie Hoeber[3], Petra M. A. Fransson[4] and Martin Weih[3]*

[1] Soil Science, Faculty of Agricultural and Environmental Sciences, University of Rostock, Rostock, Germany, [2] Department of Microbiology, Faculty of Biology and Environmental Protection, Nicolaus Copernicus University in Toruń, Toruń, Poland, [3] Department of Crop Production Ecology, Swedish University of Agricultural Sciences, Uppsala, Sweden, [4] Uppsala BioCenter, Department of Forest Mycology and Plant Pathology, Swedish University of Agricultural Sciences, Uppsala, Sweden

OPEN ACCESS

Edited by:
Erika Kothe, Friedrich-Schiller-Universität Jena, Germany

Reviewed by:
Fred Asiegbu, University of Helsinki, Finland
Katarzyna Turnau, Jagiellonian University, Poland
Johanna Witzell, Southern Swedish Forest Research Centre, Swedish University of Agricultural Sciences, Sweden

***Correspondence:**
Christel Baum
christel.baum@uni-rostock.de

Specialty section:
This article was submitted to Fungi and Their Interactions, a section of the journal Frontiers in Microbiology

Received: *13 October 2017*
Accepted: *30 April 2018*
Published: *18 May 2018*

Citation:
Baum C, Hrynkiewicz K, Szymańska S, Vitow N, Hoeber S, Fransson PMA and Weih M (2018) Mixture of Salix Genotypes Promotes Root Colonization With Dark Septate Endophytes and Changes P Cycling in the Mycorrhizosphere. Front. Microbiol. 9:1012. doi: 10.3389/fmicb.2018.01012

The roots of *Salix* spp. can be colonized by two types of mycorrhizal fungi (ectomycorrhizal and arbuscular) and furthermore by dark-septate endophytes. The fungal root colonization is affected by the plant genotype, soil properties and their interactions. However, the impact of host diversity accomplished by mixing different *Salix* genotypes within the site on root-associated fungi and P-mobilization in the field is not known. It can be hypothesized that mixing of genotypes with strong eco-physiological differences changes the diversity and abundance of root-associated fungi and P-mobilization in the mycorrhizosphere based on different root characteristics. To test this hypothesis, we have studied the mixture of two fundamentally eco-physiologically different *Salix* genotypes (*S. dasyclados* cv. 'Loden' and *S. schwerinii* × *S. viminalis* cv. 'Tora') compared to plots with pure genotypes in a randomized block design in a field experiment in Northern Germany. We assessed the abundance of mycorrhizal colonization, fungal diversity, fine root density in the soil and activities of hydrolytic enzymes involved in P-mobilization in the mycorrhizosphere in autumn and following spring after three vegetation periods. Mycorrhizal and endophytic diversity was low under all *Salix* treatments with *Laccaria tortilis* being the dominating ectomyorrhizal fungal species, and *Cadophora* and *Paraphaeosphaeria* spp. being the most common endophytic fungi. Interspecific root competition increased richness and root colonization by endophytic fungi (four taxa in the mixture vs. one found in the pure host genotype cultures) more than by ectomycorrhizal fungi and increased the activities of hydrolytic soil enzymes involved in the P-mineralization (acid phosphatase and β-glucosidase) in mixed stands. The data suggest selective promotion of endophytic root colonization and changed competition for nutrients by mixture of *Salix* genotypes.

Keywords: arbuscular mycorrhizal fungi, ectomycorrhiza, soil enzymes, phosphorus, fine root density, short rotation coppice, willows

INTRODUCTION

Mycorrhizal fungi are central to soil fertility and can affect both crop productivity and cropping security (Rooney et al., 2009). Both arbuscular mycorrhizal (AM) and ectomycorrhizal (EM) fungi are known to increase the uptake of nutrients like phosphorus (P) and nitrogen (N) by the host plants, especially in infertile soils. However, their functions and benefits for the host plants might not be equivalent (Jones et al., 1998). For this reason, a change in the proportions of mycorrhizal colonization, or type of mycorrhizal association when the host plant can form dual mycorrhiza, might affect the mycorrhizal benefit of the host plant. The mycorrhizal colonization of plants can be affected by soil nutrient level and water content, site management as well as the diversity of the vegetation composition. An increased host plant diversity is known to influence the nutrient fluxes and the interactions with soil microorganisms (Courty et al., 2011). Endophytic fungi and mycorrhizal fungi can interact in their impact on the plant growth (Rillig et al., 2014). For example, AM fungi were revealed to be able to modulate the impact of endophytic fungi beneficially for the plant growth (Wężowicz et al., 2017).

Although the majority of higher plants form mycorrhizal associations, only a low number is dual mycorrhizal, forming both AM and EM associations (Smith and Read, 2008). *Salix* belongs to the dual mycorrhizal plant genera, and can also harbor diverse endophytic fungi, which may affect the hosts growth and ecophysiological traits (An et al., 2015). Although *Salix* spp. were mainly shown to be pre-dominantly EM (Püttsepp et al., 2004; Hrynkiewicz et al., 2010b), the opposite has also been shown with a dominance of AM colonization, e.g., in response to flooding (Lodge, 1989). The ability to change their mycorrhizal association in response to the environmental conditions makes them well-suitable model plants to investigate the changes in the mycorrhizosphere in response to a changed host diversity.

Fast growing *Salix* genotypes have been cultivated successfully in short rotation coppice (SRC) for a long time, mainly for biomass production for energy purposes in boreal climates (Weih, 2004). They are viewed as a sustainable source of biomass with a positive greenhouse gas balance due to their potential to fix and accumulate carbon (Cunniff et al., 2015). Furthermore, compared to annual systems grown on arable land, the management of perennial *Salix* stands in SRC leads to decreased mechanical disturbance of the soil and changed biochemical soil properties; along with changes in the abundance and diversity of soil organisms including mycorrhizal fungi (Baum et al., 2009a; Hrynkiewicz et al., 2010a; Fransson et al., 2013; Toju et al., 2013a; Goldmann et al., 2015). In addition, *Salix* genotype identity can significantly affect the soil enzyme activities at the same site (Baum and Hrynkiewicz, 2006), and *Salix* stands grown in a floodplain revealed higher activities of the soil enzyme β-glucosidase compared to perennial grassland (Zimmer et al., 2012). Changed soil enzyme activities are considered to be a direct expression of the soil community to metabolic requirements and available nutrients, and can therefore be used as indicators of soil functional diversity. Enzyme activities might be more indicative for ecosystem productivity and stability than the taxonomic diversity of soil microorganisms (Caldwell, 2005). Acid phosphatases and β-glucosidases are hydrolytic soil enzymes involved in P- and C-cycling of the soil and originate from plant roots and microorganisms. Mycorrhizal fungi can significantly increase the activities of these enzymes in the soil (Burke et al., 2011).

In SRC, *Salix* is usually planted with single genotypes, but this could possibly make them less resistant to pest organisms, diseases and abiotic stress. This is a major concern as a SRC must remain viable for up to 20 years to be profitable (Aravanopoulos et al., 1999). For this reason, an increased host plant diversity within *Salix* stands would be advantageous, but it will also change the below-ground plant–plant interactions within the stand. The soil ecological consequences of mixed *Salix* stands on former arable land are scarcely known so far (Hoeber et al., 2017).

We hypothesize that the mixture of genotypes with strong eco-physiological differences changes the mycorrhiza formation and activities in the mycorrhizosphere, based on different root characteristics of the genotypes involved. To test this hypothesis we have studied the mixture of two fundamental eco-physiological different *Salix* genotypes (*S. schwerinii* × *S. viminalis* cv. 'Tora' and *S. dasyclados* cv. 'Loden') grown in pure and mixed cultures in a field experiment in Northern Germany. Specifically, we expected (1) a higher diversity of root-associated fungi under mixed culture than in culture with the pure genotypes; and (2) changed fine root growth, abundance of root-associated fungi and enzymatic activities in the mycorrhizosphere under host genotype mixtures resulting from changed competitive conditions for the individual genotypes. Such insights into the overall structure of belowground plant–fungal associations will help to understand mechanisms that regulate the coexistence of eco-physiological diverse dual mycorrhizal plant species.

MATERIALS AND METHODS

Study Site and Test Plants

The field site Rostock (54°04′12″ N, 12°04′58″ E) has been established in spring 2014 on former arable soil and is one out of three experimental field sites within the ECOLINK-*Salix* project (Hoeber et al., 2018), which is part of a global tree diversity network (TreeDivNet, Verheyen et al., 2016; Paquette et al., 2018). The plantation is a SRC stand with two willow genotypes ['Tora,' Svalöf-Weibull (SW) Cultivar No. 910007, *S. schwerinii* E. Wolf × *S. viminalis* L.; and 'Loden' SW 890129, *S. dasyclados*] grown in plots with one genotype being present (pure) and the combination (mixture) of the two. 'Tora' and 'Loden' in pure culture ('Tora P' and 'Loden P') were monocultures. In the mixture the two genotypes ('Tora M' and 'Loden M') were planted alternating one by one within the rows. Therefore, each genotype was directly associated with plants of the other genotype in the mixture.

Shoot biomass was harvested for the first time after 3 years of growth (in winter 2016/2017). The overall goal of the ECOLINK-*Salix* project is to assess the effects of genotype identity and diversity in willow SRC on various ecosystem functions. The

experiment has a randomized block design, with three replicates (blocks, plot size: 92.16 m^2). Planting density was c. 15600 plants ha^{-1}. Each plot contains nine subplots (3.2 m × 3.2 m, 16 plants each).

The dominating soil type at the test site is a Stagnic Cambisol (FAO classification). The annual mean temperature is 8.5°C; the annual mean precipitation 592 mm. The texture class of the topsoil is predominantly loamy sand. General soil chemical properties (0–10 cm soil depth) were: pH ($CaCl_2$) 6.2, C_{org} 6.89 g kg^{-1}, N_{total} 0.86 g kg^{-1}, C/N 8.01, P_{total} 0.11 g kg^{-1}, and S_{total} 0.09 g kg^{-1}.

Soil and Fine Root Sample Collection

Soil and fine root sampling was done in November 2016 (at the end of the first rotation period after 3 years of growth) and in April 2017 (after the first shoot biomass harvest during the winter rest in February 2017). Nine soil cores (diameter 30 mm, depth 0–100 mm) per treatment were collected per genotype (2), sampling date (2), and planting layout (2: mono- [pure] and di-clonal [mix]) in the center of the plots for the determination of the fine root density, and of soil chemical and biochemical analyses (72 soil samples in total). The same number of samples and the same sampling design was used to collect the samples for the mycorrhizal analyses, but using 10 cm × 10 cm × 10 cm soil cubes taken with a sharp knife. The samples were collected from the uppermost 0–10 cm of soil, c. 20 cm from the stem base of willow plants and kept at 4°C until analyses. The majority of fine roots were found in 0–10 cm under diverse *Salix* species in SRC (Cunniff et al., 2015). For this reason the upper part of the topsoil seems to be most relevant for investigations of the mycorrhizosphere.

Soil Properties

The soil analyses were done using air-dried < 2 mm soil. Determination of soil pH was performed electrometrically using a glass electrode in 0.01 M $CaCl_2$ with a soil:solution ratio of 1:2.5. Total carbon (C_{total}), total nitrogen (N_{total}), and total sulfur (S_{total}) contents of the soils were determined with a Vario EL elemental analyzer (Elementar Analysensysteme GmbH, Hanau, Germany). All C was organic C (C_{org}) due to the acidic pH. The total phosphorus (P_{total}) content was extracted from 0.5 g dry soil material by microwave-assisted digestion with aqua regia solution (3:1 hydrochloric acid–nitric acid) (Chen and Ma, 2001). The P concentrations in the digests were measured by inductively coupled plasma optical emission spectroscopy (ICP-OES) (Optima 8300, PerkinElmer LAS GmbH, Rodgau, Germany).

Soil Enzyme Activities

The activities of acid phosphatases (EC 3.1.3.2) and β-glucosidases (EC 3.2.1.3) in the soil were determined colorimetrically according to Tabatabai (1982) and Eivazi and Tabatabai (1988). The enzyme activities were expressed as μg *p*-nitrophenol (pNP) g^{-1} soil h^{-1} released from the pre-given substrate solution (*p*-nitrophenyl-phosphate for acid phosphatases and *p*-nitrophenyl-β-D-glucosid for β-glucosidase) within 1 h of incubation.

Fine Root Density

Soil cores with plant roots were soaked in tap water for 1 h in a bowl and then carefully separated with forceps and washed with the help of a sieve. Roots were dried at 65°C for 48 h and the dry weights were calculated per soil volume and m^2 within the upper 0–10 cm soil depth.

Fungal Colonization of Fine Roots

For analyses of AM and other endophytic colonization roots were rinsed and cut into 10 mm segments. The segments were cleared with 10% (w/v) KOH for 15 min at 90°C, bleached in 10% H_2O_2 for 1 h, acidified with 1% HCl (van der Heijden, 2001) and stained with 0.05% (w/v) chlorazol black E for 90 min at 80°C. The AM colonization was quantified microscopically using the intersection method of McGonigle et al. (1990), considering arbuscle formation as indicator of AM fungi vs. formation of sclerotia as indicator of dark septate endophytes (DSE). A minimum of 200 fine root intersections for AM colonization and a minimum of 200 fine root tips for DSE colonization were observed per plot.

For EM colonization and morphological characterization, 10 sub-samples of root fragments were randomly chosen on a grid for microscopical quantification of EM colonization. The numbers of living non-colonized root tips vs. obviously colonized EM root tips were counted using the method of Agerer (1991). In total c. 4800 root tips were scanned. A minimum of 200 root tips per genotype and treatment was investigated for each sampling date.

A minimum of two root tips per sub-sample was selected for subsequent molecular identification of the fungal partners. The morphological EM types were distinguished by macroscopical characteristics of the fungal mantle, such as color, surface appearance, presence of emanating hyphae and hyphal strands (Agerer, 1987–2002). Two to five root tips per sub-sample were separately frozen in Eppendorf-tubes and stored at −20°C for molecular analysis.

Molecular and Phylogenetic Identification of Root Colonizing Fungi

The fungal taxa from the root samples were identified using analysis of DNA sequences of the internal transcribed spacer (ITS) region. DNA was isolated from root tips using the Plant & Fungi Purification Kit (EurX, Poland) according to the manufacturer's instructions. The ITS region within the ribosomal RNA genes was amplified using the primer pair ITS1F and ITS4 (White et al., 1990; Gardes and Bruns, 1993). Amplification of the ITS region was performed in a 25 μl final volume containing 50 ng of DNA, 0.125 μl of each primer (100 pM/μl), 10 μl of Master Mix (Qiagen) and 13 μl of nuclease-free water. The amplification protocol was as follows: 5 min at 94°C, 40 cycles of 30 s at 94°C,

1 min at 50°C, and 1 min at 72°C, and a final step at 72°C for 5 min. The PCR products obtained were purified using GeneMATRIX PCR/DNA Clean-Up Purification Kit protocol (EurX, Poland) and sequenced using primers ITS1F and ITS4. Sequence editing was performed using Sequencher TW Version 5.1 (Gene Codes, Ann Arbor, MI, United States). BLAST searching with ITS-sequences was performed on the GenBank (Altschul et al., 1990). If the sequence of the fungus showed 98% identities over the whole length of the sequence (about 600 to 700 bp) with a known fungus, this fungus was assumed to be the fungal root colonizing taxa. Contigs of ITS sequences were edited with EditSeq and aligned using Clustal W (DNASTAR®). DNA sequences were submitted to GenBank and accession numbers are presented in **Table 1**.

Statistical Analyses

The effect of the genotype-, the growth design (pure vs. mixed) and the interaction of both on biological and biochemical properties were analyzed by two-way ANOVA. The Detrended correspondence analysis (DCA) was used to disclose the effects of different host plant diversity (pure vs. mixed culture) on the root fungal colonization and soil enzyme activities in the mycorrhizosphere of *Salix*. Statistical analyses were computed using the software PAST (Hammer et al., 2001).

RESULTS

Fine Root Biomass and Fungal Colonization

The fine root biomass was significantly affected by the interaction of genotype × growth design (pure vs. mixture) (**Table 2**). In pure culture 'Loden P' revealed higher fine root biomass than 'Tora P,' but under the mixture no significant differences between the two genotypes were observed (**Figure 1**). The means of the fine root biomass decreased in all treatments from autumn 2016 to spring 2017.

The AM colonization was relatively small (<12% of the total fine root length) in all treatments, but higher under 'Tora M and P,' than under 'Loden M and P' (**Figure 2**). The AM colonization of the fine roots was not significantly affected by the growth design (pure or mixed culture; **Table 2**). It was higher in spring than in autumn (**Figure 2**).

The EM colonization was significantly larger under 'Loden M and P' than under 'Tora M and P,' and significantly

TABLE 1 | Molecular identification of fungal partners in fine roots of *Salix* genotypes 'Tora' and 'Loden' in pure (P) and mixed (M) growth design in 0–10 cm soil depth at the short rotation coppice Rostock in autumn 2016 and spring 2017.

Growth design	Clone	T bp	Closest BLAST match in GenBank (NCBI)* [Accession No.]/UNITE** or description of morphological features	Similarity %	Classified as [Accession No.]
Ectomycorrhizal fungi					
M	Loden	703	*Laccaria tortilis* voucher GMM7635 [KM067859]* *Laccaria tortilis* voucher DG05-14 [JQ888175]*	702/703 (99%) 683/684 (99%)	*Laccaria tortilis* [MG076771]
M	Tora	721	*Laccaria tortilis voucher GMM7635 [KM067859]** *Laccaria tortilis voucher DG05-14 [JQ888175]** *Laccaria tortilis [KM067859]***	710/710 (100%) 684/684 (100%) 710/710 (100%)	*Laccaria tortilis* [MG076772]
Endophytes					
M	Loden	645	*Cadophora* sp. OTU097 AN-2016 (rhizosphere of *Plantago lanceolata*) [KU556579]* *Leptodontidium orchidicola* strain ZT98 022 [AF486133]* Dark septate endophyte DS16b [AH008235]* *Cadophora* [KU556579]**	641/642 (99%) 639/640 (99%) 640/643 (99%) 641/642 (99%)	*Cadophora* sp. [MG076773]
M	Loden	541^	*Rhodotorula mucilaginosa* culture-collection CBS:329 *[KY104884]** *Rhodotorula mucilaginosa [KY104887]***	474/511 (93%) 494/541 (91%)	*Rhodotorula mucilaginosa* [MG076774]
P	Tora	605	Uncultured fungus clone 99_NA1_P32_E12 isolated from the North American Arctic [KF297051]* (Timling et al., 2014) Uncultured endophytic fungus clone 374C-02 isolated from *Chorisodontium aciphyllum* (Antarctica) [KC457179]* (Zhang et al., 2013) *Eocronartium* sp. I12F-02262 isolated from *Sanionia uncinata* (Antarctica) [JX852332]* (Zhang et al., 2013) Pucciniomycetes [KF297051]**	554/583 (95%) 502/530 (95%) 493/536 (92%) 554/583 (95%)	Pucciniomycotina [MG076775]
M	Tora	566	*Paraphaeosphaeria* sp. *sedF2 [KT265808]** *Paraphaeosphaeria* sp. *OTU072 AN-2016 [KU556554]** *Paraphaeosphaeria sporulosa [GU566257]***	556/561 (99%) 559/565 (99%) 557/561 (99%)	*Paraphaeosphaeria* sp. [MG076776]
M	Tora	590	*Pyrenochaeta* sp. strain P6099 [KT270292]* Fungal endophyte (*Holcus lanatus*) [FN392316]* *Pyrenochaeta* sp. strain P2916 [KT270113]* Pleosporales [KF385302]**	522/523 (99%) 518/518 (100%) 522/524 (99%) 570/587 (97%)	Pleosporales [MG076777]

**NCBI, ***UNITE.*

TABLE 2 | Results of two-way analysis of variance (ANOVA) on the effect of the genotype, the growth design (with different host plant diversity; pure vs. mixture) and their interactions (genotype × growth design) on root and soil properties in the mycorrhizosphere of *Salix* from autumn 2016 (autumn) and spring 2017 (spring).

Parameter		Genotype		Growth design		Genotype × growth design	
		Autumn	Spring	Autumn	Spring	Autumn	Spring
Fine root biomass	*p*	0.142	0.056	0.207	0.352	**0.012**	**0.008**
	F	2.264	3.900	1.653	0.893	7.043	7.804
AM colonization	*p*	**<0.001**	**<0.001**	0.793	0.923	0.104	0.217
	F	130.400	9.500	0.070	0.009	2.796	1.587
ECM colonization	*p*	**<0.001**	**<0.001**	**0.005**	0.129	0.089	0.129
	F	96.340	84.250	8.898	2.418	3.064	2.418
DSE colonization	*p*	**0.009**	**0.012**	**<0.001**	**<0.001**	**0.022**	**<0.001**
	F	7.599	7.109	27.410	66.590	5.831	21.960
Activity of acid phosphatase	*p*	0.388	0.387	**<0.001**	**<0.001**	0.388	0.387
	F	0.766	0.763	25.110	25.110	0.766	0.763
Activity of β-glucosidase	*p*	**<0.001**	**<0.001**	**0.002**	**0.001**	**<0.001**	**<0.001**
	F	19.170	19.190	11.430	11.460	19.170	19.190

p- Significance value (in bold are p < 0.05).

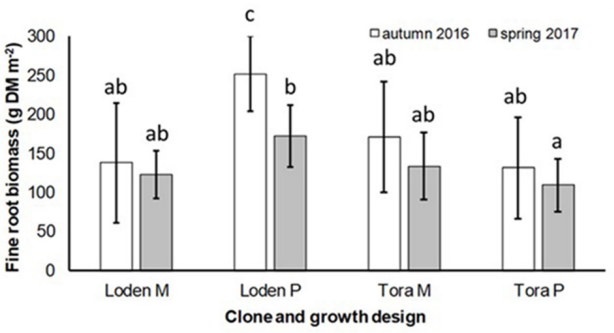

FIGURE 1 | Fine root biomass (g DM per m^2) under *Salix* genotypes 'Tora' and 'Loden' in pure (P) and mixed (M) growth in 0–10 cm soil depth at the short rotation coppice (SRC) Rostock in autumn 2016 and spring 2017 (means ± standard deviation, $n = 9$). Bars with different small letters (a, b, c) indicate significant differences among different treatments or sampling dates as defined by Duncan's test ($p < 0.05$).

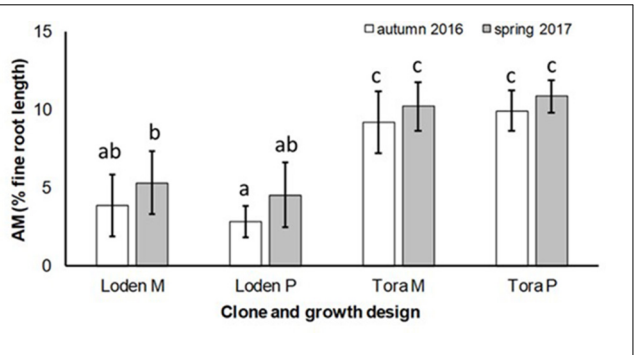

FIGURE 2 | Arbuscular mycorrhizal colonization (% root length) and spore density (number of spores per 10 g DM soil) under *Salix* genotypes 'Tora' and 'Loden', in pure (P) and mixed (M) growth in 0–10 cm soil depth at the SRC Rostock in autumn 2016 and spring 2017 (means ± standard deviation, $n = 9$). Bars with different small letters (a, b, c) indicate significant differences among different treatments or sampling dates as defined by Duncan's test ($p < 0.05$).

higher under the mixture in autumn 2016. In spring 2017 no significant impact of the growth design on the EM colonization was observed was (**Figure 3A** and **Table 2**). The EM colonization was in the mean slightly higher in autumn than in spring.

The DSE colonization was significantly larger in the mixture of genotypes ('Loden M' and 'Tora M') than in their pure cultures ('Loden P' and 'Tora P') (**Figure 3B**).

Fungal Diversity on the Fine Roots

With more than 95% of the total EM colonization (data not shown), *Laccaria tortilis* dominated as the single fungal partner in EM formation in all plots and was isolated from the roots of both genotypes (**Table 1**). Sporocarps of *Laccaria tortilis* were observed in all plots during the autumn sampling 2016. Other rarely occurring EM morphotypes observed were morphologically–anatomically determined to belong to *Inocybe* and *Russula* spp. and were found under both clones.

One endophytic fungal taxa was identified from the genotype 'Tora' in pure culture (Pucciniomycotina) and four endophytic fungal taxa from the genotypes in mixed culture (*Cadophora* sp., *Paraphaeosphaeria* sp., *Rhodotorula mucilaginosa*, Pleosporales) (**Table 1** and Supplementary Figure 1).

Soil Enzyme Activities

The activity of acid phosphatase in the soil was significantly higher under the mixed growth design, but not significantly affected by the genotype and the interaction of genotype x growth design (**Figure 4A** and **Table 2**). The activities of β-glucosidase in the soil were higher under the genotype 'Loden P' in pure culture than under 'Tora P' in pure culture (**Figure 4B** and **Table 2**).

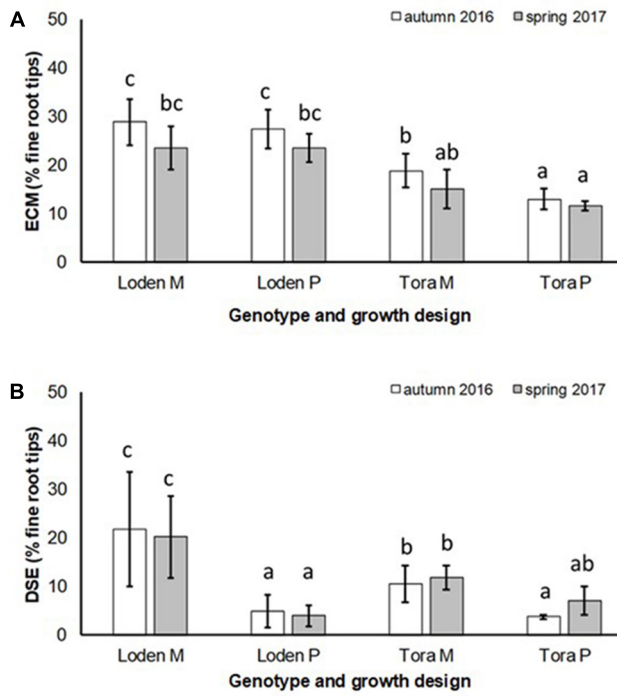

FIGURE 3 | (A) Ectomycorrhizal colonization (ECM) and **(B)** dark septate endophytic colonization (DSE) of fine roots of *Salix* genotypes 'Tora' and 'Loden in pure (P) and mixed (M) growth in 0–10 cm soil depth at the SRC Rostock in autumn 2016 and spring 2017 (means ± standard deviation, $n = 9$). Bars with different small letters (a, b, c) indicate significant differences among different treatments or sampling dates as defined by Duncan's test ($p < 0.05$).

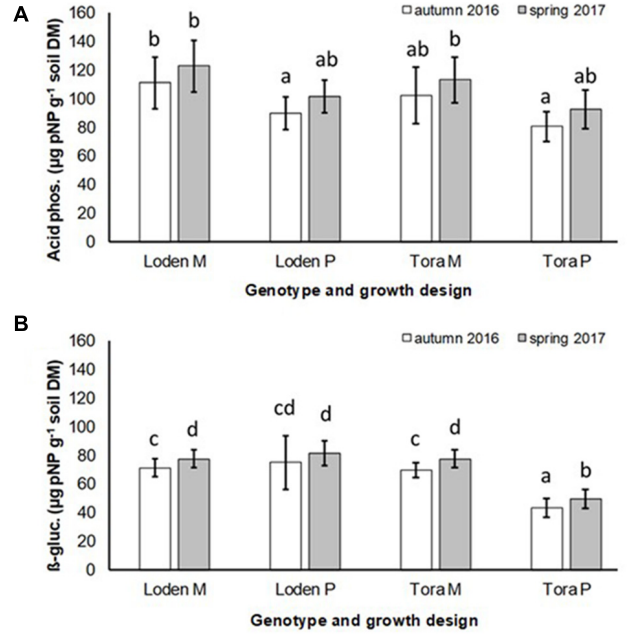

FIGURE 4 | Soil enzyme activities of **(A)** acid phosphatase and **(B)** β-glucosidases of *Salix* genotypes 'Tora' and 'Loden' in pure (P) and mixed (M) growth in 0–10 cm soil depth at the SRC Rostock in autumn 2016 and spring 2017 (means ± standard deviation, $n = 9$). Bars with different small letters (a, b, c, d) indicate significant differences among different treatments or sampling dates as defined by Duncan's test ($p < 0.05$).

Comparison Between Plots With Pure Host Genotypes and Genotype Mixtures

The mixed growth design of the genotypes increased significantly the colonization of fine roots by DSE, and the activities of acid phosphatases and β-glucosidases in the soil (**Table 2**).

The DCA of all fungal parameters and the two soil enzyme activities (acid phosphatase and β-glucosidase) clearly differentiated the genotypes (L for 'Loden,' T for 'Tora') and the host genotype mixture (M) from the two pure cultures (P) in autumn 2016 (**Figure 5A**) and spring 2017 (**Figure 5B**). The difference between the pure and the mixed culture was larger in spring 2017 than in autumn 2016, since the data differentiate the treatments along axis 2 (explaining about one quarter of the variation) in autumn, but along axis 1 in spring (explaining about half of the variation). The pure culture 'Tora P' was always closer to the mixture than the pure culture 'Loden P.'

DISCUSSION

The present results confirm the significant impact of the *Salix* genotype on its phenotypical traits (Cunniff et al., 2015) including the mycorrhizal (see **Figures 2**, **3A**) and endophytic (see **Figure 3B**) fungal colonization and host-specific differences in the fungal root colonization within a plant community as described by Toju et al. (2013b). The soil properties of the test site indicated P-deficiency (see section "Study Site and Test Plants"), which increases the importance of mycorrhizal fungi for the P-supply of the host plants (Smith et al., 2011). Assuming that plant neighbors with a faster growth rate can increase the competition for plants with slower growth, in the present mixture 'Tora M' had an advantage over 'Loden M.' Both, decreased fine root biomass under 'Loden M' grown in a mixture (see **Figure 1**) and greater similarity of the root traits and soil enzyme activities of the mixture compared with pure cultures 'Tora P' or 'Loden P' support this assumption (see **Figure 5**). These results are in line with our hypothesis that fine root growth, fungal abundance and activities are changed under host genotype mixtures, caused by changed competitive conditions for the individual genotypes and thereby changed interactions between them. However, the genotype-effect on the mycorrhizal colonization exceeds the impact of the plant design (pure or mixture of genotypes) on the mycorrhizal abundance (see **Figures 2**, **3A** and **Table 2**).

We predicted that the increased diversity of host plants in the genotype mixture will increase the diversity of root associated fungi too, since aboveground and belowground diversity can be linked (De Deyn and Van der Putten, 2005). However, we found increased fungal diversity only in endophytic fungi, not in mycorrhizal ones. This increased diversity was associated with increased colonization of the roots with DSE. Generally, low mycorrhizal diversity on *Salix* found here by only one

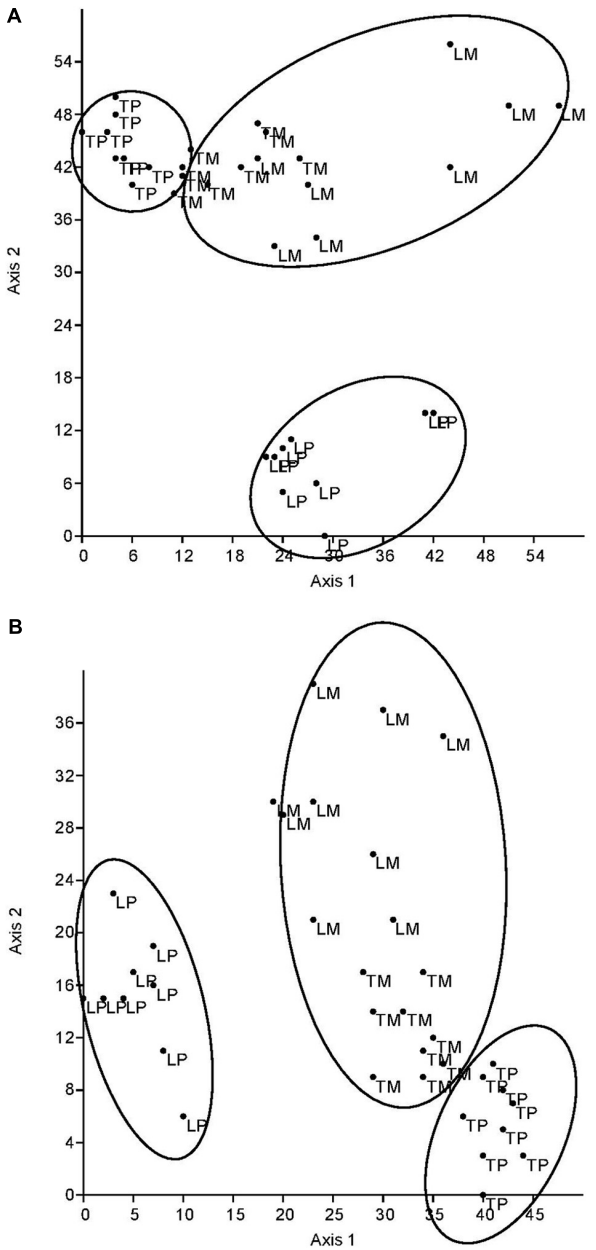

FIGURE 5 | Detrended correspondence analysis (DCA) plot based on square root transformed, normalized data and Euclidean distance matrix. Comparison of the two planting designs [pure (P) and mixture (M)] of *Salix* ['Loden' (L) and 'Tora' (T)] by root and soil properties **(A)** in autumn 2016 (axis 1: Eigenvalue = 581.9, variance explained: 52.1%, axis 2: Eigenvalue = 281.9, variance explained: 25.2%) and **(B)** in spring 2017 (axis 1: Eigenvalue = 501.2, variance explained: 56.6%, axis 2: Eigenvalue = 230.8, variance explained: 26.1%).

dominating EM fungal species (*Laccaria tortilis*; see **Table 1**) causes problems when interpreting the results. However, the low EM diversity is in line with the results on other genotypes of *Salix* (Püttsepp et al., 2004; Hrynkiewicz et al., 2012). It might be caused by the genotypic-specificity of this plant genus and additionally by the former arable site-conditions with lack of EM host plants. Therefore, we have focused rather on the ratios of root associations than on total mycorrhizal and endophytic diversity.

For the first time, we disclosed that increased host diversity of *Salix* genotypes can promote endophytic root colonization and increase soil enzyme activities involved in P-mobilization (see **Figures 2**–**4**). These results of a Continental SRC support the assumption of Pérez-Izquierdo et al. (2017) taken for Mediterranean forests, who highlighted the importance of structural shifts in fungal communities for their possible functional consequences. Functional consequences were revealed in an increased enzymatic P mobilization (see **Figure 4**) in the mycorrhizosphere with increased host plant diversity (mixture). These increased enzymatic activities can be caused directly by fungal impact, but also by the plant impact or most probably by a combination of both.

Dark septate endophytes were previously described to be the dominating root associated fungi under *S. caprea* on heavy metal contaminated sites (Likar and Regvar, 2013). In agreement with the results of these authors, we also found *Cadophora* spp. as a very common DSE in the roots of the two tested *Salix* genotypes at the non-contaminated arable site. This endophyte revealed plant growth promotion in heavy metal contaminated soils (Likar and Regvar, 2013). Also the second most common DSE in the present study (*Paraphaeosphaeria* sp., see **Table 1**), revealed plant growth promoting traits on another *Salix* sp. in heavy metal contaminated soil (An et al., 2015). The endophytic yeast *Rhodotorula mucilaginosa,* found under mixed *Salix* growth in the present study, was revealed to be plant growth promoting in *Populus* (Xin et al., 2009). However, from the present data no statement can be made on the growth response of *Salix* on the different fungal root colonization and the impact of DSE can vary from growth promotion to growth suppression of host plants (Aguilar-Trigueros and Rillig, 2016).

Increased colonization of the roots with DSE combined with consistent colonization with AM fungi in the mixture (see **Figures 1**, **3B**) were accompanied by increased soil enzyme activities involved in P-mobilization (see **Figure 4**). Della Monica et al. (2015) assumed, that DSE can be more effective to mobilize organic P, than AM fungi. However, in the present study increased enzyme activities might be stronger affected directly by the changed nutrient competition of the host plants in the mixture. Increased abundance of DSE without suppression of mycorrhiza formation supports that these fungal groups can interact beneficially in a joint host plant (Wężowicz et al., 2017). This might be caused by exudates of DSE, which can even stimulate the growth of mycorrhizal fungi (Scervino et al., 2009). Oppositely to the promotion of DSE in the mixture of different *Salix* genotypes, Becklin et al. (2012) revealed promoted of EM fungi on *Salix* in increased plant diversity by combination with herbaceous plants in an alpine meadow. However, these results have in common that host plant diversity changes the fungal root colonization of *Salix*.

The present data on dual mycorrhizal colonization of AM and EM fungi on *Salix* clearly confirmed the assumption of Lodge and Wentworth (1990), that these types of mycorrhizal fungi colonize

roots with an antagonistic behavior. Interestingly, Chen et al. (2000) found that antagonistic behavior of AM and EM fungi was most severe when the EM fungus *Laccaria* was present, which was the dominating EM fungus in the present study. Low fungal diversity was observed also in the sporocarp production in other SRCs (Baum et al., 2002).

The slow-growing genotype 'Loden' seems to be rather EM dominated, whereas the fast-growing genotype 'Tora' seems to promote AM formation (see **Figures 2**, **3**). This might be affected by the different litter quality of these genotypes, since the litter quality affects mycorrhizal communities (Lambers et al., 1998). In a pot experiment, leaves of 'Loden' revealed higher phenolic concentrations in the later growth than 'Tora' under the same environmental conditions (Baum et al., 2009b). Leaf litter with higher phenolic concentrations was described to support EM formation, whereas low phenolic concentrations were found to promote AM colonization of the host plants (Lambers et al., 1998).

Interestingly, the colonization of the roots with DSE was stronger affected by the host plant diversity than by the genotype-specific differences, which was revealed by an increased colonization of the roots (see **Figure 3B**) combined with increased species richness (see **Table 1**) in the mixture. Increased stress tolerance of *Salix* spp. was previously linked to colonization by several DSE (An et al., 2015). However, root endophytes can also include potential pathogens and each plant species and combination with different fungal strains might respond differently in plant growth (Aguilar-Trigueros and Rillig, 2016). Furthermore, the colonization of roots with DSE is also affected by edaphic properties of the site (Xie et al., 2017). The impact of edaphic differences within the present test site was initially balanced between the treatments by the randomized plot design in the present study. However, the increased colonization by DSE might also lead back to changed nutrient mobilization caused by the changed root growth of at least one of the mixed genotypes (see **Figure 1**) and indicated by changed enzymatic P mobilization under the mixture (see **Figure 4**).

Based on our results, it can be concluded that increased genotype diversity in *Salix* cultivation can lead to changed root competition, fungal association and enzymatic P-mobilization in the mycorrhizosphere. Subsequent investigations should assess the generality of promotion of DSE and P-mobilization in increased host diversity.

AUTHOR CONTRIBUTIONS

MW conceived and designed the field experiment within the frame of ECOLINK-*Salix*. CB managed the field site Rostock, collected the samples, did soil and root analyses and statistical analyses and wrote the first draft of the manuscript; did all soil chemical and biochemical analyses and wrote part of Section "Materials and Methods." NV and KH isolated the ectomycorrhizal fungi, created figures and tables and did statistical analyses. KH and SS identified the fungal species. NV analyzed the colonization density of mycorrhizal fungi and analyzed these parts of the results. SH and PF evaluated and discussed the mycorrhizal and endophytic results. All authors edited and revised the manuscript and approved the publication.

FUNDING

The authors gratefully acknowledge the German Federal Ministry of Education and Research (BMBF) for funding the BonaRes project InnoSoilPhos (Project No. 031A558). The work of MW and PF was partly funded by the Swedish Energy Agency (Project Nos. 36654-1 and 36654-2). Partial support to SH was provided by the Swedish Research Council Formas (Project No. 2016-00998).

ACKNOWLEDGMENTS

We are grateful to Ms. E. Heilmann (University of Rostock, Germany) for valuable technical assistance during the chemical soil analyses. This research was performed within the scope of the Leibniz ScienceCampus Phosphorus Research Rostock. We are grateful for the very valuable comments of the reviewers.

SUPPLEMENTARY MATERIAL

The Supplementary Material for this article can be found online at: https://www.frontiersin.org/articles/10.3389/fmicb.2018.01012/full#supplementary-material

REFERENCES

Agerer, R. (1987–2002). *Color Atlas of Ectomycorrhizae*. Schwäbisch Gmünd: Einhorn-Verlag.

Agerer, R. (1991). "Characterization of ectomycorrhiza," in *Techniques for the Study of Mycorrhiza. Methods Microbiology*, Vol. 23, eds J. R. Norris, D. J. Read, and A. K. Varma (London: Academic Press), 25–73.

Aguilar-Trigueros, C. A., and Rillig, M. C. (2016). Effect of different root endophytic fungi on plant community structure in experimental microcosms. *Ecol. Evol.* 6, 8149–8158.

Altschul, S. F., Gish, W., Miller, W., Myers, E. W., and Lipman, D. J. (1990). Basic local alignment search tool. *J. Mol. Biol.* 215, 403–410.

An, H., Liu, Y., Zhao, X., Huang, Q., Yuan, S., Yang, X., et al. (2015). Characterization of cadmium-resistant endophytic fungi from *Salix variegata* Franch. in Three Gorges Reservoir Region. *China. Microbiol. Res.* 176, 29–37. doi: 10.1016/j.micres.2015.03.013

Aravanopoulos, F. A., Kim, K. H., and Zsuffa, L. (1999). Genetic diversity of superior Salix clones selected for intensive forestry plantations. *Biomass Bioenergy* 16, 249–255.

Baum, C., and Hrynkiewicz, K. (2006). Clonal and seasonal shifts in communities of saprotrophic microfungi and soil enzyme activities in the mycorrhizosphere of *Salix* spp. *J. Plant Nutr. Soil Sci.* 169, 481–487.

Baum, C., Leinweber, P., Weih, M., Lamersdorf, N., and Dimitriou, I. (2009a). Effects of short rotation coppice with willows and poplar on soil ecology. *Agric. Forest Res.* 59, 183–196.

Baum, C., Toljander, Y. K., Eckhardt, K.-U., and Weih, M. (2009b). The significance of host-fungus combinations in ectomycorrhizal symbioses in the chemical quality of willow foliage. *Plant Soil* 323, 213–224.

Baum, C., Weih, M., Verwijst, T., and Makeschin, F. (2002). The effects of nitrogen fertilization and soil properties on mycorrhizal formation of Salix viminalis. *For. Ecol. Manage.* 160, 35–43.

Becklin, K. M., Pallo, M. L., and Galen, C. (2012). Willows indirectly reduce arbuscular mycorrhizal fungal colonization in understorey communities. *J. Ecol.* 100, 343–351. doi: 10.1111/j.1365-2745.2011.01903.x

Burke, D. J., Weintraub, M. N., Hewins, C. R., and Kalisz, S. (2011). Relationship between soil enzyme activities, nutrient cycling and soil fungal communities in a northern hardwood forest. *Soil Biol. Biochem.* 43, 795–803. doi: 10.1016/j.soilbio.2010.12.014

Caldwell, B. A. (2005). Enzyme activities as a component of soil biodiversity: a review. *Pedobiologia* 49, 637–644.

Chen, M., and Ma, L. Q. (2001). Comparison of three aqua-regia methods for twenty Florida soils. *Soil Sci. Soc. Am. J.* 65, 491–499.

Chen, Y. L., Brundrett, M. C., and Dell, B. (2000). Effects of ectomycorrhizas and vesicular-arbsucular mycorrhizas, alone and in competition, on root colonization and growth of Eucalyptus globules and *E. urophylla*. *New Phytol.* 146, 545–556.

Courty, P. E., Labbe, J., Kohler, A., Marçais, B., Bastien, C., Churin, J. L., et al. (2011). Effect of poplar genotypes on mycorrhizal infection and secreted enzyme activities in mycorrhizal and non-mycorrhizal roots. *J. Exp. Bot.* 62, 249–260. doi: 10.1093/jxb/erq274

Cunniff, J., Purdy, S. J., Barraclough, T. J., Castle, M., Maddison, A. L., Jones, L. E., et al. (2015). High yielded biomass genotypes of willow (*Salix* spp.) show differences in below ground biomass allocation. *Biomass Bioenergy* 80, 114–127.

De Deyn, G. B., and Van der Putten, W. H. (2005). Linking aboveground and belowground diversity. *Trends Ecol. Evol.* 20, 625–663.

Della Monica, I. F., Saparrat, M. C., Godeas, A. M., and Scervino, J. M. (2015). The co-existence between DSE and AMF symbionts affects plant P pools through P mineralization and solubilization processes. *Fungal Ecol.* 17, 10–17.

Eivazi, F., and Tabatabai, M. A. (1988). Glucosidases and galactosidases in soils. *Soil. Biol. Biochem.* 20, 601–606.

Fransson, P. M. A., Toljander, Y. K., Baum, C., and Weih, M. (2013). Plant genotype - ectomycorrhizal fungus combination drives resource allocation in willow - evidence for complex genotype-genotype interaction from a simple experiment. *Ecoscience* 20, 112–121.

Gardes, M., and Bruns, T. D. (1993). ITS primers with enhanced specificity for basidiomycetes—Application to identification of mycorhizae and rusts. *Mol. Ecol.* 2, 113–118. doi: 10.1111/j.1365-294X.1993.tb00005.x

Goldmann, K., Schöning, I., Buscot, F., and Wubet, T. (2015). Forest management type influences diversity and community composition of soil fungi across temperate forest ecosystems. *Front. Microbiol.* 6:1300. doi: 10.3389/fmicb.2015.01300

Hammer, Ø., Harper, D. A. T., and Ryan, P. D. (2001). PAST: Paleontological statistics software package for education and data analysis. *Palaeontol. Electron.* 4:9.

Hoeber, S., Arranz, C., Nordh, N.-E., Baum, C., Low, M., Nock, C., et al. (2018). Genotype identity has a more important influence than genotype diversity on shoot biomass productivity in willow short rotation coppices. *GCB Bioenergy* doi: 10.1111/gcbb.12521

Hoeber, S., Fransson, P., Prieto-Ruiz, I., Mazoni, S., and Weih, M. (2017). Two salix genotypes differ in productivity and nitrogen economy when grown in monoculture and mixture. *Front. Plant Sci.* 8:231. doi: 10.3389/fpls.2017.00231

Hrynkiewicz, K., Baum, C., Leinweber, P., Weih, M., and Dimitriou, I. (2010a). The significance of rotation periods for mycorrhiza formation in Short Rotation Coppice. *For. Ecol. Manag.* 260, 1943–1949.

Hrynkiewicz, K., Ciesielska, A., Haug, I., and Baum, C. (2010b). Ectomycorrhiza formation and willow growth promotion as affected by associated bacteria: role of microbial metabolites and use of C sources. *Biol. Fertil. Soils* 46, 139–150.

Hrynkiewicz, K., Toljander, Y., Baum, C., Fransson, P., Taylor, A., and Weih, M. (2012). Correspondence of ectomycorrhizal diversity and colonisation of willows (*Salix* spp.) grown in Short Rotation Coppice on arable sites and adjacent natural stands. *Mycorrhiza* 22, 603–613. doi: 10.1007/s00572-012-0437-z

Jones, M. D., Durall, D. M., and Tinker, P. B. (1998). A comparison of arbuscular and ectomycorrhizal *Eucalyptus coccifera*: growth response, phosphorus uptake efficiency and external hyphal production. *New Phytol.* 140, 125–134.

Lambers, H., Chapin, F. S., and Pons, T. L. (eds). (1998). "Role in ecosystem and global processes," in *Plant Physiological Ecology* (New York, NY: Springer).

Likar, M., and Regvar, M. (2013). Isolates of dark septate endophytes reduce metal uptake and improve physiology of *Salix caprea* L. *Plant Soil* 370, 593–604.

Lodge, D. J. (1989). The influence of soil moisture and flooding on formation of VA- endo- and ectomycorrhizae in Populus and Salix. *Plant Soil* 117, 255–262.

Lodge, D. J., and Wentworth, T. R. (1990). Negative associations among VA-mycorrhizal fungi and some ectomycorrhizal fungi inhabiting the same root system. *Oikos* 57, 347–356.

McGonigle, T. P., Miller, M. H., Evans, D. G., Fairchild, G. L., and Swan, J. A. (1990). A new method which gives an objective measure of colonization of roots by vesicular-arbuscular mycorrhizal fungi. *New Phytol.* 115, 495–501. doi: 10.1111/nph.1990.115.issue-3

Paquette, A., Hector, A., Castagneyrol, B., Vanhellemont, M., Koricheva, J., Scherer-Lorenzen, M., et al. (2018). A million and more trees for science. *Nat. Ecol. Evolut.* 2, 763–766. doi: 10.1038/s41559-018-0544-0

Pérez-Izquierdo, L., Zabal-Aguirre, M., Flores-Rentería, D., Gonzáles-Martínez, S. C., Buée, M., and Rincón, A. (2017). Functional outcomes of fungal community shifts driven by tree genotype and spatial-temporal factors in Mediterranean pine forests. *Environ. Microbiol.* 19, 1639–1652. doi: 10.1111/1462-2920.13690

Püttsepp, Ü., Rosling, A., and Taylor, A. F. S. (2004). Ectomycorrhizal fungal communities associated with *Salix viminalis* L. and *S. dasyclados* Wimm. Clones in a short-rotation forestry plantation. *For. Ecol. Manag.* 196, 413–424.

Rillig, M., Wendt, S., Antonovics, J., Hempel, S., Kohler, J., Wehner, J., et al. (2014). Interactive effects of root endophytes and arbuscular mycorrhizal fungi on an experimental plant community. *Oecologia* 174, 263–270. doi: 10.1007/s00442-013-2759-8

Rooney, D. C., Killham, K., Bending, G. D., Baggs, E., Weih, M., and Hodge, A. (2009). Mycorrhizas and biomass crops: opportunities for future sustainable development. *Trends Plant Sci.* 14, 542–549. doi: 10.1016/j.tplants.2009.08.004

Scervino, J. M., Gottlieb, A., Silvani, V. A., Pérgola, M., Fernández, L., and Godeas, A. M. (2009). Exudates of dark septate endophyte (DSE) modulate the development of the arbuscular mycorrhizal fungus (AMF) *Gigaspora rosea*. *Soil Biol. Biochem.* 41, 1753–1756. doi: 10.1016/j.soilbio.2009.04.021

Smith, S. E., Jakobsen, I., Gronlund, M., and Smith, F. A. (2011). Roles of arbuscular mycorrhizas in plant phosphorus nutrition; interactions between pathways of phosphorus uptake in arbuscular mycorrhizal roots have important implications for understanding and manipulating plant phosphorus acquisition. *Plant Physiol.* 156, 1050–1057.

Smith, S. E., and Read, D. J. (2008). *Mycorrhizal Symbiosis*. Cambridge: Academic Press.

Tabatabai, M. A. (1982). "Soil enzymes," in *Methods of Soil Analysis. Part 2, Agronomy 9*, eds A. L. Page, R. H. Miller, and D. R. Keeney (Madison, WI: American Society of Agronomy), 903–947. doi: 10.1016/j.tplants.2009.08.004

Timling, I., Walker, D. A., Nusbaum, C., Lennon, N. J., and Taylor, D. L. (2014). Rich and cold: diversity, distribution and drivers of fungal communities in patterned-ground ecosystems of the North American Arctic. *Mol. Ecol.* 23, 3258–3272. doi: 10.1111/mec.12743

Toju, H., Sato, H., Yamamoto, S., Kohmei, K., Tanabe, A. S., Yazawa, S., et al. (2013a). How are plant and fungal communities linked to each other in belowground ecosystems? A massively parallel pyrosequencing analysis of the association specificity of root-associated fungi and their host plants. *Ecol. Evol.* 3, 3112–3124. doi: 10.1002/ece3.706

Toju, H., Yamamoto, S., Sato, H., and Tanabe, A. S. (2013b). Sharing of diverse mycorrhizal and root-endophytic fungi among plant species in an oak-dominated cool–temperate forest. *PLoS One* 8:e78248. doi: 10.1371/journal.pone.0078248

van der Heijden, E. (2001). Differential benefits of arbuscular mycorrhizal and ectomycorrhizal infection of *Salix repens*. *Mycorrhiza* 10, 185–193. doi: 10.1007/s005720000077

Verheyen, K., Vanhellemont, M., Auge, H., Baeten, L., Baraloto, C., Barsoum, N., et al. (2016). Contributions of a global network of tree diversity experiments to sustainable forest plantations. *Ambio* 45, 29–41. doi: 10.1007/s13280-015-0685-1

Weih, M. (2004). Intensive short rotation forestry in boreal climates: present and future perspectives. *Can. J. For. Res.* 34, 1369–1378.

Wężowicz, K., Rozpądek, P., and Turnau, K. (2017). Interactions of arbuscular mycorrhizal and endophytic fungi improve seedling survival and growth in post-mining waste. *Mycorrhiza* 27, 499–511. doi: 10.1007/s00572-017-0768-x

White, T. J., Bruns, T., Lee, S., and Taylor, J. W. (1990). "Amplification and direct sequencing of fungal ribosomal RNA genes for phylogenetics," in *PCR Protocols: A Guide to Methods and Applications*, eds M. A. Innis, D. H. Gelfand, J. J. Sninsky, and T. J. White (New York, NY: Academic Press Inc), 315–322.

Xie, L., He, X., Wang, K., Hou, L., and Sun, Q. (2017). Spatial dynamics of dark septate endophytes in the roots and rhizospheres of *Hedysarum scoparium* in northwest China and the influence of edaphic variables. *Fungal Ecol.* 26, 135–143.

Xin, G., Glawe, D., and Doty, S. L. (2009). Characterization of three endophytic, indole-3-acetic acid producing yeasts occurring in Populus trees. *Mycol. Res.* 113, 973–980. doi: 10.1016/j.mycres.2009.06.001

Zhang, T., Xiang, H. B., Zhang, Y. Q., Liu, H. Y., Wei, Y. Z., Zhao, L. X., et al. (2013). Molecular analysis of fungal diversity associated with three bryophyte species in the Fildes Region, King George Island, maritime Antarctica. *Extremophiles* 17, 757–765. doi: 10.1016/j.mycres.2009.06.001

Zimmer, D., Baum, C., Meissner, R., and Leinweber, P. (2012). Soil-ecological evaluation of willows in a floodplain. *J. Plant Nutr. Soil Sci.* 175, 245–252.

Conflict of Interest Statement: The authors declare that the research was conducted in the absence of any commercial or financial relationships that could be construed as a potential conflict of interest.

frontiers in Microbiology

ORIGINAL RESEARCH
published: 12 July 2017
doi: 10.3389/fmicb.2017.01262

Piriformospora indica Reprograms Gene Expression in Arabidopsis Phosphate Metabolism Mutants But Does Not Compensate for Phosphate Limitation

*Madhunita Bakshi[1], Irena Sherameti[1], Doreen Meichsner[1], Johannes Thürich[1], Ajit Varma[2], Atul K. Johri[3], Kai-Wun Yeh[4] and Ralf Oelmüller[1]**

[1] Institute of General Botany and Plant Physiology, Friedrich-Schiller-University Jena, Jena, Germany, [2] Amity Institute of Microbial Technology, Amity University, Noida, India, [3] School of Life Sciences, Jawaharlal Nehru University, New Delhi, India, [4] Institute of Plant Biology, Taiwan National University, Taipei, Taiwan

OPEN ACCESS

Edited by:
Katarzyna Turnau,
Jagiellonian University, Poland

Reviewed by:
Vito Valiante,
Leibniz-Institute for Natural Product Research and Infection Biology - Hans Knöll Institute, Germany
Susana Rodriguez-Couto,
Ikerbasque, Spain

***Correspondence:**
Ralf Oelmüller
b7oera@uni-jena.de

Specialty section:
This article was submitted to Fungi and Their Interactions, a section of the journal Frontiers in Microbiology

Received: 24 February 2017
Accepted: 23 June 2017
Published: 12 July 2017

Citation:
Bakshi M, Sherameti I, Meichsner D, Thürich J, Varma A, Johri AK, Yeh K-W and Oelmüller R (2017) Piriformospora indica Reprograms Gene Expression in Arabidopsis Phosphate Metabolism Mutants But Does Not Compensate for Phosphate Limitation. Front. Microbiol. 8:1262. doi: 10.3389/fmicb.2017.01262

Piriformospora indica is an endophytic fungus of Sebacinaceae which colonizes the roots of many plant species and confers benefits to the hosts. We demonstrate that approximately 75% of the genes, which respond to *P. indica* in Arabidopsis roots, differ among seedlings grown on normal phosphate (Pi) or Pi limitation conditions, and among wild-type and the *wrky6* mutant impaired in the regulation of the Pi metabolism. Mapman analyses suggest that the fungus activates different signaling, transport, metabolic and developmental programs in the roots of wild-type and *wrky6* seedlings under normal and low Pi conditions. Under low Pi, *P. indica* promotes growth and Pi uptake of wild-type seedlings, and the stimulatory effects are identical for mutants impaired in the PHOSPHATE TRANSPORTERS1;1, -1;2 and -1;4. The data suggest that the fungus does not stimulate Pi uptake, but adapts the expression profiles to Pi limitation in Pi metabolism mutants.

Keywords: root expression profiles, PHT1, WRKY6, *Piriformospora indica*, phosphate starvation

INTRODUCTION

Piriformospora indica, an endophytic fungus of Sebacinaceae, colonizes the roots of many plant species and promotes their growth and performance (Peškan-Berghöfer et al., 2004; Waller et al., 2005, 2008; Shahollari et al., 2007; Oelmüller et al., 2009; Camehl et al., 2010; Nongbri et al., 2012; Varma et al., 2012; Jogawat et al., 2013; Ye et al., 2014). The fungus improves nutrition uptake from the soil to the host roots (Sherameti et al., 2005; Shahollari et al., 2005; Kumar et al., 2011) suggesting a strong fungal influence on the plant transport processes and metabolism. Mycorrhizal and beneficial root-colonizing fungi deliver phosphate (Pi) to the roots. Pi is taken up by the plants through Pi transporters, and low- and high-affinity Pi transporters of the PHOSPHATE TRANSPORTER1 (PHT1) family have been reported to be involved in the mycorrhizal pathway (Harrison et al., 2002; Garcia et al., 2016). While mycorrhizal plants contain fungus-inducible *PHT1* genes (Bucher, 2007; Chen et al., 2007; Walder et al., 2015), plants which do not interact

Abbreviations: LP, low phosphate concentration; NP, normal phosphate concentration; Pi, phosphate; WT, wild-type.

with mycorrhizal fungi, such as Arabidopsis, lack inducible *PHT1* genes. The expression of their Pi transporter genes is independent of root colonization by endophytic root-colonizing microbes, but some members of the *PHT1* gene family respond to Pi deficiency (e.g., Chiou et al., 2001; Ai et al., 2009; Ayadi et al., 2015). In return, up to 50% of the carbon fixed by photosynthesis can be delivered to mycorrhizal fungi associated with the roots in natural ecosystems (Nehls et al., 2010).

Root colonization and nutrient exchange by *P. indica* results in substantial alterations in the root architecture, an effect which is highly host specific (cf. Lee et al., 2011; Dong et al., 2013). In Arabidopsis, *P. indica* stimulates root growth: while the primary root length is slightly reduced, lateral root growth and root hair development is promoted (e.g., Varma et al., 1999; Barazani et al., 2005; Vadassery et al., 2008, 2009a; Johnson and Oelmüller, 2009; Fakhro et al., 2010; Das et al., 2012, 2014; Lahrmann and Zuccaro, 2012; Lahrmann et al., 2013; Prasad et al., 2013; Venus and Oelmüller, 2013; Bakshi et al., 2015; Vahabi et al., 2015). Secondary metabolites, such as indole-3-acetaldoxime derivatives, hormones, and different defense compounds/pathways control the colonization of roots during Arabidopsis/*P. indica* interaction and thus influence root development (Sherameti et al., 2008; Camehl et al., 2011; Hilbert et al., 2012; Nongbri et al., 2012; Bakshi et al., 2015; Matsuo et al., 2015). *P. indica* also protects the roots by stimulating the antioxidant system under stress, which again influences developmental programs in response to environmental cues and the redox state of the roots (Baltruschat et al., 2008; Vadassery et al., 2009b; Harrach et al., 2013). To what extend root developmental and genetic programs are altered by endophytes such as *P. indica* is not completely understood. The quite different root responses of various plant species to *P. indica* demonstrate the important role of the host genetic programs (discussed in Lee et al., 2011; Dong et al., 2013).

Here, we investigate the role of Pi availability and the Arabidopsis transcription factor WRKY6 involved in the regulation of the plant Pi metabolism in the *P. indica*/Arabidopsis symbiosis. The Arabidopsis mutant lacking the WRKY6 transcription factor shows an altered response to LP stress (Chen et al., 2009; Bakshi et al., 2015), since WRKY6 is involved in regulating *PHOSPHATE1* (*PHO1*) expression. PHO1 is a Pi exporter and required for the transfer of Pi from root epidermal and cortical cells to the xylem. The *pho1* mutant has low shoot Pi and shows Pi deficiency symptoms, including poor shoot growth and overexpression of numerous Pi-deficiency responsive genes (cf. Wege et al., 2016). LP treatment reduced WRKY6 binding to the *PHO1* promoter and thus allows *PHO1* expression (Chen et al., 2009). Therefore, deletion of WRKY6 alters the root development of WT seedlings in a Pi-dependent manner (Bakshi et al., 2015). We compared the expression profiles of WT and *wrky6* seedlings grown under normal Pi (NP) and low Pi (LP) conditions and found that the response to *P. indica* is quite different in the roots of WT and *wrky6* seedlings, both under NP and LP conditions. This suggests that the genetic response of Arabidopsis to *P. indica* is highly dependent on the nutrient availability and genotype of the host. We also investigated the role of Arabidopsis Pi transporters in the symbiosis and demonstrate that Pi limitation, due to inactivation of the plant Pi transporters, cannot be compensated by *P. indica* colonization.

MATERIALS AND METHODS

Growth Conditions of Plant and Fungus

WT, *wrky6*, *pht1;1* (At5g43350), *pht1;2* (At5g43370), and *pht1;4* (At2g38940) seeds and seeds of the *pht1;1 pht1;4* double knock-out line were surface sterilized and placed on Petri dishes containing MS (Murashige and Skoog, 1962) nutrient medium (with 13,7 g/l sucrose). After cold treatment for 48 h at 4°C, the plates were incubated for 10 days at 22°C under continuous illumination (100 μmol m^{-2} s^{-1}). *P. indica* was cultured as described previously on Aspergillus minimal medium (Johnson et al., 2011). After 10 days of growth, all seedlings were either transferred to fresh plates (MS or plant nutrient medium (PNM) as indicated in the figure legends, or to soil, cf. **Figure 6**) for the different treatments. The procedure has been described in details in Johnson et al. (2011)[1]. For the arsenate assay, they were transferred to fresh MS medium containing 1 mM Pi (KH_2PO_4) and 200 μM sodium arsenate (V) for 3 weeks (cf. **Table 2**). Alternatively, they were transferred to PNM medium (without sucrose) for 2 weeks. The PNM medium contained a fungal *P. indica* plaque in the middle (co-cultivation with *P. indica*) or an agar plaque without fungal hyphae (control, without *P. indica*), as described previously (Vadassery et al., 2009a). The fungus was allowed to grow on the PNM medium for 1 week before the seedlings were transferred to the fungal lawn. Control plates were treated in the same way. To test whether simultaneous inactivation of *PHT1;1* and *PHT1;4* has a long-term effect on plant performance, the 10-day old seedlings were transferred from MS plants (cf. above) to soil and kept in a greenhouse for 4 weeks. For the plate experiments shown in **Figure 6** (TOP), the seedlings were transferred to PNM medium with NP for 3 weeks.

Generation of the Homozygous Knock-Out Lines

The following SALK insertion lines were used for the *PHT1* genes: *pht1;1* (At5g43350; SALK_088586C/N666665), *pht1;2* (At5g43370; SALK_110194) and *pht1;4* (At2g38940; SALK_103881). Homozygocity was tested with gene-specific primer pairs (cf. Supplementary Table S1) and primers given on the SALK homepage[2]. The *pht1;1 pht1;4* double knock-out line was generated by crossing the two homozygote single knock-out lines. After confirmation of homozygocity of the two inactivated genes, the lack of PHT transporters was also confirmed with the arsenate resistance assay. The *wrky6* line was described in Bakshi et al. (2015).

[1]http://pubman.mpdl.mpg.de/pubman/item/escidoc:1587455/component/escidoc:1674163/IMPRS056.pdf

[2]www.arabidopsis.org

Arsenate Resistance Assay

Seeds were germinated on full MS medium. After 10 days they were transferred to MS medium with 1 mM Pi (KH_2PO_4) and 200 μM sodium arsenate (V) for 3 weeks. Growth occurred in continuous white light (80 μmol m^{-2} s^{-1}).

Co-cultivation Experiments

Co-cultivation of *A. thaliana* (WT, *wrky6*, as well as *pht1* single and double knock-out lines) with *P. indica* was performed under *in vitro* culture conditions on a nylon membrane placed on top of solidified PNM media (Johnson et al., 2011). For Pi stress treatment PNM media with two different Pi concentrations [2.5 mM (NP, control) and 0.25 mM (LP, Pi stress)] were used. For expression profiling, square Petri dishes were divided into two equal parts. On one plate two *P. indica* disks on Aspergillus medium, one in each part, and on another plate two disks without the fungus, were placed on each part and kept for 7 days. The disks were used for mock treatment. After 48 h of cold treatment and 10 days of growth as described above on MS medium, seedlings of equal sizes were used for the co-cultivation assays or mock treatment, using the pre-prepared plates. For each Pi concentration, 4 treatments were compared: WT, WT + *P. indica*, *wrky6* and *wrky6* + *P. indica*. Seedlings were maintained under two different Pi concentrations with and without *P. indica* as mentioned above for 3 days at 22°C and 70–80% humidity in a 16-h light/8-h dark cycle. Roots were harvested and frozen in liquid nitrogen for total RNA extraction. They were used for gene expression analyses.

For analysis of the *pht1* mutants, the same treatment was performed except that the seedlings were maintained in the two different Pi concentrations in normal Petri dishes for 14 days, before harvest for further analysis.

Microarray Analyses

Total RNA from roots of colonized/uncolonized WT and *wrky6* mutants from three independent biological experiments grown under NP and LP conditions were harvested 3 days after transfer to the fresh plates. RNA from roots of mock-treated WT and *wrky6* mutants (agar plaques instead of *P. indica* plaques) were used as control. The 3-day time point was chosen because in preliminary experiments, we observed a strong regulation of a selected number of genes. For each treatment, identical amounts of RNA from three independent biological replicates were labeled and hybridized according to Agilent's One-Color Microarray-Based Gene Expression Analysis (OAK Lab GmBH, Hennigdorf, Germany). Quality of RNA samples were checked by photometrical measurements with the Nanodrop 2000 spectrophotometer (Thermo Scientific) and then analyzed on agarose gels (2%) as well as by using the 2100 Bioanalyser (Agilent Technologies, CA, United States) for determining the RNA integrity and the exclusion of potential contaminants. After verifying the quality of RNA, the Low Input Quick Amp Labeling Kit (Agilent Technologies) was used for generation of fluorescent complementary RNA (cRNA). Default cRNAs were amplified by using oligo-dT primers labeled with cyanine 3-CTP (Cye-3) according to the manufacturer's protocol. Cye-3-labeled probes were hybridized to 8 ×60 k custom-designed Agilent microarray chips. For hybridization, the Agilent Gene Expression Hybridization Kit (Agilent Technologies) was used. The hybridized slides were washed and scanned using the SureScan Microarray Scanner (Agilent Technologies) at a resolution of 3 micron generating a 20 bit TIFF file, respectively.

Microarray Data Analysis

Data extractions from Images were performed using the Agilent's Feature Extraction software version 11. Feature extracted data were analyzed using the DirectArray Version 2.1 software from Agilent. Normalization of the data was performed with DirectArray using the ranked median quantiles according to Bolstad et al. (2003). To identify significantly differentially expressed genes $\log_2$-fold changes are calculated and Student's *t*-test was performed. In summary, raw data were normalized by rank median quantiles, intensity values from replicate probes were averaged, $\log_2$-ratios between the treatments were calculated and Student's *t*-statistics applied to test for significance. Genes with $\log_2$-fold change <-1 or >1 and p-value < 0.05 were considered to be significantly different. All data show expression levels of genes regulated by *P. indica* relative to the control levels without *P. indica*. Differentially expressed genes were then assigned using the A. *thaliana* Gene Ontology software (TAIR's GO annotations) (Berardini et al., 2004) and transcript abundance were classified based on their functional categories and pathways using the MapMan[3] software.

The microarray data have been submitted to NCBI (GEO) under the accession number GSE63500.

Real Time PCR Analyses

RNA was isolated from root tissues of WT and mutant seedlings at the time points indicated in the Sections "Result" and "Figure Legends" using the RNeasy Plant Mini Kit (Qiagen), and reverse-transcribed for quantitative real-time PCR (qRT- PCR) analyses, using an iCycler iQ real-time PCR detection system and iCycler software (version 2.2; Bio-Rad). cDNA was synthesized using the Omniscript cDNA synthesis kit (Qiagen, Hilden, Germany) with 1 μg of RNA. For the amplification of the reverse-transcription PCR products, iQ SYBR Green Supermix (Bio-Rad) was used according to the manufacturer's protocol in a final volume of 20 μl. The iCycler was programmed to 95°C for 3 min; 40 x (95°C 30 sec, 57°C 15 s, 72°C 30 sec), 72°C for 10 min, followed by a melting curve program from 55°C to 95°C in increasing steps of 0.5°C. All reactions were performed from three biological and three technical replicates. The mRNA levels for each cDNA probe were normalized with respect to the plant *ACTIN2* mRNA level. Fold-induction values of target genes were calculated with the ΔΔCP equation of Pfaffl (2001) and related to the mRNA level of target genes as indicated in the Result section. Primer pairs used in this study are given in Supplementary Table S2. They were designed using the CLC Main Workbench program[4].

[3]http://mapman.gabipd.org/web/guest/mapman

[4]http://www.clcbio.com/products/clc-main-workbench

Pi Content Analysis

For Pi content analyses, the samples were dried in an oven at 105°C overnight. The samples were mixed with 2 ml of 65% HNO_3 and kept for one hour at 160°C. The final volume was adjusted to 10 ml and the pH to 3.0–4.0. Finally, samples were mixed with ascorbic acid reagent and ammonium molybdate reagent (DIN 38405) and the Pi content was analyzed by the phosphomolybdenum blue reaction using the UV-160A spectrophotometer. Total Pi concentration was determined for the complete seedlings and expressed in nmol/g dry weight. Experiments were repeated three times with different biological replicas.

Chlorophyll Fluorescence Measurements

Plant performance was measured for WT and the *pht1;1 pht1;4* double knock-out line using chlorophyll fluorescence measurements. After germination and 10 days on MS medium (cf. above), the seedlings were transferred to fresh PNM plates with LP or NP concentrations under high light intensity (300 μmol m^{-2} s^{-1}) for 1 week. This high light intensity confers stress to the seedlings. The efficiency of the photosynthetic electron transfer describing the fitness of the plants was measured as Fv/Fm described by Maxwell and Johnson (2000) after dark adaptation of the seedlings for 20 min. The fluorescence parameters were measured with a FluorCam 700MF instrument and analyzed with the Flucam 5.0 software. The data are averages for 30 seedlings and three independent biological experiments.

RESULTS

P. indica Regulates Different Genes in WT and *wrky6* Roots Under LP and NP Conditions

The root architecture of WT and *wrky6* seedlings differs substantially and the differences become stronger under Pi limitation conditions (Chen et al., 2009; Bakshi et al., 2015). This is reflected by different expression profiles in the roots. Here we analyze how the expression profiles of the roots of WT and *wrky6* seedlings grown on either NP or LP respond to *P. indica* colonization.

Figure 1 shows that *P. indica* affects the expression of ∼ 3000 genes (regulation > 2-fold) in WT and *wrky6* roots under NP or LP conditions. The vast majority of the responsive genes are specific for a given genotype and Pi condition, since the number of genes which are equally regulated in any comparison of the four conditions is less than 25% (**Figures 1–3**). Interestingly, only 13 genes are common in the four datasets. (for details on individual genes, cf. accession number GSE63500 at NCBI, GEO). This shows an enormous flexibility of the roots to respond to the fungus, and the response is strongly dependent on the genotype (WT vs. *wrky6* mutant) and the Pi availability (LP *vs.* NP) (**Figure 2**).

Functional categorization of the identified gene products using the *A. thaliana* Gene Ontology program (TAIR's GO annotations; Berardini et al., 2004) demonstrates that the overall number of genes belonging to one of the four categories codes for proteins with similar functions. The strongest differences among the four categories were found for genes involved in DNA/RNA metabolism and extracellular functions, or for genes which code for mitochondrial, plastid and plasma membrane proteins. Less than 20% of these genes are common in all four categories (**Figure 3**, and GSE63500 at NCBI). Among them are hydrolases and transferases, transcription factors and numerous transporters (**Figure 3**). In each of the four datasets, different genes for proteins involved in the perception of internal and external signals, abiotic and biotic stress responses, primary protein metabolism, transcription, developmental processes and cell organization respond to *P. indica* (**Figure 3**). This is further supported by the PageMan analysis for genes differentially responding to *P. indica* in WT and *wrky6* roots under NP and LP conditions (Supplementary Figures S1–S4). For example, many DNA-related genes are down-regulated in *P. indica*-colonized WT roots under NP conditions and *P. indica*-colonized *wrky6* roots exposed to LP, but are up-regulated in colonized WT roots exposed to LP. Many genes involved in diverse signaling processes are down-regulated by *P. indica* in WT under Pi limitation, while signaling-related genes in WT roots grown under NP are up-regulated. Stress-related genes are down-regulated by *P. indica* in WT roots under Pi limitation, but up-regulated under the other three conditions (Supplementary Figures S1–S4). Categorization of the gene products according to enzyme families also demonstrates enormous differences under the four conditions, and often, the genes for one enzyme family are up-regulated under one condition and down-regulated or not regulated under other conditions (Supplementary Figure S1). Big differences can be observed for the large cytochrome P_{450} enzyme family, but also for peroxidases, phosphatases and glutathione-S-transferases. The identification of genes for GDSL lipases (Dong et al., 2016) suggests that *P. indica* also affects lipid metabolism. Finally, *P. indica* targets different members of the glucosidase gene family under NP and LP conditions and this is particularly striking for the *wrky6* mutant.

It is also obvious from Supplementary Figures S1–S4 that interfering with the Pi metabolism by either inactivating *WRKY6* or growth under Pi limitation conditions has severe consequences on many genes involved in transport processes (Supplementary Figure S2), cellular responses (Supplementary Figure S3), and regulatory functions (Supplementary Figure S4). Besides the expected effects on Pi transporters, genes for nitrate, ammonium and sulfate transporters are differentially regulated under the four conditions. We also observe big differences on genes for sugar, potassium and amino acid transporters, P- and V-ATPases and lipid transfer proteins. Genes related to calcium transport processes are up-regulated under all conditions, although to different extents (Supplementary Figure S2). Overall, the data indicate that inactivation of *WRKY6* activates biotic stress response genes under NP conditions (Supplementary Figures S3, S4). Furthermore, growth under LP conditions results in the down-regulation of many biotic-stress-related genes which are up-regulated under NP conditions, and this is observed for both WT and *wrky6* roots. The latter observation holds also true for abiotic stress-related genes (Supplementary Figure S3)

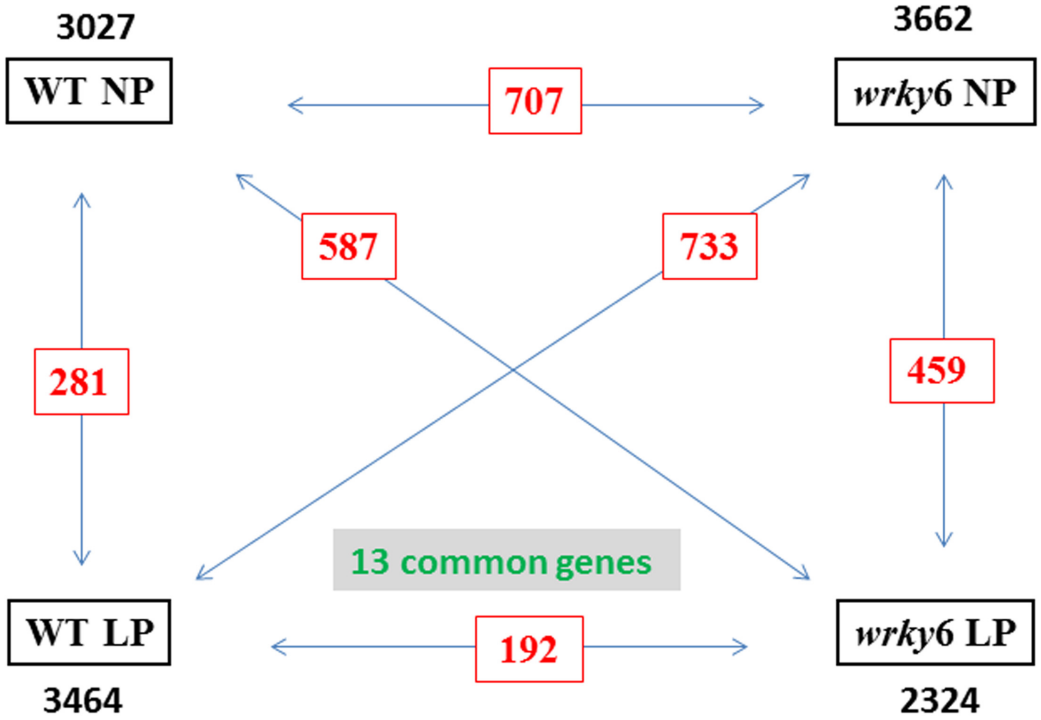

FIGURE 1 | Total number of differentially regulated genes which responded to *Piriformospora indica* in the roots of WT or *wrky6* seedlings grown on either NP or LP. The black numbers show all genes regulated more than 2-fold in the roots of WT or *wrky6* seedlings grown on either NP or LP media. Common genes among the two datasets are in red. Thirteen genes are common to all datasets. For specific genes, see data submitted to NCBI.

and those with diverse functions (categorized as "miscellaneous") in WT roots. Peroxiredoxin genes are preferentially down-regulated by *P. indica* in LP, and osmotic stress related genes (categorized as "drought/salt", Supplementary Figure S3) are downregulated in the *wrky6* mutant under NP relative to the WT control. Finally, many genes related to the cell cycle are downregulated by *P. indica* in LP-grown WT seedlings when compared to those grown under NP conditions. As expected, the changes in the gene expression patterns for cellular responses (Supplementary Figure S3) are reflected by corresponding changes in regulatory pathways (Supplementary Figure S4). It is particularly striking that members of the receptor kinase gene family are downregulated by *P. indica* in LP-grown WT roots relative to roots grown under NP conditions. Taken together, the fungus activates quite different signaling pathways, as well as metabolic and developmental programs under the four conditions tested.

PHT1 and Pi Regulator Genes in the Arabidopsis/*P. indica* Interaction

Pi uptake from the soil and distribution of Pi within the Arabidopsis plant is mediated by nine PHT1 family members (Ayadi et al., 2015). While some *PHT1* genes are regulated in response to beneficial fungi in mycorrhizal plants, it is believed that the non-mycorrhizal plant Arabidopsis does not contain fungus-inducible *PHT1* genes (cf. Tamura et al., 2012; Sisaphaithong et al., 2012). This is consistent with our observations that most of the *PHT1* transporter genes do not respond to *P. indica* (>2-fold) under NP or LP conditions, or are only mildly regulated (*PHT1;5*; *PHT1;6* and *PHT1;8*; cf. Discussion) (**Table 1**). Furthermore, WRKY42 modulates Pi homeostasis through regulating Pi translocation and acquisition (Su et al., 2015) and the transcription factor also regulates *PHO1* expression (Su et al., 2015). WRKY45 activates *PHT1;1* expression under Pi starvation (Wang et al., 2014). Both *WRKY* genes do not respond to *P. indica* (**Table 1**). Recently, the importance of posttranscriptional processes for PHT1 proteins has been shown (Cardona-López et al., 2015), and NITROGEN LIMITATION ADAPTATION (NLA) targets Pht1;4 for degradation during the regulation of Pi homeostasis (Lin et al., 2013; Park et al., 2014). Furthermore, ESCRT-III-associated protein ALIX mediates high-affinity Pi transporter trafficking to maintain Pi homeostasis in Arabidopsis (Cardona-López et al., 2015). **Table 1** demonstrates that only *PHO1* responds to *P. indica* (> 2-fold) in both WT and *wrky6* roots under LP, but not NP conditions. This demonstrates that *PHO1* is not only regulated under Pi limitation conditions, but also a mild target of signals from *P. indica* (cf. Discussion).

P. indica Does Not Compensate for Pi Limitation in *PHT1* Mutants

Although *PHT1;1*, *PHT1;2* and *PHT1;4* do not respond (>2-fold) to *P. indica* under all tested conditions, they show the highest expression level in roots (Shin et al., 2004; Ayadi et al.,

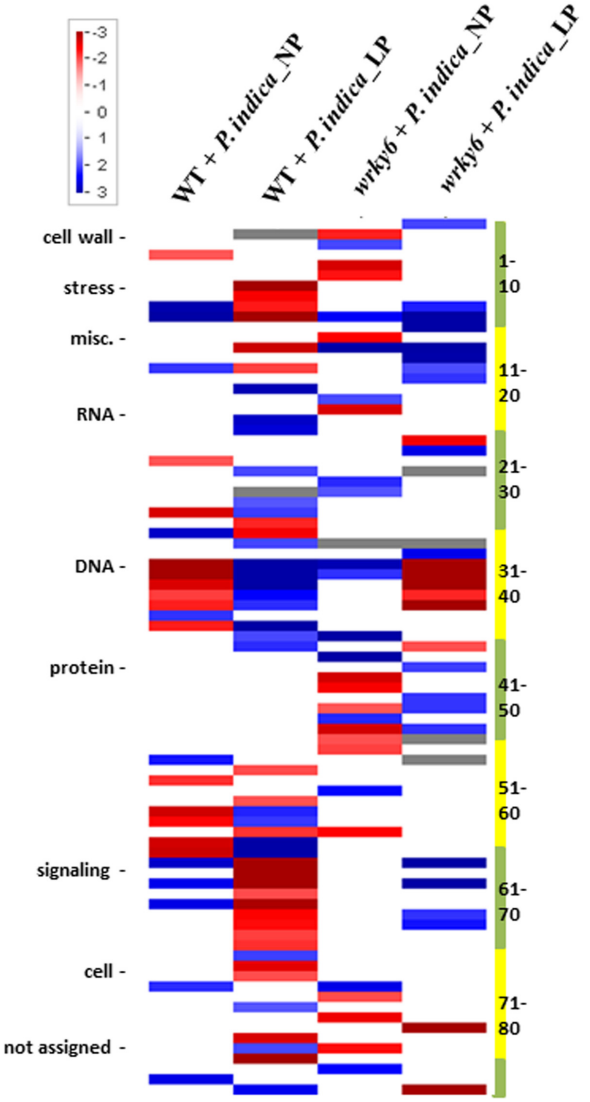

FIGURE 2 | PageMan analysis of differentially expressed genes (>2-fold) by *P. indica* in WT or *wrky6* roots grown on either NP or LP. Scale depicts level of expression with blue being high and red being low. Only significantly regulated (p-value <0.05) categories are shown. Numbers on the right refer to the categories defined by the PageMan program, which are presented in Supplementary Table S1. For specific genes, see data submitted to NCBI. For more detailed information on the program, cf. the MapMan software at http://mapman.gabipd.org/web/guest/ mapman.

2015). Therefore, we generate homozygote knock-out lines for these three transporters, and confirmed their homozygosity using standard techniques, gene-specific primer pairs as well as a primer combination with the T-DNA insertion (Supplementary Table S2). Furthermore, *pht1;1* and *pht1;4* were crossed to generate a double knock-out line. In addition to the molecular analyses (**Figure 4**), confirmation of homozygosity for all lines can easily be tested by growth of the seedlings in the presence of arsenate (V), because this heavy metal is transported into the roots via PHT1 transporters (DiTusa et al., 2016, and references therein). After 3 weeks on MS medium with 200 μM arsenate, the fresh weight of WT seedlings was reduced by 86% compared to seedlings grown without arsenate (**Table 2**). The fresh weights of the single mutants *pht1;1* and *pht1;2* were similarly reduced (79%). This demonstrates that inactivation of these Pi transporter genes has little effect on arsenate (and probably also Pi) uptake. The performance of *pht1;4* is significantly better, suggesting that PHT1;4 is more important for arsenate (and probably Pi) uptake than PHT1;1 and PHT1;2. The fresh weight of the double knock-out line is reduced by 43% in the presence of arsenate, compared to growth without arsenate. This suggests that simultaneous inactivation of the two Pi transporters is more effective in restricting arsenate (and Pi) uptake than the effects observed for the single knock-out lines. The degree of resistance can be taken as indication for the contribution of the transporter to the Pi/arsenate uptake. Although different growth conditions and arsenate concentrations were used, our results resemble those described by Shin et al. (2004).

WT seedlings and all mutants and were grown on NP and LP medium in the absence or presence of *P. indica* for 2 weeks. Shoots and roots were harvested and weighed (**Figures 5A,B**). The fresh weights of the shoots and roots of the *pht1;1* and *pht1;2* seedlings did not differ significantly from those of the WT, the weights of the shoots and roots of the *pht1;4* seedlings were slightly reduced and those of the double knock-out line ∼ half of the weights of the WT. Only little differences can be observed for seedlings grown on NP or LP medium. This might be due to the pre-cultivation of the seedlings on full MS medium: the Pi that is taken up during this period might be sufficient for the seedling's growth during the next 2 weeks. In all cases, we observed an increase in the shoot and root fresh weights for seedlings grown in the presence of *P. indica*. However, the relative increases (% increase) among the different mutant and WT seedlings are comparable. Thus, *P. indica* does not compensate for the absence of specific PHT1s by transferring more Pi from the soil to the roots. This is particularly striking for the double knock-out mutant. Although the weight of the mutant is approximately half of the weight of a WT seedling, the % increases in their fresh weights induced by *P. indica* are approximately the same (∼ 20%). This indicates that *P. indica* promotes growth of all seedlings grown under LP and NP conditions, and this is independent of the presence or absence of the tested PHT1 transporters.

To test whether *P. indica* participates in Pi allocation, we used the same growth conditions and measured the total Pi content in the seedlings (**Figure 5C**). Similar to previous reports (Shahollari et al., 2005), we observed that all *P. indica*-exposed seedlings contained more Pi than the seedlings not exposed to the fungus. Closer inspection of the data shows that the % increase in the Pi content is not different between WT and mutant seedlings. This again is consistent with the idea that *P. indica* does not compensate for the lower Pi uptake of the Pi mutants. The higher Pi content in colonized seedlings might be caused by better access to the nutrient in the presence of the hyphal mycelium, and/or because Pi from the fungal hyphae is delivered to the host.

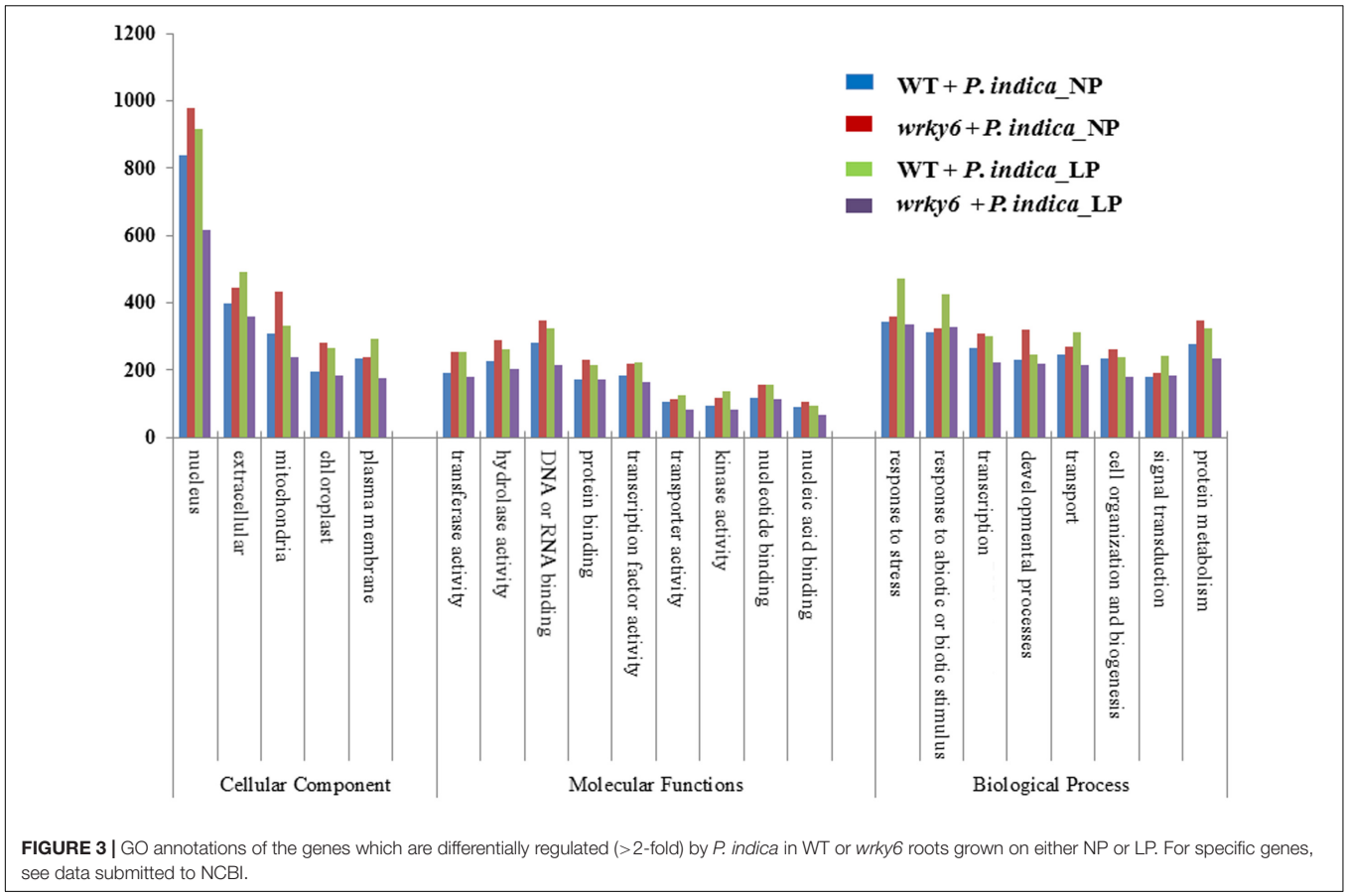

FIGURE 3 | GO annotations of the genes which are differentially regulated (>2-fold) by *P. indica* in WT or *wrky6* roots grown on either NP or LP. For specific genes, see data submitted to NCBI.

TABLE 1 | Regulation of the 9 *PHOSPHATE TRANSPORTER1* (*PHT1*) genes and genes for regulatory proteins involved in *PHT1* gene and PHT1 protein regulation by *Piriformospora indica* in WT and *wrky6* roots under NP and LP conditions.

		Fold induction [colonized/uncolonized roots]			
Gene name	**Annotation**	**WT NP**	**WT LP**	***wrky6* NP**	***wrky6* LP**
PHT1;1	At5g43350	0.027 (1.02)	0.168 (1.12)	0.060 (1.04)	0.270 (1.21)
PHT1;2	At5g43370	−0.239 (0.85)	0.311 (1.24)	−0.365 (0.78)	0.038 (1.03)
PHT1;3	At5g43360	−0.046 (0.97)	0.223 (1.17)	−0.299 (0.81)	0.104 (1.08)
PHT1;4	At2g38940	−0.710 (0.61)	−0.471 (0.72)	−0.331 (0.80)	−0.304 (0.81)
PHT1;5	At2g32830	**1.656 (3.15) [3.43 ± 0.43]**	**1.184 (2.27) [2.77 ± 0.34]**	−0.221 (0.86)	0.500 (1.41)
PHT1;6	At5g43340	**−1.248 (0.42) [0.40 ± 0.03]**	**1.730 (3.32) [3.71 ± 0.49]**	**−1.278 (0.41) [0.44 ± 0.04]**	−0.991 (0.50) **[0.42 ± 0.04]**
PHT1;7	At3g54700	−0.715 (0.61)	−0.125 (0.92)	0.177 (1.13)	−0.061 (0.96)
PHT1;8	At1g20860	1.246 **(2.37) [2.13 ± 0.37]**	−0.055 (0.96)	−0.546 (0.69)	−1.076 **(0.47) [0.40 ± 0.03]**
PHT1;9	At1g76430	−0.194 (0.87)	−0.143 (0.91)	−0.161 (0.89)	0.064 (1.05)
ALIX	At1g15130	−0.066 (0.96)	0.035 (1.03)	0.188 (1.14)	0.070 (1.07)
WRKY42	At4g04450	0.202 (1.15)	0.349 (1.27)	−0.470 (0.72)	0.060 (1.04)
WRKY45	At3g01970	0.130 (1.09)	−0.716 (0.61)	0.098 (1.07)	−0.395 (0.76)
NLA	At1g02860	−0.134 (0.91)	0.210 (1.16)	−0.308 (0.81)	0.178 (1.13)
PHO1	At3g23430	0.397 (1.32)	**1.019 (2.03) [3.23 ± 0.26]**	0.250 (1.19)	**1.420 (2.68) [2.90 ± 0.31]**

The numbers represent log_2 values of the mRNA levels in colonized roots vs. uncolonized roots, the numbers in brackets show fold-induction (colonized/uncolonized roots). Conditions with >2-fold regulation are in bold. The data from the microarray analysis (NCBI under the accession number GSE63500) are compared with qRT-PCR data shown in square brackets. Only those data are shown where a more than twofold regulation was observed. The primer pairs are given in Supplementary Table S1. Microarray and qRT-PCR data are based on three independent experiments, errors are SEs.

TABLE 2 | Arabidopsis *pht1* mutants are more resistant to arsenate (V) than the WT. After 10 days, the seedlings were transferred to MS medium with 1 mM Pi and 200 μM arsenate.

Plants	Fresh weight (mg) (+ arsenate)	Fresh weight (mg) (– arsenate)	% inhibition of fresh weight (%)
WT	19.4 ± 1.1	138.6 ± 7.1	86
pht1;1	25.5 ± 3.1	121.4 ± 6.5	79
pht1;2	24.4 ± 2.3	116.1 ± 5.4	79
pht1;4	32.5 ± 3.9	105.8 ± 5.2	69
pht1;1 pht1;4	51.1 ± 2.9	89.6 ± 2.4	43

The fresh weights of 3-week-old Arabidopsis WT, pht1;1, pht1;2, pht1;4 and pht1;1 pht1;4 single and double mutants are given. % fresh weight is calculated relative to the fresh weight of the seedlings grown without arsenate. Based on three independent experiments with 30 seedlings each, errors are SEs.

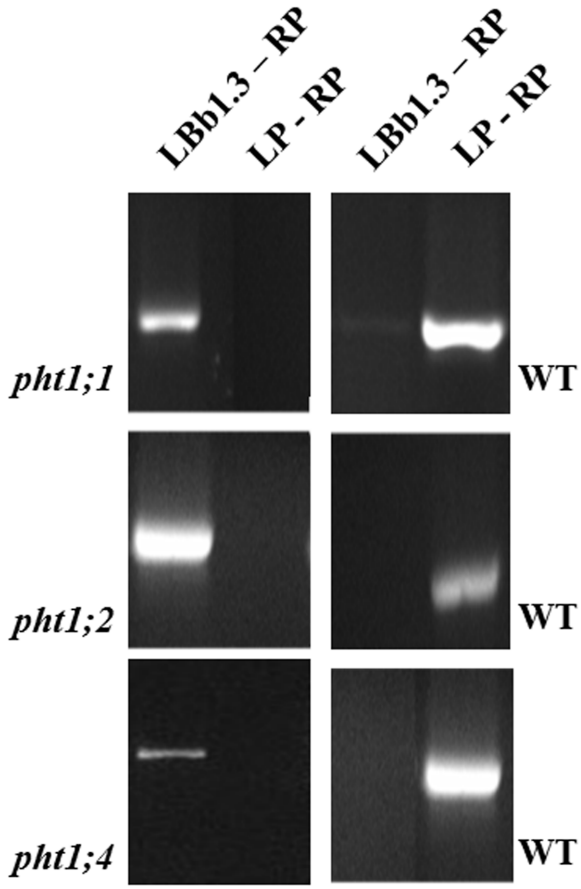

FIGURE 4 | Homozygosity test for *pht1;1*, *pht1;2*, and *pht1;4* by PCR. Only one plant per knock-out line is shown. The gene-specific primers LP (left primer) and RP (right primer) amplify the expected fragments for the *PHT1;1*, *PHT1;2*, and *PHT1;4* genes in DNA preparations from WT plants, which is used as a positive control. The T-DNA specific primer LBb1.3 (TGGTTCACGTAGTGGGCCATCG) in combination with the gene-specific RPs (cf. Supplementary Table S1) amplifies a PCR fragment only when the T-DNA is inserted into the respective gene close to the RP. The PCR samples were run on a 1% agarose gel next to a size ladder and the predicted sizes of the fragments were confirmed.

Since the double knock-out line showed the strongest phenotype, we grew the seedlings under LP conditions in the absence or presence of *P. indica* and tested whether the mutant respond to Pi limitation by activating Pi starvation-response and transporter genes and whether *P. indica* has an effect on the regulation of these genes in the mutant. **Table 3** shows that the expression of several unrelated Pi starvation-response and transporter genes are up-regulated in the double mutant under LP and that their expression is not significantly affected by *P. indica*. This includes *PHOSPHATE STARVATION RESPONSE1* (*PSR1*) which codes for a MYB transcription factor involved in the Pi starvation response (Rubio et al., 2001), *PHOSPHATE STARVATION RESPONSE1* (*PHR1*), a master regulator of Pi homeostasis (e.g., Linn et al., 2017), which balances between nutrition and immunity in plants (Motte and Beeckman, 2017), the gene for the zinc-finger transcription factor ZAT6, which controls Pi homeostasis in roots (Devaiah et al., 2007a), for MYB62 involved in Pi homeostasis and hormone actions (Devaiah et al., 2009) and for WRKY45 which activates *PHT1;1* expression in response to Pi starvation (Wang et al., 2014). Thus, the fungus does not interfere with the regulation of these genes in the LP-grown *pht1;1 pht1;4* mutant.

The double mutant is impaired in long-term growth experiments on natural soil (**Figure 6**). After germination and initial growth in Petri dishes for 10 days, the seedlings were transferred to soil for additional 3 weeks. We observed an approximately 50% reduction in the fresh weight compared to WT control plants (**Figure 6** lower panel). This suggests the combination of the two transporters is important for growth on natural soil.

To test whether *P. indica* promotes the performance of the double knock-out line, we transferred the seedlings to PNM medium and high light intensity (300 μmol m^{-2} s^{-1}). The chlorophyll fluorescence parameters Fv/Fm showing the efficiency of the photosynthetic electron transport were measured daily under LP and NP conditions over a period of 7 days (**Figure 7**). Under NP conditions, no difference between colonized and uncolonized WT and double knock-out seedlings can be detected (data not shown). However, under LP conditions, a decline in the Fv/Fm values can be detected for uncolonized *pht1;1 pht1;4* seedlings, and this stress response is partially compensated in the presence of the fungus. Thus, *P. indica* partially promotes the performance of the double knock-out line under Pi limitation conditions.

DISCUSSION

The Genotype and Pi Availability Have a Strong Influence on *P. indica*-Targeted Genes

Previous interaction studies of root-colonizing microbes with plants have shown that the mutualistic interaction and the benefits for the two partners is strongly dependent on environmental conditions (e.g., Pánková et al., 2011; Moeller

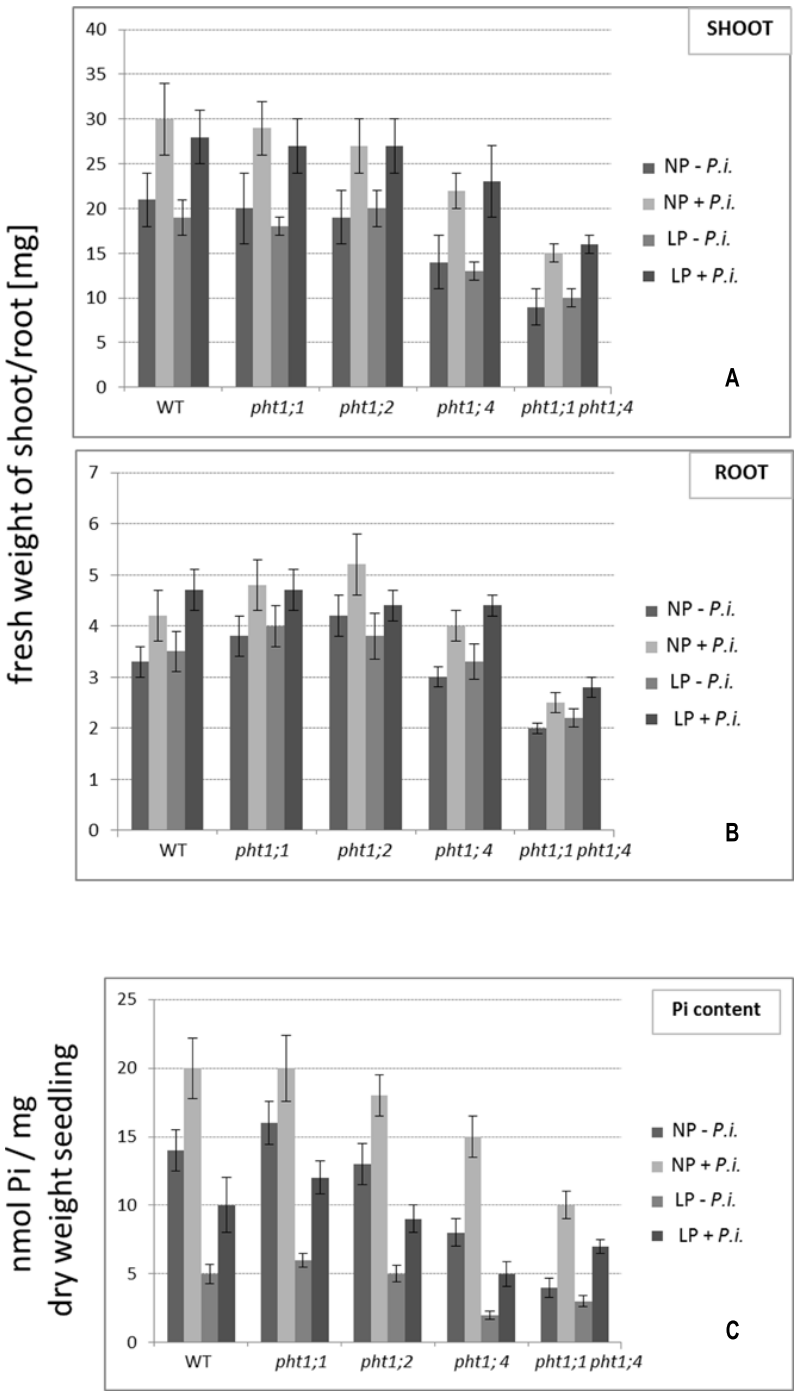

FIGURE 5 | The effect of *P. indica* on the fresh weights **(A,B)** and Pi content **(C)** of WT and *pht1* mutant seedlings grown on NP and LP medium. Seedlings were transferred to PNM medium with either NP or LP and with or without *P. indica* and the shoots and roots were harvested separately after 2 weeks. Based on five independent co-cultivation experiments with 60 seedlings per treatment and genotype. Bars represent SEs.

et al., 2014) and differ between plant species when they are colonized by the same microbe (Lee et al., 2011; Lahrmann et al., 2013). Here, we compare a WT Arabidopsis line with a mutant impaired in the WRKY6 transcription factor which is a central regulator of Pi metabolism in Arabidopsis (Hamburger et al., 2002; Liu et al., 2012). By growing these seedlings under NP and LP conditions, we show that *P. indica* targets quite different genes in both genotypes and under the two Pi conditions. Genotype-dependent alterations in gene expression profiles in response to various biotic and abiotic stresses have been described

TABLE 3 | Pi starvation response-genes are up-regulated in LP-grown *pht1;1 pht1;4* mutant seedlings, in the presence and absence of *P. indica*.

Gene	WT, LP, - *P. indica*	WT, LP, + *P. indica*	*pht1;1 pht1;4*, LP, – *P. indica*	*pht1;1 pht1;4*, LP, + *P. indica*
WRKY45	1.00 ± 0.2	0.80 ± 0.09	2,20 ± 0,25	2.32 ± 0,19
PHT1;5	1.00 ± 0,12	0.77 ± 0.11	2.33 ± 0,27	2,40 ± 0,23
PHR1	1.00 ± 0,21	0.93 ± 0.09	1.96 ± 0,24	2,11 ± 0,26
ZAT6	1.00 ± 0,27	1.11 ± 0.12	2.45 ± 0,20	2,20 ± 0,17
MYB62	1. 00 ± 0,11	1.06 ± 0.07	2.66 ± 0,21	2.45 ± 0,22

WT and double knock-out seedlings were grown in LP for 2 weeks in the presence or absence of P. indica before RNA extraction for qRT-PCR. Primer pairs for the analyzed genes are given in Supplementary Table S1. The mRNA level of a given gene from WT seedlings grown under LP without P. indica was set as 1.0 and the other values are expressed relative to it. For additional information about the genes not discussed in this paper: PHR1 (Rubio et al., 2001), ZAT6 (Devaiah et al., 2007a), and MYB62 (Devaiah et al., 2009). Based on three independent RNA extraction and two technical repetitions per RNA. Errors are SEs.

for many ecotypes, varieties, lines and mutants impaired in regulatory loci. Genotype-specific expression of miRNAs might explain distinct cold (Zhang et al., 2014) or salt sensitivities (Ding et al., 2009; Beritognolo et al., 2011; Yin et al., 2012). Genotype-specific defense gene expression programs were reported for two cultivars of *Glycine max* (Klink et al., 2011). In *Sorghum bicolor* a genotype-specific expression atlas for vegetative tissues was published (Shakoor et al., 2014). Ashraf et al. (2009) described comparative analyses of genotype-dependent expressed sequence tags and stress-responsive transcriptome for chickpea wilt. Here, we show that a mutation in the *WRKY6* gene which strongly affects plant performance under Pi limitation conditions, results in a severe reprogramming of the root transcriptome after *P. indica* infection. The altered gene expression profile affects many biochemical, signaling and metabolic processes, which are not related to the Pi metabolism (**Figures 2**, **3** and Supplementary Figures S1–S4). To our knowledge this is the first report on a comprehensive analysis of gene reprogramming in response to *P. indica* in roots of two genotypes, the WT and the *wrky6* mutant. The huge difference in the expression profiles clearly indicates that the fungus targets different genes and consequently induces completely different physiological responses in the roots of WT and *wrky6* seedlings under the two different Pi conditions. This might have important implication for the application of the fungus in agriculture, since its interaction with different cultivars of a crop plant might differ and this again is dependent on environmental and soil conditions.

Analysis of genes involved in Pi starvation have been analyzed in many plant species (e.g., Nilsson et al., 2010). Interesting in the study performed here the number of *P. indica* stimulated genes in roots of both WT and *wrky6* seedlings is quite different in LP compared to NP conditions Not only Pi-related signaling and metabolic pathways, but also developmental programs, defense strategy and transport processes are affected in WT and *wrky6* roots. Under our standardized conditions, ∼70–80% of the plant genes are differentially expressed in response to *P. indica* by inactivation of *WRKY6* and/or change in the amount of available Pi (**Figure 2**). We assume that similar phenomena could be observed for agriculturally important crops interacting with beneficial root-colonizing fungi. Therefore, the interplay between root-colonizing microbes with different cultivars, the soil quality and fertilizations may have a strong influence on the root metabolism.

PHT1 Genes and *P. indica*

The members of the AtPHT1 protein family share a high degree of similarity with overlapping expression patterns (Ayadi et al., 2015). PHT1;1 and PHT1;4 form homomeric and heteromeric complexes (Fontenot et al., 2015) and both transporters play a major role in Pi acquisition from low- and high-Pi environments (Shin et al., 2004). Their genes show the highest expression of all *PHT1* genes in Arabidopsis roots (Shin et al., 2004), but PHT1;1 also plays an important role in Pi translocation from roots to leaves in high Pi conditions (Ayadi et al., 2015). PHT1;2 cooperates with PHT1;1 and PHT1;4 in Pi uptake from the soil (Ayadi et al., 2015) and *PHT1;6* is mainly expressed in flower tissue (Karandashov et al., 2004). Members of the *PHT1* gene family are up-regulated by mycorrhizal fungi in mycorrhiza-forming plant species (e.g., Ceasar et al., 2014; Walder et al., 2015; Kariman et al., 2016; for some recent publications), however the Arabidopsis homologs (*pht1;5*, *pht1;6*, and *pht1;8*) do not or barely respond to *P. indica.* The slight response of *pht1;5* to *P. indica* might be related to the role of PHT1;5 as mobilizer of Pi between source and sink organs (Nagarajan et al., 2011). Under low Pi conditions, *pht1;5* mutants show reduced Pi allocation to the shoots and elevated transcript levels for several Pi starvation-response genes (Nagarajan et al., 2011). *P. indica* might interfere with the translocation and regulation of Pi under Pi limitation. Karandashov et al. (2004) identified six *cis*-regulatory elements which are present in different combinations and numbers in mycorrhiza-inducible *PHT1* genes from different plant species. None of these elements were found in the *P. indica*-responsive *AtPHT1;5* and *AtPHT1;6* promoters, but four of them are present in the root-specific *AtPHT1;8* promoter which shows a low response to *P. indica* (**Table 1**). Whether these elements are involved in *P. indica* -mediated *PHT1;8* expression, is unclear.

Co-cultivation of *pht1* mutants with *P. indica* demonstrates that the fungus does not compensate for Pi shortage by stimulating the expression of specific *PHT1* family members (**Table 1** and **Figure 5**) or promoting Pi uptake via other ways. The % growth promotion and Pi uptake in the presence of the fungus is comparable for WT and mutant seedlings. Even for the double knock-out line, the positive effects of the fungus are comparable to the WT (**Figure 5**). Together with the observation that the *PHT1* genes are not or barely regulated by *P. indica*, it is conceivable that the fungus targets additional genetic programs, which are not directly related to Pi availability.

PHO1 Respond to *P. indica*

Besides *PHT1* genes (Wasaki et al., 2003; Wu et al., 2003; Misson et al., 2005), the mRNA levels for several transcription factors involved in controlling Pi homeostasis, such as AtPHR1 (Rubio et al., 2001), the rice Pi starvation-induced transcription factor1 (Yi et al., 2005), AtWRKY75 (Devaiah et al., 2007a), the Arabidopsis zinc finger family member 6 (AtZAT6; Devaiah et al., 2007b), AtMYB62 (Devaiah et al., 2009), and AtWRKY6

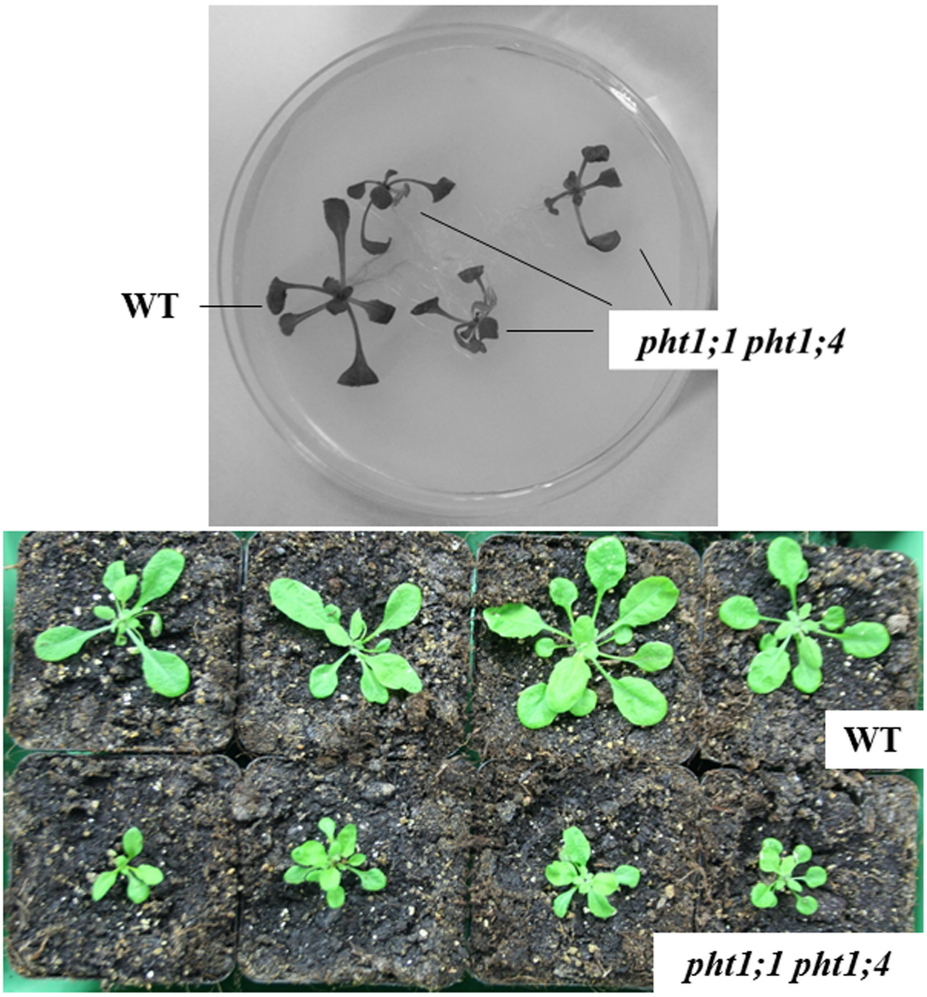

FIGURE 6 | Phenotype of WT and *pht1;1 pht1;4* seedlings/plants. Top: After 10 days, WT and *pht1;1 pht1;4* seedlings were transferred to PNM medium with NP for 3 weeks. Bottom: Arabidopsis WT (upper 4 plants) and *pht1;1 pht1;4* double knock-out lines (lower 4 plants) were grown in Petri dishes for 10 days before transfer to soil for additional 4 weeks. Growth occurred in a greenhouse.

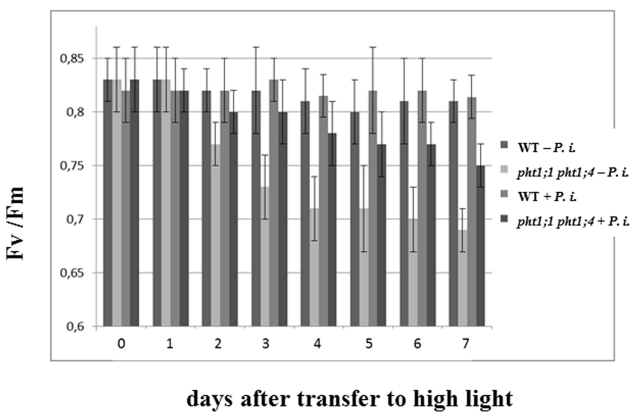

FIGURE 7 | *Piriformospora indica* promotes the efficiency of the photosynthetic electron transport of the double knock-out line exposed to high light stress under Pi limitation. Chlorophyll fluorescence measurements (Fv/Fm) for *P. indica*-exposed WT and *pht1;1 pht1;4* seedlings which were transferred to fresh PNM plates with LP and high light intensity (300 μmol m^{-2} s^{-1}) for 1 week (cf. Materials and Methods). Based on three independent experiments with 16 plants each. Bars represent SEs.

(Chen et al., 2009) are upregulated under Pi limitation in different plant species (Wang et al., 2014). Also, PHO1 has been shown to be an important regulator in controlling Pi homeostasis (Chen et al., 2007). We observed a mild, but significant upregulation of the *PHO1* mRNA level by *P. indica* in LP-exposed Arabidopsis roots (**Table 1**). PHO1 plays an important role in Pi translocation from roots to shoots (Poirier et al., 1991; Wang et al., 2014), is located primarily in root stellar cells and controls Pi xylem loading from root stellar cells (Hamburger et al., 2002). Thus, the protein is mainly involved in long distance Pi transport in Arabidopsis (Su et al., 2015). The *pho1* mutant is impaired in loading Pi to the xylem vessel in the roots (Poirier et al., 1991). Taken together, our data suggest that *P. indica* interferes primarily with the Pi distribution and metabolism in Arabidopsis under Pi limitations rather than by promoting Pi uptake from the soil.

AUTHOR CONTRIBUTIONS

MB: performed most of the experiments, except those described for others authors. IS: generated the ko lines. DM: analysed microarray data, performed low Pi experiments with Arabidopsis. JT: performed Pi experiments with the double mutant. AJ: supervision of Ph.D. students together with RO (common India-Germany DAAD project). AV: supervision of Ph.D. students together with RO (common India-Germany DAAD project). K-WY: supervision of microarray analyses. RO: supervision of Ph.D. students together with RO (common India-Germany DAAD project)

ACKNOWLEDGMENT

This work was supported by CRC 1127 to RO and collaborative DAAD grants to RO, Germany and AV, India and K-WY, Taiwan.

SUPPLEMENTARY MATERIAL

The Supplementary Material for this article can be found online at: http://journal.frontiersin.org/article/10.3389/fmicb.2017.01262/full#supplementary-material

REFERENCES

Ai, P., Sun, S., Zhao, J., Fan, X., Xin, W., Guo, Q., et al. (2009). Two rice phosphate transporters, OsPht1;2 and OsPht1;6, have different functions and kinetic properties in uptake and translocation. *Plant J.* 57, 798–809. doi: 10.1111/j.1365-313X.2008.03726.x

Ashraf, N., Ghai, D., Barman, P., Basu, S., Gangisetty, N., Mandal, M. K., et al. (2009). Comparative analyses of genotype dependent expressed sequence tags and stress-responsive transcriptome of chickpea wilt illustrate predicted and unexpected genes and novel regulators of plant immunity. *BMC Genomics* 10:415. doi: 10.1186/1471-2164-10-415

Ayadi, A., David, P., Arrighi, J. F., Chiarenza, S., Thibaud, M. C., Nussaume, L., et al. (2015). Reducing the genetic redundancy of Arabidopsis PHOSPHATE TRANSPORTER1 transporters to study phosphate uptake and signaling. *Plant Physiol.* 167, 1511–1526. doi: 10.1104/pp.114.252338

Bakshi, M., Vahabi, K., Bhattacharya, S., Sherameti, I., Varma, A., Baldwin, I. T., et al. (2015). WRKY6 restricts *Piriformospora indica*-mediated stimulation of root development in Arabidopsis under low phosphate conditions. *BMC Plant Biol.* 15:305. doi: 10.1186/s12870-015-0673-4

Baltruschat, H., Fodor, J., Harrach, B. D., Niemczyk, E., Barna, B., Gullner, G., et al. (2008). Salt tolerance of barley induced by the root endophyte *Piriformospora indica* is associated with a strong increase in antioxidants. *New Phytol.* 180, 501–510. doi: 10.1111/j.1469-8137.2008.02583.x

Barazani, O., Benderoth, M., Groten, K., Kuhlemeier, C., and Baldwin, I. T. (2005). *Piriformospora indica* and *Sebacina vermifera* increase growth performance at the expense of herbivore resistance in *Nicotiana attenuata*. *Oecologia* 146, 234–243. doi: 10.1007/s00442-005-0193-2

Berardini, T. Z., Mundodi, S., Reiser, L., Huala, E., Garcia-Hernandez, M., Zhang, P., et al. (2004). Functional annotation of the Arabidopsis genome using controlled vocabularies. *Plant Physiol.* 135, 745–755. doi: 10.1104/pp.104.040071

Beritognolo, I., Harfouche, A., Brilli, F., Prosperini, G., Gaudet, M., Brosché, M., et al. (2011). Comparative study of transcriptional and physiological responses to salinity stress in two contrasting *Populus alba* L. genotypes. *Tree Physiol.* 31, 1335–1355. doi: 10.1093/treephys/tpr083

Bolstad, B. M., Rafael, A. I., Magnus, A., and Terence, P. S. (2003). A comparison of normalization methods for high density oligonucleotide array data based on variance and bias. *Bioinformatics* 19, 185–193. doi: 10.1093/bioinformatics/19.2.185

Bucher, M. (2007). Functional biology of plant phosphate uptake at root and mycorrhiza interfaces. *New Phytol.* 173, 11–26. doi: 10.1111/j.1469-8137.2006.01935.x

Camehl, I., Drzewiecki, C., Vadassery, J., Shahollari, B., Sherameti, I., Forzani, C., et al. (2011). The OXI1 kinase pathway mediates *Piriformospora indica*-induced growth promotion in Arabidopsis. *PLoS Pathog.* 7:e1002051. doi: 10.1371/journal.ppat.1002051

Camehl, I., Sherameti, I., Venus, Y., Bethke, G., Varma, A., Lee, J., et al. (2010). Ethylene signalling and ethylene-targeted transcription factors are required to balance beneficial and non-beneficial traits in the symbiosis between the endophytic fungus *Piriformospora indica* and *Arabidopsis thaliana*. *New Phytol.* 185, 1062–1073. doi: 10.1111/j.1469-8137.2009.03149.x

Cardona-López, X., Cuyas, L., Marín, E., Rajulu, C., Irigoyen, M. L., Gil, E., et al. (2015). ESCRT-III-associated protein ALIX mediates high-affinity phosphate transporter trafficking to maintain phosphate homeostasis in Arabidopsis. *Plant Cell* 27, 2560–2581. doi: 10.1105/tpc.15.00393

Ceasar, S. A., Hodge, A., Baker, A., and Baldwin, S. A. (2014). Phosphate concentration and arbuscular mycorrhizal colonisation influence the growth, yield and expression of twelve PHT1 family phosphate transporters in foxtail millet (*Setaria italica*). *PLoS ONE* 9:e108459. doi: 10.1371/journal.pone.0108459

Chen, A., Hu, J., Sun, S., and Xu, G. (2007). Conservation and divergence of both phosphate- and mycorrhiza-regulated physiological responses and expression patterns of phosphate transporters in solanaceous species. *New Phytol.* 173, 817–831. doi: 10.1111/j.1469-8137.2006.01962.x

Chen, Y. F., Li, L. Q., Xu, Q., Kong, Y. H., Wang, H., and Wu, W. H. (2009). The WRKY6 transcription factor modulates *PHOSPHATE1* expression in response to low Pi stress in Arabidopsis. *Plant Cell* 21, 3554–3566. doi: 10.1105/tpc.108.064980

Chiou, T.-J., Liu, H., and Harrison, M. J. (2001). The spatial expression patterns of a phosphate transporter (MtPT1) from *Medicago truncatula* indicate a role in phosphate transport at the root/soil interface. *Plant J.* 25, 281–293. doi: 10.1046/j.1365-313x.2001.00963.x

Das, A., Kamal, S., Shakil, N. A., Sherameti, I., Oelmüller, R., Dua, M., et al. (2012). The root endophyte fungus *Piriformospora indica* leads to early flowering, higher biomass and altered secondary metabolites of the medicinal plant, *Coleus forskohlii*. *Plant Signal. Behav.* 7, 103–112. doi: 10.4161/psb.7.1.18472

Das, J., Ramesh, K. V., Maithri, U., Mutangana, D., and Suresh, C. K. (2014). Response of aerobic rice to *Piriformospora indica*. *Indian J. Exp. Biol.* 52, 237–251.

Devaiah, B. N., Karthikeyan, A. S., and Raghothama, K. G. (2007b). WRKY75 transcription factor is a modulator of phosphate acquisition and root development in Arabidopsis. *Plant Physiol.* 143, 1789–1801. doi: 10.1104/pp.106.093971

Devaiah, B. N., Madhuvanthi, R., Karthikeyan, A. S., and Raghothama, K. G. (2009). Phosphate starvation responses and gibberellic acid biosynthesis are regulated by the MYB62 transcription factor in Arabidopsis. *Mol. Plant.* 2, 43–58. doi: 10.1093/mp/ssn081

Devaiah, B. N., Nagarajan, V. K., and Raghothama, K. G. (2007a). Phosphate homeostasis and root development in Arabidopsis are synchronized by the zinc finger transcription factor ZAT6. *Plant Physiol.* 145, 147–159. doi: 10.1104/pp.107.101691

Ding, D., Zhang, L., Wang, H., Liu, Z., Zhang, Z., and Zheng, Y. (2009). Differential expression of miRNAs in response to salt stress in maize roots. *Ann. Bot.* 103, 29–38. doi: 10.1093/aob/mcn205

DiTusa, S. F., Fontenot, E. B., Wallace, R. W., Silvers, M. A., Steele, T. N., Elnagar, A. H., et al. (2016). A member of the Phosphate transporter 1 (Pht1) family from the arsenic-hyperaccumulating fern *Pteris vittata* is a high-affinity arsenate transporter. *New Phytol.* 209, 762–772. doi: 10.1111/nph.13472

Dong, S., Tian, Z., Chen, P. J., Kumar, S. K. R., Shen, C. H., Cai, D., et al. (2013). The maturation zone is an important target of *Piriformospora indica* in *Chinese cabbage* roots. *J. Exp. Bot.* 64, 4529–4540. doi: 10.1093/jxb/ert265

Dong, X., Yi, H., Han, C. T., Nou, I. S., and Hur, Y. (2016). GDSL esterase/lipase genes in *Brassica rapa* L.: genome-wide identification and expression analysis. *Mol. Genet. Genomics* 291, 531–542. doi: 10.1007/s00438-015-1123-6

Fakhro, A., Andrade-Linares, D. R., von Bargen, S., Bandte, M., Büttner, C., Grosch, R., et al. (2010). Impact of *Piriformospora indica* on tomato growth and on interaction with fungal and viral pathogens. *Mycorrhiza* 20, 191–200. doi: 10.1007/s00572-009-0279-5

Fontenot, E. B., Ditusa, S. F., Kato, N., Olivier, D. M., Dale, R., Lin, W. Y., et al. (2015). Increased phosphate transport of *Arabidopsis thaliana* Pht1;1 by site-directed mutagenesis of tyrosine 312 may be attributed to the disruption of homomeric interactions. *Plant Cell Environ.* 38, 2012–2022. doi: 10.1111/pce.12522

Garcia, K., Doidy, J., Zimmermann, S. D., Wipf, D., and Courty, P. E. (2016). Take a trip through the plant and fungal transportome of mycorrhiza. *Trends Plant Sci.* 1456, 1360–1385. doi: 10.1016/j.tplants.2016.07.010

Hamburger, D., Rezzonico, E., Petétot, J. M. C., Somerville, C., and Poirier, Y. (2002). Identification and characterization of the Arabidopsis *PHO1* gene involved in phosphate loading to the xylem. *Plant Cell* 14, 889–902. doi: 10.1105/tpc.000745

Harrach, B. D., Baltruschat, H., Barna, B., Fodor, J., and Kogel, K. H. (2013). The mutualistic fungus *Piriformospora indica* protects barley roots from a loss of antioxidant capacity caused by the necrotrophic pathogen *Fusarium culmorum*. *Mol. Plant-Microbe Interact.* 26, 599–605. doi: 10.1094/MPMI-09-12-0216-R

Harrison, M. J., Dewbre, G. R., and Liu, J. (2002). A phosphate transporter from *Medicago truncatula* involved in the acquisition of phosphate released by arbuscular mycorrhizal fungi. *Plant Cell* 14, 2413–2429. doi: 10.1105/tpc.004861

Hilbert, M., Voll, L. M., Ding, Y., Hofmann, J., Sharma, M., and Zuccaro, A. (2012). Indole derivative production by the root endophyte *Piriformospora indica* is not required for growth promotion but for biotrophic colonization of barley roots. *New Phytol.* 196, 520–534. doi: 10.1111/j.1469-8137.2012.04275.x

Jogawat, A., Saha, S., Bakshi, M., Dayaman, V., Kumar, M., Dua, M., et al. (2013). *Piriformospora indica* rescues growth diminution of rice seedlings during high salt stress. *Plant Signal. Behav.* 8:e26891. doi: 10.4161/psb.26891

Johnson, J. M., and Oelmüller, R. (2009). Mutualism or parasitism: life in an unstable continuum. What can we learn from the mutualistic interaction between *Piriformospora indica* and *Arabidopsis thaliana*? *Endocyt. Cell Res.* 19, 81–111.

Johnson, J. M., Sherameti, I., Ludwig, A., Nongbri, P. L., Sun, C., Lou, B., et al. (2011). Protocols for *Arabidopsis thaliana* and *Piriformospora indica* co-cultivation - a model system to study plant beneficial traits. *Endocyt. Cell Res.* 21, 101–113.

Karandashov, V., Nagy, R., Wegmüller, S., Amrhein, N., and Bucher, M. (2004). Evolutionary conservation of a phosphate transporter in the arbuscular mycorrhizal symbiosis. *Proc. Natl. Acad. Sci. U.S.A.* 101, 6285–6290. doi: 10.1073/pnas.0306074101

Kariman, K., Barker, S. J., Jost, R., Finnegan, P. M., and Tibbett, M. (2016). Sensitivity of jarrah (*Eucalyptus marginata*) to phosphate, phosphite, and arsenate pulses as influenced by fungal symbiotic associations. *Mycorrhiza* 26, 401–415. doi: 10.1007/s00572-015-0674-z

Klink, V. P., Hosseini, P., Matsye, P. D., Alkharouf, N. W., and Matthews, B. F. (2011). Differences in gene expression amplitude overlie a conserved transcriptomic program occurring between the rapid and potent localized resistant reaction at the syncytium of the *Glycine max* genotype Peking (PI 548402) as compared to the prolonged and potent resistant reaction of PI 88788. *Plant Mol. Biol.* 75, 141–165. doi: 10.1007/s11103-010-9715-3

Kumar, M., Yadav, V., Kumar, H., Sharma, R., Singh, A., Tuteja, N., et al. (2011). *Piriformospora indica* enhances plant growth by transferring phosphate. *Plant Signal. Behav.* 6, 723–725. doi: 10.4161/psb.6.5.15106

Lahrmann, U., Dinga, Y., Banharab, A., Rathc, M., Hajirezaeid, M. R., Döhlemanna, S., et al. (2013). Host-related metabolic cues affect colonization strategies of a root endophyte. *Proc. Natl. Acad. Sci. U.S.A.* 110, 13965–13970. doi: 10.1073/pnas.1301653110

Lahrmann, U., and Zuccaro, A. (2012). Opprimo ergo sum-evasion and suppression in the root endophytic fungus *Piriformospora indica*. *Mol. Plant-Microbe Interact.* 25, 727–737. doi: 10.1094/MPMI-11-11-0291

Lee, Y. C., Johnson, J. M., Chien, C. T., Sun, C., Cai, D., Lou, B., et al. (2011). Growth promotion of Chinese cabbage and Arabidopsis by *Piriformospora indica* is not stimulated by mycelium-synthesized auxin. *Mol. Plant-Microbe Interact.* 24, 421–431. doi: 10.1094/MPMI-05-10-0110

Lin, W. Y., Huang, T. K., and Chiou, T. J. (2013). Nitrogen limitation adaptation, a target of microRNA827, mediates degradation of plasma membrane-localized phosphate transporters to maintain phosphate homeostasis in Arabidopsis. *Plant Cell* 25, 4061–4074. doi: 10.1105/tpc.113.116012

Linn, J., Ren, M., Berkowitz, O., Ding, W., Van Der Merwe, M. J., Whelan, J., et al. (2017). Root cell-specific regulators of phosphate-dependent growth. *Plant Physiol.* doi: 10.1104/pp.16.01698 [Epub ahead of print].

Liu, T., Huang, T., Tseng, C., Lai, Y., Lin, S., Lin, W., et al. (2012). PHO2-dependent degradation of PHO1 modulates phosphate homeostasis in Arabidopsis. *Plant Cell* 24, 2168–2183. doi: 10.1105/tpc.112.096636

Matsuo, M., Johnson, J. M., Hieno, A., Tokizawa, M., Nomoto, M., Tada, Y., et al. (2015). High redox responsive transcription factor1 levels result in accumulation of reactive oxygen species in *Arabidopsis thaliana* shoots and roots. *Mol. Plant* 8, 1253–1273. doi: 10.1016/j.molp.2015.03.011

Maxwell, K., and Johnson, G. N. (2000). Chlorophyll fluorescence: a practical guide. *J. Exp. Bot.* 51, 659–668. doi: 10.1093/jexbot/51.345.659

Misson, J., Raghothama, K. G., Jain, A., Jouhet, J., Block, M. A., Bligny, R., et al. (2005). A genome-wide transcriptional analysis using *Arabidopsis thaliana* affymetrix gene chips determined plant responses to phosphate deprivation. *Proc. Natl. Acad. Sci. U.S.A.* 102, 11934–11939. doi: 10.1073/pnas.0505266102

Moeller, H. V., Peay, K. G., and Fukami, T. (2014). Ectomycorrhizal fungal traits reflect environmental conditions along a coastal California edaphic gradient. *FEMS Microbiol. Ecol.* 87, 797–806. doi: 10.1111/1574-6941.12265

Motte, H., and Beeckman, T. (2017). PHR1 balances between nutrition and immunity in plants. *Dev. Cell* 41, 5–7. doi: 10.1016/j.devcel.2017.03.019

Murashige, T., and Skoog, F. (1962). A revised medium for rapid growth and bioassays with tobacco tissue cultures. *Physiol. Plant.* 15, 473–497. doi: 10.1111/j.1399-3054.1962.tb08052.x

Nagarajan, V. K., Jain, A., Poling, M. D., Lewis, A. J., Raghothama, K. G., and Smith, A. P. (2011). Arabidopsis Pht1;5 mobilizes phosphate between source and sink organs and influences the interaction between phosphate homeostasis and ethylene signaling. *Plant Physiol.* 156, 1149–1163. doi: 10.1104/pp.111.174805

Nehls, U., Ghringer, F., Wittulsky, S., and Dietz, S. (2010). Fungal carbohydrate support in the ectomycorrhizal symbiosis: a review. *Plant Biol.* 12, 292–301. doi: 10.1111/j.1438-8677.2009.00312.x

Nilsson, L., Müller, R., and Nielsen, T. H. (2010). Dissecting the plant transcriptome and the regulatory responses to phosphate deprivation. *Physiol. Plant.* 139, 129–143. doi: 10.1111/j.1399-3054.2010.01356.x

Nongbri, P. L., Johnson, J., Sherameti, I., Glawischnig, E., Halkier, B. A., and Oelmüller, R. (2012). Indole-3-acetaldoxime-derived compounds restrict root colonization in the beneficial interaction between Arabidopsis roots and the endophyte *Piriformospora indica*. *Mol. Plant-Microbe Interact.* 25, 1186–1197. doi: 10.1094/MPMI-03-12-0071-R

Oelmüller, R., Sherameti, I., Tripathi, S., and Varma, A. (2009). *Piriformospora indica*, a cultivable root endophyte with multiple biotechnological applications. *Symbiosis* 49, 1–17. doi: 10.1007/s13199-009-0009-y

Pánková, H., Münzbergová, Z., Rydlová, J., and Vosátka, M. (2011). The response of *Aster amellus* (Asteraceae) to mycorrhiza depends on the origins of both the soil and the fungi. *Am. J. Bot.* 98, 850–858. doi: 10.3732/ajb.0900350

Park, B. S., Seo, J. S., and Chua, N.-H. (2014). Nitrogen limitation adaptation recruits phosphate2 to target the phosphate transporter PT2 for degradation during the regulation of Arabidopsis phosphate homeostasis. *Plant Cell* 26, 454–464. doi: 10.1105/tpc.113.120311

Peškan-Berghöfer, T., Shahollari, B., Giong, P. H., Hehl, S., Markert, C., Blanke, V., et al. (2004). Association of *Piriformospora indica* with *Arabidopsis thaliana* roots represents a novel system to study beneficial plant-microbe interactions and involves early plant protein modifications in the endoplasmic reticulum and at the plasma membrane. *Physiol. Plant.* 122, 465–477. doi: 10.1111/j.1399-3054.2004.00424.x

Pfaffl, M. W. (2001). A new mathematical model for relative quantification in real-time RT-PCR. *Nucleic Acids Res.* 29:e45. doi: 10.1093/nar/29.9.e45

Poirier, Y., Thoma, S., Somerville, C., and Schiefelbein, J. (1991). Mutant of arabidopsis deficient in xylem loading of phosphate. *Plant. Physiol.* 97, 1087–1093. doi: 10.1104/pp.97.3.1087

Prasad, R., Kamal, S., Sharma, P. K., Oelmüller, R., and Varma, A. (2013). Root endophyte *Piriformospora indica* DSM 11827 alters plant morphology, enhances biomass and antioxidant activity of medicinal plant *Bacopa monniera*. *J. Basic Microbiol.* 53, 1016–1024. doi: 10.1002/jobm.201200367

Rubio, V., Linhares, F., Solano, R., Martín, A. C., Iglesias, J., Leyva, A., et al. (2001). A conserved MYB transcription factor involved in phosphate starvation signaling both in vascular plants and in unicellular algae. *Genes Dev.* 15, 2122–2133. doi: 10.1101/gad.204401

Shahollari, B., Vadassery, J., Varma, A., and Oelmüller, R. (2007). A leucine-rich repeat protein is required for growth promotion and enhanced seed production mediated by the endophytic fungus *Piriformospora indica* in *Arabidopsis thaliana*. *Plant J.* 50, 1–13. doi: 10.1111/j.1365-313X.2007.03028.x

Shahollari, B., Varma, A., and Oelmüller, R. (2005). Expression of a receptor kinase in Arabidopsis roots is stimulated by the basidiomycete *Piriformospora indica* and the protein accumulates in Triton X-100 insoluble plasma membrane microdomains. *Plant Physiol.* 162, 945–958. doi: 10.1016/j.jplph.2004.08.012

Shakoor, N., Nair, R., Crasta, O., Morris, G., Feltus, A., and Kresovich, S. (2014). A sorghum bicolor expression atlas reveals dynamic genotype-specific expression profiles for vegetative tissues of grain, sweet and bioenergy sorghums. *BMC Plant Biol.* 14:35. doi: 10.1186/1471-2229-14-35

Sherameti, I., Shahollari, B., Venus, Y., Altschmied, L., Varma, A., and Oelmüller, R. (2005). The endophytic fungus *Piriformospora indica* stimulates the expression of nitrate reductase and the starch-degrading enzyme glucan-water dikinase in tobacco and Arabidopsis roots through a homeodomain transcription factor that binds to a conserved motif in their promoters. *J. Biol. Chem.* 280, 26241–26247. doi: 10.1074/jbc.M500447200

Sherameti, I., Tripathi, S., Varma, A., and Oelmüller, R. (2008). The root-colonizing endophyte *Pirifomospora indica* confers drought tolerance in Arabidopsis by stimulating the expression of drought stress-related genes in leaves. *Mol. Plant-Microbe Interact.* 21, 799–807. doi: 10.1094/MPMI-21-6-0799

Shin, H., Shin, H. S., Dewbre, G. R., and Harrison, M. J. (2004). Phosphate transport in Arabidopsis: Pht1;1 and Pht1;4 play a major role in phosphate acquisition from both low- and high-phosphate environments. *Plant J.* 39, 629–642. doi: 10.1111/j.1365-313X.2004.02161.x

Sisaphaithong, T., Kondo, D., Matsunaga, H., Kobae, Y., and Hata, S. (2012). Expression of plant genes for arbuscular mycorrhiza-inducible phosphate transporters and fungal vesicle formation in sorghum, barley, and wheat roots. *Biosci. Biotechnol. Biochem.* 76, 2364–2367. doi: 10.1271/bbb.120782

Su, T., Xu, Q., Zhang, F. C., Chen, Y., Li, L. Q., Wu, W. H., et al. (2015). WRKY42 modulates phosphate homeostasis through regulating phosphate translocation and acquisition in Arabidopsis. *Plant Physiol.* 167, 1579–1591. doi: 10.1104/pp.114.253799

Tamura, Y., Kobae, Y., Mizuno, T., and Hata, S. (2012). Identification and expression analysis of arbuscular mycorrhiza-inducible phosphate transporter genes of soybean. *Biosci. Biotechnol. Biochem.* 76, 309–313. doi: 10.1271/bbb.110684

Vadassery, J., Ranf, S., Drzewiecki, C., Mithöfer, A., Mazars, C., Scheel, D., et al. (2009a). A cell wall extract from *Piriformospora indica* promotes growth of Arabidopsis seedlings and induces intracellular calcium elevation in roots. *Plant J.* 59, 193–206. doi: 10.1111/j.1365-313X.2009.03867.x

Vadassery, J., Ritter, C., Venus, Y., Camehl, I., Varma, A., Shahollari, B., et al. (2008). The role of auxins and cytokinins in the mutualistic interaction between Arabidopsis and *Piriformospora indica*. *Mol. Plant-Microbe Interact.* 21, 1371–1383. doi: 10.1094/MPMI-21-10-1371

Vadassery, J., Tripathi, S., Prasad, R., Varma, A., and Oelmüller, R. (2009b). Monodehydroascorbate reductase 2 and dehydroascorbate reductase 5 are crucial for a mutualistic interaction between *Piriformospora indica* and Arabidopsis. *Plant Physiol.* 166, 1263–1274. doi: 10.1016/j.jplph.2008.12.016

Vahabi, K., Sherameti, I., Bakshi, M., Mrozinska, A., Ludwig, A., Reichelt, M., et al. (2015). The interaction of Arabidopsis with *Piriformospora indica* shifts from initial transient stress induced by fungus-released chemical mediators to a mutualistic interaction after physical contact of the two symbionts. *BMC Plant Biol.* 15:58. doi: 10.1186/s12870-015-0419-3

Varma, A., Bakshi, M., Lou, B., Hartmann, A., and Oelmüller, R. (2012). *Piriformospora indica*: a novel plant growth-promoting mycorrhizal fungus. *Agric. Res.* 1, 117–131. doi: 10.1007/s40003-012-0019-5

Varma, A., Verma, S., Sudha, Sahay, N., Büttehorn, B., and Franken, P. (1999). *Piriformospora indica*, a cultivable plant-growth-promoting root endophyte. *Appl. Environ. Microbiol.* 65, 2741–2744.

Venus, Y., and Oelmüller, R. (2013). *Arabidopsis* ROP1 and ROP6 influence germination time, root morphology, the formation of F-actin bundles, and symbiotic fungal interactions. *Mol. Plant.* 6, 872–886. doi: 10.1093/mp/sss101

Walder, F., Brulé, D., Koegel, S., Wiemken, A., Boller, T., and Courty, P.-E. (2015). Plant phosphorus acquisition in a common mycorrhizal network: regulation of phosphate transporter genes of the Pht1 family in sorghum and flax. *New Phytol.* 205, 1632–1645. doi: 10.1111/nph.13292

Waller, F., Achatz, B., Baltruschat, H., Fodor, J., Becker, K., Fischer, M., et al. (2005). The endophytic fungus *Piriformospora indica* reprograms barley to salt-stress tolerance, disease resistance, and higher yield. *Proc. Natl. Acad. Sci. U.S.A.* 102, 13386–13391. doi: 10.1073/pnas.0504423102

Waller, F., Mukherjee, K., Deshmukh, S. D., Achatz, B., Sharma, M., Schäfer, P., et al. (2008). Systemic and local modulation of plant responses by *Piriformospora indica* and related Sebacinales species. *Plant Physiol.* 165, 60–70. doi: 10.1016/j.jplph.2007.05.017

Wang, H., Xu, Q., Kong, Y. H., Chen, Y., Duan, J. Y., Wu, W. H., et al. (2014). Arabidopsis WRKY45 transcription factor activates *PHOSPHATE TRANSPORTER1;1* expression in response to phosphate starvation. *Plant Physiol.* 164, 2020–2029. doi: 10.1104/pp.113.235077

Wasaki, J., Yonetani, R., Kuroda, S., Shinano, T., Yazaki, J., Fujii, F., et al. (2003). Transcripomic analysis of metabolic changes by phosphorus stress in rice plant roots. *Plant Cell Environ.* 26, 1515–1523. doi: 10.1186/1471-2229-12-161

Wege, S., Khan, G. A., Jung, J. Y., Vogiatzaki, E., Pradervand, S., Aller, I., et al. (2016). The EXS domain of PHO1 participates in the response of shoots to phosphate deficiency via a root-to-shoot signal. *Plant Physiol.* 170, 385–400. doi: 10.1104/pp.15.00975

Wu, P., Ma, L., Hou, X., Wang, M., Wu, Y., Liu, F., et al. (2003). Phosphate starvation triggers distinct alterations of genome expression in Arabidopsis roots and leaves. *Plant Physiol.* 132, 1260–1271. doi: 10.1104/pp.103.021022

Ye, W., Shen, C. H., Lin, Y., Chen, P. J., Xu, X., Oelmüller, R., et al. (2014). Growth promotion-related miRNAs in Oncidium orchid roots colonized by the endophytic fungus *Piriformospora indica*. *PLoS ONE* 9:e84920. doi: 10.1371/journal.pone.0084920

Yi, K., Wu, Z., Zhou, J., Du, L., Guo, L., Wu, Y., et al. (2005). OsPTF1, a novel transcription factor involved in tolerance to phosphate starvation in rice. *Plant Physiol.* 138, 2087–2096. doi: 10.1104/pp.105.063115

Yin, Z., Li, Y., Yu, J., Liu, Y., Li, C., Han, X., et al. (2012). Difference in miRNA expression profiles between two cotton cultivars with distinct salt sensitivity. *Mol. Biol. Rep.* 39, 4961–4970. doi: 10.1007/s11033-011-1292-2

Zhang, Y., Zhu, X., Chen, X., Song, C., Zou, Z., Wang, Y., et al. (2014). Identification and characterization of cold-responsive microRNAs in tea plant (*Camellia sinensis*) and their targets using high-throughput sequencing and degradome analysis. *BMC Plant Biol.* 14:271. doi: 10.1186/s12870-014-0271-x

Conflict of Interest Statement: The authors declare that the research was conducted in the absence of any commercial or financial relationships that could be construed as a potential conflict of interest.

frontiers in Microbiology

ORIGINAL RESEARCH
published: 05 June 2018
doi: 10.3389/fmicb.2018.01169

Genetic Diversity Studies Based on Morphological Variability, Pathogenicity and Molecular Phylogeny of the *Sclerotinia sclerotiorum* Population From Indian Mustard (*Brassica juncea*)

*Pankaj Sharma[1], Amos Samkumar[2], Mahesh Rao[2], Vijay V. Singh[1], Lakshman Prasad[3], Dwijesh C. Mishra[4], Ramcharan Bhattacharya[2] and Navin C. Gupta[2]**

[1] Sclerotinia Lab, ICAR, Directorate of Rapeseed and Mustard Research, Bharatpur, India, [2] Brassica Lab, ICAR, National Research Centre on Plant Biotechnology, New Delhi, India, [3] ICAR, Indian Agricultural Research Institute, New Delhi, India, [4] ICAR, Indian Agricultural Statistics Research Institute, New Delhi, India

OPEN ACCESS

Edited by:
Katarzyna Turnau,
Jagiellonian University, Poland

Reviewed by:
Zbigniew Miszalski,
The Franciszek Górski Institute of Plant Physiology (PAS), Poland
Sylwia Różalska,
University of Łódź, Poland

***Correspondence:**
Navin C. Gupta
navinbtc@gmail.com

Specialty section:
This article was submitted to Fungi and Their Interactions, a section of the journal Frontiers in Microbiology

Received: 14 September 2017
Accepted: 14 May 2018
Published: 05 June 2018

Citation:
Sharma P, Samkumar A, Rao M, Singh VV, Prasad L, Mishra DC, Bhattacharya R and Gupta NC (2018) Genetic Diversity Studies Based on Morphological Variability, Pathogenicity and Molecular Phylogeny of the Sclerotinia sclerotiorum Population From Indian Mustard (Brassica juncea). Front. Microbiol. 9:1169. doi: 10.3389/fmicb.2018.01169

White mold or stem rot disease are ubiquitously distributed throughout the world and the causal organism of this disease *Sclerotinia sclerotiorum* (Lib.) de Bary, is known to infect over 400 plant species. Sclerotinia stem rot is one of the most devastating fungal diseases and poses a serious threat to the worldwide cultivation of oilseed *Brassica* including India. *S. sclerotiorum* pathogen usually infects the stem but in severe cases leaves and pods also affected at different developmental stages that deteriorate not only the oil quality but also causing the seed and oil yield losses up to 90% depending on the severity of the disease infestation. This study investigated the morphological and molecular characterization of pathogenic *S. sclerotiorum* (Lib) de Bary geographical isolates from oilseed *Brassica* including *Brassica juncea* (Indian mustard). The aim of this study was to compare isolates of *S. sclerotiorum* originated from different agro-climatic conditions and to analyse similarity or differences between them as well as to examine the virulence of this pathogen specifically in *Brassica* for the first time. The collection of *S. sclerotiorum* isolates from symptomatic *Brassica* plants was done and analyzed for morphological features, and molecular characterization. The virulence evaluation test of 65 isolates on four *Brassica* cultivars has shown 5 of them were highly virulent, 46 were virulent and 14 were moderately virulent. Phylogenetic analysis encompassing all the morphological features, SSR polymorphism, and ITS sequencing has shown the existence of high genetic diversity among the isolates that categorized all the isolates in three evolutionary lineages in the derived dendrogram. Further, genetic variability analysis based on sequences variation in ITS region of all the isolates has shown the existence of either insertions or deletions of the nucleotides in the ITS region has led to the interspecies variability and observed the variation were in a clade-specific manner. Together this analysis observed the existence of higher heterogeneity and genetic variability in *S. sclerotiorum* isolates collection and indicates the presence of clonal and sexual progenies

of the pathogen in the mustard growing regions of India surveyed in this study. With a higher level of genetic variability and diversity among the *S. sclerotiorum* population needs robust screening approaches to identify the donor parent and utilize them in resistance breeding program for effectively counter the menace of stem rot disease in *Brassica*.

Keywords: morphological, molecular, phylogeny, *Sclerotinia sclerotiorum*, stem rot, *Brassica*, diversity

INTRODUCTION

Globally India continues to be at a 3rd position after Canada and China in acreage (19.3%) and after China and Canada in production (11.1%) of rapeseed-mustard. In India, among nine edible oilseed crops, the share of rapeseed-mustard is about one-fourth of total area and one-third of total oil production in the country. During 2015–2016, production (6.82 mt) and productivity (1184 kg/ha) was achieved (Anonymous, 2016). Rapeseed-mustard is the major source of income especially for the marginal and small farmers in rainfed areas which are about 25% of the total cultivated area. In spite of its increase in demand for the year the production of oilseed Brassica remains to stagnate over the year and most of the demands are being met through import from outside the India. The main reason behind productivity stagnation in Indian Brassica is its susceptibility and damages caused to the crop by various insect pests and disease infestation in addition to the other yield-limiting factors. Out of thirty diseases known to infest the Brassica crops in India, stem rot has been found one of the most devastating diseases that heavily damages the crops during the flowering stage of development. The stem rot disease which is caused by fungal pathogens, *Sclerotinia sclerotiorum* (Lib) de Bary, ubiquitously found throughout the world is a polyphagous, soil-borne plant pathogen that infects more than 400 plant species of diverse phylogenetic origin (Boland and Hall, 1994; Saharan and Mehta, 2008; Sharma et al., 2015). In India, during the eighties and nineties, the stem rot (SR) disease in rapeseed-mustard was of a minor importance, because of its seldom appearance over the ground level of the isolated plants after mycelial infection. A widely adopted monocropping practices and cultivation of rapeseed-mustard under irrigated condition has significantly increased the sclerotial population in the soil that has made SR very serious disease of oilseed *Brassica* crops in states including Rajasthan, Haryana, Punjab, Uttar Pradesh, Bihar, Assam, West Bengal and Madhya Pradesh (Sharma et al., 2015). This fungus has been long considered as prototypical necrotrophs as it begins highly pathogenic phase by releasing oxalic acids and cellulolytic enzymes immediately upon host cuticle penetration followed by mycelial proliferation inside the host cell followed by a saprophytic phase that supports the sclerotia formation (Hegedus and Rimmer, 2005). However, the recent studies decipher the fact of evidence for the occurrence of a brief biotrophic phase just within the apoplastic space next after the establishment of the host-pathogen connection and hence based on these it is more appropriately classified as a hemibiotroph (Kabbage et al., 2015). The information related to the genetic diversity of the pathogen and their effective virulence over the target crop is the foremost requirement for taking the breeding program for development of pathogen resistance in the release of the region-specific cultivars. Various diversity analysis tools based on the molecular methods like microsatellite haplotype (Aldrich-Wolfe et al., 2015), SSR (simple sequence repeat or microsatellite-based marker; Meinhardt et al., 2002), AFLP (amplified fragment length polymorphism; Cubeta et al., 1997), and SRAP (sequence-related amplified polymorphism technique; Li et al., 2009) have been used in analyzing the genetic diversity of the pathogen *S. sclerotiorum* from different host species. Very limited variability was observed in ITS (internal transcribed spacer) sequences in *S. sclerotiorum* isolates from various host species (Njambere et al., 2008) and thus a universal barcode markers were developed from the nearly conserved nature of the nuclear ribosomal internal transcribed spacer (ITS) region for imparting the individual identity to the fungus up to genus level (Schoch et al., 2012). Furthermore, MCGs is another diversity analysis method based on the mycelial compatibility grouping (MCG) has been used in establishing the kinship among *S. sclerotiorum* isolates from chickpea (Kull et al., 2004; Li et al., 2008). In addition to it, the diversity based on the morphological appearance of sclerotia, mycelial growth, and ascospores formation have also been reported in analyzing the genetic diversity of *S. sclerotiorum* isolates in previous studies (Li et al., 2008; Sharma et al., 2013). However, polymorphism and genetic diversity of the *S. sclerotiorum* isolates at the morphological and DNA sequence level has not been comprehensively studied so far especially for the isolates from Brassica species of India.

Being a polyphagous nature, *S. sclerotiorum* pathogen is usually infecting not only the majority of the economically important dicotyledonous species but also serve as the major pathogen for several monocotyledonous plant species (Boland and Hall, 1994). The yield loss estimated with the *S. sclerotiorum* infestation has exceeded hundred million dollars annually because of the lack of resistance cultivar of the crop species and also because of lack of the effective management practices (Tok et al., 2016). In general, the management of *S. sclerotiorum* borne disease is not much easy because of its widespread existence, irregular incidence, and the long-term survival by producing huge numbers of sclerotia in the soil. Although several control measures like chemical and cultural methods have been devised and adopted for countering the Sclerotinia stem rot menace (Rousseau et al., 2007) none of them were found fully effective in preventing either the process of disease infection or pathogenesis progression after infection. The extent of genetic diversity of the pathogen and their widespread distribution among host species across the growing regions play an important role in determining and devising the control strategies to efficiently control the

diseases in the more effective way. Hence, the availability of the genetic variability information related to the target pathogen is the foremost requirement for designing the management means to counter the disease incidence more effectively. In plant-pathogen interactions, development of new pathogenic races, and the breakdown of host resistance are the limiting factors in resistance deployment against plant diseases. The pathogen's life history characteristics and evolutionary potential are major factors leading to the pathogen overcoming host resistance. Therefore, major efforts should be focused not only in understanding the genetic structure of the fungal populations but also to determine how populations will evolve in response to different control strategies (McDonald and Linde, 2002).

In recent past, India observed the frequent incidence of the *S. sclerotiorum* infestation on cereals and horticultural species that draws the wide attention of the researcher over this fungal pathogen. In pursuance of basic understanding about pathogenicity, diversity and distribution pattern of the *S. sclerotiorum* were extensively studied on isolates collected from various host species like chickpea (Mandal and Dubey, 2012), vegetable crops (Choudhary and Prasad, 2012), cumin (Prasad et al., 2017), carnation (Kumar et al., 2015), oilseed *Brassica* (Sharma et al., 2013), and their identity were established on the basis of morphological features and cultural conditions. However, major variation in the growth characteristics has been reported in the growing collection of *S. sclerotiorum* isolates even as they belong to the same *Sclerotinia* species. Indeed, as projected with diversity analysis *S. sclerotiorum* isolates has been reported of possessing the variation in morpho-physiological, biochemical properties, molecular features and pathogenicity in terms of virulence because of the presence of clonal and sexual progenies together even in the same crop and in same region (Atallah et al., 2004; Sexton and Howlett, 2004; Irani et al., 2011). For establishing the console features of the pathogen especially in *Brassica* growing regions of India, the present study was aimed at determining the genetic diversity within *S. sclerotiorum* population from various *Brassica* species based on morphological characteristics, genotyping with simple sequence repeats (SSR) markers and molecular phylogeny by ITS sequence analysis.

MATERIALS AND METHODS

Sclerotinia sclerotiorum Isolates

Brassica growing areas in 10 states of India (Rajasthan, Haryana, Punjab, Delhi, U.P., Bihar, Uttarakhand, Himachal Pradesh, Jammu & Kashmir, and Jharkhand) were surveyed and stem rot disease infected plants were collected from 65 different locations (**Table 1**). The sclerotia obtained from the stem rot infested Indian mustard plant samples were first washed with sterile water than surface sterilized with 70% ethanol for 2 min and again washed two times with sterile water. The drained sclerotia over pre-sterilized filter papers were placed on nutrient media (Potato Dextrose Agar; PDA) plates supplemented with 50 μg/ml tetracycline antibiotics to prevent the growth of bacterial contamination. The samples were wrapped in a brown envelope and kept for incubation at 20° ± 2°C in dark for 4–5 days. After the development of the white fluffy mass of mycelial growth of *S. sclerotiorum,* the mycelial plaques were used to sub-culture the isolates on PDA slants and pure culture of them was stored at 4°C for future use. Morphological identification of the isolates was based on cultural characteristics of the *S. sclerotiorum* and morphology of the mycelial mat and sclerotia formation traits.

Morphological Characterization of *S. sclerotiorum* Isolates

Freshly grown 3–4 days old cultures of *Sclerotinia* isolates were used for analyzing the morphological features like the radial spread of mycelial growth (mm) at 72 and 96 h after inoculation. Whereas, the number of sclerotia produced from each inoculum per Petri plates (90 mm), length and diameter of the sclerotia (mm) and weight of individual sclerotia (mg) was measured 10–15 days after inoculation.

Pathogenicity of Isolates

An experiment to study pathogenicity and pathogenic variability among 65 geographical isolates of *S. sclerotiorum* were conducted during 2016–2017 post-rainy season at ICAR-Directorate of Rapeseed-Mustard Research, Bharatpur, India. Seven different oilseed *Brassica species* were selected for this study. The crop was destroyed after the experiment by cutting and collecting the debris followed by autoclaving before disposing of them.

Inoculation

The inoculum was mass multiplied in the laboratory on autoclaved sorghum grains in glass jars and incorporated into the soil prior to sowing. Further, the plants were inoculated at 60 days after sowing on the stem with the pathogen growing on agar blocks. Stem inoculation procedure was followed as described by Buchwaldt et al. (2003). A single 5 mm mycelial bit cut from *S. sclerotiorum* colony of 4–5 days old culture growing on potato dextrose agar was used to inoculate each plant. The mycelial bit along with cotton swab soaked in sterilized distilled water was placed on a small piece of parafilm (5–7 cm). Mycelial bit touching the stem at 15 cm height was then secured by wrapping the parafilm strip around the stem. Wet cotton swab maintained high humidity during the infection period (Sharma et al., 2013).

Disease

Disease incidence was assessed by recording the size of stem lesion length (cm) and disease severity (%) 15–21 days after inoculation. This has been shown to be an ideal time to demonstrate the host response to the pathogen (Li et al., 2007). The disease parameters recorded were statistically verified by data analysis using Duncan's test ($P < 0.05$) and analysis of variance (ANOVA).

DNA Extraction

Sclerotinia sclerotiorum isolates were grown on PDA medium at 20° ± 2°C in BOD incubator for 5 days. Mycelial mat was harvested by scraping with a sterile spatula and ∼2 g of the mycelial mat was used for DNA extraction using modified CTAB method. The fine powder of the grounded mycelial mat in liquid nitrogen was transferred in preheated 10 ml DNA extraction

TABLE 1 | *Sclerotinia sclerotiorum* (Lib) de Bary population used for studying the virulence and genetic diversity within isolates based on morphological features, SSR profiling, and ITS sequence analysis.

Strain No.	Source (Host)	Geographic origin	Latitude and Longitude	Province	Disease severity observed in *Brassica* cultivars (Lesion length cm)				
					B. juncea (NRCDR-2)	*B. rapa var* Toria (Uttara)	*B. rapa var yellow sarson* (NRCYS 5-2)	*B. rapa var brown sarson*	Mean
ESR 1	*B. juncea*	DRMR, Bharatpur	27°15′N; 77°30′E	Rajasthan	14.0	18.7	21.0	17.0	17.7
ESR 2	*B. juncea*	Oraiya	26°46′N; 79°51′ E	UP	13.7	13.0	18.7	13.0	14.6
ESR 3	*B. rapa*	Imlia, Varansai	26°4′N; 77°9′E	UP	15.7	13.7	20.0	14.7	16.0
ESR 4	*B. juncea*	CSA, Kanpur	26°28′N; 80° 24′E	UP	6.5	8.0	8.0	8.3	7.7
ESR 5	*B.rapa*	Allahbad	25°28′N; 81° 54′E	UP	12.5	16.0	17.3	12.0	14.5
ESR 6	*B. juncea*	BHU, Varanasi	25°26′N; 82°9′E	UP	12.0	10.0	18.7	16.7	14.4
ESR 7	*B. juncea*	Akbarpur, Kanpur	26°26′N; 52° 33′E	UP	14.7	13.0	23.0	12.7	15.9
ESR 8	*B. juncea*	Etawah	26°47′N; 79° 02′E	UP	5.7	12.7	16.7	10.0	11.3
ESR 9	*B. juncea*	Firozabad	27°09′N; 78° 24′E	UP	14.0	18.3	25.0	14.3	17.9
ESR 10	*B. juncea*	Khaga	25°47′N; 81°07′E	UP	9.7	8.7	13.7	8.7	10.2
ESR 11	*B. juncea*	Kokhraj	26°55′N; 80°59′E	UP	5.0	4.7	6.3	4.7	5.2
ESR 12	*B. juncea*	Koshambi	25°48′N; 81°66′E	UP	16.7	14.0	22.7	15.0	17.1
ESR 13	*B. rapa*	Meghipur	24°94′N; 85.69 E	Bihar	11.7	13.7	19.3	14.3	14.8
ESR 14	*B. juncea*	Morena	26°49′N; 77°76′E	MP	8.0	6.3	8.0	4.7	6.8
ESR 15	*B. juncea*	Handia	25°38′N; 82°18′E	UP	19.0	24.3	25.0	21.0	22.3
ESR 16	*B. juncea*	Bawal	28°08′N; 76°58′E	Haryana	14.0	13.3	18.0	19.0	16.1
ESR 17	*B. juncea*	Maluka	30°21′N; 74°96′E	Punjab	17.7	17.0	24.0	20.7	19.9
ESR 18	*B. juncea*	Bhatinda	30°11′N; 75°00′E	Punjab	27.7	22.7	32.7	20.0	25.8
ESR 19	*B. juncea*	Moga	30°48′N; 75°10′E	Punjab	16.0	14.0	21.7	11.3	15.8
ESR 20	*B. juncea*	PAU, Ludhiana	30°55′N; 75°54′E	Punjab	15.0	13.3	25.7	14.0	17.0
ESR 21	*B. juncea*	Faridkot	30°67′N; 74°73′E	Punjab	11.3	15.0	19.3	10.0	13.9
ESR 22	*B. juncea*	Mahalkalan, Sangrur	30°75′N; 76°78′E	Punjab	13.7	16.3	20.7	17.3	17.0
ESR 23	*B. juncea*	Rajoana, Ludhiana	30°72′N; 75°6′E	Punjab	8.0	15.0	22.7	12.7	14.6
ESR 24	*B. juncea*	Ranchi	23°23′N; 85° 23′E	Jharkhand	4.3	4.0	9.0	4.0	5.3
ESR 25	*B. juncea*	Mathura	27°28′N; 77°41′E	UP	19.7	26.0	28.7	24.7	24.8
ESR 26	*B. juncea*	CCSHAU Hisar	29°14′N; 75°72′E	Haryana	13.0	16.0	20.0	17.0	16.5
ESR 27	*B. juncea*	Sirsa	29°53′N; 75°01′E	Haryana	14.0	12.3	20.0	14.0	15.1
ESR 28	*B. juncea*	Bassi, Jaipur	26°91′N; 75°78′E	Rajasthan	5.3	4.0	9.0	4.3	5.7
ESR 29	*B. juncea*	Shahganj, Janunpur	24°70′N; 82°95′E	UP	6.0	11.7	18.7	10.7	11.8
ESR 30	*B. juncea*	Jammu	31°14′29″N; 77°2′12″E	J & K	14.3	18.0	25.3	18.7	19.1
ESR 31	*B. juncea*	Bansur, Alwar	27°71′N; 76°28′E	Rajasthan	15.3	15.0	21.7	15.3	16.8
ESR 32	*B. juncea*	Badodamev, Alwar	27°34′N; 76° 38′E	Rajasthan	13.7	12.3	23.7	9.7	14.9
ESR 33	*B. juncea*	DU, SC	28°36′N; 77°22′E	Delhi	11.7	16.0	18.0	14.3	15.0
ESR 34	*B. juncea*	Pantnagar	29°02′N; 79°48′E	Uttarakhand	11.0	15.0	15.7	10.0	12.9
ESR 35	*B. juncea*	Kherli	27°20′N; 77°03′E	Rajasthan	23.7	23.3	31.3	22.0	25.1
ESR 36	*B. juncea*	Amoli	27°09′N; 77°08′E	Rajasthan	49.0	46.3	55.0	42.3	48.2
ESR 37	*B. juncea*	Dausa	26°89′N; 76°33′E	Rajasthan	11.5	11.3	19.0	12.0	13.5
ESR 38	*B. juncea*	Nadbai	27°21′N; 77°20′E	Rajasthan	4.3	14.7	14.7	13.3	11.8
ESR 39	*B. juncea*	Ludhawai	27°21′N; 77°2′E	Rajasthan	11.3	18.7	21.3	14.0	16.3
ESR 40	*B. juncea*	Sangaria,SGN	29°79′N; 74°46′E	Rajasthan	5.7	12.7	16.7	10.0	11.3
ESR 41	*B. juncea*	Sri Ganga nagar	29°90′N; 73°87′E	Rajasthan	8.0	12.7	16.7	10.0	11.9
ESR 42	*B. juncea*	Kumher	27°34′N; 77°37′E	Rajasthan	5.3	7.0	13.0	10.0	8.8
ESR 43	*B. juncea*	Gajsinghpur	29°65′N; 73°43′E	Rajasthan	8.3	16.0	17.7	12.0	13.5
ESR 44	*B. juncea*	Halena	27°10′N; 77°15′E	Rajasthan	8.0	11.7	15.3	10.0	11.3
ESR 45	*B. juncea*	Bajoli	26°86′N; 74°4′E	Rajasthan	9.7	18.3	15.3	13.3	14.2
ESR 46	*B. juncea*	Mahua	27°05′N; 76°92′E	Rajasthan	7.3	12.3	17.0	15.3	13.0
ESR 47	*B. juncea*	Kiratpura, Jaipur	31°18′N; 76°.56′E	Punjab	4.7	11.0	11.3	12.7	9.9

(Continued)

TABLE 1 | Continued

Strain No.	Source (Host)	Geographic origin	Latitude and Longitude	Province	Disease severity observed in *Brassica* cultivars (Lesion length cm)				
					B. juncea (NRCDR-2)	*B. rapa var* Toria (Uttara)	*B. rapa var yellow sarson* (NRCYS 5-2)	*B. rapa var brown sarson*	Mean
ESR 48	*B. juncea*	Pathredi	27°59′N; 76°09′E	Rajasthan	8.7	10.7	12.0	11.0	10.6
ESR 49	*B. juncea*	Bhadubha	26°89′N; 75°81′E	Rajasthan	4.3	13.7	14.0	14.0	11.5
ESR 50	*B. juncea*	Tulsipura	27°57′N; 82°45′E	UP	2.0	14.0	12.0	11.3	9.8
ESR 51	*B. juncea*	Chhonkarwara	27°10′N; 77°04′E	Rajasthan	9.7	14.3	19.7	14.3	14.5
ESR 52	*B. juncea*	Kaimasi	27°08′N; 77°38′E	Rajasthan	5.0	14.3	16.0	10.7	11.5
ESR 53	*B. juncea*	Habibpur	25°21′N; 86°98′E	UP	1.7	12.3	12.3	12.3	9.7
ESR 54	*B. juncea*	Baansi	24°32′N; 74°38′E	Rajasthan	2.3	6.3	10.0	10.7	7.3
ESR 55	*B. juncea*	Jhalatala	27°08′N; 77°01′E	Rajasthan	1.7	16.0	14.7	11.7	11.0
ESR 56	*B. juncea*	Gundwa	27°24′N; 77°46′E	Rajasthan	1.3	2.0	7.3	4.3	3.7
ESR 57	*B. juncea*	Deeg	27°34′N; 77°37′E	Rajasthan	4.0	1.3	4.7	2.7	3.2
ESR 58	*B. juncea*	Sewar	27°18′N; 77°44′E	Rajasthan	8.0	12.0	13.0	8.7	10.4
ESR 59	*B. juncea*	Hantra	27°12′N; 77°24′E	Rajasthan	2.7	4.3	6.0	4.0	4.3
ESR 60	*B. juncea*	Kanma	27°08′N; 77°1′E	Rajasthan	2.0	10.0	13.0	9.0	8.5
ESR 61	*B. juncea*	Baansi	24°32′N; 74°38′E	Rajasthan	12.7	11.3	18.7	11.7	13.6
ESR 62	*B. juncea*	Dehra mod	27°21′N; 77°49′E	Rajasthan	2.0	2.0	6.0	4.7	3.7
ESR 63	*B. juncea*	Aroda	23°75′N; 72°89′E	Rajasthan	15.0	15.0	25.7	15.0	17.7
ESR 64	*B. juncea*	Bhandor	27°26′N; 77°45′E	Haryana	6.0	8.7	12.3	11.0	9.5
ESR 65	*B. juncea*	Basua	25°02′N; 87°32′E	Rajasthan	16.0	18.0	26.0	18.0	19.5

The severity of disease assessed on Brassica cultivars was measured in lesion length (cm). Disease index for the strains listed, accessed on length of the lesion developed on stem (in cm). Lesion size 0.0 cm: Non-virulent; 0.1–3.0 cm: less virulent; 3.1–10.0: Moderately virulent; 10.1–20.0 cm: virulent; >20.0 cm: highly virulent. NRCDR-02 stands for National Research Centre Disease Resistance-02, YS stands for yellow sarson

buffer (1% Cetyltrimethylammonium bromide; 250 mM NaCl; 100 mM Tris-HCl, pH 8.0; 100 mM EDTA, pH 8.0; along with 4 mM Spermidine) and incubated at 65°C with intermittent mixing at regular interval for 60 min. Denatured proteins were removed by extracting once with an equal volume of Tris-saturated phenol: chloroform: isoamyl alcohol (25:24:1, v/v/v), followed by repeated extractions with an equal volume of Tris-saturated chloroform: isoamyl alcohol (24:1, v/v). The aqueous phase obtained after centrifugation was added with 0.6 volume of chilled isopropanol and stored overnight at −20°C for DNA precipitation. DNA was pelleted, dried and resuspended in 500 µl of Tris–EDTA buffer [10 mM Tris-HCl, pH 7.5; 1 mM EDTA (ethylenediaminetetraacetic acid)]. The purity and concentration of the DNA were determined through NanoDrop (Thermo Scientific, USA) and stored in aliquots at −20°C.

Species-Specific PCR Assay

Sclerotinia-specific primers as described by Freeman et al. (2002) (**Table 2**) were used to carry out PCR amplification in all the isolates. The PCR reaction of 15 µL contained 1.5 µL of 10x PCR buffer with 15 mM $MgCl_2$, 50 µM dNTPs, 10 µM forward and reverse primers, 1 U Taq DNA polymerase (Bangalore Genei, India) and 50 ng of template DNA was performed in a thermal cycler (Biometra, ILS, USA) and the program made with initial denaturation at 95°C for 4 min followed by 35 cycles of denaturation at 94°C for 45 s, annealing at 57°C for 45 s and extension at 72°C for 1 min, and a final extension at 72°C for 10 min. The PCR amplicons were resolved on 1% agarose gel along with 1 kb standard DNA ladder and visualized in a UV transilluminator. Gels were photographed using Alpha image (Alpha innotech, USA) Gel Doc system.

TABLE 2 | Details of the primers used for identification of *Sclerotinia* species, rDNA conserved sequence, and ITS analysis.

Primer	Primer Sequence (5′-3′)	Amplification size	Reference
SSFWD	GCTGCTCTTCGGGGCCTTGTATGC	278 bp	Freeman et al., 2002
SSREV	TGACATGGACTCAATACCAAGCTG		
ITS4	TCCTCCGCTTATTGATATGC	600 bp	White et al., 1990
ITS5	GGAAGTAAAAGTCGTAACAAGG		

Genetic Diversity

Simple Sequence Repeat (SSR) Marker Analysis

The pathogenicity tested 65 *S. sclerotiorum* isolates were subjected to SSR fingerprinting. A total of 25 SSR primers (Sirjusingh and Kohn, 2001; **Table 3**) were synthesized from IDT, Agrigenome, Bengaluru, India and used for amplification of

microsatellite loci. PCR reactions were performed using a BioRad C1000 thermocycler (BioRad, USA). The PCR reaction was set up in a 25 μL reaction volume with 2.5 μL of 10x Taq buffer (with 15 mM $MgCl_2$), 0.25 mM dNTPs (10 mM dNTPs mix), 10 nM of forward and reverse primers, 1 U of Taq polymerase and 200 ng template DNA. The reproducibility of the amplification was confirmed by repeated PCR with a similar set of ingredients and condition. For each experiment, negative controls were taken with sterile water in place of the template. The thermal cycler program consisted of an initial denaturation for 4 min at 95°C, followed by 35 cycles of denaturation at 94°C for 45 s, optimized annealing temperature for 45 s, and extension at 72°C for 1 min with a final extension of 72°C for 10 min. The PCR amplicons were resolved on 3.5% agarose gel in 1x TAE buffer by electrophoresis at 60 V cm^{-1}.

SSR Profiling and Data Analysis:

The standard binomial matrices were followed in SSR profiling and the presence and absence of the allele at a particular locus was scored as 1 and 0, respectively. Though Jaccard's coefficient pairwise distance were calculated and the resultant distance matrices were further used in NTSYSpc2 software version 2.0 (Rohlf, 2000) for clustering the isolates under investigation based on the Unweighted Pair Group method using arithmetic means (UPGMA) method. Allele frequency and Polymorphism information content (PIC) value for each marker was also calculated based on the formula: $Hn = 1 - \Sigma pi2$, where *pi* is the allele frequency of the *i*th allele (Nei, 1973).

Internal Transcribed Spacer (ITS) Amplification

The universal primers pair ITS4 and ITS5 (White et al., 1990; **Table 2**) were used for amplifying the ITS region of the rDNA. The PCR was carried out in a total volume of 50 μL with 1xPCR buffer (with 15 mM $MgCl_2$), 250 μM each dNTPs, 1 μL of each primer (10 nmol), 1.5 U Taq DNA polymerase, and 200 ng of genomic DNA. The thermal cycler program consisted of an initial denaturation at 95°C for 4 min followed by cycling conditions included denaturation at 94°C for 45 s, annealing at 49°C for 45 s, and elongation at 72°C for 1 min (35 cycles), followed by a final extension at 72°C for 10 min. All the PCR reactions were set up along with a negative control (without template DNA). The amplification product was analyzed on 1% agarose gels by running a standard DNA molecular weight 1 kb marker parallel to it.

rDNA Sequence Analysis

The PCR amplified internal transcribed (ITS) rDNA region from each of the isolates was purified using Favorgen PCR purification kit (FAVORGEN Biotech Corp, Taiwan), as per the manufacturer's instructions. The purified ITS amplicons were sequenced by Agrigenome, Bengaluru, India and then the sequences were analyzed in GenBank (http://www.ncbi.nlm.nih.gov/) by using the Mega BLAST sequence analysis tool. The full length ITS sequences were used as queries for establishing kinship with the published sequences and search result with maximum homology and highest score were marked for further analysis. All the ITS sequences obtained from the isolates used in the present study were submitted to GenBank. ClustalW program of the Bioedit sequence alignment editor (Thompson et al., 1994; Hall, 1999) was used to align all the obtained sequences. The resulting multiple-alignment file was used for phylogenetic analyses which were performed using Molecular Evolutionary Genetics Analysis (MEGA 7.0) with Neighbour-Joining method (Kumar et al., 2016).

RESULTS AND DISCUSSION

Morphological Identification

All the 65 *S. sclerotiorum* isolates collected from the major *Brassica* growing regions of India were observed exhibited morphological characteristics specific to *Sclerotinia sclerotiorum*. The mycelia of *S. sclerotiorum* isolates produced abundantly and appeared white to off-white, fluffy, delicate and generally with a brownish to blackish tinge. Sclerotia produced by the fungus were often dark brown to black and appeared concentrically in some case and at the periphery in others. The sclerotia were formed in abundant at the terminal stage of the growth and vary in its shape and size viz. oval-ellipsoid, straight to curved, 1.8–2.4 × 2.9–6.2 mm in size (**Table 4**). Usually, the sclerotia were produced solitary in the chain of ring-shaped either at the periphery or in the center and occasionally also formed in pairs randomly. Substantial variability in culture and morphology were exhibited by the *S. sclerotiorum* isolates during their growth in a controlled environment (**Figure 1**).

Species-Specific PCR Assay

For ascertaining the originality, the *S. sclerotiorum* isolates was tested by using the species-specific PCR assay. For this, the species-specific primers designed and verified by Freeman et al. (2002) were used and a single 278 bp DNA fragment amplified by PCR was specific to *S. sclerotiorum*, which confirms the species-specific identity of the isolates (Figure S10).

Morphological Variability

The growth rates of mycelia in all the 65 isolates of *S. sclerotiorum* were varied irrespective of their collection from the similar host species and they were prominently distinct in terms of the morphological characteristics. Depending on the growth characteristics of mycelium after 72 h of incubation the isolates were categorized into 3 groups: (i) Fast growing (ESR-01, 02, 03, 05, 06, 07, 09, 12, 13, 15, 17–22, 25, 27, 31, 32, 35, 36 and 37); (ii) Intermediate (ESR-08, 11, 14, 16, 23, 26, 28, 29, 34, 38, 40, 42, 43, 46, 48, 50, 53, 55–58, and 64); and (iii) Slow growing (ESR-04, 10, 24, 30, 33, 39, 41, 44, 47, 49, 51, 52, 54, 59, 60–63, and 65). Although most of the *S. sclerotiorum* isolates has attained full mycelial growth and filled up the 90 mm Petri plates within 4–5 days whereas other isolates namely ESR-04, 10, 24, 26, 28, 30, 49, 52, and 62 were taken 7–9 days for attaining the full growth and in filling the 90 mm Petri plate with the mycelial mat. Among these *S. sclerotiorum* isolates collection, most of them were had whitish mycelial growth with a smooth texture but the remaining isolates ESR-02, 06, 08, 12, 14, 17, 21, 31, 42, and 48 had an off-white color.

TABLE 3 | Optimized annealing temperature (Tm), Polymorphism information content (PIC), product size and a total number of bands observed for the SSR markers used to check the presence genetic diversity among *S. sclerotiorum* isolates.

Primer ID	Primer sequence (5′-3′)	Locus*	Repeat motif #	Tm (ÂoC)	PIC	Amplicon size range	Allele frequency
SS 1A	CCGAGCATAATATACATCC AAGGTTATATTTCCCTCGC	41-1	(TA)5 and (CA)10	50	0.663	494–504	1
SS 2B	GTAACACCGAAATGACGGC GATCACATGTTTATCCCTGGC	5-2	(GT)8	55	0.467	318–325	1
SS 3C	GGGGGAAAGGGATAAAGAAAAG CAGACAGGATTATAAGCTTGGTCAC	6-2	(TTTTTC)2(TTTTTG)2(TTTTTC)	55	0.564	479–484	1
SS 4D	TTTGCGTATTATGGTGGGC ATGGCGCAACTCTCAATAGG	7-2	(GA)14	50	0.345	160–172	1
SS 5E	GCCGATATGGACAATGTACACC TCTTCGCAGCTCGACAAGG	9-2	(CA)9(CT)9	50	0.243	358–382	1
SS 6F	CTTTCCTTTCGTTTGAGGG GGCAGGTAATGTTGCTTGG	11-2	(GA)6GG(GA)6(GGGA)2	47	0.806	276–284	1
SS 7G	CGATAATTTCCCCTCACTTGC GGAAGTCCTGATATCGTTGAGG	12-2	(CA)9	55	0.260	215–225	1
SS 8H	TCTACCCAAGCTTCAGTATTCC GAACTGGTTAATTGTCTCGG	13-2	(GTGGT)6	50	0.391	284–304	1
SS 9I	CAGACGAATGAGAAGCGAAC TTCAAAACAACGCTCCTGG	5-3	[(GT)2GAT]3(GT)14GAT(GT)5[GAT(GT)4]3(GAT)3	55	0.343	245–320	2
SS 10J	CCTGATATCGTTGAGGTCG ATTTCCCCTCACTTGCTCC	7-3	GT10	55	0.207	202–212	1
SS 11K	CACTCGCTTCTCCATCTCC GCTTGATTAGTTGGTTGGCA	8-3	CA12	55	0.190	251–271	1
SS 12L	TCATAGTGAGTGCATGATGCC CAGGGATGACTTTGGAATGG	17-3	(TTA)9	55	0.603	345–390	4
SS 13M	GACGCCTTGAAGTTCTCTTCC CGAACAAGTATCCTCGTACCG	20-4	(GT)7GG(GT)5	50	0.030	268–278	1
SS 14N	CTTCTAGAGGACTTGGTTTTGG CGGAGGTCATTGGGAGTACG	23-4	(TG)10	60	0.360	384–388	4
SS 15O	GAATCTCTGTCCCACCATCG AGCCCATGTTTGGTTGTACG	36-4	CA6(CGCA)2CAT2	50	0.097	415–429	1
SS 16P	GGTCTCATACAGTCTACACACA CTCTAGAGGATCTGCTGACA	42-4	GA9	60	0.360	410–414	1
SS 17Q	CCCTACAATATCCCATGGAGTC CCTCGTCTATCCGTCCATC	50-4	CA7(TACA)2	50	0.243	419–527	2
SS 18R	GTTTTCGGTTGTGTGCTGG GCTCGTTCAAGCTCAGCAAG	55-4	TACA10	50	0.153	173–221	1
SS 19S	TCGCCTCAGAAGAATGTGC AGCGGGTTACAAGGAGATGG	92-4	(CT)12	50	0.153	374–378	1
SS 20T	CTCATTTCATCCCATCTCTCC AATTCAAGCCTTCCTCAGCC	99-4	(GTAA)2(GCAA)(GTAA)3	50	0.243	402–422	1
SS 21 U	TGCATCTCGATGCTTGAATC CCTGCAGGGAGAAACATCAC	106-4	(CATA)25	55	0.391	491–571	1
SS 22V	ATCCCTAACATCCCTAACGC GGAGAATTGAAGAATTGAATGC	110-4	(TATG)9	50	0.294	362–378	1
SS 23W	GCTCCTGTATACCATGTCTTG GGACTTTCGGACATGATGAT	114-4	(AGAT)14(AAGC)4	50	0.294	351–391	1
SS 24X	TCAAGTACAGCATTTGC TTCCAGTCATTACCTACTAC	117-4	(TAC)6C(TAC)3	55	0.564	376–388	1
SS 25Y	GTAACAAGAGACCAAAATTCGG TGAACGAGCTGTCATTCCC	119-4	(GTAT)6 and (TACA)5	50	0.135	369–391	1

*****Locus names; #Repeat motifs as mentioned by Sirjusingh and Kohn (2001).*

TABLE 4 | Variability in mycelial growth and sclerotia formation (on PDA) in a different geographical isolate of *Sclerotinia sclerotiorum*.

Isolate	Mycelium				Sclerotia						
	Growth on PDA (mm)		Color	Texture	Scl. Ini. (Days)	Days of formation	Scl./plate	Color	Pattern	Dia. (mm)	Length (mm)
	72 h	96 hr									
SR-1	85	90	Whitish	Scattered	4	5	40	Black	Peripheral (Spread)	1.9	3.6
SR-2	90	83	Off White	Scattered	5	5	36	Black	Peripheral	1.9	4.9
SR-3	84	90	Whitish	Scattered	4	5	33	Black	Peripheral	2.0	4.3
SR-4	34	84	Whitish	Scattered	4	6	49	Black	Peripheral (Spread)	1.8	4.2
SR-5	90	90	Whitish	Fluffy	4	5	33	Black	Peripheral	2.2	4.7
SR-6	87	90	Off White	Smooth	4	5	35	Black	Peripheral	2.3	4.1
SR-7	87	90	Dirty White	Scattered	4	5	44	Black	Peripheral	2.0	4.4
SR-8	64	90	Off White	Smooth	5	6	39	Black	Peripheral	2.2	3.5
SR-9	87	90	Whitish	Smooth	4	5	40	Black	Peripheral	1.8	4.6
SR-10	44	61	Whitish	Scattered	5	7	33	Black	Peripheral (Spread)	2.2	2.9
SR-11	80	90	Whitish	Scattered	4	5	35	Black	Peripheral	2.0	4.0
SR-12	87	90	Off White	Scattered	4	5	39	Black	Peripheral (Spread)	2.0	4.2
SR-13	90	90	Whitish	Scattered	4	5	41	Black	Peripheral	1.8	3.5
SR-14	67	90	Off White	Smooth	5	6	38	Black	Peripheral	2.1	6.2
SR-15	87	90	Whitish	Smooth	4	5	40	Black	Peripheral (dou. ring)	2.0	3.4
SR-16	64	80	Whitish	Scattered	5	5	38	Black	Peripheral (dou. ring)	2.1	3.5
SR-17	90	90	Off White	Scattered	4	5	48	Black	Peripheral	2.1	3.1
SR-18	80	90	Whitish	Smooth	4	5	38	Black	Peripheral	1.9	4.9
SR-19	90	90	Whitish	Scattered(fluffy)	4	5	30	Black	Peripheral (Spread)	2.1	2.9
SR-20	90	90	Whitish	Smooth	4	5	62	Black	Peripheral	2.0	3.7
SR-21	90	90	Off White	Scattered	4	5	37	Black	Peripheral	2.1	3.7
SR-22	87	90	Whitish	Smooth	4	5	45	Black	Peripheral (Spread)	2.2	4.4
SR-23	80	90	Whitish	Smooth	4	5	55	Black	Peripheral	2.1	4.5
SR-24	11	34	Whitish	Smooth	6	7	34	Black	Peripheral	2.0	5.9
SR-25	90	90	Whitish	Smooth	4	5	39	Black	Peripheral	2.3	6.3
SR-26	64	84	Dirty White	Scattered(fluffy)	5	5	53	Black	Peripheral (dou. ring)	2.4	4.7
SR-27	84	90	Whitish	Scattered	4	5	37	Black	Peripheral	2.4	5.8
SR-28	67	83	Whitish	Smooth	4	5	39	Black	Peripheral	2.1	4.8
SR-29	70	90	Whitish	Smooth	5	5	32	Black	Peripheral	2.0	6.2
SR-30	47	64	Dirty White	Fluffy	5	5	27	Black	Peripheral	2.1	5.7
SR-31	90	90	Off White	Scattered	4	5	40	Black	Peripheral	2.3	4.6
SR-32	87	90	Dirty White	Smooth	4	5	42	Black	Peripheral	2.1	3.5
SR-33	57	87	Whitish	Fluffy(Scattered)	5	6	44	Black	Peripheral	2.1	4.5
SR-34	73	90	Whitish	Fluffy	5	6	42	Black	Peripheral	2.0	4.6
SR-35	90	90	Dirty White	Smooth	4	5	36	Black	Peripheral	2.3	4.8
SR-36	87	90	Whitish	Scattered	4	5	34	Black	Peripheral (dou. ring)	2.1	4.7
SR-37	90	90	Dirty White	Scattered	4	5	42	Black	Peripheral (Spread)	2.0	4.4
SR-38	70	90	Whitish	Smooth	4	5	50	Black	Peripheral (Spread)	2.2	3.5
SR-39	57	90	Whitish	Scattered	4	5	55	Black	Peripheral (Spread)	2.2	3.7
SR-40	60	90	Whitish	Scattered	5	5	34	Black	Peripheral	2.2	5.3
SR-41	34	87	Whitish	Scattered	5	5	47	Black	Spread (Scatter)	2.2	3.7
SR-42	77	90	Off White	Smooth	5	5	38	Black	Peripheral	2.3	5.4
SR-43	71	90	Whitish	Scattered	5	6	47	Black	Peripheral (dou. ring)	2.1	4.5
SR-44	54	90	Whitish	Fluffy	4	5	32	Black	Peripheral	2.4	3.5
SR-45	70	90	Whitish	Smooth	4	5	47	Black	Peripheral	2.3	4.7
SR-46	60	90	Whitish	Scattered	4	5	52	Black	Peripheral (dou. ring)	2.2	3.1
SR-47	34	87	Whitish	Scattered	5	6	44	Black	Peripheral (dou. ring)	2.0	3.7
SR-48	70	90	Off White	Smooth	4	5	48	Black	Peripheral	2.3	3.5

(Continued)

TABLE 4 | Continued

Isolate	Mycelium				Sclerotia						
	Growth on PDA (mm)		Color	Texture	Scl. Ini. (Days)	Days of formation	Scl./plate	Color	Pattern	Dia. (mm)	Length (mm)
	72 h	96 hr									
SR-49	20	77	Whitish	Smooth	5	6	49	Black	Peripheral (dou. ring)	2.4	4.2
SR-50	64	90	Whitish	Fluffy	5	6	25	Black	Peripheral (Spread)	2.0	3.1
SR-51	47	90	Whitish	Scattered	5	5	51	Black	Peripheral (Spread)	2.1	4.5
SR-52	24	77	Whitish	Smooth	5	6	42	Black	Peripheral	2.1	4.9
SR-53	80	90	Whitish	Scattered	4	5	40	Black	Peripheral (dou. ring)	2.2	3.1
SR-54	54	90	Whitish	Scattered	4	5	38	Black	Spread	2.3	3.9
SR-55	60	90	Dirty White	Smooth	5	6	40	Black	Peripheral	2.4	4.3
SR-56	70	90	Whitish	Fluffy	4	5	40	Black	Peripheral (dou. ring)	2.2	4.0
SR-57	67	84	Whitish	Scattered	5	5	36	Black	Peripheral	2.0	3.3
SR-58	77	90	Whitish	Scattered	4	5	59	Black	Peripheral (dou. ring)	2.2	4.5
SR-59	57	90	Whitish	Smooth	4	5	46	Black	Peripheral	2.1	5.3
SR-60	47	90	Whitish	Scattered	5	6	47	Black	Peripheral (dou. ring)	2.1	3.5
SR-61	30	84	Whitish	Fluffy	5	6	50	Black	Peripheral	2.2	3.9
SR-62	50	67	Dirty White	Smooth	4	5	35	Black	Peripheral	2.1	6.3
SR-63	57	90	Whitish	Smooth	4	5	45	Black	Peripheral	2.2	4.7
SR-64	60	90	Whitish	Scattered	4	5	49	Black	Peripheral (Spread)	2.2	4.7
SR-65	40	87	Whitish	Fluffy	4	5	56	Black	Peripheral	2.5	6.6
SE	9.43	5.36			0.24	0.25	5.26			0.14	0.88
CD at 5%	6.50	5.11			0.33	0.33	4.97			0.18	1.17
CV	3.05	0.76			0.03	0.02	1.53			0.02	0.41

Scl. Ini, Sclerotia initiation; Dia, Diameter; dou. Ring, double ring.

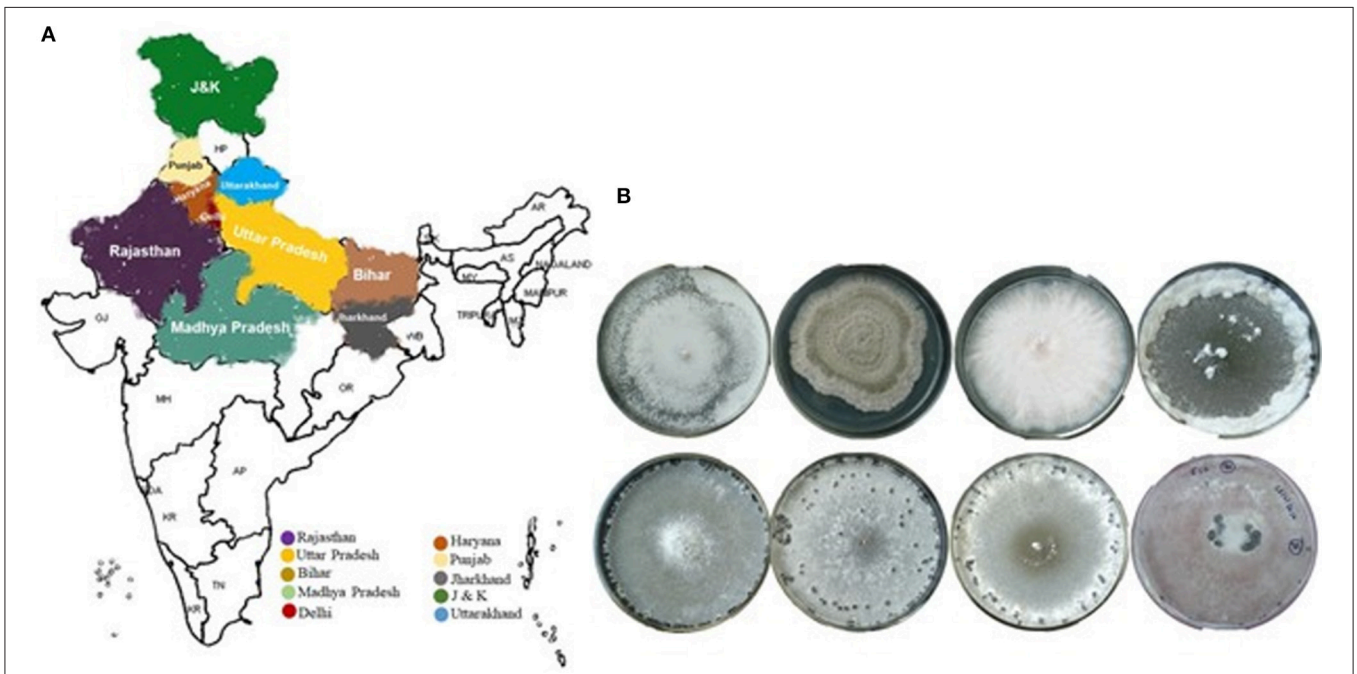

FIGURE 1 | Geographic distribution map of isolates of *Sclerotinia sclerotiorum* from the 10 different states of India. There were 65 isolates collected from *Brassica* field of these states **(A)**, and representative images of the *S. sclerotiorum* isolates with morphological variabilities **(B)**.

All the distinct *Sclerotinia* isolates were categorized based on the number and rate of sclerotia produced by them at a given time point into three groups: (i) High producer (ESR-20, 23, 26, 39, 46, 51, 58, and 65), (ii) Intermediate (ESR-01–19, 21, 22, 24, 25, 27–29, 31–38, 40–45, 47–49, 52–57, 59–64), and (iii) Low producer (ESR-30 and 50). In the majority of the isolates, sclerotia were observed produced within 6–9 days after growth. The sclerotia of isolates ESR-26, 27, 44, 49, 55 and 65 were larger in size (2.4–2.5 mm in diameter), while those of ESR-01, 02, 04, 09, 13, 18 were smallest (1.8–1.9 mm in diameter). The isolates varied in their sclerotial length (2.9–6.6 mm), however, the sclerotia of isolate ESR-65 had a maximum length (6.6 mm) (Table S1).

The morphological features among *S. sclerotiorum* collections from *Brassica* field of different agronomic regions in India (**Figure 1**), were used in genetic diversity analysis. The dendrogram generated (Jaccard's coefficient) have three distinct clusters at 65% of distance (**Figure 2**). Cluster I, with the highest degree of genetic variation, comprises 60 isolates from different regions; cluster II has four isolates, collected from distinct geographical locations or provinces, and cluster III contains one isolate, from Haryana. The robustness of the tree was estimated by bootstrap resampling, and the bootstrap values for clusters I, II, and III were very high, 100, 99, and 100%, respectively. Out of three clusters, cluster I was the largest and differentiated into seven distinct sub-clusters: IA-IG. Almost 99% of the isolates from different provinces fell under these sub-clusters. The majority of the *S. sclerotiorum* isolates from Rajasthan were grouped in the sub-cluster IC to IG (83%) and rest were distributed across the dendrogram. Cluster II had 4 isolates were grouped into two sub-clusters IIA and IIB. All the four isolates one in IIA and three in IIB were from four different states whereas single isolate present in cluster III was from Haryana region. Individual isolates from Jharkhand and J&K distributed in sub-cluster IIB. Interestingly out of 4 isolates in cluster II, 2 of the isolates one each from Rajasthan and Jharkhand was moderately virulent. One notable thing in the dendrogram was the distribution of the highly virulent isolates, one from each states UP, Punjab and Rajasthan had clustered into sub-clad ID whereas another highly virulent isolates one each from UP and Rajasthan falls under IA and IB, respectively.

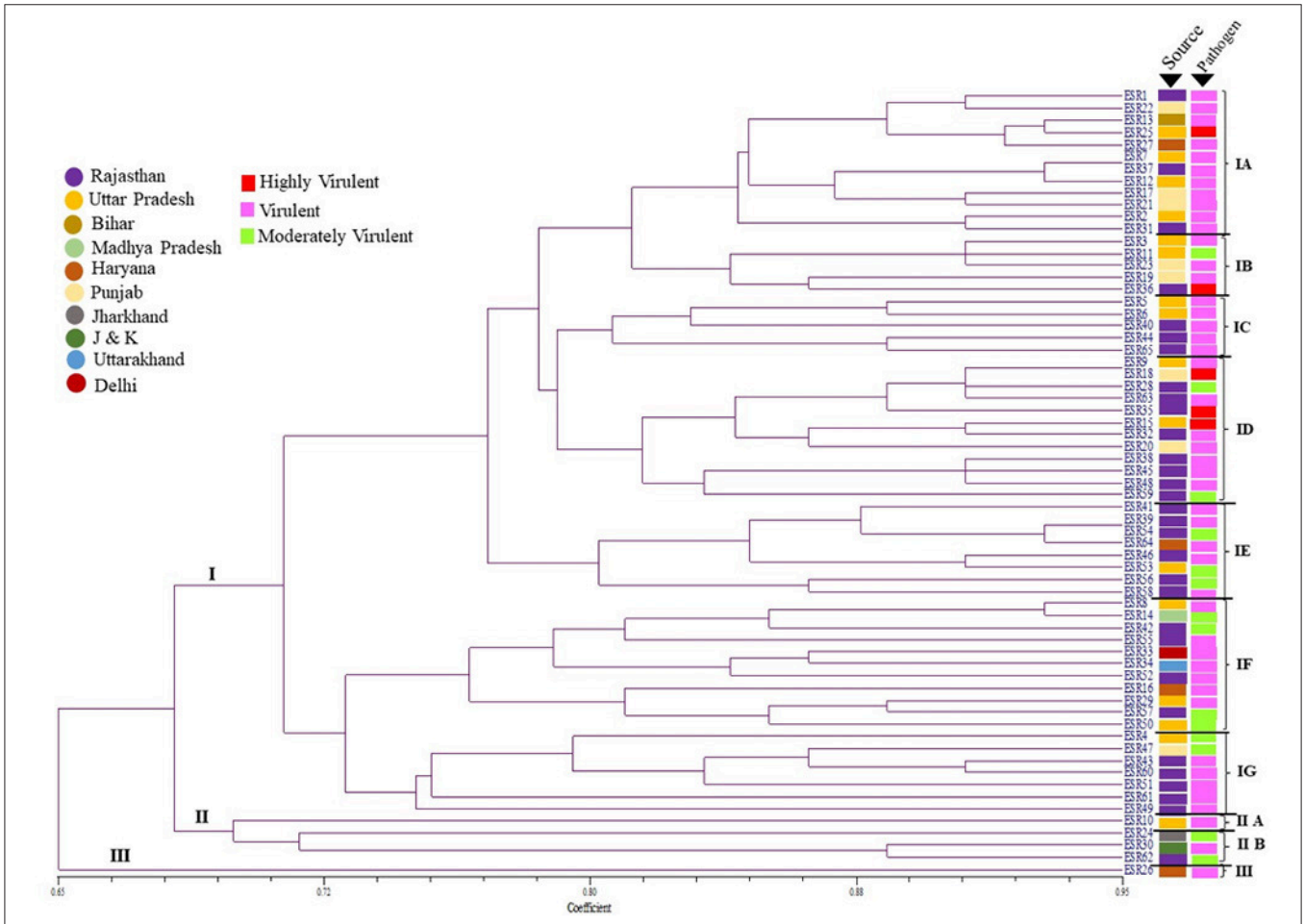

FIGURE 2 | Dendrogram derived from the morphological characters of 65 different *S. sclerotiorum* isolates, based on growth, color, texture, shape and size of the mycelia and sclerotia grown on PDA medium and their respective pathogenicity over *Brassica* species.

Pathogenicity

Plants inoculated with *S. sclerotiorum* developed necrotic and bleached lesions 6–9 days after inoculation, and white cottony mycelial growth appeared on stem surface after successful infestation. Pathogenic variability test conducted on 4 *Brassica* differentials has shown that all the isolates collected were pathogenic and able to develop stem rot disease after infection. However, the aggressiveness of the isolates was observed varies contrarily on all the host differentials and thus diverse groups were identified for each character by comparing the pathologically quantitative characteristics i.e., stem lesion length and percentage of disease incidence on different host differentials. All the 65 *S. sclerotiorum* isolates from different geographical regions showed variations in pathogenicity in respect of stem lesion length. After artificial inoculation of *S. sclerotiorum*, the typical water-soaked lesion was observed on the stems of host differentials. On the basis of longest and shortest stem lesion formed by different geographical isolates of four *Brassica* species, following 4 groups were made: Group I: (*Brassica juncea* var. NRCDR-02), Group II: (*B. rapa* var. toria), Group III: (*B. rapa* var. yellow sarson), and Group IV: (*B. rapa* var. brown sarson). Group I, composed of 9 isolates viz., ESR−12, 15, 17–19, 25, 35, 36, 65 produced longer stem lesion and among them ESR-36 produced the longest lesion i.e., 49.0 cm, while ESR-26, 40 and 64 isolates produced shortest stem lesion i.e., 1.0 cm (range:1.0–49.0 cm). Similarly, other 6 groups also showed pathogenic variability. Based on the stem lesion formation, out of 7 groups, ESR-36 and ESR-60 isolates were found producing longest and shortest stem lesion on the inoculated stem, respectively.

The results of pathogenicity tests conducted by using the 65 isolates of *S. sclerotiorum* over the 4 different *Brassica* differential has shown that the isolates had differences in their pathogenicity, infectivity and disease severity on tested *Brassica* cultivars and are presented in **Table 1**. The disease severity was measured in terms of Mean Disease Severity (MDS) by measuring the lesion length appeared on infected stem and that provides the basis for recording the virulence of individual isolate as low (MDS: < 3 cm), medium (MDS: < 3–10 cm) and high (MDS: > 10 cm). Thus, based on the disease severity index of the isolates *S. sclerotiorum* collection was distributed into three groups viz., highly virulent (5 isolates), virulent (46 isolates), and moderately virulent (14 isolates) based on the variations observed by analyzing the mean disease severity index in the treated mustard variety (**Table 5**). The un-inoculated and control plants of test variety inoculated with plain agar media showed no symptoms. The *Sclerotinia* isolates were further re-isolated and cultured from the infected *Brassica* plants following Koch's postulates.

SSR Genotyping

The population dynamics study of the pathogen plays a vital role in deciphering the mechanism behind behavioral pattern as well as in understanding the distribution pattern of the pathogen in distinct geographical areas where host species envisioned frequently by the infective pathogen. In this direction, the genetic diversity of *S. sclerotiorum* isolates were analyzed by simple sequence repeat (SSR) based fingerprinting. All the 25 SSR primers were analyzed after optimizing the melting temperature (Tm) for polymorphism assay on collective set of 65 isolates comprising representatives from the major *Brassica* growing states of India included in the study: Rajasthan (31), Uttar Pradesh (16), Punjab (8), Haryana (4), Delhi (1), Bihar (1), Madhya Pradesh (1), Uttarakhand (1), Jharkhand (1), and Jammu & Kashmir (1). Among the genome-wide distributed primers, only four primers (9I, 12L, 14N, and 17Q) has generated multiple bands whereas remaining primers were produced a single polymorphic band (**Table 3**). Two primers 9I and 17Q were observed produced 2 polymorphic bands of 100–500 bp size range per isolate. Subsequently other two primers 12L and 14N have produced 4 polymorphic bands within a range of 200–1,000 bp (Figures S1–S9). The differences in genetic diversity among the *S. sclerotiorum* pathogen population obtained through SSR fingerprinting in this study were found reproducible. Subsequently, UPGMA dendrogram drawn based on presence and absence of the banding patterns showed substantial diversity among the isolates. Based on the topology and similarity indices of the dendrogram, the isolates were grouped into three major clades and each clade was signified by a roman numeral (group I to III; **Figure 3**).

The detailed analysis of the dendrogram revealed, maximum numbers of isolates grouped in clade I and it was the largest and based on the similarity indices the clade I was further separated into seven divergent sub-clades: IA-IG. Among these sub-clades, IA, IF and IG harbors nearly 60% of the *S. sclerotiorum* isolates from Rajasthan whereas, remaining 40% were distributed in other clades of the dendrogram. The other two major clades, clade II and III had 2 and 4 isolates and in which 1 isolate in clade II and 2 isolates in clade III were from Rajasthan. Almost all the isolates from UP were clustered in clade I under sub-clades IA, IB, IC, IE, and IG. But, isolates from Punjab has a different trend of distribution across the dendrogram. All the isolates from Haryana were clustered in sub-clades IA and IC. Individual isolates from Delhi and J&K distributed in sub-clade IA, from Bihar, Jharkhand, and MP distributed in IC, and one isolate from Uttarakhand distributed in the major Clade II. The distribution of highly virulent isolates in dendrogram was found interesting were two from UP and one isolates from each Rajasthan and Punjab had clustered into IA sub-clade whereas another highly virulent isolate from Rajasthan was clustered in clade III. The prominent genetic diversity feature in clustering was observed in sub-clade IE, IF, IG and clade II, III those included exclusively virulent or highly virulent isolates and more interestingly these clades had at least one isolate from individual state included in this study.

ITS Sequence Analysis

The fungal-specific ITS4-ITS5 universal primers pair was used in amplifying the internal transcribed spacer (ITS) region from the DNA of all the 65 *S. sclerotiorum* isolates collected from infected *Brassica* crop grown in the diverse genetic background. The amplicon lengths and purity was estimated by gel electrophoresis and found about 600 bp in size (Figure S11). The sequence analysis result of the rRNA data by NCBI BLAST tool observed connoted the morphological variability and supported their individual existence. Further, in NCBI GenBank database the

TABLE 5 | Virulence grade for *Sclerotinia sclerotiorum* population assigned based on disease severity assessment and GenBank accession numbers for the ITS sequences.

Strain No.	Source (Host)	Province	Pathogenicity of the isolate	GenBank accession no.
ESR 1	*B. juncea*	Rajasthan	Virulent	MF408233
ESR 2	*B. juncea*	UP	Virulent	MF408234
ESR 3	*B. rapa*	UP	Virulent	MF408235
ESR 4	*B. juncea*	UP	Moderately Virulent	MF408236
ESR 5	*B. rapa*	UP	Virulent	MF408237
ESR 6	*B. juncea*	UP	Virulent	MF408238
ESR 7	*B. juncea*	UP	Virulent	MF408239
ESR 8	*B. juncea*	UP	Virulent	MF408240
ESR 9	*B. juncea*	UP	Virulent	MF408241
ESR 10	*B. juncea*	UP	Virulent	MF408242
ESR 11	*B. juncea*	UP	Moderately Virulent	MF408243
ESR 12	*B. juncea*	UP	Virulent	MF408244
ESR 13	*B. rapa*	Bihar	Virulent	MF408245
ESR 14	*B. juncea*	MP	Moderately Virulent	MF408246
ESR 15	*B. juncea*	UP	Highly Virulent	MF408247
ESR 16	*B. juncea*	Haryana	Virulent	MF408248
ESR 17	*B. juncea*	Punjab	Virulent	MF408249
ESR 18	*B. juncea*	Punjab	Highly Virulent	MF408250
ESR 19	*B. juncea*	Punjab	Virulent	MF408251
ESR 20	*B. juncea*	Punjab	Virulent	MF408252
ESR 21	*B. juncea*	Punjab	Virulent	MF408253
ESR 22	*B. juncea*	Punjab	Virulent	MF408254
ESR 23	*B. juncea*	Punjab	Virulent	MF408255
ESR 24	*B. juncea*	Jharkhand	Moderately Virulent	MF408256
ESR 25	*B. juncea*	UP	Highly Virulent	MF408257
ESR 26	*B. juncea*	Haryana	Virulent	MF408258
ESR 27	*B. juncea*	Haryana	Virulent	MF408259
ESR 28	*B. juncea*	Rajasthan	Moderately Virulent	MF408260
ESR 29	*B. juncea*	UP	Virulent	MF408261
ESR 30	*B. juncea*	J & K	Virulent	MF408262
ESR 31	*B. juncea*	Rajasthan	Virulent	MF408263
ESR 32	*B. juncea*	Rajasthan	Virulent	MF408264
ESR 33	*B. juncea*	Delhi	Virulent	MF408265
ESR 34	*B. juncea*	Uttarakhand	Virulent	MF408266
ESR 35	*B. juncea*	Rajasthan	Highly Virulent	MF408267
ESR 36	*B. juncea*	Rajasthan	Highly Virulent	MF408268
ESR 37	*B. juncea*	Rajasthan	Virulent	MF408269
ESR 38	*B. juncea*	Rajasthan	Virulent	MF408270
ESR 39	*B. juncea*	Rajasthan	Virulent	MF408271
ESR 40	*B. juncea*	Rajasthan	Virulent	MF408272
ESR 41	*B. juncea*	Rajasthan	Virulent	MF408273
ESR 42	*B. juncea*	Rajasthan	Moderately Virulent	MF408274
ESR 43	*B. juncea*	Rajasthan	Virulent	MF408275
ESR 44	*B. juncea*	Rajasthan	Virulent	MF408276
ESR 45	*B. juncea*	Rajasthan	Virulent	MF408277
ESR 46	*B. juncea*	Rajasthan	Virulent	MF408278
ESR 47	*B. juncea*	Punjab	Moderately Virulent	MF408279
ESR 48	*B. juncea*	Rajasthan	Virulent	MF408280
ESR 49	*B. juncea*	Rajasthan	Virulent	MF408281
ESR 50	*B. juncea*	UP	Moderately Virulent	MF408282

(Continued)

TABLE 5 | Continued

Strain No.	Source (Host)	Province	Pathogenicity of the isolate	GenBank accession no.
ESR 51	*B. juncea*	Rajasthan	Virulent	MF408283
ESR 52	*B. juncea*	Rajasthan	Virulent	MF408284
ESR 53	*B. juncea*	UP	Moderately Virulent	MF408285
ESR 54	*B. juncea*	Rajasthan	Moderately Virulent	MF408286
ESR 55	*B. juncea*	Rajasthan	Virulent	MF408287
ESR 56	*B. juncea*	Rajasthan	Moderately Virulent	MF408288
ESR 57	*B. juncea*	Rajasthan	Moderately Virulent	MF408289
ESR 58	*B. juncea*	Rajasthan	Virulent	MF408290
ESR 59	*B. juncea*	Rajasthan	Moderately Virulent	MF408291
ESR 60	*B. juncea*	Rajasthan	Virulent	MF408292
ESR 61	*B. juncea*	Rajasthan	Virulent	MF408293
ESR 62	*B. juncea*	Rajasthan	Moderately Virulent	MF408294
ESR 63	*B. juncea*	Rajasthan	Virulent	MF408295
ESR 64	*B. juncea*	Haryana	Virulent	MF408296
ESR 65	*B. juncea*	Rajasthan	Virulent	MF408297

GenBank accession IDs of each isolate based on ITS sequence information.

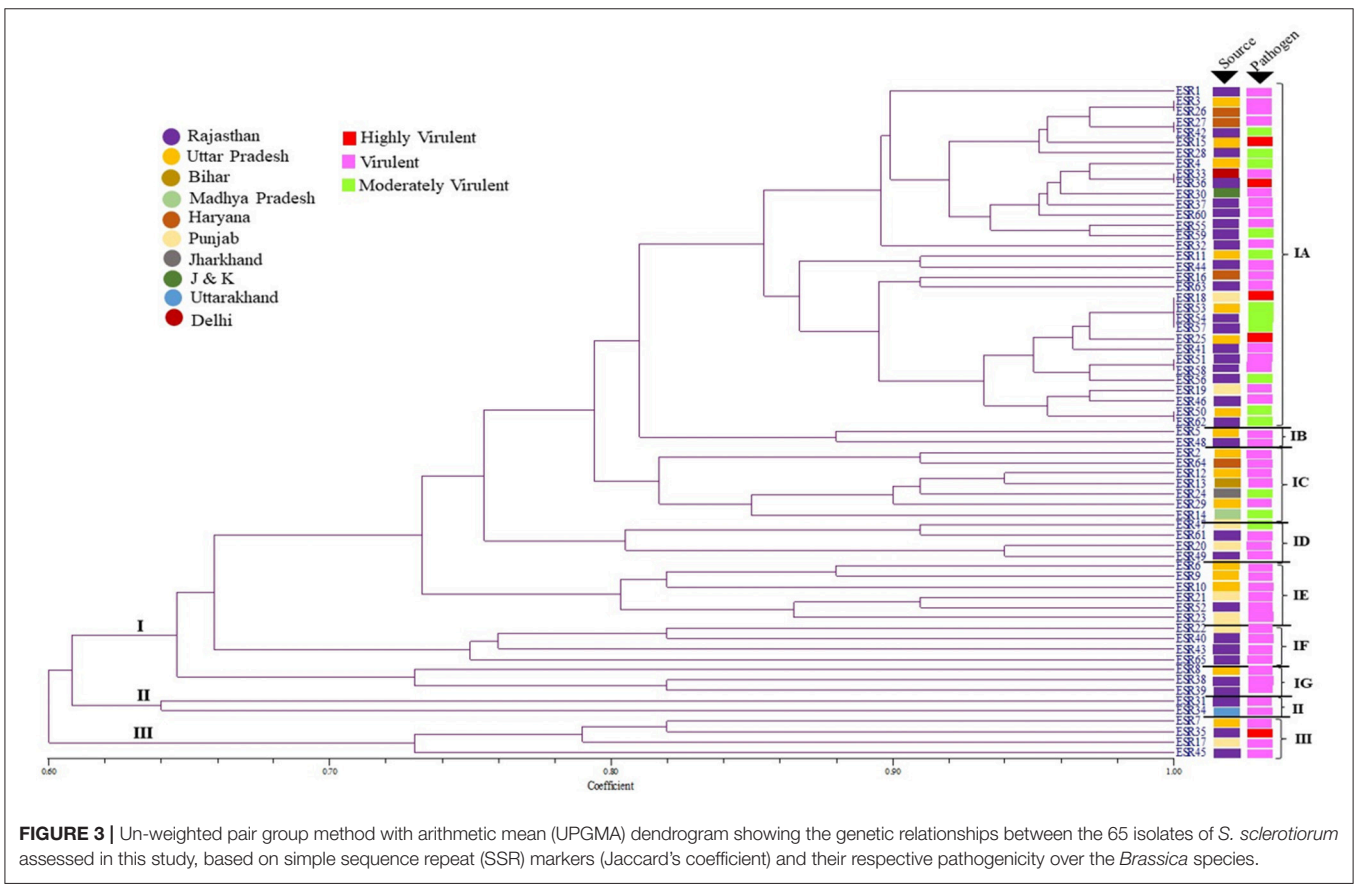

FIGURE 3 | Un-weighted pair group method with arithmetic mean (UPGMA) dendrogram showing the genetic relationships between the 65 isolates of *S. sclerotiorum* assessed in this study, based on simple sequence repeat (SSR) markers (Jaccard's coefficient) and their respective pathogenicity over the *Brassica* species.

99–100% closest match was found with *S. sclerotiorum*. The sequence data information for the ITS rDNA region of all the 65 *S. sclerotiorum* isolates obtained in this study were submitted in the GenBank database of the NCBI (GenBank Accession numbers MF408233-MF408297; **Table 5**).

Based on the ITS sequence information a dendrogram was constructed by using the ClustalW and Mega7.0 software with the Neighbor-Joining method (**Figure 4**). The resulted phylogenetic tree was clustered in total 11 clades and six of them were formed major clades, four clades with two members each and one clade

with a single member that clearly indicates the distribution of the isolates across dendrogram irrespective of their properties of pathogenicity or geographic origin. Isolates from Rajasthan and UP were found distributed in nine and six different clades, respectively, whereas isolates from Punjab were found distributed in five different clades. Clade I was found to be the largest and consisted of 21 divergent isolates from Rajasthan, UP, Punjab, Bihar, and Delhi with varied pathogenicity (highly virulent, virulent and moderately virulent). Clade II had virulent and moderately virulent isolates from Rajasthan and UP whereas isolates from Haryana were all virulent and distributed in clades IV, V and VI. Clade VII had only two isolates and both of them were from Rajasthan and virulent. Interestingly, the clade IV and V were also found heterogeneous as of clade I in terms of the isolates of different region and their virulence features. The isolate from Jharkhand was found distinctly in the clade VIII and was moderately virulent. Remarkably clade X had four isolates from the four different states. Two pathogenic isolate each from Rajasthan and Punjab were formed clade III, from UP and Punjab have formed clade IX and from UP and Rajasthan were formed clade X. One moderately pathogenic isolate from Jharkhand formed the single member clade VIII. The highly pathogenic isolates from UP, Rajasthan, and Punjab were distributed in Clades I, V, and VI.

The ITS sequence analysis of all the isolates in the study depicted on an average 95–100% of sequence similarity that entails conspecific nature of the isolates and their host from which the isolates were collected irrespective of different geographic regions.

DISCUSSION

The incidence of stem rot disease in India, especially in oilseed *Brassica*, has been known to damage the crops since from the mid-1990 but the genetic diversity of the pathogen especially in oilseed *Brassica* has not been comprehensively studied so far which is primarily required for understanding the mechanism of the pathogenesis and virulence of the pathogen. From the last decade, the stem rot disease in *Brassica* poses a serious threat to the crop every year in India and causes significant damage to the crop in terms of yield and economic losses to the farmers due to lack of effective management practices and other control measures. From the frequent disease occurring reports and extent of its severity over the oilseed crops, this pathogen has drawn attention and interest of the researchers to analyze the host-pathogen interaction in a broader spectrum as the mustard growing farmers experiencing this problem almost every years during the cropping season. The present investigation thoroughly reporting the existence of *S. sclerotiorum* pathogen in mustard fields and the genetic diversity among the population distributed throughout the *Brassica* growing regions of India.

The field-based crop-specific disease survey in different states of the India has shown the high occurrence and well-dispersed existence of the stem rot disease that commonly associated with the scorched lesion on the stem of the infected plants and sclerotia infested soil samples in the severely affected crop field. The regular appearance of the stem rot disease in *Brassica* indicates it is a recurrent menace for the crop and the lack of promising resistance source to the pathogen in existing cultivated varieties. Although the isolates in the present investigation were collected from *Brassica* field only but even though they were found genetically diverse in terms of their culture conditions and in morphological appearance as well. This might be due to the divergent geographical location from where the isolates have been collected. The evaluation of the pathogenicity of different *Brassica* cultivars has revealed that there was differential susceptibility in host species against different isolates of the *S. sclerotiorum* and thus based on the pathogenicity assay and virulence properties the pathogen population was grouped into three subgroups highly virulent, virulent and moderately virulent isolates. Depending on their virulence all the isolates resulted in the development of lesions of white patches of a different length over the infected stem of the *Brassica* cultivars that indicates the existence of genetically diverse and variable population of *S. sclerotiorum*. The pathogenicity assay and virulence variability test have shown that out of 65 *S. sclerotiorum* isolates 5 of them were highly virulent, 46 were virulent and 14 isolates were falls under moderately virulent category and they disseminated through either contaminated soil or seed across *Brassica* growing regions in India. The genetic diversity analysis by all the means followed in this study has clearly shown there were not many differences exists in terms of virulence and in groups that comprised from the isolates of different virulence nature belongs to different localities. Our results are in accordance with the observations made in previous studies where aggressiveness of the isolates are being independent of their geographic distribution (Atallah et al., 2004; Xie et al., 2014). Hence, the nature of the virulence of the *S. sclerotiorum* pathogen possesses a potential threat to the planting of *Brassica* cultivars susceptible to the stem rot disease.

Sclerotinia sclerotiorum apart from reproducing asexually by myceliogenic germination of sclerotia it is also able to produce sexually through apothecia and ascospores formation. The diversity analysis and genetic architecture of *S. sclerotiorum* have shown the existence of homogeneity across the isolates with little variation in 18 and 28 s rDNA regions (Kohli et al., 1995). The genetic diversity of the pathogen, severity of the disease and frequency of its occurrence are the important factors that directly correlates with the epidemics of the disease at the regional level and hence their comprehensive studies are the foremost requirement for understanding the behavioral pattern of the pathogens for effectively design the management practices for the control of this disease more efficiently. The polymorphism assay with the genome-wide distributed SSR markers has been proven effective in studying the existence of genetic diversity within the pathogen population. The SSR is the co-dominant molecular markers and it is a PCR-based robust technique that amplifies the putative repeat regions of the DNA and therefore it is able to identify a higher level of polymorphism than PCR-based another less robust markers like RAPD and hence it has been extensively used for analyzing the fungal population. The genetic diversity among *S. sclerotiorum* isolates based on the morphological features and SSR fingerprinting had observed

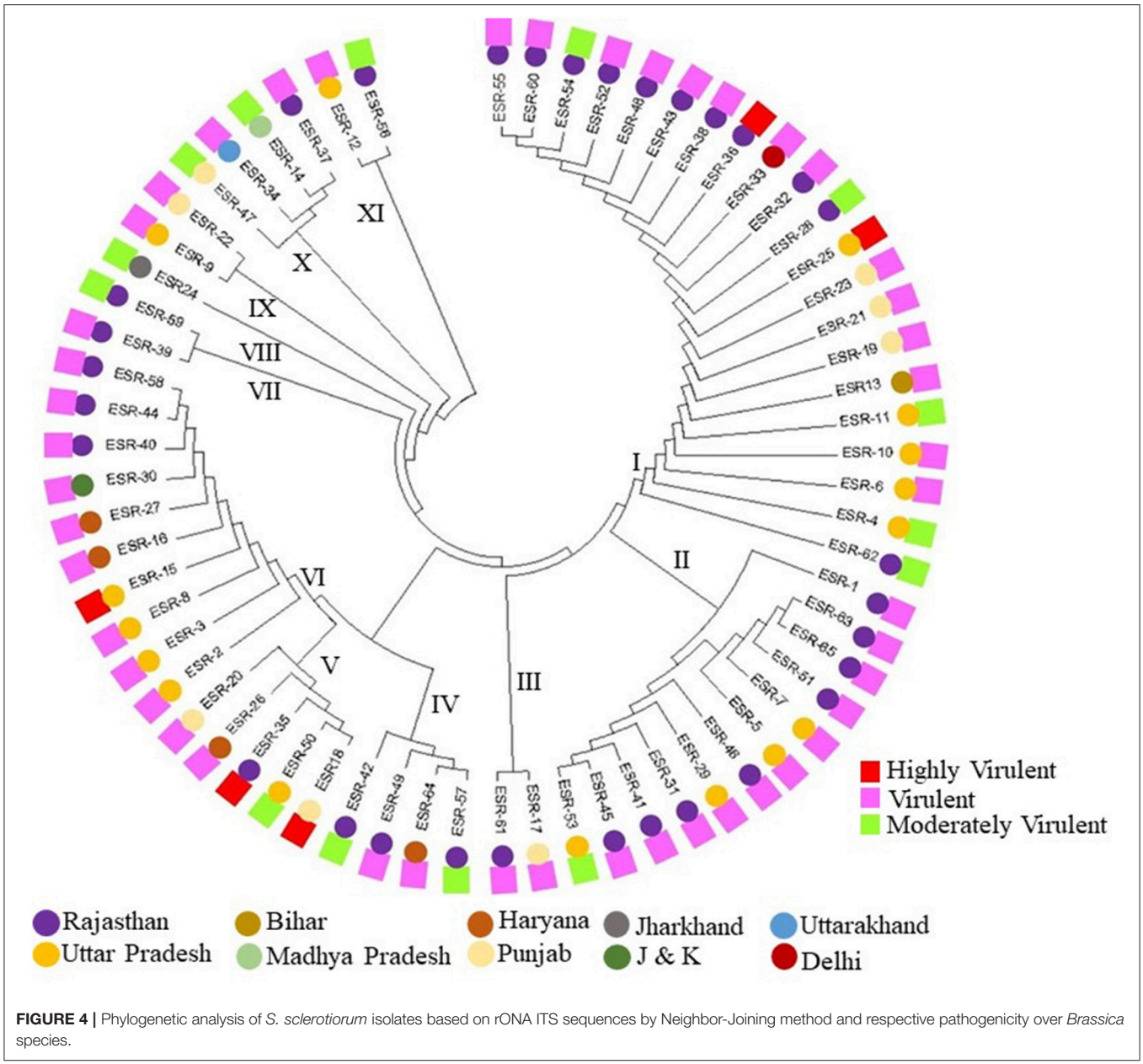

FIGURE 4 | Phylogenetic analysis of *S. sclerotiorum* isolates based on rONA ITS sequences by Neighbor-Joining method and respective pathogenicity over *Brassica* species.

quite diverse and reveals that some of the isolates grouped together belonging to the same region while others from the same region distributed across the dendrogram. The morphological features of the isolates and their SSR fingerprinting confirms the existence of a highly variable population of *S. sclerotiorum* even within the same crop and the region. However, among some isolates of *S. sclerotiorum* those belonging to the same geographic regions has been found having lower genetic diversity and that might be due to the locally adapted cropping system where introduction of newer varieties are usually not preferred over the existing one and hence diversity of the pathogen remained to stagnate due to lack of introduction of the newer genotypes of the pathogen in the area under cultivation.

The result of the present investigation depicting the genetic diversity of *S. sclerotiorum* population based on the morphological parameters and SSR analysis has been observed in coherence with earlier findings of the studies made on the same pathogen but in different host species. In eggplant, the genetic diversity analysis of *S. sclerotiorum* population by using the SSR and RAPD molecular markers, Tok et al. (2016) had shown the existence of high level of heterogeneity in the pathogen populations and presence of different isolates of *S. sclerotiorum* pathogen in the same regions. The presence of high heterogeneity in genetic composition of the *S. sclerotiorum* isolates in different regions of Turkey has reflected by their distribution across the dendrogram in different groups made

from the RAPD and SSR profiling. In a similar study, Barari et al. (2013) have characterized the genetic diversity within the population of *S. sclerotiorum* isolates from Iran and the variations among them were projected by SSR profiling. The depiction of variability in closely related isolates by SSR markers demonstrated its effectiveness in analyzing the genetic diversity among *S. sclerotiorum* pathogen. In chickpea, the use of RAPD, ITS-RFLP, ITS sequencing, and mycelial compatibility groupings (MCG) has shown the limited variability among the distinct *S. sclerotiorum* isolates possess the higher genetic homogeneity and partially correlated with their geographical origin (Mandal and Dubey, 2012). The robustness and reproducibility features of the SSR markers make it more effective and reliable marker for deciphering the genetic relationship among population studies and thus the phylogenetic analysis of *S. sclerotiorum* based on the SSR genotyping revealed the existence of wider genetic diversity among its population. The present findings are in connotation with the earlier reports that molecular typing by SSR is an efficient technique for establishing the genetic relationship among the diverse population and it is being preferred over other molecular tools for diversity analysis.

Further, the ITS (internal transcribed spacer) sequence based molecular phylogeny was established by using the ITS region as a genetic marker to investigate the genetic association within the *S. sclerotiorum* isolates. This phylogenetic study has facilitated the revelation of the evolutionary relationship within *S. sclerotiorum* species collected from a single host *Brassica* species from different geographical regions of India. Based on the ITS phylogeny all the 65 isolates investigated in the present study were observed grouped into six major and five minor evolutionary lineages of *S. sclerotiorum* isolates collected from different mustard growing states of India. In all the lineages deviation in virulence was not so evident and this suggests that the isolates from single host species may not differ ominously in their pathogenicity. The least variation in virulence of the pathogen has been observed in the case where isolates from defined geographical regions were taken into the investigation (Alvarez and Molina, 2000; Atallah et al., 2004; Sexton and Howlett, 2004). The differences in virulence can be more evident and conclusive when isolates from the widely distant geographical area will be taken for comparison. Kull et al. (2004) has found the conclusive evidence for the host specialization among *S. sclerotiorum* isolates.

Although, there is no report of any toxin is usually produced by the *S. sclerotiorum* pathogen it has been observed the production of oxalic acid (Cessna et al., 2000) and extracellular lytic enzymes production (Riou et al., 1991) invariably by all the isolates during pathogenesis. However, extensive biochemical and physiological studies are required to investigate the production of any natural mycotoxins by the pathogen if any like other fungus and further needs to find the effect of those toxins on the host plants and in herbivores consuming those plants. In this study, we attempted to verify the authenticity of *S. sclerotiorum* isolates by using the *Sclerotinia*-specific PCR primers and found all the geographical isolates (65) investigated were genetically diverse.

Development of the Genetic fingerprinting database for distinguishing the pathogen diversity between and within the fungal species is one of the foremost requirement for determining the origin and evaluation of the pathogen. Unequivocally, environmental factors are also influencing the properties of the pathogen and play crucial roles in determining the genetic differentiation within the pathogen population (Weller, 1988). The existence of a mixed population of *S. sclerotiorum* within a region could be due to the possible human interventions like the movement of infested soil through seeds, packaging materials or agricultural equipment that might carry the pathogen from one region to another. Results of the present study, as well as evidence from the previous studies, indicates the minute changes in physiological properties of the pathogen like changes in virulence due to evolutionary changes happening in due course of time that brings changes among genetically distinct populations of *S. sclerotiorum* isolates. Such changes may happen because of the varying force of selection over pathogen imposed by the selected set of genes of the host germplasm being tolerant to the invasive pathogen. The genes involved in host defense system and coding for the virulence factors in pathogen have been observed comparatively much more vulnerable for accumulating the mutation under positive selection pressure than the genes those regulating the basic physiological processes in the organism (Matute et al., 2008). As a consequence, in most of the host-pathogen interaction pathogen often adapts themselves to the evolutionary changes arises in response to the variation in the host genotype.

CONCLUSION

The current investigation reports the studies on morphological features, pathogenicity variance over the *Brassica* cultivars, and genetic diversity based on molecular characteristics of the *S. sclerotiorum* isolates population collected from 65 locations of the 10 major *Brassica* growing states of India. This is the first comprehensively studied report on *S. sclerotiorum* isolates especially from *Brassica* field of India that indicates the existence of broader genetic variations among the pathogen and this would facilitate the plant breeders to use the information in *Brassica* breeding program for stem rot disease resistance development. The SSR-based markers utilized in present investigation for diversity analysis can be effectively used for identification and analysis of *S. sclerotiorum* population from various host species. The present study offers the basis for increasing the basic understanding of host-pathogen interaction and also for deciphering the genes and associated pathways involved in combating the pathogen invasion. The evidence of the present study may provide a broader understanding of the pathogen virulence and that will facilitate the development of the effective disease management strategies based on molecular breeding and other advanced approaches.

AUTHOR CONTRIBUTIONS

PS, NG, and LP conceived and obtained funding from ICAR-EMR project for Sclerotinia work in Indian mustard. PS and VS collected isolates from diseased plants and along with

LP done the morphological characterization and pathogenicity evaluation. AS and MR obtained isolates from PS, carried out microsatellite genotyping. NG and RB do the ITS sequencing of *S. sclerotiorum* isolates and wrote the paper. NG and DM carried out clustering and phylogenetic analyses of microsatellite data and ITS sequences. RB and VS edited the manuscript.

FUNDING

The authors are grateful to ICAR (Indian Council for Agricultural Research), New Delhi, India for providing the financial support under ICAR-Extramural research Project F. No.: CS/18(15)/2015-O&P and Director, IARI, New Delhi, Director, DRMR, Bharatpur; Project Director, NRCPB, New Delhi for providing facilities to conduct these experiments.

SUPPLEMENTARY MATERIAL

The Supplementary Material for this article can be found online at: https://www.frontiersin.org/articles/10.3389/fmicb.2018.01169/full#supplementary-material

REFERENCES

Aldrich-Wolfe, L., Travers, S., and Nelson, B. D. Jr. (2015). Genetic variation of *Sclerotinia sclerotiorum* from multiple crops in the North Central United States. *PLoS ONE* 10:e0139188. doi: 10.1371/journal.pone.0139188

Alvarez, E., and Molina, M. L. (2000). Characterizing the *Sphaceloma* fungus, the causal agent of super-elongation disease in Cassava. *Plant Dis.* 84, 423–428. doi: 10.1094/PDIS.2000.84.4.423

Anonymous (2016). *Agricultural Statistics at a Glance 2016*. Directorate of Economics and Statstics, Govt. of India. Available online at: www.agricoop.nic.in & http:// eands.dacnet.nic.in

Atallah, Z. K., Larget, B., Chen, X., Johnson, D. A. (2004). High genetic diversity, phenotypic uniformity, and evidence of outcrossing in *Sclerotinia sclerotiorum* in the Columbia Basin of Washington state. *Phytopathology* 94, 737–742. doi: 10.1094/PHYTO.2004.94.7.737

Barari, H., Dalili, S. A., Rezaii, S. A. A., and Badalian, S. M. (2013). Genetic structure analysis of *Sclerotinia sclerotiorum* (Lib.) de bary population from different host plant species in North of Iran. *Rom. Biotechnol. Lett.* 18, 8197–8205. doi: 10.2298/ABS1301171B

Boland, G. J., and Hall, R. (1994). Index of plant hosts of *Sclerotinia sclerotiorum*. *Can. J. Plant Pathol*. 16, 93–100. doi: 10.1080/07060669409500766

Buchwaldt, L., Yu, F. Q., Rimmer, S. R., and Hegedus, D. D. (2003). Resistance to *Sclerotinia sclerotiorum* in a Chinese Brassica napus cultivar," in *International Congress of Plant Pathology*, (Christchurch).

Cessna, S. G., Sears, V. E., Dickman, M. B., and Low, P. S. (2000). Oxalic acid, a pathogenicity factor for *Sclerotinia sclerotiorum*, suppresses the oxidative burst of the host plant. *Plant Cell* 12, 2191–2200. doi: 10.1105/tpc.12.11.2191

Choudhary, V., and Prasad, L. (2012). Morpho-pathological, genetic variations and population structure of *Sclerotinia sclerotiorum*. *Vegetos Int. J. Plant Res.* 25, 178–183.

Cubeta, M. A., Cody, B. R., Kohli, Y., and Kohn, L. M. (1997). Clonality in *Sclerotinia sclerotiorum* on infected cabbage in eastern North Carolina. *Phytopathology* 87, 1000–1004. doi: 10.1094/PHYTO.1997.87.10.1000

Freeman, J., Ward, E., Calderon, C., and McCartney, A. (2002). A polymerase chain reaction (PCR) assay for the detection of inoculum of *Sclerotinia sclerotiorum*. *Eur. J. Plant Pathol.* 108, 877–886. doi: 10.1023/A:1021216720024

Hall, T. A. (1999). BioEdit: a user-friendly biological sequence alignment editor and analysis program for Windows 95/98/NT. *Nucleic Acids Symp. Ser*. 41, 95–98.

Hegedus, D. D., and Rimmer, S. R. (2005). *Sclerotinia sclerotiorum*: when "to be or not to be" a pathogen? *Fed. Eur. Microbiol. Soc. Microbiol. Lett*. 251, 177–184. doi: 10.1016/j.femsle.2005.07.040

Irani, H., Heydari, A., Javan-Nikkhah, M., and Ibrahimov, A. S. (2011). Pathogenicity variation and mycelial compatibility groups in *Sclerotinia sclerotiorum*. *J. Plant Prot. Res*. 51, 329–336. doi: 10.2478/v10045-011-0054-4

Kabbage, M., Yarden, O., and Dickman, M. B. (2015). Pathogenic attributes of *Sclerotinia sclerotiorum*: switching from a biotrophic to necrotrophic lifestyle. *Plant Sci*. 233, 53–60. doi: 10.1016/j.plantsci.2014.12.018

Kohli, Y., Brunner, L., Yoell, H., Milgroom, M., Anderson, J., Morrall, R., et al. (1995). Clonal dispersal and spatial mixing in populations of the plant pathogenic fungus, *Sclerotinia sclerotiorum*. *Mol. Ecol.* 4, 69–77. doi: 10.1111/j.1365294x.1995.tb00193.x

Kull, L. S., Pedersen, W. L., Palmquist, D., and Hartman, G. L. (2004). Mycelial compatibility grouping and aggressiveness of *Sclerotinia sclerotiorum*. *Plant Dis.* 88, 325–332. doi: 10.1094/PDIS.2004.88.4.325

Kumar, S., Stecher, G., and Tamura, K. (2016). MEGA7: molecular evolutionary genetics analysis version 7.0 for bigger datasets. *Mol. Biol. Evol*. 33, 1870–1874. doi: 10.1093/molbev/msw054

Kumar, S. V., Rajeshkumar, P., Senthilraja, C., and Nakkeran, S. (2015). First report of *Sclerotinia sclerotiorum* causing Stem Rot of Carnation (Dianthus caryophyllus) in India. *Plant Dis.* 99:1280. doi: 10.1094/PDIS-02-15-0240-PDN

Li, C. X., Li, H., Siddique, A. B., Sivasithamparam, K., Salisbury, P., Banga, S. S., Banga, S., et al. (2007). The importance of the type and time of inoculation and assessment in the determination of resistance in Brassica napus and *B. juncea* to *Sclerotinia sclerotiorum*. *Austr. J. Agric. Res.* 58, 1198–1203. doi: 10.1071/AR07094

Li, Z., Wang, Y., Chen, Y., Zhang, J., and Fernando, W. G. D. (2009). Genetic diversity and differentiation of *Sclerotinia sclerotiorum* populations in sunflower. *Phytoparasitica* 37, 77–85. doi: 10.1007/s12600-008-0003-6

Li, Z., Zhang, M., Wang, Y., Li, R., and Dilantha Fernando, W. G.(2008). Mycelial compatibility group and pathogenicity variation of *Sclerotinia sclerotiorum* populations in sunflower from China, Canada, and England. *Plant Pathol. J.* 2, 131–139. doi: 10.3923/ppj.2008.131.139

Mandal, A. K., and Dubey, S. C. (2012). Genetic diversity analysis of *Sclerotinia sclerotiorum* causing stem rot in chickpea using RAPD, ITS-RFLP, ITS sequencing and mycelial compatibility grouping. *World J. Microbiol. Bioethanol*. 28, 1849–1855. doi: 10.1007/s11274-011-0981-2

Matute, D. R., Quesada-Ocampo, L. M., Rauscher, J. T., and McEwen, J. G. (2008). Evidence for positive selection in putative virulence factors within the *Paracoccidioides brasiliensis* species complex. *PLoS Negl. Trop. Dis*. 2:296. doi: 10.1371/journal.pntd.0000296

McDonald, B. A., and Linde, C. (2002). Pathogen population genetics, evolutionary potential, and durable resistance. *Annu. Rev. Phytopathol*. 40, 349–379. doi: 10.1146/annurev.phyto.40.120501.101443

Meinhardt, L. W., Wulff, N. A., Bellato, C. M., and Tsai, S. M. (2002). Telomere and microsatellite primers reveal diversity among *Sclerotinia sclerotiorum* isolates from Brazil. *Fitopatol. Bras*. 27, 211–215. doi: 10.1590/S0100-41582002000200015

Nei, M. (1973). Analysis of gene diversity in subdivided populations. *Proc. Natl. Acad. Sci. U.S.A.* 70, 3321–3323. doi: 10.1073/pnas.70.12.3321

Njambere, E. N., Chen, W., Frate, C., Wu, B. M., Temple, S. R., and Muehlbauer, F. J. (2008). Stem and crown rot of chickpea in California caused by *Sclerotinia trifoliorum*. *Plant Dis.* 92, 917–922. doi: 10.1094/PDIS-92-6-0917

Prasad, L., Kamil, D., Solanki, R. K., and Singh, B. (2017). First report of *Sclerotinia sclerotiorum* infecting cumin (*Cuminum cyminum*) in India. *Plant Dis.* 101:833. doi: 10.1094/PDIS-08-16-1089-PDN

Riou, C., Freyssinet, G., and Fèvre, M. (1991). Production of cell wall degrading enzymes by the phytopathogenic fungus *Sclerotinia sclerotiorum*. *Appl. Environ. Microbiol*. 54, 1478–1484.

Rohlf, F. J. (2000). *NTSYS-pc: Numerical Taxonomy and Multivariate Analysis System. Version 2.1*. Setauket, NY: Exeter Biological Software.

Rousseau, G., Rioux, S., and Dostaler, D. (2007). Effect of crop rotation and soil amendments on *Sclerotinia* stem rot on soybean in two soils. *Can. J. Plant Sci.* 87, 605–614. doi: 10.4141/P05-137

Saharan, G. S., and Mehta, N. (2008). *Sclerotinia Diseases of Crop Plants: Biology, Ecology and Disease Management*. The Netherlands: Springer Science+Busines Media B.V. 485.

Schoch, C. L., Seifert, K. A., Huhndorf, S., Robert, V., Spouge, J. L., Levesque, C. A., et al. (2012). Fungal barcoding consortium. nuclear ribosomal internal transcribed spacer (ITS) region as a universal DNA barcode marker for fungi. *Proc. Natl. Acad. Sci. U.S.A.* 109, 6241–6246. doi: 10.1073/pnas.1117018109

Sexton, A. C., and Howlett, B. J. (2004). Microsatellite markers reveal genetic differentiation among populations of *Sclerotinia sclerotiorum* from Australian fields. *Curr. Genet.* 46, 357–365. doi: 10.1007/s00294-004-0543-3

Sharma, P., Meena, P. D., Kumar, S., and Chauhan, J. S. (2013). Genetic diversity and morphological variability of *Sclerotinia sclerotiorum* isolates of oilseed Brassica in India. *Afr. J. Microbiol. Res.* 7, 1827–1833. doi: 10.5897/AJMR12.1828

Sharma, P., Meena, P. D., Verma, P. R., Saharan, G. S., Mehta, N., Singh, D., et al. (2015). *Sclerotinia sclerotiorum* (Lib.) de Bary causing *Sclerotinia* rot in oilseed Brassicas: a review. *J. Oilseed Brass.* 6, 1–44.

Sirjusingh, C., and Kohn, L. M. (2001). Characterization of microsatellites in the fungal plant pathogen, *Sclerotinia sclerotiorum*. *Mol. Ecol. Notes* 1, 267–269. doi: 10.1046/j.1471-8278.2001.00102.x

Thompson, J. D., Higgins, D. G., and Gibson, T. J. (1994). CLUSTAL W: improving the sensitivity of progressive multiple sequence alignment through sequence weighting, position-specific gap penalties, and weight matrix choice. *Nucleic Acids Res.* 22, 4673–4680. doi: 10.1093/nar/22.22.4673

Tok, F. M., Dervis, S., and Arslan, M. (2016). Analysis of genetic diversity of *Sclerotinia sclerotiorum* from eggplant by mycelial compatibility, random amplification of polymorphic DNA (RAPD) and simple sequence repeat (SSR) analysis. *Biotechnol. Biotechnol. Equip.* 30, 921–928. doi: 10.1080/13102818.2016.1208059

Weller, D. M. (1988). Biological control of soilborne plant pathogens in the rhizosphere with bacteria. *Ann. Rev. Phytopathol.* 26, 379–407. doi: 10.1146/annurev.py.26.090188.002115

White, T. J., Bruns, T., Lee, S., and Taylor, J. (1990). "Amplification and direct sequencing of fungal ribosomal RNA genes for phylogenetics," in *PCR Protocols. A Guide to Methods and Applications,* eds M. A. Innis, D. H. Gelfand, J. J. Sninsky and T. J. White (San Diego, CA: White Academic Press), 315–322.

Xie, C., Huang, C. H., and Vallad, G. E. (2014). Mycelial compatibility and pathogenic diversity among *Sclerotium rolfsii* isolates in the southern United States. *Plant Dis.* 98, 1685–1694. doi: 10.1094/PDIS-08-13-0861-RE

Conflict of Interest Statement: The authors declare that the research was conducted in the absence of any commercial or financial relationships that could be construed as a potential conflict of interest.

frontiers in Microbiology

REVIEW
published: 29 August 2017
doi: 10.3389/fmicb.2017.01602

Integrated Translatome and Proteome: Approach for Accurate Portraying of Widespread Multifunctional Aspects of *Trichoderma*

Vivek Sharma[1], Richa Salwan[2], P. N. Sharma[1] and Arvind Gulati[3]*

[1] Department of Plant Pathology, Choudhary Sarwan Kumar Himachal Pradesh Agricultural University, Palampur, India, [2] Department of Veterinary Microbiology, Choudhary Sarwan Kumar Himachal Pradesh Agricultural University, Palampur, India, [3] Institute of Himalayan Bioresource Technology, Palampur, India

Genome-wide studies of transcripts expression help in systematic monitoring of genes and allow targeting of candidate genes for future research. In contrast to relatively stable genomic data, the expression of genes is dynamic and regulated both at time and space level at different level in. The variation in the rate of translation is specific for each protein. Both the inherent nature of an mRNA molecule to be translated and the external environmental stimuli can affect the efficiency of the translation process. In biocontrol agents (BCAs), the molecular response at translational level may represents noise-like response of absolute transcript level and an adaptive response to physiological and pathological situations representing subset of mRNAs population actively translated in a cell. The molecular responses of biocontrol are complex and involve multistage regulation of number of genes. The use of high-throughput techniques has led to rapid increase in volume of transcriptomics data of *Trichoderma*. In general, almost half of the variations of transcriptome and protein level are due to translational control. Thus, studies are required to integrate raw information from different "omics" approaches for accurate depiction of translational response of BCAs in interaction with plants and plant pathogens. The studies on translational status of only active mRNAs bridging with proteome data will help in accurate characterization of only a subset of mRNAs actively engaged in translation. This review highlights the associated bottlenecks and use of state-of-the-art procedures in addressing the gap to accelerate future accomplishment of biocontrol mechanisms.

Keywords: transcripts, active mRNA, regulation, integrated omic, translatome

OPEN ACCESS

Edited by:
Katarzyna Turnau, Jagiellonian University, Poland

Reviewed by:
Somayeh Dolatabadi, Westerdijk Fungal Biodiversity Institute, Netherlands
Ravindra Nath Kharwar, Banaras Hindu University, India

****Correspondence:***
Vivek Sharma
ankvivek@gmail.com

Specialty section:
This article was submitted to Fungi and Their Interactions, a section of the journal Frontiers in Microbiology

Received: *21 April 2017*
Accepted: *07 August 2017*
Published: *29 August 2017*

Citation:
Sharma V, Salwan R, Sharma PN and Gulati A (2017) Integrated Translatome and Proteome: Approach for Accurate Portraying of Widespread Multifunctional Aspects of Trichoderma. Front. Microbiol. 8:1602. doi: 10.3389/fmicb.2017.01602

INTRODUCTION

Trichoderma is a cosmopolitan and cardinal representative soil microflora of various climatic conditions (Herrera-Estrella, 2014). The biocontrol role of *Trichoderma* spp. have emerged as an attractive choice in agriculture sector due to their environmentally friendly nature over synthetic pesticides (Mukherjee et al., 2012, 2013). Among different biocontrol agents (BCAs),

the genus *Hypocrea*/*Trichoderma* containing *Trichoderma harzianum*, *Trichoderma atroviride*, *Hypocrea virens* are probably the most explored BCAs (Schuster and Schmoll, 2010; Sharma and Shanmugam, 2012; Sharma and Salwan, 2017) and occupies over 60% of all registered biopesticides (Mukherjee et al., 2013). The continuous efforts on the evaluation of biocontrol potential of *Trichoderma* have led to the identification of several promising species/strains including *T. harzianum* (Yedidia et al., 1999; Cloyd et al., 2007), *Trichoderma virens* (Hermosa et al., 2000; Howell, 2006), *Trichoderma viride* (Papavizas, 1985), *T. atroviride* (Longa et al., 2009), *Trichoderma polysporum* (Zhang et al., 2015), and *Trichoderma asperellum* GDFS1009 (Wu et al., 2017). In recent studies, another potential strains of *Trichoderma saturnisporum* has been identified for its biocontrol potential (Sharma and Shanmugam, 2012; Diánez Martínez et al., 2016). In addition to primary application in agriculture, *Hypocrea jecorina*/*Trichoderma reesei* strains are molecular factory for cellulolytic enzymes (Merino and Cherry, 2007; Singh et al., 2015). The natural potential to secrete lytic enzymes, antibiotics, and defeating opponent for space and nutrition are largely considered responsible for its success against plant pathogenic fungi (Viterbo et al., 2002; Benítez et al., 2004). The root colonization and intimate association of *Trichoderma* spp. with plant roots are known to promote plant growth and boost immune response against a number of plant pathogens (Contreras-Cornejo et al., 2011; Brotman et al., 2012; Mukherjee, 2012). Biocontrol strains of *Trichoderma* are used worldwide for the management of various plant pathogens like vascular wilt caused *Fusarium* (Al-Ani et al., 2013), Botrytis blight or gray mold caused by *Botrytis* (Elad and Kapat, 1999), anthracnose caused by *Colletotrichum* spp., and several other plant fungal diseases (Sharma et al., 2016a,b, 2017a). The improvement of *Trichoderma* species as BCAs for various agricultural applications required, detailed understanding of its active biological repertoire involved in mycoparasitism antibiosis as well as others components (**Table 1**). Genome sequencing and its annotation in mycoparasitic species have depicted genome sizes of 38.8 and 36.1 Mb for *T. viride* and of *T. atroviride* for biocontrol strains, respectively, compared to 34 Mb of *T. reesei* an industrial strain. Annotation of complete genome depicted a gene pool of 11,800 genes for *T. atroviride* and 12,400 genes for *T. viride*, compared to 9,143 genes in saprophytic strain *T. reesei*. The abundance of gene pool in mycoparasitic strains of *Trichoderma* genome (Lin et al., 2012; Atanasova et al., 2013) and expression of over 60% of the encoding transcripts during interaction of *T. virens* and *T. atroviride* against *Rhizoctonia solani* have revealed a complex nature of biocontrol mechanisms (Atanasova et al., 2013). Liu and Yang (2005) using simulated mycoparasitic conditions and cDNA libraries identified a total of 3,298 expressed sequence tags (ESTs) which corresponds to 1,740 transcripts. Using inducible conditions for *T. harzianum* CECT 2413, Vizcaíno et al. (2006) characterized, nearly 8,710 ESTs whereas Yao et al. (2013) identified 1,386 ESTs for *T. harzianum* 88. Among different ESTs, significant differential expression was observed only for limited transcripts. These EST represents a fragment of mRNA have several biotechnological applications and are being explored for either complementing the sequenced genome projects or cost effective alternatives for identification of genes as well as elucidation of functional genomics of plant–microbe interactions (Vieira et al., 2013). Advancement in molecular tools such as transcriptome profiling using RNA-seq and quantitative real-time PCR (RT-qPCR) technologies also predicted a large number of genes (14,095) for *T. harzianum* during augmentation on plant pathogen such as *Sclerotinia sclerotiorum* cell wall and only 297 were found differentially expressed among them (Steindorff et al., 2012, 2014). In addition to plant diseases management potential of biocontrol strains of *Trichoderma*, its growth promotion abilities in plants have been identified which are significantly enhanced during their antagonistic interactions with pathogens in soil. The molecular action of its biocontrol arsenal is mediated through adaptive recruitment and reprogramming of unique reservoir of several transcripts (Shaw et al., 2016). A comparative account using bioinformatic approaches such as BLAST analysis has revealed a very low overlap for different ESTs libraries (Yao et al., 2013). Therefore, the microarrays set designed based on genome coverage and ESTs may not provide accurate information.

The comprehensive analyses using different molecular approaches including ESTs (Chambergo et al., 2002), subtractive hybridization (Carpenter et al., 2005; Scherm et al., 2009; Vieira et al., 2013), microarray (Chambergo et al., 2002; Breakspear and Momany, 2007; Samolski et al., 2009), and transcriptomes (Atanasova et al., 2013) have established the complex response of *Trichoderma* species in biocontrol process which induces numerous genes having morphogenetic or other functions as well (Mehrabi-Koushki et al., 2012; Puglisi et al., 2012; Cacciola et al., 2015; Cetz-Chel et al., 2016). The complexity in different attributes may not be related to a particular stress and hence can lead to either imperfect transcriptional representation or a complex response. The continuous development in molecular technologies and advent of cloning free libraries using genome sequencing, deep RNA sequencing and proteomics has played vital role in the accurate identification and enhancing our capabilities of cataloging mRNA and protein populations exclusive to *Trichoderma* strains in response to changing environmental conditions (Shentu et al., 2014; Xie et al., 2015; Schmoll et al., 2016).

The *Trichoderma*–plant–pathogen interaction can produce significant amount of noise. Therefore one can speculate that the substantial amount of response at the gene expression level represents noise and that only a few changes are adaptive. Also, the microbes in the environment are continuously subjected to challenges and respond simultaneously to these factors in a complex way. Understanding the regulatory interactions necessitates an approach that can encompasses simultaneous both the transcriptome and proteome to observe and systematically view the adaptive expression at RNA and protein level. The integrated studies based on translatome and proteome level can provide a better state of these adaptive responses during biocontrol interaction. The regulation of mRNA at transcriptional and post-transcriptional levels contributes to reprogramming the behavior of BCAs through protein and secondary bioactive metabolites secretion to counter the pathogen associated challenges.

TABLE 1 | List of a few selected glycosyl hydrolases, secondary metabolites, and different transcripts of biocontrol strains/species of *Trichoderma* characterized for their role in biocontrol.

S. no.	Responsible biocontrol metabolites	Reference	Biological function
Lytic enzymes	**Chitinases** Endochitinases, chitobiosidase, *N*-acetyl-β-D-glucosaminidase	Faize et al., 2003; Hoell et al., 2005; Seidl et al., 2005; de las Mercedes Dana et al., 2006; Ike et al., 2006; Klemsdal et al., 2006; Lopez-Mondejar et al., 2009; Ihrmark et al., 2010; Gruber et al., 2011; Loc et al., 2011; Sharma and Shanmugam, 2012; Xie et al., 2014; Sharma et al., 2016a	• Targeted breakdown of pathogen's cell wall through mycoparasitism • Induces resistance against biotic and abiotic stress responses • Root colonization
	Glucanases- Exo-β-D-(1,3/4/6)-glucanases, endo-β-D-(1,3/4/6)-glucanases	De la Cruz et al., 1995; Vazqez-Garciduen et al., 1998; De la Cruz and Llobell, 1999; Kulminskaya et al., 2001; Kim et al., 2002; Teresa et al., 2003; Nobe et al., 2004; Djonović et al., 2006; Grun et al., 2006; Montero et al., 2005, 2007; Xie et al., 2014	
	Proteases	Elad and Kapat, 1999; De Marco and Felix, 2002; Szekeres et al., 2004; Viterbo et al., 2004; Simkovi et al., 2008; Atanasova et al., 2013; Dou et al., 2014; Sharma et al., 2016b, 2017a; Wu et al., 2017	
	Amylase	de Azevedo et al., 2000	
Secondary metabolites	**Antibiotics** Gliotoxin, viridin, gliovirin, glisoprenin, hepteledic acid. **VOCs and other metabolites** 6-Pentyl-α-pyrone, hydrocarbons, alcohols, ketones, aldehydes, alkanes, alkenes, esters, aromatic compounds, heterocyclic compounds, and terpenes, koninginins, anthraquinones, trichodermamides, polyketides, terpenoids, trichodermaides, azaphilones and harzialactones, massoilactone, glisoprenins, heptelidic acid, etc.	Reino et al., 2008; Zhang et al., 2014; Garnica-vergara et al., 2015; Kottb et al., 2015; Bae et al., 2016; Chen et al., 2016; Lee et al., 2016; Zeilinger et al., 2016	• Antimicrobial action • Plant defense stimulator • Mycoparasitism/competition • Root morphogenesis • Promote plant growth and growth regulator changes
	AMPs Non-ribosomal-derived antimicrobial peptides such as peptaibols, harzianic acid, Trichopolyn VI, alamethicins, harzianin HA V and saturnisporin SA IV, etc.	Garo et al., 2003; Viterbo et al., 2007; Maischak et al., 2010; Shi et al., 2012, 2016; Panizel et al., 2013; Röhrich et al., 2015	• Antimicrobial and insecticidal • Induces plant resistance • Inhibition of primary roots • Programmed cell death • Electrical long distance signaling in plants
	Siderophores and organic acids Phenolate type, organic acids such as gluconic, citric, or fumaric acid	Anke et al., 1991; Qi and Zhao, 2013	• Mineral acquisition through chelation and acidification of soil
Root colonization	**Hydrophobins**	Sanna, 2006; Espino-rammer et al., 2013; Ruocco et al., 2015; Przylucka et al., 2017	• Biotic and abiotic stresses • *Trichoderma*–plant–pathogen three-way interaction • Potential role in stimulating the activity of cutinases on poly(ethylene terephthalate)
Miscellaneous	**Transporters**	Ruocco et al., 2009; Reithner et al., 2011; Shentu et al., 2014; Steindorff et al., 2014; Morán-Diez et al., 2015; Sharma et al., 2017a,b	• Tolerance to phytotoxins/and their detoxification

So far studies on *Trichoderma* have been conducted extensively using ESTs and transcriptome approach revealed the expression of several genes related to mycoparasitism of BCAs directly (Reithner et al., 2011; Sharma et al., 2017b) or indirectly through the modulation of host transcriptome (Morán-Diez et al., 2012; Perazzolli et al., 2012). In our previous studies, attempts were made to identify the role of different transcripts related to lytic enzymes, transporter system, and other gene related to metabolites of *T. harzianum* (Sharma et al., 2016a,b, 2017b) and characterization of extracellular proteins from *T. saturnisporum* (Sharma and Shanmugam, 2012) using autoclaved mycelium of different plant pathogenic fungi. These studies revealed only a limited number of proteins compared to transcripts. The approaches used for cDNA cloning and other array technologies have also created artifacts in accurate identification of candidate transcripts. Therefore, the integrated translatome and proteome based studies can help in a better and accurate depiction of key regulators involved in *Trichoderma*–plant–pathogen interaction (**Figure 1**). Recent studies showed that the gene expression of mycoparasitic *T. harzianum* and *T. atroviride* strains changes not only to plant-pathogenic fungi (Sharma et al., 2016a, 2017b) but also to itself (Reithner et al., 2011). Thus translational response is a key determinant contributing to adaptation under such interaction stress (Picard

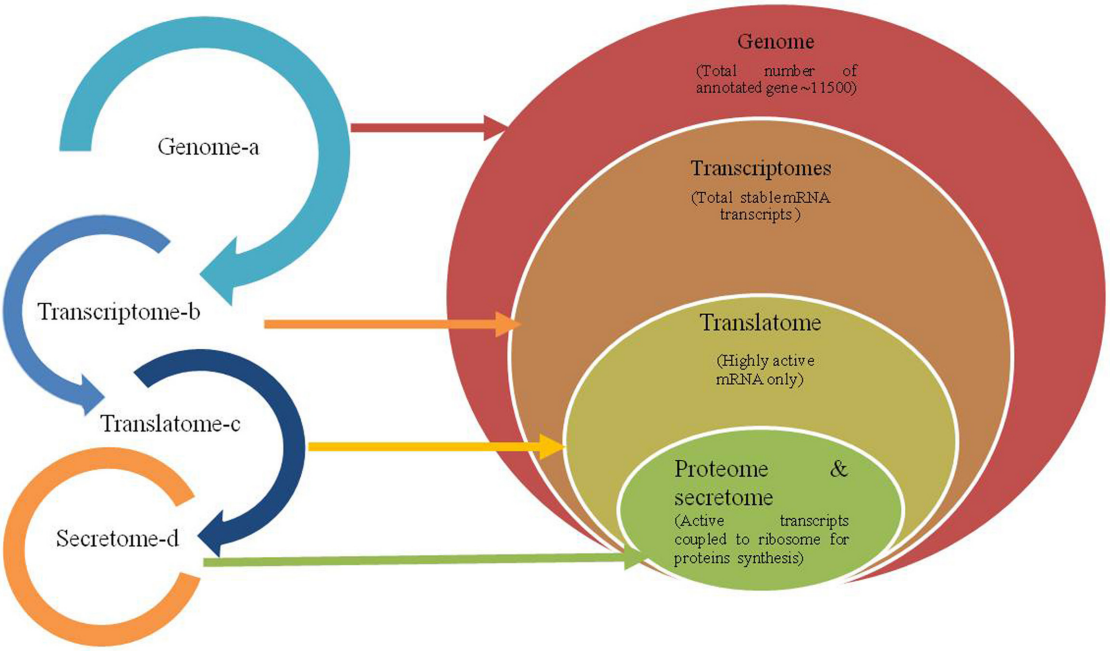

FIGURE 1 | Schematic flow of genetic information from genome to proteome level. A- Relationship of different omic approaches in *Trichoderma*–plant–plant pathogen interaction. B- Hierarchal relationship of total gene predicted using stacked ven diagram in the genome to the total mRNA transcribed (transcriptome) representing both stable and highly active mRNAs population under a stress response. Here depending upon the conditions and alternate splicing a > b > c > d or a > b > c = d or rarely a >b = c=d; a > b = c < d.

et al., 2013). Therefore, present review emphasizes the role of translatome based approach in accurate determination of active mRNA population in a complex dialog coupled to proteome data in a three way interaction of *Trichoderma*–plant–pathogen.

MECHANISMS OF *Trichoderma*

Trichoderma strains are used as BCAs in agriculture largely due to their abilities to directly antagonize plant-pathogenic fungi through the production of hydrolases (Benítez et al., 2004; Gruber and Seidl-Seiboth, 2012), antibiotics (Rubio et al., 2009; Vinale et al., 2014) and their tolerance to toxin produced by plant pathogens (Sharma et al., 2013) (**Table 1**). The interaction of *Trichoderma* with host plants reprograms not only the gene expression of biocontrol strains but also of its associated host plant (Harman, 2011; **Figure 2**). For example, strains of *Trichoderma* are explored for growth promotion and boosting immune responses, root development, and activation of seed germination or amelioration of abiotic stresses (Harman et al., 2004; Lorito et al., 2010; Shoresh et al., 2010; Hermosa et al., 2012). The immune responses in host plant are primed through systemic resistance (Tucci et al., 2011), involving a complex signaling of jasmonic acid/ethylene-induced systemic resistance and/or salicylic acid-dependent pathways which may behave differently in plant–*Trichoderma* interactions (Shoresh et al., 2010). The three way interaction between biocontrol, host plant, and pathogen from initial root colonization is known to change both the transcripts and proteome of host plants (Alfano et al., 2007; Segarra et al., 2007; Shoresh and Harman, 2008; Palmieri et al., 2012; Gomes et al., 2017; Martínez-Medina et al., 2017a,b; Pelagio-Flores et al., 2017). The availability of microarrays, next generation DNA sequencing, RNA-seq, and genome annotation have provided a global insight into the transcriptome response of plant–*Trichoderma* and *Trichoderma*–plant pathogen interaction.

Omics APPROACHES IN UNCOUPLING GENOME AND TRANSCRIPTOME PROFILE

The characterization of candidate transcripts involved in various biological functions using transcriptome is one of the best approach. In comparison to stable nature of the genome, transcriptome is more dynamic and vary in response to different stimuli. The massive transcriptome response to various factors can be tentatively identified, quantified, and correlated to a biological process using ESTs, subtractive libraries, and DNA microarrays (Herrera-Estrella, 2014). A number of studies have been done at genome-wide and transcriptional level to understand the molecular behavior of different *Trichoderma* strains under contrasting conditions ranging from mycoparasitism of plant pathogens to imparting direct beneficial aspects to plants under stress conditions (Arvas et al., 2006; Vizcaíno et al., 2007; Seidl et al., 2009). The transcriptome analysis of *T. atroviride* IMI206040 at different stages of

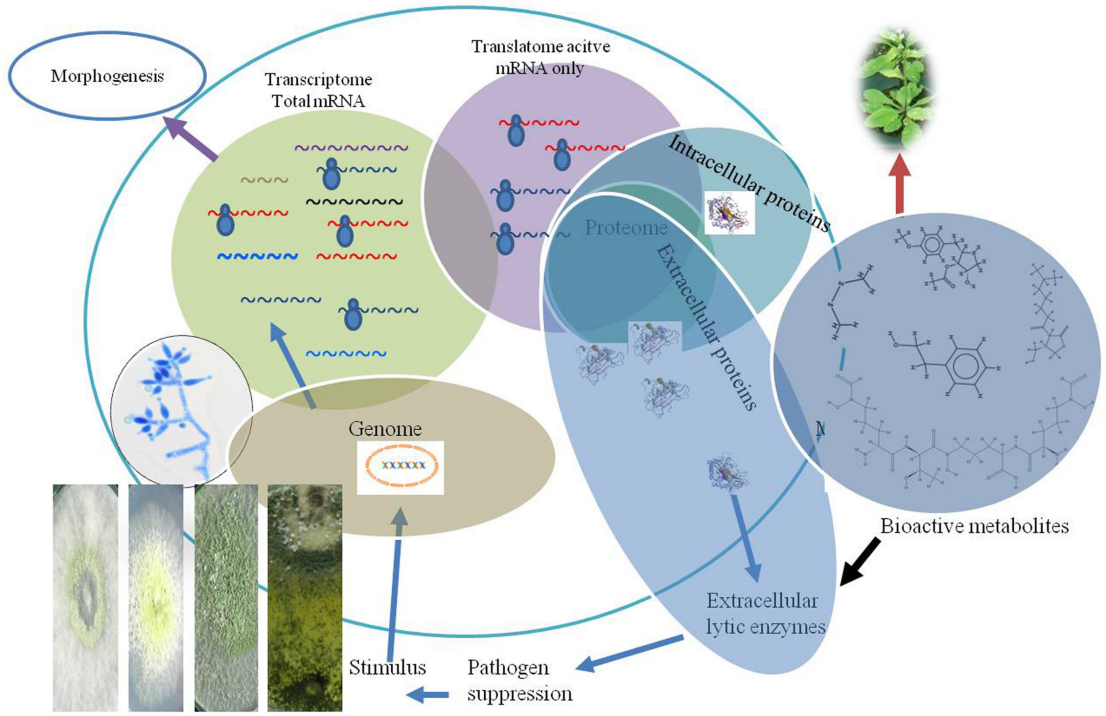

FIGURE 2 | Pictorial representation of total mRNA transcripts, active mRNA involved in protein and bioactive metabolites synthesis during interaction with plant or plant pathogens. The figure explains that transcriptome based study in general represents a higher level of mRNA, compared to total translatome which represents only ribosomal loaded active mRNAs during interaction.

interaction with *R. solani* identified 7,797 out of 11,863 estimated genes which represented over 65% of total gene of the organism genome whereas only 1.47% of total gene (175) transcripts were found significantly differentially expressed in mycoparasitic interactions. The differentially expressed transcripts were also investigated during pathogenic attack on *Phytophthora capsici*, *Botrytis cinerea*, and *R. solani* (Reithner et al., 2011). In comparison to a large number of transcribed genes predicted for *T. atroviride* based on genomic data, only 38.4% of genes involved in interaction with *R. solani*, were expressed before contact whereas 52.8% were found responsible for *Trichoderma* confrontation with itself (Reithner et al., 2011).

The use of EST (Vizcaíno et al., 2006, 2007), subtractive cDNA libraries and DNA array (Rosales-Saavedra et al., 2006; Alfano et al., 2007; Mathys et al., 2012) based studies carried under environmental conditions have helped dramatically to the global-scale identification of active genes of *Trichoderma* which are not directly linked to plant pathogens but are required for colonization and imparting other beneficial aspects to the host plant. For example, hydrophobins, aspartyl proteases, expansin-like protein of *Trichoderma* origin have been explored for their involvement in the mycoparasitism mediated biocontrol of these microbes (Brotman et al., 2008; Samolski et al., 2009). Subsequently, the sequencing of complete genome and high-throughput transcriptome using 454 sequencing (Barakat et al., 2009) has enhanced our understanding on investigation of mechanisms at global cellular level under different conditions in better way (Reithner et al., 2011). The transcriptome based approach is far more robust, dynamic, and refined technique compared to genome sequencing which is stable as described below.

Trichoderma Genome Organization

Since the genome sequencing of *T. reesei* industrial strain nine years back (Martinez et al., 2008), presently the genome of a number of strains representing *T. virens*, *T. harzianum*, *T. atroviride*, *T. asperellum*, *Trichoderma longibrachiatum*, and *Trichoderma citrinoviride* have been sequenced and revised (http://genome.jgi.doe.gov/). A comparative account of genome revealed presence of seven chromosomes in industrial strain *T. reesei* (Carter et al., 1992; Mantyla et al., 1992; Herrera-Estrella et al., 1993) whereas six chromosomes in biocontrol strains *T. harzianum* and *T. viride* (Gómez et al., 1997; Martinez et al., 2008). The genomic annotation of *T. virens*, *T. atroviride*, and *T. reesei* also unveiled lack of transposons and remarkable similarity of genes up to 78–96% among them. In the genome of *T. virens* and *T. atroviride* no true orthodox were reported for 2,756 and 2,510 genes, respectively in other species. The genome of *T. virens* and *T. atroviride* share 1,273 exclusive orthologs and 26 expanded families which were missing in *T. reesei* genome that may be a probable answer to mycoparasitic nature of *T. atroviride* and *T. virens* (Kubicek et al., 2011; Herrera-Estrella, 2014). A comparative study of genome organization of two *Trichoderma* species has revealed the expansion of considerable expansion

genes involved in mycoparasitic *T. virens* strain which are missing in *T. reesei* (Kubicek et al., 2011).

Transcriptome

The development of modern sophisticated omics technologies has played a vital role in developing better system-level understanding of gene expression. In particular, transcriptome based studies have proved a yardstick in the investigation of global cellular mechanisms and identification of several key genes involved in mycoparasitism and imparting other benefits to the host by *Trichoderma* strains. The measurement of the entire set of RNAs through transcriptome coupled with DNA microarrays or high-throughput RNA sequencing is a reliable and reproducible tool for wide analysis of transcripts. A number of transcriptome studies have been done on *Trichoderma*–plant–pathogen interaction (Marra et al., 2006; Chacon et al., 2007; Samolski et al., 2009; Mehrabi-Koushki et al., 2012; Rubio et al., 2012).

Stating from initial use of EST for the determination of glucose metabolism in *T. reesei* (Chambergo et al., 2002) and TrichoEST project (Vizcaíno et al., 2006), ESTs based studies have been done in *T. harzianum* (Liu and Yang, 2005; Vizcaíno et al., 2006; Suárez et al., 2007; Yao et al., 2013), *T. atroviride*, *T. asperellum* (Vizcaíno et al., 2007; Liu et al., 2010), *T. virens* (Vizcaíno et al., 2007; Morán-Diez et al., 2010), *Trichoderma aggressivum*, *T. viride*, and *T. longibrachiatum* (Vizcaíno et al., 2007) for the identification of transcripts induced during mycoparasitism and other environmental conditions. From a total of unique sequences (3,478), in *T. harzianum* CECT2413, 23% were found related to secretory chitinases, glucanases, and proteases. A large number of transcripts expressed (9478 ESTs containing 2,734 unique sequences) during the early interaction of *T. atroviride* with *B. cinerea* and *R. solani* were identified (Seidl et al., 2009) whereas 66 genes covering 442 ESTs were induced under mycoparasitic interaction (Herrera-Estrella, 2014).

Similarly, the analysis of transcriptomics changes in *T. harzianum*, *T. virens*, and *T. hamatum* during interactions with tomato plants revealed expression of 1,077 genes and only six of them being common to all three. The majority of genes encoding enzymes belong to chitin degradation during early interactions with tomato plants whereas genes encoding other secreted proteins were likely to involve in the signaling between *Trichoderma* and plants. Transcriptome based studies have led to the identification of new candidate genes having role in redox reaction, possible elicitors, transporters (Sharma et al., 2017b), lipid metabolism and detoxification (Chacon et al., 2007; Sharma et al., 2013), small secreted proteins (Ruocco et al., 2009; Samolski et al., 2009; Rubio et al., 2014). The *de novo* sequencing of *T. atroviride* IMI206040 transcriptome obtained during mycoparasitic interaction in presence of plant-pathogenic fungus *R. solani* revealed thousands of high-quality reads. An account of transcripts expressed during interaction to the total number of genes predicted in the genome of *T. atroviride* revealed that almost 45% were induced during interaction with *R. solani* and only 175 of them were host responsive (Reithner et al., 2011; Gupta et al., 2016).

Microarray analysis of *T. harzianum* T34 strain interaction with *Arabidopsis* identified approximately 24,000 transcripts of the host plant which were modulated by the BCA. The significance and global impact of this beneficial microbe in reprogramming the molecular physiology of host plant to stress responses through the regulation of transcription, signal transduction pathways has been reported in different studies (Morán-Diez et al., 2012; Lamdan et al., 2015). Further host specific response of *Trichoderma* strain with plants representing monocot and dicot hosts under the same conditions have also been explored to identify signature transcriptome repertoires and answer the widely prevalent questions of specificity of responses and role of secreted proteins in mutualistic interaction, root colonization, and induction of immune responses (Morán-Diez et al., 2015; Ho et al., 2016; Sharma et al., 2017b). These studies indicate the limitations of transcriptome based studies in precise estimation of ribosome loaded active mRNA population involved in complex mycoparasitic behavior of *Trichoderma* species as BCAs.

Translatomes

The mRNA and protein levels do not perfectly correlate in native or engineered systems (Tian et al., 2004; Jayapal et al., 2008; Vogel and Marcotte, 2012; Payne, 2015). The post-transcriptional regulation of transcripts is a complex process and may not be compared with transcription level regulation of genes. Therefore, the post-transcriptional regulation is of great significance for better characterization of functional role of genes (Picard et al., 2013). Although ESTs and transcriptome based experimental studies have provided valuable information in mining genes incited by various stress responses in *Trichoderma* interaction with plants and plant pathogens, its application is limited because the levels of the proteins and their encoding mRNA are not correlated to each other. Therefore considering the use of the cutoff standards in transcriptome based studies and appearance of artifacts in the differential expression of genes, translatome based studies offers potential choice and a better alternative involving only active mRNA populations (Picard et al., 2013; Yanguez et al., 2013; Piccirillo Ciriaco et al., 2014; King and Gerber, 2016; Meteignier et al., 2017).

Studies involving translational regulation of gene expression are emerging as a prominent tool for the understanding the regulation of protein abundance in adaptive responses of the host (Halbeisen and Gerber, 2009; Spriggs et al., 2010). In the genetic flow of information, the translational regulation reprograms the cell activities by protein synthesis. In last decade due to rapid advancements in technology, efforts on understanding the modulatory role of translation in gene expression have increased significantly. The translatome referring to the active mRNAs population associated with ribosomes has facilitated the removal of background noise and useful for the accurate determination of active mRNA. Originally used in oocytes and embryos (Terman, 1970; Gurdon et al., 1971), translational control has emerged as a key point of eukaryotes. The process is executed by loading of ribosomes on mRNA followed by translation elongation (Groppo and Richter, 2009; Jackson et al.,

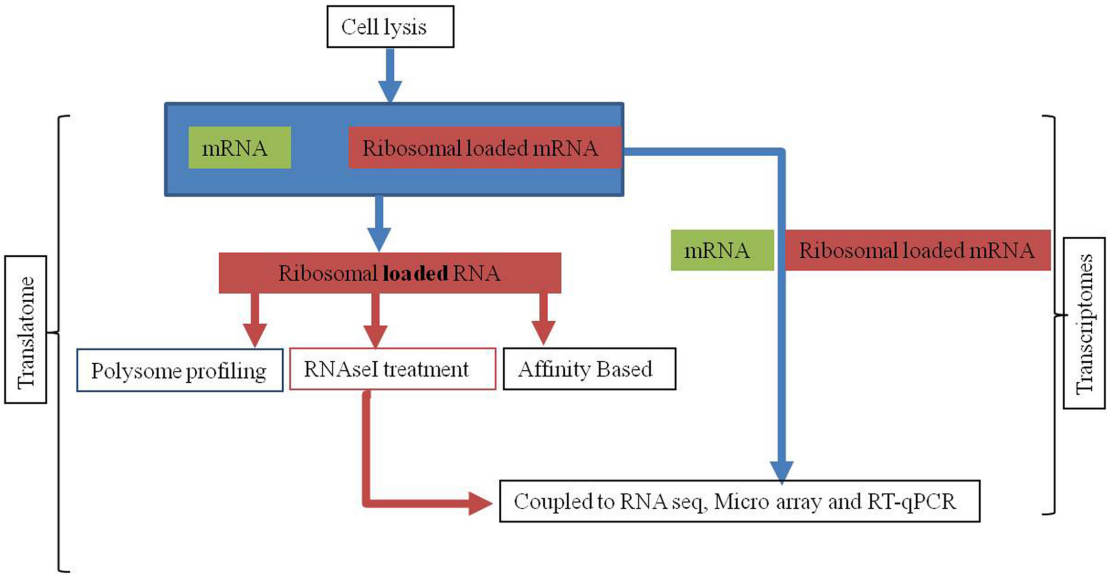

FIGURE 3 | The experimental procedure of transcriptome and translatome for genome wide studies. In translatome ribosomal loaded or protected fragments of RNA are size or affinity fractionated, recovered, and ligated to adaptors for reverse transcription, amplification, and high-throughput RNA-seq whereas in transcriptome complete mRNA is used for subsequent analysis.

2010). Since, the translatome based studies are focused only on the pools of genome-wide translated mRNA and therefore have helped in identification of key regulatory factors that are under translational control (Zupanic et al., 2013). This technique offers immense potential in the targeting key regulators which are active during interaction and play important role for the host plant in combating various stress responses. Translatome studies also help in determination of the ribosome number on active mRNA molecule in response to stress in the cellular genes (Koritzinsky and Wouters, 2007; Thomas and Johannes, 2007; Picard et al., 2013; **Figure 3**).

Presently, there are three methods used for translatome analysis; (a) polysomal profiling, (b) ribosomal profiling, and (c) ribosome affinity purification (RAP) (**Figure 3**). Polysomal profiling discovered in 1960s involves the separation of actively translated mRNAs bound by several ribosomes from free RNA by sucrose gradient centrifugation and then mRNAs can be coupled to northern blot or RT-qPCR or cDNA microarrays, or RNA-seq on a global level (Karginov and Hannon, 2013; Spangenberg et al., 2013). The second method known as ribosomal profiling was developed by Weissman group in *Saccharomyces cerevisiae*, determines the location of ribosomes at codon or nucleotide scale (Ingolia et al., 2009). The advantage of this technique is acquisition of information at global scale with respect to the position of the ribosomes on translated mRNA.

The deep nucleotide sequencing of ribosome protected RNA fragments obtained after RNase I treatment of cell lysate helps in accurate determination of ribosome position and its densities along RNA (Ingolia et al., 2012). Both polysome and ribosome based profiling need relatively large sample size to obtain enough RNA for microarray/RNA-seq analysis. The third method known as RAP developed by Inada et al. (2002) in *S. cerevisiae* capture monosomes and polysomes by using antiFLAG affinity resin. The RAP also known as translating RAP provides a better approximation of the translated mRNA population if coupled with transcriptome analysis (Halbeisen and Gerber, 2009; Jiao and Meyerowitz, 2010).

Integrating Translatome and Proteomic Study

The post-transcriptional events such as translation regulation and protein stability are the principle causes of weak correlations and variations in proteomic, transcriptomic, and genomic data. The associated errors in transcriptome analysis are subjected to arise from the suppression by microarrays which can further impede the identification of active candidate transcripts. On the other side, methods opted for protein staining, limitations associated in visualizing low-abundant and co-migrating proteins seriously hampers proteomic based study. The recent developments in proteomics methods such as use of mass spectrometric (MS) and liquid chromatography (LC) techniques have made quantitative proteomic profiling, currently a driving force for identification of proteins. The highly stable and reproducible performance of mass spectrometers such as Q Exactive hybrid quadrupole-Orbitrap mass spectrometer MS and Triple TOF 5600 MS is capable of identification of both proteomics (Chang et al., 2014) and characterization of bioactive metabolites. Integrated analyses of active mRNAs coupled with protein expression are available for bacteria, yeast, mice, and humans. Similar to transcriptome, the translatome based studies are focused only on transcripts level which are intracellular in nature. The coupling of multiomic approaches based on active mRNA, proteomes,

and protein turnover of both intra as well extracellular proteins and biologically active metabolites under different environmental conditions will provide a better answer of reprogramming biocontrol to various plant beneficial attribute and its resiliencies to combat different environmental conditions (**Figure 2**).

CONCLUSION

The availability of the fully sequenced genomes of *Trichoderma* spp. has accelerated our research on understanding of the behavior of different species of this genus and how the information on their gene pool determines their capabilities and limitations. The genomes of *Trichoderma* which is known to contain thousands of genes encoding different glycosyl hydrolases, secondary metabolites, antibiotics, lectins with insecticidal properties, and transporters with potential in bioremediation involved in antibiotics biosynthesis, and several other candidate genes (Druzhinina et al., 2012; Atanasova et al., 2013). Exploration of genes and their encoding proteins involved in developing tolerance against various stresses such as cold, below-average precipitation, salty conditions, pH, herbicide resistance as well biotic factor are an active field of research. The predicted genome of *Trichoderma* strains are known to encode a large number genes therefore coupling of translatome studies with proteomics of both extracellular and intracellular proteins offers a wide scope for better understanding the complex behaviors of *Trichoderma* as BCA.

The genomic comparison of mycoparasitic species of *T. harzianum* with non-mycoparasitic strains of *T. reesei* already provides evidences of the expansion of several genes in biocontrol strains. The secretion of a large number of cell wall targeting enzymes and bioactive secondary metabolites require adaptive molecular reprogramming of *Trichoderma* transcriptome. The variation at genomic, transcriptomics, and proteomic levels is a challenging task and difficult to correlate due to complex and non-systematic post-transcriptional and limitation of proteomic techniques. Further, the translational control is a widespread phenomenon with intense effect; nevertheless it is underestimated for its regulatory roles. In general, extensive uncoupling of both RNA movements and inferred cell activities has been observed for 19 different transcriptome and translatome. Therefore, coupled quantitative transcript and protein abundance studies can serve as a gold standard for proper and accurate depiction of interaction involving *Trichoderma*–plant–plant pathogens. Although detecting changes in the transcriptome level (total mRNAs), translatome level (ribosome loaded mRNAs) and the proteome is experimentally feasible in a high-throughput way, the integration of these omic technologies is still far away. Systematic global analyses aims at integrating transcriptome, translatome, and proteome level can provide accurate view of widespread adaptive mechanisms of interaction between *Trichoderma*–plant–pathogen.

In future, integrated efforts will help us to better understand, identify, and then explore the molecular behavior of *Trichoderma* arsenal involved in its success as BCAs as well as industrial sectors. In such instances, the integration of the translatome using ribosomal profiling and coupling it with proteomic approaches such as liquid chromatography-tandem mass spectrometry (LC-MS/MS) for both extracellular and intracellular proteins offers a lot of scope for accurate characterization of active molecular components involved in biocontrol and then subsequently their utilization of various applications.

FUTURE DIRECTIONS

A comparative multiomic coupled insights of *Trichoderma*–plant–plant pathogens in three way interaction will play vital role in accurate characterization of transcripts responsible for cosmopolitan nature of *Trichoderma* and then targeting the promising one for agricultural based applications. The latest advancements and complete genome sequencing have already provided a platform of gene pool. Further integration with latest functional techniques such as translatome will lead another step close to identification of targets in the form of active transcripts involved in a complex interaction of plant–BCA–plant pathogens.

AUTHOR CONTRIBUTIONS

VS and RS prepared the manuscript. PS and AG edited the manuscript.

ACKNOWLEDGMENT

The authors are thankful to SERB, Department of Science and Technology-New Delhi India for providing funding under DST-FAST Track young scientist scheme (award letter NO. SB/FT/LS-365/2012).

REFERENCES

Al-Ani, L., Salleh, B., and Ghazali, A. H. A. (2013). "Biocontrol of *Fusarium* wilt of banana by *Trichoderma* spp," in *Proceedings of the Conference Paper International Symposium on Tropical Fungi (ISTF) IPB International Convention Center*, Bogor.

Alfano, G., Ivey, M. L. L., Cakir, C., Bos, J. I. B., Miller, S. A., Madden, L. V., et al. (2007). Systemic modulation of gene expression in tomato by *Trichoderma hamatum* 382. *Phytopathology* 97, 429–437. doi: 10.1094/PHYTO-97-4-0429

Anke, H., Kinn, J., Bergquist, K.-E., and Sterner, O. (1991). Production of siderophores by strains of the genus *Trichoderma*, isolation and characterization of the new lipophilic coprogen derivative, palmitoylcoprogen. *Biol. Met.* 4, 176–180. doi: 10.1007/BF01141311

Arvas, M., Pakula, T., Lanthaler, K., Saloheimo, M., Valkonen, M., Suortti, T., et al. (2006). Common features and interesting differences in transcriptional responses to secretion stress in the fungi *Trichoderma reesei* and *Saccharomyces cerevisiae*. *BMC Genomics* 7:32. doi: 10.1186/1471-2164-7-32

Atanasova, L., Crom, S. L., Gruber, S., Coulpier, F., Seidl-Seiboth, V., Kubicek, C. P., et al. (2013). Comparative transcriptomics reveals different strategies of *Trichoderma* mycoparasitism. *BMC Genomics* 14:121. doi: 10.1186/1471-2164-14-121

Bae, S., Kumar, T., Young, J., Ryu, M., Park, G., Shim, S., et al. (2016). *Trichoderma* metabolites as biological control agents against *Phytophthora* pathogens. *Biol. Control* 92, 128–138. doi: 10.1111/j.1472-765X.2009.02599.x

Barakat, A., DiLoreto, D. S., Zhang, Y., Smith, C., Baier, K., Powell, W. A., et al. (2009). Comparison of the transcriptomes of American chestnut (*Castanea dentata*) and Chinese chestnut (*Castanea mollissima*) in response to the chestnut blight infection. *BMC Plant Biol.* 9:51. doi: 10.1186/1471-2229-9-51

Benítez, T., Rincón, A. M., Limón, M. C., and Codón, A. C. (2004). Biocontrol mechanisms of *Trichoderma* strains. *Int. Microbiol.* 7, 249–260.

Breakspear, A., and Momany, M. (2007). The first fifty microarray studies in filamentous fungi. *Microbiology* 153, 7–15. doi: 10.1099/mic.0.2006/002592-0

Brotman, Y., Briff, E., Viterbo, A., and Chet, I. (2008). Role of Swollenin, an expansin-like protein from *Trichoderma*, in plant root colonization. *Plant Physiol.* 147, 779–789. doi: 10.1104/pp.108.116293

Brotman, Y., Lisec, J., Méret, M., Chet, I., Willmitzer, L., and Viterbo, A. (2012). Transcript and metabolite analysis of the *Trichoderma*-induced systemic resistance response to *Pseudomonas syringae* in *Arabidopsis thaliana*. *Microbiology* 158, 139–46. doi: 10.1099/mic.0.052621-0

Cacciola, S. O., Puglisi, I., Faedda, R., Sanzaro, V., Pane, A., Lo Piero, A. R., et al. (2015). Cadmium induces cadmium-tolerant gene expression in the filamentous fungus *Trichoderma harzianum*. *Mol. Biol. Rep.* 42, 1559–1570. doi: 10.1007/s11033-015-3924-4

Carpenter, M. A., Stewart, A., and Ridgway, H. J. (2005). Identification of novel *Trichoderma hamatum* genes expressed during mycoparasitism using subtractive hybridisation. *FEMS Microbiol. Lett.* 251, 105–112. doi: 10.1016/j.femsle.2005.07.035

Carter, G. L., Allison, D., Rey, M. W., and Dunn-Coleman, N. S. (1992). Chromosomal and genetic analysis of the electrophoretic karyotype of *Trichoderma reesei*: mapping of the cellulase and xylanase genes. *Mol. Microbiol.* 6, 2167–2174. doi: 10.1111/j.1365-2958.1992.tb01390.x

Cetz-Chel, J. E., Balcázar-López, E., Esquivel-Naranjo, E. U., and Herrera-Estrella, A. (2016). The *Trichoderma atroviride* putative transcription factor Blu7 controls light responsiveness and tolerance. *BMC Genomics* 17:327. doi: 10.1186/s12864-016-2639-9

Chacon, M. R., Rodriguez-Galan, O., Benitez, T., Sousa, S., Rey, M., Llobell, A., et al. (2007). Microscopic and transcriptome analyses of early colonization of tomato roots by *Trichoderma harzianum*. *Int. Microbiol.* 10, 19–27.

Chambergo, F. S., Bonaccorsi, E. D., Ferreira, A. J., Ramos, A. S., Ferreira, J. R. J. J. R., Abrahao-Neto, J., et al. (2002). Elucidation of the metabolic fate of glucose in the filamentous fungus *Trichoderma reesei* using expressed sequence tag (EST) analysis and cDNA microarrays. *J. Biol. Chem.* 277, 13983–13988. doi: 10.1074/jbc.M107651200

Chang, C., Li, L., Zhang, C., Wu, S., Guo, K., Zi, J., et al. (2014). Systematic analyses of the transcriptome, translatome, and proteome provide a global view and potential strategy for the C-HPP. *J. Proteome Res.* 13, 38–49. doi: 10.1021/pr4009018

Chen, J., Sun, S., Miao, C., Wu, K., Chen, Y., Xu, L., et al. (2016). Endophytic *Trichoderma gamsii* YIM PH30019: a promising biocontrol agent with hyperosmolar, mycoparasitism, and antagonistic activities of induced volatile organic compounds on root-rot pathogenic fungi of *Panax notoginseng*. *J. Ginseng Res.* 40, 315–324. doi: 10.1016/j.jgr.2015.09.006

Cloyd, R. A., Dickinson, A., and Kemp, K. E. (2007). Effect of diatomaceous earth and *Trichoderma harzianum* T-22 (Rifai strain KLR-AG2) on the fungus gnat *Bradysia* sp. nr. *coprophila* (Diptera: Sciaridae). *J. Econ. Entomol.* 100, 1353–1359. doi: 10.1093/jee/100.4.1353

Contreras-Cornejo, H. A., Macías-Rodríguez, L., Beltrán-Peña, E., Herrera-Estrella, A., and López-Bucio, J. (2011). Trichoderma-induced plant immunity likely involves both hormonal- and camalexin-dependent mechanisms in *Arabidopsis thaliana* and confers resistance against necrotrophic fungus *Botrytis cinerea*. *Plant Signal. Behav.* 6, 1554–1563. doi: 10.4161/psb.6.10.17443

de Azevedo, A. M. C., De Marco, J. L., and Felix, C. R. (2000). Characterization of an amylase produced by a *Trichoderma harzianum* isolate with antagonistic activity against *Crinipellis perniciosa*, the causal agent of witches' broom of cocoa. *FEMS Microbiol. Lett.* 188, 171–175. doi: 10.1016/S0378-1097(00)00231-7

De la Cruz, J., and Llobell, A. (1999). Purification and properties of a basic endo-β-1,6-glucanase (BGN16.1) from the antagonistic fungus *Trichoderma harzianum*. *FEBS J.* 265, 145–151. doi: 10.1046/j.1432-1327.1999.00698.x

De la Cruz, J., Pintor-Toro, J. A., Benítez, T., and Llobell, A. (1995). Purification and characterization of an endo- β -1,6-glucanase from *Trichoderma harzianum* that is related to its mycoparasitism. *J. Bacteriol.* 177, 1864–1871. doi: 10.1128/jb.177.7.1864-1871.1995

de las Mercedes Dana, M., Pintor-Toro, J. A., and Cubero, B. (2006). Transgenic tobacco plants overexpressing chitinases of fungal origin show enhanced resistance to biotic and abiotic stress agents. *Plant Physiol.* 142, 722–730. doi: 10.1104/pp.106.086140

De Marco, J. L., and Felix, C. R. (2002). Characterization of a protease produced by a *Trichoderma harzianum* isolate which controls cocoa plant witches' broom disease. *BMC Biochem.* 3:3.

Diánez Martínez, F., Santos, M., Carretero, F., and Marín, F. (2016). *Trichoderma saturnisporum*, a new biological control agent. *J. Sci. Food Agric.* 96, 1934–1944. doi: 10.1002/jsfa.7301

Djonović, S., Pozo Maria, J., and Kenerley, C. M. (2006). Tvbgn3, a β-1, 6-Glucanase from the biocontrol fungus *Trichoderma virens*, is involved in mycoparasitism and control of *Pythium ultimum*. *Appl. Microbiol. Biotechnol.* 72, 7661–7670.

Dou, K., Wang, Z., Zhang, R., Wang, N., Fan, H., Diao, G., et al. (2014). Cloning and characteristic analysis of a novel aspartic protease gene Asp55 from *Trichoderma asperellum* ACCC30536. *Microbiol. Res.* 169, 915–923. doi: 10.1016/j.micres.2014.04.006

Druzhinina, I. S., Shelest, E., and Kubicek, C. P. (2012). Novel traits of *Trichoderma* predicted through the analysis of its secretome. *FEMS Microbiol. Lett.* 337, 1–9. doi: 10.1111/j.1574-6968.2012.02665.x

Elad, Y., and Kapat, A. (1999). The role of *Trichoderma harzianum* protease in the biocontrol of *Botrytis cinerea*. *Eur. J. Plant Pathol.* 105, 177–189. doi: 10.1128/AEM.02486-10

Espino-rammer, L., Ribitsch, D., Przylucka, A., Marold, A., Greimel, K. J., and Acero, H. (2013). Two novel class II hydrophobins from *Trichoderma* spp. stimulate enzymatic hydrolysis of poly(ethylene terephthalate) when expressed as fusion proteins. *Appl. Environ. Microbiol.* 79, 4230–4238. doi: 10.1128/AEM.01132-13

Faize, M., Malnoy, M., Dupuis, F., Chevalier, M., Parisi, L., and Chevreau, E. (2003). Chitinases of *Trichoderma atroviride* Induce scab resistance and some metabolic changes in two cultivars of apple. *Genet. Resist.* 93, 1496–1504. doi: 10.1094/PHYTO.2003.93.12.1496

Garnica-vergara, A., Barrera-ortiz, S., Mu, E., and Raya-gonz, J. (2015). The volatile 6-pentyl-2H-pyran-2-one from *Trichoderma atroviride* regulates *Arabidopsis thaliana* root morphogenesis via auxin signaling and ethylene insensitive 2 functioning. *New Phytol.* 209, 1469–1512. doi: 10.1111/nph.13725

Garo, E., Starks, C. M., Jensen, P. R., Fenical, W., Lobkovsky, E., and Clardy, J. (2003). Trichodermamides A and B, cytotoxic modified dipeptides from the marine-derived fungus *Trichoderma virens*. *J. Nat. Prod.* 66, 423–426. doi: 10.1021/np0204390

Gomes, E. V., Ulhoa, C. J., Cardoza, R. E., Silva, R. N., and Gutiérrez, S. (2017). Involvement of *Trichoderma harzianum* Epl-1 protein in the regulation of botrytis virulence- and tomato defense-related genes. *Front. Plant Sci.* 29:880. doi: 10.3389/fpls.2017.00880

Gómez, I., Chet, I., and Herrera-Estrella, A. (1997). Vegetative compatibility and molecular variation among *Trichoderma harzianum* isolates. *Mol. Gen. Genet.* 256, 127–135. doi: 10.1007/s004380050554

Groppo, R., and Richter, J. D. (2009). Translational control from head to tail. *Curr. Opin. Cell. Biol.* 21, 444–451. doi: 10.1016/j.ceb.2009.01.011

Gruber, S., Kubicek, C. P., and Seidl-seiboth, V. (2011). Differential regulation of orthologous chitinase genes in mycoparasitic *Trichoderma* species. *Appl. Environ. Microbiol.* 77, 7217–7226. doi: 10.1128/AEM.06027-11

Gruber, S., and Seidl-Seiboth, V. (2012). Self versus non-self: fungal cell wall degradation in *Trichoderma*. *Microbiology* 158, 26–34. doi: 10.1099/mic.0.052613-0

Grun, C. H., Dekker, N., Nieuwland, A. A., Klis, F. M., Kamerling, J. P., Vliegenthart, J. F. G., et al. (2006). Mechanism of action of the *endo*-(1→3)-α-glucanase MutAp from the mycoparasitic fungus *Trichoderma harzianum*. *FEBS Lett.* 580, 3780–3786. doi: 10.1016/j.febslet.2006.05.062

Gupta, V. K., Steindorff, A. S., de Paula, R. G., Silva-Rocha, R., Mach-Aigner, A. R., Mach, R. L., et al. (2016). The post-genomic era of *Trichoderma reesei*: What's next? *Trends Biotechnol.* 34, 970–982. doi: 10.1016/j.tibtech.2016.06.003

Gurdon, J. B., Lane, C. D., Woodland, H. R., and Marbaix, G. (1971). Use of frog eggs and oocytes for the study of messenger RNA and its translation in living cells. *Nature* 233, 177–182. doi: 10.1038/233177a0

Halbeisen, R. E., and Gerber, A. P. (2009). Stress-dependent coordination of transcriptome and translatome in yeast. *PLoS Biol.* 7:e1000105. doi: 10.1371/journal.pbio.1000105

Harman, G. E. (2011). Multifunctional fungal plant symbionts: new tools to enhance plant growth and productivity. *New Phytol.* 189, 647–649. doi: 10.1111/j.1469-8137.2010.03614.x

Harman, G. E., Howell, C. R., Viterbo, A., Chet, I., and Lorito, M. (2004). *Trichoderma* species-opportunistic, avirulent plant symbionts. *Nat. Rev. Microbiol.* 2, 43–56. doi: 10.1038/nrmicro797

Hermosa, M. R., Grondona, I., Iturriaga, E. A., Diaz-Minguez, J. M., Castro, C., Monte, E., et al. (2000). Molecular characterization and identification of biocontrol isolates of *Trichoderma* spp. *Appl. Environ. Microbiol.* 66, 1890–1898. doi: 10.1128/AEM.66.5.1890-1898.2000

Hermosa, R., Viterbo, A., Chet, I., and Monte, E. (2012). Mini-review plant-beneficial effects of *Trichoderma* and of its genes. *Microbiology* 158, 17–25. doi: 10.1099/mic.0.052274-0

Herrera-Estrella, A. (2014). "Genome-wide approaches toward understanding mycotrophic *Trichoderma* species," in *Biotechnology and Biology of Trichoderma*, eds V. Gupta, M. Schmoll, A. Herrera-Estrella, R. S. Upadhyay, and M. G. Tuohy (Oxford: Elsevier), 455–464. doi: 10.1111/j.1365-2958.1993.tb01142.x

Herrera-Estrella, A., Goldman, G. H., van Montagu, M., and Geremia, R. A. (1993). Electrophoretic karyotype and gene assignment to resolved chromosomes of *Trichoderma* spp. *Mol. Microbiol.* 7, 515–521.

Ho, C.-L., Tan, Y.-C., Yeoh, K.-A., Ghazali, A.-K., Yee, W.-Y., and Hoh, C.-C. (2016). *De novo* transcriptome analyses of host-fungal interactions in oil palm (*Elaeis guineensis* Jacq.). *BMC Genomics* 17:66. doi: 10.1186/s12864-016-2368-0

Hoell, I. A., Klemsdal, S. S., Vaaje-Kolstad, G., Horn, S. J., and Eijsink, V. G. H. (2005). Overexpression and characterization of a novel chitinase from *Trichoderma atroviride* strain P1. *Biochim. Biophys. Acta* 1748, 180–190. doi: 10.1016/j.bbapap.2005.01.002

Howell, C. R. (2006). Understanding the mechanisms employed by *Trichoderma virens* to effect biological control of cotton diseases. *Phytopathology* 96, 178–180. doi: 10.1094/PHYTO-96-0178

Ihrmark, K., Asmail, N., Ubhayasekera, W., Melin, P., Stenlid, J., and Karlsson, M. (2010). Comparative molecular evolution of *Trichoderma* chitinases in response to mycoparasitic interactions. *Evol. Bioinform.* 6, 1–26. doi: 10.1017/S1355838202026018

Ike, M., Nagamatsu, K., Shioya, A., Nogawa, M., Ogasawara, W., Okada, H., et al. (2006). Purification, characterization, and gene cloning of 46 kDa chitinase (Chi46) from *Trichoderma reesei* PC-3-7 and its expression in *Escherichia coli*. *Appl. Microbiol. Biotechnol.* 71, 294–303. doi: 10.1007/s00253-005-0171-y

Inada, T., Winstall, E., Tarun, S. Z. Jr., Yates, J. R. III, Schieltz, D., and Sachs, A. B. (2002). One-step affinity purification of the yeast ribosome and its associated proteins and mRNAs. *RNA* 8, 948–958.

Ingolia, N. T., Brar, G. A., Rouskin, S., McGeachy, A. M., and Weissman, J. S. (2012). The ribosome profiling strategy for monitoring translation in vivo by deep sequencing of ribosome-protected mRNA fragments. *Nat. Protoc.* 7, 1534–1550. doi: 10.1038/nprot.2012.086

Ingolia, N. T., Ghaemmaghami, S., Newman, J. R., and Weissman, J. S. (2009). Genome-wide analysis in vivo of translation with nucleotide resolution using ribosome profiling. *Science* 324, 218–223. doi: 10.1126/science.1168978

Jackson, R. J., Hellen, C. U., and Pestova, T. V. (2010). The mechanism of eukaryotic translation initiation and principles of its regulation. *Nat. Rev. Mol. Cell Biol.* 11, 113–127. doi: 10.1038/nrm2838

Jayapal, K. P., Philp, R. J., Kok, Y. J., Yap, M. G., Sherman, D. H., Griffin, T. J., et al. (2008). Uncovering genes with divergent mRNA–protein dynamics in *Streptomyces coelicolor*. *PLoS ONE* 3:e2097. doi: 10.1371/journal.pone.0002097

Jiao, Y., and Meyerowitz, E. M. (2010). Cell-type specific analysis of translating RNAs in developing flowers reveals new levels of control. *Mol. Syst. Biol.* 6, 419. doi: 10.1038/msb.2010.76

Karginov, F. V., and Hannon, G. J. (2013). Remodeling of Ago2-mRNA interactions upon cellular stress reflects miRNA complementarity and correlates with altered translation rates. *Genes Dev.* 27, 1624–1632. doi: 10.1101/gad.215939.113

Kim, D. J., Baek, J. M., Uribe, P., Kenerley, C. M., and Cook, D. R. (2002). Cloning and characterization of multiple glycosyl hydrolase genes from *Trichoderma virens*. *Curr. Genet.* 40, 374–384. doi: 10.1007/s00294-001-0267-6

King, H. A., and Gerber, A. P. (2016). Translatome profiling: methods for genome-scale analysis of mRNA translation. *Brief. Funct. Genomics* 15, 22–31. doi: 10.1093/bfgp/elu045

Klemsdal, S. S., Clarke, J. L., Hoell, I., Eijsink, V. G. H., and Brurberg, M. B. (2006). Molecular cloning, characterization, and expression studies of a novel chitinase gene (*ech30*) from the mycoparasite *Trichoderma atroviride* strain P1. *FEMS Microbiol. Lett.* 256, 282–289. doi: 10.1111/j.1574-6968.2006.00132.x

Koritzinsky, M., and Wouters, B. G. (2007). Hypoxia and regulation of messenger RNA translation. *Methods Enzymol.* 435, 247–273. doi: 10.1016/S0076-6879(07)35013-1

Kottb, M., Gigolashvili, T., Großkinsky, D. K., and Piechulla, B. (2015). *Trichoderma* volatiles effecting *Arabidopsis*: from inhibition to protection against phytopathogenic fungi. *Front. Microbiol.* 6:995. doi: 10.3389/fmicb.2015.00995

Kubicek, C. P., Herrera-Estrella, A., Seidl-seiboth, V., Martinez, D. A., Druzhinina, I. S., Thon, M., et al. (2011). Comparative genome sequence analysis underscores mycoparasitism as the ancestral life style of *Trichoderma*. *Genome Biol.* 12:R40. doi: 10.1186/gb-2011-12-4-r40

Kulminskaya, A. A., Thomsen, K. K., Shabalin, K. A., Sidorenko, I. A., Eneyskaya, E. V., Savel, A. N., et al. (2001). Isolation, enzymatic properties, and mode of action of an exo-1,3-β-glucanase from *T. viride*. *FEBS J.* 268, 6123–6131.

Lamdan, N.-L., Shalaby, S., Ziv, T., Kenerley, C. M., and Horwitz, B. A. (2015). Secretome of *Trichoderma* interacting with maize roots: role in induced systemic resistance. *Mol. Cell Proteomics* 14, 1054–1063. doi: 10.1074/mcp.M114.046607

Lee, S., Yap, M., Behringer, G., Hung, R., and Bennett, J. W. (2016). Volatile organic compounds emitted by *Trichoderma* species mediate plant growth. *Fungal Biol. Biotechnol.* 3:7. doi: 10.1186/s40694-016-0025-7

Lin, Y. R., Lo, C. T., Liu, S. Y., and Peng, K. C. (2012). Involvement of pachybasin and emodin in self-regulation of *Trichoderma harzianum* mycoparasitic coiling. *J. Agric. Food Chem.* 60, 2123–2128. doi: 10.1021/jf202773y

Liu, P. G., and Yang, Q. (2005). Identification of genes with a biocontrol function in *Trichoderma harzianum* mycelium using the expressed sequence tag approach. *Res. Microbiol.* 156, 416–423. doi: 10.1016/j.resmic.2004.10.007

Liu, Z., Yang, X., Sun, D., Song, J., Chen, G., Juba, O., et al. (2010). Expressed sequence tags-based identification of genes in a biocontrol strain *Trichoderma asperellum*. *Mol. Biol. Rep.* 37, 3673–3681. doi: 10.1007/s11033-010-0019-0

Loc, N. H., Quang, H. T., Hung, N. B., Huy, N. D., Phuong, T. T. B., and Ha, T. T. T. (2011). *Trichoderma asperellum* Chi42 genes encode chitinase. *Mycobiology* 39, 182–186. doi: 10.5941/MYCO.2011.39.3.182

Longa, C. M., Savazzini, F., Tosi, S., Elad, Y., and Pertot, I. (2009). Evaluating the survival and environmental fate of the biocontrol agent *Trichoderma atroviride* SC1 in vineyards in northern Italy. *J. Appl. Microbiol.* 106, 1549–1557. doi: 10.1111/j.1365-2672.2008.04117.x

Lopez-Mondejar, R., Catalano, V., Kubicek, C. P., and Seidl, V. (2009). The β-*N*-acetylglucosaminidases NAG1 and NAG2 are essential for growth of *Trichoderma atroviride* on chitin. *FEBS J.* 276, 5137–5148. doi: 10.1111/j.1742-4658.2009.07211.x

Lorito, M., Woo, S. L., Harman, G. E., and Monte, E. (2010). Translational research on *Trichoderma*: from 'omics to the field. *Annu. Rev. Phytopathol.* 48, 395–417. doi: 10.1146/annurev-phyto-073009-114314

Maischak, H., Zimmermann, M. R., Felle, H. H., and Boland, W. (2010). Alamethicin-induced electrical long distance signaling in plants. *Plant Signal. Behav.* 5, 988–990. doi: 10.1104/pp.108.133884

Mantyla, A. L., Rossi, K. H., Vanhanen, S. A., Penttila, M. E., Suominen, P. L., and Nevalainen, K. M. H. (1992). Electrophoretic karyotyping of wild-type and mutant *Trichoderma longibrachiatum* (reesei) strains. *Curr. Genet.* 21, 471–477. doi: 10.1007/BF00351657

Marra, R., Ambrosino, P., Carbone, V., Vinale, F., Woo, S. L., Ruocco, M., et al. (2006). Study of the three- way interaction between *Trichoderma atroviride*, plant and fungal pathogens by using a proteomic approach. *Curr. Genet.* 50, 307–321. doi: 10.1007/s00294-006-0091-0

Martinez, D., Berka, R. M., Henrissat, B., Saloheimo, M., Arvas, M., Baker, S. E., et al. (2008). Genome sequencing and analysis of the biomass-degrading fungus *Trichoderma reesei* (syn. *Hypocrea Jecorina). Nat. Biotechnol.* 26, 553–560. doi: 10.1038/nbt1403

Martínez-Medina, A., Appels, F. V. W., and Van Wees, S. C. M. (2017a). Impact of salicylic acid- and jasmonic acid-regulated defences on root colonization by *Trichoderma harzianum* T-78. *Plant Signal. Behav.* doi: 10.1080/15592324.2017.1345404 [Epub ahead of print].

Martínez-Medina, A., Van Wees, S. C. M., and Pieterse, C. M. J. (2017b). Airborne signals by *Trichoderma* fungi stimulate iron uptake responses in roots resulting in priming of jasmonic acid-dependent defences in shoots of *Arabidopsis thaliana* and *Solanum lycopersicum*. *Plant Cell Environ.* doi: 10.1111/pce.13016 [Epub ahead of print].

Mathys, J., De Cremer, K., Timmermans, P., Van Kerckhove, S., Lievens, B., Vanhaecke, M., et al. (2012). Genome-Wide characterization of ISR induced in *Arabidopsis thaliana* by *Trichoderma hamatum* T382 against *Botrytis cinerea* infection. *Front. Plant Sci.* 3:108. doi: 10.3389/fpls.2012.00108

Mehrabi-Koushki, M., Rouhani, H., and Mahdikhani-Moghaddam, E. (2012). Differential display of abundantly expressed genes of *Trichoderma harzianum* during colonization of tomato-germinating seeds and roots. *Curr. Microbiol.* 65, 524–533. doi: 10.1007/s00284-012-0189-1

Merino, S., and Cherry, J. (2007). "Progress and challenges in enzyme development for biomass utilization," in *Biofuels*, ed. L. Olsson (Berlin: Springer), 95–120.

Meteignier, L. V., El Oirdi, M., Cohen, M., Barff, T., Matteau, D., Lucier, J. F., et al. (2017). Translatome analysis of an NB-LRR immune response identifies important contributors to plant immunity in Arabidopsis. *J. Exp. Bot.* 68, 2333–2344. doi: 10.1093/jxb/erx078

Montero, M., Sanz, L., Rey, M., Llobell, A., and Monte, E. (2007). Cloning and characterization of bgn16.3, coding for a β-1,6-glucanase expressed during *Trichoderma harzianum* mycoparasitism. *J. Appl. Microbiol.* 103, 1291–1300. doi: 10.1111/j.1365-2672.2007.03371.x

Montero, M., Sanz, L., Rey, M., Monte, E., and Llobell, A. (2005). BGN16.3, a novel acidic β-1,6-glucanase from mycoparasitic fungus *Trichoderma harzianum* CECT 2413. *FEBS J.* 272, 3441–3448. doi: 10.1111/j.1742-4658.2005.04762.x

Morán-Diez, E., Rubio, B., Domínguez, S., Hermosa, R., Monte, E., and Nicolás, C. (2012). Transcriptomic response of *Arabidopsis thaliana* after 24h incubation with the biocontrol fungus *Trichoderma harzianum*. *J. Plant Physiol.* 169, 614–620. doi: 10.1016/j.jplph.2011.12.016

Morán-Diez, M. E., Cardoza, R. E., Gutiérrez, S., Monte, E., and Hermosa, R. (2010). TvDim1 of *Trichoderma virens* is involved in redox-processes and confers resistance to oxidative stresses. *Curr. Genet.* 56, 63–73. doi: 10.1007/s00294-009-0280-8

Morán-Diez, M. E., Trushina, N., Lamdan, N. L., Rosenfelder, L., Mukherjee, P. K., Kenerley, C. M., et al. (2015). Host-specific transcriptomic pattern of *Trichoderma virens* during interaction with maize or tomato roots. *BMC Genomics* 16:8. doi: 10.1186/s12864-014-1208-3

Mukherjee, M. (2012). "*Trichoderma* genes involved in interactions with fungi and plants," in *Biotechnology of Fungal Genes*, eds V. K. Gupta and M. Ayyachamy (New York, NY: CRC Press), 153–171.

Mukherjee, P. K., Horwitz, B. A., Herrera-Estrella, A., Schmoll, M., and Kenerley, C. M. (2013). *Trichoderma* research in the genome era. *Annu. Rev. Phytopathol.* 51, 105–129. doi: 10.1146/annurev-phyto-082712-102353 doi: 10.1099/mic.0.053629-0

Mukherjee, P. K., Horwitz, B. A., and Kenerley, C. M. (2012). Secondary metabolism in *Trichoderma* - a genomic perspective. *Microbiology* 158, 35–45. doi: 10.1099/mic.0.053629-0

Nobe, R., Sakakibara, Y., Ogawa, K., and Suiko, M. (2004). Cloning and expression of a novel *Trichoderma viride* laminarinase AI gene (*lamAI*). *Biosci. Biotechnol. Biochem.* 68, 2111–2119. doi: 10.1271/bbb.68.2111

Palmieri, M. C., Perazzolli, M., Matafora, V., Moretto, M., Bachi, A., and Pertot, I. (2012). Proteomic analysis of grapevine resistance induced by *Trichoderma harzianum* T39 reveals specific defence pathways activated against downy mildew. *J. Exp. Bot.* 63, 6237–6251. doi: 10.1093/jxb/ers279

Panizel, I., Yarden, O., Ilan, M., and Carmeli, S. (2013). Eight new peptaibols from sponge-associated *Trichoderma atroviride*. *Mar. Drugs* 11, 4937–4960. doi: 10.3390/md11124937

Papavizas, G. C. (1985). *Trichoderma* and *Gliocladium*: biology, ecology, and potential for biocontrol. *Annu. Rev. Phytopathol.* 23, 23–54. doi: 10.1146/annurev.py.23.090185.000323

Payne, S. H. (2015). The utility of protein and mRNA correlation. *Trends Biochem. Sci.* 40, 1–3. doi: 10.1016/j.tibs.2014.10.010

Pelagio-Flores, R., Esparza-Reynoso, S., Garnica-Vergara, A., López-Bucio, J., and Herrera-Estrella, A. (2017). *Trichoderma*-induced acidification is an early trigger for changes in *Arabidopsis* root growth and determines fungal phytostimulation. *Front. Plant Sci.* 17:822. doi: 10.3389/fpls.2017.00822

Perazzolli, M., Moretto, M., Fontana, P., Ferrarini, A., Velasco, R., Moser, C., et al. (2012). Downy mildew resistance induced by *Trichoderma harzianum* T39 in susceptible grapevines partially mimics transcriptional changes of resistant genotypes. *BMC Genomics* 13:660. doi: 10.1186/1471-2164-13-660

Picard, F., Loubière, P., Girbal, L., and Cocaign-Bousquet, M. (2013). The significance of translation regulation in the stress response. *BMC Genomics* 14:588. doi: 10.1186/1471-2164-14-588

Piccirillo Ciriaco, A., Bjur, E., Topisirovic, I., Sonenberg, N., and Larsson, O. (2014). Translational control of immune responses: from transcripts to translatomes. *Nat. Immunol.* 15, 503–511. doi: 10.1038/ni.2891

Przylucka, A., Bayram, G., Chenthamara, K., Cai, F., Grujic, M., Karpenko, J., et al. (2017). HFB7 – a novel orphan hydrophobin of the *Harzianum* and *Virens* clades of *Trichoderma*, is involved in response to biotic and abiotic stresses. *Fungal Genet. Biol.* 102, 63–76. doi: 10.1016/j.fgb.2017.01.002

Puglisi, I., Faedda, R., Sanzaro, V., Lo Piero, A. R., Petrone, G., and Cacciola, S. O. (2012). Identification of differentially expressed genes in response to mercury I and II stress in *Trichoderma harzianum*. *Gene* 15, 325–330. doi: 10.1016/j.gene.2012.06.091

Qi, W., and Zhao, L. (2013). Study of the siderophore-producing *Trichoderma asperellum* Q1 on cucumber growth promotion under salt stress. *J. Basic Microbiol.* 53, 355–364. doi: 10.1002/jobm.201200031

Reino, J. L., Guerrero, R. F., Hernández-Galan, R., and Collado, I. G. (2008). Secondary metabolites from species of the biocontrol agent *Trichoderma*. *Phytochemistry* 7, 89–123. doi: 10.1007/s11101-006-9032-2

Reithner, B., Ibarra-Laclette, E., Mach, R. L., and Herrera-Estrella, A. (2011). Identification of mycoparasitism-related genes in *Trichoderma atroviride*. *Appl. Environ. Microbiol.* 77, 4361–4370. doi: 10.1128/AEM.00129-11

Röhrich, C. R., Voglmayr, H., Iversen, A., and Vilcinskas, A. (2015). Front line defenders of the ecological niche! Screening the structural diversity of peptaibiotics from saprotrophic and fungicolous *Trichoderma*/*Hypocrea* species. *Fungal Divers.* 69, 117–146. doi: 10.1007/s13225-013-0276-z

Rosales-Saavedra, T., Esquivel-Naranjo, E. U., Casas-Flores, S., Martinez-Hernandez, P., Ibarra-Laclette, E., Cortes-Penagos, C., et al. (2006). Novel light-regulated genes in *Trichoderma atroviride*: a dissection by cDNA microarrays. *Microbiology* 152, 3305–3317. doi: 10.1099/mic.0.29000-0

Rubio, M. B., Dominguez, S., Monte, E., and Hermosa, R. (2012). Comparative study of *Trichoderma* gene expression in interactions with tomato plants using high-density oligonucleotide microarrays. *Microbiology* 158(Pt 1), 119–128. doi: 10.1099/mic.0.052118-0

Rubio, M. B., Hermosa, R., Reino, J. L., Collado, I. G., and Monte, E. (2009). *Thctf1* transcription factor of *Trichoderma harzianum* is involved in 6-pentyl-2*H*-pyran-2-one production and antifungal activity. *Fungal Genet. Biol.* 46, 17–27. doi: 10.1016/j.fgb.2008.10.008

Rubio, M. B., Quijada, N. M., Pérez, E., Domínguez, S., Monte, E., and Hermosa, R. (2014). Identifying beneficial qualities of *Trichoderma parareesei* for plants. *Appl. Environ. Microbiol.* 80, 1864–1873. doi: 10.1128/AEM.03375-13

Ruocco, M., Lanzuise, S., Lombardi, N., Woo, S. L., Vinale, F., and Marra, R. (2015). Multiple roles and effects of a novel *Trichoderma* hydrophobin. *Mol. Plant Microbe Interact.* 28, 167–179. doi: 10.1094/MPMI-07-14-0194-R

Ruocco, M., Lanzuise, S., Vinale, F., Marra, R., Turrà, D., Woo, S. L., et al. (2009). Identification of a new biocontrol gene in *Trichoderma atroviride*: the role of an ABC transporter membrane pump in the interaction with different plant-pathogenic fungi. *Mol. Plant Microbe Interact.* 22, 291–301. doi: 10.1094/MPMI-22-3-0291

Samolski, I., de Luis, A., Vizcaino, J. A., Monte, E., and Suarez, M. B. (2009). Gene expression analysis of the biocontrol fungus *Trichoderma harzianum* in the presence of tomato plants, chitin, or glucose using a high-density oligonucleotide microarray. *BMC Microbiol.* 9:217. doi: 10.1186/1471-2180-9-217

Sanna, A. (2006). *Characterization of the Trichoderma reesei Hydrophobins HFBI and HFBII*. Doctoral dissertation, Helsinki University of Technology, Espoo. doi: 10.1007/s00294-008-0226-6

Scherm, B., Schmoll, M., Balmas, V., Kubicek, C. P., and Migheli, Q. (2009). Identification of potential marker genes for *Trichoderma harzianum* strains with high antagonistic potential against *Rhizoctonia solani* by a rapid subtraction hybridization approach. *Curr. Genet.* 55, 81–91. doi: 10.1007/s00294-008-0226-6

Schmoll, M., Dattenböck, C., Carreras-Villaseñor, N., Mendoza-Mendoza, A., Tisch, D., Alemán, M. I., et al. (2016). The genomes of three uneven siblings: footprints of the lifestyles of three *Trichoderma* species. *Microbiol. Mol. Biol. Rev.*? 80, 205–327. doi: 10.1128/MMBR.00040-15

Schuster, A., and Schmoll, M. (2010). Biology and biotechnology of *Trichoderma*. *Appl. Microbiol. Biotechnol.* 87, 787–799. doi: 10.1007/s00253-010-2632-1

Segarra, G., Casanova, E., Bellido, D., Odena, M. A., Oliveira, E., and Trillas, I. (2007). Proteome, salicylic acid, and jasmonic acid changes in cucumber plants inoculated with *Trichoderma asperellum* strain T34. *Proteomics* 7, 3943–3952. doi: 10.1002/pmic.200700173

Seidl, V., Huemer, B., Seiboth, B., and Kubicek, C. P. (2005). A complete survey of *Trichoderma* chitinases reveals three distinct subgroups of family 18 chitinases. *FEBS J.* 272, 5923–5939. doi: 10.1111/j.1742-4658.2005.04994.x

Seidl, V., Song, L., Lindquist, E., Gruber, S., Koptchinskiy, A., Zeilinger, S., et al. (2009). Transcriptomic response of the mycoparasitic fungus *Trichoderma atroviride* to the presence of a fungal prey. *BMC Genomics* 10:567. doi: 10.1186/1471-2164-10-567

Sharma, V., Bhandari, P., Singh, B., Bhatacharya, A., and Shanmugam, V. (2013). Chitinase expression due to reduction in fusaric acid level in an antagonistic *Trichoderma harzianum* S17TH. *Indian J. Microbiol.* 53, 214–220. doi: 10.1007/s12088-012-0335-2

Sharma, V., and Salwan, R. (2017). "Molecular markers and their use in taxonomic characterization of *Trichoderma* spp," in *Molecular Markers in Mycology. Fungal Biology*, eds B. Singh and V. Gupta (Cham: Springer).

Sharma, V., Salwan, R., and Sharma, P. N. (2017a). The comparative mechanistic aspects of *Trichoderma* and probiotics: scope for future research. *Physiol. Mol. Plant Pathol.* 100, 84–96. doi: 10.1016/j.pmpp.2017.07.005

Sharma, V., Salwan, R., and Sharma, P. N. (2016a). Differential response of extracellular proteases of *Trichoderma harzianum* against fungal phytopathogens. *Curr. Microbiol.* 73, 419–425. doi: 10.1007/s00284-016-1072-2

Sharma, V., Salwan, R., Sharma, P. N., and Kanwar, S. S. (2017b). Elucidation of biocontrol mechanisms of *Trichoderma harzianum* against different plant fungal pathogens: universal yet host specific response. *Int. J. Biol. Macromol.* 95, 72–79. doi: 10.1016/j.ijbiomac.2016.11.042

Sharma, V., Salwan, R., Sharma, P. N., and Kanwar, S. S. (2016b). Molecular cloning and characterization of ech46 endochitinase from *Trichoderma harzianum*. *Int. J. Biol. Macromol.* 92, 615–624. doi: 10.1016/j.ijbiomac.2016.07.067

Sharma, V., and Shanmugam, V. (2012). Purification and characterization of an extracellular 24 kDa chitobiosidase from the mycoparasitic fungus *Trichoderma saturnisporum*. *J. Basic Microbiol.* 52, 324–331. doi: 10.1002/jobm.201100145

Shaw, S., Cocq, K. L., Paszkiewicz, K., Moore, K., Winsbury, R., de Torres Zabala, M., et al. (2016). Transcriptional reprogramming underpins enhanced plant growth promotion by the biocontrol fungus *Trichoderma hamatum* GD12 during antagonistic interactions with *Sclerotinia sclerotiorum* in soil. *Mol. Plant Pathol.* 17, 1425–1441. doi: 10.1111/mpp.12429

Shentu, X.-P., Liu, W.-P., Zhan, X.-H., Xu, Y. P., Xu, J. F., Yu, X. P., et al. (2014). Transcriptome sequencing and gene expression analysis of *Trichoderma brevicompactum* under different culture conditions. *PLoS ONE* 9:e94203. doi: 10.1371/journal.pone.0094203

Shi, M., Chen, L., Wang, X., Zhang, T., Zhao, P., Song, X., et al. (2012). Antimicrobial peptaibols from *Trichoderma pseudokoningii* induce programmed cell death in plant fungal pathogens. *Microbiology* 158, 166–175. doi: 10.1099/mic.0.052670-0

Shi, W.-L., Chen, X.-L., Wang, L.-X., Gong, Z.-T., Li, S., Li, C.-L., et al. (2016). Cellular and molecular insight into the inhibition of primary root growth of Arabidopsis induced by peptaibols, a class of linear peptide antibiotics mainly produced by *Trichoderma* spp. *J. Exp. Bot.* 67, 2191–2205. doi: 10.1093/jxb/erw023

Shoresh, M., and Harman, G. E. (2008). The molecular basis of shoot responses of maize seedlings to *Trichoderma harzianum* T22 inoculation of the root: a proteomic approach. *Plant Physiol.* 147, 2147–2163. doi: 10.1104/pp.108.123810

Shoresh, M., Harman, G. E., and Mastouri, F. (2010). Induced systemic resistance and plant responses to fungal biocontrol agents. *Annu. Rev. Phytopathol.* 48, 21–43. doi: 10.1146/annurev-phyto-073009-114450

Simkovi, M., Kurucová, A., Hunová, M., and Vare, Ľ. (2008). Induction of secretion of extracellular proteases from *Trichoderma viride*. *Acta Chim. Slovaca* 1, 250–264.

Singh, A., Taylor, L. E. II, Vander Wall, T. A., Linger, J., Himmel, M. E., Podkaminer, K., et al. (2015). Heterologous protein expression in *Hypocrea jecorina*: a historical perspective and new developments. *Biotechnol. Adv.* 33, 142–154. doi: 10.1016/j.biotechadv.2014.11.009

Spangenberg, L., Shigunov, P., Abud, A. P., Cofré, A. R., Stimamiglio, M. A., Kuligovski, C., et al. (2013). Polysome profiling shows extensive posttranscriptional regulation during human adipocyte stem cell differentiation into adipocytes. *Stem Cell Res.* 11, 902–912. doi: 10.1016/j.scr.2013.06.002

Spriggs, K. A., Bushell, M., and Willis, A. E. (2010). Translational regulation of gene expression during conditions of cell stress. *Mol. Cell.* 40, 228–237. doi: 10.1016/j.molcel.2010.09.028

Steindorff, A. S., Ramada, M. H., Coelho, A. S., Miller, R. N., Pappas, G. J. Jr., Ulhoa, C. J., et al. (2014). Identification of mycoparasitism-related genes against the phytopathogen *Sclerotinia sclerotiorum* through transcriptome and expression profile analysis in *Trichoderma harzianum*. *BMC Genomics* 15:204. doi: 10.1186/1471-2164-15-204

Steindorff, A. S., Silva, R. N., Coelho, A. S. G., Nagata, T., Noronha, E. F., and Ulhoa, C. J. (2012). *Trichoderma harzianum* expressed sequence tags for identification of genes with putative roles in mycoparasitism against *Fusarium solani*. *Biol. Control* 61, 134–140. doi: 10.1016/j.biocontrol.2012.01.014

Suárez, M. B., Vizcaíno, J. A., Llobell, A., and Monte, E. (2007). Characterization of genes encoding novel peptidases in the biocontrol fungus *Trichoderma harzianum* CECT 2413 using the TrichoEST functional genomics approach. *Curr. Genet.* 51, 331–342. doi: 10.1007/s00294-007-0130-5

Szekeres, A., Kredics, L., Antal, Z., Kevei, F., and Manczinger, L. (2004). Isolation and characterization of protease overproducing mutants of *Trichoderma harzianum*. *FEMS Microbiol. Lett.* 233, 215–222. doi: 10.1111/j.1574-6968.2004.tb09485.x

Teresa, M., Bara, F., Lima, A. L., and Ulhoa, C. J. (2003). Purification and characterization of an exo- β-1,3-glucanase produced by *Trichoderma asperellum*. *FEMS Microbiol. Lett.* 219, 81–85. doi: 10.1016/S0378-1097(02)01191-6

Terman, S. A. (1970). Relative effect of transcription-level and translation-level control of protein synthesis during early development of the sea urchin. *Proc. Natl. Acad. Sci. U.S.A.* 65, 985–992. doi: 10.1073/pnas.65.4.985

Thomas, J. D., and Johannes, G. J. (2007). Identification of mRNAs that continue to associate with polysomes during hypoxia. *RNA* 13, 1116–1131. doi: 10.1261/rna.534807

Tian, Q., Stepaniants, S. B., Mao, M., Mao, M., Weng, L., Feetham, M. C., et al. (2004). Integrated genomic and proteomic analyses of gene expression in Mammalian cells. *Mol. Cell. Proteomics* 3, 960–969. doi: 10.1074/mcp.M400055-MCP200

Tucci, M., Ruocco, M., De Masi, L., De Palma, M., and Lorito, M. (2011). The beneficial effect of *Trichoderma* spp. on tomato is modulated by the plant genotype. *Mol. Plant Pathol.* 12, 341–354. doi: 10.1111/j.1364-3703.2010.00674.x

Vazqez-Garciduen, S., Leal-morales, C. A., and Herrera-Estrella, A. (1998). Analysis of the β-1,3-glucanolytic system of the biocontrol agent *Trichoderma harzianum*. *Appl. Environ. Microbiol.* 64, 1442–1446.

Vieira, P. M., Coelho, A. S. G., Steindorff, A. S., de Siqueira, S. J. L., Silva, R., do, N., et al. (2013). Identification of differentially expressed genes from *Trichoderma harzianum* during growth on cell wall of *Fusarium solani* as a tool for biotechnological application. *BMC Genomics* 14:177. doi: 10.1186/1471-2164-14-177

Vinale, F., Sivasithamparam, K., Ghisalberti, E. L., Woo, S. L., Nigro, M., Marra, R., et al. (2014). *Trichoderma* secondary metabolites active on plants and fungal pathogens. *Open Mycol. J.* 8, 127–139. doi: 10.1111/j.1472-765X.2009.02599.x

Viterbo, A., Harel, M., and Chet, I. (2004). Isolation of two aspartyl proteases from *Trichoderma asperellum* expressed during colonization of cucumber roots. *FEMS Microbiol. Lett.* 238, 151–158.

Viterbo, A., Wiest, A., Brotman, Y., Chet, I., and Kenerley, C. (2007). The 18mer peptaibols from *Trichoderma virens* elicit plant defence responses. *Mol. Plant. Pathol.* 8, 737–746. doi: 10.1111/j.1364-3703.2007.00430.x

Viterbo, A., Ramot, O., Chemin, L., and Chet, I. (2002). Significance of lytic enzymes from *Trichoderma* spp. in the biocontrol of fungal plant pathogens. *Antonie Van Leeuwenhoek* 81, 549–556. doi: 10.1023/A:1020553421740

Vizcaíno, J. A., González, F. J., Suárez, M. B., Redondo, J., Heinrich, J., Delgado-Jarana, J., et al. (2006). Generation, annotation and analysis of ESTs from *Trichoderma harzianum* CECT 2413. *BMC Genomics* 7:193. doi: 10.1186/1471-2164-7-193

Vizcaíno, J. A., Redondo, J., Suárez, M. B., Cardoza, R. E., Hermosa, R., González, F. J., et al. (2007). Generation, annotation, and analysis of ESTs from four different *Trichoderma* strains grown under conditions related to biocontrol. *Appl. Microbiol. Biotechnol.* 75, 853–862. doi: 10.1007/s00253-007-0885-0

Vogel, C., and Marcotte, E. M. (2012). Insights into the regulation of protein abundance from proteomic and transcriptomic analyses. *Nat. Rev. Genet.* 13, 227–232. doi: 10.1038/nrg3185

Wu, Q., Sun, R., Ni, M., Yu, J., Li, Y., Yu, C., et al. (2017). Identification of a novel fungus, *Trichoderma asperellum* GDFS1009, and comprehensive evaluation of its biocontrol efficacy. *PLoS ONE* 12:e0179957. doi: 10.1371/journal.pone.0179957

Xie, B.-B., Li, D., Shi, W.-L., Qin, Q. L., Wang, X., Rong, J. C., et al. (2015). Deep RNA sequencing reveals a high frequency of alternative splicing events in the fungus *Trichoderma longibrachiatum*. *BMC Genomics* 16:54. doi: 10.1186/s12864-015-1251-8

Xie, B.-B., Qin, Q.-L., Shi, M., Chen, L.-L., Shu, Y.-L., Luo, Y., et al. (2014). Comparative genomics provide insights into evolution of *Trichoderma* nutrition style. *Genome Biol. Evol.* 6, 379–390. doi: 10.1093/gbe/evu018

Yanguez, E., Castro-Sanz, A. B., Ferna´ndez-Bautista, N., Oliveros, J. C., and Castellano, M. M. (2013). Analysis of genome-wide changes in the translatome of Arabidopsis seedlings subjected to heat stress. *PLoS ONE* 8:e71425. doi: 10.1371/journal.pone.0071425

Yao, L., Yang, Q., Song, J., Tan, C., Guo, C., Wang, L., et al. (2013). Cloning, annotation and expression analysis of mycoparasitism-related genes in *Trichoderma harzianum* 88. *J. Microbiol.* 51, 174–182. doi: 10.1007/s12275-013-2545-7

Yedidia, I. I., Benhamou, N., and Chet, I. I. (1999). Induction of defense responses in cucumber plants (*Cucumis sativus* L.) by the biocontrol agent *Trichoderma harzianum*. *Appl. Environ. Microbiol.* 65, 1061–1070.

Zeilinger, S., Gruber, S., Bansal, R., and Mukherjee, P. K. (2016). Secondary metabolism in *Trichoderma* – chemistry meets genomics. *Fungal Biol. Rev.* 30, 74–90. doi: 10.1016/j.fbr.2016.05.001

Zhang, F., Yang, X., Ran, W., and Shen, Q. (2014). *Fusarium oxysporum* induces the production of proteins and volatile organic compounds by *Trichoderma harzianum* T-E5. *FEMS Microbiol. Lett.* 359, 116–123. doi: 10.1111/1574-6968.12582

Zhang, T., Chaturvedi, V., and Chaturvedi, S. (2015). Novel *Trichoderma polysporum* strain for the biocontrol of *Pseudogymnoascus destructans*, the fungal etiologic agent of bat white nose syndrome. *PLoS ONE* 10:e0141316. doi: 10.1371/journal.pone.0141316

Zupanic, A., Meplan, C., Grellscheid, S. N., Mathers, J. C., Kirkwood, T. B., Hesketh, J. E., et al. (2013). Detecting translational regulation by change point analysis of ribosome profiling data sets. *RNA* 20, 1507–1518. doi: 10.1261/rna.045286.114

Conflict of Interest Statement: The authors declare that the research was conducted in the absence of any commercial or financial relationships that could be construed as a potential conflict of interest.

frontiers in Microbiology

ORIGINAL RESEARCH
published: 13 February 2018
doi: 10.3389/fmicb.2018.00217

Verticillium dahliae-Arabidopsis Interaction Causes Changes in Gene Expression Profiles and Jasmonate Levels on Different Time Scales

*Sandra S. Scholz[1], Wolfgang Schmidt-Heck[2], Reinhard Guthke[2], Alexandra C. U. Furch[1], Michael Reichelt[3], Jonathan Gershenzon[3] and Ralf Oelmüller[1]**

[1] Department of Plant Physiology, Matthias Schleiden Institute of Genetics, Bioinformatics and Molecular Botany, Friedrich-Schiller-University Jena, Jena, Germany, [2] Systems Biology and Bioinformatics Group, Leibniz Institute for Natural Product Research and Infection Biology—Hans-Knöll-Institute, Jena, Germany, [3] Department of Biochemistry, Max-Planck Institute for Chemical Ecology, Jena, Germany

Verticillium dahliae is a soil-borne vascular pathogen that causes severe wilt symptoms in a wide range of plants. Co-culture of the fungus with *Arabidopsis* roots for 24 h induces many changes in the gene expression profiles of both partners, even before defense-related phytohormone levels are induced in the plant. Both partners reprogram sugar and amino acid metabolism, activate genes for signal perception and transduction, and induce defense- and stress-responsive genes. Furthermore, analysis of *Arabidopsis* expression profiles suggests a redirection from growth to defense. After 3 weeks, severe disease symptoms can be detected for wild-type plants while mutants impaired in jasmonate synthesis and perception perform much better. Thus, plant jasmonates have an important influence on the interaction, which is already visible at the mRNA level before hormone changes occur. The plant and fungal genes that rapidly respond to the presence of the partner might be crucial for early recognition steps and the future development of the interaction. Thus they are potential targets for the control of *V. dahliae*-induced wilt diseases.

Keywords: ***Arabidopsis*, calcium, JA, defense, *Verticillium dahliae***

OPEN ACCESS

Edited by:
Katarzyna Turnau, Jagiellonian University, Poland

Reviewed by:
Sotiris Tjamos, Agricultural University of Athens, Greece
Sergio Casas-Flores, Institute for Scientific and Technological Research, Mexico

****Correspondence:***
Ralf Oelmüller
ralf.oelmueller@uni-jena.de

Specialty section:
This article was submitted to Fungi and Their Interactions, a section of the journal Frontiers in Microbiology

Received: *30 September 2017*
Accepted: *30 January 2018*
Published: *13 February 2018*

Citation:
Scholz SS, Schmidt-Heck W, Guthke R, Furch ACU, Reichelt M, Gershenzon J and Oelmüller R (2018) Verticillium dahliae-Arabidopsis Interaction Causes Changes in Gene Expression Profiles and Jasmonate Levels on Different Time Scales. Front. Microbiol. 9:217. doi: 10.3389/fmicb.2018.00217

INTRODUCTION

Vascular wilts caused by members of the genus *Verticillium* are among the most devastating fungal diseases worldwide, and these soil-borne ascomycete fungi attack a large variety of plant hosts in many parts of the world (Decetelaere et al., 2017) which leads to massive yield losses (Pegg and Brady, 2002). Among the 10 species within the *Verticillium* genus, *Verticillium dahliae* has the broadest host range with the ability to infect >200 plant species worldwide (Agrios, 1997; Inderbitzin et al., 2011; Inderbitzin and Subbarao, 2014). *Verticillium* species produce microsclerotia, which can survive in soil or dead plant material for more than 10 years, but they also form resting mycelia which survive in dead plant material. Newly growing hyphae rapidly penetrate the roots of their hosts, reach the vascular tissue and ultimately propagate in the xylem (Puhalla and Bell, 1981; Schnathorst, 1981). Initially, these hemibiotrophic fungi show biotrophic behavior that does not lead to severe reductions in plant performance. However, at later stages, they shift to a necrotrophic interaction characterized by the reprogramming of phytohormone metabolism (Veronese et al., 2003; Thaler et al., 2004; Tjamos et al., 2005), synthesis of hydrogen peroxide

(H_2O_2) and nitric oxide (NO, Yao et al., 2011, 2012), and defense gene activation which ultimately induces host cell death (Reusche et al., 2012; Zhang et al., 2016). A typical symptom of these pathogens is wilting, which occurs as a consequence of impaired vascular transportation (Reusche et al., 2012).

Arabidopsis is an ideal model plant to study the *Verticilllium* infection process at the molecular level. Sun et al. (2014) showed that jasmonate phytohormones are highly induced upon *V. dahliae* infection, including the jasmonic acid (JA) pre-cursor *cis*-(+)-12-oxo-phytodienoic acid (*cis*-OPDA) and the jasmonic acid-isoleucine conjugate (JA-Ile). JA-Ile, synthesized by the enzyme JASMONATE RESISTANT 1 (JAR1), is the active signaling compound that binds to the JA receptor CORONATINE INSENSITIVE 1 (COI1) to initiate the downstream signaling cascade (Xie et al., 1998; Staswick and Tiryaki, 2004; Fonseca et al., 2009). Hydroxylation of JA-Ile by a P450 enzyme leads to the deactivation of the molecule (Koo et al., 2011). Previous observations on JA-deficient *def1* tomato plants showed decreased fitness after *V. dahliae* treatment (Thaler et al., 2004), while external application of methyl JA (MeJA) to cotton and tomato plants partially blocked disease development due to the reduced growth of the fungus (Li et al., 1996). Recent RNA-seq analysis in cotton showed that in addition to the biosynthesis of JA, also other components of the JA signaling cascade are targets of *Verticillium*. For instance, the gene of a repressor protein of COI1, *GhJAZ10*, was significantly upregulated in a *V. dahliae*-resistant cotton cultivar (Chini et al., 2007; Thines et al., 2007; Zhang W. W. et al., 2017). On the other hand, *Verticillium* itself needs an activated COI1 signaling pathway in the plant to cross the root-shoot barrier and to induce disease symptoms in the leaf. Consequently, *V. dahliae*-infected *coi1* mutant plants showed less severe wilt symptoms (Ralhan et al., 2012).

Besides jasmonates, *Verticillium*-infested plants also accumulate other phytohormones like salicylic acid (SA) and ethylene (ET), (Fradin and Thomma, 2006; Ratzinger et al., 2009; Sun et al., 2014). SA plays an important role in plant defense against pathogens by activation of systemic acquired resistance (SAR) (Metraux, 2001). In *Brassica napus* the concentration of SA increased after infection with *Verticillium longisporum* in the xylem sap of the plants (Ratzinger et al., 2009). Also in *Arabidopsis,* a significant increase of SA could be detected in *V. dahliae*-infested plants (Sun et al., 2014). Exogenous application of SA protected cotton callus cells against a *V. dahliae (VD)*-toxin preparation by increase of chitinase and β-1,3-glucanase activities (Li et al., 2003; Zhen and Li, 2004). Interestingly, several *Arabidopsis* genotypes affected in different steps of SA signaling did not show altered resistance against *V. dahliae* infection (Veronese et al., 2003).

The role of ET in pathogen responses is still controversial although it was shown that ET can increase resistance and control symptom expression in some hosts. In soybean, tobacco and *Aarabidopsis,* ET is involved in host resistance against particular classes of pathogens (Knoester et al., 1998; Hoffman et al., 1999; Thomma et al., 1999), while a tomato mutant impaired in ET perception exhibited a significant reduction in disease symptoms after inoculations with different bacterial and fungal pathogens (Lund et al., 1998). Similarly, a tomato mutant with decreased ET biosynthesis showed significantly reduced symptom development (Robinson et al., 2001). The involvement of ET in response to *Verticillium* infection and *VD*-toxins has been shown repeatedly (Pegg and Cronshaw, 1976; Mansoori and Smith, 2005; Sun et al., 2014). Also the ET-resistant *Arabidopsis* mutant *etr1-1* was found to display less chlorosis upon *Verticillium* inoculation (Veronese et al., 2003; Tjamos et al., 2005; Pantelides et al., 2010).

A growing number of other chemical compounds of both plant and fungal origin have been identified that participate in disease development of infected host plants. For *Verticillium*, a range of peptides, hormones like cytokinins, and other metabolites were shown to confer partial resistance to infection (Reusche et al., 2013; Bu et al., 2014; Gaspar et al., 2014; Roos et al., 2014). In addition, the *Ve* gene provides resistance against isolates of *V. dahliae* in tomato and *Arabidopsis* (Kawchuk et al., 2001; Fradin et al., 2009, 2011) and the *VET1* gene was able to convey increased tolerance with milder chlorosis symptoms (Veronese et al., 2003).

Due to the vascular location of the growing fungus, *Verticillium* wilt of agricultural plants is difficult to control by chemicals or molecular tools. Even after removal of infected plants from agricultural fields, the resting structures (microsclerotia) remain in soil making them a hazard for future plantings (Fradin and Thomma, 2006). Biocontrol studies with bacterial and fungal isolates like *Pseudomonas putida* B E2, *Pseudomonas chlororaphis* K15, *Serratia plymuthica* R12 or *Paenibacillus alvei* K165 on *Solanaceae, Malvaceae*, and *Brassicaceae* have been shown to be an alternative strategy to restrict *Verticillium*-induced wilts (Berg et al., 2001; Tjamos et al., 2005; Li et al., 2012). Sun et al. (2014) showed that *Piriformospora indica*, a beneficial endophytic fungus of Sebacinales which colonizes the roots of many plant species, is an efficient biocontrol agent that restricts *V. dahliae* growth in the model plant *Arabidopsis thaliana*.

V. dahliae rapidly and efficiently colonizes *Arabidopsis* roots within 24 h post germination. In order to identify plant and fungal genes involved in these early recognition processes we performed an RNA-seq analysis under standardized co-cultivation conditions. We found a massive reprogramming of both the plant and fungal expression profiles that occurred before pathogen induced, defense-related phytohormone levels changed in the host. This alteration in expression profiles clearly indicates that both plant and pathogen respond very rapidly to the presence of the other.

MATERIALS AND METHODS

Growth Conditions of Seedlings

A. thaliana wild-type (ecotype Columbia-0) seeds, and seeds of the *jar1, coi1-16,* and *cyp94B3* mutants (kindly provided by Axel Mithöfer, MPI-CE, Jena) were surface-sterilized and placed on Petri dishes with MS media supplemented with 0.3% gelrite (Murashige and Skoog, 1962). After cold treatment at 4°C for 48 h, plates were incubated vertically for 9 or 14 days at 22°C under long day conditions (16 h light/8 h dark; 80 μmol m^{-2} s^{-1}, for experimental setup, cf. Figure S1).

Growth Conditions of Fungi and Preparation of Spore Solutions

V. dahliae wild-type (FSU-343, Jena Microbial Resource Center, Germany) and a GFP-labeled strain (IPP0860, kindly provided by Prof. Tiedemann, University of Göttingen) were grown for 1–2 weeks on Potato-Dextrose-Agar (PDA) medium (Bains and Tewari, 1987) at 23°C in the dark. To obtain high spore production, the still white mycelia (with low amount of microsclerotia) were transferred to liquid KM medium (Hill and Kaefer, 2001) and incubated for 4–5 days at room temperature (RT) in the dark and 110 rpm. The cultures were filtered through two layers of a nylon membrane (75 µm pore size), pelleted and washed with water. The spore concentration was determined with a hemocytometer and adjusted to 5×10^6 per ml.

Co-cultivation Assays

For short time co-cultivation assays, 9 day-old *A. thaliana* seedlings of equal sizes were used. Co-cultivation of *A. thaliana* and the fungus was performed under *in vitro* culture conditions on a nylon membrane on PNM medium (Johnson et al., 2011). Two days prior to use, 100 µl of the generated spore solutions (in water) or an equal amount of water were plated on six sterile membrane stripes (4 × 1 cm) placed on PDA plates and incubated at room temperature (Figure S1). For the co-cultivation the membrane stripes with fungus or water were placed on the PNM plates together with two plants per membrane. The plants were placed in the way that the roots were in contact with the fungus while the leaves were not (Figure S1). Plates were sealed with 3M™ Micropore tape and incubated for 24 h at 80 µmol m^{-2} s^{-1} with light from one side (leaves directed to light). Roots and leaves were harvested separately for further analysis. All experiments were performed three times independently (≈120 seedlings per replicate).

For long term co-cultivation [10 and 20 *days post infection* (*dpi*)], 14 day-old *A. thaliana* seedlings of equal size were used. Plants were grown and infected as described above and transferred to Magenta boxes (Sigma-Aldrich, Germany) after 24 h. One plant was added per box which contained 30 g sterile vermiculite mixed with 100 ml liquid PNM medium. The boxes were incubated at 23°C under short day conditions (9 h light/15 h dark; 80 µmol m^{-2} s^{-1}). After 10 or 20 *dpi*, plants were visually examined and photographed. The performance of the plants [n = 6 (control) and 9 (*VD*-infected)] was quantified based on the efficiency of the photosynthetic electron transfer measured with the Fluorcam as described before (Matsuo et al., 2015).

RNA Isolation and RNA-Seq

RNA of both plant and fungus was isolated from 100 mg root material (≈ 120 seedlings per replicate, $n = 3$). The frozen roots were finely ground with mortar and pistil and weighed. The RNA from the samples was extracted with peqGOLD TriFast™ FL (VWR, Darmstadt, Germany) according to the manufacturer's protocol. The RNA was further processed by use of the PureLink™ RNA Mini Kit (Thermo Fisher Scientific, Dreieich, Germany) with on-column DNAse treatment. RNA was dissolved in water and checked for quality. The isolated RNA was shipped to GeneCore (Heidelberg, Germany) where library construction was performed using the mRNA sequencing Sample Preparation Guide (Illumina, Cat#RS-930-1001), followed by a validation of the library and RNA sequencing (Hi Seq 2000, single-end 75 bp, ∼50 Mill. reads/sample). The removal of low quality reads and Illumina adapters was performed using Trimmomatic (Bolger et al., 2014). The remaining reads were then aligned to the *A. thaliana* (TAIR10.33) and *V. dahliae* (ASM15067v2.37) reference genomes using the RNA-seq aligner STAR (Dobin et al., 2013). Differential gene expression analysis was performed using DESeq2 (Love et al., 2014) with the raw counts obtained from FeatureCounts (Liao et al., 2014). Differentially Expressed Genes (DEGs) of both interaction partners were analyzed [FoldChange $\geq$ 2 and p-Value (FDR) $\leq$ 0.05]. The function of the DEGs was analyzed with the TAIR (www.arabidopsis.org) and the Fungi Ensembl (http://fungi.ensembl.org/Verticillium_dahliae) databases. Pathway analysis for the plant and the fungus was executed with the KEGG (Kyoto Encyclopedia of Genes and Genomes) Mapper tool (http://www.genome.jp/kegg/tool/map_pathway2.html; RRID:SCR_012773).

Analysis of Gene Expression and Fungal Colonization

The RNA ($n = 3$) was isolated as described above. One µg of RNA was transcribed to cDNA using the Omniscript RT Kit (Qiagen, Hilden, Germany). Fifty nanograms of synthesized cDNA was used as template for RT-qPCR in a CFX Connect™ Real-Time PCR Detection System (Bio-Rad, Munich, Germany) with the Brilliant II SYBR® Mastermix (Agilent, Böblingen, Germany). The mRNA levels for each cDNA probe were normalized with respect to the *RPS18B* (plant) or *VD_Actin2* (fungus, e.g., Klimes and Dobinson, 2006; Yang et al., 2013) mRNA levels. The normalized fold expression of GOIs was calculated according to ΔΔCP (Pfaffl, 2001). The primer pairs are given in Table S5. To analyze fungal colonization of different mutant plants, normalized fungal housekeeping gene expression was compared to that in WT plants.

Confocal Microscopy

Samples for confocal laser scanning microscopy were prepared according to the method for the short time co-cultivation described above. The GFP-labeled *V. dahliae* strain on *Arabidopsis* seedlings was imaged using a LSM 880 (Zeiss Microscopy GmbH, Jena, Germany) with the 488 nm laser line of an argon multiline laser (11.5 mW). Images were taken with a 40x objective (Plan-Apochromat 40x/0.8). Lambda stacks were created using the 32 channel GaAsP detector followed by Linear Unmixing with ZEN software (Zeiss, Jena, Germany). Z-stacks were taken from specific areas of the sample and Maximum Intensity Projections were produced with ZEN software. Cross-sections of the roots with a width of 14 µm were done with a Microm HM560 Cryostar (Southeast Pathology Instrument Service, Charleston, USA).

Quantification of Phytohormones

Phytohormones were extracted from the green parts of co-cultivated seedlings (1 sample = seedlings from 1 plate, ≈ 50–100 mg, $n = 10$). Frozen samples were homogenized for

30 s at 1000 rpm in a 2010 Geno/Grinder® (Spex SamplePrep, Stanmore, UK) and mixed with 1 ml methanol containing 40 ng/ml of D_6-JA, D_6-ABA, D_4-SA, and 8 ng/ml of D_6-JA-Ile (Scholz et al., 2017). All samples were shaken for 30 min at 4°C and centrifuged at 13,000 rpm for 20 min at 4°C. The supernatants were collected and the sample re-extracted with 500 µl methanol. The combined supernatants were evaporated to dryness at 30°C using a vacuum concentrator. Residues were re-suspended in 200 µl methanol and centrifuged at 13,000 rpm for 10 min. The supernatants were collected and measured with the API 5000 LC-MS/MS system (Applied Biosystems, Framingham, USA) as previously described (Vadassery et al., 2012). Since it was observed that both the D_6-labeled JA and JA-Ile contained 40% of the corresponding D_5-labeled compounds, both peaks were combined for analysis.

Statistics

Experiments were repeated three times to ensure reproducibility and 120–150 seedlings were used in each treatment for each mutant. Data of all independent experiments were pooled and analyzed. For comparison of two groups, the Mann Whitney U-test was applied. For statistical analyses of multiple groups, one-way analysis of variance (one-way ANOVA) was used as indicated in the figure legends. Different letters indicate significant differences between treatments. SigmaPlot13 and Origin Pro were used for data analysis and graph composition.

RESULTS

Co-cultivation of *Arabidopsis* Seedlings with *V. dahliae* for 24 H

Verticillium species are considered as hemibiotrophs, where a biotrophic phase—within the root xylem without a visible disease phenotype—is followed by a necrotrophic phase in the aerial parts of the plant (Reusche et al., 2012). We focused on the very early phase of infection, the pre-vascular growth phase, and analyzed the plant and fungal expression profiles during the first 24 h of fungal root colonization in *Arabidopsis*. By developing a stable co-cultivation method (scheme in Figure S1), a reproducible colonization of the seedlings by the fungus was achieved. Confocal microscopic pictures taken 24 h after co-culture demonstrate that *Arabidopsis* roots are already heavily colonized by the GFP-labeled *V. dahliae* (**Figure 1**). The hyphae of the fungus form a net over the root surface and root tip while the first spores can be observed at the site of lateral root formation (**Figures 1G–I**). In cross-sections of the colonized root (**Figures 1J–O**) it can be observed that the fungus penetrates the root surface, but did not yet invade the vascular tissue after 24 h of co-culture.

Dual-RNA-Seq of *Arabidopsis-Verticillium* Co-culture Reveals High Number of Differentially-Expressed Genes (DEGs)

Recent studies of plant-*Verticillium* co-cultures focus on analysis of the plant transcriptome by RNA-seq and indicate major changes in nearly 19% of pathways in early phases of infection (1 or 4 *dpi*, e.g., Faino et al., 2012; Zhang W. W. et al., 2017). The RNA-seq data generated in this study 24 h after co-cultivation was analyzed for changes in both the plant and fungal transcriptomes and revealed a total number of 4432 DEGs for both organisms (**Table 1**). Compared to *Arabidopsis* seedlings grown alone, co-cultivation with *Verticillium* results in 1143 DEGs, 903 of them are significantly up-regulated and 240 down-regulated (Tables S1, S2). For the fungus, 3289 DEGs were detected with 1695 significantly up-regulated (Table S3) and 1594 significantly down-regulated genes (Table S4). This suggests that the fungal expression profile responds more strongly to the presence of a host than the plant genome to a pathogen. The results for selected genes were verified by RT-qPCR (**Figures 7**, **8**, WT).

Multiple *Arabidopsis* Pathways Are Affected by *V. dahliae* Infection

Previous studies during longer co-cultivation times have shown that infection of *Arabidopsis* plants with *Verticillium* species results in disruption of water transport and massive accumulation of phytohormones like jasmonates (JAs), ethylene (ET), salicylic acid (SA), or abscisic acid (ABA), as well as stomata closure (Pegg and Brady, 2002; Fradin and Thomma, 2006; Klosterman et al., 2009; Ralhan et al., 2012; Sun et al., 2014). To identify early targets of the fungus in *Arabidopsis* and to analyze and classify the plant DEGs, we chose the 24 h co-cultivation time point and mapped the identified plant DEGs to distinct pathways in the KEGG database (Kanehisa, 1997). In total, 78 pathways were affected by the fungus (**Table 2** and **Figure 2A**). Metabolic pathways involved in carbon and amino acid metabolism seemed to be the major targets, such as *SWEET* genes and sugar efflux transporters, which often respond to pathogens and symbionts for nutritional gain (Chen et al., 2010). In our study, *SWEET11*, *−3,* and *−12* were down-regulated. Genes involved in plant development were also affected. So was ROOT CAP POLYGALACTURONASE28, a crucial player in root tip growth, which was also down-regulated at the mRNA level (Kamiya et al., 2016). Defense-related genes, genes involved in the synthesis and propagation of defense signals like JA, SA, NO, and reactive oxygen species (ROS), membrane-associated receptor kinases are up-regulated while pathways involved in or related to photosynthesis, carotenoid and flavonoid biosynthesis are down-regulated. We observed the activation of genes for various defense-related WRKY transcription factors (WRKY18, −28, −30, −33, −41, −45, −53, −55, −71). It has been shown that WRKY71 promotes shoot branching, acceleration of flowering and cell death (cf. references in TAIR, www.Arabidopsis.org); WRKY33 is a target of *Botrytis* to repress defense in *Arabidopsis* (Liu et al., 2017), WRKY53 is involved in disease resistance against *Verticillium longisporium* (Reusche et al., 2013), and WRKY30 confers general abiotic stress response to the plant (Scarpeci et al., 2013). Upregulation of these genes suggest that the plant reprograms its metabolism for defense. Also candidate genes for the perception of pathogen-associated molecular patterns, and enzymes as well as signaling components which might lead to the activation

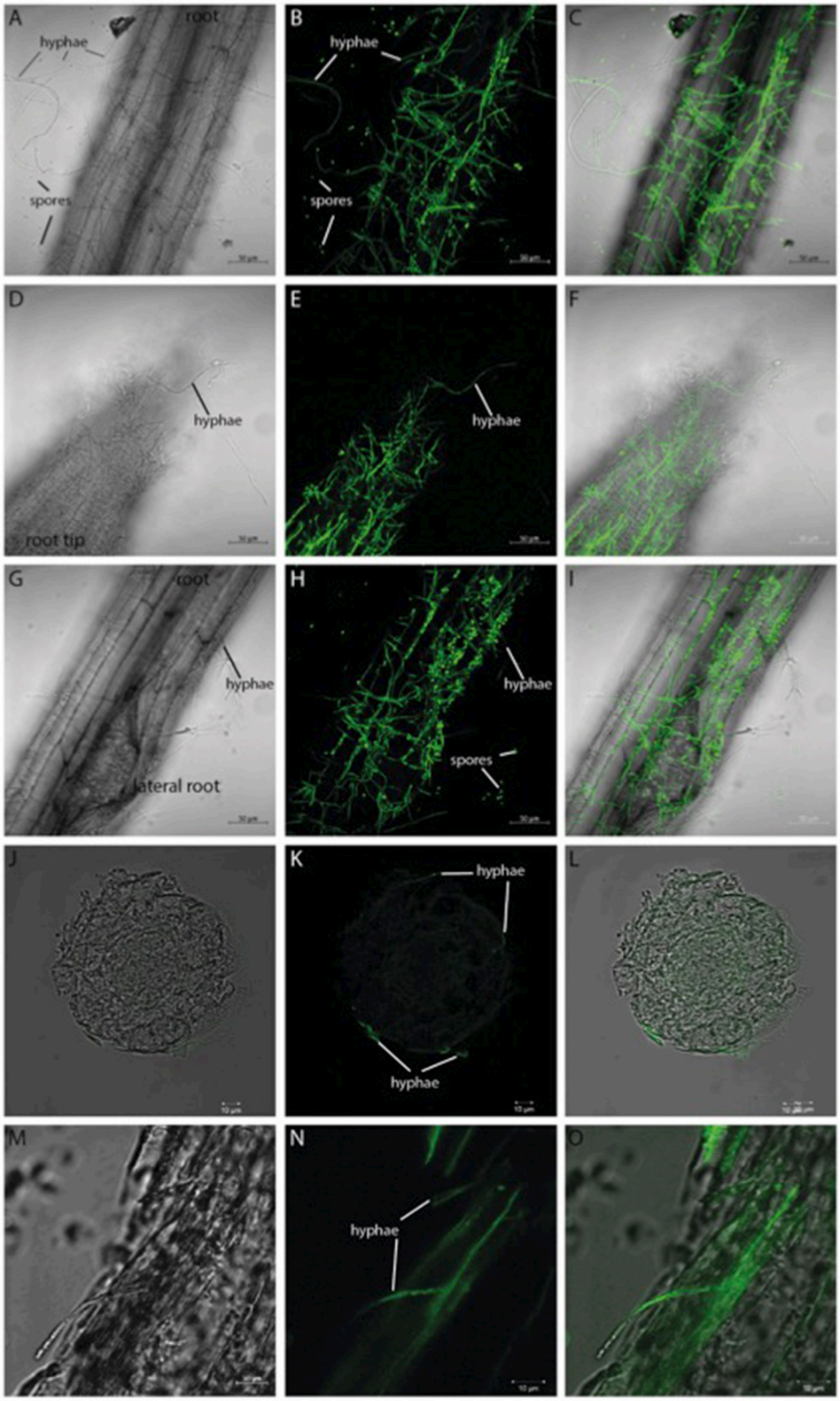

FIGURE 1 | GFP-labeled *Verticillium dahliae* colonizing roots of 10 day-old seedlings of *Arabidopsis thaliana* after 24 h co-culture. Shown are pictures (obtained from confocal microscopy) of the colonized *Arabidopsis* root surface **(A–C)**, root tip **(D–F)**, area around lateral roots **(G–I)** as well as a cross-section **(J–L)** and longitudinal section **(M–O)**. A bright field image (left), the GFP image (middle), and the overlay of both (right) are shown for each analyzed area. Both the hyphae and the spores of *V. dahliae* show a GFP fluorescence.

TABLE 1 | Overview of differentially regulated genes in *A. thaliana* (ATH) and *V. dahliae* (VDA) co-culture compared to organisms grown separately.

	Up	Down
ATH grown with VDA vs. ATH alone	903	240
VDA grown with ATH vs. VDA alone	1695	1594

of defense compounds in the host were upregulated in the presence of the fungus. This includes six genes for receptor-like protein kinases (RLP7, −15, −19, −20, −35, −38) and seven genes for proteins with TIR-NBS-LRR domains involved in disease resistance responses (At1g57630; At1g66090; At5g45240; At5g41750; At1g63750; At1g72900, At1g72920). For the RLP genes, no clear function has been described yet. The mRNAs for the Toll and Interleukin-1 Receptor (TIR)-Nucleotide-Binding Site (NBS)-Leucine-Rich Repeat (LRR) proteins (TIR-NBS-LRR), At1g66090 and At1g72920, have been shown to travel to distant tissue upon stress and thus might be involved in systemic signal propagation (Thieme et al., 2015). Furthermore, numerous genes for cytochrome P450 enzymes responded to the fungus. Of these, 17 are up-regulated and 11 have a described role in plant defense (cf. TAIR). Two of the three down-regulated genes (CYP87A2 and CYP705A12) are involved in cytokinin signaling (cf. TAIR). Many of the *cyp* mRNAs are also known to be mobile within the plant. Finally, defense gene activation is often mediated via Ca^{2+} signaling and Ca^{2+}-binding proteins. The majority of genes that code for proteins with Ca^{2+}-related functions are involved in signaling, ion uptake and distribution. Many of these are also up-regulated in *Arabidopsis* upon *V. dahliae* infection. At an early phase of interaction with the pathogen, the plant appears to shift its resources from primary metabolism to defense processes (cf. Discussion).

Interestingly, two genes for SNARE proteins (soluble N-ethylmaleimide-sensitive-factor attachment receptor, At5g39630, and At1g16225) also responded to the fungus. SNARE proteins are involved in vesicle trafficking and membrane fusion and deliver defense products to infection sites during exocytosis-associated immune responses (Wang et al., 2017, and references cited therein). Stimulation of *EXO70H4* and *EXO70A3* for EXOCYST subunits is consistent with the stimulation of exocytosis-mediated callose deposition and cell wall maturation by the fungus (Li et al., 2010; Kulich et al., 2015).

V. dahliae Pathways Respond to the Interaction with *Arabidopsis*

Many genes annotated in the 117 fungal pathways that were affected by co-cultivation with *Arabidopsis* (**Table 3** and **Figure 2B**), are still uncharacterized or with unknown function, which limits our analysis on the fungal side. However, like on the plant side, the majority of the affected pathways involved in primary metabolism, e.g., genes for the amino acid metabolism, were highly down-regulated, while those for sugar metabolism and sugar transport processes were up-regulated. This suggests that the fungus starts quite early to reprogram its primary

TABLE 2 | KEGG pathway classification of genes differentially expressed in *Arabidopsis* alone vs. co-culture with *V. dahliae*.

KEGG Pathway	Number	Percent	Pathway ID
Metabolic pathways	113	21.3	ath01100
Biosynthesis of secondary metabolites	81	15.3	ath01110
Phenylpropanoid biosynthesis	25	4.7	ath00940
Biosynthesis of amino acids	20	3.8	ath01230
Plant-pathogen interaction	18	3.4	ath04626
Glutathione metabolism	17	3.2	ath00480
Phenylalanine. tyrosine and tryptophan biosynthesis	13	2.4	ath00400
Amino sugar and nucleotide sugar metabolism	11	2.1	ath00520
Photosynthesis	10	1.9	ath00195
MAPK signaling pathway—plant	10	1.9	ath04016
Plant hormone signal transduction	9	1.7	ath00380
Photosynthesis—antenna proteins	9	1.7	ath04075
Nitrogen metabolism	8	1.5	ath01200
Carbon metabolism	8	1.5	ath00460
Tryptophan metabolism	8	1.5	ath00910
Cyanoamino acid metabolism	7	1.3	ath00966
Starch and sucrose metabolism	6	1.1	ath00500
Glucosinolate biosynthesis	6	1.1	ath00966
Glycine. serine and threonine metabolism	6	1.1	ath00260
Pentose and glucuronate interconversions	5	0.9	ath00040
2-Oxocarboxylic acid metabolism	5	0.9	ath01210
Flavonoid biosynthesis	5	0.9	ath00941
Glycolysis/Gluconeogenesis	5	0.9	ath00010
Carotenoid biosynthesis	5	0.9	ath00906
Cysteine and methionine metabolism	5	0.9	ath00270
Protein processing in endoplasmic reticulum	5	0.9	ath04141
Phenylalanine metabolism	4	0.8	ath00360
Tropane. piperidine and pyridine alkaloid biosynthesis	4	0.8	ath00960
Sulfur metabolism	4	0.8	ath00920
Purine metabolism	4	0.8	ath00230
Valine. leucine and isoleucine degradation	4	0.8	ath00280
Sesquiterpenoid and triterpenoid biosynthesis	4	0.8	ath00909
Beta-Alanine metabolism	3	0.6	ath00410
SNARE interactions in vesicular transport	3	0.6	ath04130
Fatty acid degradation	3	0.6	ath00071
Fatty acid metabolism	3	0.6	ath01212
Pentose phosphate pathway	3	0.6	ath00030
Ubiquinone and other terpenoid-quinone biosynthesis	3	0.6	ath00130
Propanoate metabolism	3	0.6	ath00640
Pyruvate metabolism	3	0.6	ath00620
Taurine and hypotaurine metabolism	3	0.6	ath00430

(Continued)

TABLE 2 | Continued

KEGG Pathway	Number	Percent	Pathway ID
Ascorbate and aldarate metabolism	3	0.6	ath00053
Alpha-Linolenic acid metabolism	3	0.6	ath00592
Fatty acid biosynthesis	3	0.6	ath00061
Carbon fixation in photosynthetic organisms	3	0.6	ath00710
Steroid biosynthesis	3	0.6	ath00100
Galactose metabolism	3	0.6	ath00052
Tyrosine metabolism	3	0.6	ath00350
Inositol phosphate metabolism	2	0.4	ath00562
Selenocompound metabolism	2	0.4	ath00450
Monobactam biosynthesis	2	0.4	ath00261
Isoquinoline alkaloid biosynthesis	2	0.4	ath00950
Protein export	2	0.4	ath03060
Linoleic acid metabolism	2	0.4	ath00591
RNA degradation	2	0.4	ath03018
Peroxisome	2	0.4	ath04146
Fructose and mannose metabolism	2	0.4	ath00051
Arachidonic acid metabolism	1	0.2	ath00590
Citrate cycle (TCA cycle)	1	0.2	ath00020
Alanine. aspartate and glutamate metabolism	1	0.2	ath00250
Transporters	1	0.2	ath02010
Riboflavin metabolism	1	0.2	ath00740
Lysine degradation	1	0.2	ath00310
Flavone and flavonol biosynthesis	1	0.2	ath00944
Glyoxylate and dicarboxylate metabolism	1	0.2	ath00630
Zeatin biosynthesis	1	0.2	ath00908
Vitamin B6 metabolism	1	0.2	ath00750
Valine. leucine and isoleucine biosynthesis	1	0.2	ath00290
Terpenoid backbone biosynthesis	1	0.2	ath00900
Biosynthesis of unsaturated fatty acids	1	0.2	ath01040
Circadian rhythm—plant	1	0.2	ath04712
Stilbenoid. diarylheptanoid and gingerol biosynthesis	1	0.2	ath00945
Pantothenate and CoA biosynthesis	1	0.2	ath00770
Butanoate metabolism	1	0.2	ath00650
Indole alkaloid biosynthesis	1	0.2	ath00901
Phagosome	1	0.2	ath04145
Glycerophospholipid metabolism	1	0.2	ath00564
Lysine biosynthesis	1	0.2	ath00310

metabolism and adapts amino acid and sugar metabolism to being inside a host. mRNA for several enzymes employed in degradation of the plant cell wall, such as the cell wall glycosyl-hydrolase *YteR* (Moore et al., 2016), were up-regulated as shown previously. Genes involved in processes such as oxidative phosphorylation, ribosome formation, RNA transport and degradation or proteasome functions were preferentially down-regulated in the co-cultivated fungus. Closer inspection of the data supports the idea that the fungus down-regulates genes for essential processes (primary sucrose, N and P metabolism, ion homeostasis, redox processes, defense, and secondary metabolites) perhaps because of its increasing reliance on the plant. Reduced defense gene activation may indicate that the fungus prevents the synthesis of compounds that restrict its growth and propagation in the host.

V. dahliae Growth Is Reduced in *Arabidopsis* JA Mutants

Former studies indicate that the accumulation and perception of jasmonates are key events for both plant and fungal responses to the interaction. The plant defense machinery is activated by an elevation of jasmonates and activation of the receptor COI1, while the fungus activates the plant COI1-dependent JA pathway to induce disease symptom development in the host (Feys et al., 1994; Xie et al., 1998; Ralhan et al., 2012). Upregulation of genes involved in JA biosynthesis and responses within the first 24 h of co-cultivation demonstrates that the course is already set even before significant changes in the plant hormone levels can be detected (cf. below). We observed several DEGs involved in the α-linolenic acid pathway as well as in plant hormone signal transduction pathways (**Table 2** and **Figure 2A**). While the expression of growth-associated genes like the auxin-responsive genes *ARF5* (Krogan et al., 2016) and several members of the *GH3*-family (e.g., *GH3.17, GH3.4, DFL2, WES1*, Staswick et al., 2005) was decreased, an up-regulation of the JA biosynthetic genes *LIPOXYGENASE 3* and *4* (*LOX3* and *4*, Acosta and Farmer, 2010; Umate, 2011) and *OXOPHYTODIENOATE-REDUCTASE 3* (*OPR3*, Müssig et al., 2000) as well as of an ET response factor (*ERF1*, Fujimoto et al., 2000) was observed.

To further investigate the role of JA in the *Arabidopsis-V. dahliae* interaction, we analyzed the phenotype and vitality of *Verticillium*-infected JA mutants *jar1* (Staswick et al., 1992; Staswick and Tiryaki, 2004), *coi1-16* (Ellis and Turner, 2002), and *cyp94B3* (Koo et al., 2011). Although there was no visual difference between the mutants and the WT plants 10 *dpi*, the WT plants were dead after 20 *dpi*, while the mutant plants showed disease symptoms in leaves but were still vital and alive (**Figure 3**). This result was confirmed by analysis of the efficiency of the electron transfer during photosynthesis using chlorophyll fluorescence measurements, a sensitive marker for plant vitality (**Figure 4**). At 10 *dpi*, there were only small differences between the mutants and the WT, and chlorophyll fluorescence values around 0.81 indicate that the plants were capable of photosynthesis. At 20 *dpi*, the JA mutants still possessed a fluorescence value between 0.81 and 0.83, while WT plants were at 0.24 corresponding to very low levels of electron transport and photosynthetic efficiency. Thus, these non-invasive measurements provide an efficient tool to determine and quantify disease development in *Verticillium*-infected hosts. To obtain further insight into the colonization efficiency of *V. dahliae*, the content of fungal RNA—in the plants previously analyzed for chlorophyll fluorescence—was determined in roots and shoots separately, and the levels

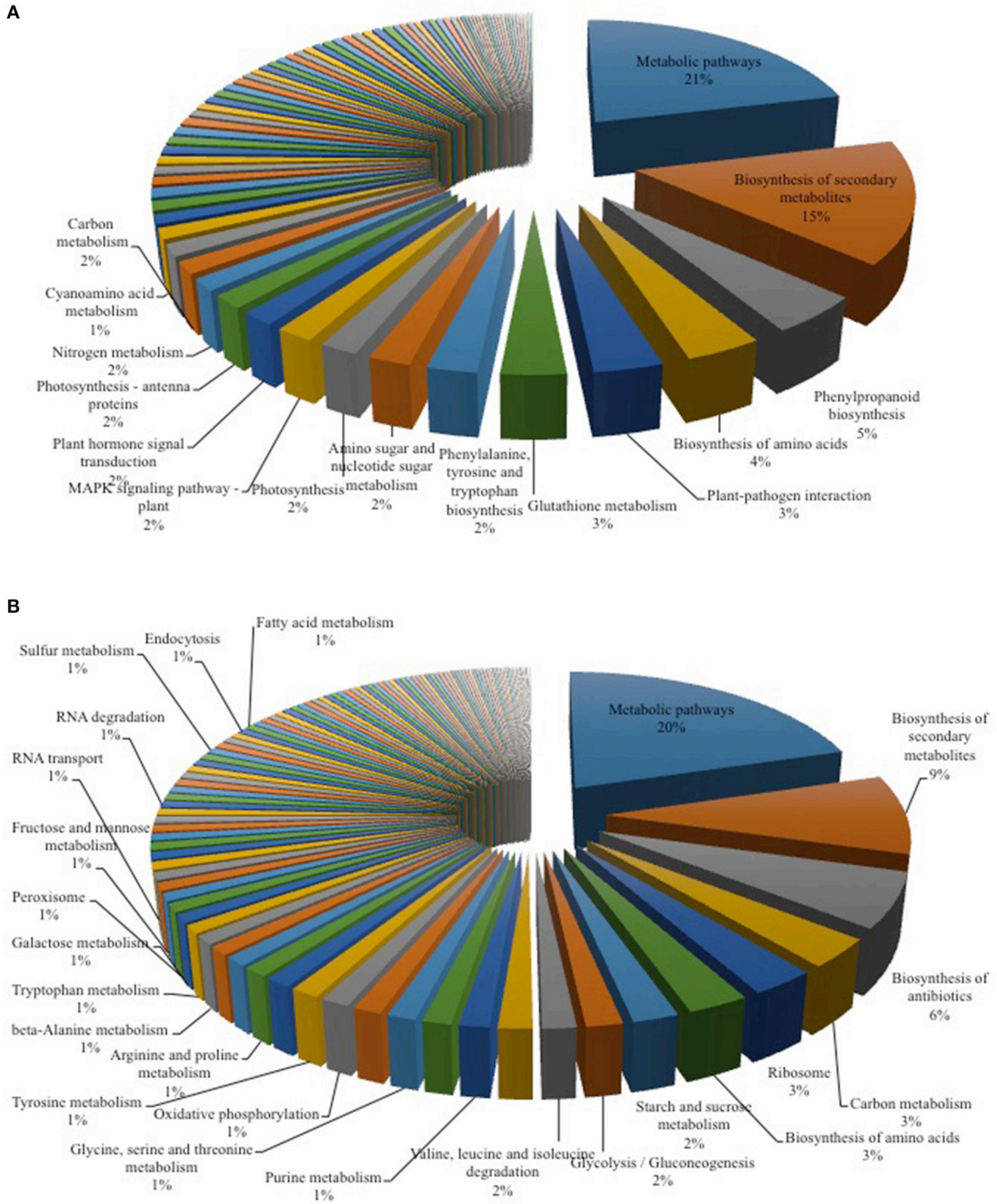

FIGURE 2 | KEGG Mapper analysis of RNA-seq data for *Arabidopsis-Verticillium* co-culture. Shown are the mapped pathways ($n = 3$) for differentially expressed genes in *Arabidopsis* alone vs. co-culture **(A)** and *Verticillium* alone vs. co-culture **(B)**. A full list of the other regulated pathways is shown in **Tables 2**, **3**.

were compared to those in WT plants (Figure S2). The colonization pattern at the two tested time points was very different. While *coi1-16* and *cyp94B3* roots showed a significantly lower colonization at 10 *dpi* compared to WT (38 and 30%, respectively), *jar1* roots showed an intermediate level with 83% (Figure S2A). The respective shoots of the plants show the same trend (Figure S2B). At 20 *dpi*, no difference in colonization of the mutant shoots was detectable; all of them showed significantly lower fungal RNA levels compared to the WT (Figure S2D). The levels of fungal RNA in the roots of *coi1-16* plants was significantly lower compared to those of all other genotypes.

TABLE 3 | KEGG pathway classification of genes differentially expressed in *Verticillium* alone vs. co-culture.

KEGG Pathway	Number	Percent	Pathway ID
Metabolic pathways	344	20.4	vda01100
Biosynthesis of secondary metabolites	151	9.0	vda01110
Biosynthesis of antibiotics	104	6.2	vda01130
Carbon metabolism	55	3.3	vda01200
Ribosome	50	3.0	vda03010
Biosynthesis of amino acids	47	2.8	vda01230
Starch and sucrose metabolism	35	2.1	vda00500
Glycolysis/Gluconeogenesis	28	1.7	vda00010
Valine. leucine and isoleucine degradation	26	1.5	vda00280
Pentose and glucuronate interconversions	26	1.5	vda00040
Purine metabolism	23	1.4	vda00230
Amino sugar and nucleotide sugar metabolism	22	1.3	vda00520
Glycine. serine and threonine metabolism	22	1.3	vda00260
Pyruvate metabolism	22	1.3	vda00620
Oxidative phosphorylation	22	1.3	vda00190
Tyrosine metabolism	22	1.3	vda00350
Cysteine and methionine metabolism	20	1.2	vda00270
Arginine and proline metabolism	19	1.1	vda00330
Glycerolipid metabolism	18	1.1	vda00561
Propanoate metabolism	17	1.0	vda00640
Beta-Alanine metabolism	17	1.0	vda00410
Tryptophan metabolism	16	0.9	vda00380
Galactose metabolism	16	0.9	vda00052
Peroxisome	16	0.9	vda04146
Methane metabolism	15	0.9	vda00680
Fructose and mannose metabolism	15	0.9	vda00051
Butanoate metabolism	15	0.9	vda00650
Cyanoamino acid metabolism	15	0.9	vda00460
RNA transport	14	0.8	vda03013
2-Oxocarboxylic acid metabolism	14	0.8	vda01210
Histidine metabolism	13	0.8	vda00340
Protein processing in endoplasmic reticulum	13	0.8	vda04141
Alanine. aspartate and glutamate metabolism	13	0.8	vda00250
Ribosome biogenesis in eukaryotes	12	0.7	vda03008
RNA degradation	12	0.7	vda03018
Steroid biosynthesis	12	0.7	vda00100
Phenylalanine metabolism	12	0.7	vda00360
Lysine degradation	12	0.7	vda00310
Pentose phosphate pathway	12	0.7	vda00030
Fatty acid degradation	11	0.7	vda00071
Glyoxylate and dicarboxylate metabolism	11	0.7	vda00630
Glycerophospholipid metabolism	11	0.7	vda00564
Sulfur metabolism	11	0.7	vda00920
Pantothenate and CoA biosynthesis	11	0.7	vda00770
Nicotinate and nicotinamide metabolism	10	0.6	vda00760
Autophagy—yeast	9	0.5	vda04138
Endocytosis	9	0.5	vda04144
Fatty acid metabolism	9	0.5	vda01212
Phenylalanine. tyrosine and tryptophan biosynthesis	8	0.5	vda00400
Ubiquinone and other terpenoid-quinone biosynthesis	8	0.5	vda00130
Valine. leucine and isoleucine biosynthesis	8	0.5	vda00290
Porphyrin and chlorophyll metabolism	8	0.5	vda00860
Spliceosome	8	0.5	vda03040
Pyrimidine metabolism	7	0.4	vda00240
Arginine biosynthesis	7	0.4	vda00220
Nitrogen metabolism	7	0.4	vda00910
Aminoacyl-tRNA biosynthesis	7	0.4	vda00970
Glutathione metabolism	6	0.4	vda00480
Folate biosynthesis	6	0.4	vda00790
Ubiquitin mediated proteolysis	6	0.4	vda04120
Terpenoid backbone biosynthesis	6	0.4	vda00900
Nucleotide excision repair	6	0.4	vda03420
Citrate cycle (TCA cycle)	6	0.4	vda00020
Other glycan degradation	5	0.3	vda00511
Mitophagy—yeast	5	0.3	vda04139
Base excision repair	5	0.3	vda03410
Taurine and hypotaurine metabolism	5	0.3	vda00430
Proteasome	5	0.3	vda03050
Sphingolipid metabolism	5	0.3	vda00600
MAPK signaling pathway—yeast	5	0.3	vda04011
Various types of N-glycan biosynthesis	5	0.3	vda00513
Phagosome	5	0.3	vda04145
Ascorbate and aldarate metabolism	5	0.3	vda00053
Fatty acid elongation	4	0.2	vda00062
Riboflavin metabolism	4	0.2	vda00740
SNARE interactions in vesicular transport	4	0.2	vda04130
N-Glycan biosynthesis	4	0.2	vda00510
One carbon pool by folate	4	0.2	vda00670
Vitamin B6 metabolism	4	0.2	vda00750
mRNA surveillance pathway	4	0.2	vda03015
Carotenoid biosynthesis	4	0.2	vda00906
Linoleic acid metabolism	3	0.2	vda00591
Ether lipid metabolism	3	0.2	vda00565
Meiosis—yeast	3	0.2	vda04113
Synthesis and degradation of ketone bodies	3	0.2	vda00072
Cell cycle—yeast	3	0.2	vda04111
Glycosylphosphatidylinositol (GPI)-anchor biosynthesis	3	0.2	vda00563
Arachidonic acid metabolism	3	0.2	vda00590
Sulfur relay system	3	0.2	vda04122
Basal transcription factors	3	0.2	vda03022
Thiamine metabolism	3	0.2	vda00730
Selenocompound metabolism	3	0.2	vda00450
Glycosphingolipid biosynthesis—globo and isoglobo series	3	0.2	vda00603
Phosphonate and phosphinate metabolism	2	0.1	vda00440
Non-homologous end-joining	2	0.1	vda03450
RNA polymerase	2	0.1	vda03020
Autophagy—other	2	0.1	vda04136

(Continued)

TABLE 3 | Continued

KEGG Pathway	Number	Percent	Pathway ID
Biosynthesis of unsaturated fatty acids	2	0.1	vda01040
Alpha-Linolenic acid metabolism	2	0.1	vda00592
Lysine biosynthesis	2	0.1	vda00300
DNA replication	2	0.1	vda03030
Protein export	2	0.1	vda03060
Inositol phosphate metabolism	2	0.1	vda00562
Biotin metabolism	2	0.1	vda00780
Mismatch repair	2	0.1	vda03430
Mannose type O-glycan biosynthesis	1	0.1	vda00515
Lipoic acid metabolism	1	0.1	vda00785
Other types of O-glycan biosynthesis	1	0.1	vda00514
Phosphatidylinositol signaling system	1	0.1	vda04070
Monobactam biosynthesis	1	0.1	vda00261
Fatty acid biosynthesis	1	0.1	vda00061
Sesquiterpenoid and triterpenoid biosynthesis	1	0.1	vda00909
Caffeine metabolism	1	0.1	vda00232
AGE-RAGE signaling pathway in diabetic complications	1	0.1	vda04933
Carbapenem biosynthesis	1	0.1	vda00332
ABC transporters	1	0.1	vda02010
Glycosaminoglycan degradation	1	0.1	vda00531

Root Colonization and Plant Hormone Levels Are Not Altered after the First 24 h of Co-culture with *V. dahliae*

To compare the colonization of the mutant plants in the very early phase, the content of fungal RNA was also analyzed 24 h after co-cultivation (**Figure 5**). All plants showed a similar fungal colonization with no statistically significant differences (**Figure 5A**). Compared to the WT colonization level (set as 100%), *jar1* plants showed a colonization of 90.0%, *coi1-16,* and *cyp94B3* of 121.4 and 129.8%, respectively (**Figure 5B**). These results suggest that there are also no differences in plant JA levels during the first 24 h of co-culture.

In a previous study we demonstrated that *V. dahliae* infection leads to an elevation of JA, JA-Ile, and SA 21 *dpi* (Sun et al., 2014). To analyze whether the accumulation of these phytohormones was already induced in the first 24 h, leaf tissue of WT and the mutants was analyzed, but the content of SA (**Figure 6A**) and JA-Ile (**Figure 6C**) were found not to be significantly induced by the fungus. There was also no difference in the JA content in WT, *coi1-16* and *cyp94B3*, while a slight difference was observed in *jar1* plants. Accumulation of JA in this mutant is caused by the inactivation of the Ile-conjugating enzyme. These data confirm that the changes in the gene expression profiles described above occur before the fungus induces changes in the plant phytohormone levels. Thus, the identified genes respond most likely to fungal signals and not to fungus-induced phytohormone changes in the plant. JA signaling in the host is necessary for disease development only during later phases of the interaction, which can be strongly repressed or retarded when JA function is impaired.

Gene Expression in JA Mutants Is Different to That in the WT in the Early Phase of Colonization

To validate the RNA-seq results obtained, the expression of selected regulated genes in the data set was analyzed by RT-qPCR for co-cultivated WT plants (**Figure 7**) and for the fungus (**Figure 8**). Highly regulated members of the SWEET family (Chen et al., 2010) and a Wall-Associated Kinase-like gene (*WAKL10*, Meier et al., 2010) were chosen for the plant and *VDAG_02979* (a glucose transporter) and *VDAG_06565* (poly-A-ribonuclease, PARN) for the fungus. In the RNA-seq analysis, the expression of *WAKL10* was 56-fold induced in *V. dahliae*-infested plants compared to plants grown alone. A 10-fold induction was observed in the RT analysis (**Figure 7A**). *SWEET11* and *-3* were 20- and 10-fold downregulated in the RNA-seq data set, respectively, while a 9.7- and 6.8-fold decrease was detected by RT-qPCR (**Figures 7B,C**). Interestingly, the expression of these genes was differently regulated in the JA mutants. The expression of *WAKL10* was induced ∼100-fold in *jar1*, i.e., significantly higher than in WT seedlings, while *SWEET3*, which is down-regulated in the WT, was induced 17-fold in the mutant (**Figure 7**). Additionally, *SWEET11* was less repressed in the mutants: for *jar1*, the repression was 50% lower compared to WT plants. This clearly indicates that the expression of interaction-specific plant genes is influenced by JA content.

The RNA-seq results for the fungal genes were also validated by RT-qPCR analysis (**Figure 8**). The mRNA levels of *VDAG_02979* (RNA-seq: + 200-fold; RT-qPCR: + 120-fold) and *VDAG_06565* (RNA-seq: + 3-fold; RT-qPCR: + 27-fold) in response to the fungus showed the same trend. Again, when co-cultivation was performed with the JA mutants, the expression of both genes was less induced compared to WT plants (**Figure 8**). Thus, both partners require plant JA for the typical regulation of genes that respond to the symbiotic interaction.

DISCUSSION

V. dahliae Is in the Pre-vascular Growth Phase 24 h after Co-cultivation with *Arabidopsis*

The propagation of *Verticillium* species within their hosts is characterized by a biphasic interaction: initially a biotrophic phase allows rapid growth of the microbe in the xylem without major effects on plant performance followed by a necrotrophic phase in which the host is ultimately killed (Reusche et al., 2012). Analysis of the initial contact and early phase of the interaction between both partners could lead to the identification of target genes that will help understand further phases of the interaction and provide useful targets for pest control. Confocal analysis 24 h after co-cultivation demonstrated that the pathogen colonizes the root efficiently (**Figure 1**) by developing a dense hyphal network at the root surface and root tip. In areas of lateral

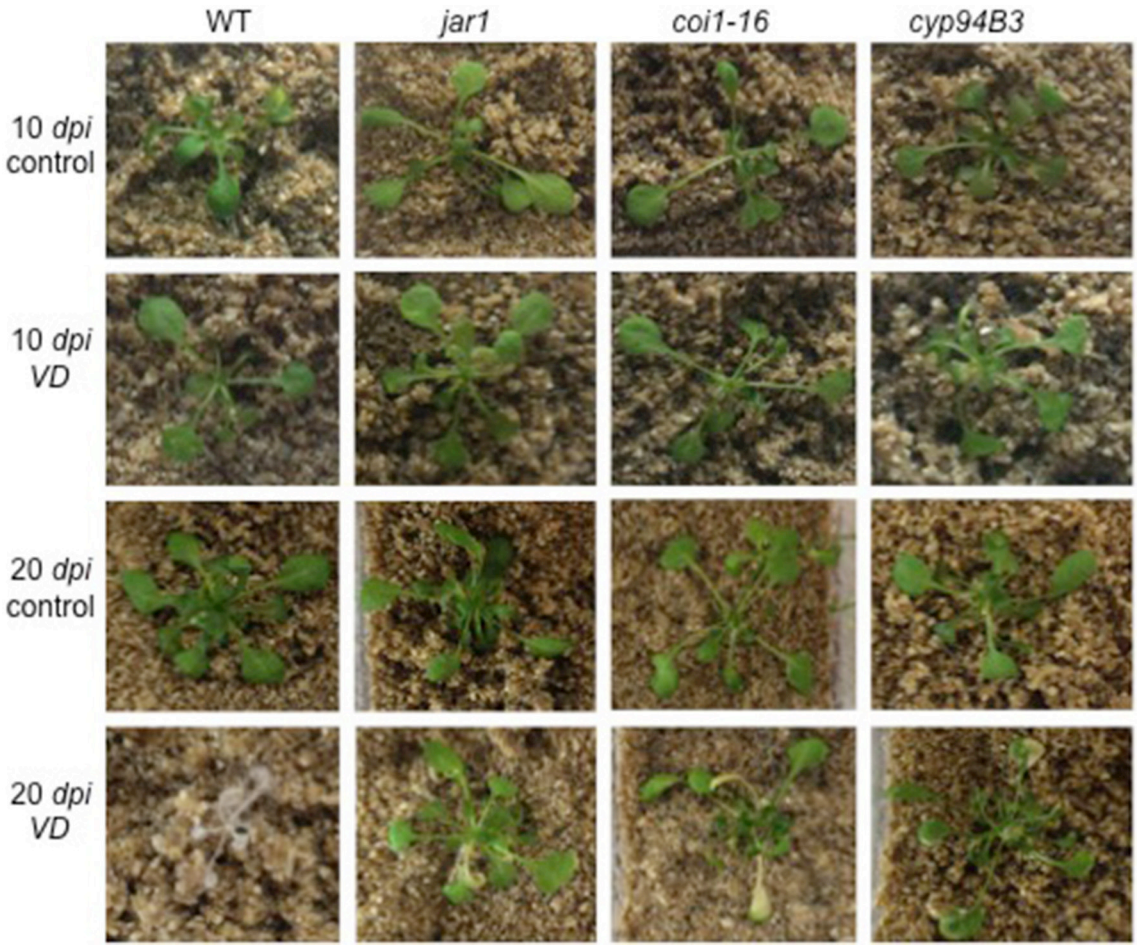

FIGURE 3 | Phenotype of *V. dahliae (VD)*-infected *Arabidopsis* WT and JA mutant plants. Shown are representative phenotypes of WT, *jar1*, *coi1-16,* and *cyp94B3* plants 10 (upper two rows) and 20 *dpi* (lower two rows) grown in Magenta boxes. 14 day-old plants were treated with water (control, $n = 6$) or *VD* ($n = 9$) for 24 h and then transferred to the boxes.

root formation, an accumulation of conidia spores was detectable (**Figures 1G–I**). This matches previous observations that showed the lateral root to be a primary area of *Verticillium* infection in diverse host plants (Zhou et al., 2006; Vallad and Subbarao, 2008; Zhao et al., 2014). Further analyses of root cross-sections demonstrated that the fungus invades the plant tissue but did not reach the vascular system within the first 24 h of co-culture (**Figures 1J–O**). We conclude that the fungus was still growing in the pre-vascular phase during our experiments, optimal for the identification of genes regulated during the very early interaction phase. During this period we also did not observe significant differences in phytohormone levels, which is consistent with the microscopic information.

Initial Contact of *Arabidopsis* and *V. dahliae* Leads to Reprogramming of Primary Metabolism in Both Organisms

Plant-pathogen interactions involve an adaptation of both partners. While the plant typically recognizes the pathogen and induces appropriate defense responses, the fungus manipulates the biology of its host to gain sufficient nutrients for growth and reproduction (Boyd et al., 2013). To identify early targets in the *Arabidopsis—V. dahliae* interaction, an RNA-seq analysis after 24 h of co-cultivation was performed for both partners. This time point was chosen because no structural changes were detected in plant and fungal tissues under the microscope, and because the phytohormone levels in the plant were not yet altered, thereby avoiding secondary effects due to the response of the plant genome to an altered phytohormone environment. We detected 4432 DEGs for both organisms (**Table 1,** Tables S1–S4), 1143 DEGs in *Arabidopsis* belong mainly to primary metabolic pathways (21%, **Figure 2A**). This result is comparable to a recent study in cotton where 26% of the DEG reads could be assigned to metabolic pathways (Zhang W. W. et al., 2017). Comparably, in both studies, pathways associated with plant-pathogen interaction (3%) and plant hormone signal transduction (2%) were also regulated upon *Verticillium* stress.

Several members of the plant sucrose efflux transporters of the SWEET family were highly regulated in the analyzed interaction.

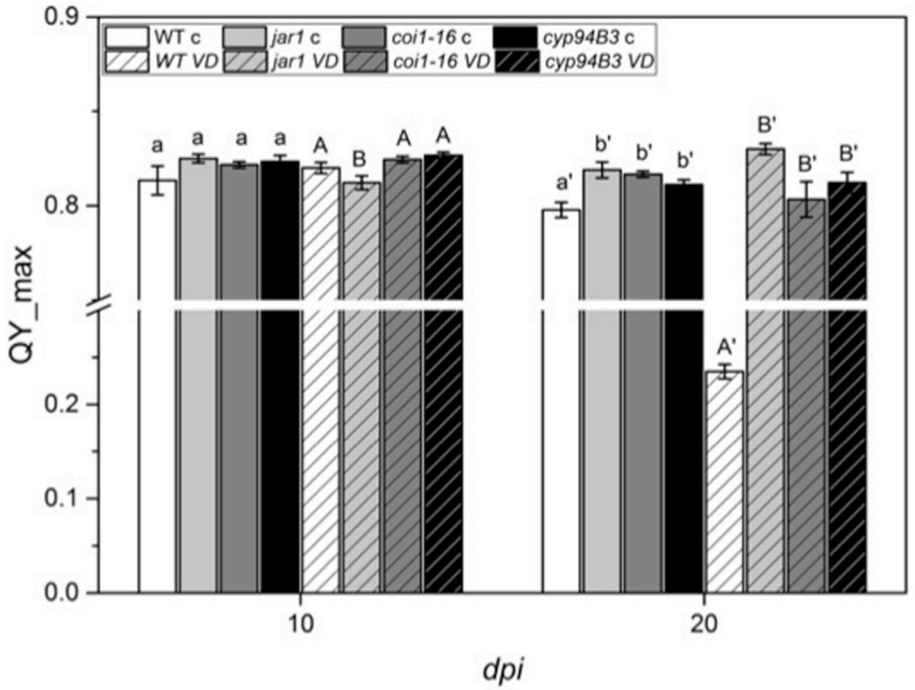

FIGURE 4 | Chlorophyll fluorescence (QY_max) analysis of *Arabidopsis* WT and JA mutant plants after 24 h of *V. dahliae* infection. Shown are the QY_max values [± SE, $n = 6$ (control) and 9 (*VD*-infected)] in control (plain color) and *VD*-infected (stripes) plants 10 and 20 *dpi*. QY_max was analyzed in WT (white), *jar1* (light gray), *coi1-16* (dark gray) and *cyp94B3* (black) plants. Statistically significant differences between controls and between infected plants were analyzed by one-way ANOVA separately, $p < 0.05$ (Sidak). Different letters indicate a statistically significant difference.

SWEET11 as well as *–3, −12, −15,* and *–8* were downregulated in decreasing order (Table S2). SWEET11 and −12 are involved in phloem loading with sugars (Chen et al., 2010, 2012; Boyd et al., 2013). By silencing of *OsSWEET11* in rice it could be demonstrated that the growth of *Xanthomonas oryzae pv. oryzae* (Xoo) is decreased which resulted in more resistant plants (Yang et al., 2006). Also *SWEET3* was reported to be involved in defense and was downregulated after Geminivirus infection (Ascencio-Ibá-ez et al., 2008). These observations suggest that the plant is trying to prevent export of its sugars to restrict fungal growth.

Besides the defense genes discussed above, members of the *WAK* family are also highly represented in our data sets. *WAK-L10 and WAK3*, *–5*, *−1,* and *−4* responded to *Verticillium* treatment (in declining order, Table S1). *WAK1* is induced upon infection with *Ps. maculicola* ES4326 and the protein stimulated *PR1* expression (He et al., 1998). Additionally, *WAK1*, *−2*, *−3,* and *−5* are inducible by SA which accumulated during pathogen infection (He et al., 1999). Likewise, the WAK-like gene *WAKL10* is SA-induced and involved in defense against bacteria and fungi (Meier et al., 2010). Among the genes involved in controlling Ca^{2+} homeostasis, genes for in- and efflux transporters of the cyclic nucleotide-gated channel (CNGC), autoinhibited Ca^{2+}-ATPase (ACA), and glutamate-like receptor (GLR) protein families responded to the fungus, indicating that many signaling events induced during the early phase of the interaction are Ca^{2+}-dependent. Consistent with this idea, genes for Ca^{2+}-binding proteins involved in signal perception and propagation showed increased expression, especially members of the calmodulin-like (CML) protein family. However, closer inspection of the genes did not allow any meaningful conclusion about which pathways are major targets of the fungus. Besides regulation of defense responses, many genes for Ca^{2+}-binding proteins are involved in ion homeostasis, enzyme activity control, and biotrophic plant/microbe interactions (for details compare genes in Table S1 with the TAIR database). An induction of defense genes is always accompanied by a lower investment in plant growth (Huot et al., 2014). This is reflected by the down-regulation of *ROOT CAP POLYGALACTURONASE28* and enzymes involved in cytokinin signaling. The phase of reprogramming of plant primary metabolism lasts for several days, as in *Verticillium*-infected tomato plants where it was shown that both gene expression and protein synthesis of metabolic pathways proteins are still down-regulated at 7 *dpi* (van Esse et al., 2009; Witzel et al., 2017). The global transcriptome analysis performed in this study provides significant insights into components involved in early phases of the *Arabidopsis—V. dahliae* interaction and suggests a number of genes and pathways that could be employed as markers in breeding for wilt tolerance.

In contrast to previous studies focusing on analysis of the plant's reaction to the fungus (van Esse et al., 2009; Faino et al., 2012; Witzel et al., 2017; Zhang W. W. et al., 2017), we present also DEGs from the fungus caused by response to the plant. The majority of the 3289 DEGs code for proteins with unknown

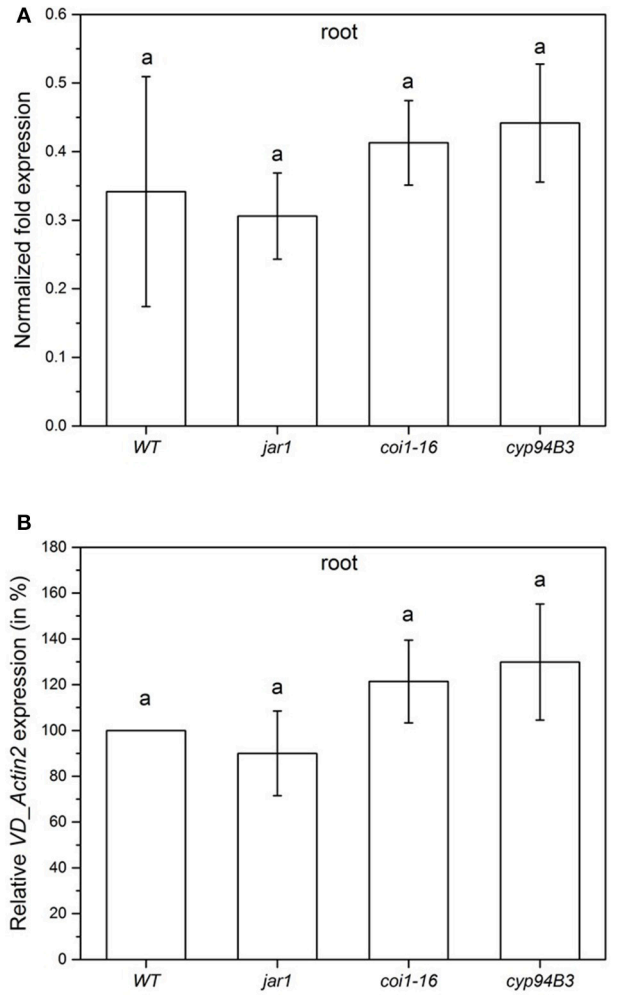

FIGURE 5 | Colonization of *Arabidopsis* WT and JA mutant plants by *V. dahliae* after 24 h. Shown is the normalized fold expression (± SE, $n = 3$) of *VD_Actin2* in *VD*-infected WT, *jar1*, *coi1-16* and *cyp94B3* plants **(A)** and the relative expression in % **(B)**. The expression level of *VD_Actin2* in *VD*-infected WT plants was used as control and set to 1.0. The mRNA levels for each cDNA probe were normalized with respect to the *RPS18B* mRNA level. Statistically significant differences between the mutants were analyzed by one-way ANOVA, $p < 0.05$ (Sidak). Different letters indicate a statistically significant difference.

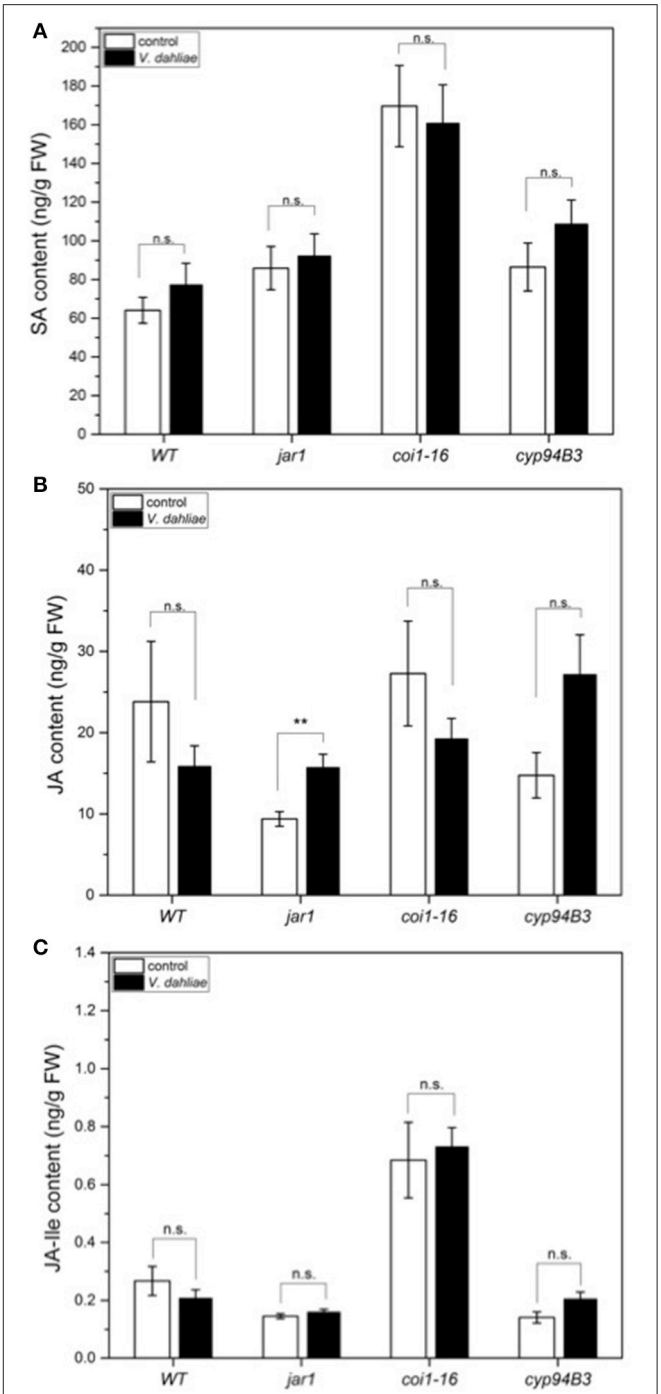

FIGURE 6 | Phytohormone levels in *Arabidopsis* WT and JA mutant plants after 24 h of *V. dahliae* infection. Shown is the content (± SE, $n = 10$) of SA **(A)**, JA **(B),** and JA-Ile **(C)** in control (white) and *VD*-infected (black) WT, *jar1*, *coi1-16,* and *cyp94B3* plants. Statistically significant differences were analyzed by Mann Whitney U-test, $p < 0.05$; n.s. not significant, $^{**}p < 0.01$.

functions (Tables S3, S4). The up-regulation of *VDAG_02979*, which encodes for a glucose transporter, suggests that it might play an important role in the early interaction. Besides this initial observation, a huge number of identified genes belong to families which might become important targets after elucidation of their function in *V. dahliae*. Therefore, this list might provide useful information for genes with interaction-specific functions, in particular since the knowledge about the function of *V. dahliae* genes is strongly increasing. For example, very recent studies revealed that homeodomain and bZIP transcription factors (Fang et al., 2017; Sarmiento-Villamil et al., 2017), two less characterized transcription factors (Sarmiento-Villamil et al., 2010; Zhang W. Q. et al., 2017), polyketide synthases (Zhang T. et al., 2017), endochitinases (Cheng et al., 2017), a novel *V. dahliae* protein that targets the plant nucleus (Zhang L. et al., 2017), LysM effectors (Kombrink et al., 2017), a isochorismatase hydrolase (Zhu et al., 2017), a factor involved in the fungal

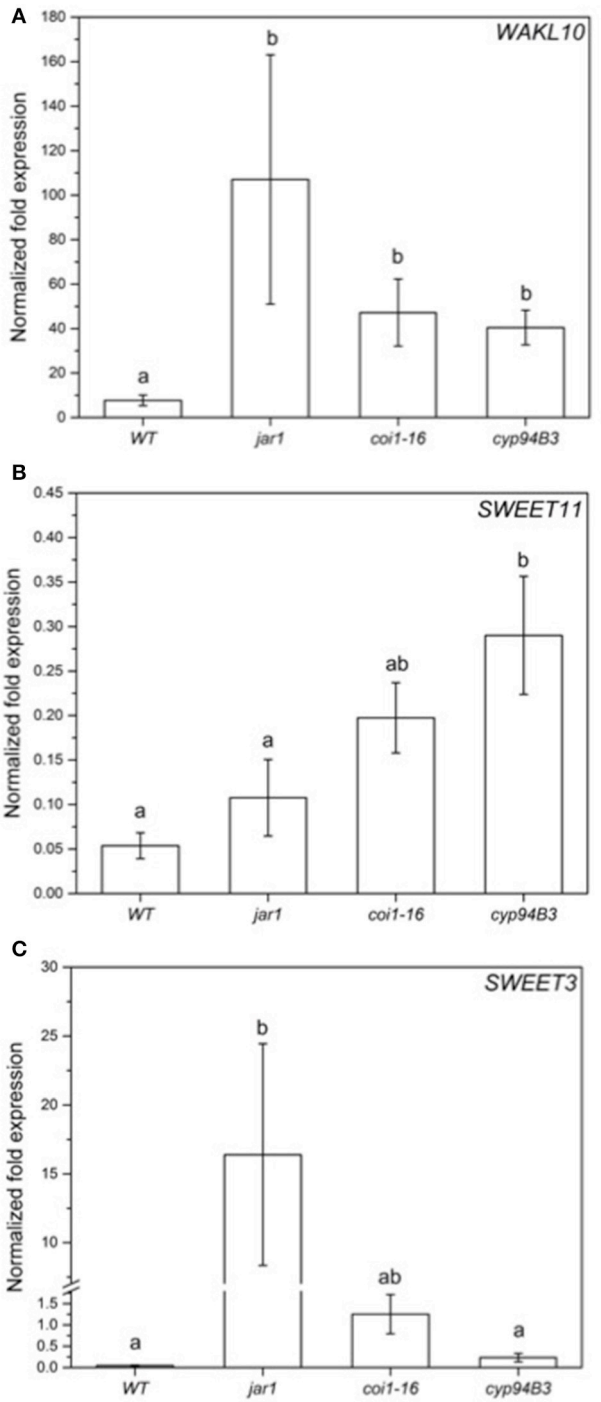

FIGURE 7 | Expression of selected genes in *Arabidopsis* WT and JA mutant plants after 24 h of *V. dahliae* infection. Shown is the normalized fold expression (± SE, $n = 3$) of *WAKL10* **(A)**, *SWEET11* **(B),** and *SWEET3* **(C)** in *VD*-infected WT, *jar1*, *coi1-16,* and *cyp94B3* plants. The expression level of genes of interest (GOIs) in water-treated plants was used as control and set to 1.0. The mRNA levels for each cDNA probe were normalized with respect to the *RPS18B* mRNA level. Statistically significant differences between the mutants were analyzed by one-way ANOVA, $p < 0.05$ (Sidak). Different letters indicate a statistically significant difference.

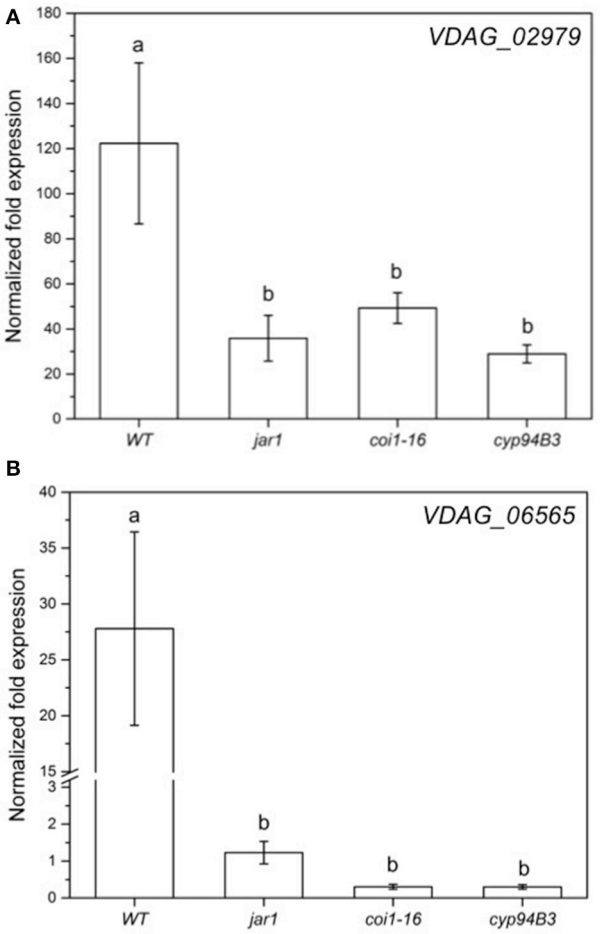

FIGURE 8 | Expression of selected genes in *V. dahliae* after colonizing *Arabidopsis* WT and JA mutant plants for 24 h. Shown is the normalized fold expression (± SE, $n = 3$) of *VDAG_02979* **(A)** and *VDAG_06565 (PARN)* **(B)** in *VD*-colonized WT, *jar1*, *coi1-16,* and *cyp94B3* plants. The expression level of GOIs in *VD* alone was used as control and set to 1.0. The mRNA levels for each cDNA probe were normalized with respect to the *VD_Actin2* mRNA level. Statistically significant differences between the mutants were analyzed by one-way ANOVA, $p < 0.05$ (Sidak). Different letters indicate a statistically significant difference.

secretory pathway (Xie et al., 2017), a RACK1-like protein involved in root entry (Yuan et al., 2017), pathogenesis-related exudated proteins (Chen et al., 2016), and the mitogen-activated protein kinase 2 (Tian et al., 2016) are important components in controlling *V. dahliae*-induced disease development in various plant species. Members of all these protein families can be found in the list of *V. dahliae* genes up-regulated after infection of *Arabidopsis*.

JA Mutants Are Less Susceptible to *Verticillium* Infection

Various studies have shown the involvement of several classes of plant hormones in the control of *Verticillium* growth and

propagation in *Arabidopsis*. While ET perception mutants are more susceptible to *Verticillium* infection, an elevation of cytokinins enhances plant resistance (Pantelides et al., 2010; Reusche et al., 2013; Sun et al., 2014). Downregulation of plant genes involved in cytokinin signaling might therefore be induced by the fungus. Interestingly, jasmonates are not only accumulated by the plant to induce defense, but the fungus also requires a JA-independent COI1 function in roots to elicit disease symptoms in *Arabidopsis* shoots (Ralhan et al., 2012). To further analyze the role of JA levels in the interaction of *Arabidopsis* and *V. dahliae*, JA biosynthesis (*jar1*), perception (*coi1-16*) and degradation (*cyp94B3*) mutants were studied. All of these mutants performed better, showed less severe disease symptom development in the leaves at 20 *dpi* compared to the WT control, which were already dead at this time point (**Figure 3**), and had a higher photosynthetic potential, as demonstrated by their QY_max value above 0.80 (F_v/F_m, **Figure 4**) (e.g., Kim et al., 2009; Sztatelman et al., 2015). The observation, that *jar1* plants performed better than WT plants, contradicts earlier findings where *jar1* plants were as susceptible as WT plants (Fradin et al., 2011). To analyze this contradiction, the colonization of the mutants used was compared to WT plants (Figure S2). While there was no difference to the WT colonization level after 10 *dpi* in the roots and the shoots, there was a significant difference at 20 *dpi*. The colonization level of the root was similar to WT while the colonization in the shoots was significantly lower in *jar1* (Figure S2D). This observation could explain the better performance of the aerial parts of the *jar1* plants. Taken together, the altered expression of the interaction-specific genes of plant and fungal origin in the JA mutants confirms the important role of this phytohormone also during early phases. Apparently, the altered expression profile occurs before a significant change in phytohormone levels become detectable.

To gain insight into the growth behavior of *V. dahliae* on JA mutants during the first 24 h of co-cultivation, the colonization of the roots was analyzed. The detected differences in the colonization (**Figure 5**) were not significant at this time point, but may have a greater impact in later phases where a clear difference is obvious. After 24 h of co-cultivation, there was also no detectable difference in the levels of the phytohormones SA, JA and JA-Ile (**Figure 6**). Since changes in phytohormone levels upon pathogen attack are normally very rapid in plants, *Arabidopsis* might have not yet recognized the microbe as friend or foe, in spite of the already initiated reprogramming of its gene expression pattern. It is also conceivable that the penetration rate is still too low to induce the accumulation of JA and JA-Ile, since this is often associated with wounding or pathogen-induced cell disruption, which was not visible in our microscopic studies (e.g., Suza and Staswick, 2008; Koo et al., 2009). The biphasic interaction with an initial biotrophic period followed by a necrotrophic period may also leave the plant undecided whether it responds to the pathogen with SA- or JA-dependent defense strategies. Furthermore, both phytohormones cross-talk (Thaler et al., 2012; Proietti et al., 2013).

The low content of active JA-Ile in *jar1* plants and the reduced perception in the receptor mutant *coi1-16* lead to a decreased activation of the downstream signaling pathway by the receptor complex SCF^{COI1} (Thines et al., 2007). Since *Verticillium* propagation from the roots to the leaves depends on an activated COI pathway (Ralhan et al., 2012), this could be a reason why *Verticillium* causes a reduced leaf growth rate of the JA mutant plants (**Figure 3**). The reduced spread in the green parts of the JA mutants is also reflected in the gene expression analysis of chosen genes for both the plant and the fungus (**Figures 7**, **8**). In the mutant plants, the SA-induced defense gene *WAKL10* is more highly expressed than in WT plants and the downregulation of *SWEET11* is less pronounced (**Figure 7**). In the fungus, both target genes *VDAG_02979* and *VDAG_06565* are more weakly expressed in the mutants than in the WT plants (**Figure 8**). *VDAG_02979* codes for a glucose transporter (http://fungi.ensembl.org/Verticillium_dahliae), which contributes to the nutrient supply of the fungus. The lower growth rate in the mutants may be a consequence of this transporter being less expressed.

In conclusion, biotrophic plant-microbe interactions are characterized by the stimulation of SA, but not JA levels, while the opposite hormone regulation occurs during nectrophophic interactions (reviewed in Chanclud and Morel, 2016). Within the first 24 h of interaction studied here, none of these phytohormone levels increase significantly, while hormone-synthesis related genes, as well as defense-related genes responding to both hormone types are already up-regulated in the host. This suggests that no clear decision has been taken yet about which strategy will follow initial contact. The numerous genes identified during early reprogramming of the fungal and plant development might be crucial for the initiation and propagation of the pest, and thus may be helpful for developing strategies which potentially restrict fungal development after infection. Considering our results, identification of crucial players which control the interaction at early stage is apparently difficult, because many metabolomic pathways are already re-adjusted within the first 24 h of the contact of the two partners.

The strong retardation of disease symptom development in host plants impaired in jasmonate mutants has been attributed to the fact that *Verticillium* stimulates the host JA functions in order to promote host cell death during the later necrotrophic phase. There is a substantial crosstalk between JA and SA signaling in which each hormone inhibits the accumulation and/or function of the other. Complete or strong inhibition of JA functions in the mutants may favor SA accumulation and/or SA signaling function which—in turn—may prolong the biotrophic phase and thus retard necrosis and disease development.

AUTHOR CONTRIBUTIONS

SS: designed and performed the experiments; WS-H: analyzed the RNA-seq data and DEGs; AF: prepared, analyzed, and evaluated samples for confocal microscopy; MR: analyzed the phytohormones; RG, JG, and RO: supervised the projects; RO: coordinated the project; SS, JG, and RO: wrote the manuscript; All authors read and approved the final manuscript.

DATA ACCESS

Raw and calculated RNA-seq data was submitted to NCBIs Gene Expression Omnibus (GEO, http://www.ncbi.nlm.nih.gov/geo/) under the accession number GSE104590.

ACKNOWLEDGMENTS

We like to thank Anna-Sophie Enke for technical assistance and Julia Starke for pre-experiments and set-up of the cultivation method. Special thanks go to Dr. Vladimir Benes and co-workers at GeneCore (http://genecore3.genecore.embl.de/genecore3/index.cfm) for RNA sequencing. This work was supported by the DFG (CRC1127, projects A03 and INF).

SUPPLEMENTARY MATERIAL

The Supplementary Material for this article can be found online at: https://www.frontiersin.org/articles/10.3389/fmicb.2018.00217/full#supplementary-material

REFERENCES

Acosta, I. F., and Farmer, E. E. (2010). Jasmonates. *Arabidopsis Book* 8:e0129. doi: 10.1199/tab.0129

Agrios, G. N. (1997). *Plant Pathology, 4th Edn*. San Diego, CA: Academic Press.

Ascencio-Ibá-ez, J. T., Sozzani, R., Lee, T. J., Chu, T. M., Wolfinger, R. D., Cella, R., et al. (2008). Global analysis of Arabidopsis gene expression uncovers a complex array of changes impacting pathogen response and cell cycle during geminivirus infection. *Plant Physiol.* 148, 436–454, doi: 10.1104/pp.108.121038

Bains, P. S., and Tewari, J. P. (1987). Purification, chemical characterization and host-specificity of the toxin produced by *Alternaria brassicae*. *Physiol. Mol. Plant Pathol.* 30, 259–271. doi: 10.1016/0885-5765(87)90039-7

Berg, G., Fritze, A., Roskot, N., and Smalla, K. (2001). Evaluation of potential biocontrol rhizobacteria from different host plants of *Verticillium dahliae* Kleb. *J. Appl. Microbiol.* 91, 963–971. doi: 10.1046/j.1365-2672.2001.01462.x

Bolger, A. M., Lohse, M., and Usadel, B. (2014). Trimmomatic: a flexible trimmer for Illumina sequence data. *Bioinformatics* 30, 2114–2120. doi: 10.1093/bioinformatics/btu170

Boyd, L. A., Ridout, C., O'Sullivan, D. M., Leach, J. E., and Leung, H. (2013). Plant–pathogen interactions: disease resistance in modern agriculture. *Trends Genet.* 29, 233–240 doi: 10.1016/j.tig.2012.10.011

Bu, B., Qiu, D., Zeng, H., Guo, L., Yuan, J., and Yang, X. (2014). A fungal protein elicitor PevD1 induces Verticillium wilt resistance in cotton. *Plant Cell Rep.* 33, 461–470. doi: 10.1007/s00299-013-1546-7

Chanclud, E., and Morel, J. B. (2016). Plant hormones: a fungal point of view. *Mol. Plant Pathol.* 17 ,1289–1297. doi: 10.1111/mpp.12393

Chen, J. Y., Xiao, H. L., Gui, Y. J., Zhang, D. D., Li, L., Bao, Y. M., et al. (2016). Characterization of the *Verticillium dahliae* exoproteome involves in pathogenicity from cotton-containing medium. *Front Microbiol.* 7:1709. doi: 10.3389/fmicb.2016.01709

Chen, L. Q., Hou, B. H., Lalonde, S., Takanaga, H., Hartung, M. L., Qu, X. Q., et al. (2010). Sugar transporters for intercellular exchange and nutrition of pathogens. *Nature* 468, 527–532. doi:10.1038/nature09606

Chen, L. Q., Qu, X. Q., Hou, B. H., Sosso, D., Osorio, S., Fernie, A. R., et al. (2012). Sucrose efflux mediated by SWEET proteins as a key step for phloem transport. *Science* 335, 207–211. doi: 10.1126/science.1213351

Cheng, X. X., Zhao, L. H., Klosterman, S. J., Feng, H. J., Feng, Z. L., Wie, F., et al. (2017). The endochitinase VDECH from *Verticillium dahliae* inhibits spore germination and activates plant defense responses. *Plant Sci.* 259, 12–23. doi: 10.1016/j.plantsci.2017.03.002

Chini, A., Fonseca, S., Fernandez, G., Adie, B., Chico, J. M., Lorenzo, O., et al. (2007). The JAZ family of repressors is the missing link in JA signalling. *Nature* 448, 666–674. doi: 10.1038/nature06006

Decetelaere , S., Tyvaert, L., França, S. C., and Höfte, M. (2017). Desirable traits of a good biocontrol agent against Verticillium wilt. *Front. Microbiol.* 8:1186. doi: 10.3389/fmicb.2017.01186

Dobin, A., Davis, C. A., Schlesinger, F., Drenkow, J., Zaleski, C., Jha, S., et al. (2013). STAR: ultrafast universal RNA-seq aligner. *Bioinformatics* 29, 15–21. doi: 10.1093/bioinformatics/bts635

Ellis, C., and Turner, J. G. (2002). A conditionally fertile coi1 allele indicates cross-talk between plant hormone signalling pathways in *Arabidopsis thaliana* seeds and young seedlings. *Planta* 215, 549–556. doi: 10.1007/s00425-002-0787-4

Faino, L., de Jonge, R., and Thomma, B. P. H. J. (2012). The transcriptome of *Verticillium dahliae*-infected *Nicotiana benthamiana* determined by deep RNA sequencing. *Plant Signal. Behav.* 7, 1065–1069. doi: 10.4161/psb.21014

Fang, Y., Xiong, D., Tian, L., Tang, C., Wang, Y., and Tian, C. (2017). Functional characterization of two bZIP transcription factors in *Verticillium dahliae*. *Gene* 626, 386–394. doi: 10.1016/j.gene.2017.05.061

Feys, B., Benedetti, C. E., Penfold, C. N., and Turner, J. G. (1994). Arabidopsis mutants selected for resistance to the phytotoxin coronatine are male sterile, insensitive to Methyl JA, and resistant to a bacterial pathogen. *Plant Cell.* 6, 751–759. doi: 10.1105/tpc.6.5.751

Fonseca, S., Chico, J. M., and Solano, R. (2009). The JA pathway: the ligand, the receptor and the core signalling module. *Curr. Opin. Plant Biol.* 12, 539–547. doi: 10.1016/j.pbi.2009.07.013

Fradin, E. F., Abd-El-Haliem, A., Masini, L., van den Berg, G. C., and Joosten, M. H. (2011). Interfamily transfer of tomato Ve1 mediates Verticillium resistance in Arabidopsis. *Plant Physiol.* 156, 2255–2265. doi: 10.1104/pp.111.180067

Fradin, E. F., and Thomma, B. P. (2006). Physiology and molecular aspects of Verticillium wilt diseases caused by *V. dahliae* and *V. albo-atrum*. *Mol. Plant Pathol.* 7, 71–86. doi: 10.1111/j.1364-3703.2006.00323.x

Fradin, E. F., Zhang, Z., Ayala, J. C., Castroverde, C. D., Nazar, R. N., Robb, J., et al. (2009). Genetic dissection of Verticillium wilt resistance mediated by tomato Ve1. *Plant Physiol.* 150, 320–332. doi: 10.1104/pp.109.136762

Fujimoto, S. Y., Ohta, M., Usui, A., Shinshi, H., and Ohme-Takagi, M. (2000). Arabidopsis ethylene-responsive element binding factors act as transcriptional activators or repressors of GCC box-mediated gene expression. *Plant Cell.* 12, 393–404. doi: 10.1105/tpc.12.3.393

Gaspar, Y. M., McKenna, J. A., McGinness, B. S., Hinch, J., Poon, S., Connelly, A. A., et al. (2014). Field resistance to *Fusarium oxysporum* and *Verticillium dahliae* in transgenic cotton expressing the plant defensin NaD1. *J. Exp. Bot.* 65, 1541–1550. doi: 10.1093/jxb/eru021

He, Z. H., Cheeseman, I., He, D., and Kohorn, B. D. (1999). A cluster of five cell wall-associated receptor kinase genes, Wak1-5, are expressed in specific organs of Arabidopsis. *Plant Mol. Biol.* 39, 1189–1196. doi: 10.1023/A:1006197318246

He, Z.-H., He, D., and Kohorn, B. D. (1998). Requirement for the induced expression of a cell wall associated receptor kinase for survival during the pathogen response. *Plant J.* 14, 55–64. doi: 10.1046/j.1365-313X.1998.00092.x

Hill, T. W., and Kaefer, E. (2001). Improved protocols for Aspergillus minimal medium: trace element and minimal medium salt stock solutions. *Fungal Genet. Newsl.* 48, 20–21. doi: 10.4148/1941-4765.1173

Hoffman, T., Schmidt, J. S., Zheng, X., and Bent, A. F. (1999). Isolation of ethylene-insensitive soybean mutants that are altered in pathogen susceptibility and gene-for-gene disease resistance. *Plant Physiol.* 119, 935–950.

Huot, B., Yao, J., Montgomery, B. L., and He, S. (2014). Growth–defense tradeoffs in plants: a balancing act to optimize fitness. *Mol. Plant.* 7, 1267–1287. doi: 10.1093/mp/ssu049

Inderbitzin, P., Bostock, R. M., Davis, R. M., Usami, T., Platt, H. W., and Subbarao, K. V. (2011). Phylogenetics and taxonomy of the fungal vascular wilt pathogen Verticillium, with the descriptions of five new species. *PLoS ONE* 6:e28341. doi: 10.1371/journal.pone.0028341

Inderbitzin, P., and Subbarao, K. V. (2014). Verticillium systematics and evolution: how confusion impedes Verticillium wilt management and how to resolve it. *Phytopathology* 104, 564–574. doi: 10.1094/PHYTO-11-13-0315-IA

Johnson, J. M., Sherameti, I., Ludwig, A., Nongbri, P. L., Sun, C., Lou, B., et al. (2011). Protocols for *Arabidopsis thaliana* and *Piriformospora indica* co-cultivation - a model system to study plant beneficial traits. *Endocyt. Cell Res.* 21, 101–113.

Kamiya, M., Higashio, S. Y., Isomoto, A., Kim, J. M., Seki, M., Miyashima, S., et al. (2016). Control of root cap maturation and cell detachment by BEARSKIN transcription factors in Arabidopsis. *Development* 143, 4063–4072. doi: 10.1242/dev.142331

Kanehisa, M. (1997). A database for post-genome analysis. *Trends Genet*. 9, 375–376. doi: 10.1016/S0168-9525(97)01223-7

Kawchuk, L. M., Hachey, J., Lynch, D. R., Kulcsar, F., van Rooijen, G., Waterer, D. R., et al. (2001). Tomato Ve disease resistance genes encode cell surface-like receptors. *Proc. Natl. Acad. Sci. U.S.A*. 98, 6511–6515. doi: 10.1073/pnas.091114198

Kim, E.-H., Li, X.-P., Razeghifard, R., Anderson, J. M., Niyogi, K. K., Pogson, B. J., et al. (2009). The multiple roles of light-harvesting chlorophyll a/b-protein complexes define structure and optimize function of Arabidopsis chloroplasts: a study using two chlorophyll b-less mutants. *Biochim. Biophys. Acta* 1787, 973–984. doi: 10.1016/j.bbabio.2009.04.009

Klimes, A., and Dobinson, K. F. (2006). A hydrophobin gene, VDH1, is involved in microsclerotial development and spore viability in the plant pathogen *Verticillium dahliae*. *Fungal Genet. Biol*. 43, 283–294. doi: 10.1016/j.fgb.2005.12.006

Klosterman, S. J., Atallah, Z. K., Vallad, G. E., and Subbarao, K. V. (2009). Diversity, pathogenicity, and management of Verticillium species. *Ann. Rev. Phytopathol*. 47, 39–62. doi: 10.1146/annurev-phyto-080508-081748

Knoester, M., Van Loon, L. C., Van Den Heuvel, J., Hennig, J., Bol, J. F., and Linthorst, H. J. M. (1998). Ethylene-insensitive tobacco lacks nonhost resistance against soil-borne fungi. *Proc. Nat. Acad. Sci. U.S.A*. 95, 1933–1937.

Kombrink, A., Rovenich, H., Shi-Kunne, X., Rojas-Padilla, E., van den Berg, G. C., Domazakis, E., et al. (2017). *Verticillium dahliae* LysM effectors differentially contribute to virulence on plant hosts. *Mol. Plant Pathol.* 18, 596–608. doi: 10.1111/mpp.12520

Koo, A. J. K., Cooke, T. F., and Howe, G. A. (2011). Cytochrome P450 CYP94B3 mediates catabolism and inactivation of the plant hormone jasmonoyl-L-isoleucine. *Proc. Natl. Acad. Sci. U.S.A.* 108, 9298–9303. doi: 10.1073/pnas.1103542108

Koo, A. J., Gao, X., Jones, A. D., and Howe, G. A. (2009). A rapid wound signal activates the systemic synthesis of bioactive JAs in Arabidopsis. *Plant J.* 59, 974–986. doi: 10.1111/j.1365-313X.2009.03924.x

Krogan, N. T., Marcos, D., Weiner, A. I., and Berleth, T. (2016). The auxin response factor MONOPTEROS controls meristem function and organogenesis in both the shoot and root through the direct regulation of PIN genes. *New Phytol*. 212, 42–50. doi: 10.1111/nph.14107

Kulich, I., Vojtíková, Z., Glanc, M., Ortmannová, J., Rasmann, S., and Žárský, V. (2015). Cell wall maturation of *Arabidopsis* trichomes is dependent on exocyst subunit EXO70H4 and involves callose deposition. *Plant Physiol*. 168, 120–131. doi: 10.1104/pp.15.00112

Li, C. H., Shi, L., Han, Q., Hu, H. L., Zhao, M. W., Tang, C. M., et al. (2012). Biocontrol of Verticillium wilt and colonization of cotton plants by an endophytic bacterial isolate. *J. Appl. Microbiol*. 113, 641–651. doi: 10.1111/j.1365-2672.2012.05371.x

Li, J., Zingen-Sell, I., and Buchenauer, H. (1996). Induction of resistance of cotton plants to Verticillium wilt and of tomato to Fusarium wilt by 3-aminobutyric acid and methyl JA. *J. Plant Dis. Plant Prot*. 103, 288–299.

Li, S., van Os, G. M., Ren, S., Yu, D., Ketelaar, T., Emons, A. M., et al. (2010). Expression and functional analyses of EXO70 genes in Arabidopsis implicate their roles in regulating cell type-specific exocytosis. *Plant Physiol*. 154, 1819–1830. doi: 10.1104/pp.110.164178

Li, Y., Zheng, X., Tang, H., Zhu, J., and Yang, J. (2003). Increase of β-1,3-glucanase and chitinase activities in cotton callus cells treated by salicylic acid and toxin of *Verticillium dahliae*. *Kleb. Acta Bot Sin.* 45, 802–808. Available online at: http://www.jipb.net/Abstract_old.aspx?id=2235

Liao, Y., Smyth, G. K., and Shi, W. (2014). featureCounts: an efficient general purpose program for assigning sequence reads to genomic features. *Bioinformatics* 30, 923–930. doi: 10.1093/bioinformatics/btt656

Liu, S., Ziegler, J., Zeier, J., Birkenbihl, R. P., and Somssich, I. E. (2017). *Botrytis cinerea* B05.10 promotes disease development in Arabidopsis by suppressing WRKY33-mediated host immunity. *Plant Cell Environ*. 40, 2189–2206. doi: 10.1111/pce.13022

Love, M. I., Huber, W., and Anders, S. (2014). Moderated estimation of fold change and dispersion for RNA-seq data with DESeq2. *Genome Biol.* 15, 550. doi: 10.1186/s13059-014-0550-8

Lund, S. T., Stall, R. E., and Klee, H. J. (1998). Ethylene regulates the susceptible response to pathogen infection in tomato. *Plant Cell* 10, 371–382. doi: 10.1105/tpc.10.3.371

Mansoori, B., and Smith, C. J. (2005). Elicitation of ethylene by *Verticillium albo-atrum* phytotoxins in potato. *J. Phytopathol*. 153, 143–149. doi: 10.1111/j.1439-0434.2005.00943.x

Matsuo, M., Johnson, J. M., Hieno, A., Tokizawa, M., Nomoto, M., Tada, Y., et al. (2015). High REDOX RESPONSIVE TRANSCRIPTION FACTOR1 levels result in accumulation of reactive oxygen species in *Arabidopsis thaliana* shoots and roots. *Mol. Plant*. 8, 1253–1273. doi: 10.1016/j.molp.2015.03.011

Meier, S., Ruzvidzo, O., Morse, M., Donaldson, L., Kwezi, L., and Gehring, C. (2010). The Arabidopsis wall associated kinase-like 10 gene encodes a functional guanylyl cyclase and is co-expressed with pathogen defense related genes. *PLoS ONE*. doi: 10.1371/journal.pone.0008904

Metraux, J. P. (2001). Systemic acquired resistance and salicylic acid: current state of knowledge. *Eur. J. Plant Pathol*. 107, 13–18. doi: 10.1023/A:1008763817367

Moore, G. G., Mack, B. M., Beltz, S. B., and Gilbert, M. K. (2016). Draft genome sequence of an aflatoxigenic aspergillus species, A. *bombycis. Genome Biol. Evol*. 8, 3297–3300. doi: 10.1093/gbe/evw238

Murashige, T., and Skoog, F. (1962). A revised medium for rapid growth and bioassays with tobacco tissue cultures. *Physiol. Plant*. 15, 473–497. doi: 10.1111/j.1399-3054.1962.tb08052.x

Müssig, C., Biesgen, C., Lisso, J., Uwer, U., Weiler, E. W., and Altmann, T. (2000). A novel stress-inducible 12-oxophytodienoate reductase from Arabidopsis thaliana provides a potential link between Brassinosteroid-action and Jasmonic-acid synthesis. *J. Plant Physiol.* 157, 143–152. doi: 10.1016/S0176-1617(00)80184-4

Pantelides, I. S., Tjamos, S. E., and Paplomatas, E. J. (2010). Ethylene perception via ETR1 is required in Arabidopsis infection by *Verticillium dahliae*. *Mol. Plant Pathol.*. 11, 191–202. doi: 10.1111/j.1364-3703.2009.00592.x

Pegg, G. F., and Brady, B. L. (2002). *Verticillium Wilts*. Wallingford: CABI Publishing.

Pegg, G. F., and Cronshaw, D. K. (1976). Ethylene production in tomato plants infected with Verticillium albo-atrum. *Physiol. Plant Pathol*. 8, 279–295. doi: 10.1016/0048-4059(76)90022-9

Pfaffl, M. W. (2001). A new mathematical model for relative quantification in real-time RT-PCR. *Nucleic Acids Res*. 29:e45.

Proietti, S., Bertini, L., Timperio, A. M., Zolla, L., Caporale, C., and Caruso, C. (2013). Crosstalk between salicylic acid and JA in Arabidopsis investigated by an integrated proteomic and transcriptomic approach. *Mol. Biosyst*. 9, 1169–1187. doi: 10.1039/c3mb25569g

Puhalla, J. E., and Bell, A. A. (1981). "Genetics and biochemistry of Wilt of pathogens," in *Fungal Wilt Diseases of Plants*, eds M. E. Mace, A. A. Bell, and C. H. Beckman (New York, NY: Academic Press Inc.), 146–192.

Ralhan, A., Schöttle, S., Thurow, C., Iven, T., Feussner, I., Polle, A., et al. (2012). The vascular pathogen *Verticillium longisporum* requires a jasmonic acid-independent COI1 function in roots to elicit disease symptoms in Arabidopsis shoots. *Plant Physiol*. 159, 1192–1203. doi: 10.1104/pp.112.198598

Ratzinger, A., Riediger, N., von Tiedemann, A., and Karlovsky, P. (2009). Salicylic acid and salicylic acid glucoside in xylem sap of *Brassica napus* infected with *Verticillium longisporum*. *J. Plant Res.* 122, 571–579. doi: 10.1007/s10265-009-0237-5

Reusche, M., Klásková, J., Thole, K., Truskina, J., Novák, O., Janz, D., et al. (2013). Stabilization of cytokinin levels enhances Arabidopsis resistance against *Verticillium longisporum*. *Mol. Plant Microbe Interact*. 26, 850–860. doi: 10.1094/MPMI-12-12-0287-R

Reusche, M., Thole, K., Janz, D., Truskina, J., Rindfleisch, S., Drübert, C., et al. (2012). Verticillium infection triggers VASCULAR-RELATED NAC DOMAIN7-dependent de novo xylem formation and enhances drought tolerance in Arabidopsis. *Plant Cell* 24, 3823–3837. doi: 10.1105/tpc.112.103374

Robinson, M. M., Shah, S., Tamot, B., Pauls, K. P., Moffatt, B. A., and Glick, B. R. (2001). Reduced symptoms of Verticillium wilt in transgenic

tomato expressing a bacterial ACC deaminase. *Mol. Plant Pathol.* 2, 135–145. doi: 10.1046/j.1364-3703.2001.00060.x

Roos, J., Bejai, S., Oide, S., and Dixelius, C. (2014). RabGAP22 is required for defense to the vascular pathogen *Verticillium longisporum* and contributes to stomata immunity. *PLoS ONE* 9:e88187. doi: 10.1371/journal.pone.0088187

Sarmiento-Villamil, J. L., García-Pedrajas, N. E., Baeza-Monta-ez, L., and García-Pedrajas, M. D. (2010). The APSES transcription factor Vst1 is a key regulator of development in microsclerotium- and resting mycelium-producing Verticillium species. *Mol Plant Pathol.* 19, 59–76. doi: 10.1111/mpp.12496

Sarmiento-Villamil, J. L., Prieto, P., Klosterman, S. J., and García-Pedrajas, M. D. (2017). Characterization of two homeodomain transcription factors with critical but distinct roles in virulence in the vascular pathogen *Verticillium dahliae*. *Mol Plant Pathol.* doi: 10.1111/mpp.12584. [Epub ahead of print].

Scarpeci, T. E., Zanor, M. I., Mueller-Roeber, B., and Valle, E. M. (2013). Overexpression of AtWRKY30 enhances abiotic stress tolerance during early growth stages in *Arabidopsis thaliana*. *Plant Mol. Biol.* 83, 265–277. doi: 10.1007/s11103-013-0090-8

Schnathorst, W. C. (1981). "Life cycle and epidemiology of Verticillium," in *Fungal Wilt Diseases of Plants*, eds M. E. Mace, A. A. Bell, and C. H. Beckman (New York, NY: Academic Press Inc.), 81–111.

Scholz, S. S., Malabarba, J., Reichelt, M., Heyer, M., Ludewig, F., and Mithöfer, A. (2017). Evidence for GABA-induced systemic GABA accumulation in arabidopsis upon wounding. *Front. Plant Sci.* 8:388. doi: 10.3389/fpls.2017.00388

Staswick, P. E., and Tiryaki, I. (2004). The oxylipin signal jasmonic acid is activated by an enzyme that conjugates it to isoleucine in Arabidopsis. *Plant Cell*. 16, 2117–2127. doi: 10.1105/tpc.104.023549

Staswick, P. E., Serban, B., Rowe, M., Tiryaki, I., Maldonado, M. T., Maldonado, M. C., et al. (2005). Characterization of an Arabidopsis enzyme family that conjugates amino acids to indole-3-acetic acid. *Plant Cell*. 17, 616–627. doi: 10.1105/tpc.104.026690

Staswick, P. E., Su, W., and Howell, S. H. (1992). Methyl jasmonate inhibition of root growth and induction of a leaf protein are decreased in an *Arabidopsis thaliana* mutant. *Proc. Natl Acad. Sci. U.S.A.* 89, 6837–6840. doi: 10.1073/pnas.89.15.6837

Sun, C., Shao, Y., Vahabi, K., Lu, J., Bhattacharya, S., Dong, S., et al. (2014). The beneficial fungus *Piriformospora indica* protects Arabidopsis from *Verticillium dahliae* infection by downregulation plant defense responses. *BMC Plant Biol.* 14, 268–283. doi: 10.1186/s12870-014-0268-5

Suza, W. P., and Staswick, P. E. (2008). The role of JAR1 in Jasmonoyl-L-isoleucine production during Arabidopsis wound response. *Planta* 227, 1221–1232. doi: 10.1007/s00425-008-0694-4

Sztatelman, O., Grzyb, J., Gabryś, H., and Banaś, A. K. (2015). The effect of UV-B on Arabidopsis leaves depends on light conditions after treatment. *BMC Plant Biol.* 15, 281. doi: 10.1186/s12870-015-0667-2

Thaler, J. S., Humphrey, P. T., and Whiteman, N. K. (2012). Evolution of JA and salicylate signal crosstalk. *Trends Plant Sci.* 17, 260–270. doi: 10.1016/j.tplants.2012.02.010

Thaler, J. S., Owen, B., and Higgins, V. J. (2004). The role of the JA response in plant susceptibility to diverse pathogens with a range of lifestyles. *Plant Physiol.* 135, 530–538. doi: 10.1104/pp.104.041566

Thieme, C. J., Rojas-Triana, M., Stecyk, E., Schudoma, C., Zhang, W., Yang, L., et al. (2015). Endogenous Arabidopsis messenger RNAs transported to distant tissues. *Nat. Plants* 1:15025. doi: 10.1038/nplants.2015.25

Thines, B., Katsir, L., Melotto, M., Niu, Y., Mandaokar, A., Liu, G., et al. (2007). JAZ repressor proteins are targets of the SCF(COI1) complex during JA signalling. *Nature* 448, 661–665. doi: 10.1038/nature05960

Thomma, B. P. H. J., Eggermont, K., Tierens, K. F. M.-J., and Broekaert, W. F. (1999). Requirement of functional ethylene-insensitive 2 gene for efficient resistance of Arabidopsis to infection by Botrytis cinerea. *Plant Physiol.* 121, 1093–1101.

Tian, L., Wang, Y., Yu, J., Xiong, D., Zhao, H., and Tian, C. (2016). The mitogen-activated protein kinase kinase VdPbs2 of *Verticillium dahliae* regulates microsclerotia formation, stress response, and plant infection. *Front. Microbiol.* 7:1532. doi: 10.3389/fmicb.2016.01532

Tjamos, S. E., Flemetakis, E., Paplomatas, E. J., and Katinakis, P. (2005). Induction of resistance to *Vericillium dahliae* in *Arabidopsis thaliana* by biocontrol agent K-165 and pathogenesis-related proteins gene expression. *Mol. Plant Microbe. Interact.* 18, 555–561. doi: 10.1094/MPMI-18-0555

Umate, P. (2011). Genome-wide analysis of lipoxygenase gene family in Arabidopsis and rice. *Plant Signal Behav.* 6, 335–338. doi: 10.4161/psb.6.3.13546

Vadassery, J., Reichelt, M., Hause, B., Gershenzon, J., Boland, W., and Mithöfer, A. (2012). CML42-mediated calcium signaling coordinates responses to Spodoptera herbivory and abiotic stresses in Arabidopsis. *Plant Physiol.* 159, 1159–1175. doi: 10.1104/pp.112.198150

Vallad, G. E., and Subbarao, K. V. (2008). Colonization of resistant and susceptible lettuce cultivars by a green fluorescent protein-tagged isolate of *Verticillium dahliae*. *Phytopathology*. 98, 871–885. doi: 10.1094/PHYTO-98-8-0871

van Esse, H. P., Fradin, E. F., de Groot, P. J., de Wit, P. J., and Thomma, B. P. (2009). Tomato transcriptional responses to a foliar and a vascular fungal pathogen are distinct. *Mol. Plant Microbe Interact.* 22, 245–258. doi: 10.1094/MPMI-22-3-0245

Veronese, P., Narasimhan, M. L., Stevenson, R. A., Zhu, J. K., and Weller, S. C. (2003). Identification of a locus controlling Verticillium disease symptom response in *Arabidopsis thaliana. Plant J.* 35, 574–587. doi: 10.1046/j.1365-313X.2003.01830.x

Wang, P., Zhang, X., Ma, X., Sun, Y., Liu, N., Li, F., et al. (2017). Identification of CkSNAP33, a gene encoding synaptosomal-associated protein from *Cynanchum komarovii* that enhances *Arabidopsis* resistance to *Verticillium dahliae*. *PLoS ONE* 12:e0178101. doi: 10.1371/journal.pone.0178101

Witzel, K., Buhtz, A., and Grosch, R. (2017). Temporal impact of the vascular wilt pathogen *Verticillium dahliae* on tomato root proteome. *J. Proteomics* 169, 215–224. doi: 10.1016/j.jprot.2017.04.008

Xie, C., Li, Q., and Yang, X. (2017). Characterization of VdASP F2 secretory factor from *Verticillium dahliae* by a fast and easy gene knockout system. *Mol. Plant Microbe Interact.* 30, 444–454. doi: 10.1094/MPMI-01-17-0007-R

Xie, D.-X., Feys, B. F., James, S., Nieto-Rostro, M., and Turner, J. G. (1998). COI1: an arabidopsis gene required for JA-regulated defense and fertility. *Science* 280, 1091–1094.

Yang, B., Sugio, A., and White, F. F. (2006). Os8N3 is a host disease-susceptibility gene for bacterial blight of rice. *Proc. Natl. Acad. Sci. U.S.A.* 103, 10503–10508. doi: 10.1073/pnas.0604088103

Yang, X., Ben, S., Sun, Y., Fan, X., Tian, C., and Wang, Y. (2013). Genome-wide identification, phylogeny and expression profile of vesicle fusion components in *Verticillium dahliae*. *PLoS ONE* 8:e68681. doi: 10.1371/journal.pone.0068681

Yao, L. L., Pei, B. L., Zhou, Q., and Li, Y. Z. (2012). NO serves as a signaling intermediate downstream of H2O2 to modulate dynamic microtubule cytoskeleton during responses to VD-toxins in Arabidopsis. *Plant Signal. Behav.* 7, 174–177. doi: 10.4161/psb.18768

Yao, L. L., Zhou, Q., Pei, B. L., and Li, Y. Z. (2011). Hydrogen peroxide modulates the dynamic microtubule cytoskeleton during the defence responses to *Verticillium dahliae* toxins in Arabidopsis. *Plant Cell Environ.* 34, 1586–1598. doi: 10.1111/j.1365-3040.2011.02356.x

Yuan, L., Su, Y., Zhou, S., Feng, Y., Guo, W., and Wang, X. (2017). A RACK1-like protein regulates hyphal morphogenesis, root entry and *in vivo* virulence in *Verticillium dahliae. Fungal Genet. Biol.* 99, 52–61. doi: 10.1016/j.fgb.2017.01.003

Zhang, H. C., Zhang, W. W., Jian, G. L., Qi, F. J., and Si, N. (2016). The genes involved in the protective effects of phytohormones in response to *Verticillium dahliae* infection in *Gossypium hirsutum. J. Plant Biol.* 59, 194–202. doi: 10.1007/s12374-016-0568-4

Zhang, L., Ni, H., Du, X., Wang, S., Ma, X. W., Nürnberger, T., et al. (2017). The Verticillium-specific protein VdSCP7 localizes to the plant nucleus and modulates immunity to fungal infections. *New Phytol.* 215, 368–381. doi: 10.1111/nph.14537

Zhang, T., Zhang, B., Hua, C., Meng, P., Wang, S., Chen, Z., et al. (2017). VdPKS1 is required for melanin formation and virulence in a cotton wilt pathogen *Verticillium dahliae*. *Sci. China Life Sci.* 60, 868–879. doi: 10.1007/s11427-017-9075-3

Zhang, W. Q., Gui, Y. J., Short, D. P. G., Li, T. G., Zhang, D. D., Zhou, L., et al. (2017). *Verticillium dahliae* transcription factor VdFTF1 regulates the expression of multiple secreted virulence factors and is required for full virulence in cotton. *Mol. Plant Pathol.* doi: 10.1111/mpp.12569. [Epub ahead of print].

Zhang, W. W., Zhang, H. C., Liu, K., Jian, G. L., Qi, F. J., and Si, N. (2017). Large-scale identification of *Gossypium hirsutum* genes associated with *Verticillium dahliae* by comparative transcriptomic and reverse genetics analysis. *PLoS ONE* 12:e0181609. doi: 10.1371/journal.pone.0181609

Zhao, P., Zhao, Y.-L., Jin, Y., Zhang, T., and Guo, H.-S. (2014). Colonization process of *Arabidopsis thaliana* roots by a green fluorescent protein-tagged isolate of *Verticillium dahliae*. *Protein Cell* 5, 94–98. doi: 10.1007/s13238-013-0009-9

Zhen, X., and Li, Y. (2004). Ultrastructural changes and location of b-1,3-glucanase in resistant and susceptible cotton callus cells in response to treatment with toxin of *Verticillium dahliae* and salicylic acid. *J. Plant Physiol.* 161, 1367–1377. doi: 10.1016/j.jplph.2004.04.007

Zhou, L., Hu, Q., Johansson, A., and Dixelius, C. (2006). *Verticillium longisporum* and *V. dahliae*: infection and disease in *Brassica napus*. *Plant Pathol.* 55, 137–144. doi: 10.1111/j.1365-3059.2005.01311.x

Zhu, X., Soliman, A., Islam, M. R., Adam, L. R., and Daayf, F. (2017). *Verticillium dahliae's* isochorismatase hydrolase is a virulence factor that contributes to interference with Potato's Salicylate and jasmonate defense signaling. *Front. Plant Sci.* 8:399. doi: 10.3389/fpls.2017.00399

Conflict of Interest Statement: The authors declare that the research was conducted in the absence of any commercial or financial relationships that could be construed as a potential conflict of interest.

frontiers in Microbiology

ORIGINAL RESEARCH
published: 09 January 2018
doi: 10.3389/fmicb.2017.02647

Metabolomics Investigation of an Association of Induced Features and Corresponding Fungus during the Co-culture of *Trametes versicolor* and *Ganoderma applanatum*

*Xiao-Yan Xu[1†], Xiao-Ting Shen[1†], Xiao-Jie Yuan[1], Yuan-Ming Zhou[2], Huan Fan[3], Li-Ping Zhu[1], Feng-Yu Du[4], Martin Sadilek[5], Jie Yang[6], Bin Qiao[7] and Song Yang[1,8]**

[1] Shandong Province Key Laboratory of Applied Mycology, Qingdao International Center on Microbes Utilizing Biogas, School of Life Science, Qingdao Agricultural University, Qingdao, China, [2] Central Laboratory, Qingdao Agricultural University, Qingdao, China, [3] Tianjin Animal Science and Veterinary Research Institute, Tianjin Academy of Agricultural Sciences, Tianjin, China, [4] School of Chemistry and Pharmacy, Qingdao Agricultural University, Qingdao, China, [5] Department of Chemistry, University of Washington, Seattle, WA, United States, [6] Department of Biochemistry and Molecular Biology, School of Basic Medical Sciences, Tianjin Medical University, Tianjin, China, [7] School of Chemical Engineering and Technology, Tianjin University, Tianjin, China, [8] Key Laboratory of Systems Bioengineering, Ministry of Education, Tianjin University, Tianjin, China

OPEN ACCESS

Edited by:
Erika Kothe, Friedrich Schiller Universität Jena, Germany

Reviewed by:
Nico Jehmlich, Helmholtz-Zentrum für Umweltforschung (UFZ), Germany
Martin Taubert, Friedrich Schiller Universität Jena, Germany

***Correspondence:**
Song Yang
yangsong1209@163.com

[†]These authors have contributed equally to this work.

Specialty section:
This article was submitted to Fungi and Their Interactions, a section of the journal Frontiers in Microbiology

Received: *03 September 2017*
Accepted: *19 December 2017*
Published: *09 January 2018*

Citation:
Xu X-Y, Shen X-T, Yuan X-J, Zhou Y-M, Fan H, Zhu L-P, Du F-Y, Sadilek M, Yang J, Qiao B and Yang S (2018) Metabolomics Investigation of an Association of Induced Features and Corresponding Fungus during the Co-culture of Trametes versicolor and Ganoderma applanatum. Front. Microbiol. 8:2647. doi: 10.3389/fmicb.2017.02647

The co-culture of *Trametes versicolor* and *Ganoderma applanatum* is a model of intense basidiomycete interaction, which induces many newly synthesized or highly produced features. Currently, one of the major challenges is an identification of the origin of induced features during the co-culture. Herein, we report a ^{13}C-dynamic labeling analysis used to determine an association of induced features and corresponding fungus even if the identities of metabolites were not available or almost nothing was known of biochemical aspects. After the co-culture of *T. versicolor* and *G. applanatum* for 10 days, the mycelium pellets of *T. versicolor* and *G. applanatum* were sterilely harvested and then mono-cultured in the liquid medium containing half fresh medium with ^{13}C-labeled glucose as carbon source and half co-cultured supernatants collected on day 10. ^{13}C-labeled metabolome analyzed by LC-MS revealed that 31 induced features including 3-phenyllactic acid and orsellinic acid were isotopically labeled in the mono-culture after the co-culture stimulation. Twenty features were derived from *T. versicolor*, 6 from *G. applanatum*, and 5 features were synthesized by both *T. versicolor* and *G. applanatum*. ^{13}C-labeling further suggested that 12 features such as previously identified novel xyloside [N-(4-methoxyphenyl)formamide 2-O-beta-D-xyloside] were likely induced through the direct physical interaction of mycelia. Use of molecular network analysis combined with ^{13}C-labeling provided an insight into the link between the generation of structural analogs and producing fungus. Compound **1** with m/z 309.0757, increased 15.4-fold in the co-culture and observed ^{13}C incorporation in the mono-culture of both *T. versicolor* and *G. applanatum*, was purified and identified as a phenyl polyketide, 2,5,6-trihydroxy-4,

6-diphenylcyclohex-4-ene-1,3-dione. The biological activity study indicated that this compound has a potential to inhibit cell viability of leukemic cell line U937. The current work sets an important basis for further investigations including novel metabolites discovery and biosynthetic capacity improvement.

Keywords: basidiomycete, interaction, ^{13}C-labeling, origin of induced features, phenyl polyketide, metabolite identification, LC-MS

INTRODUCTION

Secondary metabolites are an important source of valuable drug leads, of which compounds derived from various fungi, especially medicinal fungi of basidiomycetes, represent an important part. To explore chemical diversity, several approaches such as epigenetic modification or non-targeted metabolic pathway manipulation have recently been developed in the *Aspergillus* and *Streptomyces* species (Scherlach and Hertweck, 2009; Chiang et al., 2011). In the case of basidiomycetes, the induction of novel secondary metabolites or enhancement of secreting extracellular enzymes can be achieved by activating cryptic biosynthetic pathways through establishment of a fungi interaction in the co-culture (Peiris et al., 2008; Hiscox et al., 2010). This co-culture strategy mimics natural ecosystem, in which interspecies interaction of basidiomycetes is very common (Hiscox et al., 2015, 2017). Recently, Zheng et al. demonstrated that co-culture of basidiomycetes *Inonotus obliquus* and *Phellinus punctatus* resulted in the accumulation of lanostane-type triterpenoids, polyphenols, and melanins, compounds capable of scavenging free radicals and inhibiting tumor cell proliferation (Zheng et al., 2011). The co-culture of *Trichoderma Reesei* with *Coprinus comatus* was an important approach for an on-site generation of lignocellulolytic enzyme leading to the increase of lignocellulose degradation rate as described by Ma and Ruan (2015). In our previous work, fifteen wood-decaying basidiomycetes and two straw-decaying basidiomycetes were used to establish 136 pairwise co-cultures on agar plates (Yao et al., 2016). The co-culture system of *Trametes versicolor* and *Ganoderma applanatum* showed an interaction zone, in which the accumulation of a series of known carboxylic acids as well as novel xylosides were observed.

The application of co-culture has enhanced the number of discovered novel secondary metabolites but also raises several challenges. One of the major challenges is how to timely and accurately identify the species responsible for the newly induced metabolites during the microorganism interaction. Typically, the structure of compounds and related biochemical information were required to verify the unique secondary metabolite and its particular producer (Riedlinger et al., 2006). Recently, a combined technique of nanospray desorption electrospray ionization and matrix-assisted laser desorption/ionization-time of flight mass spectrometry has been developed as a platform to reveal many unknown metabolites produced by *Streptomyces coelicolor* when paired with five other actinomycetes (Traxler et al., 2013). However, this approach was limited to associate the novel metabolites with corresponding producer grown on agar plates and was not suitable to the co-culture in the liquid medium. The metabolic incorporation of stable isotopes ^{13}C or ^{15}N is a powerful approach used for quantitative proteome and metabolome studies (Julka and Regnier, 2004; Yang et al., 2010). Moreover, ^{13}C-dynamic labeling analysis has been applied for analyzing the metabolite turnover rates, distinguishing the flux distribution between two pathways starting from the same metabolic point, and interpreting the synthetic process of novel metabolites (Yang et al., 2012; Shlomi et al., 2014; Hammerl et al., 2017). With the advantage of a ^{13}C-labeling approach, the current study reports on the identification of the producer of novel induced metabolites in liquid medium after the two interactive mycelia were sterilely separated and mono-cultured after the induction by the co-culture.

The research of the interspecies crosstalk expands our possibilities to discover novel metabolites, and also increases our understanding of how these metabolites are induced in microbial consortia. A chemical warfare in the fungal-fungal communication is often described as diffusion of harmful and chemically complex metabolites from one partner to the other (Bertrand et al., 2014). For instance, the interaction between the *Aspergillus niger* and *Aspergillus flavus* led to the inhibition of aflatoxin B1 produced by *A. flavus* through signal molecules downregulating expression of major biosynthetic genes (Xing et al., 2017). Under some conditions, co-cultivation appears to trigger production and accumulation of novel metabolites without the involvement of released signaling molecules. For instance, co-cultivation with *Corynebacteria glutamicum* or *Tsukamurella pulmonis* was indicated to stimulate a novel pathway in *S. endus*, contributing to a new heterocyclic chromophore-containing antibiotics alchivemycin A (Onaka et al., 2011). Notably, the mono-culture of *S. endus* did not generate the same compound with or without the addition of filter sterilized supernatants from bacterial culture. The production of alchivemycin A therefore appeared to require a direct physical interaction between *S. endus* and the coryneform bacteria cells. For this research, ^{13}C dynamic labeling was further utilized to suggest the potential mechanism of the induction of increased and newly synthesized features.

In this work, we built upon the characteristic of mycelial pellets of basidiomycetes and ^{13}C-labeling analysis, to analyze and catalog a broad range of ^{13}C-labeled features, which were highly accumulated in the co-culture of *T. versicolor* and *G. applanatum*. ^{13}C dynamic labeling further suggested two potential mechanism of the induction of these features. Ultimately, compound **1** with $M+H^+$ m/z 309.0757, that displayed ^{13}C incorporation in the mono-culture of both *T. versicolor* and *G. applanatum*, was isolated and identified as novel phenyl polyketide, and its biological activity was evaluated.

MATERIALS AND METHODS

Chemicals

All chemicals including standards (ascorbic acid and phenolic antioxidant 2,6-di-*tert*-butyl-4-methoxyphenol) were purchased from either Sigma-Aldrich (St. Louis, MO, USA) or TCI (Kita-ku, Tokyo, Japan). Millipore water (Billerica, MA, USA) was used for the preparation of all the media and sample solutions.

Fungi Material and Culture Conditions

G. applanatum (CGMCC No. 5.249) and *T. versicolor* (CGMCC No. 12241) were deposited at the Shandong Province Key Lab of Applied Mycology in China. The culture medium was supplied at concentrations as follows: 2 g glucose, 0.2 g KH_2PO_4, 0.1 g $MgSO_4$, 0.4 g peptone, and 4 g agar (only in solid medium) in 200 mL of sterilized water.

Mono-culture of *T. versicolor* and *G. applanatum* on Agar Plate

The mono-culture procedure was adapted from our previous publication (Yao et al., 2016), and mono-culture medium was the same as above. Briefly, a 5 mm agar plug of each fungus scraped from agar slant culture-medium was cultured on a Petri dish (9 cm diameter), and were incubated at 28°C for 10 days.

Co-culture of *T. versicolor* and *G. applanatum* in Liquid Medium and Sample Preparation

Eight 5 mm agar plugs of *T. versicolor* and *G. applanatum* were separately pre-cultured in 500 mL shake flask containing 200 mL of culture medium at 28°C for 4 days on orbital shakers at 180 rpm. Then 100 mL culture broth of *G. applanatum* was transferred into the culture of 100 mL *T. versicolor*, and co-cultivated up to 18 days. All the co-cultures had three independent biological replicates. At the harvest time, 10 mL of co -culture broth was filtered by using MILLEX-GP PES membrane filters (0.22 μm, 33 mm, Merck Millipore, Germany) and the filtrate was dried in a freeze-dryer ALPHA 1-2LDplus (Christ, Osterode, Germany). Five milliliters of freshly prepared dichloromethane/methanol/water (64:36:8, v/v) solvent mixture was added to the dried samples (Yao et al., 2016). The sample extractions were carried out in a water bath sonicator (KQ-300GVDV, Kunshan, China) at 25°C for 20 min, and were centrifuged at 12,000 rpm for 10 min. Finally, the extracts were dried on a rotational vacuum concentrator (Christ, Osterode, Germany) and stored in a −80°C freezer.

Measurement of the Metabolome

The extracts were dissolved in 200 μL methanol, and then were centrifuged at 12,000 rpm for 15 min. The supernatants were transferred into 250 μL Agilent autosampler vials. The samples were analyzed on an Agilent liquid chromatograph-quadrupole time-of-flight mass spectrometer (LC-QTOF-MS, Agilent 1290 Infinity-6530B, Agilent Technologies, Santa Clara, CA, USA) as previously described (Cui et al., 2016; Hu et al., 2016). Briefly, 10 μL of the samples was separated on an Acquity UPLC BEH C18 column (100 × 2.1 mm, 1.7 μm, Waters, Milford, MA, USA). The mobile phase A was water with 0.1% formic acid. The mobile phase B was pure acetonitrile. The reversed-phase liquid chromatographic elution gradient was optimized in order to maximize the resolution of the induced features. The gradient was the following: 0–3 min, 5% B, 3–12 min, 5–40% B, 12–38 min, 40–95% B, 38–46 min, 95% B, 46–48 min, 95–5% B, 48–55 min, 5% B. This shallow gradient provided reproducible separation for many co-eluting compounds in a time window from 5.0 to 8.0 min. The TOF m/z range was set to 50–1,200 amu in centroid mode with a scan rate of 1.5 spectra/s. All the samples had three independent biological replicates. Each biological replicate had two analytical replicates.

Data Pre-processing and Principal Component Analysis

LC-QTOF-MS data were converted into mzML format using MS Convert software (Holman et al., 2014). Data pre-processing and statistical analysis were performed with MZmine 2 (Version 2.11) (Pluskal et al., 2010) and SIMCA-P 11.5. For the MZmine 2, the peak detection threshold for MS signal intensity was set to 1.0×10^3. The chromatogram building was realized using a minimum time span of 0.01 min, minimum height of 2.5×10^3, and m/z tolerance of 0.005 (or 10 ppm). Chromatograms were deconvoluted with the following settings: search minimum in absolute retention time (RT) range 0.1 min, minimum relative height 10%, minimum absolute height 2.5×10^3 and baseline level 1.2. The chromatogram isotopic peaks grouper algorithm was set as m/z tolerance of 0.005 (or 10 ppm) and absolute RT tolerance of 0.10 min. Chromatograms were peak aligned with m/z tolerance at 0.008 (or 15 ppm) and absolute RT tolerance 1 min. The peak list was eventually gap-filled with m/z tolerance at 0.008 (or 15 ppm), and absolute RT tolerance of 0.20 min. To classify m/z in the peak list, principal component analysis (PCA) was carried out by using SIMCA-P (version 11.5). Two steps were required to perform PCA. The first step was to set the variables m/z and RT as Primary ID and Secondary ID. The secondary step was to do the normalization of the variables with Pareto scaling. This normalized method was embedded in SIMPCA-P, which did not require further parameter tuning. After that, PCA were displayed by a scores plot, mainly observing the overall cluster of the different treatments as well as the presence of outliers. The correlation coefficient loading plot was used to identify the variables responsible for the clustering or separation of the treatments.

Molecular Network Analysis

MS/MS data for molecular network analysis were acquired in targeted MS/MS mode on the same LC-QTOF-MS system (the precursor ions are listed in **Table 1**). The collision energy and m/z range for different precursor ions were optimized based on their own characteristics as our previous publication (Yao et al., 2016). MS/MS data were converted to mzML format, and then were subjected to the Molecular Networking workflow of Global Natural Products Social Molecular (GNPS at gnps.ucsd.edu) using the Group Mapping feature (Watrous et al., 2012; Wang et al., 2016). The subnetworks were generated with settings of minimum pairs cosine 0.65, parent mass tolerance 1.0 Dalton,

TABLE 1 | List of induced features in the co-culture of *T. versicolor* and *G. applanatum* analyzed by LC-MS in the positive/negative mode and corresponding production fungus.

m/z(–)	RT /min	Predictive elemental composition	Difference	Produced by fungus	^{12}C signal intensity in the co-culture	Features discovered with the current, optimized chromatography
136.0403	3.91	$C_7H_7NO_2$	Newly synthesized	*G. applanatum*	4.00E+04	
165.0554	9.79	$C_9H_{10}O_3$	Fold increase 15.8 ± 0.7	*T. versicolor and G. applanatum*	2.50E+04	
166.0507	8.65	$C_8H_9NO_3$	Newly synthesized	NA	6.00E+04	
167.0348	9.90	$C_8H_8O_4$	Fold increase 5.8 ± 0.6	*G. applanatum*	5.00E+03	
181.0615	6.46	$C_8H_{10}N_2O_3$	Newly synthesized	*T. versicolor*	4.00E+03	
195.0505	8.37	$C_6H_{12}O_4$	Fold increase 25.3 ± 1.2	NA	ND	
244.0612	6.86	$C_{13}H_{11}NO_4$	Newly synthesized	NA	7.00E+03	
249.1497	16.33	$C_{15}H_{22}O_3$	Newly synthesized	*T. versicolor*	1.50E+04	+
251.0712	15.72	$C_{16}H_{12}O_3$	Fold increase 7.3 ± 1.3	*T. versicolor*	6.00E+03	
269.0577	11.75	$C_{14}H_{10}N_2O_4$	Newly synthesized	*G. applanatum*	9.00E+03	+
271.0716	7.03	$C_{14}H_{12}N_2O_4$	Newly synthesized	*G. applanatum*	1.00E+05	
271.0725	10.25	$C_{14}H_{12}N_2O_4$	Newly synthesized	*G. applanatum*	7.00E+04	
279.0656	13.25	$C_{17}H_{12}O_4$	Fold increase 5.2 ± 1.3	*T. versicolor*	2.50E+05	+
281.0808	11.93	$C_{17}H_{14}O_4$	Fold increase 102.2 ± 4.8	*T. versicolor*	5.00E+04	
298.0928	8.65	$C_{13}H_{17}NO_7$	Newly synthesized	NA	2.30E+04	
304.0626	3.33	$C_9H_{13}N_3O_9$	Newly synthesized	NA	ND	
306.0775	10.46	$C_{18}H_{13}NO_4$	Newly synthesized	NA	ND	+
309.0756	12.04	$C_{18}H_{14}O_5$	Fold increase 15.4 ± 1.2	*T. versicolor* and *G. applanatum*	2.50E+05	+
311.0931	11.49	$C_{18}H_{16}O_5$	Fold increase 400 ± 7.1	*T. versicolor*	4.00E+04	
314.0899	3.32	$C_{14}H_{13}N_5O_4$	Newly synthesized	NA	ND	
330.2656	14.03	$C_{18}H_{37}NO_4$	Fold increase 59.7 ± 8.1	*T. versicolor*	6.00E+04	
334.0733	11.44	$C_{20}H_9N_5O_4$	Newly synthesized	NA	ND	
337.0712	10.59	$C_{20}H_{10}N_4O_2$	Newly synthesized	NA	ND	+
341.1046	16.16	$C_{20}H_{14}N_4O_2$	Newly synthesized	*T. versicolor*	5.00E+03	+
342.2654	15.17	$C_{19}H_{37}NO_4$	Newly synthesized	*T. versicolor* and *G. applanatum*	6.00E+04	
387.1926	20.12	$C_{19}H_{36}N_2S_3$	Newly synthesized	NA	ND	
389.2072	20.07	$C_{19}H_{38}N_2S_3$	Newly synthesized	NA	ND	
397.223	19.42	$C_{21}H_{34}O_7$	Newly synthesized	NA	1.25E+04	
398.1058	13.53	$C_{25}H_{13}N_5O$	Newly synthesized	NA	ND	+
399.2386	20.07	$C_{21}H_{36}O_7$	Fold increase 103.3 ± 4.2	NA	3.00E+03	
405.0737	12.83	$C_{22}H_{10}N_6O_3$	Newly synthesized	NA	ND	
406.1043	7.89	$C_{22}H_{13}N_7O_2$	Newly synthesized	NA	ND	
415.2338	10.40	$C_{21}H_{36}O_8$	Newly synthesized	NA	ND	
436.2698	15.86	$C_{24}H_{39}NO_6$	Newly synthesized	*T. versicolor*	2.50E+04	+
454.2817	15.86	$C_{24}H_{41}NO_7$	Newly synthesized	*T. versicolor*	1.50E+04	+
455.1685	8.64	$C_{21}H_{24}N_6O_6$	Newly synthesized	NA	ND	
472.2923	15.86	$C_{24}H_{43}NO_8$	Newly synthesized	*T. versicolor*	1.25E+04	+
490.3025	15.06	$C_{24}H_{45}NO_9$	Newly synthesized	*T. versicolor*	3.40E+04	+
567.3139	15.87	$C_{25}H_{48}N_2O_{12}$	Newly synthesized	*T. versicolor*	7.00E+03	+
581.1208	13.24	$C_{36}H_{22}O_8$	Newly synthesized	NA	ND	+
586.2857	16.44	$C_{28}H_{45}NO_{12}$	Newly synthesized	NA	2.00E+03	+
597.1968	8.63	$C_{31}H_{34}O_{12}$	Newly synthesized	NA	ND	
629.1419	11.77	$C_{30}H_{22}N_4O_{12}$	Newly synthesized	NA	ND	+
641.1461	12.65	$C_{19}H_{29}N_7O_{18}$	Newly synthesized	NA	ND	
138.0555	3.93	$C_7H_7NO_2$	Newly synthesized	*G. applanatum*	8.00E+04	

(Continued)

TABLE 1 | Continued

m/z(+)	RT /min	Predictive elemental composition	Difference	Produced by fungus	^{12}C signal intensity in the co-culture	Features discovered with the current, optimized chromatography
140.0708	8.64	$C_7H_9NO_2$	Fold increase 14.9 ± 1.3	*G. applanatum*	1.10E+04	
150.0548	8.53	$C_8H_7NO_2$	Newly synthesized	NA	1.00E+05	
160.0377	3.84	$C_4H_5N_3O_4$	Newly synthesized	NA	ND	
168.0653	8.65	$C_8H_9NO_3$	Newly synthesized	NA	8.00E+04	+
196.0944	9.16	$C_{10}H_{13}NO_3$	Newly synthesized	NA	2.00E+03	+
216.1021	14.2	$C_{13}H_{14}NO_2$	Newly synthesized	NA	1.00E+04	+
230.1177	19.07	$C_{14}H_{15}NO_2$	Newly synthesized	NA	2.60E+03	
257.0919	9.18	$C_{14}H_{12}N_2O_3$	Newly synthesized	NA	ND	+
265.0860	11.92	$C_{17}H_{12}O_3$	Fold increase 802.4 ± 9.6	NA	ND	+
268.2277	15.96	$C_{16}H_{29}NO_2$	Newly synthesized	NA	4.00E+03	+
270.0979	3.27	$C_{13}H_{11}N_5O_2$	Newly synthesized	NA	ND	
272.1129	3.58	$C_{12}H_{17}NO_6$	Newly synthesized	NA	ND	
273.0871	10.22	$C_{14}H_{12}N_2O_4$	Newly synthesized	*G. applanatum*	1.10E+05	
286.1436	14.85	$C_{17}H_{19}NO_3$	Newly synthesized	NA	ND	
287.1030	10.61	$C_{16}H_{10}N_6$	Newly synthesized	NA	ND	
288.2900	20.88	$C_{17}H_{37}NO_2$	Fold increase 50.5 ± 3.3	*T. versicolor*	1.90E+04	+
298.2744	18.56	$C_{18}H_{35}NO_2$	Newly synthesized	*T. versicolor*	4.00E+04	+
300.1076	8.65	$C_{13}H_{17}NO_7$	Newly synthesized	*NA*	3.00E+04	
302.3069	21.38	$C_{18}H_{39}NO_2$	Fold increase 24.4 ± 3.1	*T. versicolor and G. applanatum*	4.80E+05	
322.0898	8.7	$C_{11}H_{11}N_7O_5$	Newly synthesized	NA	ND	+
330.3371	26.77	$C_{20}H_{43}NO_2$	Fold increase 152.3 ± 1.6	*T. versicolor*	5.60E+03	
332.2800	14.05	$C_{18}H_{37}NO_4$	Fold increase 74.3 ± 4.6	*T. versicolor*	3.60E+04	
334.2953	14.95	$C_{18}H_{39}NO_4$	Newly synthesized	*T. versicolor*	1.60E+04	
344.2803	15.17	$C_{19}H_{37}NO_4$	Newly synthesized	*T. versicolor and G. applanatum*	1.25E+05	
348.1430	11.71	$C_{20}H_{17}N_3O_3$	Newly synthesized	NA	ND	
358.2955	15.66	$C_{20}H_{39}NO_4$	Fold increase 25.2 ± 2.3	*T. versicolor*	3.00E+04	+
369.2269	13.47	$C_{16}H_{28}N_6O_4$	Newly synthesized	NA	ND	
372.3113	19.96	$C_{21}H_{41}NO_4$	Newly synthesized	*T. versicolor and G. applanatum*	3.60E+05	
377.2302	20.09	$C_{18}H_{28}N_6O_3$	Newly synthesized	NA	ND	+
400.1019	7.96	$C_{17}H_9N_{11}O_2$	Newly synthesized	NA	ND	
432.1504	8.68	$C_{19}H_{21}N_5O_7$	Newly synthesized	NA	ND	
474.3068	15.86	$C_{24}H_{43}NO_8$	Newly synthesized	*T. versicolor*	1.25E+04	+
492.3176	15.04	$C_{24}H_{45}NO_9$	Newly synthesized	*T. versicolor*	1.50E+04	+
496.2886	16.43	$C_{15}H_{41}N_2O_4$	Newly synthesized	*T. versicolor*	4.00E+04	+
506.3332	15.85	$C_{25}H_{47}NO_9$	Newly synthesized	*T. versicolor*	3.00E+04	+
599.2043	8.63	$C_{31}H_{34}O_{12}$	Newly synthesized	NA	ND	
716.5259	18.91	$C_{42}H_{69}NO_8$	Newly synthesized	NA	ND	

Yellow label, the features were observed by LC-MS in both negative and positive modes. These features were only counted once. Plus mark, the features discovered in this work were tagged with plus mark. NA, the features had no ^{13}C incorporation. ND, the features had weak MS signal intensity or no signal in the supernatants from the co-culture on day 10. Fold increase, fold value was the ratio of MS signal intensity of increased feature in the co-culture to that in the control mono-culture. Data show the mean with standard deviation calculated from three independent biological replicates.

ion tolerance 0.5 Dalton, maximum connected components 50, minimum matched peaks 6, minimum cluster size 2. The results were then visualized using Cytoscape (Version 3.1.1) (Su et al., 2014).

^{13}C-Labeling Analysis

T. versicolor and *G. applanatum* were co-cultivated up to 10 days as described above. Then mycelium pellets of *T. versicolor* and *G. applanatum* were respectively harvested using sterilized tweezers based on the difference of diameter size and color. The mycelium pellets of *T. versicolor* had the size ranging from 6 to 8 mm with the color of faint yellow and those of *G. applanatum* had the size ranging from 2 to 4 mm with red color. The harvested mycelium pellets were washed with sterile water three times and then mono-cultured in 50 ml shake flask containing 10 mL fresh medium with ^{13}C-labeled glucose at the final concentration of 5 g L^{-1} and 10 mL of co-cultured supernatants collected on day 10. For the control experiment no co-culture supernatants

were added, only 20 mL of fresh medium with ^{13}C-labeled glucose as carbon source. After the mono-culture for 10 or 20 days, 10 mL of *T. versicolor* and *G. applanatum* culture broths were harvested for analysis of ^{13}C-labeling. All samples had three independent biological replicates and two analytical replicates. Samples were extracted and analyzed by LC-QTOF-MS as described above. The mass isotopomer distributions were corrected for the contribution from natural isotopes by a matrix-based method (Jennings and Matthews, 2005). The total ^{13}C-incorporation for each feature was obtained by normalizing to its total carbon number as in our previous publication (Yang et al., 2013). Relative isotopic abundance (*M*i) for a feature in which *i* ^{13}C atoms were incorporated was calculated by the Equation (1):

$$\mathrm{M}i(\%) = \frac{m_i}{\sum_{j=0}^{n} m_j} \quad (1)$$

where m_i represents the isotopic abundance for a feature in which *i* ^{13}C atoms were incorporated and *n* represents the maximum number of ^{13}C atoms incorporated.

Total ^{13}C-incorporation of a feature with N carbon atoms was obtained by normalizing to its total carbon number according to the Equation (2):

$$\text{Total } ^{13}\text{C} - \text{incorporation } (\%) = \frac{\sum_{i=1}^{\mathrm{N}} i \times \mathrm{M}i}{\mathrm{N}} \quad (2)$$

The significance of difference of ^{13}C-incorporation between experimental data points was determined by *t*-tests (Origin 8.0). A *P*-value <0.05 was considered to be statistically significant.

Isolation and Purification of Compound 1

Twenty liters of the co-cultured supernatant was extracted three times with ethyl acetate (EtOAc). 2.5 g of crude EtOAc extract was concentrated under reduced pressure and purified on a silica gel (200–300 mesh) column and then eluted with petroleum ether/ethyl acetate and chloroform/methanol system to yield ten fractions (Song et al., 2014). Eight hundred and fifty milligrams of fraction 6 and 7 from the chloroform/methanol elution (20:1 and 10:1, v/v) was used to a medium pressure liquid chromatography (Flash CO140080-0, Agela Technologies, China) and eluted with methanol/water (the elution gradient was 10–90% methanol in 65 min) to generate a mixture of 216 mg. This mixture was purified on a silica gel (200–300 mesh, Qingdao Haiyang Chem. Ind. Co. Ltd. China) column by eluting with petroleum ether/ethyl acetate/ methanol (3:3:1, v/v) and then separated on a preparative column (Venusil XBP C18, Agela Technologies, China) by eluting with methanol/water (the elution gradient was 10–50% methanol in 40 min and flow rate was 8 mL/min) to obtain 10 mg of compound **1**.

NMR Analysis of Purified Compound 1

^{1}H, ^{13}C, and 2D NMR spectra of the purified compound **1** were all performed by using a Bruker Avance 600 MHz spectrometer (Karlsruhe, Germany) at 25°C. The compound **1** was accurately weighted, and dissolved in 0.5 mL of deuterated methanol as the internal lock. The resulting spectra were manually phased and baseline corrected and calibrated to methanol, using TOPSPIN (Version 2.1, Bruker).

Cell Viability Assay

The human leukemic cell line U937 and lung cancer cell line A549 were purchased from American Type Culture Collection (Manassas, VA, USA). They were cultured in RPMI-1640 (HyClone, USA) with 10% FBS (fetal bovine serum, Gibco). Cells were inoculated in 96-well plates at a density of 3,000 cells per well overnight and then treated to different concentrations of compound **1** for 48 h. The compound **1** was solved in ethanol. At a concentration of 300 μM of compound **1**, the ethanol was 0.8% (v/v) in the cell culture medium, showing minimal effect on the viability of both cell lines. The effect of compound **1** on the viability of U937 and A549 cells was evaluated with CellTiter 96® AQueous One Solution (Promega, Madison, WI, USA) (Soman et al., 2009). The absorbance was read at 490 nm with a microplate spectrophotometer (Multiskan FC, Thermo scientific, USA). Three independent experiments were performed and each one had six replicates. Data show the mean with error bar indicating standard deviation calculated from biological replicates by Origin 8.0. IC_{50} defined as the concentration with the inhibition of 50% cells was calculated by using SPSS (Statistical Package for Social Sciences) package 6, version 15.0.

Antioxidant Activity Assay

The 2,2′-azinobis-(3-ethylbenzothiazoline-6-sulfonic acid) (ABTS) method used is based on the reduction of the $ABTS^{\bullet+}$ radical action by the antioxidants present in the sample (Rigano et al., 2014). Three biological replicates were performed. A solution of 7.4 mM $ABTS^{\bullet+}$ (5 mL) mixed with 140 mM $K_2S_2O_8$ (88 μL) was prepared and stabilized for 12 h at 4°C in the dark. This mixture was then diluted by mixing $ABTS^{\bullet+}$ solution with ethanol (1:88) to obtain an absorbance of 0.70 ± 0.10 unit at 734 nm using a spectrophotometer (Multiskan FC, Thermo scientific, USA). Compound **1** (100 μL) and the standard controls (ascorbic acid and phenolic antioxidant 2,6-di-*tert*-butyl-4-methoxyphenol) reacted with 1 mL of diluted $ABTS^{\bullet+}$ solution for 2.5 min, and then the absorbance was taken at 734 nm against a blank constituted by $ABTS^{\bullet+}$ solution added with 100 μL of ethanol. $ABTS^{\bullet+}$ scavenging activity was calculated by the Equation (3):

$$\text{Scavenging effect } (\%) = \left(1 - \frac{Abs.sample}{Abs.blank}\right) \times 100 \quad (3)$$

where Abs blank = 100 μL of ethanol+1 mL of diluted $ABTS^{\bullet+}$ solution.

RESULTS

Induced Feature Discovery in Fungal Interaction

Unsupervised PCA is well-suited for comparing different biological samples and identifying statistically significant differences (Chen et al., 2007). As shown in **Figure 1** (left figure), examination of the scores plot showed that the co-culture treatment is clearly separated from the two mono-cultures. The variable features responsible for discriminating these three groups are shown in the loading plots (**Figure 1**, right). More

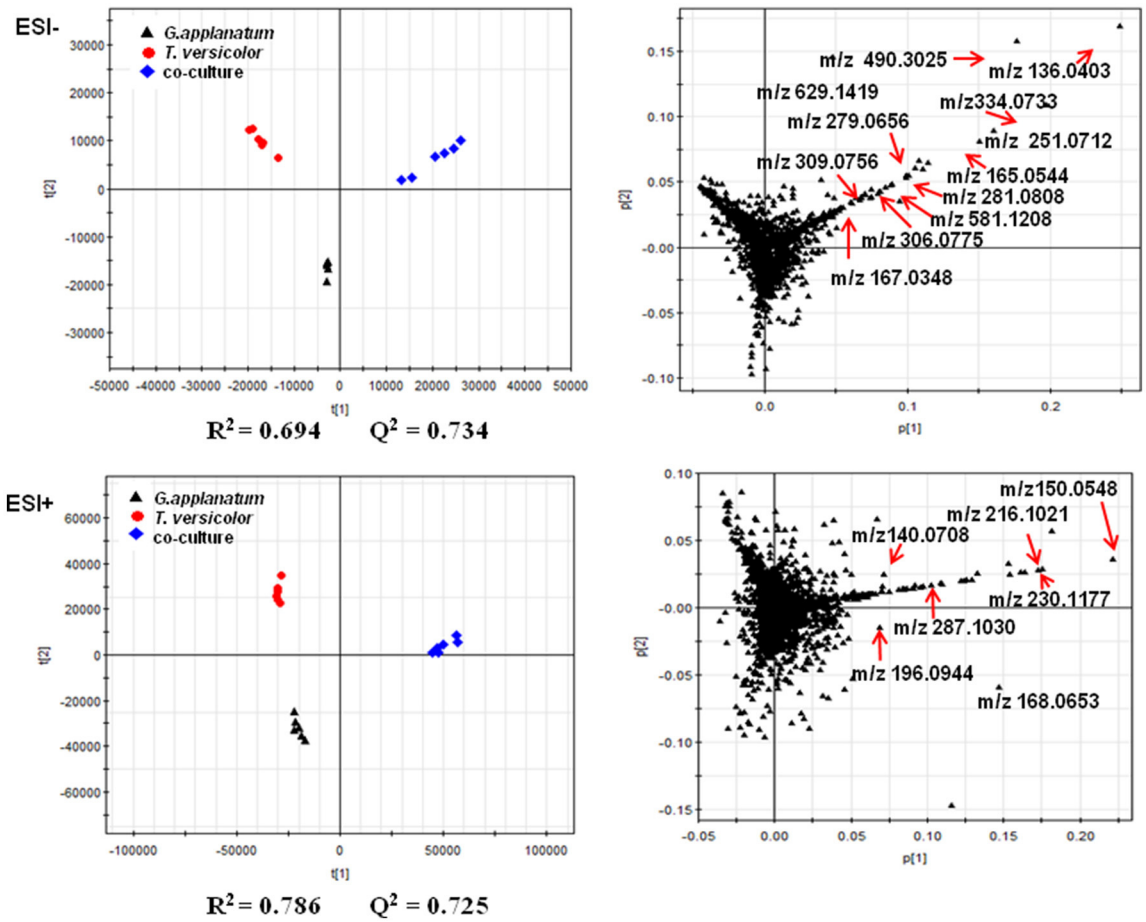

FIGURE 1 | PCA of metabolomics data of co-culture and their corresponding mono-cultures on day 18 is shown. The score and loading plots of the data analyzed by LC-QTOF-MS in the negative mode (2287 features) and positive mode (2076 features), respectively. The parameters (R^2 and Q^2) of the score plots demonstrated the discriminative ability of this model. The scattered dots labeled with m/z were representative features mentioned in the Results section.

than 4,000 features were recorded, out of which 58 features were detected only in the co-culture and 16 features were at least 5-fold more abundant in the co-culture than those in the control mono-culture (**Table 1**, **Figure 2**). Compared to our previous work (Yao et al., 2016), 28 additional features were discovered mainly due to the optimized chromatography (**Table 1**, **Figure 2**).

^{13}C-Labeling Analysis to Associate Induced Features with Corresponding Fungus

To associate induced features with corresponding fungus, we initially harvested individual mycelium pellets of *T. versicolor* and *G. applanatum* after the co-culture for 10 days and then detected the abundance of *in vivo* induced features. Many of the induced features were observed for both samples of *T. versicolor* and *G. applanatum* (data not shown). This made it impossible to distinguish if individual or both fungi were induced to generate the compounds in the co-culture. To overcome this issue, we designed a ^{13}C-labeling approach in the liquid co-cultivation. The workflow is shown in **Figure 3**. First, *T. versicolor* and *G. applanatum* were co-cultivated for 10 days to activate the cryptic genes. Next, their mycelia were sterilely separated and mono-cultivated in the liquid medium which contained half of fresh medium with ^{13}C-labeled glucose as carbon source and half of co-cultured supernatants collected on day 10. Then, the samples were harvested in the mono-cultures of *T. versicolor* and *G. applanatum* on days 10 and 20 and analyzed by LC-QTOF-MS. In the preliminary experiments, the samples were also harvested after 5 days of mono-culture with the addition of the supernatants. However, many of induced features were only slightly labeled. It was likely due to a relatively long lag phase and low growth rate in the mono-culture of *T. versicolor* and *G. applanatum* after the stimulation of the co-culture. In addition, for the unlabeled features, ^{13}C-labeling was not detected on day 5 either. Therefore, the samples were harvested later in order to obtain the strong MS signal. As the incorporation of ^{13}C-labeled carbons from glucose increases the molecular weight of metabolites, the mass shift determined from the mass spectra

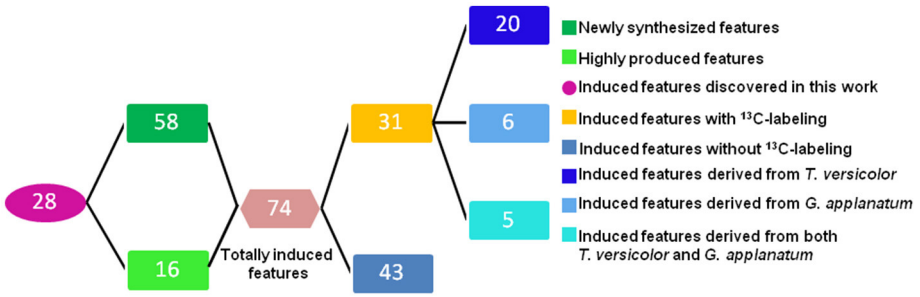

FIGURE 2 | Overview of the number of the induced features in the co-culture of *T. versicolor* and *G. applanatum*.

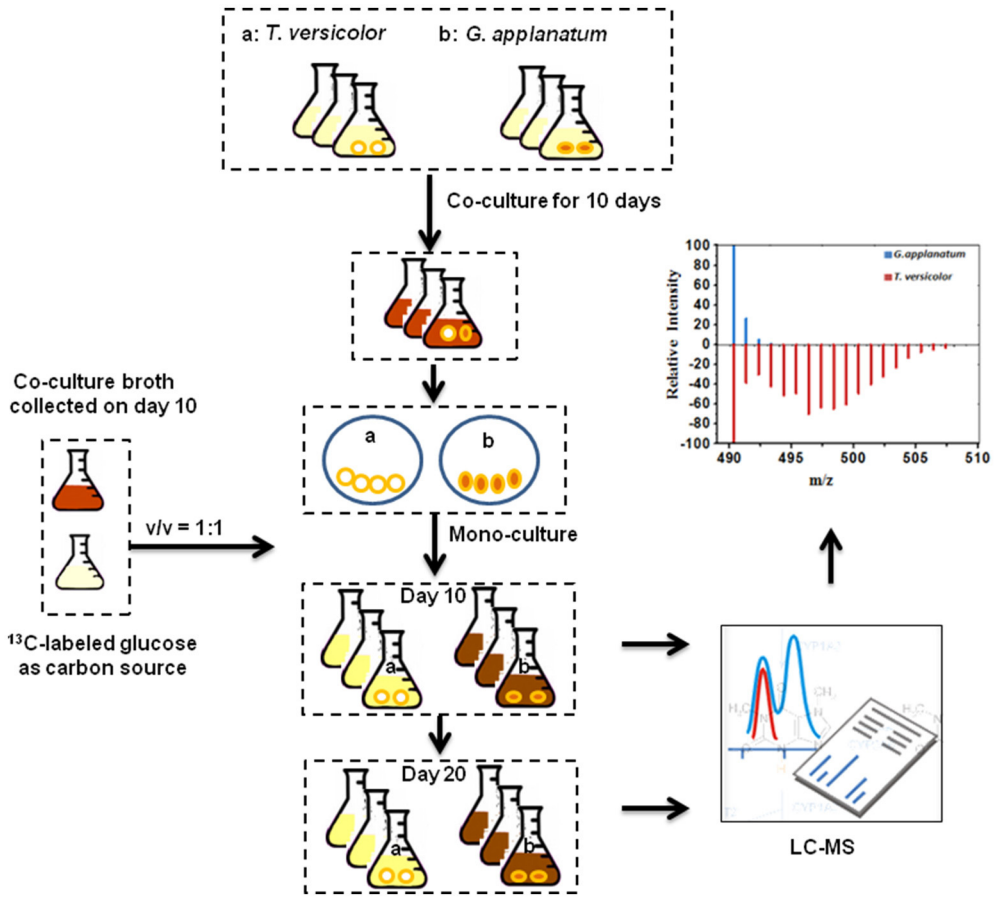

FIGURE 3 | ^{13}C-labeling analysis procedure. *T. versicolor* and *G. applanatum* were co-cultivated for 10 days, and then their mycelia were sterilely separated and mono-cultivated in the liquid medium which contained half of fresh medium with ^{13}C-labeled glucose as carbon source and half of co-cultured supernatants. Then samples were harvested in the mono-cultures of *T. versicolor* and *G. applanatum* and analyzed on LC-QTOF-MS.

provides then the information about which fungi generated the induced features.

Total 31 induced features were found to have ^{13}C incorporation in the mono-culture, and 43 features did not incorporate any label (**Figure 2**). Among the labeled features activated by the co-culture, 20 originated from *T. versicolor* and 6 features were derived from *G. applanatum*. Five features were induced by both *T. versicolor* and *G. applanatum* (**Figure 2**). Several representative ^{13}C labeling results are shown in **Figure 4**. In **Figure 4A**, the m/z 490 (experimental m/z 490.3025, predicted elemental component $C_{24}H_{45}NO_9$, error 0.3 ppm) was a newly synthesized feature in the co-culture. As ^{13}C-labeled carbon was incorporated into the feature m/z 490, intensity of m/z 491 (m/z + 1) up to m/z 506 (m/z + 16) increased. This change

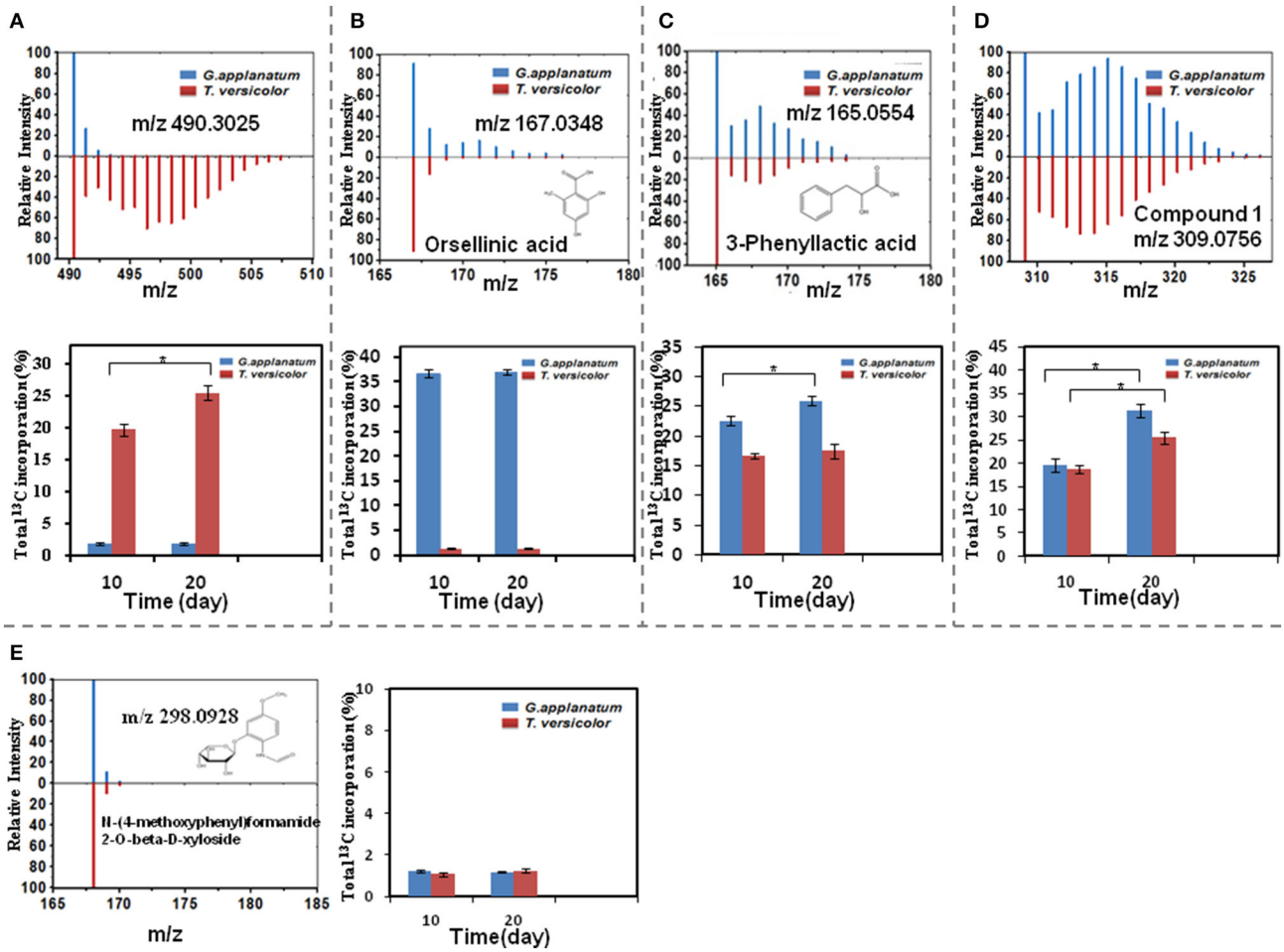

FIGURE 4 | A comparison of relative MS intensity suggests that the induced features have ^{13}C incorporation with time. **(A–D)** Upper figures: representative mass spectral data for 10 day time point showing that mass intensity caused by ^{13}C incorporation in the mono-culture of *T. versicolor* or *G. applanatum*, Lower figures: comparison of total ^{13}C incorporation shows that induced feature was produced by either *T. versicolor* or *G. applanatum*, or both. Data show the mean with error bars indicating standard deviation calculated from three independent replicates (*$P \leq 0.05$, *t*-test). **(E)** There was no ^{13}C incorporation for N-(4-methoxyphenyl)formamide 2-O-beta-D-xyloside on day 10 and 20.

was observed only in the mono-culture of *T. versicolor* and indicates that m/z 490 was particularly induced in this species. The calculation of total ^{13}C incorporation indicated that about 19 and 25% carbon was replaced with ^{13}C on days 10 and 20, respectively (bottom part of **Figure 4A**). The m/z 167.0348 in **Figure 4B** was highly produced during the co-culture and identified as orsellinic acid in the previous publication (Yao et al., 2016). In contrast to the above example, the m/z 167 incorporated ^{13}C-labels in the same time frame only in the mono-culture of *G. applanatum*, resulting in the parent ions shifted from m/z 167 to m/z 174 in the ^{13}C-labeled mass spectra and total ^{13}C incorporation level reached 14% on day 20 (**Figure 4B**). The m/z 165.0554 was previously identified as 3-phenyllactic acid (Yao et al., 2016), and ^{13}C-labeled mass spectra ranging from m/z 165 to m/z 174 were observed in both mono-cultures of *T. versicolor* and *G. applanatum* (**Figure 4C**). Similar example, feature with m/z 309 (experimental m/z 309.0756, $C_{18}H_{14}O_5$, error 0.37 ppm) increased 15.4-fold during the co-culture in comparison with MS signal in the control mono-culture and ^{13}C-labeling was observed for both fungi (**Figure 4D**). It is worth mentioning that a contamination from the undesired fungus cannot be absolutely excluded during the transfer from the co-culture to the mono-culture, but that it does not affect the identification of the fungus producing a feature only found in the mono-culture of either *T. versicolor* or *G. applanatum* based on the ^{13}C-labeling analysis.

^{13}C incorporation could be due to the induction of features which have been released into the medium during the co-culture. To confirm whether diffusible features were involved in triggering the silent gene expression in this study, we treated *T. versicolor* and *G. applanatum* with fresh medium containing ^{13}C labeled glucose as carbon source but without the addition of the supernatant of co-culture on day 10. As shown in **Figure 5** as an example, ^{13}C labeling of m/z 490.3025 and 136.0403

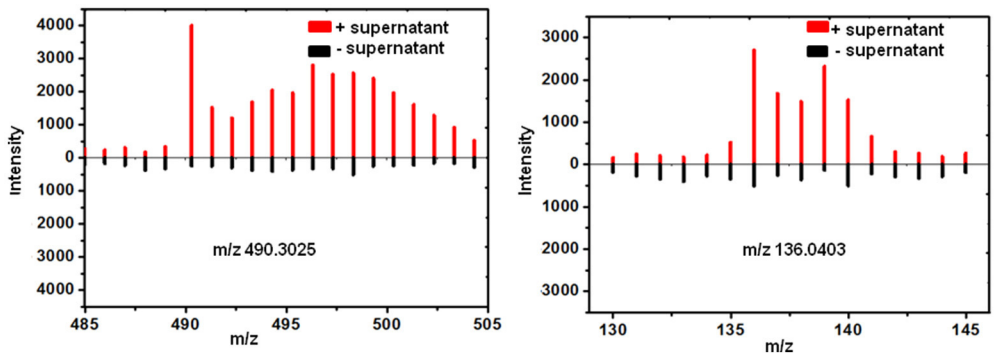

FIGURE 5 | ^{13}C incorporation was not observed for the induced features on day 20 in the mono-culture of *T. versicolor* **(Left)** or *G. applanatum* **(Right)** without the addition of the supernatant of co-culture.

was not observed up to 20 days but when the supernatant was added the features were significantly labeled. Notably, for 12 induced features with high signal intensities, including newly synthesized xyloside [N-(4-methoxyphenyl)formamide 2-O-beta-D-xyloside; Yao et al., 2016], we did not detected any ^{13}C incorporation in the mono-culture of either fungus (**Table 1**, **Figure 4E**, Supplementary Figure 1D). Therefore, it was not possible to assign their origin to a specific fungus.

Dereplication of Newly Discovered Features by Molecular Network Analysis

To investigate the structural similarities occurring for 28 newly discovered features in this study, MS/MS fragmentation spectra of the induced features in **Table 1** were processed and organized as molecular network with the previously identified features. **Figure 6** (upper part) shows a constructed subnetwork to dereplicate m/z 196.0944 and 216.1021. These two new features likely possessed similar backbone structure with the previously identified N-(2-hydroxy-4-methoxyphenyl) formamide (m/z 168.0653) and its analogous features (m/z 140.0708, 150.0548, 230.1177, 287.1030) due to their close fragmentation patterns (Supplementary Figure 2). This data was also in agreement with ^{13}C-labeling analysis, in which most of features involved in this subnetwork were not labeled either. In another example, five newly identified features and three previous features (m/z 251.0712, 281.0808, and 334.0733) were clustered together with high scores (**Figure 6**, bottom part). Comparison of the fragment ions of m/z 306.0775, 334.0733, 581.1208, 629.1419, and 279.0656 showed some common ions of m/z 77.04, 117.03, 235.08 which were likely derived from fragmentation of m/z 279.0656, suggesting that these features probably had the same backbone structure and belonged to a series of structural derivatives (Supplementary Figure 2). Moreover, ^{13}C incorporation of m/z 279.0656, 251.0712, and 281.0808 were clearly detected in the mono-culture of *T. versicolor* with the addition of the supernatant of co-culture (Supplementary Figure 1), suggesting that the derivatives of m/z 279.0656 (i.e., m/z 306.0775, 334.0733, 581.1208, and 629.1419, which did not show ^{13}C incorporation due to the weak signals in the mono-culture) were also likely biosynthesized by *T. versicolor* under the co-cultured condition.

Identification of Induced Compound 1 and Analysis of Its Biological Activity

Since compound **1** was derived from both *T. versicolor* and *G. applanatum* (**Figure 4D**), and 15.4-fold more abundant in the co-culture, we isolated and purified sufficient amount for detailed characterization. Compound **1** was a pale yellow powder with the molecular formula of $C_{18}H_{14}O_5$. The ^{1}H, ^{13}C-NMR and HSQC spectrum showed the presence of two carbonyl carbon, one oxygen connected CH, one oxygen connected to quaternary carbon, two single benzene rings and two olefinic carbon atoms (one with oxygen attached to it) (Supplementary Table 1 and Supplementary Figure 3). All the information suggested that the basic skeleton of the compound **1** is a terphenyl derivative with two mono-substituted benzene rings. The COSY spectrum showed the ^{1}H–^{1}H spin systems of H-2′/H-3′/H-4′/H-5′/H-6′ and H-2″/H-3″/H-4″/H-5″/H-6″, assigned two mono-substituted benzene rings (A and B). The HMBC correlations from H-2 (δ_H 4.49) to C1 (δ_C 203.4), C3 (δ_C 197.4), C4 (δ_C 113.5), and C6 (δ_C 90.9), and from OH-6 (δ_H 5.44, dimethylsulfoxide (DMSO-d_6) to C1 (δ_C 202.45), C5 (δ_C 191.28) and C6 (δ_C 90.9) established the ring C. The fragment ring A was linked to C-6 of ring C supported by the HMBC correlations from H-6' (δ_H 7.98) to the carbonyl C1 (δ_C 203.4). Likewise, the linkage of the ring B to the ring C at C-4 was confirmed by HMBC correlations from H-2″ (δ_H 7.88) to C4 (δ_C 113.5) and C-1″(δ_C 135.4). Therefore, the structure of compound **1** was identified as a phenyl polyketide, 2,5,6-trihydroxy-4,6-diphenylcyclohex-4-ene-1,3-dione (**Figure 7**).

We further tested biological activity of compound **1**. The human lung cancer cell lines A549 and leukemic cell lines U937 were treated with compound **1** at various concentrations for 48 h. As shown in **Figure 8A**, no visible changes in cell viability were detected for human lung cancer cell line A549 when the concentrations were increased to 300 μM. In contrast, compound **1** inhibited the viability of leukemic cells in a dose-dependent manner. The IC_{50} at 48 h was determined

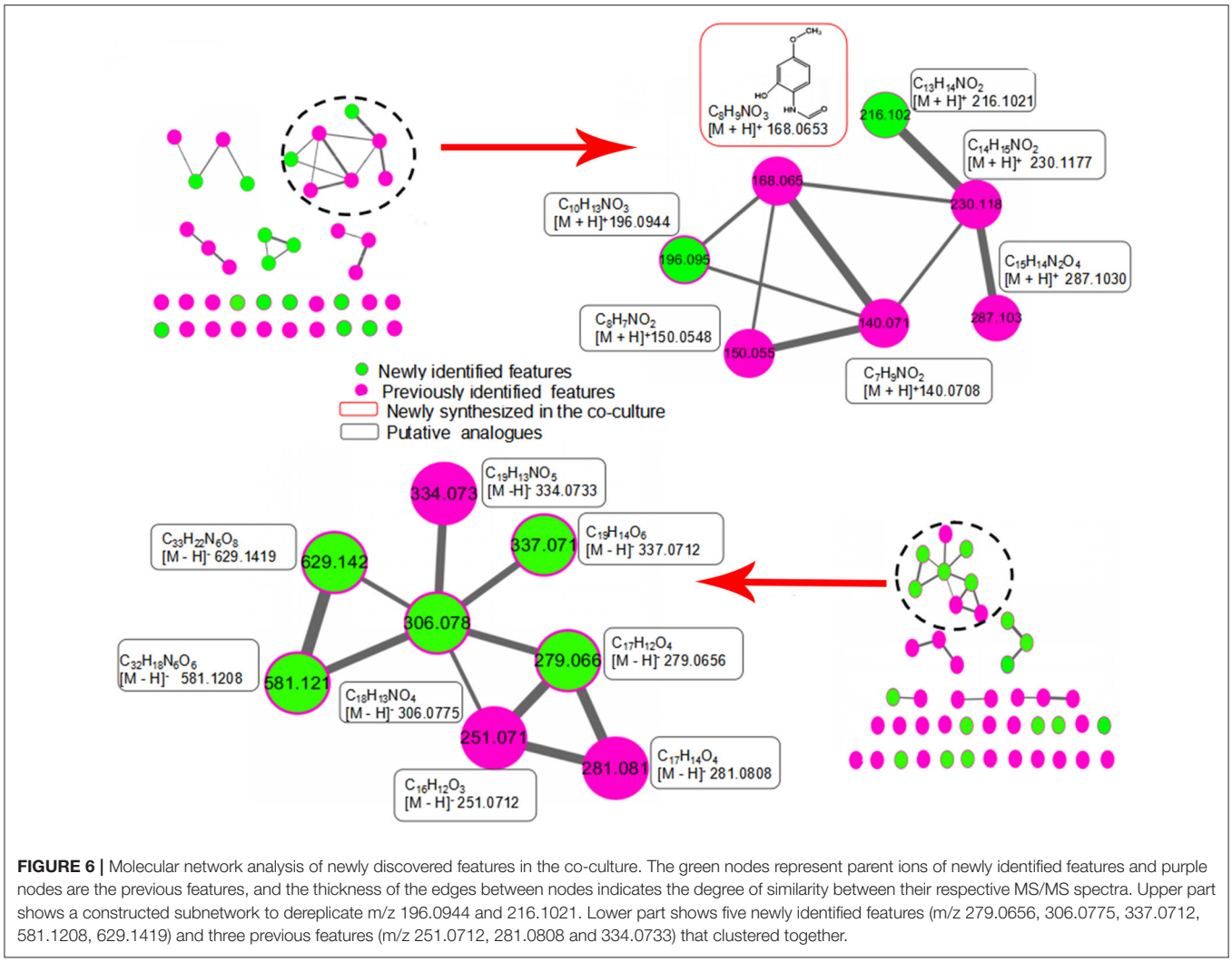

FIGURE 6 | Molecular network analysis of newly discovered features in the co-culture. The green nodes represent parent ions of newly identified features and purple nodes are the previous features, and the thickness of the edges between nodes indicates the degree of similarity between their respective MS/MS spectra. Upper part shows a constructed subnetwork to dereplicate m/z 196.0944 and 216.1021. Lower part shows five newly identified features (m/z 279.0656, 306.0775, 337.0712, 581.1208, 629.1419) and three previous features (m/z 251.0712, 281.0808 and 334.0733) that clustered together.

to be 276 ± 5 μM (equal to 85 mg/L). In addition, based on the structural characteristics of compound **1**, we also studied whether compound **1** had antioxidant properties using ABTS assay (**Figure 8B**). The highest percentage of antioxidant capacities (82.65 ± 1.25%) was observed for compound **1** at the concentration of 200 μg/mL. This is comparable with the report of crude extracts from berries (Abu-Bakar et al., 2016). The comparison of the antioxidant activity with ascorbic acid (VC) and phenolic antioxidant 2,6-di-*tert*-butyl-4-methoxyphenol (BHT) revealed that ascorbic acid> compound **1** > BHT.

DISCUSSION

Determining the origin of induced features in the co-culture remains a large challenge, because it generally requires the chemical structures with their biological information. Previously Bertrand et al. discovered five *de novo* induced compounds from the co-culture of *Trichophyton rubrum* and *Bionectria ochroleuca*, and elucidated the origin of one of them based on its non-sulfated form detected in the mono-culture of *B. ochroleuca* (Bertrand et al., 2013). However, other four compounds could not be associated with corresponding fungi due to the lack of their structures. In another study Ola et al. isolated nine compounds and speculated that four of them detected only in the co-culture originated from *Fusarium tricinctum* in terms of structural analogies with the known fungal products from the Xylariaceae family, but the producer of remaining five compounds was still unclear because of insufficient biochemical evidences (Ola et al., 2013). In this work, among 74 induced features, 31 features were shown to be produced specifically by either *T. versicolor* or *G. applanatum,* or by both fungi using a ^{13}C-based labeling analysis. This methodology was able to distinguish the origin even if the identities of compounds were not available or almost nothing was known about biochemical aspects. In more detail, the total ^{13}C incorporation in the same fungal culture varied noticeably among features. Isotopic steady state is the state that ^{13}C-labeling signatures in metabolites become time invariant (Antoniewicz et al., 2007). In current

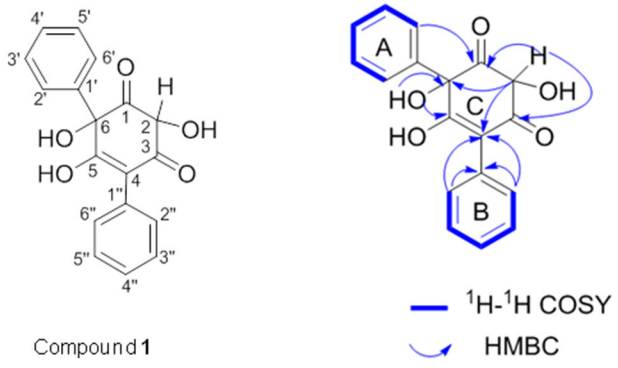

FIGURE 7 | 1H−1H COSY (blue bold lines) and key HMBC (blue arrows) correlations of compound **1.** COSY is two-dimensional spectrum which is used to identify spins coupled to each other, and HMBC is two-dimensional inverse H,C correlation technique that allow for the determination of carbon to hydrogen connectivity.

work, ^{13}C incorporation into 20 features (e.g., orsellinic acid) had the similar abundance levels between days 10 and 20 and these features had the similar ^{13}C-labeling pattern (data not shown), indicating that they likely reached isotopic steady state around 10 days (**Figure 4B**, Supplementary Figure 1). In contrast, ^{13}C incorporation level of 11 features including novel phenyl polyketide (compound **1**) increased from day 10 to day 20 (**Figures 4A,C,D**, Supplementary Figure 1), suggesting either the fluxes via their synthetic pathways were low or their metabolite pools were relatively large (Zamboni et al., 2009).

By comparison of ^{13}C-labeling patterns between with and without the addition of the supernatant of co-culture, it was demonstrated that the induction of gene expression and synthesis of corresponding metabolites during the co-culture of *T. versicolor* and *G. applanatum* depended indeed on the signaling molecules released into the medium. Forty-three induced features in the supernatant of co-culture on day 10 were detected with signal intensity ranging from 10^3 to 10^5 (**Table 1**), but in the current work we were not able to determine which features were responsible for signaling to activate gene expression in *T. versicolor* or *G. applanatum*. Additional studies will be needed to confirm this link as well as to elucidate the structure and function of signaling molecules. Notably, the previous report also demonstrated that an intimate physical interaction of the actinomycete *S. hygroscopicus* and fungal mycelia of *Aspergillus nidulans* was required to induce specific stimulation of the silent polyketide synthases and non-ribosomal peptide synthetases gene clusters (Schroeckh et al., 2009). In our research, we found 12 highly produced features that did not incorporate ^{13}C labeling in the mono-culture. One potential explanation is that these features were also produced in the co-culture via mycelium physical interaction to elicit the specific response. In addition, compound **1** had over 15-fold higher MS signal intensity in the co-culture than in the control mono-culture of *T. versicolor* where the mycelia were not pre-induced by the co-culture. It was not detected in the control mono-culture of *G. applanatum*, yet ^{13}C incorporation in *G. applanatum* was 1.3-fold higher than that in *T. versicolor* on day 20 (**Figure 4D**). This finding suggests that the co-culture could significantly activate the encoding genes or gene clusters related to the synthesis of Compound **1** in *G. applanatum*. This provides an important insight into possible manipulation of *G. applanatum* to enhance biosynthesis of novel metabolites.

Comparing MS fragmentation similarity including common losses, molecular network analysis is able to obtain a simultaneous visual investigation of identical molecules, analogs, or metabolite families, thereby assisting the structural analysis (Winnikoff et al., 2014; Cabral et al., 2016). In our previous research, this method was utilized to show that the common neutral loss of 132 Dalton resulted from the deglycosylation reaction, which helped to find a series of novel xylosides generated during the co-culture (Yao et al., 2016). Here, combined molecular network analysis and ^{13}C-labeling analysis suggested further that some newly discovered features were not only structurally analogous but also had similar induction mechanism and were likely produced by the same fungus. Thus, combination of network analysis and ^{13}C labeling shows promise to accelerate the elucidation of biosynthetic pathways of novel metabolites.

Several type II polyketides have been reported to be high-value medicals (Zhang W. et al., 2012). In antioxidant assay, compound **1** had better activity than BHT. More interestingly, compound **1** at micromolar concentration was able to inhibit the viability of leukemic cells. For comparison, Zhang et al. reported that matrine extracted from *Sophora flavescens* inhibited the proliferation of acute myeloid leukemia cell lines U937 in a dose- and time-dependent manner with the IC_{50} of 590 mg/L at 24 h, and resulted in the maximal apoptosis rates with 37.2% for 24 h (Zhang S. et al., 2012). Wang et al. also demonstrated that 100 μg/mL of *Ganoderma lucidum* extracts could greatly suppress leukemic cell growth with the inhibition rate of 75% (Wang et al., 1997). In our case, the IC_{50} of compound **1** was at the same level with matrine and crude extracts from *G. lucidum*. Thus, it can become a starting point for development of lead compounds to cure leukemia or other cancers.

CONCLUSION

The application of ^{13}C-labeling analysis produced valuable insight into the role of individual partners in the co-culture in production of known or unknown induced metabolites. Moreover, ^{13}C-labeling approach combined with molecular network analysis can reveal whether certain structural analogs were produced by the same fungus or through the similar activation mechanism. The current ^{13}C-labeling information sets an important foundation for further studies in the basidiomycetes, including but not limited to novel metabolites discovery and biosynthetic capacity improvement.

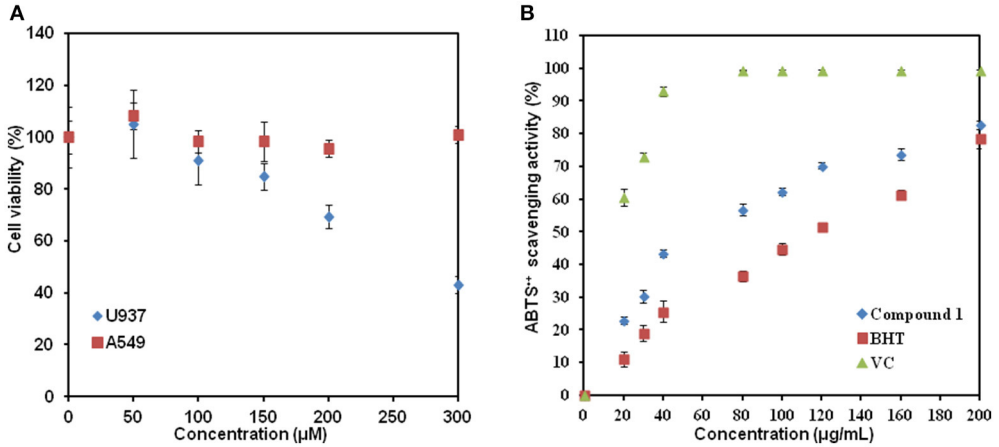

FIGURE 8 | The biological activity study of compound **1**. **(A)** Addition of compound **1** affected the cell viability of U937 but not of A549. **(B)** Graph of $ABTS^{\bullet+}$ scavenging activity vs. concentration. Data show the mean with error bars indicating standard deviation calculated from three independent biological replicates. VC, ascorbic acid; BHT, 2,6-di-*tert*-butyl-4-methoxyphenol.

AUTHOR CONTRIBUTIONS

X-YX, BQ, and SY: conceived and designed the project; X-YX, X-TS, X-JY, Y-MZ, HF, and JY: performed the experiments; X-YX, X-TS, L-PZ, F-YD, MS, and SY: interpreted the data. All authors contributed to the preparation of the manuscript, read and approved the final manuscript.

FUNDING

This work was supported by a grant from the Petrochemical Joint Fund of National Natural Science Foundation of China (No. U1462109), a grant from Shandong Province Natural Science Foundation (No. ZR2013CM024), a grant from National Natural Science Foundation of China (No. 31600028), a grant from Qingdao Applied Basic Research Program (No. 16-5-1-76-jch), a grant from Key Laboratory for Industrial Biocatalysis (Tsinghua University) Ministry of Education (No. 2015102) and a grant from Shandong provincial key research and development plan (Grant No. 2016GSF121010).

ACKNOWLEDGMENTS

We thank Dr. Yan Li at the University of Texas Health Science Center for his assistance with NMR analysis.

SUPPLEMENTARY MATERIAL

The Supplementary Material for this article can be found online at: https://www.frontiersin.org/articles/10.3389/fmicb.2017.02647/full#supplementary-material

REFERENCES

Abu-Bakar, M. F., Ismail, N. A., Isha, A., and Mei-Ling, A. L. (2016). Phytochemical composition and biological activities of selected wild berries (*Rubus moluccanus* L., *R. fraxinifolius* Poir., and *R. alpestris* Blume). *Evid. Based Complement. Alternat. Med.* 2016:2482930. doi: 10.1155/2016/2482930

Antoniewicz, M. R., Kelleher, J. K., and Stephanopoulos, G. (2007). Elementary Metabolite Units (EMU): a novel framework for modeling isotopic distributions. *Metab. Eng.* 9, 68–86. doi: 10.1016/j.ymben.2006.09.001

Bertrand, S., Bohni, N., Schnee, S., Schumpp, O., Gindro, K., and Wolfender, J. L. (2014). Metabolite induction via microorganism co-culture: a potential way to enhance chemical diversity for drug discovery. *Biotechnol. Adv.* 32, 1180–1204. doi: 10.1016/j.biotechadv.2014.03.001

Bertrand, S., Schumpp, O., Bohni, N., Monod, M., Gindro, K., and Wolfender, J. L. (2013). *De novo* production of metabolites by fungal co-culture of *Trichophyton rubrum* and *Bionectria ochroleuca*. *J. Nat. Prod.* 76, 1157–1165. doi: 10.1021/np400258f

Cabral, R. S., Allard, P. M., Marcourt, L., Young, M. C., Queiroz, E. F., and Wolfender, J. L. (2016). Targeted isolation of indolopyridoquinazoline alkaloids from Conchocarpus fontanesianus based on molecular networks. *J. Nat. Prod.* 79, 2270–2278. doi: 10.1021/acs.jnatprod.6b00379

Chen, C., Gonzalez, F. J., and Idle, J. R. (2007). LC-MS-based metabolomics in drug metabolism. *Drug Metab. Rev.* 39, 581–597. doi: 10.1080/03602530701497804

Chiang, Y. M., Chang, S. L., Oakley, B. R., and Wang, C. C. (2011). Recent advances in awakening silent biosynthetic gene clusters and linking orphan clusters to natural products in microorganisms. *Curr. Opin. Chem. Boil.* 15, 137–143. doi: 10.1016/j.cbpa.2010.10.011

Cui, J., Good, N. M., Hu, B., Yang, J., Wang, Q., Sadilek, M., et al. (2016). Metabolomics revealed an association of metabolite changes and defective growth in *Methylobacterium extorquens* AM1 overexpressing ecm during growth on methanol. *PLoS ONE* 11:e0154043. doi: 10.1371/journal.pone.0154043

Hammerl, R., Frank, O., and Hofmann, T. (2017). Differential off-line LC-NMR (DOLC-NMR) metabolomics to monitor tyrosine-induced metabolome alterations in *Saccharomyces cerevisiae*. *J. Agric. Food Chem.* 65, 3230–3241. doi: 10.1021/acs.jafc.7b00975

Hiscox, J., Baldrian, P., Rogers, H. J., and Boddy, L. (2010). Changes in oxidative enzyme activity during interspecific mycelial interactions involving the white-rot fungus *Trametes versicolor*. *Fungal Genet. Biol.* 47, 562–571. doi: 10.1016/j.fgb.2010.03.007

Hiscox, J., Savoury, M., Müller, C. T., Lindahl, B. D., Rogers, H. J., and Boddy, L. (2015). Priority effects during fungal community establishment in beech wood. *ISME J.* 9, 2246–2260. doi: 10.1038/ismej.2015.38

Hiscox, J., Savoury, M., Toledo, S., Kingscott-Edmunds, J., Bettridge, A., Waili, N. A., et al. (2017). Threesomes destabilise certain relationships: multispecies interactions between wood decay fungi in natural resources. *FEMS Microbiol. Ecol*. 93:fix 014. doi: 10.1093/femsec/fix014

Holman, J. D., Tabb, D. L., and Mallick, P. (2014). Employing ProteoWizard to convert raw mass spectrometry data. *Curr. Protoc. Bioinformatics* 46, 1–9. doi: 10.1002/0471250953.bi1324s46

Hu, B., Yang, Y. M., Beck, D. A., Wang, Q. W., Chen, W. J., Yang, J., et al. (2016). Comprehensive molecular characterization of *Methylobacterium extorquens* AM1 adapted for 1-butanol tolerance. *Biotechnol. Biofuels* 9:84. doi: 10.1186/s13068-016-0497-y

Jennings, M. E., and Matthews, D. E. (2005). Determination of complex isotopomer patterns in isotopically labeled compounds by mass spectrometry. *Anal. Chem.* 77, 6435–6444. doi: 10.1021/ac0509354

Julka, S., and Regnier, F. (2004). Quantification in proteomics through stable isotope coding: a review. *J. Proteome Res.* 3, 350–363. doi: 10.1021/pr0340734

Ma, K., and Ruan, Z. (2015). Production of a lignocellulolytic enzyme system for simultaneous bio-delignification and saccharification of corn stover employing co-culture of fungi. *Bioresour. Technol.* 175, 586–593. doi: 10.1016/j.biortech.2014.10.161

Ola, A. R., Thomy, D., Lai, D., Brötz-Oesterhelt, H., and Proksch, P. (2013). Inducing secondary metabolite production by the endophytic fungus *Fusarium tricinctum* through coculture with *Bacillus subtilis*. *J. Nat. Prod.* 76, 2094–2099. doi: 10.1021/np400589h

Onaka, H., Mori, Y., Igarashi, Y., and Furumai, T. (2011). Mycolic acid-containing bacteria induce natural-product biosynthesis in Streptomyces species. *Appl. Environ. Microbiol.* 77, 400–406. doi: 10.1128/AEM.01337-10

Peiris, D., Dunn, W. B., Brown, M., Kell, D. B., Roy, I., and Hedger, J. N. (2008). Metabolite profiles of interacting mycelial fronts differ for pairings of the wood decay basidiomycete fungus, *Stereum hirsutum* with its competitors *Coprinus micaceus* and *Coprinus disseminatus*. *Metabolomics* 4, 52–62. doi: 10.1007/s11306-007-0100-4

Pluskal, T., Castillo, S., Villar-Briones, A., and Oresic, M. (2010). MZmine 2: modular framework for processing, visualizing, and analyzing mass spectrometry-based molecular profile data. *BMC Bioinformatics* 11:395. doi: 10.1186/1471-2105-11-395

Riedlinger, J., Schrey, S. D., Tarkka, M. T., Hampp, R., Kapur, M., and Fiedler, H. P. (2006). Auxofuran, a novel metabolite that stimulates the growth of fly agaric, is produced by the mycorrhiza helper bacterium Streptomyces strain AcH 505. *Appl. Environ. Microbiol.* 72, 3550–3557. doi: 10.1128/AEM.72.5.3550-3557.2006

Rigano, M. M., Raiola, A., Tenore, G. C., Monti, D. M., Del-Giudice, G. R., Frusciante, L., et al. (2014). Quantitative trait loci pyramiding can improve the nutritional potential of tomato (*Solanum lycopersicum*) fruits. *J. Agri. Food Chem*. 62, 11519–11527. doi: 10.1021/jf502573n

Scherlach, K., and Hertweck, C. (2009).Triggering cryptic natural product biosynthesis in microorganisms. *Organ. Biomol. Chem*. 7, 1753–1760. doi: 10.1039/b821578b

Schroeckh, V., Scherlach, K., Nützmann, H. W., Shelest, E., Schmidt-Heck, W., Schuemann, J., et al. (2009). Intimate bacterial–fungal interaction triggers biosynthesis of archetypal polyketides in *Aspergillus nidulans*. *Proc. Natl. Acad. Sci. U.S.A*. 106, 14558–14563. doi: 10.1073/pnas.0901870106

Shlomi, T., Fan, J., Tang, B., Kruger, W. D., and Rabinowitz, J. D. (2014). Quantitation of cellular metabolic fluxes of methionine. *Anal. Chem.* 86, 1583–1591. doi: 10.1021/ac4032093

Soman, G., Yang, X., Jiang, H., Giardina, S., Vyas, V., Mitra, G., et al. (2009). MTS dye based colorimetric CTLL-2 cell proliferation assay for product release and stability monitoring of interleukin-15: assay qualification, standardization and statistical analysis. *J. Immunol. Methods* 348, 83–94. doi: 10.1016/j.jim.2009.07.010

Song, A. R., Sun, X. L., Kong, C., Zhao, C., Qin, D., Huang, F., et al. (2014). Discovery of a new sesquiterpenoid from Phellinus ignarius with antiviral activity against influenza virus. *Arch. Virol*. 159, 753–760. doi: 10.1007/s00705-013-1857-6

Su, G., Morris, J. H., Demchak, B., and Bader, G. D. (2014). Biological network exploration with cytoscape 3. *Curr. Protoc. Bioinformatics* 47, 1–24. doi: 10.1002/0471250953.bi0813s47

Traxler, M. F., Watrous, J. D., Alexandrov, T., Dorrestein, P. C., and Kolter, R. (2013). Interspecies interactions stimulate diversification of the *Streptomyces coelicolor* secreted metabolome. *MBio* 4:e00459–e00413. doi: 10.1128/mBio.00459-13

Wang, M., Carver, J. J., and Phelan, V. V. (2016). Sharing and community curation of mass spectrometry data with global natural products social molecular networking. *Nat. Biotechnol.* 34, 828–837. doi: 10.1038/nbt.3597

Wang, S. Y., Hsu, M. L., Hsu, H. C., Tzeng, C. H., Lee, S. S., Shiao, M. S., et al. (1997). The antitumor effect of *Ganoderma lucidum* is mediated by cytokines released from activated macrophages and T lymphocytes. *Int. J. Cancer* 70, 699–705. doi: 10.1002/(SICI)1097-0215(19970317)70:6<699::AID-IJC12>3.0.CO;2-5

Watrous, J., Roach, P., Alexandrov, T., Heath, B. S., Yang, J. Y., Kersten, R. D., et al. (2012). Mass spectral molecular networking of living microbial colonies. *Proc. Natl. Acad. Sci. U.S.A*. 109, 1743–1752. doi: 10.1073/pnas.1203689109

Winnikoff, J. R., Glukhov, E., Watrous, J., Dorrestein, P. C., and Gerwick, W. H. (2014). Quantitative molecular networking to profile marine cyanobacterial metabolomes. *J. Antibiot*. 67, 105–112. doi: 10.1038/ja.2013.120

Xing, F., Wang, L., Liu, X., Selvaraj, J. N., Wang, Y., Zhao, Y., et al. (2017). Aflatoxin B1 inhibition in *Aspergillus flavus* by *Aspergillus niger* through down-regulating expression of major biosynthetic genes and AFB1 degradation by atoxigenic *A. flavus*. *Int. Food Microbiol*. 256, 1–10. doi: 10.1016/j.ijfoodmicro.2017.05.013

Yang, S., Matsen, J. B., Konopka, M., Green-Saxena, A., Clubb, J., Sadilek, M., et al. (2013). Global molecular analyses of methane metabolism in methanotrophic Alphaproteobacterium, Methylosinus trichosporium OB3b. Part II. metabolomics and 13C-labeling study. *Front. Microbial.* 4:70. doi: 10.3389/fmicb.2013.00070

Yang, S., Nadeau, J. S., Humston-Fulmer, E. M., Hoggard, J. C., Lidstrom, M. E., and Synovec, R. E. (2012). Gas chromatography-mass spectrometry with chemometric analysis for determining ^{12}C and ^{13}C labeled contributions in metabolomics and ^{13}C flux analysis. *J. Chromatogr. A*. 1240, 156–164. doi: 10.1016/j.chroma.2012.03.072

Yang, S., Sadilek, M., and Lidstrom, M. E. (2010). Streamlined pentafluorophenylpropyl column liquid chromatography-tandem quadrupole mass spectrometry and global 13C-labeled internal standards improve performance for quantitative metabolomics in bacteria. *J. Chromatogr. A* 1217, 7401–7410. doi: 10.1016/j.chroma.2010.09.055

Yao, L., Zhu, L. P., Xu, X. Y., Tan, L. L., Sadilek, M., Fan, H., et al. (2016). Discovery of novel xylosides in co-culture of basidiomycetes *Trametes versicolor* and *Ganoderma applanatum* by integrated metabolomics and bioinformatics. *Sci. Rep*. 6:33237. doi: 10.1038/srep33237

Zamboni, N., Fendt, S. M., Rühl, M., and Sauer, U. (2009). 13C-based metabolic flux analysis. *Nat. Protoc*. 4, 878–892. doi: 10.1038/nprot.2009.58

Zhang, S., Zhang, Y., Zhuang, Y., Wang, J., Ye, J., Zhang, S., et al. (2012). Matrine induces apoptosis in human acute myeloid leukemia cells via the mitochondrial pathway and Akt inactivation. *PLoS ONE* 7:e46853. doi: 10.1371/journal.pone.0046853

Zhang, W., Wang, L., Kong, L., Wang, T., Chu, Y., Deng, Z., et al. (2012). Unveiling the post-PKS redox tailoring steps in biosynthesis of the type II polyketide antitumor antibiotic xantholipin. *Chem. Biol*. 19, 422–432. doi: 10.1016/j.chembiol.2012.01.016

Zheng, W., Zhao, Y., Zheng, X., Liu, Y., Pan, S., Dai, Y., et al. (2011). Production of antioxidant and antitumor metabolites by submerged cultures of *Inonotus obliquus* cocultured with *Phellinus punctatus*. *Appl. Microbiol. Biotechnol.* 89, 157–167. doi: 10.1007/s00253-010-2846-2

Conflict of Interest Statement: The authors declare that the research was conducted in the absence of any commercial or financial relationships that could be construed as a potential conflict of interest.

The reviewer MT and handling Editor declared their shared affiliation.

frontiers in Microbiology

ORIGINAL RESEARCH
published: 18 April 2018
doi: 10.3389/fmicb.2018.00651

How Does Salinity Shape Bacterial and Fungal Microbiomes of *Alnus glutinosa* Roots?

*Dominika Thiem[1,2], Marcin Gołębiewski[2,3], Piotr Hulisz[4], Agnieszka Piernik[5] and Katarzyna Hrynkiewicz[1,2]**

[1] Department of Microbiology, Faculty of Biology and Environmental Protection, Nicolaus Copernicus University in Toruń, Toruń, Poland, [2] Centre for Modern Interdisciplinary Technologies, Nicolaus Copernicus University in Toruń, Toruń, Poland, [3] Chair of Plant Physiology and Biotechnology, Faculty of Biology and Environmental Protection, Nicolaus Copernicus University in Toruń, Toruń, Poland, [4] Department of Soil Science and Landscape Management, Faculty of Earth Sciences, Nicolaus Copernicus University in Toruń, Toruń, Poland, [5] Chair of Geobotany and Landscape Planning, Faculty of Biology and Environmental Protection, Nicolaus Copernicus University in Toruń, Toruń, Poland

Black alder (*Alnus glutinosa* Gaertn.) belongs to dual mycorrhizal trees, forming ectomycorrhizal (EM) and arbuscular (AM) root structures, as well as represents actinorrhizal plants that associate with nitrogen-fixing actinomycete *Frankia* sp. We hypothesized that the unique ternary structure of symbionts can influence community structure of other plant-associated microorganisms (bacterial and fungal endophytes), particularly under seasonally changing salinity in *A. glutinosa* roots. In our study we analyzed black alder root bacterial and fungal microbiome present at two forest test sites (saline and non-saline) in two different seasons (spring and fall). The dominant type of root microsymbionts of alder were ectomycorrhizal fungi, whose distribution depended on site (salinity): *Tomentella*, *Lactarius*, and *Phialocephala* were more abundant at the saline site. *Mortierella* and *Naucoria* (representatives of saprotrophs or endophytes) displayed the opposite tendency. Arbuscular mycorrhizal fungi belonged to Glomeromycota (orders Paraglomales and Glomales), however, they represented less than 1% of all identified fungi. Bacterial community structure depended on test site but not on season. Sequences affiliated with *Rhodanobacter*, *Granulicella*, and *Sphingomonas* dominated at the saline site, while *Bradyrhizobium* and *Rhizobium* were more abundant at the non-saline site. Moreover, genus *Frankia* was observed only at the saline site. In conclusion, bacterial and fungal community structure of alder root microsymbionts and endophytes depends on five soil chemical parameters: salinity, phosphorus, pH, saturation percentage (SP) as well as total organic carbon (TOC), and seasonality does not appear to be an important factor shaping microbial communities. Ectomycorrhizal fungi are the most abundant symbionts of mature alders growing in saline soils. However, specific distribution of nitrogen-fixing *Frankia* (forming root nodules) and association of arbuscular fungi at early stages of plant development should be taken into account in further studies.

Keywords: salinity, ectomycorrhiza, arbuscular mycorrhiza, *Frankia* sp., metagenomics, Illumina MiSeq

OPEN ACCESS

Edited by:
Katarzyna Turnau,
Jagiellonian University, Poland

Reviewed by:
Christopher Blackwood,
Kent State University, United States
Christel Baum,
University of Rostock, Germany

***Correspondence:**
Katarzyna Hrynkiewicz
hrynk@umk.pl;
hrynkiewicz.katarzyna@gmail.com

Specialty section:
This article was submitted to Fungi and Their Interactions, a section of the journal Frontiers in Microbiology

Received: *09 October 2017*
Accepted: *20 March 2018*
Published: *18 April 2018*

Citation:
Thiem D, Gołębiewski M, Hulisz P, Piernik A and Hrynkiewicz K (2018) How Does Salinity Shape Bacterial and Fungal Microbiomes of Alnus glutinosa Roots? Front. Microbiol. 9:651. doi: 10.3389/fmicb.2018.00651

INTRODUCTION

The global scarcity of water resources, environmental pollution and increased salinization of soil and water are the most pressing problems of the 21st century. Salinity affects more than 7% of global land surface and 70% of all irrigated agricultural soils worldwide (Bencherif et al., 2015). Current predictions indicate that salinity is expected to be responsible for 30% land loss within the next 25 years, and up to 50% within the next 35 years (Chandrasekaran et al., 2014). Afforestation may contribute to solving the problem of soil reclamation, as it is a sustainable land use system that serves as an alternative to agriculture. In general, trees are more tolerant to salt stress than herbaceous crops (Chen et al., 2014). Among them, representatives of Betulaceae family are the most widely planted around the world for the rehabilitation of salinity affected lands (Diagne et al., 2013).

Alnus glutinosa Gaertn., commonly known as black alder, belongs to this plant family and is an actinorrhizal plant that forms symbiosis with nitrogen-fixing actinomycete *Frankia* sp. (McEwan et al., 2017; Roy et al., 2017). Additionally, *A. glutinosa* can be colonized by both ectomycorrhizal (EM) and arbuscular (AM) fungi at the same time (Pritsch et al., 1997). *Alnus* sp. has high potential in forestry, land reclamation and biomass production (Roy et al., 2007). Alder trees belong to pioneer tree species and can grow in poor or disturbed soils and are well adapted to abiotic stresses, e.g., drought, salinity, and flooding (Diagne et al., 2013).

The ability of alders to form multifactorial symbiotic association can be a key factor improving their tolerance to saline stress conditions. The symbiotic relationship with *Frankia* sp. increases the soil fertility and enhances the performance of tree during their plantation under unfavorable conditions (Diagne et al., 2013). *Alnus* plants inoculated with *Frankia* sp. in general display improved plant growth, total biomass, nitrogen supply, and chlorophyll content in leaves tissues under saline conditions (Oliveira et al., 2005; Ngom et al., 2016). However, the selection of tolerant *Frankia* sp. strains is needed because this symbiosis is facultative for the actinobacteria (Põlme et al., 2013). *Frankia* strains vary in their sensitivity and response to salinity (Ngom et al., 2016) and the number of root nodules, vesicle production and nitrogenase activity is affected under saline stress conditions (Oshone et al., 2013).

Mycorrhizal fungi – ectomycorrhizal and arbuscular – play an important role in protection of plants against abiotic stress in the environment (Schützendübel and Polle, 2002; Meharg, 2003; Ruotsalainen et al., 2009). Mycorrhizal fungi prevent Na^+ and Cl^- translocation to shoot and leaf tissues and enhance nutrients uptake, e.g., phosphorus (P) and nitrogen (N), in moderately salt-tolerant plants, e.g., black alder (Tang et al., 2009; Evelin et al., 2012), which indirectly increases plant growth and subsequent diminution of toxic ion effects (Tang et al., 2009). Mycorrhiza indirectly increase salinity tolerance by other mechanisms, e.g., by synthesis of phytohormones, amelioration of rhizosphere and bulk soil conditions (Asghari et al., 2005), enhancement of photosynthetic activity, water uptake (Hajiboland et al., 2010), accumulation of compatible solutes (Evelin and Kapoor, 2013), and production of higher levels of antioxidant enzymes (Manchanda and Garg, 2011). However, saline stress can affect mycorrhizal association (Hrynkiewicz et al., 2015) by decreasing fungal colonization capacity, the growth of fungal hyphae and germination of fungal spores in soil (Hameed et al., 2014). A broad taxonomic range of EM fungi can grow at ∼170 mM NaCl, although at a lower rate than in the absence of salt (Chen et al., 2001). This fact can suggest high salt resistance of many EM fungi (e.g., Dixon et al., 1993). Many reports describe successful application of salt-tolerant mycorrhizal fungi in plants protection against saline stress (Langenfeld-Heyser et al., 2007; Estrada et al., 2013; Talaat and Shawky, 2014; Sarwat et al., 2016). High concentrations of soluble salts have negative effect on microorganisms, e.g., decrease microbial activity and biomass and affect microbial community structure (Yan et al., 2015). However, this environmental factor can also predominantly stimulate occurrence of some salt tolerant bacterial and fungal strains, and the knowledge of changes in microbial community under salt stress conditions can be useful in development of new technologies used in forestry.

The aim of our study was to assess the effect of the unique ternary structure of alder symbionts on community of other root-associated microorganisms (bacterial and fungal endophytes), particularly under seasonally changing salinity. Specifically, we hypothesize that: (i) one type of symbiosis will dominate, (ii) salinity and seasonality will affect diversity and species richness of plant-associated bacteria and fungi, and (iii) salinity can preferentially promote occurrence of certain groups of symbionts or halotolerant bacterial and/or fungal taxa. Broadening of the knowledge on alder's endophytes can open new horizons in plant-microbial interactions occurring in forests.

MATERIALS AND METHODS

Site Description and Sampling

The study was carried out in mid-northern Poland at two test sites: a non-saline one in Pszczółczyn (53° 00′22.9″ N, 17° 54′57.2″ E; NS) and a saline one in Słonawy (53° 01′26.6″ N, 17° 37′47.3″ E; S) (Thiem et al., 2017). Salinity of soils in this area results from the impact of saline springs contacting with the Zechstein (Permian) salt deposits (Dadlez and Jaroszewski, 1994). The investigated saline site is located in the close vicinity of salt marshes (Solniska Szubińskie) belonging to the European Ecological Network Nature 2000. Analyzed sites belong to the State Forests, outside of any protected areas. The control site Pszczółczyn (NS) is located 18 km away from the saline test site (S). Both sites are located in Odra drainage basin, elevation is 100 m over the sea level and the sites are flat (<1° slope). They are characterized by similar climatic, hydrological and pedological conditions and harbor tree stands of similar age [about 20 years old, planted in 1995 (S) and 1996 (NS), respectively]. Climate is temperate, mean annual temperature is 8.4°C, and precipitation 520 mm. Groundwater table usually lies at lower than 1 m depth, the sites are located ∼1.5 km from the nearest river, and as such are not flooded by river waters. Soils are mineral-mucky developed on sands. Groundcover at

the NS site is typical for riparian forest and consists mainly of *Urtica dioica*, *Stachys sylvatica,* and *Ranunculus lanuginosus,* but also *Rubus occidentalis* could be found. At the S site the groundcover was even less diverse consisting almost exclusively of *U. dioica*.

Roots and soil samples (20 cm × 20 cm, 20 cm depth, litter layer was first removed) were collected from two test sites (NS and S) in two seasons of 2015 (spring – April and fall – September). In each test site three plots (10 m × 10 m) were selected, and within them three randomly selected trees were analyzed (9 trees per site). In total, 36 samples were analyzed (9 × 4 variants of experiment: NS-spring, NS-fall, S-spring, S-fall) (Supplementary Figure 1).

Soil Description and Analysis

The air-dried soil samples were passed through a 2 mm mesh and analyzed using the following methods: soil moisture content – gravimetrically, total organic carbon (TOC) and total nitrogen (TN) content using a CNS Vario MAX analyzer, pH (in H_2O and 1 M KCl) by potentiometric method, and phosphorus in 1% citric acid solution (P_{ca}) by colorimetric method. The saturation paste extracts were prepared to evaluate the soil salinity level. The electrical conductivity (EC_e) was measured conductometrically and saturation percentage (SP) – gravimetrically (van Reeuwijk, 2006). Soil moisture content (M) was determined by drying to constant weight at 105°C.

Metagenomic Analysis

Roots Cleaning and Preparation

First, soil was gently separated from roots to obtain rhizosphere soil for analysis of physico-chemical properties. Next, the pre-cleaned roots were thoroughly washed with sterile distilled water. Residual soil was separated from the roots with a sterile dissecting needle under magnifying glass and the roots were washed again with sterile distilled water. All steps were performed under sterile conditions. Ca. 500 mg samples were randomly collected from pools of cleaned roots and lyophilized.

Isolation of Metagenomic DNA

Total DNA was extracted from 50 mg of lyophilized black alder roots with the use of Plant & Fungi DNA Purification Kit (EURx, Poland) according to the manufacturer's protocol with the number of washing steps increased to four. Three technical replicates (independent DNA isolations) were prepared for each sample. Tubes with sterile glass beads (Mo Bio Laboratories) were used for plant material homogenization. The amount of isolated DNA was quantified fluorometrically (Qubit 2.0) and the quality was assessed spectrophotometrically (NanoDrop 2000) and the preparations were diluted to 1 ng/μl.

PCR Amplification of 16S rRNA Gene as Well as ITS Fragments and Sequencing

Bacterial 16S rRNA and fungal ITS amplicon libraries were generated in two-step PCR, first with the specific primers bearing M13/M13R overhangs (Gołębiewski et al., 2014) (bacteria: u357f and u786r; fungi: uITS1 and uITS2) then with M13 and M13R primers with P5/P7 adapters and barcodes (different MID sequences for each sample) (**Table 1**). Mock community sample with known composition of bacterial species (Human Microbiome Project Mock Community A, BEI Resources) was also processed. Negative control (without DNA) and positive control (*Escherichia coli* K12 DH10B [NC_00930.1] and *Paxillus involutus* [GQ389624.1] purified DNA) were included in each PCR round.

The first PCR reaction mix consisted of: 1 ng of DNA, 5 pmol of each primer, 4 nmol of each dNTP, 0.4 U of Phusion polymerase (Thermo Scientific), 100 μg of BSA and 1× concentrated buffer with 1.5 mM $MgCl_2$ in 20 μl. The cycling conditions were as follows: 98°C – 30 s; 30 cycles of: 98°C – 10 s, either 55°C (bacteria) or 53°C (fungi) – 15 s, 72°C for 20 s; then 5 min at 72°C. The PCR products were checked on 1.5% agarose gels in TBE and then they were purified using DNA Clean-Up Purification Kit (EURx) according to the manufacturer's protocol. Next, PCR products were quantified on Qubit 2.0 and diluted to 1 ng/μl.

The second PCR round was performed using Taq PCR Master Mix Kit (Qiagen) according to the manufacturer's protocol. The cycling conditions were as follows: 95°C – 5 min, 14 cycles of: 95°C – 30 s, 54°C –15 s, 72°C – 30 s; and finally 72°C for 1 min. The products were checked again on 1.5% agarose gel, quantified with Qubit 2.0 (Thermo Scientific) and pooled in equimolar amounts.

Libraries were purified twice with Agencourt AMPure XP (Beckman Coulter) according to the manufacturer's protocol. The quality of the pooled libraries was assessed on a Bioanalyzer chip (Agilent) and they were quantified with KAPA Library Quantification Kit for Illumina Platform using LightCycler 480 (Roche) according to the manufacturers' protocols. The final pool was diluted to 4 nM, denaturated, mixed with 5% of PhiX control library and sequenced with the use of 2 × 300 cycles kit v.3 on a MiSeq machine (Illumina). Sequencing was performed using HPLC-purified versions of forward and reverse primers as well as reverse-complement of the reverse primer (**Table 1**).

Bioinformatic and Statistical Analyzes

The resulting read pairs were quality filtered with Sickle (Joshi and Fass, 2011), merged with Pandaseq (Masella et al., 2012) and denoised with BayesHammer (Nikolenko et al., 2013). The sequences were classified with naive Bayesian classifier (Wang et al., 2003) with SILVA Seed v.123 database then bacterial and non-bacterial ones were separated.

In case of the bacterial 16S rRNA sequences, the processing was performed essentially as described in Gołębiewski et al. (2014). In brief: the sequences set was dereplicated, aligned to a template alignment (SILVA v. 123) and screened for the sequences covering the desired region of the alignment. Gap-only and terminal gap-containing columns were filtered out of the alignment, the set was pre-clustered to reduce the error rate and putative chimeras were identified with UCHIME (Edgar et al., 2011). The fungal sequences were processed with ITSx (Bengtsson-Palme et al., 2013), and all fungal ITS1 sequences were used in the downstream analyzes. The reads were dereplicated and OTUs were constructed using vsearch (Rognes

TABLE 1 | Primer sequences.

Name1	Sequence 5′ → 3′2	Paired with	Target	Reference
u357f	GTTTTCCCAGTCACGACCCTACGGGAGGCAGCAG	B786rU	Bacterial 16S	Neefs et al., 1993
u786r	CAGGAAACAGCTATGACACCAGGGTATCTAAWCC	B357fU		Deja-Sikora, 2012
uITS1	**GTTTTCCCAGTCACGA**CTCCGTAGGTGAACCTGCGG	uITS2	Fungal ITS	This work
uITS2	**CAGGAAACAGCTATGAC**TTYGCTGYGTTCTTCATCG	uITS1		This work
M13-x-A3,4	CCATCTCATCCCTGCGTGTCTCCGAC*TCAG*XGTTTTCCCAGTCACGAC	M13R-B	M13-tagged amplicons	This work
M13-x-A3,4	CCATCTCATCCCTGCGTGTCTCCGAC*TCAG*XGTTTTCCCAGTCACGAC	M13R-B		This work

1 – u denotes M13/M13R tagged sequences; 2 – M13 and M13R sequences are given in boldface font; 3 – key sequence in italics; 4 – X denotes barcode (MID sequence).

et al., 2016) at 0.03 dissimilarity level, then singletons as well as doubletons (OTUs consisting of one or two sequences only) were removed. The sequences were classified with naive Bayesian classifier (minimum 80% bootstrap support was required; Wang et al., 2003) using SILVA v.123 (bacteria) and ITS1 extracted from UNITE v.7 (fungi), and the non-bacterial and non-fungal sequences were removed from the respective sets. The final data were subsampled to 500 (bacteria) and 300 (fungi) sequences per sample twenty times, sequences names were mangled to reflect the iteration, the sets were pooled, dereplicated, and OTUs were constructed as described earlier. OTU tables were then averaged over the twenty subsamples and the entries were rounded to the nearest integer with a Perl script to yield the final tables. Bray–Curtis distance matrices based on Wisconsin double-standardized OTU tables were calculated with vegdist in R. Non-metric multidimensional scaling (NMDS) and canonical correspondence analysis (CCA) analyzes were performed within R with vegan's metaMDS and cca functions. In case of CCA, forward selection procedure implemented in ordistep was used for model building. Significance of differences between sample clusters was assessed with ANOSIM and PERMANOVA in vegan's anosim and adonis functions, respectively. p-value < 0.05 was considered significant. Variance partitioning was performed with the varpart function.

Differences between soil parameters were analyzed by the non-parametric Kruskal–Wallis test and the Dunn test for *post hoc* comparison (Statistica ver. 7.1, StatSoft et al., 2006). Significance of differences in means (number of observed OTUs, Shannon's H', Shannon's E, taxa and functional groups distribution) was assessed with ANOVA with *post hoc* Tukey's HSD analysis, unless assumptions of normality of data and/or homogeneity of variance were violated, in which case Robust ANOVA implemented in raov of the Rfit package was used to check for general p-value. All figures were plotted with standard R graphic functions.

Bacterial sequences were classified to functional groups (nitrogen-fixing, nitrifying, denitrifying, halotolerant/halophilic) based on a BLAST analysis. Matches were considered significant when the alignment spanned over 99% of query length and identity was over 99% (details in Supplementary Material).

Fungal sequences classified down to the species level were assigned to functional groups [saprophytic (S), parasitic/pathogenic (P), endophytic (E), mycorrhizal (M)] based on information contained in NCBI's databases including source of isolation, host and data contained in references pertaining to a given sequence (details in Supplementary Material).

Possible metagenomes were imputed based on 16S rRNA fragments data with PICRUSt v.1.1.3 (Langille et al., 2013). Briefly, sequences were reclassified using Greengenes v.13_8_99 (DeSantis et al., 2006), then a BIOM file was produced with MOTHUR and made compatible with PICRUSt using BIOM tools[1]. Then, the BIOM file was normalized with normalize_by_copy_number.py and metagenomes were predicted as well as NSTI scores calculated with predict_metagenomes.py, using KEGG Orthology[2] as the base for predictions. Finally, an.spf file was prepared with biom_to_stamp.py. Predicted metagenomes were analyzed at the KEGG Orthologs (KO) level with STAMP v.2.1.3 (Parks et al., 2014), using the following parameters: remove unclassified reads, analysis of two groups, two sided Welch's test with Benjamini-Hochberg FDR correction. Q-value threshold was set to 0.01 and minimum ratio of proportions of five was used as a filter. PCA plot as well as barplot for the most significantly different categories were prepared.

RESULTS

Soil Physico-Chemical Parameters Differ Between Test Sites and Seasons

Physico-chemical soil parameters of samples are presented in **Table 2**. The EC_e values at the S site ranged between 2.4 and 5 $dS{\cdot}m^{-1}$ in spring, and they were significantly lower ($\sim$1 $dS{\cdot}m^{-1}$) in fall. At the NS site the values ranged between 0.55 to 1.13 $dS{\cdot}m^{-1}$. We supposed that the low EC_e values at the saline site in fall were due to heavy rainfalls occurring right before sampling, which caused increase of soil water content and decreased salinity. It was confirmed by the higher level of soil moisture (M) at the S site, close to the values of SP. Similar phenomenon was observed at the NS site (**Table 2**). The soil samples from the S site were more acidic (pH-H_2O 6.1 and 5.6 in spring and fall, respectively) than the NS ones (pH-H_2O 6.7 and 6.5 in spring and fall, respectively). Soils at both sites were mineral, but the nutrients content (TOC, TN, and P_{ca}) was consistently higher at the NS site (**Table 2**).

[1]https://github.com/rprops/PICRUSt_from_mothur

[2]www.genome.jp

TABLE 2 | Physicochemical and chemical parameters of the studied soils (mean ± standard deviation) and Kruskal–Wallis test with the Dunn *post hoc* comparisons for analyzed variants (site: NS, non-saline; S, saline; season – fall, spring).

	NS		S		
Season	**Spring**	**Fall**	**Spring**	**Fall**	***p***
EC_e ($dS \cdot m^{-1}$)	0.90 ± 0.23^{a}	0.80 ± 0.25^{a}	3.70 ± 1.29^{b}	1.10 ± 0.34^{a}	0.0001
pH-H_2O	6.5 ± 0.5^{ab}	6.7 ± 0.3^{b}	6.1 ± 0.7^{ab}	5.6 ± 1.0^{a}	0.0196
pH-KCl	6.1 ± 0.6^{bc}	6.3 ± 0.4^{c}	5.0 ± 0.8^{ab}	4.3 ± 0.9^{a}	0.0001
TOC (%)	8.18 ± 2.34^{b}	9.90 ± 4.81^{b}	3.74 ± 1.36^{a}	5.31 ± 2.05^{ab}	0.0005
TN (%)	0.72 ± 0.18^{b}	0.84 ± 0.38^{b}	0.36 ± 0.12^{a}	0.49 ± 0.17^{ab}	0.0004
P_{ca} ($mg \cdot kg^{-1}$)	90.8 ± 30.2^{b}	83.6 ± 33.9^{b}	36.7 ± 4.60^{a}	34.7 ± 8.13^{a}	0.0000
M (%)	37.4 ± 13.4^{ab}	73.8 ± 15.4^{c}	27.6 ± 7.68^{a}	64.7 ± 22.6^{bc}	0.0000
SP (%)	79.2 ± 20.3^{a}	76.1 ± 22.5^{a}	64.1 ± 12.8^{a}	83.3 ± 26.7^{a}	0.3318

Variants labeled with the same letters are not significantly different ($p \leq 0.05$). EC_e, electrical conductivity of the saturated extract; pH-H_2O – pH in water; pH-KCl, pH in 1M KCl; TOC, total organic carbon; TN, total nitrogen; P_{ca}, phosphorus in 1% citric acid solution, M, soil moisture, SP, saturation percentage.

Sequencing Statistics

3 158 772 read pairs were obtained, of which 2 317 906 met the quality criteria and were merged. Of these, 546 961 sequences were classified as bacterial, and the rest (1 770 945) was regarded to be ITS sequences. 319 355 putative chimeras and 43 184 doubletons and singletons were removed from the bacterial dataset, leaving 184 422 sequences in the analysis (1–29 056 per sample).

ITSx correctly identified fungal ITS1 region in 863 931 putative ITS sequences. After classification with naive Bayesian classifier using the UNITE database, 588 198 non-fungal sequences were culled. They originated mainly from the host (*Alnus glutinosa*), demonstrating that the primers amplify not only fungal sequences. Finally, after removal of 11 264 singletons and doubletons 264 499 sequences were included in downstream analyses (2–18 341 per sample).

The reads, bacterial and fungal separately, were deposited in NCBI's SRA under accession no. SRP119174.

Microbial Community – Species Richness and Diversity Indices

Bacterial diversity, species richness as well as evenness for OTUs constructed at 0.03 dissimilarity threshold were lower at the S site both in spring and fall (**Figures 1A–C**). The opposite tendency was observed for fungal community, however, in fall the values were comparable at both sites, and they decreased at the S site and increased at the NS site (**Figures 1D–F**). Parameters measured for the bacterial community were always higher than for the fungal one: diversity ∼fourfold (bacteria: 4.3–5.0, fungi: 0.6–1.2), species richness ∼100 times (bacteria: 180–350, fungi: 18–34), and evenness ∼threefold (bacteria: 0.84–0.86, fungi: 0.21–0.34) (**Figure 1**).

Bacterial and Fungal Community Structure

Bacterial community was dominated by bacteria belonging to proteobacterial classes Alphaproteobacteria (NS: 36.4–38.7%, S: 27.0–28.3%) and Gammaproteobacteria (NS: 9.1–9.9%, S: 14.4–17.1%), Actinobacteria (NS: 18.0–19.4%, S: 16.0–16.6%) and Acidobacteria (NS:1.7–2.1%, S: 9.4–11.7%) (**Figure 2A**), however, the observed differences between the test sites were not significant. To the contrary, significant differences were observed at the genus level, where the most abundant genera differed between the NS and S sites: *Bradyrhizobium* and *Rhizobium* were more frequent at the NS site, while an unknown actinobacterial genus, *Rhodanobacter*, *Granulicella,* and *Sphingomonas* were more abundant at the S site (**Figure 2B**). At the level of order, sites differed significantly in abundance of Frankiales, comprising bacteria of genus *Frankia*, and greater abundance was observed at the S site (Supplementary Figure 2B). No significant differences between seasons were observed for all taxonomic levels.

Fungal community was dominated by Agaricomycetes (NS: 34.5–60.9%, S: 50.6–57.2%), Leotiomycetes (NS: 3.3–10.9, S: 13.7–17.4%), Mortierellomycotina Incertae Sedis (NS: 3.2–8.5%, S: 0.6–3.7%), and Sordariomycetes (NS: 06–2.1%, S: 0.9–1.7%) (**Figure 3A**). Similarly to bacteria, differences between sites and seasons at the class level were not significant, however, in general, greater abundance of Agaricomycetes was observed in fall, and Leotiomycetes were more frequent at the S site, and at the NS site in fall, while Mortierellomycotina Incertae Sedis and Sordariomycetes were most abundant at the NS site in fall, and at the S site in spring. At the genus level, *Tomentella*, *Lactarius*, *Phialocephala*, and *Mortierella* were the most frequent taxa, however, their share depended on site. *Tomentella*, *Lactarius*, and *Phialocephala* were more abundant at the S site, while *Mortierella* and *Naucoria* displayed the opposite tendency (**Figure 3B**). *Tomentella*, *Lactarius*, *Thelephora,* and *Naucoria* were the most frequently identified ectomycorrhizal fungi in all variants of the experiment (**Figure 3B**). Smaller number of sequences was noted for other EM fungal genera, such as *Cortinarius* or *Amanita* that were confounded within 'other fungi' group due to the low number of reads. Arbuscular mycorrhizal fungi were found in all samples and represented less than 1% of all identified fungi in each of them. They belonged to Glomeromycota (orders Paraglomales and Glomales, data not shown).

Microbial Communities Ordinations

Unconstrained ordination of bacterial community matrix (Bray–Curtis distance-based NMDS) demonstrated that the samples

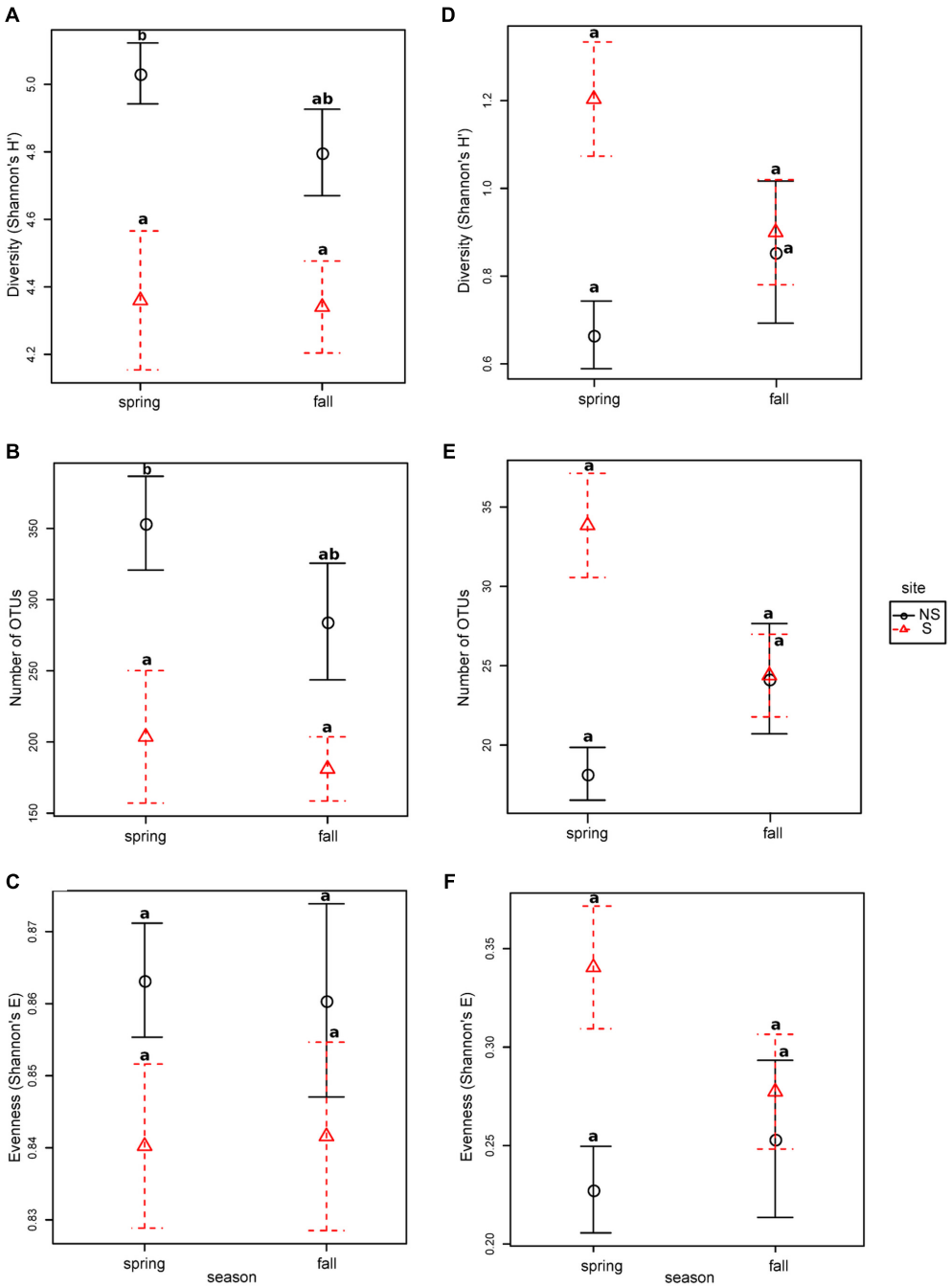

FIGURE 1 | Species richness, diversity and evenness in different seasons and sites for OTUs constructed at 0.03 dissimilarity for bacterial and fungal sequences: panels **(A,D)** Shannon's H', **(B,E)** – observed number of OTUs, **(C,F)** – Shannon's E. Robust ANOVA test with the Tukey's *post hoc* analysis were used to assess significance of differences between sites and seasons. Variants labeled with the same letters are not significantly different ($p \leq 0.05$).

were divided according to site and this grouping appeared to be significant according to ANOSIM and PERMANOVA analyses ($p < 0.001$) (**Figure 4A**). Notably, grouping according to season was not significant ($p > 0.05$). CCA, a method of constrained ordination (i.e., showing which environmental variables explain observed differences in community composition), showed that site together with P_{ca}, pH, and TOC were significant environmental factors shaping the structure of bacterial communities in analyzed samples (**Figure 4B**). Percent variance explained by the variables found in the CCA analysis was assessed with variance partitioning. Total variance explained by the variable in question is followed by variance explained solely by this variable: site – 25.00% (7.00%), P_{ca} – 15.60% (0.10%), pH – 14.40% (3.20%), TOC – 9.30% (1.00%).

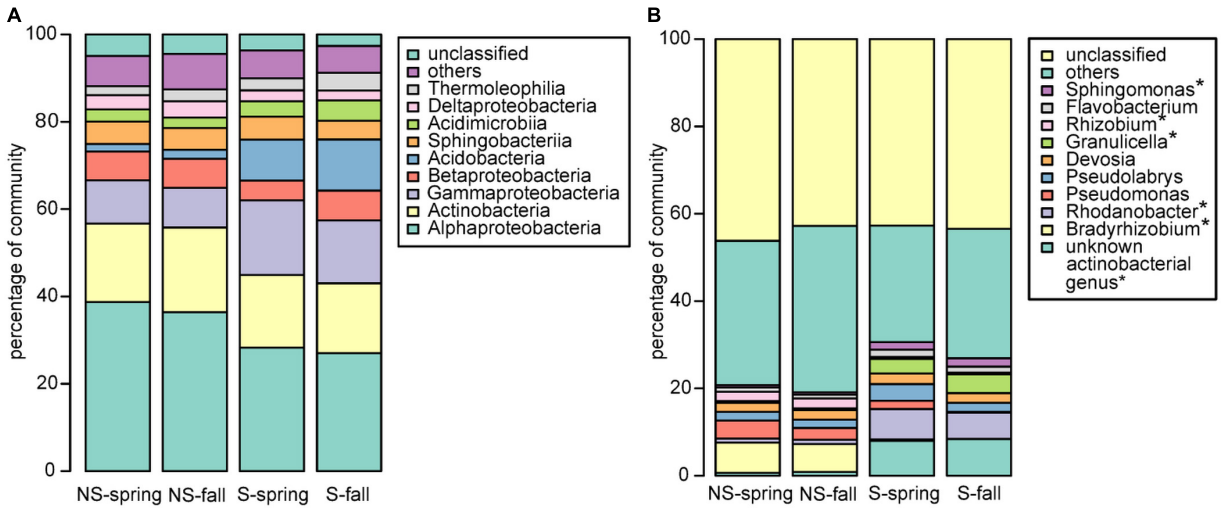

FIGURE 2 | Bacterial community structure at the **(A)** class and **(B)** genus level. *significant differences in the distribution.

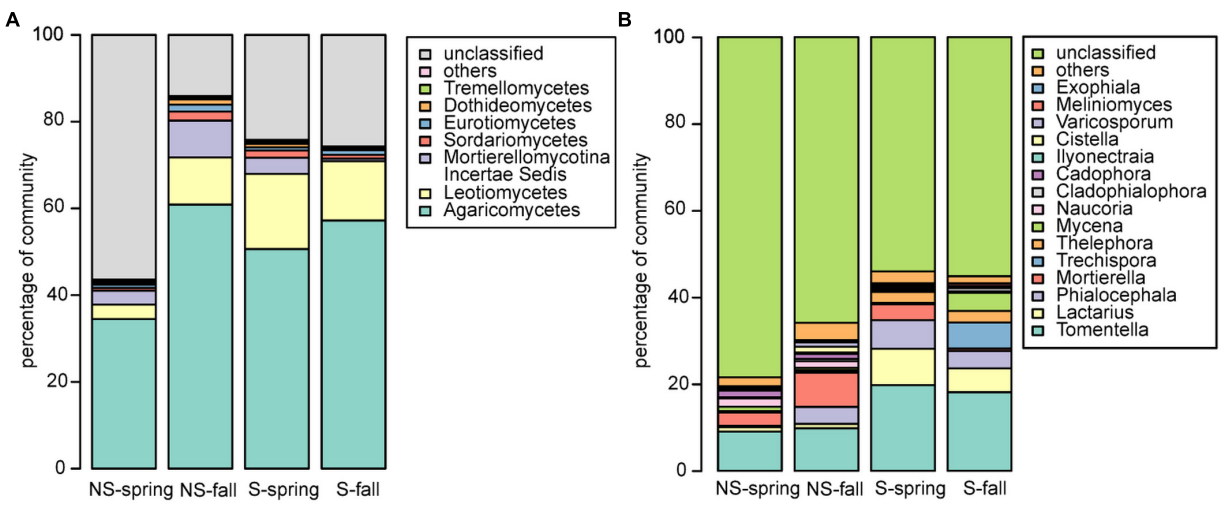

FIGURE 3 | Fungal community structure at the **(A)** class and **(B)** genus level.

Fungal communities, like bacterial ones, were grouped according to test site, and the grouping was significant (ANOSIM and PERMANOVA analyses, $p < 0.001$) (**Figure 4C**). Similarly to bacterial communities, CCA analysis revealed significant effect of site, P_{ca} and pH (**Figure 4D**). Variance partitioning showed that season site explained 7.90% (3.70%), SP – 6.10% (3.90%), P_{ca} – 5.80% (0.70%), pH – 5.10% (4.30%) of variance.

Functional Analysis of Bacterial and Fungal Communities

Bacterial sequences were classified to functional groups potentially involved in nitrogen cycling based on their similarity to 16S rRNA genes of organisms of known function (**Figure 5A**). Sequences similar to those coming from denitrifiers were more frequent at the S site, while nitrifying and nitrogen-fixing ones were more abundant at the NS site. Counter intuitively, the potentially halotolerant taxa were more frequent at the NS site in spring (data not shown).

Fungal sequences were classified based on descriptions of species found in NCBI's databases (**Figure 5B**). The percentage of saprophytic and parasitic/pathogenic taxa appeared to be consistently low. Occurence of endophytes and mycorrhizal fungi turned out to be negatively correlated, although the correlation was not significant (Spearman's $\rho = -0.14$, p-value = 0.2351). Endophytes were more frequent in fall and at the NS site, while the opposite was true for mycorrhizal fungi.

PICRUSt Analysis

PCA analysis demonstrated that sets of KOs were different in genomes of organisms coming from the two investigated sites (Supplementary Figure 4).

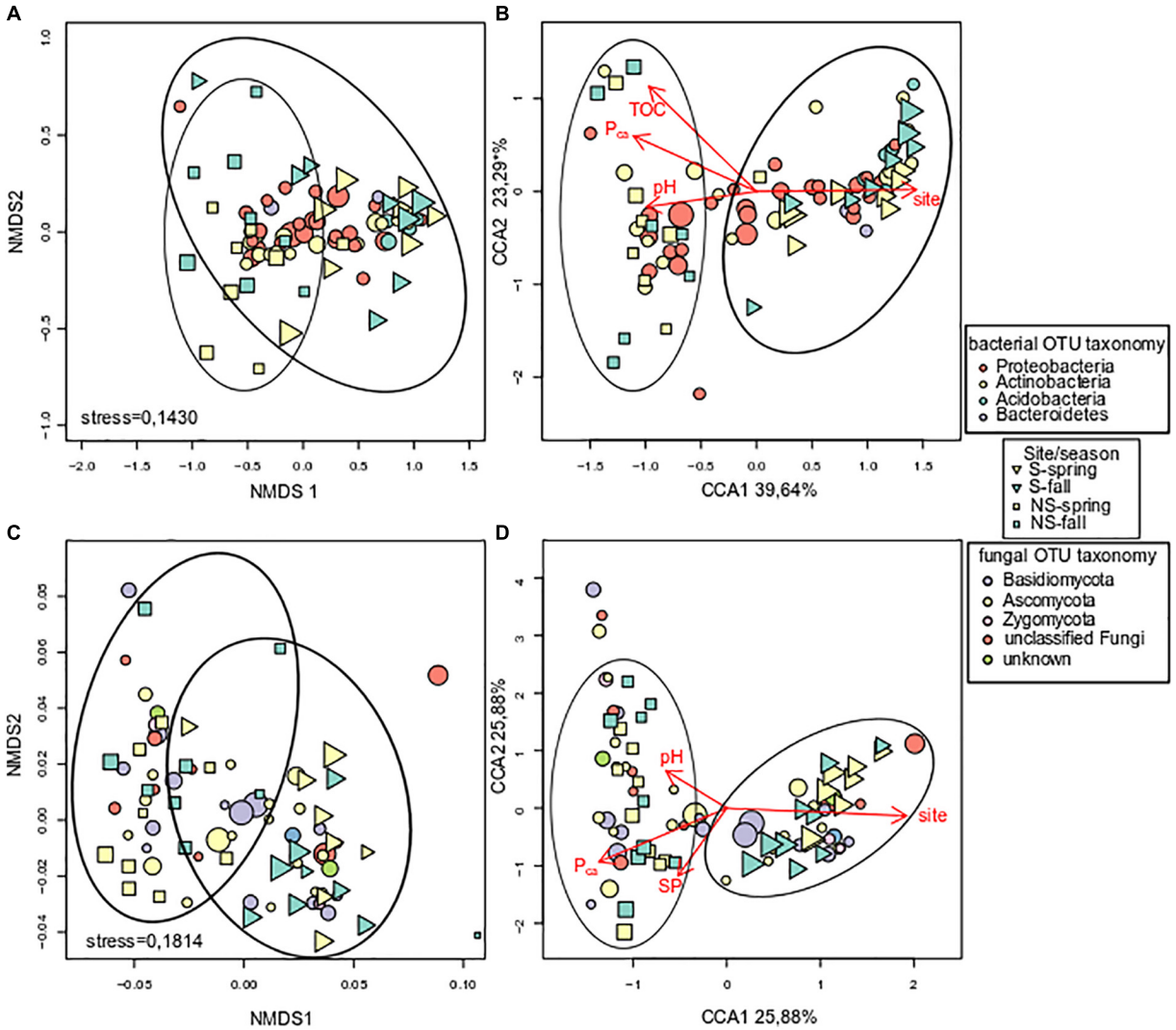

FIGURE 4 | Analysis of log-transformed and Wisconsin double-standardized Bray–Curtis dissimilarity matrix for bacterial and fungal communities, respectively: **(A)** stress = 0.1430 and **(C)** stress = 0.1814 – NMDS (non-metric multidimensional scaling analysis), **(B,D)** – CCA (canonical correspondence analysis). Circles represent OTUs, their fill color denotes consensus taxonomy at the phylum level. Fifty most abundant OTUs were plotted in each case. Squares and triangles represent sites, their fill color means season. Area of figures is proportional to square root of EC_e (electrical conductivity) in soil samples.

Altogether, 5101 KO categories were found by PICRUSt to be encoded in genomes of organisms thriving in alder root samples. Functional diversity (measured as the number of categories) did not differ significantly between samples groups, nor between sites (Kruskal–Wallis test, $p > 0.05$, Supplementary Table 1). Sixty-six KO categories were significant (**Figure 6**), five of them were represented more frequently in genomes of organisms coming from the S site. They were responsible for DNA replication and repair, biosynthesis and metabolism of pyrimidines as well as CoA biosynthesis. The remaining 61 categories were more frequent at the NS site. They were engaged in a plethora of processes, such as amino acids, peptides, carbohydrates, opines, and aromatic hydrocarbons metabolism, as well as type IV secretion, resistance to antibiotics and their biosynthesis (Supplementary Table 3).

DISCUSSION

Each plant species hosts a genotype-specific microbiome (i.e., endophytic microbiome) that dynamically responds to the environment, e.g., soil quality (Podolich et al., 2015). A recent meta-analysis of soil microbial communities revealed that the global microbial composition in saline soils is affected more by salinity than by extremes of any other abiotic factor, e.g., pH or temperature (Lozupone and Knight, 2007). There is a direct relationship between soil and root salinity levels, which may significantly influence endophytic microbial community structure (Yaish et al., 2016b). However, the effect of salinity on endophytic communities is largely unexplored. Most of the studies on the endophytes were focused on non-woody crops, moreover most of them used culture-dependent

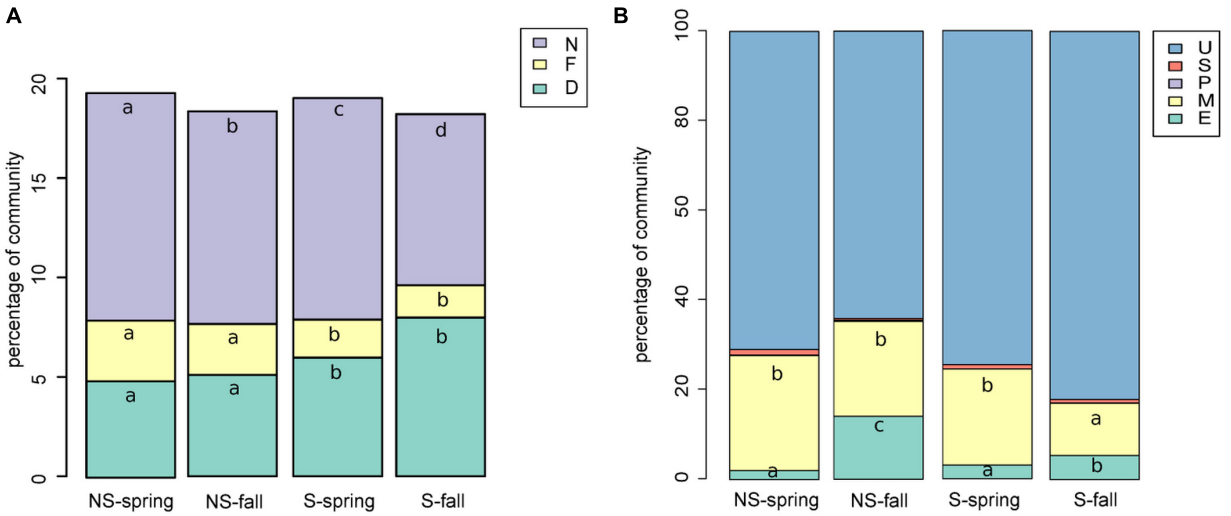

FIGURE 5 | Functional classification of **(A)** bacterial sequences: shares of bacterial functional groups potentially involved in nitrogen cycling, D, denitrifying; N, nitrifying; NF, nitrogen-fixing **(A)**; **(B)** fungal sequences, E, endophytic; M, mycorrhizae forming; P, parasitic/pathogenic; S, saprophytic; U, unknown/unclassifiable **(B)**. Classification results were added to the OTU table and graphs were prepared and Kruskal–Wallis tests were performed.

methods (Shen and Fulthorpe, 2015; Szymańska et al., 2016). Data on bacterial and fungal endophytes in roots of forest trees under saline stress are very limited (Ju et al., 2014; Hrynkiewicz et al., 2015; Thiem et al., 2017), and our work is the first report describing application of metagenomics to such a community with particular emphasis on root symbionts.

In general, we have noted more bacterial than fungal OTUs in alder roots, which may be caused by the 10-fold greater number of bacterial than fungal species observed in most soils (Larsen et al., 2017). Consistently bacteria showed higher diversity (measured as Shannon's H') than fungi. Moreover, our findings demonstrated significant differences in the endophytic microbial community composition due to the level of salt in the soil. Bacterial diversity, species richness, and evenness of black alder roots was decreased at the saline site (S), an effect similar to that observed by Yaish et al. (2016a) in *Phoenix dactylifera*. The lower average number of OTUs observed at the S site can be due to the fact that only a fraction of endophytes can thrive under conditions of increased salinity.

Black alder roots endophytic bacterial community was dominated by three phyla: Proteobacteria, Actinobacteria, and Acidobacteria that are the most common groups found in studies concerning soils (e.g., Gołębiewski et al., 2014; Canfora et al., 2017), including saline ones (Valenzuela-Encinas et al., 2009; Ma and Gong, 2013). Our results are also in agreement with studies of Shakya et al. (2013) concerning root endophytes of *Populus deltoides*. Moreover, our studies showed that Alphaproteobacteria, Actinobacteria, and Betaproteobacteria were found more frequently at the NS site, which is consistent with report of Yaish et al. (2016b). Decrease of Alphaproteobacteria and Actinobacteria level in response to environmental stress is a common observation in soil studies (e.g., Chodak et al., 2013; Gołębiewski et al., 2014). In our study, Acidobacteria and Gammaproteobacteria were more frequently found at the S site. It can be related to the higher abundance of this bacteria in saline soils (e.g., Yang et al., 2016; Yaish et al., 2016b).

Bacteria belonging to *Rhodanobacter*, *Granulicella,* and *Sphingomonas* genera were significantly more abundant in libraries coming from black alder roots from the S site. *Rhodanobacter* is a Gram-negative, aerobic bacterium currently not regarded as halotolerant. However, this bacterial species was found as a relatively abundant organism in *A. glutinosa* nodules (McEwan et al., 2017). *Sphingomonas* sp. belongs to a group of Gram-negative, chemoheterotrophic, aerobic bacteria that are widely distributed in nature, having been isolated from many different land and water habitats as well as from plant roots (Yang et al., 2016). Representatives of this genus make up a significant proportion of endophytic community in many trees (Izumi et al., 2008). They have the capacity to survive at low nutrient concentrations, as well as to metabolize a wide variety of carbon sources and some of them showed characteristics of nitrogen fixation and denitrification (Yang et al., 2016). Moreover, different species of *Sphingomonas* were shown to be endophytes effective in protection of crops against salts stress (Khan et al., 2014, 2017). Members of the *Granulicella* genus were found in the nodules of alder, similarly to *Rhodanobacter* (McEwan et al., 2017). Interestingly, according to Marupakula (2016), *Rhodanobacter* and *Granulicella* belong to bacteria colonizing ectomycorrhiza in boreal forest, which may suggest that they are mycorrhiza helper bacteria.

Frankia was found to be scarce in our study, and was found exclusively at the saline site. This might have been caused by a specific spatial distribution of these bacteria in plant roots, namely they are found mainly in nodules (Diagne et al., 2013). Roy et al. (2017) found 12 *Frankia* OTUs in *A. glutinosa* nodules,

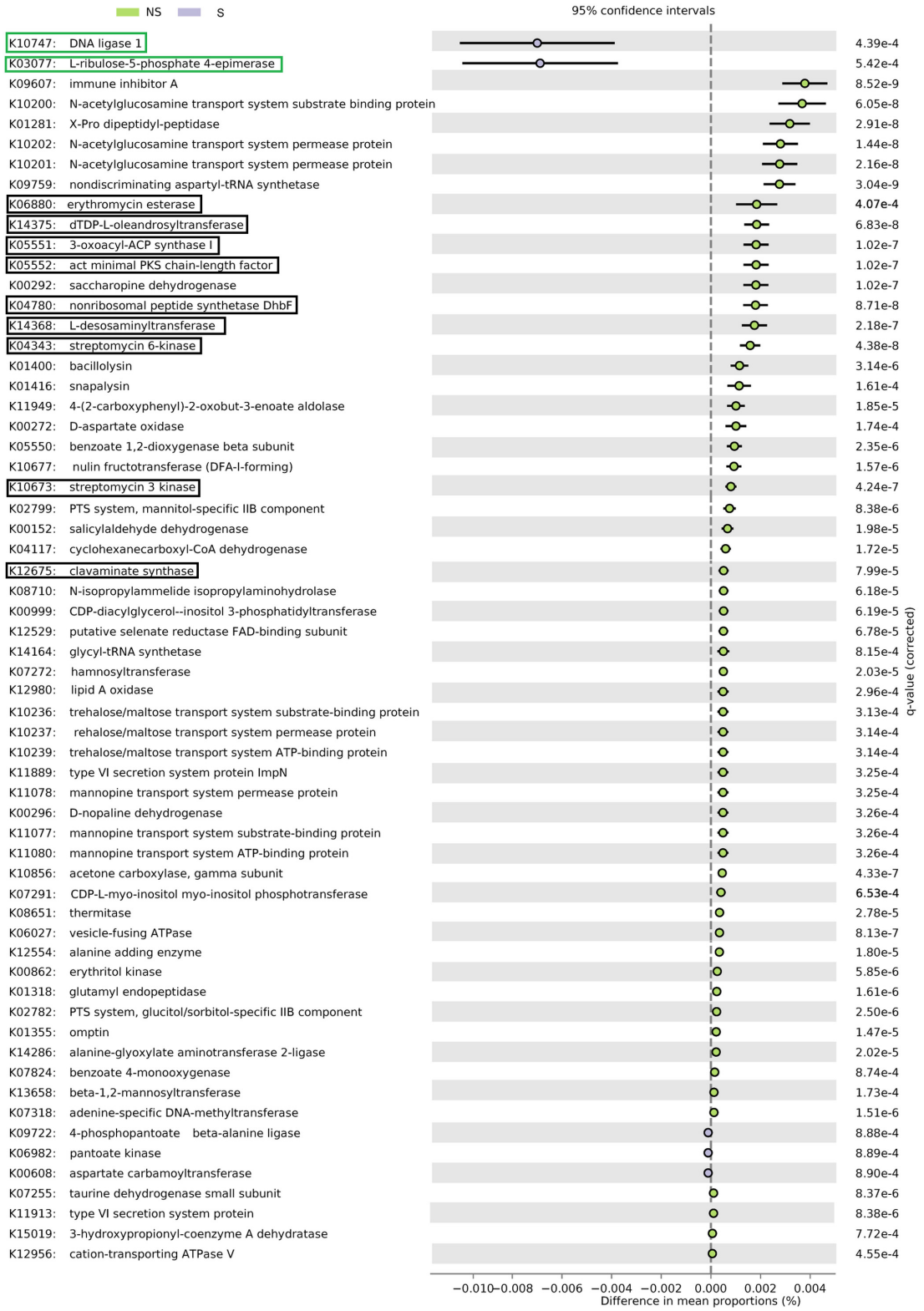

FIGURE 6 | PICRUSt analysis of bacterial sequences. Barplots for most significantly different KO categories. Error bars represent standard error of the mean of given category abundance in different sample types. Categories belonging to DNA replication and repair supercategory and are shown in green boxes, while antibiotic synthesis and resistance is displayed in black boxes. *Q*-values (False Discovery Rates, based on two-sided Welche's test with Benjamini-Hochberg correction) are given to the right of each category plot.

however, the bacteria might constitute <1% of all sequences (McEwan et al., 2017), which is similar to our results. This scarcity might have been caused by bias imposed by universal primers used. The universal primers were used to obtain broad picture of the bacterial community, at the expense of underrepresentation of certain groups.

Bradyrhizobium and *Rhizobium* were more abundant at the NS site. Members of both of these bacterial genera are common microsymbionts of nodulating legumes (Guimarães et al., 2015). However, many data indicate that non-legumes also react to the presence of bradyrhizobia and rhizobia in the rhizosphere. Root hair curling induced by these symbiotic bacteria was observed on maize, rice and oat plants (Antoun et al., 1998). To date, *Bradyrhizobium* was found to be endosymbiont of only one tree species – *Parasponia* (Trinick and Hadobas, 1988). *Bradyrhizobium* sp. is relatively sensitive to unfavorable environmental conditions, e.g., salinity (it tolerates up to 0.5–1% NaCl) (Guimarães et al., 2015) or soil pH (Rascovan et al., 2016). A member of the *Rhizobium* genus (*R. metallidurans*) was isolated from roots of silver birch and alder growing on heavy metals-contaminated sites (Złoch et al., 2016). However, representative of these genera can be also robust heterotrophs that can persist in bulk soil (Gano-Cohen et al., 2016).

Classification of bacterial OTUs into functional groups indicated that sequences from those potentially involved in nitrogen cycling comprised together ∼20% of their total number. This high percentage is in accordance with the key role of bacteria in nitrogen cycling in soil (Boyle et al., 2008). However, it must be noted that such a kind of analysis is intrinsically limited, as there may exist organisms with closely related 16S rRNA sequences, yet differing in genome content and not performing the same ecological roles. Therefore, these results should be treated with caution. Nitrogen-fixing bacteria were significantly more frequent at the NS site, and these organisms belonged to Alphaproteobacteria (*Rhizobium* and *Bradyrhizobium* genera). It might be connected to possible greater abundance of these taxa in non-saline soils, as it is known that environmental stress decreases level of Alphaproteobacteria in soils (e.g., Chodak et al., 2013).

To learn more on possible functions contained in genomes of organisms found in our samples, PICRUSt analysis was performed. Possible gene content was imputed based on Greengenes classification of OTUs. This approach allows to get insight into metagenomes without performing shotgun sequencing, which is much more expensive than amplicon sequencing. However, it has its intrinsic limits, due to the lack of certain sequences in the database and the fact that even organisms closely related in terms of 16S rRNA sequences may significantly differ when it comes to the gene content. Moreover, one has to bear in mind that this kind of analysis yields potential functions that does not need to be expressed. Nevertheless, when carefully interpreted, PICRUSt may yield interesting results at a very low cost. Our results suggest that bacterial functional diversity does not differ between sites, and, as antibiotic biosynthesis and resistance genes were more frequent at the site, that competition is more intensive. This is supported by the greater diversity observed at the NS site. On the other hand, higher salinity at the S site might have selected organisms more adapted to extreme environments requiring greater capabilities of DNA repair.

The ITS region sequencing indicated a positive relationship between higher salinity and biodiversity. We suggest that this phenomenon can be caused by two mechanisms: (i) salt-sensitive fungi may more readily enter plant roots where the environment is more stable, and (ii) plants may attract endophytes under stress conditions, as they might increase their tolerance to the stressors.

These mechanisms are connected with plant reaction to abiotic stress. Differences in the outside environment put the plant metabolism out of homeostasis and impose the necessity to harbor specific genetic and metabolic traits within its cellular system (Meena et al., 2017). Plant microbiome often facilitates reduction of abiotic stress (Singh et al., 2011; Meena et al., 2017), and endophytes from different habitats confer habitat-specific stress tolerance to plants (Rodriguez et al., 2004). It is also known that plant physiology together with environmental physico-chemical parameters determine endophytic community structure (Hardoim et al., 2015).

Alder's endophytic fungal community was dominated by members of Agaricomycetes, Leotiomycetes, and Mortierellomycotina Incertae Sedis. In spite of large differences in taxa abundances between sites and seasons, statistical analysis indicated that the differences were not significant. This effect was caused by large variability among analyzed replicates, which might have been caused by specific spatial distribution of fungal mycelia, among them the mycorrhizal ones. We observed lower abundance of Agaricomycetes and Leotiomycetes at the NS site in spring. These groups comprise many ectomycorrhizal representatives that may be less abundant under conditions of high soil phosphorus content (Balzergue et al., 2013; Nouri et al., 2014). Our analysis revealed mainly ectomycorrhizal fungi, while arbuscular ones turned out to be rare in our dataset. This is probably due to two factors: (i) primers' specificity and (ii) the age of the tree stands under study. Arbuscular mycorrhizal structures usually are formed only at early stages of seedling development (van der Heijden, 2001; Põlme et al., 2013).

Tomentella, *Lactarius*, and *Phialocephala* members were more abundant at the S site. *Tomentella* was commonly found as an ectomycorrhizal partner of many trees, such as willow, birch, or alder, with tendency to dominate at unfavorable environmental conditions (Ishida et al., 2009; Regvar et al., 2010; Hrynkiewicz et al., 2015). Our results suggest that members of this genus can be tolerant to salinity. Mechanisms involved in *Tomentella* tolerance to abiotic environmental stressors still remain to be elucidated. *Lactarius*, belonging to russula-lactarius fungal linkages (Tedersoo et al., 2009), was frequently identified in alder roots (Kennedy and Hill, 2010; Rochet et al., 2011), but never in saline environment. *Phialocephala* spp. belong to dark septate endophytes (DSE) and dominate the endophytic mycobiota in roots of conifers and members of the Ericaceae family in heathlands, forests, and alpine ecosystems (Grünig et al., 2009). *Phialocephala* spp. may form mycorrhizal structures or live as endophytes (Lukešová et al., 2015).

Contrary to the above-mentioned fungal taxa, *Mortierella* and *Naucoria* were found more frequently at the NS site. Members of the *Mortierella* genus can grow on a wide variety of substrates,

including chitin (Leake and Read, 1990), and are commonly found as soil-inhabiting saprophytes (Kirk et al., 2008), however, some species were found to adopt endophytic lifestyle (Jankowiak et al., 2016). They were also found to increase effectiveness of mycorrhiza formation and to solubilize phosphorus (Zhang et al., 2011). This fungal genus is known to prefer high organic matter content (Wagner et al., 2013) and its abundance was greater at the non-saline site. It is thus possible that the higher level of extractable phosphorus at the NS site is related to the incidence of *Mortierella*. Genus *Naucoria* (also known as *Alnicola*) comprises many closely related endophytic species that colonize *Alnus* roots (e.g., Moreau et al., 2006; Rochet et al., 2011).

As salinity and other soil physico-chemical parameters differed significantly between the test sites, we expected that the identity of sites would be the key driver of microbial diversity. Indeed, unconstrained ordinations showed that the samples coming from the same site clustered together, moreover, this grouping appeared to be significant. This was corroborated by the CCA analysis, wherein site TOC, pH, parasitic/pathogenic (P), and SP were found to be significant factors explaining variance in microbial communities. Seasonality is commonly regarded as an important parameter influencing plant-associated microbial communities (Hrynkiewicz et al., 2015; Shen and Fulthorpe, 2015). This is due to the differences in nutrients levels and temperature, both factors can change microorganisms' abundance and community structure (Carrero-Colo et al., 2006), however, we did not see significant influence of season on the communities under study. This effect might be explained by relative stability of environment within plants. Moreover, as we analyzed the communities by amplification of rDNA, we were unable to capture changes in microorganismal activity that probably fluctuated seasonally.

CONCLUSION

Salinity affects both bacterial and fungal diversity, albeit in different manners. Bacterial diversity decreases with salinity, while the response of fungi to this parameter is more complex. Bacterial and fungal community structure depends on salinity, and seasonality does not appear to be an important factor explaining variance in communities of root alder endophytes. There are taxa that are more abundant at the saline site: *Rhodanobacter*, *Sphingomonas*, and *Granulicella* (bacteria); *Tomentella*, *Lactarius*, *Phialocephala* (fungi). We found a low number of sequences coming from obvious halotolerant/halophilic bacteria and fungi in our dataset. Ectomycorrhizal fungi (*Tomentella*, *Lactarius*, and *Thelephora*) are an important component of endophytic community of alder roots at the saline site. The lasting challenge would be to evaluate microbiome influence on nutrients cycling and plant physiology of alder at a greater number of sites differing in salinity. This could be done by means of shotgun metatranscriptomic analysis coupled with marker amplicons sequencing both at the DNA and RNA levels.

AUTHOR CONTRIBUTIONS

DT did all the laboratory analyses and wrote the first version of the manuscript. MG designed the sequencing system, managed the lab experiments, performed the bioinformatic and statistical analyses, and participated in the preparation of the manuscript. PH did the soil chemical analyses and interpreted the results. AP selected the areas for field experiments, analyzed the M level in soils, and interpreted the results of soil analysis. KH designed and managed the field and lab experiments as well as participated in the preparation of the manuscript. All authors revised the manuscript and approved the publication.

FUNDING

This investigation was conducted under the framework of COST Action (European Cooperation in Science and Technology) FP1305 Linking Belowground Biodiversity and Ecosystem Function in European Forests, and financially supported by the National Science Centre (Poland) PRELUDIUM 2016/23/N/NZ8/00294.

SUPPLEMENTARY MATERIAL

The Supplementary Material for this article can be found online at: https://www.frontiersin.org/articles/10.3389/fmicb.2018.00651/full#supplementary-material

REFERENCES

Antoun, H., Beauchamp, C. J., Goussard, N., Chabot, R., and Lalande, R. (1998). Potential of *Rhizobium* and *Bradyrhizobium* species as plant growth promoting rhizobacteria on non-legumes: effects on radish (*Raphanus sativus* L.). *Plant Soil* 204, 57–67. doi: 10.1023/A:1004326910584

Asghari, H. R., Marschner, P., Smith, S. E., and Smith, F. A. (2005). Growth response of *Atriplex nummularia* to inoculation with arbuscular mycorrhizal fungi at different salinity levels. *Plant Soil* 373, 245–256. doi: 10.1007/s11104-004-7942-6

Balzergue, C., Chabaud, M., Barker, D. G., Bécard, G., and Rochange, S. F. (2013). High phosphate reduces host ability to develop arbuscular mycorrhizal symbiosis without affecting root calcium spiking responses to the fungus. *Front. Plant Sci.* 29:426. doi: 10.3389/fpls.2013.00426

Bencherif, K., Boutekrabt, A., Fontaine, J., Laruelle, F., Dalpè, Y., and Sahraoui, A. (2015). Science of the total environment impact of soil salinity on arbuscular mycorrhizal fungi biodiversity and microflora biomass associated with *Tamarix articulata* Vahll rhizosphere in arid and semi-arid Algerian areas. *Sci. Total Environ.* 533, 488–494. doi: 10.1016/j.scitotenv.2015.07.007

Bengtsson-Palme, J., Veldre, V., Ryberg, M., Hartmann, M., Branco, S., Wang, Z., et al. (2013). ITSx: improved software detection and extraction of ITS1 and ITS2 from ribosomal ITS sequences of fungi and other eukaryotes for use in environmental sequencing. *Methods Ecol. Evol.* 4, 914–919. doi: 10.1111/2041-210X.12073

Boyle, S. A., Yarwooda, R. R., Bottomley, P. J., and Myrolda, D. D. (2008). Bacterial and fungal contributions to soil nitrogen cycling under Douglas fir and red alder at two sites in Oregon. *Soil Biol. Biochem.* 40, 443–451. doi: 10.1016/j.soilbio.2007.09.007

Canfora, L., Salvati, L., Benedetti, A., and Francaviglia, R. (2017). Is soil microbial diversity affected by soil and groundwater salinity? Evidences from a coastal system in central Italy. *Environ. Monit. Assess.* 189:319. doi: 10.1007/s10661-017-6040-1

Carrero-Colo, M., Nakatsu, C. H., and Konopka, A. (2006). Effect of nutrient periodicity on microbial community dynamics. *Appl. Environ. Microbiol.* 72, 3175–3183. doi: 10.1128/AEM.72.5.3175-3183.2006

Chandrasekaran, M., Boughattas, S., Hu, S., Oh, S. H., and Sa, T. (2014). A meta-analysis of arbuscular mycorrhizal effects on plants grown under salt stress. *Mycorrhiza* 24, 611–625. doi: 10.1007/s00572-014-0582-7

Chen, D. M., Ellul, S., Herdman, K., and Cairney, J. W. G. (2001). Influence of salinity on biomass production by Australian *Pisolithus* spp. isolates. *Mycorrhiza* 11, 231–236. doi: 10.1007/s005720100126

Chen, S., Hawighorst, P., Sun, J., and Polle, A. (2014). Salt tolerance in *Populus*: significance of stress signaling networks, mycorrhization, and soil amendments for cellular and whole-plant nutrition. *Environ. Exp. Bot.* 107, 113–124. doi: 10.1016/j.envexpbot.2014.06.001

Chodak, M., Gołębiewski, M., Morawska-Płoskonka, K., Kudak, K., and Niklińska, M. (2013). Diversity of microorganisms from forest soils differently polluted with heavy metals. *Appl. Soil Ecol.* 64, 7–14. doi: 10.1016/j.apsoil.2012.11.004

Dadlez, R., and Jaroszewski, W. (1994). *Tectonics*. Warsaw: PWN.

Deja-Sikora, E. (2012). *Search for Bacterial Cadmium, Zinc, Lead, Copper and Chromium Resistance Genes in Metagenome of Soils Polluted with Heavy Metals*. Ph.D. thesis, Nicolaus Copernicus University, Torun.

DeSantis, T. Z., Hugenholtz, P., Larsen, N., Rojas, M., Brodie, E. L., Keller, K., et al. (2006). Greengens, a chimera-checked 16S rRNA gene database and workbench compatible with ARB. *Appl. Environ. Microbiol.* 72, 5069–5072. doi: 10.1128/AEM.03006-05

Diagne, N., Arumugama, K., Ngom, M., Nambiar-Veetil, M., Franche, C., Narayanan, K. K., et al. (2013). Use of *Frankia* and actinorhizal plants for degraded lands reclamation. *BioMed Res. Int.* 2013:948258. doi: 10.1155/2013/948258

Dixon, R. K., Rao, M. V., and Garg, V. K. (1993). Salt stress affects *in vitro* growth and *in situ* symbioses of ectomycorrhizal fungi. *Mycorrhiza* 3, 63–68. doi: 10.1007/BF00210694

Edgar, R. C., Haas, B. J., Clemente, J. C., Quince, C., and Knight, R. (2011). UCHIME improves sensitivity and speed of chimera detection. *Bioinformatics* 27, 2194–2200. doi: 10.1093/bioinformatics/btr381

Estrada, B., Aroca, R., Maathuis, J. M., Barea, J. M., and Ruiz-Lozano, J. M. (2013). Arbuscular mycorrhizal fungi native from a Mediterranean saline area enhance maize tolerance to salinity through improved ion homeostasis. *Plant Cell Environ.* 36, 1771–1782. doi: 10.1111/pce.12082

Evelin, H., Giri, B., and Kapoor, R. (2012). Contribution of *Glomus intraradices* inoculation to nutrient acquisition and mitigation of ionic imbalance in NaCl-stressed *Trigonella foenum-graecum*. *Mycorrhiza* 22, 203–217. doi: 10.1007/s00572-011-0392-0

Evelin, H., and Kapoor, R. (2013). Arbuscular mycorrhizal symbiosis modulates antioxidant response in salt-stressed *Trigonella foenum-graecum* plants. *Mycorrhiza* 24, 197–208. doi: 10.1007/s00572-013-0529-4

Gano-Cohen, K. A., Stokes, P. J., Blanton, M. A., Wendlandt, C. E., Hollowell, A. C., Regus, J. U., et al. (2016). Nonnodulating *Bradyrhizobium* spp. modulate the benefits of legume-*Rhizobium* mutualism. *Appl. Environ. Microbiol.* 1, 5259–5268. doi: 10.1128/AEM.01116-16

Gołębiewski, M., Deja-Sikora, E., Cichosz, M., Tretyn, A., and Wróbel, B. (2014). 16S rDNA pyrosequencing analysis of bacterial community in heavy metals polluted soils. *Microb. Ecol.* 67, 635–647. doi: 10.1007/s00248-013-0344-7

Grünig, C. R., Queloz, V., Duò, A., and Sieber, T. N. (2009). Phylogeny of *Phaeomollisia piceae* gen. sp. nov.: a dark, septate, conifer-needle endophyte and its relationships to *Phialocephala* and *Acephala*. *Mycol. Res.* 113, 207–221. doi: 10.1016/j.mycres.2008.10.005

Guimarães, A. A., Florentinoa, L. A., Almeidaa, K. A., Lebbeb, L., Silvaa, K. B., Willemsb, A., et al. (2015). High diversity of *Bradyrhizobium* strains isolated from several legume species and land uses in Brazilian tropical ecosystems. *Syst. Appl. Microbiol.* 38, 433–441. doi: 10.1016/j.syapm.2015.06.006

Hajiboland, R., Aliasgharzadeh, N., Laiegh, S. F., and Poschenreider, C. (2010). Colonization with arbuscular mycorrhizal fungi improves salinity tolerance of tomato (*Solanum lycopersicum* L.) plants. *Plant Soil* 331, 313–327. doi: 10.1007/s11104-009-0255-z

Hameed, A., Dilfuza, E., Abd-Allah, E. F., Hashem, A., Kumar, A., and Ahmad, P. (2014). "Salinity stress and arbuscular mycorrhizal symbiosis in plants," in *Use of Microbes for the Alleviation of Soil Stresses*, ed. M. Miransari (New York, NY: Springer), 139–159.

Hardoim, P. R., van Overbeek, L. S., Berg, G., Pirttilä, A. M., Compant, S., Campisano, A., et al. (2015). The Hidden world within plants: ecological and evolutionary considerations for defining functioning of microbial endophytes. *Microbiol. Mol. Biol. Rev.* 79, 293–320. doi: 10.1128/MMBR.00050-14

Hrynkiewicz, K., Szymańska, S., Piernik, A., and Thiem, D. (2015). Ectomycorrhizal community structure of *Salix* and *Betula* spp. at a saline site in central Poland in relation to the seasons and soil parameters. *Water Air Soil Pollut.* 226:99. doi: 10.1007/s11270-015-2308-7

Ishida, T. A., Nara, K., Ma, S., Takano, T., and Liu, S. (2009). Ectomycorrhizal fungal community in alkaline-saline soil in northeastern China. *Mycorrhiza* 19, 329–335. doi: 10.1007/s00572-008-0219-9

Izumi, H., Cairney, J. W., Killham, K., Moore, E., Alexander, I. J., and Anderson, I. C. (2008). Bacteria associated with ectomycorrhizas of slash pine (*Pinus elliottii*) in south-eastern Queensland, Australia. *FEMS Microbiol. Lett.* 282, 196–204. doi: 10.1111/j.1574-6968.2008.01122.x

Jankowiak, R., Bilański, P., Paluch, J., and Kołodziej, Z. (2016). Fungi associated with dieback of *Abies alba* seedlings in naturally regenerating forest ecosystems. *Fungal Ecol.* 24, 61–69. doi: 10.1016/j.funeco.2016.08.13

Joshi, N. A., and Fass, J. N. (2011). *Sickle: A Sliding-window, Adaptive, Quality-based Trimming Tool for FastQ Files (Version 1.33) [Software]*. Available at: https://github.com/najoshi/sickle

Ju, X., Ouyang, L., and Zhang, L. (2014). Endophytes community of *Populus euphratica* Oliv and the strains improving the salt tolerance of plant. *J. Pure Appl. Microbiol.* 8, 43–51.

Kennedy, P. G., and Hill, L. T. (2010). A molecular and phylogenetic analysis of the structure and specificity of *Alnus rubra* ectomycorrhizal assemblages. *Fungal Ecol.* 3, 195–204. doi: 10.1016/j.funeco.2009.08.005

Khan, A. L., Waqas, M., Asaf, S., Kamran, M., Shahzad, R., Bilal, S., et al. (2017). Plant growth-promoting endophyte *Sphingomonas* sp. LK11 alleviates salinity stress in *Solanum pimpinellifolium*. *Environ. Exp. Bot.* 133, 58–69. doi: 10.1016/j.envexpbot.2016.09.009

Khan, A. L., Waqas, M., Kang, S. M., Al-Harrasi, A., Hussain, J., Al-Rawahi, A., et al. (2014). Bacterial endophyte *Sphingomonas* sp. LK11 produces gibberellins and IAA and promotes tomato plant growth. *J. Microbiol.* 52, 689–695. doi: 10.1007/s12275-014-4002-7

Kirk, P. M., Cannon, P. F., Minter, D. W., and Stalpers, J. A. (2008). *Dictionary of the Fungi*, 10th Edn. Wallingford: CAB International.

Langenfeld-Heyser, R., Gao, J., Ducic, T., Tachd, P., Lu, C. F., Fritz, E., et al. (2007). *Paxillus involutus* mycorrhiza attenuate NaCl-stress responses in the salt-sensitive hybrid poplar *Populus* × *canescens*. *Mycorrhiza* 17, 121–131. doi: 10.1007/s00572-006-0084-3

Langille, M. G. I., Zaneveld, J., Caporaso, J. G., McDonald, D., Knights, D., A Reyes, J., et al. (2013). Predictive functional profiling of microbial communities using 16S rRNA marker gene sequences. *Nat. Biotechnol.* 31, 814–821. doi: 10.1038/nbt.2676

Larsen, B. B., Miller, E. C., Rhodes, M. K., and Wiens, J. J. (2017). Inordinate fondness multiplied and redistributed: the number of species on earth and the new pie of life. *Q. Rev. Biol.* 92, 229–265. doi: 10.1086/693564

Leake, J. R., and Read, D. J. (1990). Chitin as a nitrogen source for mycorrhizal fungi. *Mycol. Res.* 94, 993–995. doi: 10.1016/S0953-7562(09)81318-X

Lozupone, C. A., and Knight, R. (2007). Global patterns in bacterial diversity. *Proc. Natl. Acad. Sci. U.S.A.* 104, 11436–11440. doi: 10.1073/pnas.0611525104

Lukešová, T., Kohout, P., Větrovský, T., and Vohník, M. (2015). The potential of dark septate endophytes to form root symbioses with ectomycorrhizal and ericoid mycorrhizal middle European forest plants. *PLoS One* 10:e0124752. doi: 10.1371/journal.pone.0124752

Ma, B., and Gong, J. (2013). A meta-analysis of the publicly available bacterial and archaeal sequence diversity in saline soils. *World J. Microbiol. Biotechnol.* 29, 2325–2334. doi: 10.1007/s11274-013-1399-9

Manchanda, G., and Garg, N. (2011). Alleviation of salt-induced ionic, osmotic and oxidative stresses in *Cajanus cajan* nodules by AM inoculation. *Plant Biosyst.* 145, 88–97. doi: 10.1080/11263504.2010.539851

Marupakula, S. (2016). *Interactions between Ectomycorrhizal Associations and Bacteria*. Ph.D. thesis, University of Agricultural Sciences, Uppsala.

Masella, A. P., Bartram, A. K., Truszkowski, J. M., Brown, D. G., and Neufeld, J. D. (2012). PANDAseq: paired-end assembler for Illumina sequences. *BMC Bioinformatics* 14:31. doi: 10.1186/1471-2105-13-31

McEwan, N. R., Wilkinson, T., Girdwood, S. E., Snelling, T. J., Collins, T., Dougal, K., et al. (2017). Evaluation of the microbiome of decaying alder nodules by next generation sequencing. *Endocyt. Cell Res.* 28, 14–19.

Meena, K. K., Sorty, A. M., Bitla, U. M., Choudhary, K., Gupta, P., Pareek, A., et al. (2017). Abiotic stress responses and microbe-mediated mitigation in plants: the Omics strategies. *Front. Plant Sci.* 9:172. doi: 10.3389/fpls.2017.00172

Meharg, A. A. (2003). The mechanistic basis of interactions between mycorrhizal associations and toxic metal cations. *Mycol. Res.* 107, 1253–1265. doi: 10.1017/S0953756203008608

Moreau, P. A., Peintner, U., and Gardes, M. (2006). Phylogeny of the ectomycorrhizal mushroom genus *Alnicola* (Basidiomycota, Cortinariaceae) based on rDNA sequences with special emphasis on host specificity and morphological characters. *Mol. Phylogenet. Evol.* 38, 794–807. doi: 10.1016/j.ympev.2005.10.008

Neefs, J. M., Van de Peer, Y., De Rijk, P., Chapelle, S., and De Wachter, R. (1993). Compilation of small ribosomal subunit RNA structures. *Nucleic Acids Res.* 21, 3025–3049. doi: 10.1093/nar/21.13.3025

Ngom, M., Oshone, R., Diagne, N., Cissoko, M., Svistoonoff, S., Tisa, L. S., et al. (2016). Tolerance to environmental stress by the nitrogen-fixing actinobacterium *Frankia* and its role in actinorhizal plants adaptation. *Symbiosis* 70, 17–29. doi: 10.1007/s13199-016-0396-9

Nikolenko, S. I., Korobeynikov, A. I., and Alekseyev, M. A. (2013). BayesHammer: Bayesian clustering for error correction in single-cell sequencing. *BMC Genomics* 14(Suppl. 1):S7. doi: 10.1186/1471-2164-14-S1-S7

Nouri, E., Breuillin-Sessoms, F., Feller, U., and Reinhardt, D. (2014). Phosphorus and nitrogen regulate arbuscular mycorrhizal symbiosis in *Petunia hybrida*. *PLoS One* 9:e90841. doi: 10.1371/journal.pone.0090841

Oliveira, R. S., Castro, P. M. L., Dodd, J. C., and Vosátka, M. (2005). Synergistic effect of *Glomus intraradices* and *Frankia* spp. on the growth and stress recovery of *Alnus glutinosa* in an alkaline anthropogenic sediment. *Chemosphere* 60, 1462–1470. doi: 10.1016/j.chemosphere.2005.01.038

Oshone, R., Mansour, S. R., and Tisa, L. S. (2013). Effect of salt stress on the physiology of *Frankia* sp. strain CcI6. *J. Biosci.* 38, 699–702. doi: 10.1007/s12038-013-9371-2

Parks, D. H., Tyson, G. W., Hugenholtz, P., and Beiko, R. G. (2014). STAMP: statistical analysis of taxonomic and functional profiles. *Bioinformatics* 30, 3123–3124. doi: 10.1093/bioinformatics/btu494

Podolich, O., Ardanov, P., Zaets, I., Pirttilä, A. M., and Kozyrovska, N. (2015). Reviving of the endophytic bacterial community as a putative mechanism of plant resistance. *Plant Soil* 388, 367–377. doi: 10.1007/s11104-014-2235-1

Põlme, S., Bahram, M., Yamanaka, T., Nara, K., Dai, Y. C., Grebenc, T., et al. (2013). Biogeography of ectomycorrhizal fungi associated with alders (*Alnus* spp.) in relation to biotic and abiotic variables at the global scale. *New Phytol.* 198, 1239–1249. doi: 10.1111/nph.12170

Pritsch, K., Boyle, H., Munch, J. C., and Buscot, F. (1997). Characterization and identification of black alder ectomycorrhizas by PCR/RFLP analyses of the rDNA internal transcribed spacer (ITS). *New Phytol.* 137, 357–369. doi: 10.1046/j.1469-8137.1997.00806.x

Rascovan, N., Carbonetto, B., Perrig, D., Díaz, M., Canciani, W., Abalo, M., et al. (2016). Integrated analysis of root microbiomes of soybean and wheat from agricultural fields. *Sci. Rep.* 6:28084. doi: 10.1038/srep28084

Regvar, M., Likar, M., Piltaver, A., Kugonic, N., and Smith, J. E. (2010). Fungal community structure under goat willows (*Salix caprea* L.) growing at metal polluted site: the potential of screening in a model phytostabilisation study. *Plant Soil* 330, 345–356. doi: 10.1007/s11104-009-0207-7

Rochet, J., Moreau, P. A., Manzi, S., and Gardes, M. (2011). Comparative phylogenies and host specialization in the alder ectomycorrhizal fungi *Alnicola*, *Alpova* and *Lactarius* (Basidiomycota) in Europe. *BMC Evol. Biol.* 11:40. doi: 10.1186/1471-2148-11-40

Rodriguez, R. J., Redman, R. S., and Henson, J. M. (2004). The role of fungal symbioses in the adaptation of plants to high stress environments. *Mitig. Adapt. Strat. Glob. Change* 9, 261-272. doi: 10.1023/B:MITI.0000029922.31110.97

Rognes, T., Flori, T., Nichols, B., Quince, C., and Mahe, F. (2016). vSEARCH: a versatile open source tool for metagenomics. *PeerJ* 4:e2584. doi: 10.7717/peerj.2584

Roy, M., Pozzi, A. C., Gareil, R., Nagati, M., Manzi, S., Nouioui, I., et al. (2017). Alder and the Golden Fleece: high diversity of *Frankia* and ectomycorrhizal fungi revealed from *Alnus glutinosa* subsp. *barbata* roots close to a Tertiary and glacial refugium. *PeerJ* 18:e3479. doi: 10.7717/peerj.3479

Roy, S., Khasa, D. P., and Greer, C. W. (2007). Combining alders, frankiae, and mycorrhizae for soil remediation and revegetation. *Can. J. Bot.* 85, 237–251. doi: 10.1139/B07-017

Ruotsalainen, A. L., Markkola, A. M., and Kozlov, M. V. (2009). Mycorrhizal colonisation of mountain birch (*Betula pubescens* ssp. *czerepanovii*) along three environmental gradients: does life in harsh environments alter plant-fungal relationships? *Environ. Monit. Assess.* 148, 215–232. doi: 10.1007/s10661-007-0152-y

Sarwat, M., Hashem, A., Ahanger, M. A., Elsayed, F. A., Alqarawi, A. A., Alyemeni, M. N., et al. (2016). Mitigation of NaCl stress by arbuscular mycorrhizal fungi through the modulation of osmolytes, antioxidants and secondary metabolites in mustard (*Brassica juncea* L.) plants. *Front. Plant Sci.* 7:869. doi: 10.3389/fpls.2016.00869

Schützendübel, A., and Polle, A. (2002). Plant responses to abiotic stresses: heavy metal induced oxidative stress and protection by mycorrhization. *J. Exp. Bot.* 53, 1351–1365. doi: 10.1093/jexbot/53.372.1351

Shakya, M., Gottel, N., Castro, H., Yang, Z. K., Gunter, L., Labbé, J., et al. (2013). A multifactor analysis of fungal and bacterial community structure in the root microbiome of mature *Populus deltoides* trees. *PLoS One* 8:e76382. doi: 10.1371/journal.pone.0076382

Shen, S. Y., and Fulthorpe, R. (2015). Seasonal variation of bacterial endophytes in urban trees. *Front. Microbiol.* 6:427. doi: 10.3389/fmicb.2015.00427

Singh, L. P., Gill, S. S., and Tuteja, N. (2011). Unraveling the role of fungal symbionts in plant abiotic stress tolerance. *Plant Signal. Behav.* 6, 175–191. doi: 10.4161/psb.6.2.14146

StatSoft, Inc. (2006). *Statistica for Windows (Version 7.1) [Software]*. Available at: www.statsoft.com

Szymańska, S., Płociniczak, T., Piotrowska-Seget, Z., and Hrynkiewicz, K. (2016). Endophytic and rhizosphere bacteria associated with the roots of the halophyte *Salicornia europaea* L. – community structure and metabolic potential. *Microbiol. Res.* 192, 37–51. doi: 10.1016/j.micres.2016.05.012

Talaat, N. B., and Shawky, B. T. (2014). Protective effects of arbuscular mycorrhizal fungi on wheat (*Triticum aestivum* L.) plants exposed to salinity. *Environ. Exp. Bot.* 98, 20–31. doi: 10.1016/j.envexpbot.2013.10.005

Tang, M., Sheng, M., Chen, H., and Zhang, F. F. (2009). *In vitro* salinity resistance of three ectomycorrhizal fungi. *Soil Biol. Biochem.* 41, 948–953. doi: 10.1016/j.soilbio.2008.12.007

Tedersoo, L., Suvi, T., Jairus, T., Ostonen, I., and Põlme, S. (2009). Revisiting ectomycorrhizal fungi of the genus *Alnus*: differential host specificity, diversity and determinants of the fungal community. *New Phytol.* 182, 727–735. doi: 10.1111/j.1469-8137.2009.02792.x

Thiem, D., Piernik, A., and Hrynkiewicz, K. (2017). Ectomycorrhizal and endophytic fungi associated with *Alnus glutinosa* growing in a saline area of central Poland. *Symbiosis* 1–12. doi: 10.1007/s13199-017-0512-5

Trinick, M. J., and Hadobas, P. A. (1988). Biology of the *Parasponia-Bradyrhizobium* symbiosis. *Plant Soil* 110, 177–185. doi: 10.1007/BF02226797

Valenzuela-Encinas, C., Neria-Gonzalez, I., Alcantara-Hernandez, R. J., Estrada-Alvarado, I., Zavala-Diaz de la Serna, F. J., Dendooven, L., et al. (2009). Changes in the bacterial populations of the highly alkaline saline soil of the former lake Texcoco (Mexico) following flooding. *Extremophiles* 13, 609–621. doi: 10.1007/s00792-009-0244-4

van der Heijden, E. W. (2001). Differential benefits of arbuscular mycorrhizal and ectomycorrhizal infection in *Salix repens*. *Mycorrhiza* 10, 185–193. doi: 10.1007/s005720000077

van Reeuwijk, L. P. (2006). *Procedures for Soil Analysis*. Wageningen: ISRIC.

Wagner, L., Stielow, B., Hoffmann, K., Petkovits, T., Papp, T., Vágvölgyi, C., et al. (2013). A comprehensive molecular phylogeny of the *Mortierellales* (*Mortierellomycotina*) based on nuclear ribosomal DNA. *Persoonia* 30, 77–93. doi: 10.3767/003158513X666268

Wang, H., Fan, W., Yu, P. S., and Han, J. (2003). "Mining concept-drifting data streams using ensemble classifiers," in *Proceedings of the 9th ACM International Conference on Knowledge Discovery and Data Mining* (Washington, DC: SIGKDD), 226–235. doi: 10.1145/956750.956778

Yaish, M. W., Al-Harrasi, I., Alansari, A. S., Al-Yahyai, R., and Glick, B. R. (2016a). The use of high throughput DNA sequence analysis to assess the endophytic microbiome of date palm roots grown under different levels of salt stress. *Int. Microbiol.* 19, 143–155. doi: 10.2436/20.1501.01.272

Yaish, M. W., Al-Lawati, A., Jana, G. A., Vishwas Patankar, H., and Glick, B. R. (2016b). Impact of soil salinity on the structure of the bacterial endophytic community identified from the roots of Caliph medic (*Medicago truncatula*). *PLoS One* 11:e0159007. doi: 10.1371/journal.pone.0159007

Yan, N., Marschner, P., Cao, W., Zuo, C., and Qin, W. (2015). Influence of salinity and water content on soil microorganisms. *Int. Soil Water Conserv. Res.* 3, 316–323. doi: 10.1016/j.iswcr.2015.11.003

Yang, H., Hu, J., Long, X., Liu, Z., and Renge, Z. (2016). Salinity altered root distribution and increased diversity of bacterial communities in the rhizosphere soil of Jerusalem artichoke. *Sci. Rep.* 6:20687. doi: 10.1038/srep20687

Zhang, H., Wu, X., Li, G., and Qui, P. (2011). Interactions between arbuscular mycorrhizal fungi and phosphate-solubilizing fungus (*Mortierella* sp.) and their effects on *Kostelelzkya virginica* growth and enzyme activities of rhizosphere and bulk soils at different salinities. *Biol. Fertil. Soils* 47, 543–554. doi: 10.1007/s00374-011-0563-3

Złoch, M., Thiem, D., Gadzała-Kopciuch, R., and Hrynkiewicz, K. (2016). Synthesis of siderophores by plant-associated metallotolerant bacteria under exposure to (Cd^{2+}). *Chemosphere* 156, 312–325. doi: 10.1016/j.chemosphere.2016.04.130

Conflict of Interest Statement: The authors declare that the research was conducted in the absence of any commercial or financial relationships that could be construed as a potential conflict of interest.

frontiers in Microbiology

ORIGINAL RESEARCH
published: 23 April 2018
doi: 10.3389/fmicb.2018.00747

Two P_{1B-1}-ATPases of *Amanita strobiliformis* With Distinct Properties in Cu/Ag Transport

*Vojtěch Beneš, Tereza Leonhardt, Jan Sácký and Pavel Kotrba**

Department of Biochemistry and Microbiology, University of Chemistry and Technology Prague, Prague, Czechia

As we have shown previously, the Cu and Ag concentrations in the sporocarps of Ag-hyperaccumulating *Amanita strobiliformis* are correlated, and both metals share the same uptake system and are sequestered by the same metallothioneins intracellularly. To further improve our knowledge of the Cu and Ag handling in *A. strobiliformis* cells, we searched its transcriptome for the P_{1B-1}-ATPases, recognizing Cu^+ and Ag^+ for transport. We identified transcripts encoding 1097-amino acid (AA) AsCRD1 and 978-AA AsCCC2, which were further subjected to functional studies in metal sensitive *Saccharomyces cerevisiae*. The expression of As*CRD1* conferred highly increased Cu and Ag tolerance to metal sensitive yeasts in which the functional AsCRD1:GFP (green fluorescent protein) fusion localized exclusively to the tonoplast, indicating that the AsCRD1-mediated Cu and Ag tolerance was a result of vacuolar sequestration of the metals. Increased accumulation of As*CRD1* transcripts observed in *A. strobiliformis* mycelium upon the treatments with Cu and Ag (8.7- and 4.5-fold in the presence of 5 μM metal, respectively) supported the notion that AsCRD1 can be involved in protection of the *A. strobiliformis* cells against the toxicity of both metals. Neither Cu nor Ag affected the levels of As*CCC2* transcripts. Heterologous expression of As*CCC2* in mutant yeasts did not contribute to Cu tolerance, but complemented the mutant genotype of the *S. cerevisiae ccc2*Δ strain. Consistent with the role of the yeast Ccc2 in the trafficking of Cu from cytoplasm to nascent proteins via post-Golgi, the GFP fluorescence in As*CCC2*-expressing *ccc2*Δ yeasts localized among Golgi-like punctate foci within the cells. The As*CRD1*- and As*CCC2*-associated phenotypes were lost in yeasts expressing mutant transporter variants in which a conserved phosphorylation/dephosphorylation site was altered. Altogether, the data support the roles of AsCRD1 and AsCCC2 as genuine P_{1B-1}-ATPases, and indicate their important functions in the removal of toxic excess of Cu and Ag from the cytoplasm and charging the endomembrane system with Cu, respectively.

Keywords: ectomycorrhizal fungi, P_1-type ATPase, copper transporter, silver transporter, metal homeostasis, *Amanita strobiliformis*

OPEN ACCESS

Edited by:
Erika Kothe, Friedrich-Schiller-Universität Jena, Germany

Reviewed by:
Christopher Rensing, Fujian Agriculture and Forestry University, China
Michael Bölker, Philipps University of Marburg, Germany

****Correspondence:***
Pavel Kotrba
pavel.kotrba@vscht.cz

Specialty section:
This article was submitted to Fungi and Their Interactions, a section of the journal Frontiers in Microbiology

Received: *28 September 2017*
Accepted: *03 April 2018*
Published: *23 April 2018*

Citation:
Beneš V, Leonhardt T, Sácký J and Kotrba P (2018) Two P_{1B-1}-ATPases of Amanita strobiliformis With Distinct Properties in Cu/Ag Transport. Front. Microbiol. 9:747. doi: 10.3389/fmicb.2018.00747

INTRODUCTION

Studies have revealed that ectomycorrhizal (EM) fungi effectively mobilize heavy metals from soils and minerals (Gadd et al., 2012) and that ectomycorrhizae improve plant fitness in metal polluted environments also because metal tolerant mycobionts function as a barrier for the entry of metals into plant tissues (Colpaert et al., 2011; Reddy et al., 2016). High concentrations of heavy metals and

metalloids accumulated in the sporocarps further support the notion that EM fungi substantially contribute to the environmental cycling of these elements, including Cu and Ag (Falandysz and Borovička, 2013). It is noteworthy that studies indicate that macrofungi could be considered the most effective Ag accumulators among eukaryotes with two known outstanding EM species, *Amanita strobiliformis* and *Amanita solitaria* (Borovička et al., 2007, 2010). The concentrations of Ag in their sporocarps collected from unpolluted sites range from 200 to 1200 mg kg^{-1}. We have documented that the intracellular detoxification of Cu and Ag in *A. strobiliformis* largely relies upon binding with cysteinyl-rich, cytosolic metallothionein (MT) peptides, AsMT1a, 1b, and 1c (Osobová et al., 2011; Beneš et al., 2016; Hložková et al., 2016); and that two *A. strobiliformis* transporters of the copper transporter family (CTR; specifically AsCTR2 and AsCTR3) can recognize not only Cu, but also Ag for uptake (Beneš et al., 2016).

Studies in eukaryotes have revealed that while CTRs transport Cu ions into the cytoplasm, the members of P_{1B-1} subgroup of P_{1B}-type ATPases (also called heavy metal ATPases, HMA) contribute to the homeostasis and redistribution of essential Cu by exporting the metal ion from the cytoplasm into the subcellular compartments or out of the cell (Nevitt et al., 2012; Bashir et al., 2016). The homology of P_{1B}-ATPases and their characteristic sequence features suggest a division into seven subgroups (Smith et al., 2014). While the roles of the members of the P_{1B-5} to P_{1B-7} subgroups (predicted so far only in prokaryotes) remain elusive, the transporters belonging to P_{1B-1}, P_{1B-2}, prokaryote P_{1B-3}, and P_{1B-4} subgroups are known for distinct preferences for their substrate heavy metal ion(s). The transporters highly specific for monovalent Cu ions (the dominant intracellular Cu species in eukaryotes; Nevitt et al., 2012) comprise P_{1B-1}-subgroup, while P_{1B-2}, P_{1B-3}, and P_{1B-4} transport $Cd^{2+}/Zn^{2+}/Pb^{2+}$, Cu^{+}/Cu^{2+}, and Co^{2+}, respectively.

The intracellular handling of Cu involves in *Saccharomyces cerevisiae* Ccc2 protein (Bleackley and MacGillivray, 2011), and in mammals the Menkes protein ATP7A and Wilson protein ATP7B (La Fontaine and Mercer, 2007; Nevitt et al., 2012). These P_{1B-1}-ATPases are responsible for the transport of the physiological Cu into the post-Golgi. Unlike with Ccc2 in *S. cerevisiae*, the Cu overload in mammalian cells triggers trafficking of ATP7A to the plasma membrane and ATP7B to the excretory vesicles, and both transporters then facilitate the efflux of the excess metal to rescue the cell from Cu toxicity. Similar trafficking [from the endoplasmic reticulum (ER) to the plasma membrane] stimulated by Cu overload has been documented in *Arabidopsis thaliana* for its AtHMA5 and heterologously expressed SvHMA5I from *Silene vulgaris* (Li et al., 2017). It is noteworthy that several P_{1B-1}-ATPases have been shown to also recognize Ag for transport (Argüello et al., 2007; Smith et al., 2014; Migocka et al., 2015). Among fungi, the plasma membrane Cu^{+}- and Ag^{+}-efflux CaCRD1 of *Candida albicans* provides the primary source of cellular resistance against both metals (Riggle and Kumamoto, 2000; Weissman et al., 2000). Recently, the P_{1B-1}-ATPase CrpA that also localizes to the plasma membrane has been shown to confer substantial Cu- but not Ag-tolerance in filamentous fungus *Aspergillus nidulans* (Antsotegi-Uskola et al., 2017).

Since our previous studies revealed certain overlap in the cell biology of Ag and Cu in *A. strobiliformis*, we investigated whether or not this species may employ P_{1B-1}-ATPases in the intracellular handling of both Cu and Ag. We searched its transcriptome for the homologs of P_{1B-1}-ATPases and describe here the isolation and functional characterization of cDNA coding the Cu- and Ag-inducible AsCRD1 that can protect metal-sensitive yeasts against the toxicity of both metals. We also describe the second isolated P_{1B-1}-ATPase of *A. strobiliformis*, the homolog of yeast Ccc2 named AsCCC2. To our knowledge, these are the first P_{1B-1}-ATPases characterized in mycorrhizal fungi.

MATERIALS AND METHODS

Amplification of As*CRD1* and As*CCC2* Genes and Sequence Analyses

Partial sequences of As*CRD1* and As*CCC2* transcripts were obtained from tBLASTn analysis (Altschul et al., 1990) of the transcriptome of *A. strobiliformis* (Paulet ex Vittad.) isolate PRM 857486 (Hložková et al., 2016) by using characterized fungal P_{1B-1}-type ATPases as queries. The entire coding sequence information was established by 5′ and 3′ RACE, using a SMARTer RACE cDNA Amplification Kit (Clontech Labs) with 1 μg of total RNA to produce the population of the first cDNA strand; the Q5 High-Fidelity DNA polymerase (New England Biolabs) was used to obtain double-stranded cDNAs. The total RNA was isolated by using an RNeasy Plant Mini Kit and RNase free DNase set (Qiagen) from 50 mg of freeze-dried tissue of the *A. strobiliformis* PRM 857486 sporocarp. Transcript-specific primers were 5rCRD1_R1 to R5 for As*CRD1* 5′ RACE, and 5rCRD2_R1 to R3 or 3rCRD2R1 and R2 for As*CCC2* 5′ or 3′ RACE, respectively (for primer sequences see **Supplementary Table S1**), and the amplicons were subjected to 3′-A tailing with GoTaq DNA polymerase (Promega). Genomic fragments harboring As*CRD1* and As*CCC2* genes were amplified from 200 ng of chromosomal DNA template by PCR using Q5 DNA polymerase and pairs of gene-specific primers designed based on 5′ and 3′ untranslated regions of the corresponding cDNAs; the primers were CRD1_F/R for As*CRD1* and CRD2_F/R for As*CCC2* (**Supplementary Table S1**). The chromosomal DNA was isolated from 50 mg of freeze-dried tissue of *A. strobiliformis* PRM 857486 by using a NucleoSpin Plant II Kit (Macherey-Nagel). The amplicons were inserted to a pGEM-T vector (Promega) and then amplified in *E. coli* DH5α according to standard protocols. The recombinant DNAs were subjected to custom DNA sequencing on both strands with the vector-specific primers. The sequences of As*CRD1* and As*CCC2* cDNAs were deposited in GenBank under the accession numbers MF317930 and MF317931, respectively.

Sequence Analyses

The protein sequences deduced from the cDNAs were subjected to a transmembrane domain and signal peptide predictions

in silico at the CCTOP web server (Dobson et al., 2015). The signal peptide prediction was also done by submitting the sequences to SignalP 4.1 server (Pettersen et al., 2004). The homology modeling of transporter 3D structure used the Phyre2 protein homology/analogy recognition engine (Kelley et al., 2015), the Modeller (Webb and Sali, 2014), and UCSF Chimera (Pettersen et al., 2004) programs. The closest AsCRD1 and AsCCC2 homologs among the RCSB Protein Data Bank (PDB) entries used for comparative modeling were 2EW9 (N-terminal domain of ATP7B, 23% and 40% identity, respectively) and 3J09 (P_{1B-1}-ATPase of *Archaeoglobus fulgidus*; 34% and 41% identity, respectively). A MEGA 6.0 package (Tamura et al., 2013) incorporating ClustalW (Thompson et al., 1994) was used to align AsCRD1, AsCCC2, and related amino acid (AA) sequences (retrieved from UniProtKB datase by using BLASTp) and construct the corresponding unrooted phylogenetic tree using the Neighbor-joining method with Poisson correction model and 10,000 bootstrap replications.

Functional Complementation in Yeasts

The *S. cerevisiae* strains used in complementation assays were *cup1*Δ strain DTY113 (*MAT*α *trp1-1 leu2-3,-112 gal1 ura3-50 cup1*Δ*61*; Tamai et al., 1993) and the Euroscarf[1] Y00569 (*yap1*Δ; YML007w::kanMX4) and Y03629 (*ccc2*Δ; YDR270w::kanMX4) mutant strains of BY4741 (*MAT*a *his3*Δ*1 leu2*Δ*0 met15*Δ*0 ura3*Δ*0*). To constitutively express As*CRD1* and As*CCC2* in yeasts, the entire coding sequences produced by Q5 DNA polymerase from cDNA using primer pairs eifCRD1_F/R (As*CRD1*) and eifCRD2_F/R (As*CCC2*) were inserted into the HindIII-treated and EcoRI-treated yeast expression vector p416GPD (Mumberg et al., 1995), respectively, by using an In-Fusion HD Cloning Kit (Clontech Labs) according to manufacturer's instructions. Site-directed mutagenesis of As*CRD1* and As*CCC2* in p416GPD was performed by the inverse PCR method (Füzik et al., 2014) with Phusion High-Fidelity DNA Polymerase (Thermo Scientific); the overlapping primers used were mCRD1_F plus mCRD1_R and mCRD2_F plus mCRD2_R, respectively. Primer sequences are listed in **Supplementary Table S1**. The yeasts transformed with p416GPD-based plasmids were routinely grown at 30°C on *URA*$^-$ selective SD medium containing (w/v) 0.7% yeast nitrogen base (Difco), 0.005% adenine hemisulfate, 2% glucose, and 0.003% of each of the essential amino acids (Sigma-Aldrich).

For complementation plate assays, the mid-log cultures of transformed *S. cerevisiae* were adjusted to an optical density at 590 nm (OD_{590}) of 0.1, and 5 μl of serial dilutions were spotted on agar medium. The metal (added as $CuCl_2$ or $AgNO_3$) tolerance of *cup1*Δ and *yap1*Δ transformants was assayed on SD medium and non-fermentable YPEG medium [1% (w/v) yeast extract, 2% ([w/v) peptone, 2.5% (v/v) ethanol and 2.5% (v/v) glycerol], respectively. The growth tests of *ccc2*Δ transformants used non-fermentable YPEG medium.

Fluorescence Microscopy of As*CRD1:GFP* and As*CCC2:GFP*-Expressing Yeasts

To construct the translational As*CRD1*:*GFP* and As*CCC2*:*GFP* fusions, the coding sequences without the termination codons were amplified from cDNA by using primer pairs gifCRD1_F plus gifCRD2_R for As*CRD1* and gifCRD2_F plus gifCRD2_R for As*CCC2* (**Supplementary Table S1**). The amplicons were inserted into a BamHI-digested plasmid p416GFP. The plasmid p416GFP is a p416GPD derivative, harboring *GFP* from plasmid pEGFP-C1 (Clontech Labs) inserted as a BamHI/HindIII DNA fragment (Hložková et al., 2016). The cells of As*CRD1*:*GFP*-expressing *cup1*Δ and As*CCC2*:*GFP*-expressing *ccc2*Δ yeasts were obtained from mid-log cultures grown in SD medium supplemented with 0.5 $\mu g \cdot ml^{-1}$ DAPI (Invitrogen) when needed. Vacuoles were labeled at 30°C for 4 h in SD medium with 400 $\mu g \cdot ml^{-1}$ of the tonoplast-specific FM4-64 dye (Molecular Probes). The fluorescence microscopy was performed by using a BioSystems Imaging station Cell^R with a MT20 illumination and a DSU semiconfocal unit on a IX-81 microscope (Olympus BioSystems) equipped with the model C9100 EM-CCD camera (Hamamatsu Photonix). A GFP-deriving fluorescence was observed with the U-DM-DA-FI-Tx2 FITC filter (excitation band: 495/15 nm, emission band: 530/30 nm; Olympus) and nuclei stained with DAPI were visualized with the U-DM-DA-FI-Tx2 DAPI filter (excitation band: 400/15 nm, emission band: 460/20 nm). Vacuoles were observed with the U-DM-Cy5 filter (excitation band: 590–650 nm, emission band: 665–740 nm). The recorded black and white images were processed using the ImageJ software[2].

Gene Expression Analysis in *A. strobiliformis*

The mycelium isolate from the PRM 857486 pileus (Osobová et al., 2011) was grown at 25°C and routinely maintained on potato dextrose (PD) agar containing 4 $g \cdot l^{-1}$ potato extract (Sigma-Aldrich) and 10 $g \cdot l^{-1}$ glucose (0.5× PD). The metal dose-dependent growth was observed with mycelia grown for 8 weeks on 0.5× PD agar with $CuCl_2$ or $AgNO_3$ supplements. The expression of target genes was assessed in the mycelium propagated in liquid PD medium (basal Cu, Ag and Cd concentrations below the atomic absorption spectrometry detection limit of 0.21, 0.04, and 0.09 μM, respectively) for 16 weeks and then subjected to metal (added as $CuCl_2$, $AgNO_3$, or $CdCl_2$) exposures for 24 h. The gene expression analysis was performed on independent biological samples from three replicate experiments in two technical replicates. The RNA extraction from freeze-dried mycelia and quantitative reverse-transcribed PCR measurements including the quality/specificity controls were conducted essentially as described previously (Hložková et al., 2016). Briefly, the population of transcripts present in 1 μg of total RNA was reverse transcribed in a 20 μl reaction and 1.5 μl of the resulting cDNA product was used in a 12 μl quantitative PCR (qPCR) reaction for the measurements

[1] http://web.uni-frankfurt.de/fb15/mikro/euroscarf/

[2] http://imagej.nih.gov/ij/

with 0.35 μM gene-specific primers (**Supplementary Table S1**). The measurements used a DyNAmo Flash SYBR Green 2-Step qPCR Kit (Life Technologies) and a MiniOpticon Real Time PCR System (Bio-Rad). The primers were qF- plus qR-CRD1 for As*CRD1*, qF- plus qR-CRD2 for As*CRD1*, and qFtub-b plus qRtub-b for β-tubulin As*TUB-b* gene (GenBank: JX463743), which was used for normalization of the qPCR data as internal reference, stably expressed under Ag and Cu exposures (Hložková et al., 2016). A Bio-Rad CFX Manager was used to calculate the baseline range and the experiment threshold cycle (C_{te}) values recorded during the elongation period of the qPCR. The levels of gene transcription as relative to the controls (unexposed mycelium) were calculated by using the $2^{-\Delta\Delta Ct1}$ method (Livak and Schmittgen, 2001), where $C_{t1} = C_{te} \times [\log(1+E)/\log 2]$. The amplification efficiency values *(E)* were calculated using the equation $E = [10^{(-1/slope)}]-1$; the slopes were determined from the standard quantification curves obtained with serial dilutions of first strand cDNA templates. The obtained *E* values for As*CRD1*, As*CCC2* and As*TUBb* genes were 102%, 98%, and 108%, respectively.

RESULTS

Identification and Sequence Analysis of AsCRD1 and AsCCC2

To obtain information about the sequences coding for P_{1B-1}-ATPases in *A. strobiliformis*, the sporocarp transcriptome of *A. strobiliformis* was screened by using tBLASTn search with known P_{1B-1}-ATPases as queries. The screening retrieved two partial transcript sequences: one 822 nucleotides long in which a termination codon was included (a part of mRNA named As*CRD1*) and another 528 nucleotides long without a termination codon (a part of mRNA named As*CCC2*). As the deduced protein fragments showed a substantial identity with the C-terminal sequences of known P_{1B-1}-ATPases, the corresponding full-length coding sequences were established via the RACE method.

The predicted 1097-AA AsCRD1 and 978-AA AsCCC2 proteins showed the characteristic sequence features of P_{1B-1}-ATPases described in other organisms (Argüello et al., 2007; Smith et al., 2014). These involve putative N-terminal Cu/Ag-binding CxxC motifs (three in AsCRD1, two in AsCCC2) and two P_{1B-1} subgroup signature sequences in predicted transmembrane domains (TMD), Nx_6YNx_4P (x represents any AA residue), and $Px_6MxxSSx_5S$, which are in P_{1B-1}-ATPases conserved in TMD7 and TMD8, respectively (**Figure 1** and **Supplementary Figure S1**). Like other P_{1B}-type ATPases, AsCRD1 and AsCCC2 contained eight predicted TMDs with $CPCx_6P$ sequence in TMD6 and HP locus between TMD6 and TMD7. In addition, both predicted proteins possess features typical for all the members of the P-ATPase superfamily (**Figure 1**), particularly the DKTGTxT motif in the predicted large cytoplasmic loop with an aspartyl residue whose phosphorylation from ATP and dephosphorylation is prerequisite for active metal ion transport (Palmgren and Nissen, 2011). Despite the identified regions of conservancy at the protein level, the corresponding genes showed different structure and appeared dissimilar. The cDNA and genomic sequences of As*CRD1* and As*CCC2* were clearly distinct, with coding sequences interrupted with nine and three introns, respectively (**Figure 1**).

The comparison of the predicted AsCRD1 and AsCCC2 proteins revealed that along the sequence, they show lower identity and similarity with each other (25% and 38%, respectively) than they individually showed to P_{1B-1}-ATPases characterized from other species. Predicted AsCRD1 shares 38%, 36%, and 31% identity (54%, 50%, and 48% similarity) with *A. nidulans* CrpA, *C. albicans* CaCRD1, and cucumber (*Cucumis sativus*) CsHMA5.2, respectively, while AsCCC2 shows 35% identity and 51% similarity with both the *S. cerevisiae* Ccc2 and *A. thaliana* AtHMA5. As further indicated in the Neighbor-joining tree (**Supplementary Figure S2**), AsCRD1

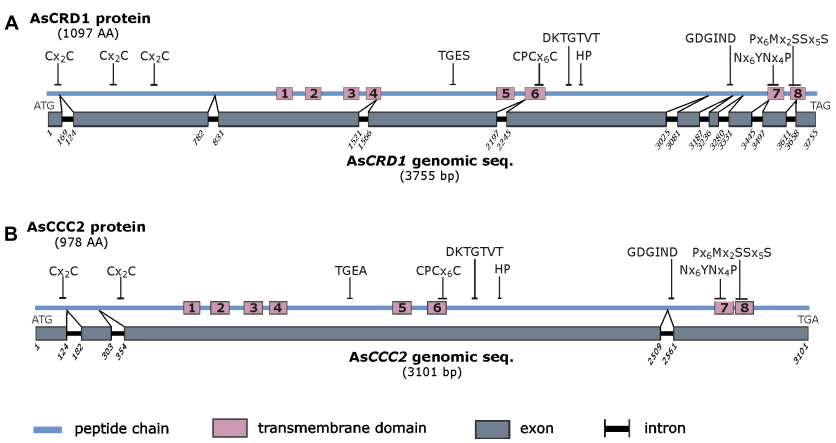

FIGURE 1 | Schematic representation of the predicted AsCRD1 protein **(A)** and AsCCC2 protein **(B)** and the corresponding genomic sequences. The characteristic amino acid sequence motifs are indicated and include Cx_2C metal binding motif, sequence features characteristic of phosphatase domain (TGE[S/A]), aspartyl kinase domain (DKTGTxT), HP locus (HP), ATP-binding domain (GDGxND), Cu translocation domain ($CPCx_5P$), and P_{1B-1}-subtype signature sequences (Nx_6YNx_4P and $Px_6MxxSSx_5S$). For the comparative amino acid sequence analysis and homology models see **Supplementary Figure S1**.

and AsCCC2 sort into two distinct clusters. The AsCRD1-containing cluster comprised the characterized CaCRD1 and a clade of predicted agaricomycete P_{1B-1}-ATPases. The second cluster involved clearly separated clades of mammalian and plant P_{1B-1}-ATPases together with the AsCCC2-containing agaricomycete clade, which was more closely related to plant than to mammalian or yeast transporters. It is noteworthy that among the characterized transporters from Ascomycetes and Basidiomycetes, the closest relatives of AsCCC2 were P_{1B-1}-ATPases from plant pathogens *Botrytis cinerea* (Saitoh et al., 2010) and *Colletotrichum lindemuthianum* (Parisot et al., 2002), and human pathogen *Cryptococcus neoformans* (Walton et al., 2005).

Functional Expression of AsCRD1 and AsCCC2 in *S. cerevisiae*

The homology to known fungal P_{1B-1}-ATPases suggested that AsCRD1 and AsCCC2 are P_{1B-1}-ATPases, which could be involved in metal tolerance and delivery of Cu to metalloproteins, respectively. In order to gain information regarding the function of AsCRD1 and AsCCC2 in handling Cu and Ag, the corresponding coding sequences were constitutively expressed in mutant *S. cerevisiae* strains grown on agar media with or without metal supplements. To attest the importance of the DKTGTxT motif in which the conserved aspartyl is in P-ATPases, a target of phosphorylation/dephosphorylation during the transport reaction cycle, the corresponding mutant As*CRD1*^{D742A} and As*CCC2*^{D555A} variants were constructed, in which the codons for aspartyl 742 (in As*CRD1*) and aspartyl 555 (in As*CCC2*) were changed to encode alanyl residues.

The Cu tolerance assays were conducted in the *cup1*Δ strain carrying a deletion of its single-copy MT gene *cup1*, which renders the cells hypersensitive to Cu. Heterologous expression in yeasts grown on SD medium containing 50 or 100 μM Cu^{2+} revealed that only As*CRD1*, but not As*CCC2*, protected the yeasts form Cu toxicity (**Figure 2A**). The protective effect of As*CRD1* became weaker when the cells were subjected to 200 μM Cu^{2+} (**Figure 2A**). Considering that Ag^{+}, particularly in respiratory conditions, acts as a potent inducer of oxidative stress (Mijnendonckx et al., 2013), and yeasts with defects in oxidative stress response proved useful in attributing Ag-detoxification functions to heterologous proteins (Sácký et al., 2014; Migocka et al., 2015), the *yap1*Δ strain, deficient in a transcription factor upregulating genes involved in oxidative stress response (Rodrigues-Pousada et al., 2010), was used in Ag toxicity assays. As documented in **Figure 2B**, the *yap1*Δ cells grown on non-fermentable YPEG medium and expressing As*CRD1* grew much better in the presence of 5–30 μM Ag^{+} than did the controls. The observation that the expression of As*CRD1*^{D742A} did not confer increased resistance against either Cu (**Figure 2A**) or Ag (**Figure 2B**) suggested that the Cu- and Ag-tolerance phenotypes associated in the model yeasts with wild-type As*CRD1* were indeed due to the metal-transport ability of the encoded protein.

The apparent lack of the Ag/Cu toxicity-related phenotype of As*CCC2* in *cup1*Δ and *yap1*Δ yeasts was congruent with the expected function of AsCCC2 as the transporter involved in handling of physiological Cu inside the cell. The properties of AsCCC2 were thus further tested in the *ccc2*Δ strain in which the absence of Ccc2 causes a severe growth defect on non-fermentable media because of the lack of sufficient mitochondrial iron (Fu et al., 1995; Yuan et al., 1997); note that high affinity iron uptake pathway in *S. cerevisiae* involves Fet1 permease that works together with Cu-dependent, plasma membrane ferroxidase Fet3 that receives its Cu ions (supplied by Ccc2) in Golgi. The growth tests on YPEG medium revealed that As*CCC2* was able to fully complement the respiratory deficiency of the *ccc2*Δ cells, whilst the control cells transformed with empty p416GPD and those expressing As*CCC2*^{D555A} (and As*CRD1*; not shown) failed to grow under the same conditions (**Figure 2C**). The

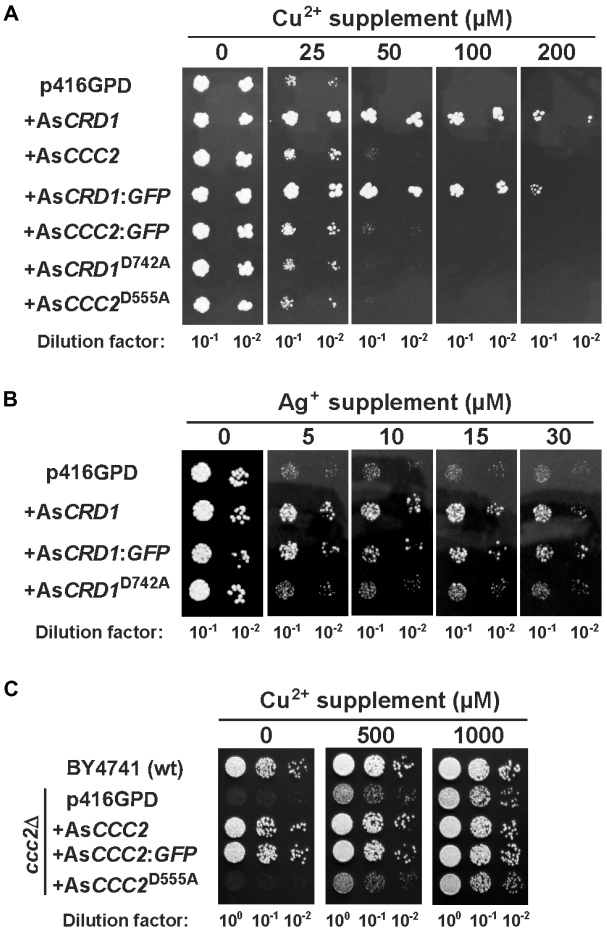

FIGURE 2 | Metal-related phenotypes of yeasts expressing As*CRD1* and As*CCC2* variants. **(A)** Cu tolerance and **(B)** Ag tolerance of the indicated transformants of Cu-hypersensitive *cup1*Δ and Ag-sensitive *yap1*Δ strains of *S. cerevisiae*, respectively. **(C)** Growth of the indicated transformants of *ccc2*Δ strain under respiratory conditions. Spotted for growth were the diluted cultures of cells transformed with the empty p416GPD vector or with the same expression vector inserted with As*CRD1* or As*CCC2,* their translational fusions with GFP, or mutant variants (As*CRD1*^{D742A}, As*CCC2*^{D555A}). Metal tolerance assays were performed using SD medium with or without indicated metal supplement and assays with *ccc2*Δ strain were conducted on non-fermentable YPEG medium.

controls, As*CRD1* (not shown), and As*CCC2*^{D555A} cells showed full growth on the YPEG medium supplemented with 1 mM Cu^{2+}, respectively.

Targeting of AsCRD1 and AsCCC2 in *S. cerevisiae*

Distinct phenotypes associated with As*CRD1* and As*CCC2* in yeasts suggested that the corresponding proteins localized to different membranes. To obtain information about the cellular localization of AsCRD1 and AsCCC2 using direct fluorescence microscopy, the proteins were translationally fused with GFP at their C-termini, and the recombinant As*CRD1*:*GFP* and As*CCC2*:*GFP* genes were expressed in *cup1*Δ and *ccc2*Δ yeasts grown in SD medium. Complementation assays revealed that the phenotypes conferred by the fusions upon the yeasts were essentially the same as those observed with the corresponding transporters without GFP (**Figure 2**), thereby indicating that AsCRD1 and AsCCC2 tagged with GFP at their C-termini remained functional.

The microscopy of As*CRD1*:*GFP*-expressing *cup1*Δ yeasts revealed strong GFP fluorescence co-localizing exclusively with the tonoplast stained with the vacuole-specific fluorophore FM4-64 (**Figure 3A**). The expression of As*CCC2*:*GFP* in the *ccc2*Δ strain resulted in a strong, punctuated GFP signal in vesicular bodies within the cell (**Figure 3B**). The absence of GFP fluorescence from the perinuclear region attributable to ER may suggest that AsCCC2:GFP localized to Golgi rather than ER. The localization of GFP fluorescence in As*CRD1*:*GFP*- and As*CCC2*:*GFP*-transformed yeasts was not affected by the presence of subtoxic concentrations of Cu or Ag or the length of culture period (not shown).

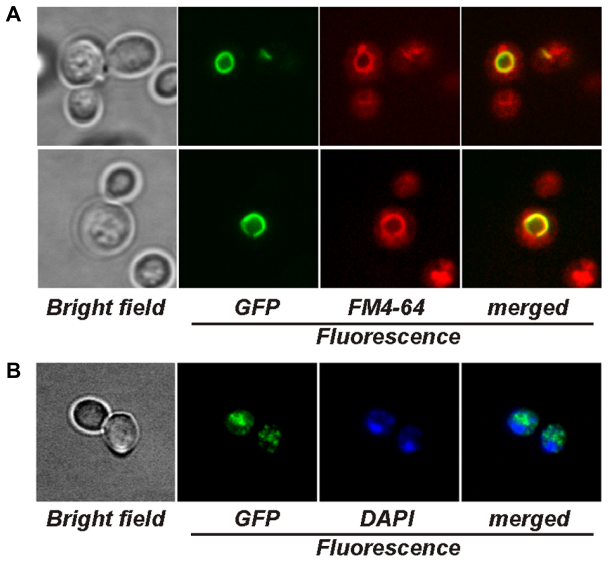

FIGURE 3 | Visualization of yeasts producing GFP-tagged AsCRD1 and AsCCC2 by fluorescence microscopy. **(A)** Cells of *cup1*Δ strain expressing As*CRD1*:*GFP*. The vacuoles were stained with FM4-64; displayed panels from left to right: green GFP fluorescence, red FM4-64 fluorescence, and GFP/FM4-64 merged image with yellow GFP and FM4-64 overlap. **(B)** Cells of *ccc2*Δ strain expressing As*CCC2*:*GFP*. The nuclei were stained with DAPI; displayed panels from left to right: green GFP fluorescence, blue DAPI fluorescence, and GFP/DAPI merged image.

Metal Responsiveness of As*CRD1* and As*CCC2* in *A. strobiliformis*

Considering the As*CRD1*-associated, metal tolerance-related phenotypes in the model yeasts and the typically induced expression of metal tolerance genes during metal overload, the transcription rates of the studied P_{1B-1}-ATPases genes were analyzed by using qRT-PCR, measuring mRNA levels in the mycelium of *A. strobiliformis* treated with 5 and 50 μM Cu^{2+}, 5, 20, and 50 μM Ag^{+}, or 5 μM Cd^{2+} for 24 h. The Cu and Ag concentrations used in the 24-h exposures proved sublethal also in long-term exposures (**Figure 4A**), although the radial growth of mycelia was strongly reduced (by 70%) in the presence of 50 μM Ag. The mycelia always developed brown zones already at 5 μM of any of the metals, presumably due to the induced production of stress-related melanin (Gostinčar et al., 2012).

As shown in **Figure 4B**, 24 h treatments of mycelia with Ag and Cu clearly elevated the expression of As*CRD1*, but not As*CCC2*, relative to the unexposed control. The average levels of As*CRD1* transcripts increased 4.5- and 8.7-fold in the presence of 5 μM Ag^{+} and Cu^{2+}, respectively, and they further nearly doubled when the concentration of the two metals was 50 μM. Neither As*CRD1* nor As*CCC2* showed significant response when the mycelia were treated with a 5 μM concentration of Cd^{2+} (**Figure 4B**), which in *A. strobiliformis* induces the expression of Zn^{2+}/Cd^{2+}-related MT gene As*MT3*, but not Cu^{+}/Ag^{+}-related As*MT1*s (Hložková et al., 2016).

DISCUSSION

Our previous studies revealed a certain overlap in the cellular biology of Cu and Ag in the EM, Ag-hyperaccumulating fungus *A. strobiliformis* – both metals can enter the cells via AsCTR2 and AsCTR3 transporters (Beneš et al., 2016) and intracellular Cu and Ag are sequestered in the cytoplasm through binding with AsMT1s (Hložková et al., 2016). It is worth noting that MTs have been considered principal in the sequestration of Cu or Ag in many EM fungi, including *Pisolithus albus* (Reddy et al., 2016), *Laccaria bicolor* (Reddy et al., 2014), *Hebeloma mesophaeum* (Sácký et al., 2014), *Hebeloma cylindrosporum* (Ramesh et al., 2009), *Amanita submembranacea* (Borovička et al., 2010), and *Paxillus involutus* (Bellion et al., 2007). The present study aimed to identify P_{1B-1}-ATPases of *A. strobiliformis* and inspect their potential role in the handling of intracellular Cu and Ag in this species. Our search of the sporocarp transcriptome suggested the presence of several putative P_{1B}-ATPases of which only two showed sequence features characteristic of the P_{1B-1} subgroup.

Unlike for Zn or Cd, information about the deposition of the excess of the accumulated Cu in fungal vacuoles is scarce. In *Aspergillus niger* (Fomina et al., 2007) and in arbuscular mycorrhizal *Rhizophagus intraradices*

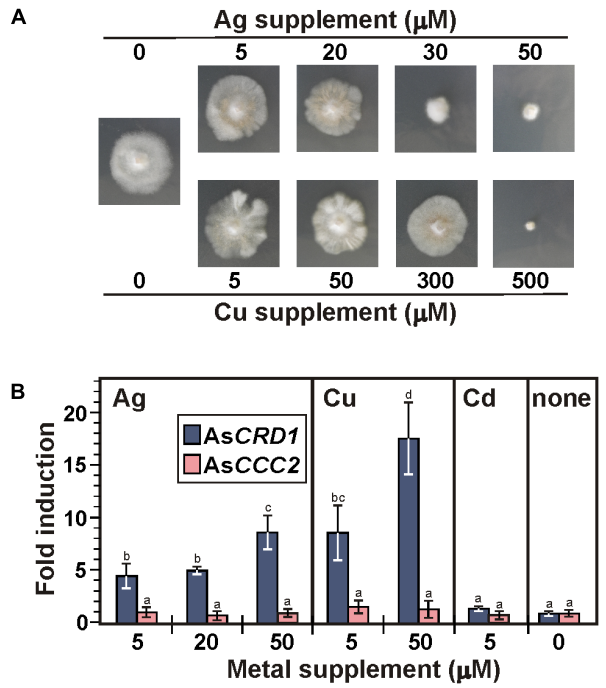

FIGURE 4 | Growth of *A. strobiliformis* and expression of As*CRD1* and As*CCC2* genes in the presence of metal ions as indicated. **(A)** Mycelia grown on 0.5× PD medium with or without metal supplement for 8 weeks (long-term exposure). **(B)** Relative transcript levels measured by qRT-PCR in mycelium incubated in liquid 0.5× PD medium for 24 h with or without (the controls) metal supplement (short term exposure). Expression of β-tubulin gene was used to calculate the relative expression and values plotted are an average of three biological replicates ± standard deviation of the mean (different letters above the bars indicate significant differences as determined by ANOVA followed by Tukey's test, $p < 0.05$).

(González-Guerrero et al., 2008), the vacuolar sequestration of excess Cu was revealed by X-ray microanalyses, which further suggested the association of Cu with vacuolar polyphosphate in *A. niger*. The vacuole is an important organelle for Cu homeostasis in *S. cerevisiae* and the strains defective in vacuolar assembly are hypersensitive to Cu (Szczypka et al., 1997). While the transporters of the CTR family responsible for the mobilization of the vacuolar Cu back into the fungal cytoplasm are well characterized (e.g., Ctr2 in *S. cerevisiae*; Bleackley and MacGillivray, 2011), the Cu-specific, high-affinity transporters that can deliver Cu into the vacuoles remained elusive.

Besides the sequence features common in P-ATPases, in particular of the P_{1B}-subtype, several lines of experimental evidence implicate that AsCRD1 can act as a detoxification P_{1B-1}-ATPase that can transport Cu^+ and Ag^+ into vacuoles in *A. strobiliformis*. First, the expression of As*CRD1*, but not As*CRD1*^{D742A}, protected the model yeasts from Cu and Ag toxicity. The observation that the replacement of aspartyl with alanyl in the DKTGTxT motif (to prevent the phosphorylation in AsCRD1^{D742A} from ATP) abolished the As*CRD1*-associated phenotype in both *cup1*Δ and *yap1*Δ yeast mutants further indicates that AsCRD1 can recognize both Cu and Ag for an active, ATP-dependent transport, and that it was the metal transport that increased the metal tolerance in the yeasts, not a mere immobilization of Cu^+ or Ag^+ through binding to cytoplasmic N-terminal metal binding motifs as it is the case, e.g., of Cu-binding to the Cd-transporting PCA1 in *S. cerevisiae* (Adle et al., 2007). Second, the functional GFP-tagged AsCRD1 was targeted to the tonoplast in model yeasts. Although vacuolar P_{1B-1}-ATPases have not been described in fungi before, such localization is not without precedent. Recent studies in plants have identified the Cu-transporting *S. vulgaris* SvHMA5II (Li et al., 2017), and cucumber (*Cucumis sativus*) Cu- and also Ag-activated CsHMA5.1 and CsHMA5.2 proteins (Migocka et al., 2015), as tonoplast-localizing P_{1B-1}-ATPases facilitating metal detoxification in root cells. Third, the observation that the expression of As*CRD1* was in *A. strobiliformis* effectively induced by Cu and Ag makes it reasonable to assume that AsCRD1 is involved in the cellular biology of both metals and the fungus raises the levels of As*CRD1* to handle excess intracellular Cu and Ag. Considering that our previous metal speciation analyses using size exclusion chromatography revealed that the majority of the Ag and Cu accumulated in *A. strobiliformis* is stably bound in 6-kDa complexes with Ag- and Cu-inducible, cytosolic AsMT1s (Osobová et al., 2011; Beneš et al., 2016; Hložková et al., 2016), one may then ask the question of what role AsCRD1 would have in metal detoxification. We propose that vacuolar storage could provide the second line of defense against high intracellular Ag and Cu levels, perhaps during a temporal deficiency of Cu^+- and Ag^+-binding AsMT1s, akin to the function of zincosome vesicles acting as transient stores of the excess accumulated Zn in *S. cerevisiae* (Devirgiliis et al., 2004). However, considering the plasma membrane localization of the closely related CaCRD1 in *C. albicans* (Riggle and Kumamoto, 2000; Weissman et al., 2000) and CrpA in *A. nidulans* (Antsotegi-Uskola et al., 2017), the possibility that AsCRD1 mislocalizes in *S. cerevisiae* and in *A. strobiliformis* acts as a transporter that exports the excess Cu and Ag out of the cells should not be excluded.

The predicted AsCCC2 and its homologs from Agaricomycetes appeared phylogenetically associated with the Ccc2 protein from the unicellular basidiomycete *C. neoformans* and to a lesser extent with Ccc2s from ascomycetes *B. cinerea*, *C. lindemuthianum* and *S. cerevisiae*. Congruent with this observation, As*CCC2* functionally complemented the *CCC2* gene in *S. cerevisiae ccc2*Δ that is unable to charge its multicopper oxidase Fet3 with Cu in Golgi to establish the Fet3-Ftr1-based iron uptake system (Bleackley and MacGillivray, 2011). The lack of the As*CCC2*-associated phenotype resulting from the D-to-A substitution in the DKTGTxT motif of the encoded protein (in the *ccc2*Δ cells expressing As*CCC2*^{D555A}), and the GFP fluorescence localizing to the intracellular punctuate bodies resembling Golgi in yeasts expressing As*CCC2:GFP* provides further support to the notion that AsCCC2 can mediate active transport of Cu into the Golgi. In *C. neoformans*, *B. cinerea*, and *C. lindemuthianum*, the corresponding functional *CCC2* gene appeared critical for the biosynthesis of melanin; the lack of CCC2 in these species lead to a disruption in the delivery of Cu to extracellular multicopper oxidases

(laccases in particular) during their trafficking through Golgi (Parisot et al., 2002; Walton et al., 2005; Saitoh et al., 2010). Multiple copies of laccase genes have been predicted in both saprobic and EM species (Kohler et al., 2015); for example, the genomes of saprobic *Amanita thiersii* and EM *Amanita muscaria* contain 15 and 18 putative non-allelic laccase genes, respectively. Recent studies indicate that laccases expressed in EM fungi are, besides the pigmentation, involved in the sporocarp development or nutrient acquisition in extraradical mycelia (Courty et al., 2009; Kües and Rühl, 2011; Ellström et al., 2015; Shah et al., 2016). Considering this and the fact that Fet3-like ferroxidase genes have been found in most sequenced basidiomycetes, including *Amanita* species (Kües and Rühl, 2011; Kohler et al., 2015), it could be possible that *A. strobiliformis* benefits from AsCCC2 for both the Fe-uptake complex and laccase(s) assembly via Cu handling.

The results obtained in this study indicate that AsCRD1 and AsCCC2 belong to two separate protein clusters of the P_{1B-1}-ATPase subgroup. The collected data strongly suggest that AsCRD1 is in *A. strobiliformis*, like AsMT1s and AsCTRs, involved in the handling of both Ag and Cu, specifically in supporting the detoxification of Ag and Cu, which is, besides efficient transport, the prerequisite for (hyper)accumulation. Our data further indicate that AsCCC2, identified as another P_{1B-1}-ATPase of *A. strobiliformis*, is a functional homolog of yeast Ccc2, involved in the delivery of physiological Cu into organelles of endomembrane system for the biosynthesis of Cu-dependent proteins. It is worth noting that BLASTp returned putative P_{1B-1}-type ATPases of Agaricomycetes species in which homologs of AsCRD1 and AsCCC2 were identified. These species belong to different orders (**Supplementary Figure S2**) of different lifestyles. It is thus tempting to speculate that the functional specialization and roles of P_{1B-1}-type ATPases, which we here discussed for AsCRD1 and AsCCC2, are widespread among Agaricomycetes.

AUTHOR CONTRIBUTIONS

VB conducted the experimental work and analyzed and interpreted data. TL and JS jointly contributed to the conception and design of the study, the bioinformatic analyses, and helped with the interpretation of data. PK was responsible for the concept and design of the work and the interpretation of the results, ensured the scientific issue was appropriately investigated, and wrote the manuscript. All of the authors assisted in writing the manuscript, discussed the results, and commented on the manuscript.

FUNDING

This work was supported by the Czech Science Foundation through grant no. 16-15065S. Publication fees of the work have been co-financed by the endowment from the Ministry of Education, Youth and Sports of Czechia for the institutional development plan at UCT Prague.

ACKNOWLEDGMENTS

We are grateful to Prof. Dennis J. Thiele (Duke University Medical Center) for the gift of DTY113 (*cup1*Δ) strain. We thank Dr. Jan Borovička (Institute of Geology and Nuclear Physic Institute, CAS) for the valuable discussions.

SUPPLEMENTARY MATERIAL

The Supplementary Material for this article can be found online at: https://www.frontiersin.org/articles/10.3389/fmicb.2018.00747/full#supplementary-material

FIGURE S1 | (A) Comparative sequence analysis of the predicted AsCRD1 and AsCCC2 proteins. Sequences were aligned by using ClustalW and the identical, conservative, and semiconservative residues were marked with asterisks, double dots, and single dots, respectively. The predicted transmembrane domains (TMD, numbered) are highlighted with light blue background and the characteristic sequence motifs are boxed in yellow (metal binding CxxC motif), green ($CPCx_6P$ in TMD6, Nx_6YNx_4P in TMD7, $Px_6MxxSSx_5S$ in TMD8, and HP locus), and red (DKTGTxT motif). The signal peptide predictions in AsCRD1 and AsCCC2 at CCTOP and Signal P 4.1 servers did not unveil any potential signal sequences. **(B)** 3D homology models of AsCRD1 and AsCCC2. The PDB entries used for the comparative modeling of AsCRD1 and AsCCC2 were 2EW9 (N-terminal domain of ATP7B, 23% and 40% identity, respectively) and 3J09 (P_{1B-1}-ATPase CopA of *Archaeoglobus fulgidus*; 34% and 41% identity, respectively). The positions of characteristic sequence motifs are indicated with arrows.

FIGURE S2 | An unrooted, neighbor-joining-based tree of characterized and predicted P_{1B-1}-ATPases. Species name and UniProt accession numbers of functionally characterized ascomycete, plant and mammalian, and predicted Agaricomycetes P_{1B-1}-ATPases (30% to 40% identical with AsCRD1 or AsCCC2; UniProt expect values of 0 to 10^{-97}) are indicated. The tree was generated by MEGA version 6.0 after the sequence alignment by using ClustalW. Bootstrap values (%; 1,000 replicates) are shown at nodes (values <40% are omitted for clarity) and branch lengths are proportional to phylogenetic distances.

TABLE S1 | Primers used in this study.

REFERENCES

Adle, D. J., Sinani, D., Kim, H., and Lee, J. (2007).A cadmium-transporting P1B-type ATPase in yeast *Saccharomycescerevisiae*. *J. Biol. Chem.* 282, 947–955. doi: 10.1074/jbc.M609535200

Altschul, S. F., Gish, W., Miller, W., Myers, E. W., and Lipman, D. J. (1990). Basic local alignment search tool. *J. Mol. Biol.* 215, 403–410. doi: 10.1016/S0022-2836(05)80360-2

Antsotegi-Uskola, M., Markina-Iñarrairaegui, A., and Ugalde, U. (2017). Copper resistance in *Aspergillus nidulans* relies on the PI-type ATPase CrpA, regulated by the transcription factor AceA. *Front. Microbiol.* 8:912. doi: 10.3389/fmicb.2017.00912

Argüello, J. M., Eren, E., and González-Guerrero, M. (2007). The structure and function of heavy metal transport P-1B-ATPases. *Biometals* 20, 233–248. doi: 10.1007/s10534-006-9055-6

Bashir, K., Rasheed, S., Kobayashi, T., Seki, M., and Nishizawa, N. K. (2016). Regulating subcellular metal homeostasis: the key to crop improvement. *Front. Plant Sci.* 7:1192. doi: 10.3389/fpls.2016.01192

Bellion, M., Courbot, M., Jacob, C., Guinet, F., Blaudez, D., and Chalot, M. (2007). Metal induction of a Paxillus involutus metallothionein and its heterologous

expression in Hebeloma cylindrosporum. *New Phytol.* 174, 151–158. doi: 10.1111/j.1469-8137.2007.01973.x

Beneš, V., Hložková, K., Matěnová, M., Borovička, J., and Kotrba, P. (2016). Accumulation of Ag and Cu in *Amanita strobiliformis* and characterization of its Cu and Ag uptake transporter genes AsCTR2 and AsCTR3. *Biometals* 29, 249–264. doi: 10.1007/s10534-016-9912-x

Bleackley, M. R., and MacGillivray, R. T. (2011). Transition metal homeostasis: from yeast to human disease. *Biometals* 24, 785–809. doi: 10.1007/s10534-011-9451-4

Borovička, J., Kotrba, P., Gryndler, M., Mihaljevič, M., Řanda, Z., Rohovec, J., et al. (2010). Bioaccumulation of silver in ectomycorrhizal and saprobic macrofungi from pristine and polluted areas. *Sci. Total Environ.* 408, 2733–2744. doi: 10.1016/j.scitotenv.2010.02.031

Borovička, J.,Řanda, Z., Jelínek, E., Kotrba, P., and Dunn, C. E. (2007). Hyperaccumulation of silver by *Amanita strobiliformis* and related species of the section *Lepidell*a. *Mycol. Res.* 111, 1339–1344. doi: 10.1016/j.mycres.2007.08.015

Colpaert, J. V., Wevers, J. H. L., Krznaric, E., and Adriaensen, K. (2011). How metal-tolerant ecotypes of ectomycorrhizal fungi protect plants from heavy metal pollution. *Ann. For. Sci.* 68, 17–24. doi: 10.1007/s13595-010-0003-9

Courty, P. E., Hoegger, P. J., Kilaru, S., Kohler, A., Buée, M., Garbaye, J., et al. (2009). Phylogenetic analysis, genomic organization, and expression analysis of multi-copper oxidases in the ectomycorrhizal basidiomycete Laccaria bicolor. *New Phytol.* 182, 736–750. doi: 10.1111/j.1469-8137.2009.02774.x

Devirgiliis, C., Murgia, C., Danscher, G., and Perozzi, G. (2004). Exchangeable zinc ions transiently accumulate in a vesicular compartment in the yeast *Saccharomyces cerevisiae*. *Biochem. Biophys. Res. Commun.* 323, 58–64. doi: 10.1016/j.bbrc.2004.08.051

Dobson, L., Reményi, I., and Tusnády, G. E. (2015). CCTOP: A Consensus Constrained TOPology prediction web server. *Nucleic Acids Res.* 43, W408–W412. doi: 10.1093/nar/gkv451

Ellström, M., Shah, F., Johansson, T., Ahrén, D., Persson, P., and Tunlid, A. (2015). The carbon starvation response of the ectomycorrhizal fungus *Paxillus involutus*. *FEMS Microbiol. Ecol.* 91:fiv027. doi: 10.1093/femsec/fiv027

Falandysz, J., and Borovička, J. (2013). Macro and trace mineral constituents and radionuclides in mushrooms: health benefits and risks. *Appl. Microbiol. Biotechnol.* 97, 477–501. doi: 10.1007/s00253-012-4552-8

Fomina, M., Charnock, J., Bowen, A. D., and Gadd, G. M. (2007). X-ray absorption spectroscopy (XAS) of toxic metal mineral transformations by fungi. *Environ. Microbiol.* 9, 308–321. doi: 10.1111/j.1462-2920.2006.01139.x

Fu, D., Beeler, T. J., and Dunn, T. M. (1995). Sequence, mapping and disruption of CCC2, a gene that cross-complements the Ca^{2+}-sensitive phenotype of csg1 mutants and encodes a P-type ATPase belonging to the Cu2+-ATPase subfamily. *Yeast* 11, 283–292. doi: 10.1002/yea.320110310

Füzik, T., Ulbrich, P., and Ruml, T. (2014). Efficient mutagenesis independent of ligation (EMILI). *J. Microbiol. Methods* 106, 67–71. doi: 10.1016/j.mimet.2014.08.003

Gadd, G. M., Rhee, Y. J., Stephenson, K., and Wei, Z. (2012). Geomycology: metals, actinides and biominerals. *Environ. Microbiol. Rep.* 4, 270–296. doi: 10.1111/j.1758-2229.2011.00283.x

González-Guerrero, M., Melville, L. H., Ferrol, N., Lott, J. N. A., Azcón-Aguilar, C., and Peterson, R. L. (2008). Ultrastructural localization of heavy metals in the extraradical mycelium and spores of the arbuscular mycorrhizal fungus *Glomus intraradices*. *Can. J. Microbiol.* 54, 103–110. doi: 10.1139/w07-119

Gostinčar, C., Muggia, L., and Grube, M. (2012). Polyextremotolerant black fungi: oligotrophism, adaptive potential, and a link to lichen symbioses. *Front. Microbiol.* 3, 390. doi: 10.3389/fmicb.2012.00390

Hložková, K., Matìnová, M., Žáčková, P., Strnad, H., Hršelová, H., Hroudová, M., et al. (2016). Characterization of three distinct metallothionein genes of the Ag-hyperaccumulating ectomycorrhizal fungus *Amanita strobiliformis*. *Fungal Biol.* 120, 358–369. doi: 10.1016/j.funbio.2015.11.007

Kelley, L. A., Mezulis, S., Yates, C. M., Wass, M. N., and Sternberg, M. J. (2015). The Phyre2 web portal for protein modeling, prediction and analysis. *Nat. Protoc.* 10, 845–858. doi: 10.1038/nprot.2015.053

Kohler, A., Kuo, A., Nagy, L. G., Morin, E., Barry, K. W., Buscot, F., et al. (2015). Convergent losses of decay mechanisms and rapid turnover of symbiosis genes in mycorrhizal mutualists. *Nat. Genet.* 47, 410–415. doi: 10.1038/ng.3223

Kües, U., and Rühl, M. (2011). Multiple multi-copper oxidase gene families in basidiomycetes - what for? *Curr. Genomics* 12, 72–94. doi: 10.2174/138920211795564377

La Fontaine, S., and Mercer, J. F. B. (2007). Trafficking of the copper-ATPases, ATP7A and ATP7B: Role in copper homeostasis. *Arch. Biochem. Biophys.* 463, 149–167. doi: 10.1016/j.abb.2007.04.021

Li, Y., Iqbal, M., Zhang, Q., Spelt, C., Bliek, M., Hakvoort, H. W. J., et al. (2017). Two Silene vulgaris copper transporters residing in different cellular compartments confer copper hypertolerance by distinct mechanisms when expressed in *Arabidopsis thaliana*. *New Phytol.* 215, 1102–1114. doi: 10.1111/nph.14647

Livak, K. J., and Schmittgen, T. D. (2001). Analysis of relative gene expression data using real-time quantitative PCR and the $2\Delta\Delta C(T)$ method. *Methods* 25, 402–408. doi: 10.1006/meth.2001.1262

Migocka, M., Posyniak, E., Maciaszczyk-Dziubinska, E., Papierniak, A., and Kosieradzaka, A. (2015). Functional and biochemical characterization of cucumber genes encoding two copper ATPases CsHMA5.1 and CsHMA5.2. *J. Biol. Chem.* 290, 15717–15729. doi: 10.1074/jbc.M114.618355

Mijnendonckx, K., Leys, N., Mahillon, J., Silver, S., and Van Houdt, R. (2013). Antimicrobial silver: uses, toxicity and potential for resistance. *Biometals* 26, 609–621. doi: 10.1007/s10534-013-9645-z

Mumberg, D., Müller, R., and Funk, M. (1995). Yeast vectors for the controlled expression of heterologous proteins in different genetic backgrounds. *Gene* 156, 119–122. doi: 10.1016/0378-1119(95)00037-7

Nevitt, T., Öhrvik, H., and Thiele, D. J. (2012). Charting the travels of copper in eukaryotes from yeast to mammals. *Biochim. Biophys. Acta Mol. Cell Res.* 1823, 1580–1593. doi: 10.1016/j.bbamcr.2012.02.011

Osobová, M., Urban, V., Jedelský, P. L., Borovička, J., Gryndler, M., Ruml, T., et al. (2011). Three metallothionein isoforms and sequestration of intracellular silver in the hyperaccumulator *Amanita strobiliformis*. *New Phytol.* 190, 916–926. doi: 10.1111/j.1469-8137.2010.03634.x

Palmgren, M. G., and Nissen, P. (2011). P-Type ATPases. *Annu. Rev. Biophys.* 40, 243–266. doi: 10.1146/annurev.biophys.093008.131331

Parisot, D., Dufresne, M., Veneault, C., Laugé, R., and Langin, T. (2002). clap1, a gene encoding a copper-transporting ATPase involved in the process of infection by the phytopathogenic fungus *Colletotrichum lindemuthianum*. *Mol. Genet. Genomics* 268, 139–151. doi: 10.1007/s00438-002-0744-8

Pettersen, E. F., Goddard, T. D., Huang, C. C., Couch, G. S., Greenblatt, D. M., Meng, E. C., et al. (2004). UCSF Chimera - a visualization system for exploratory research and analysis. *J. Comput. Chem.* 25, 1605–1612. doi: 10.1002/jcc.20084

Ramesh, G., Podila, G. K., Gay, G., Marmeisse, R., and Reddy, M. S. (2009). Different patterns of regulation for the copper and cadmium metallothioneins of the ectomycorrhizal fungus *Hebeloma cylindrosporum*. *Appl. Environ. Microbiol.* 75, 2266–2274. doi: 10.1128/AEM.02142-08

Reddy, M. S., Kour, M., Aggarwal, S., Ahuja, S., Marmeisse, R., and Fraissinet-Tachet, L. (2016). Metal induction of a *Pisolithus albus* metallothionein and its potential involvement in heavy metal tolerance during mycorrhizal symbiosis. *Environ. Microbiol.* 18, 2446–2454. doi: 10.1111/1462-2920.13149

Reddy, M. S., Prasanna, L., Marmeisse, R., and Fraissinet-Tachet, L. (2014). Differential expression of metallothioneins in response to heavy metals and their involvement in metal tolerance in the symbiotic basidiomycete *Laccaria bicolor*. *Microbiology* 160, 2235–2242. doi: 10.1099/mic.0.080218-0

Riggle, P. J., and Kumamoto, C. A. (2000). Role of a *Candida albicans* P1-type ATPase in resistance to copper and silver ion toxicity. *J. Bacteriol.* 182, 4899–4905. doi: 10.1128/JB.182.17.4899-4905.2000

Rodrigues-Pousada, C., Menezes, R. A., and Pimentel, C. (2010). The Yap family and its role in stress response. *Yeast* 27, 245–258. doi: 10.1002/yea.1752

Sácký, J., Leonhardt, T., Borovička, J., Gryndler, M., Briksí, A., and Kotrba, P. (2014). Intracellular sequestration of zinc, cadmium and silver in Hebeloma mesophaeum and characterization of its metallothionein genes. *Fungal Genet. Biol.* 64, 3–14. doi: 10.1016/j.fgb.2014.03.003

Saitoh, Y., Izumitsu, K., Morita, A., and Tanaka, C. (2010). A copper-transporting ATPase BcCCC2 is necessary for pathogenicity of *Botrytis cinerea*. *Mol. Genet. Genomics* 284, 33–43. doi: 10.1007/s00438-010-0545-4

Shah, F., Nicolás, C., Bentzer, J., Ellström, M., Smits, M., Rineau, F., et al. (2016). Ectomycorrhizal fungi decompose soil organic matter using oxidative mechanisms adapted from saprotrophic ancestors. *New Phytol.* 209, 1705–1719. doi: 10.1111/nph.13722

Smith, A. T., Smith, K. P., and Rosenzweig, A. C. (2014). Diversity of the metal-transporting P1B-type ATPases. *J. Biol. Inorg. Chem.* 19, 947–960. doi: 10.1007/s00775-014-1129-2

Szczypka, M. S., Zhu, Z., Silar, P., and Thiele, D. J. (1997). *Saccharomyces cerevisiae* mutants altered in vacuole function are defective in copper detoxification and iron-responsive gene transcription. *Yeast* 13, 1423–1435. doi: 10.1002/(SICI)1097-0061(199712)13:15<1423::AID-YEA190>3.0.CO;2-C

Tamai, K. T., Gralla, E. B., Ellerby, L. M., Valentine, J. S., and Thiele, D. J. (1993). Yeast and mammalian metallothioneins functionally substitute for yeast copper-zinc superoxide dismutase. *Proc. Natl. Acad. Sci. U. S. A.* 90, 8013–8017. doi: 10.1073/pnas.90.17.8013

Tamura, K., Stecher, G., Peterson, D., Filipski, A., and Kumar, S. (2013). MEGA6: molecular evolutionary genetics analysis version 6.0. *Mol. Biol. Evol.* 30, 2725–2729. doi: 10.1093/molbev/mst197

Thompson, J. D., Higgins, D. G., and Gibson, T. J. (1994). CLUSTAL W: Improving the sensitivity of progressive multiple sequence alignment through sequence weighting, position-specific gap penalties and weight matrix choice. *Nucleic Acids Res.* 22, 4673–4680. doi: 10.1093/nar/22.22.4673

Walton, F. J., Idnurm, A., and Heitman, J. (2005). Novel gene functions required for melanization of the human pathogen *Cryptococcus neoformans*. *Mol. Microbiol.* 57, 1381–1396. doi: 10.1111/j.1365-2958.2005.04779.x

Webb, B., and Sali, A. (2014). Comparative protein structure modeling using MODELLER. *Curr. Protoc. Bioinformatics* 47, 5.6.1–5.6.32. doi: 10.1002/0471250953.bi0506s47

Weissman, Z., Berdicevsky, I., Cavari, B. Z., and Kornitzer, D. (2000). The high copper tolerance of Candida albicans is mediated by a P-type ATPase. *Proc. Natl. Acad. Sci. U.S.A.* 97, 3520–3525. doi: 10.1073/pnas.97.7.3520

Yuan, D. S., Dancis, A., and Klausner, R. D. (1997). Restriction to copper transport in *Saccharomyces cerevisiae* to a late Golgi or post-Golgi compartments in the secretory pathway. *J. Biol. Chem.* 272, 25787–25793. doi: 10.1074/jbc.272.41.25787

Conflict of Interest Statement: The authors declare that the research was conducted in the absence of any commercial or financial relationships that could be construed as a potential conflict of interest.

Advantages of publishing in Frontiers

OPEN ACCESS
Articles are free to read for greatest visibility and readership

FAST PUBLICATION
Around 90 days from submission to decision

HIGH QUALITY PEER-REVIEW
Rigorous, collaborative, and constructive peer-review

TRANSPARENT PEER-REVIEW
Editors and reviewers acknowledged by name on published articles

Frontiers
Avenue du Tribunal-Fédéral 34
1005 Lausanne | Switzerland

Visit us: www.frontiersin.org
Contact us: info@frontiersin.org | +41 21 510 17 00

REPRODUCIBILITY OF RESEARCH
Support open data and methods to enhance research reproducibility

DIGITAL PUBLISHING
Articles designed for optimal readership across devices

FOLLOW US
@frontiersin

IMPACT METRICS
Advanced article metrics track visibility across digital media

EXTENSIVE PROMOTION
Marketing and promotion of impactful research

LOOP RESEARCH NETWORK
Our network increases your article's readership